COMBINED BIOREACTION AND SEPARATION IN CENTRIFUGAL FIELDS

STEVEN JOHN SETFORD

Doctor of Philosophy

THE UNIVERSITY OF ASTON IN BIRMINGHAM

September 1992

THE UNIVERSITY OF ASTON IN BIRMINGHAM

COMBINED BIOREACTION AND SEPARATION IN CENTRIFUGAL FIELDS

Steven John Setford PhD September 1992

SUMMARY

The aim of this work has been to investigate the principle of combined centrifugal bioreaction-separation. The production of dextran and fructose by the action of the enzyme dextransucrase on sucrose was employed to elucidate some of the principles of this type of process. Dextran is a valuable pharmaceutical product used mainly as a blood volume expander and blood flow improver whilst fructose is an important dietary product. The development of a single step process capable of the simultaneous biosynthesis of dextran and the separation of the fructose by-product should improve dextran yields whilst reducing capital and processing costs.

This thesis shows for the first time that it is possible to conduct successful bioreaction-separations using a rate-zonal centrifugation technique. By layering thin zones of dextransucrase enzyme onto sucrose gradients and centrifuging, very high molecular weight (MW) dextran-enzyme complexes were formed that rapidly sedimented through the sucrose substrate gradients under the influence of the applied centrifugal field. The low MW fructose by-product sedimented at reduced rates and was thus separated from the enzyme and dextran during the reaction.

The MW distribution of dextran recovered from the centrifugal bioreactor was compared with that from a conventional batch bioreactor. The results indicated that the centrifugal bioreactor produced up to 100% more clinical dextran with MWs of between 12 000 and 98 000 at 20% w/w sucrose concentrations than conventional bioreactors. This was due to the removal of acceptor fructose molecules from the sedimenting reaction zone by the action of the centrifugal field. Higher proportions of unwanted lower MW dextran were found in the conventional bioreactor than in the centrifugal bioreactor-separator.

The process was studied on a number of alternative centrifugal systems. A zonal rotor fitted with a reorienting gradient core proved most successful for the evaluation of bioreactor performance. Results indicated that viscosity build-up in the reactor must be minimised in order to increase the yields of dextran per unit time and improve product separation.

A preliminary attempt at modelling the process has also been made.

Key words:

Biochemical reactor, Centrifugal reactor, Dextran, Dextransucrase, Reactor-separator

DEDICATED TO ISOBEL JANE
FROM HILLHEAD TO BLA BHEINN TO WHITTLE-LE-WOODS !

ACKNOWLEDGEMENTS

The author is indebted to the following:

Dr. E L Smith, the head of the Chemical Engineering and Applied Chemistry Department for making the research facilities available.

Professor P E Barker, my research supervisor for his advice and guidance throughout this work. Also Dr. G Ganetsos, an honorary fellow of the University for his helpful comments and suggestions.

The Science and Engineering Research Council for the provision of a research studentship and also a research capital grant that allowed this work to be continued.

Dr Ian Blackburn, and Mr RM Alsop for helpful advice and discussions and Fisons Pharmaceuticals Ltd. for the donation of standard dextran 'T' fractions.

Mr Dave Walton and Mr Paul Tack for helpful advice and sample analysis. Also Mr. Mike Lea, Mr Dave Bleby, Mrs Lyn Wright, Mr Steve Ludlow and all the staff in the department for all their time and effort.

Mr Steve Howitt of Pharmaceutical Sciences for the use of the MSE centrifuge.

Dr Arthur Rowe of the National Centre for Macromolecular Hydrodynamics, University of Leicester, for his considerable time and effort in teaching me the rudiments of analytical ultracentrifugation.

Dr Eric Smith and Mr Luiz Taddei for their helpful advice and suggestions towards the development of a mathematical model for the process.

Mrs Rita Wright and Mrs Wendy Overton for typing numerous reports.

To Dr. John Ajongwen and my fellow research students in the separation and purification group for their practical help, advice and useful discussions.

Finally I Would like to thank Jane, Mum, Dad, Bill and Iris for their support and encouragement throughout this work.

LIST OF CONTENTS

LIST OF FIGURES

LIST OF TABLES

1.0 INTRODUCTION

Dextran is the collective name given to a large class of extracellular branched bacterial polysaccharides composed of repeating monomeric glucose units.

Dextran is mainly used in the pharmaceutical industry as a blood volume expander and blood flow improver [1]. The molecular weight of these products are strictly controlled. For example, the British Pharmacopoeia standard for dextran 40, that is, dextran with a molecular weight average $\overline{MW}$ of 40 000, requires 85% of its molecular weight (MW) to be between 12 000 and 98 000 [2]. Dextran is also required for the production of iron dextran, used in the treatment of anaemia.

Clinical dextran is produced from sucrose using the extracellular enzyme dextransucrase. The product of this fermentation stage is called 'native dextran'. Fructose is the main by-product of the reaction. At low sucrose concentrations the reaction is almost stoichiometric yielding similar quantities of dextran and fructose.

The industrial production of clinical dextran consists of several distinct unit operations. First is the fermentation stage, where a large fermentation vessel containing an aqueous solution of sucrose, fortified with suitable nutrients, growth stimulators, buffer salts and minerals is inoculated with a culture of the bacterium *Leuconostoc mesenteroides*, strain NRRL B-512F. The fermentation is then allowed with little process control, to reach completion. The final fermentation broth will contain native dextran, fructose, cellular debris and other impurities. Clinical dextran is produced from this broth using a combination of acid hydrolysis and ethanol fractionation stages.

The overall process suffers from high energy costs, mainly due to the need for ethanol recovery by distillation. Working with large quantities of ethanol is also hazardous. Furthermore, the initial fermentation step is inefficient, particularly for the following reasons:

(i) The dextran produced is present in a large vessel containing large quantities of impurities. A method capable of separating, purifying and concentrating the native dextrans produced in these fermentation broths could significantly reduce production costs.

(ii) No attempt is made to remove fructose from the broths. Fructose is a valuable by-product, used extensively as a sweetner in the food industry.

(iii) High equipment and operating costs.

(iv) It has been shown that the fructose molecules produced during the reaction interfere with dextran chain growth, causing premature release of the growing dextran chains from the enzyme molecules. This results in the increased production of low molecular weight (LMW) dextran. This phenomenon is most pronounced at high sucrose concentrations and is termed 'the acceptor reaction'. Alsop[3] reports that at sucrose concentrations of 20% w/v (weight per unit volume), nearly half of all the dextran produced has a molecular weight (MW) of below 5 000. LMW dextran has limited uses.

However, high sucrose concentrations are important to reduce equipment and operating costs. Ideally, a production method that minimises the acceptor reaction at high sucrose concentrations is required. This can be achieved by simultaneously removing the fructose molecules as they are produced, from the reaction zone where dextran synthesis is occurring. This has been achieved in this laboratory by Barker and co-workers[4-9] using batch and continuous chromatographic systems. Improved yields of high molecular weight (HMW) dextran were recorded.

The integration of the bioreaction and separation processes is also attractive for other reasons. Downstream processing costs can account for a substantial amount of the total production cost of a material. Therefore by limiting the number of process stages in a production process by combining two or more of the process steps, a substantial reduction in the overall operating costs can be achieved.

The purpose of this project is to develop an alternative combined bioreaction-separation process for native dextran production. The ideal process will be capable of both minimising the acceptor reaction by fructose removal and collecting a concentrated dextran rich product. This process should also be economically viable, non-hazardous and capable of continuous operation.

The powerful separation technique of centrifugation was chosen for investigation, since in theory it appeared to meet the above criteria. This process exploits differences in mass between the various reaction species.

The aims of this project can therefore be defined as follows:

(i) Study the principle of the combined centrifugal bioreaction-separation process. It was envisaged that the work undertaken would act as a foundation for further process development.

(ii) Determine the efficiency of centrifugal techniques for the separation of dextran from fermentation broths.

(iii) Study the behaviour of the dextransucrase reaction in centrifugal fields with the particular aim of minimising the acceptor reaction.

(iv) Investigate methods of operating the combined centrifugal dextransucrase bioreactor-separator on a semi-continuous or continuous basis.

(v) To mathematically model the process showing most promise as a dextransucrase bioreactor-separator.

2.0 DEXTRAN, FRUCTOSE AND THE COMBINED BIOREACTION-SEPARATION PROCESS

A brief introduction to dextran and fructose and their current methods of production are reported in this chapter. This is followed by a literature survey highlighting the use of centrifuges as combined bioreactor-separators and how centrifugation techniques could be employed in the development of a combined bioreaction-separation process for dextran production. Because dextran sedimentation in centrifugal fields is highly dependant upon dextran structure, a detailed literature review concerning dextran structure is also reported.

2.1 DEXTRAN

2.1.1 Introduction

The term 'dextran' was first used by Scheibler[10] in 1874 in connection with a carbohydrate with an empirical formula of $C_6H_{10}O_5$, found in cane and beet sugar juices. Later investigations have shown that 'dextran' can be formed by many different microorganisms and the term 'dextrans' is used when no clear definition of the bacterial origins and chemical properties are given.

Dextrans are extracellular bacterial polysaccharides, composed almost exclusively of the monomeric unit α-D-glucopyranose linked mainly by α 1→6 bonds. Many dextrans with widely different branched structures exist. The *Leuconostoc mesenteroides* B-512F strain has emerged as the bacterium of choice for the commercial production of clinical dextran and is the only strain approved medically for the synthesis of dextran for intravenous injection. This strain produces a water soluble dextran containing 95% α 1→6 linear linkages and 5% α 1→3 branch linkages. The chemical structure of dextran is shown in figure 2.1.

Alsop[3] has listed a number of potential uses for dextran, although its main use remains in the pharmaceutical industry as blood volume expanders ($\overline{MW}$ ~ 70 000) and blood flow improvers ($\overline{MW}$ ~ 40 000). The molecular weight distribution (MWD) of these fractions is controlled by various pharmacopoeial and national specifications. The advantage of dextran preparations are their stability to heat sterilisation, independence of blood type and recipients, freedom from transmissible diseases and low incidence of adverse reactions. Dextran is also used for the production of iron dextran, used in veterinary medicine for the treatment of anaemia.

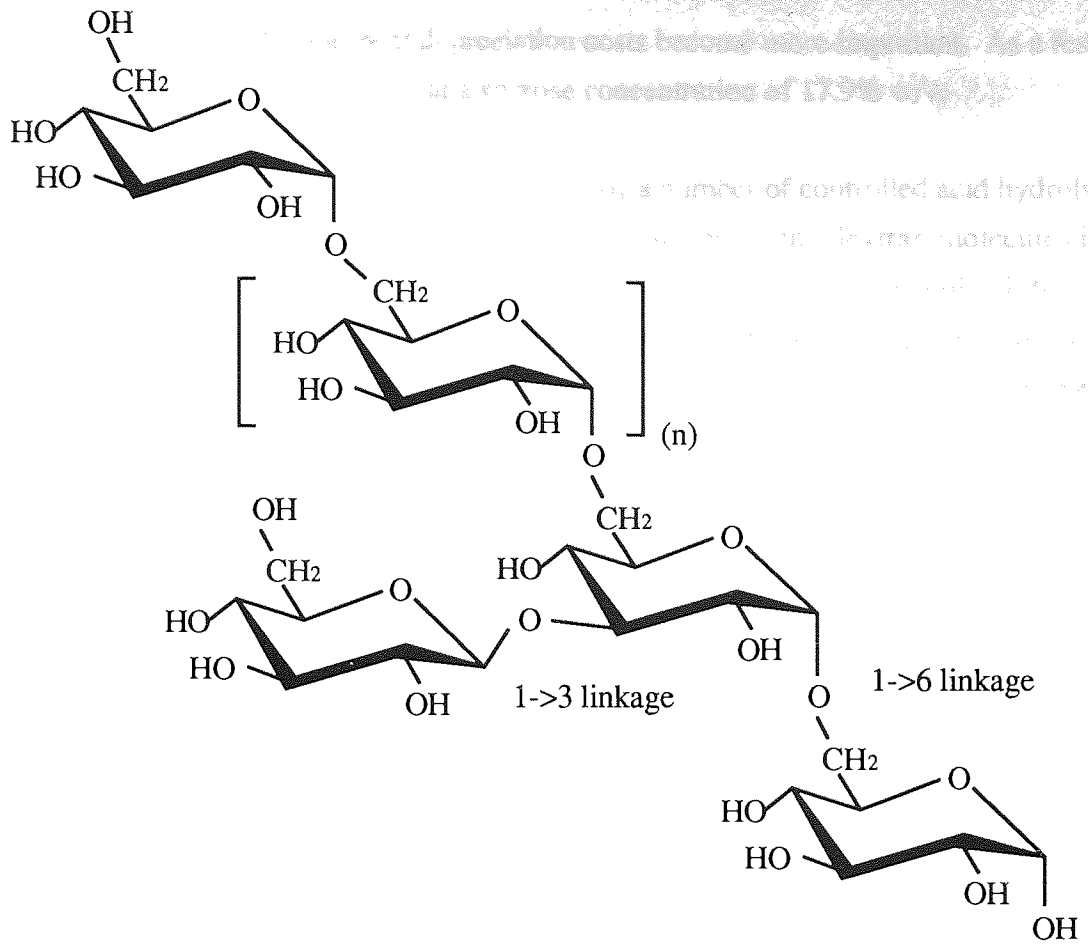

Figure 2.1 The Chemical Structure of Dextran

2.1.2 Production of Dextran

B-512F dextran is produced from sucrose by the action of dextransucrase, an extracellular enzyme, synthesised by the NRRL B-512F *Leuconostoc mesenteroides* species. Fructose is the main by-product of the reaction.

Industrially, dextran production is carried out by inoculating sucrose solutions, fortified with suitable nutrients, growth stimulators, buffer salts and mineral salts with a culture of *Leuconostoc mesenteroides*, at a temperature of 25°C and a neutral pH. Details of this process have been reported by Jeanes[11]. Only limited process control takes place and the fermentation is left to reach completion.

The dextran produced, called 'native' dextran has a broad MWD. However, the commercially important product is HMW dextran. Alsop[3] found that in the industrial process, HMW dextran yields are maximised by using initial sucrose concentrations of 17.9% w/v. When the yield is related to the direct operating costs of a plant, a decrease in the optimum level to 12.5% w/v sucrose is registered. However, at this lower optimum,

throughputs are less and equipment depreciation costs become more important. As a result, the main UK manufacturer operates at a sucrose concentration of 17.9% w/v.

Dextran is harvested from the fermentation media by a number of controlled acid hydrolysis and ethanol fractionation steps. Acid hydrolysis breaks down the dextran molecules into smaller units which can be harvested by precipitation using aqueous ethanol solutions of appropriate strengths and volumes. By controlling the hydrolysis step, dextran of the required molecular weight (MW) can be produced. The industrial process is summarised in figure 2.2.

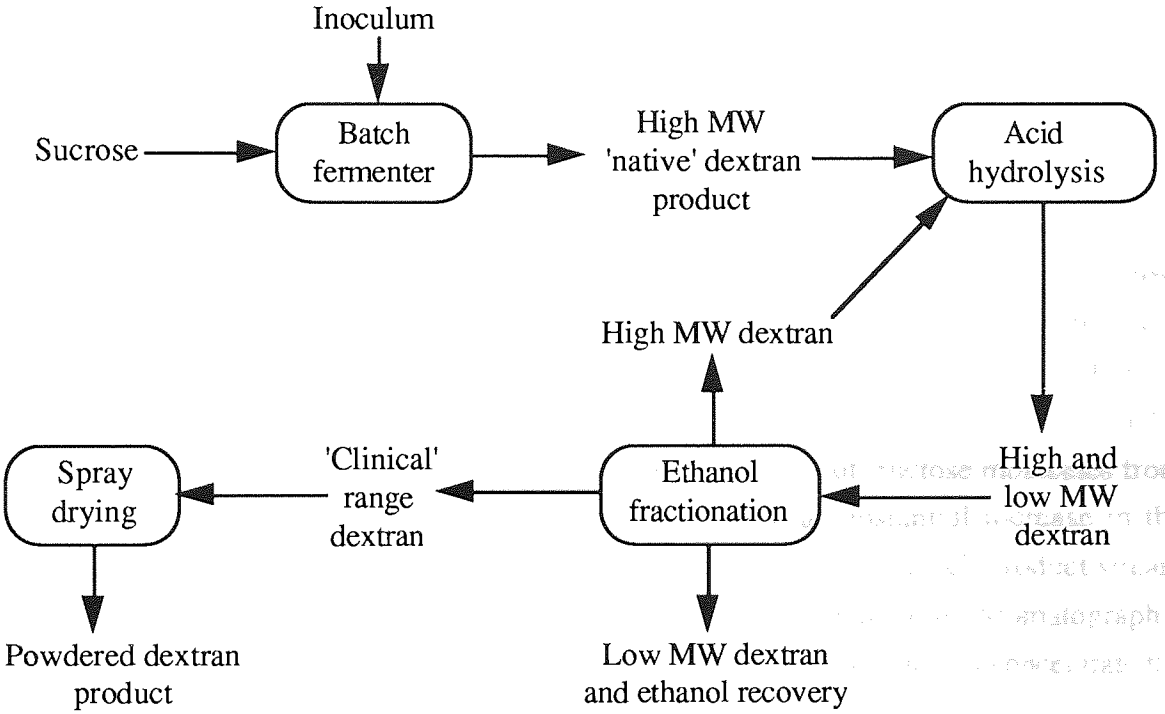

Figure 2.2 Industrial Manufacture of Dextran

The process has the disadvantage of cell, enzyme and dextran production under a set of conditions which is not constant throughout the fermentation. By maintaining a pH of 6.7 and a temperature of 23°C throughout the fermentation, Tsuchiya et al [12] were able to increase dextransucrase enzyme activities by a factor of six although the enzyme exhibited instability at this pH. Subsequent work by Alsop[3] and Barker and Ajongwen[13] have further increased enzyme activities in batch fermentations. Higher enzyme activities will result in improved product yields per unit time, which is an important consideration in commercial processes.

Further process optimisation can be achieved by removing cellular material from reacted *Leuconostoc mesenteroides* fermentation broths, leaving a cell free enzyme solution. This will be discussed in Chapter 3. This was first achieved by Hehre[14]. The enzyme solution

can then be used to synthesise dextran under controlled, optimum conditions. Cell free enzyme solutions have been used by Barker and co-workers[4-9], Zafar[15], Akintoye[16] and Ganetsos[17] in dextransucrase bioreaction-separation studies.

2.1.3 Alternative Dextran Production Processes

A number of workers [18-23] have described processes for the production of clinically specified dextran as well as dextrans of other MWD specifications without using expensive and hazardous solvent extraction procedures. Based on this work, Barker et al[24] have reported a promising alternative method for clinical dextran production (figure 2.3) In this process, the extracellular dextransucrase enzyme is produced separately and purified by ultracentrifugation (UC) and ultrafiltration (UF) before being passed into a continuous chromatographic reactor (SCCR-S), packed with calcium charged resin. The operation of the SCCR-S system has been detailed in reference 24. The bioreactor is initially charged with purified dextransucrase and then more enzyme was added continuously in the deionised water eluent and/or sucrose feed streams at the required strengths. During operation, the sucrose is converted to dextran and fructose and the acceptor fructose molecule will be simultaneously removed from the bioreaction zone due to loose complexing with the calcium ions in the resin. The fructose is retarded by being held back on the resin and thus is separated from the other components which moved preferentially with the mobile phase. Zafar [15] has showed that the removal of fructose molecules from the reaction zones in chromatographic bioreactors led to a substantial increase in the commercially important HMW native dextran product. The dextran-rich product stream from the SCCR-S can then be acid hydrolysed. The use of a continuous chromatographic separator (SCCR) and ultrafiltration and diafiltration (DF) to fractionate and concentrate the dextran product removes the need for ethanol in this production process.

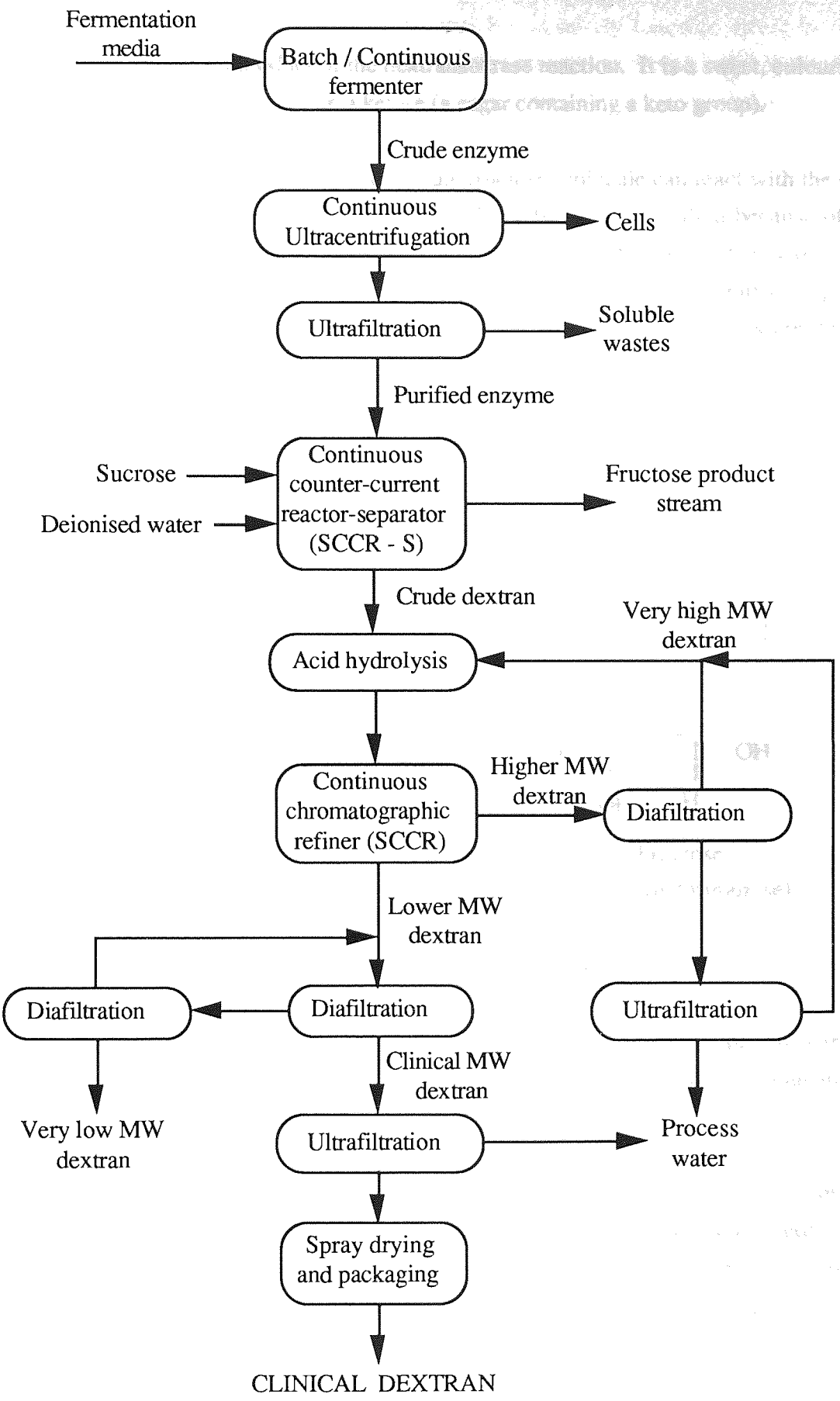

Figure 2.3 The Proposed Clinical Dextran Production Process

2.2 FRUCTOSE

Fructose is the other main product of the dextransucrase reaction. It is a sweet, colourless monosaccharide and is an example of a ketose (a sugar containing a keto group).

The C-2 keto group in the open chain form of the fructose molecule can react with the C-5 hydroxyl group to form a five membered ring called a furanose, so called because of its similarity to furan (figure 2.4) .Two furanose forms are possible, α and β. The designation α means that the hydroxyl group attached to the C-2 group is below the plane of the ring, β means that it is above the plane of the ring. The two forms are called anomers.

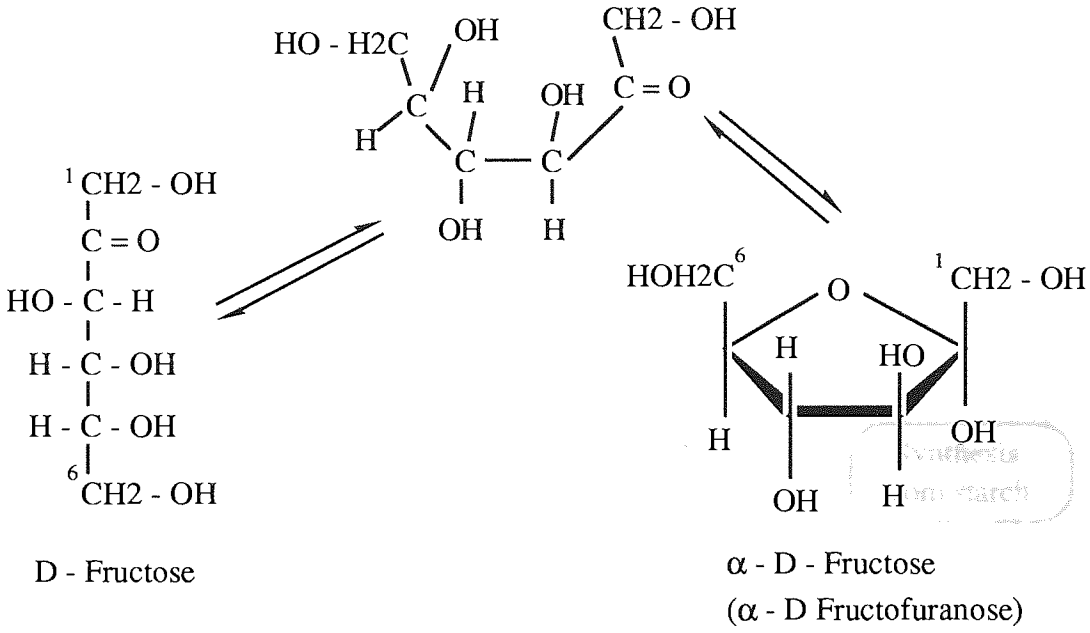

D - Fructose

α - D - Fructose
(α - D Fructofuranose)

Figure 2.4 Fructose Structure

The most common form of fructose is D-fructose, the symbol D indicating that the carbon furthest from the keto group, namely C-5, is of the same configuration as that in D-glyceraldehyde.

Fructose has found various uses in the market place as a sweetener substitute for sucrose in products as diverse as beverages, 'diet' foods, baby food and childrens medicines. Fructose is also used as a flavour enhancer and as a raw material in the manufacture of flavourings. Fructose can enhance the inherent aroma of fruits, berries and vegetables and has been added to juices, jams and desserts[25].

Fructose has a similar calorific value to sucrose but is nearly twice as sweet in cold solutions[26,27] and has been used in saccharin preparations to remove bitter aftertastes. Fructose-saccharin mixtures are generally 3 to 4 times sweeter than pure sucrose without any distinguishing taste differences. At temperatures in excess of 50°C, the sweetness of fructose is reduced to that of sucrose due to conformational changes in the molecule[26,27].

The main industrial methods of fructose production have been reviewed by Akintoye [16] and are summarised in figure 2.5.

Fructose is also the main by-product formed during the industrial conversion of sucrose to B-512F dextran in the presence of dextransucrase enzyme. Although no instances in the literature concerning the commercial recovery of fructose from dextransucrase fermentation broths were found, Barker and co-workers[24] have reported an alternative clinical dextran production process that results in the yield of 100% pure fructose product streams (see figure 2.3).

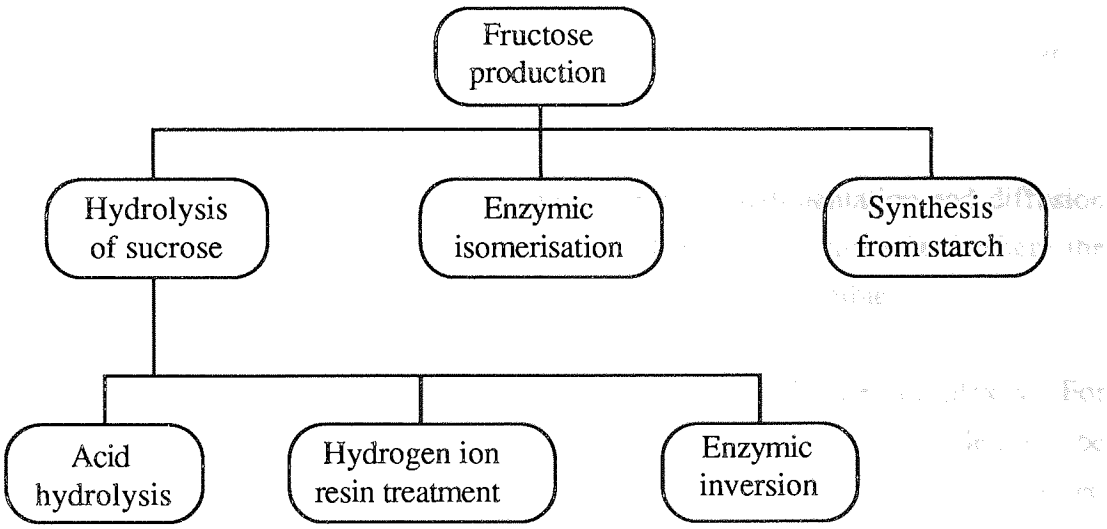

Figure 2.5 The Main Industrial Methods of Fructose Production

2.3 BIOREACTION-SEPARATION IN CENTRIFUGAL FIELDS

2.3.1 Literature survey

Centrifugation techniques are mostly used for the separation, purification, characterisation and/or clarification of solids and liquids. However, instances concerning the study of chemically reacting systems in centrifugal fields have been reported.

Cohen et al[28] studied the behaviour of an enzyme in an applied centrifugal field using the rate-zonal centrifugation technique. This technique is used to separate two or more sample

components by virtue of their different rates of sedimentation in a centrifugal field. Dense supporting solutions are overlaid with thin zones of sample solution and centrifuged so that the sample components sediment into the supporting medium at their own characteristic rates and are thus separated from each other as centrifugation proceeds. The rate-zonal centrifugation technique will be discussed in more detail in section 4.4.2. Cohen et al. chose to study the specific enzymic reaction of glutamic dehydrogenase:

$$NAD^+ + \text{Glutamic Acid} \xrightleftharpoons[\text{Glutamic Dehydrogenase}]{} NADH + NH_3 + \alpha\text{-Ketoglutaric Acid} + H^+$$

A small volume of the buffered enzyme was carefully layered onto the top of a glutamic acid solution, which served as both the supporting solution and enzyme substrate solution. The tube was then centrifuged. The substrate concentrations were sufficient to saturate the enzyme and decreased by less than 5% during the course of the reaction. Photographs of the centrifuge cell at a wavelength of 334 nm were taken at uniform time intervals. Since only NADH absorbed light of this wavelength and the decrease in optical density due to absorption was directly proportional to NADH concentration, the distribution of NADH in the centrifuge cells could be determined at any given time interval (figure 2.6).

This distribution data was then used to determine the mean sedimentation and diffusion coefficients of the enzyme using the fact that NADH was only synthesized where the enzyme was present in the cell. The back reaction was assumed negligible.

This method proved useful for the study of active enzyme-molecule complexes. For example, during a polymerisation reaction, the molecular weight of the complex will be proportional to its sedimentation and diffusion properties. Data can then be obtained concerning the possible polymerisation state of the complex and the changes that can occur under the influence of various enzyme activators and inhibitors.

The polymerisation of acrylonitrile to polyacrylonitrile in centrifugal fields was studied by Parts and Elbing[29]. The monomer was initially uniformally dispersed in a centrifuge cell and the polymerisation process was initiated by the catalytic decomposition of hydrogen peroxide by ferric nitrate solution. Experiments were performed in centrifugal fields ranging from 2 000 to 180 000 g. The reaction was followed in a laboratory centrifuge by sample collection and in an analytical ultracentrifuge by measurement of the level of sedimented polyacrylonitrile.

Figure 2.7 shows the rate of polymerisation is lower in all the centrifugal fields compared to that of the normal gravitational field. 51.2% of the monomer was polymerised after 597 minutes at 180 000 g, while the same degree of conversion was achieved in about 50 minutes at 1 g. This was because the polymer particles, due to their increase in mass, sedimented to the base of the centrifuge cell where they were subsequently covered by more polymer material and so were cut off from the supply of monomer. Hence the rate of polymerisation decreased. Similar results were obtained by Carenza et al[30] when studying the radiation induced polymerisation of vinyl chloride in centrifugal fields.

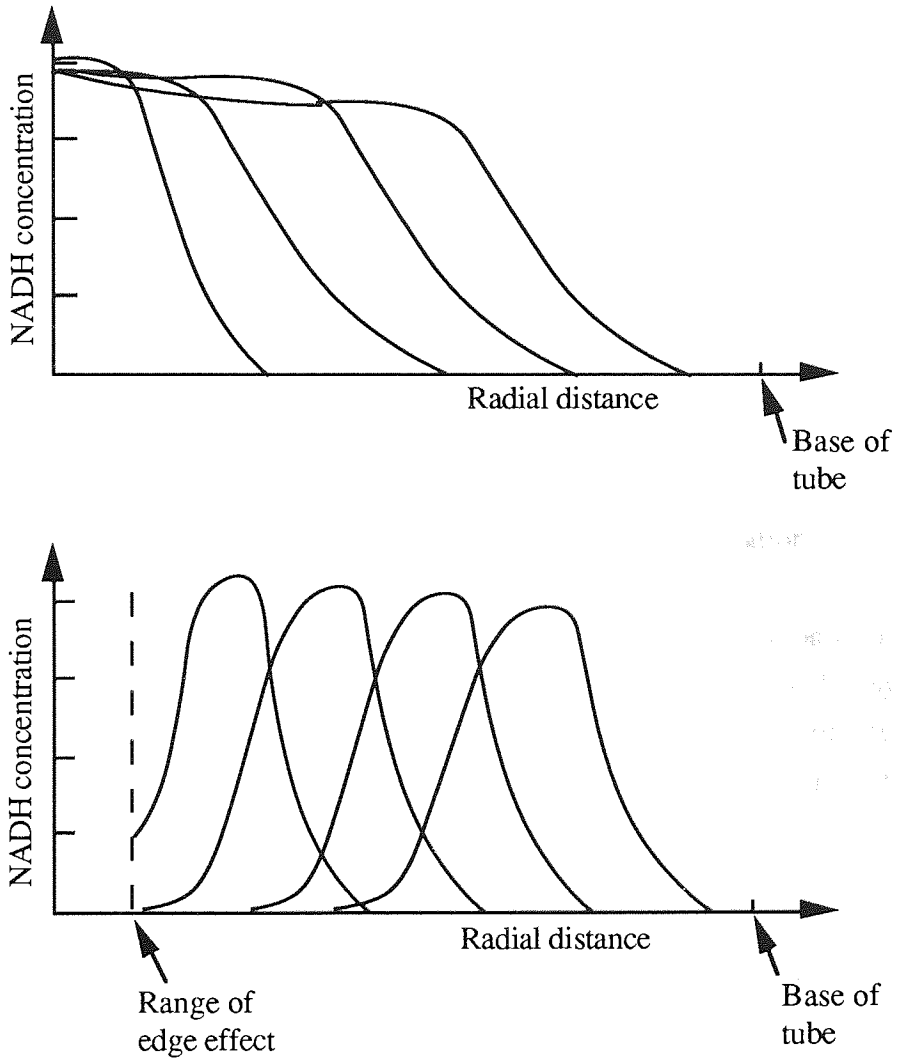

Figure 2.6 NADH Distributions. (The first plot shows the total NADH detected at four minute time intervals. The lower plot shows the NADH generated during a given time interval, corrected for sedimentation and diffusion effects.)

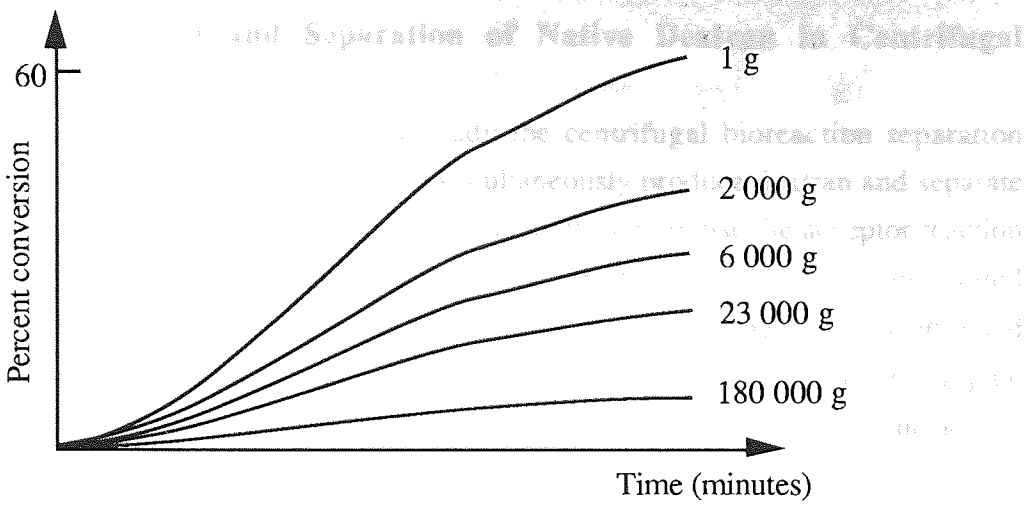

Figure 2.7 Acrylonitrile Polymerisation. Effect of centrifugal field[29]

A number of workers, most notably Gilbert and Jenkins[31-40] have studied the transport behaviour of interacting particle species in centrifugal fields. The distribution of a number of interacting particle species during centrifugation were mathematically defined by sets of particle differential equations. Each equation expressed the overall conservation of mass during transport caused by the combined diffusion and sedimentation of one of the reactants. These equations were developed from the equation of continuity in the ultracentrifuge [41]. Cann [42] has discussed the derivation of this equation.

These equations allowed the quantitative analysis of the sedimentation patterns of certain interacting systems. However, the work of these researchers was directed at systems that exhibited reversible particle interactions for the specific purpose of studying the mechanisms of enzyme action. For example, Gilbert and Müller-Hill[43,44] used sedimentation experiments to study the mechanism of enzyme induction and genetic control of lactose metabolism in the bacterium *Escherichia coli.*

Although the sedimentation patterns produced by the irreversible production of macromolecules from small molecules by enzyme synthesis was not considered by these workers, the equations that were developed may be of use when describing such a system. An excellent review concerning the interaction of molecules in centrifugal fields has been presented by Cann[42].

No instances in the literature were found concerning the behaviour of the dextransucrase reaction in centrifugal fields.

2.3.2 The Bioreaction and Separation of Native Dextran in Centrifugal Fields

The principle aims of this study were to study the centrifugal bioreaction separation principle and to develop a system that could simultaneously produce dextran and separate enzyme and fructose molecules during synthesis in order to minimise the acceptor reaction and obtain a dextran rich product. Furthermore, the development of an integrated bioreaction-separation process should reduce capital and processing costs. Combined bioreaction-separation been achieved by Barker and co-workers using chromatographic systems[4-9,15,16]. Theoretically, these aims could also be accomplished using the active-enzyme rate-zonal centrifugation technique used by Cohen et al[28]. The rate-zonal technique will be discussed in detail in subsequent chapters but the process can be summarised as follows:

A small volume of the dextransucrase enzyme is carefully layered onto a sucrose solution in a centrifuge tube and centrifuged. The action of the centrifugal force will result in the sedimentation of the enzyme molecules, which are of a relatively high MW due to the presence of high MW associated dextran material. The 'molecular weight' values of native dextran, enzyme and dextran-enzyme complexes will be discussed in more detail in subsequent chapters. When the enzyme contacts the substrate solution, reaction will occur resulting in the formation of fructose, which has a very low MW and native dextran, which can have extremely high 'MWs'. During synthesis, dextran will remain complexed with the enzyme before being released. The formation of high MW dextran-enzyme complexes should result in the rapid sedimentation of the active enzyme molecules away from the fructose rich portions of the tube. The low MW fructose and sucrose molecules will have very low rates of sedimentation. Therefore the fructose and dextran particles should be simultaneously separated as centrifugation proceeds. The analytical techniques used to evaluate the bioreaction-separation principle will be discussed in Chapter 5. A highly idealised summary of the proposed bioreaction-separation process is shown in figure 2.8.

Sedimentation of the high MW components will be dependent on a number of parameters including: rotor speed, substrate and product concentration, the density and viscosity of the sucrose supporting medium, initial enzyme volume and activity, dextran MW and the sedimentation and diffusion properties of dextran, enzyme and the dextran-enzyme complexes. These factors were considered in this study.

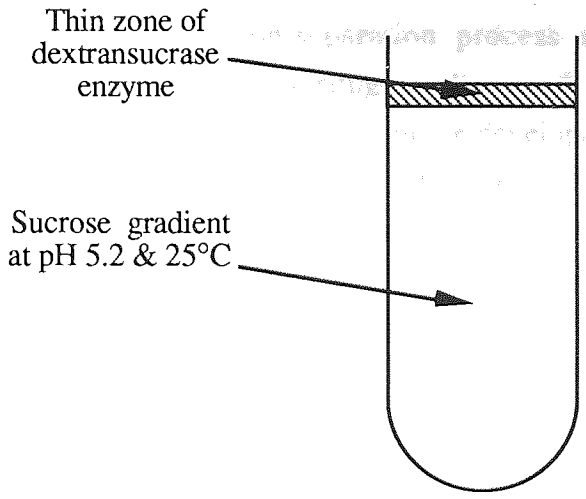

Step 1: The dextransucrase enzyme is carefully layered onto a dense sucrose gradient in a centrifuge tube.

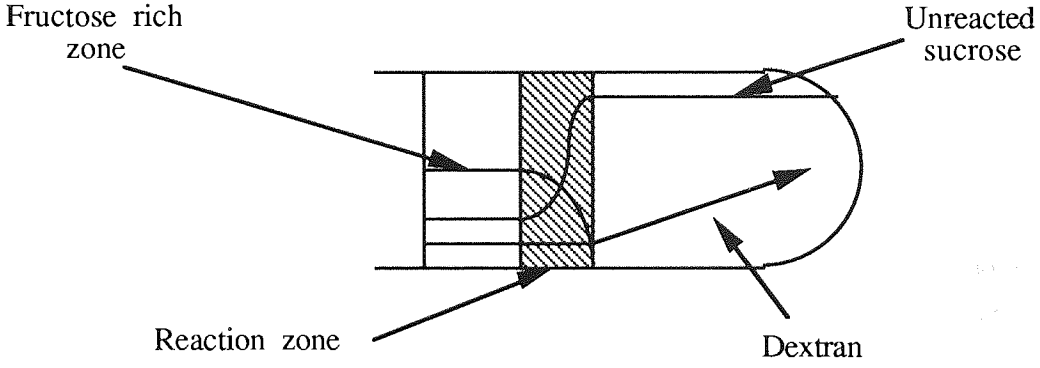

Step 2: The reaction zone sediments as a band through the sucrose gradient under the applied centrifugal field. Enzyme and dextran are separated from the fructose rich portions of the tube as the reaction proceeds.

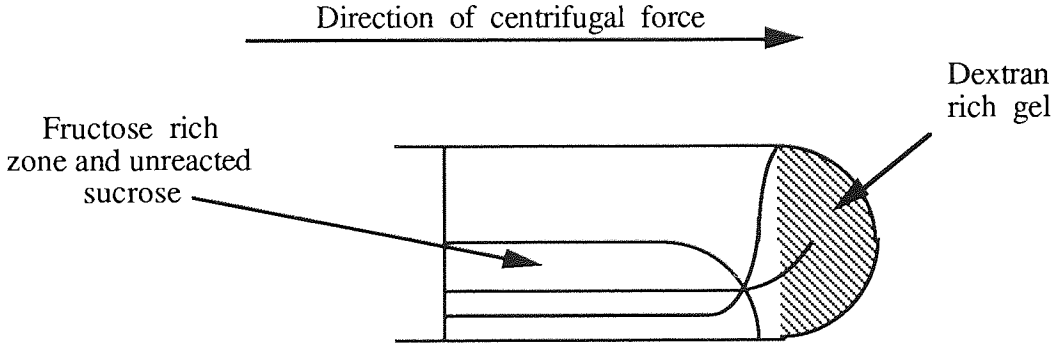

Step 3: The run is halted when the reaction reaches the base of the tube. The dextran and fructose rich portions of the tube can then be removed for analysis.

Figure 2.8 The Bioreaction-Separation Principle.

The study of the rate-zonal bioreaction-separation process using an analytical ultracentrifuge and a conventional batch centrifuge is discussed in Chapters 6 and 7 respectively. The use of tubular settling centrifuges in the development of a continuous centrifugal bioreaction-separation system is reported in Chapter 8 and the use of specially designed zonal rotors to study the bioreaction-separation process is discussed in Chapter 9. A preliminary attempt at modelling the process is presented in Chapter 10.

2.4 DEXTRAN STRUCTURE, SYNTHESIS AND SEDIMENTATION

In order to understand the effects of the various process variables, such as centrifugal force, enzyme activity and substrate concentration on the proposed bioreaction-separation process, it is necessary to have an understanding of the structure, synthesis and sedimenting properties of the dextran product and a knowledge of the sedimenting behaviour of the dextransucrase enzyme and the dextran-enzyme complexes. These factors will be discussed in the following sections.

2.4.1 Dextran structure

The B-512F type of dextran contains around 95% $\alpha 1 \rightarrow 6$ linkages, the remaining linkages being predominantly $\alpha 1 \rightarrow 3$ branch linkages. Chemical studies have indicated that most branch chains are single $\alpha 1 \rightarrow 3$ linked glucose residues[45], whereas physical studies have indicated that the branch chains are relatively long, containing 50-100 $\alpha 1 \rightarrow 6$ linked glucose residues[46,47]. Robyt, on considering the mechanism of branch formation believes that branches consist of both single glucose units and the longer branch chains[48]. At least 80% of these branches have been found to be only one glucose unit long[47]. The number of glucose units in the long branches does not appear to exceed 1% of the total number of glucose units in the molecule.

B-512F dextrans aggregate readily to form three dimensional structures known as gels[49,50]. These gels are readily soluble in water, which is believed to be due to the large number of linear $\alpha 1 \rightarrow 6$ bonds present. The observation of films formed by the evaporation of dilute solutions of B-512F dextran by electron microscopy have indicated the presence of networks of microscopic filaments[51,52], which suggests that many of the dextran molecules remain associated, presumably in some kind of network structure, even in dilute solution[53].

Evidence of crystallinity has also been observed in water soluble dextran gels[53]. Crystalline structures are formed by the regular association of polysaccharide chain segments. B-512F dextrans readily form crystalline structures, which X-ray powder

diagrams have conclusively shown to be as a result of the association of linear α1→6 chain segments [54-56].

Measurements of p.m.r. spectra indicate that dextran chains are most likely to have regular helical conformations[57]. The number of allowed conformations is likely to very large, with numbers (n) of residues per helix turn ranging from 2-7 and projected lengths (h) of the residues along the helical axis, ranging from 0-6 Ångstroms. The distribution of n and h values however, has suggested a bias towards extended 'ribbon-like' conformations where n= 2-3 and h= 4-6 Å [53] (figure 2.9). The ordered and stable crystalline structures would be possible through intermolecular hydrogen bonding that can occur between the readily spaced 3-hydroxyl group. The linearity of B-512F dextran, which is a result of the large number of α1→6 linkages, coupled with the relatively low number of long chain branches allows this high degree of hydrogen bonding to occur, which gives the associated molecules a high degree of stability.

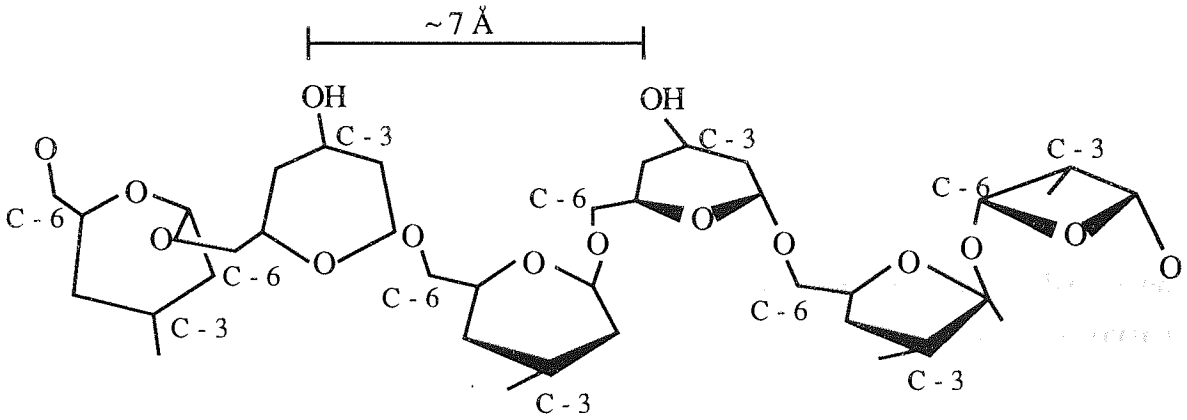

Figure 2.9 The Possible Helical Structure of Dextran

2.4.2 Dextran Particle Weights During Synthesis

The speed of formation of the dextran molecules and particles will greatly influence the rate at which the dextran and dextran-enzyme complexes will sediment and hence be separated from the fructose rich portions of the tube in the proposed bioreaction-separation process. Therefore the MW and time of formation of native dextran particles will be reviewed in this section. The actual method of dextran formation from the dextransucrase enzyme has been shown to be a single chain polymerisation process and will be discussed in Chapter 3.

Light scattering studies by Bovey[47] and Tsuchiya et al[58] showed that very high MW dextrans, typically of the order of 10^7 to $6x10^8$ were formed very soon after the start of the dextransucrase reaction. The 'MW' of these native dextran particles changed only to a relatively limited degree during the course of conversion (table 2.1). These results were

obtained using very low enzyme activities and sucrose concentrations where particle-particle interactions will be minimal. Molecular weight values of the order of 10^8 were confirmed by Arond and Franks[59] using a variety of chemical techniques.

Reaction time (mins)	Conversion (%)	Molecular weight ($x10^{-6}$)
18.0	10.2	52.5
30.0	16.7	52.5
40.0	22.2	54.6
50.0	27.8	64.0
60.0	32.4	73.0
70.0	37.7	79.5
85.0	44.7	87.4
110.0	56.8	93.6
132.5	68.2	93.6
162.5	76.4	99.9
195.0	90.0	101.0
225.0	94.5	105.0
245.0	96.5	105.0

Table 2.1 Changes in Average Dextran Particle Weight with Reaction Time during Dextran Synthesis. Data from Light Scattering Studies Carried out by Bovey [47].

The first evidence that these 'MW' values were too high was obtained by Ebert and Schenk[60] who determined the turnover number of the enzyme, which is a measure of the number of substrate molecules that a single enzyme molecule can convert to product per minute. These researchers reported that the dextransucrase enzyme, with a turnover number of 32000 min^{-1}, would require more than 20 minutes to build up a dextran molecule with a molecular weight of 10^8 under optimum conditions and that a process other than a simple single chain polymerisation mechanism was occuring. By applying several independent methods of analysis, they found the molecular weights of the dextran particles to be in the range of $3\text{-}5x10^5$. Similar results have been obtained by other workers[61]. They concluded that the high recorded dextran 'MWs' were caused by dextran molecule associations which may be of a remarkably high stability. They further concluded that by using the 'ribbon-like' helical model for the individual dextran molecules, ordered superposed structures could be formed by hydrogen bonding between the C_3-OH groups.

Assuming that the work of Ebert and Schenk is correct, then further conclusions concerning native dextran particle structures can be drawn:

A dextran molecule that is of $4x10^5$ MW is equivalent to around 2 200 glucose units. From the observation that only 1% of the total glucose units in a dextran are present on the long side branches, which have been shown to be between 50 and 100 units long, then it can be concluded than on average, between 50 and 75% of native dextran molecules will have no long branches. All of the molecules should have a number of smaller branch units. This observation further indicates why linear B-512F dextran molecules aggregate readily to form stable, ordered, crystalline structures. The low number of branches will decrease the likelihood of branch interference, allowing a high degree of bonding to occur between the C_3-OH groups on the extended molecules.

The work of Bovey[47] indicated that these large native dextran particles, with particle weights of the order of $50x10^6$, were formed very rapidly. However, no explanation was given as to why, after this initial rapid particle weight increase, only very low increases in particle weights with time were recorded. Furthermore, no data in the literature was found to explain this observation.

The dextran MW values of $3\text{-}5x10^5$ recorded by Ebert and Schenk[60] should be treated with caution, because the acceptor reaction can greatly alter the MW distribution of the dextran products from the dextransucrase reaction.

2.4.3 Native Dextran Particle Sizes

Senti et al[46] have studied the size of several acid hydrolysed dextran fractions using light scattering techniques. They found that over the observed molecular weight range, the 'molecular radius' r_p was proportional to MW such that:

$$r_p = 0.66\ MW^{0.43} \qquad (2.1)$$

A double logarithmic plot of 'molecular radius' versus molecular weight for their results is shown in figure 2.10. Bovey[47], has also studied the particle 'radii' of native dextran particles during synthesis using light scattering techniques. He found that these radii, like the observed dextran particle weights did not vary greatly during the course of the reaction, typically giving radius values of around 800 Å.

Applying equation 2.1 to a sample of Boveys results gives radial values of 1400-1800 Å for the native dextrans. Thus it appears that native dextran particles become increasingly

'compact' with increasing particle weight, which is consistent with the electron microscopic observations of native dextran particle structures[52].

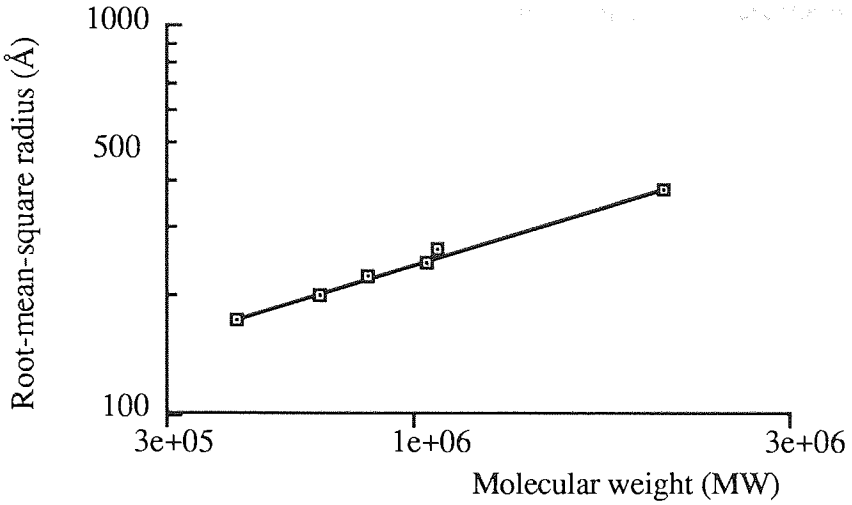

Figure 2.10 Log-Log Plot of Root Mean Square Radius Versus MW for Various Hydrolysed Dextran Fractions in Water

2.4.4 Dextran Structure : Summary

The size, shape and structure of B-512F dextran will greatly influence its sedimentation properties in a centrifugal field.

Ebert and Schenk[60] showed that HMW native dextran particles were composed of aggregates of dextran molecules with MWs of between $3\text{-}5\text{x}10^5$, that were remarkably stable. This observation explained the work of Bovey[47] who observed that HMW native dextran particles were formed very soon after the start of the dextransucrase reaction and increased in MW more rapidly than the enzyme's kinetic data would suggest.

The rapid formation and hence sedimentation of native dextran particles may be advantageous in the proposed centrifugal bioreaction-separation process by encouraging the rapid sedimentation of enzyme molecules away from fructose rich portions of the reaction vessel. Dextran, fructose and enzyme sedimentation rates will be discussed in chapter 4.

3.0 THE DEXTRANSUCRASE ENZYME

It is intended that this chapter should serve as an introduction to the *Leuconostoc mesenteroides* B-512F dextransucrase enzyme. This chapter discusses the mechanism of dextran synthesis and chain termination by the action of acceptor molecules, a knowledge of which is important for the development of a successful combined bioreaction-separation process. Practical aspects of enzyme synthesis, purification, storage, assay and optimum reaction conditions are also considered.

3.1 INTRODUCTION

Dextransucrase is an extracellular glucosyltransferase enzyme that catalyses the conversion of sucrose to dextran and fructose:

$$\underset{\text{Sucrose}}{nC_{12}H_{22}O_{11}} \xrightarrow{\text{Dextransucrase}} \underset{\text{Dextran}}{(C_6H_{10}O_5)_n} + \underset{\text{Fructose}}{nC_6H_{12}O_6}$$

Two genera of bacteria, *Leuconostoc* and *Streptococcus*, both belonging to the *Streptococceae* family are mainly used to synthesise dextransucrase [62]. Dextransucrase from the *Leuconostoc mesenteroides* NRRL B-512F strain of bacterium is the enzyme used to synthesise clinical grade dextran. The dextran produced contains 95% α 1→6 and 5% α 1→3 glucosidic linkages. Dextransucrase is an enzyme of absolute specificity, sucrose being the only substance which can act as a substrate [63].

3.2 DEXTRANSUCRASE REACTION MECHANISMS

3.2.1 Dextran Chain Growth

Robyt and co-workers[64,66-72] have extensively studied the probable dextransucrase reaction mechanisms using pulse-chase radiolabelling techniques. Their mechanism, purposes that there is an active nucleophile present in each of two active sites, X_1 and X_2 of the enzyme (figure 3.1). These two nucleophiles attack and bind two sucrose molecules, displacing the fructose units, leaving two glucosyl groups covalently linked to the nucleophiles through the C_1 carbon group (stage 1). Subsequently, the primary C_5 hydroxyl group of one glucose unit effects a nucleophilic attack on the C_1 of the other glucose unit to form an α 1→6 glucosidic link (stage 2). This transformation releases the active site nucleophile which attacks another sucrose molecule to give a new glucosyl unit attached to the active site (stage 3). The process continues with the two active sites alternately forming covalent complexes with glucose and the growing chain (stage 4). Chain growth is terminated by the action of acceptor molecules (see next section).

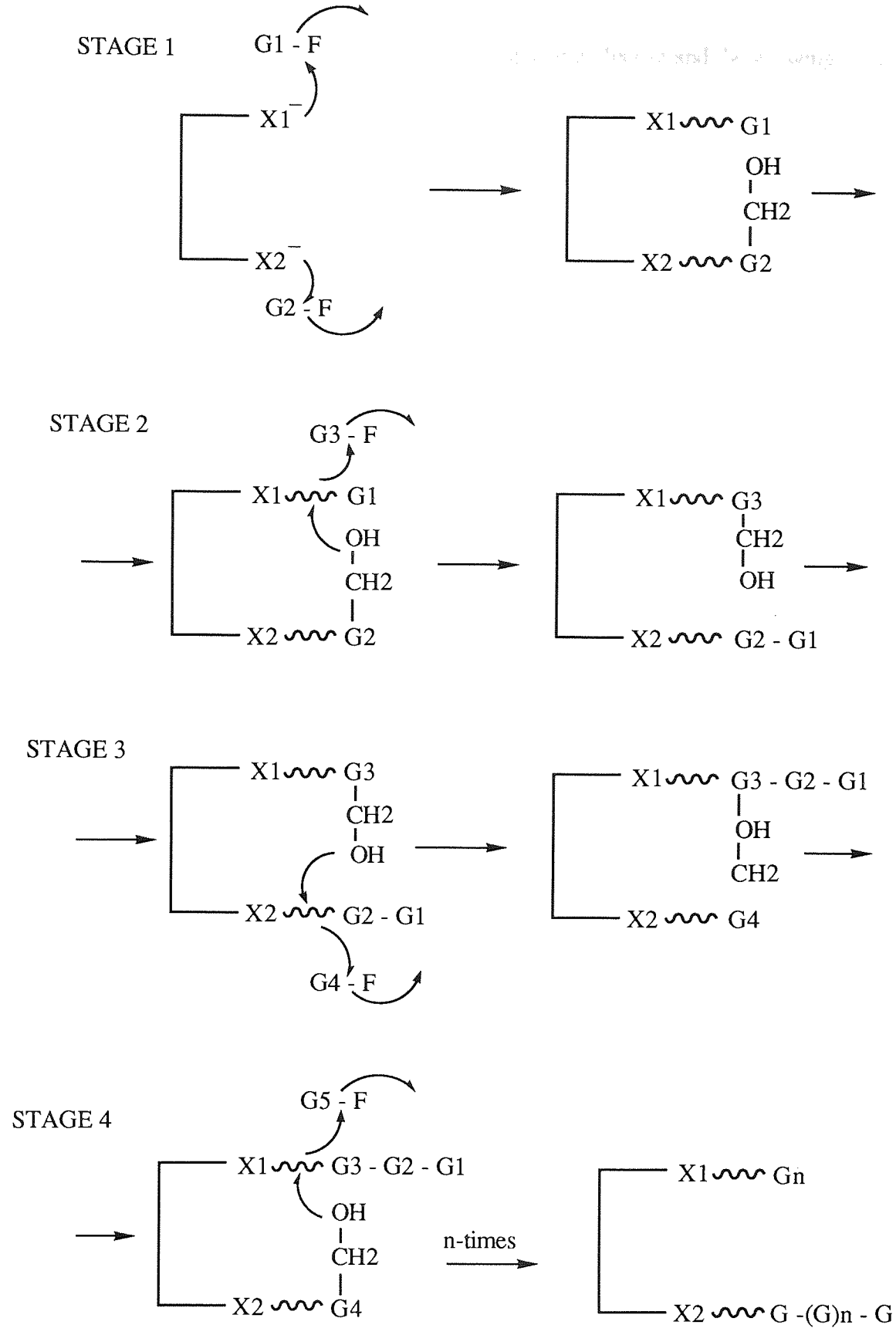

Figure 3.1 The Proposed Dextransucrase Enzyme Reaction Mechanism. After Robyt et al [64-72].

3.2.2 The Acceptor Reaction

Acceptor molecules cause chain termination by displacing glucose and the growing dextran chain from the active sites of the enzyme [58,60,64,65].

Robyt and Walseth [64] have investigated the acceptor reaction using radiolabelled acceptor molecules and established that they not only terminate dextran chain growth, but also release oligosaccharides (sugars consisting of a few monomeric units). In the presence of sucrose, this reaction can occur in competition with the normal polymerisation reaction. Robyt and Walseth established the following acceptor-oligosaccharide relationships:

ACCEPTOR	OLIGOSACCHARIDE
Glucose	Isomaltose
Fructose	Leucrose
Maltose	Panose

In the case of the above three acceptor molecules, the C_6-OH group of the glucose and maltose and the C_5-OH group of fructose can act as nucleophiles, displacing the glucosyl and dextranosyl groups from the enzyme complex, yielding the oligosaccharide and dextran product. Robyt and Walseth [66] have reported 27 different acceptor molecules. Isomaltose, for example, can displace the glucosyl unit attached to the active site of the enzyme to form isomaltotriose (a trisaccharide) and the glucosyl unit to form isomaltose-reducing end-terminated glucan as shown in figure 3.2.

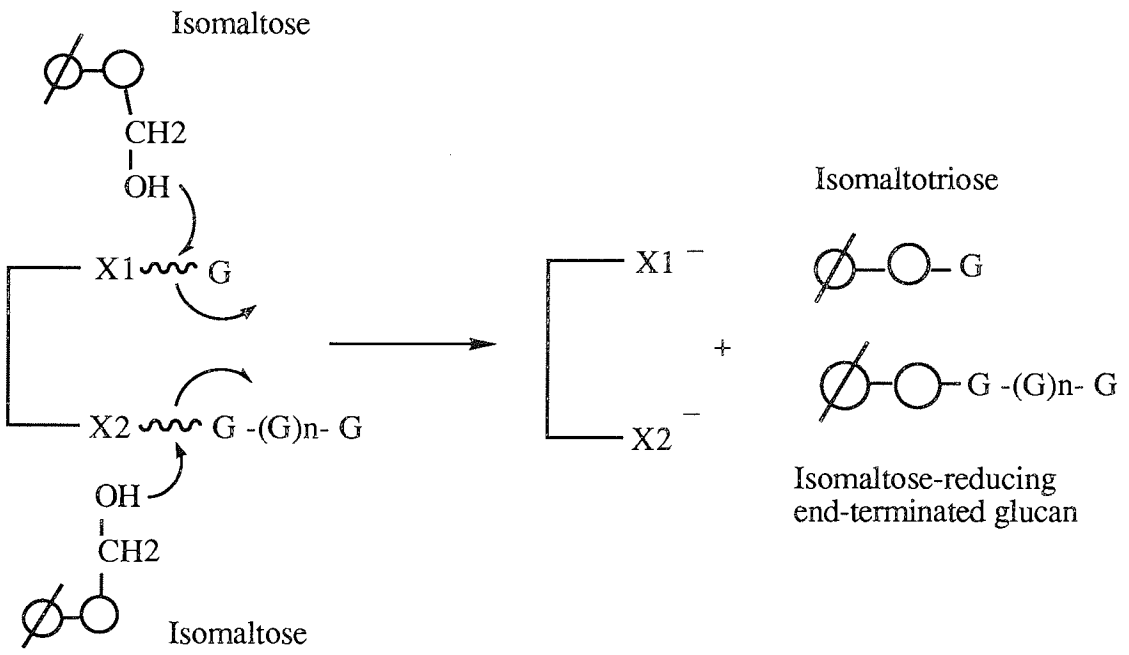

Figure 3.2 The Mechanism of Acceptor Reactions: The Isomaltose Reaction.

3.2.3 The Branching Mechanism

B-512F dextran has also been shown to act as an acceptor [67-69]. The C_3-OH groups on the dextran acceptor chain can attack the C_1 of the glucosyl or dextranosyl units of the enzyme complex to form an α 1→3 bond and release the glucose unit or dextran chain from the enzyme (figure 3.3). This mechanism is believed to be the origin of branching in dextran molecules and explains the presence of large numbers of single α 1→3 linked glucose residues observed on B-512F dextran molecules as discussed in section 2.4.1.

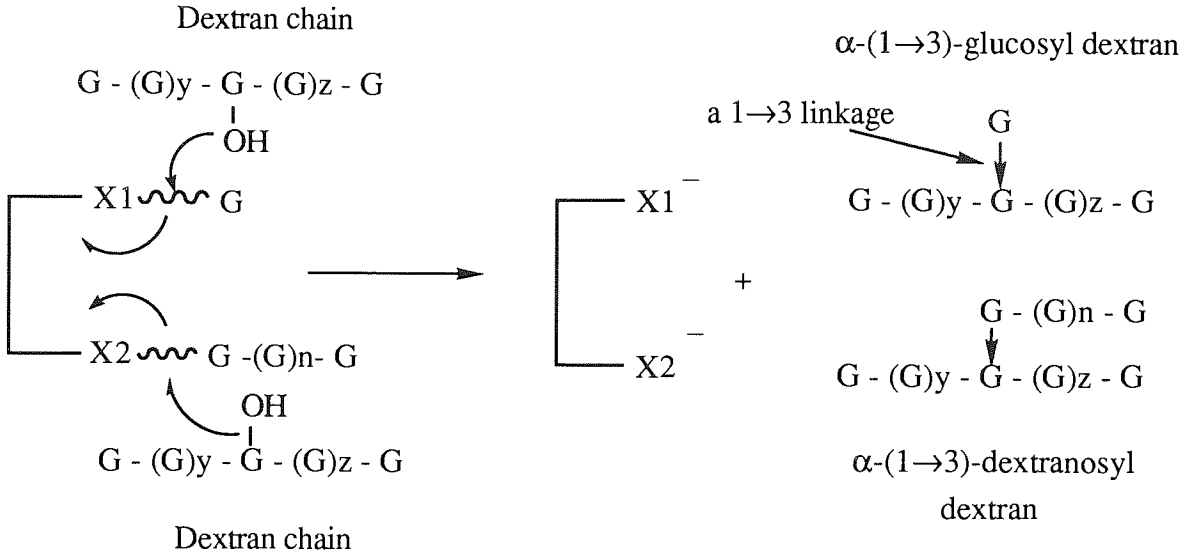

Figure 3.3 The Probable Mechanism of Branch Formation During Dextran Synthesis

3.3 THE ACTION OF DEXTRANSUCRASE ON SUCROSE UNDER INDUSTRIAL CONDITIONS.

Alsop[3] has studied the effects of a number of factors on the conversion of sucrose to dextran in an industrial situation. He found that the most important parameter controlling the yield and MW distribution (MWD) of dextran was sucrose concentration. His results, obtained by High Pressure Liquid Chromatography (HPLC) and Gel Permeation Chromatography (GPC) analysis are summarised in table 3.1.

The monosaccharides were found to be mainly fructose, but small quantities of glucose were also observed. The disaccharides consisted mainly of leucrose but some sucrose and isomaltose were also recorded. Alsop classified all the dextran above 5 000 MW to be of a high molecular weight (HMW) and below this value to be of a low molecular weight (LMW). Typical chromatograms using a TSK-PW G2000 column for 2% and 20% w/v initial sucrose solutions are shown in figure 3.4.

Sucrose % w/v	Monosaccharides	Disaccharides	Total Dextran	HMW Dextran	LMW Dextran
2	52.2	1.9	45.9	45.9	0
4	50.0	4.4	45.6	45.6	0
5	51.3	4.3	44.4	44.4	0
10	51.2	6.8	42.0	39.0	3.0
15	55.5	9.4	35.3	25.3	10.0
20	56.9	11.2	31.9	17.9	14.0
Theory	52.6	0	47.4	47.4	0

Table 3.1 Dextransucrase Reaction Products at Varying Sucrose Concentrations [3].

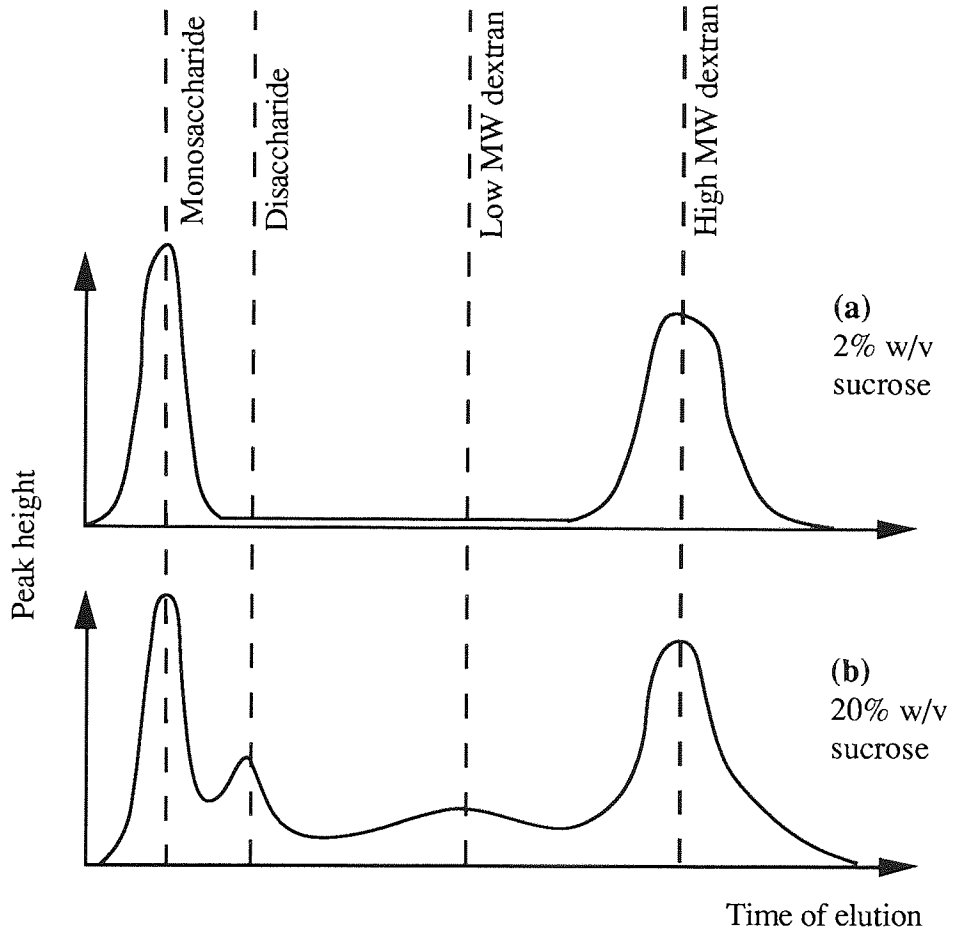

Figure 3.4 Dextransucrase Reaction Product Molecular Weight Distributions for Initial Sucrose Concentrations of (a) 2% w/v and (b) 20% w/v [3].

Stoichiometrically, the reaction should yield 52.6% fructose and 47.4% HMW dextran. At low sucrose concentrations this was approximately true. As the sucrose concentration was increased, the following trends were apparent:

(1) A marginal increase in monosaccharide levels.
(2) A marked increase in disaccharide levels, found mainly to be leucrose.
(3) A marked increase in LMW dextran and oligosaccharide levels.

As a result, the proportion of HMW dextran fell from 45.9% to 17.9% when the initial sucrose concentration was increased from 2% w/v to 20% w/v.

These results clearly showed that the acceptor reaction was more marked at high sucrose and hence high fructose and oligosaccharide concentrations. Higher concentrations of sucrose resulted in higher concentrations of fructose being synthesised, hence resulting in an increase in acceptor activity. Fructose acceptor molecules act on the glucosyl dextransucrase complex to form leucrose and on the dextranosyl dextransucrase complex to release the growing dextran chain. Dextran chain termination will be more prevalent at high fructose concentrations and thus will result in increased yields of LMW dextran.

LMW dextran has few uses. The objective of any dextan manufacturer is to maximise the yield of HMW dextran, which can then be broken down under controlled hydrolytic conditions to yield the commercially important clinical dextran product.

Clearly, HMW dextran yields can be increased by operating bioreactors at low sucrose concentrations, but this will result in a need for large bioreactors with their inherent high production and capital costs. As a result, considerable interest has been shown in the development of bioreactors that can minimise the acceptor reaction by rapidly removing acceptor molecules from the vicinity of the dextransucrase enzyme active sites. This has been achieved in recent years by Barker and co-workers in chromatographic systems [4-9,15,16].

From an academic viewpoint, it is interesting to note that the addition of acceptor molecules to dextransucrase in the presence of sucrose can alter the reaction products obtained. Koepsell and co-workers [65] have reported that the addition of α-methylglucoside, maltose or isomaltose leads to the formation of short chain oligosaccharides at the expense of HMW dextran. Alsop[3] believes that this may be a way of controlling the dextran fermentation to yield commercially important dextran products of the desired MW.

3.4 DEXTRANSUCRASE ENZYME ACTIVITY

One unit of dextransucrase enzyme activity (1 DSU) is defined as the amount of enzyme required to convert 1 mg of sucrose to product in one hour under standard conditions, that is, at a pH of 5.2 and at 25°C.

3.4.1 Enzyme Activity Determinations

The activity of the enzyme preparations used in this study were determined either by Hostettler's method[74] or by a method requiring the use of high pressure liquid chromatography (HPLC) techniques. Hostettler's method used a colourimetric technique to determine the levels fructose released during the action of the enzyme on a sucrose substrate, and the HPLC technique monitored the levels of sucrose and fructose during the enzyme assay[75].

3.4.1.1 HPLC Method

The HPLC analytical procedure is described in Chapter 5. This assay technique allows the determination of either the sucrose consumed or the fructose produced during the enzyme reaction with sucrose. The procedure is as follows:

20 cm^3 of enzyme was added to 80 cm^3 of a 2%w/v solution of sucrose at pH 5.2, maintained at 25°C. Ideally the enzyme solution should be diluted to give an approximate activity of 50 DSU cm^{-3}, so an 'educated guess' as to the original enzyme activity was required. The solution was then shaken and a sample immediately taken. This, and all subsequent samples were heated in boiling water for five minutes to denature the enzyme, filtered and injected into the HPLC system. Samples were taken at twenty minute intervals for a further two hours. Sucrose and fructose concentrations were calculated by comparing their respective areas with standard 1% w/v solutions. Figure 3.5 shows the typical sucrose consumption during an enzyme assay.

Enzyme activities were calculated using the following equations:

Activity based on sucrose consumption:

$$\text{Activity (DSU cm}^{-3}) = \frac{Ms}{1.0} \times 50 \times d \quad \text{——— (3.1)}$$

Activity based on fructose production:

$$\text{Activity (DSU cm}^{-3}) = \frac{MF}{0.524} \times 50 \times d \quad \text{——— (3.2)}$$

where Ms and M_F are the initial sucrose and fructose curve gradients obtained from plots of sucrose consumption or fructose production versus time (see figure 3.5). d is the enzyme dilution factor.

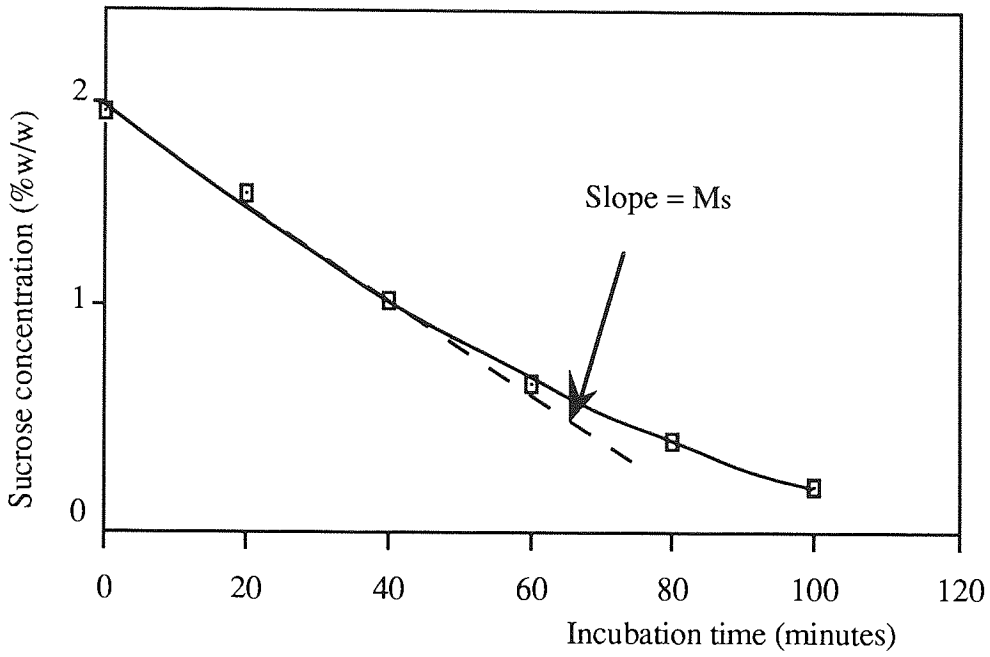

Figure 3.5 HPLC Determination of Dextransucrase Activity: Sucrose Consumption

The HPLC method is a far more time consuming process than Hostettler's method but allows the identification and quantification of any contaminating materials to be made. For example, the accumulation of glucose during analysis is indicative of invertase and levansucrase activity. Invertase converts sucrose to glucose and fructose, while levansucrase converts sucrose to levan and glucose.

3.4.1.2 Hostettler's Method

The procedure for assaying enzyme activity by Hostettler's method is as follows:

1 cm^3 of appropriately diluted enzyme (ideally between 30 and 50 DSU cm^{-3}) was added to 4 cm^3 of 6.25% w/v sucrose in 0.1M sodium acetate buffer at pH 5.2 and shaken. Immediately, 0.5 cm^3 of this mixture was taken out and the remainder incubated in a waterbath at 25°C. The 0.5 cm^3 sample was added to 1.0 cm^3 of Sumner reagent (10 g 3-5 dinitrosalicylic acid, 300 g potassium-sodium-tartrate dissolved in 1 litre of 0.5 M NaOH), placed in boiling water for exactly 5 minutes, rapidly cooled and 11 cm^3 of distilled water added. This provided the unincubated sample. Every 5 minutes, a sample was taken from the reaction mixture in the waterbath and treated in the same way for the

next 20 minutes. All the samples were stable for at least 24 hours and their optical densities were read at 530 mm (OD_{530}) against a blank on a Pye Unicam SP1800 UV/visible photospectrometer. The blank was prepared by adding 0.5 cm^3 of the sucrose stock solution to 1 cm^3 sumner reagent, boiling for 5 minutes, cooling and adding 11 cm^3 of distilled water. The enzyme activity was then calculated using the following formula.

$$DSU\ cm^{-3} = \frac{(OD_i - OD_u) \times d \times 60 \times 2}{OD_F \times 0.52 \times 0.2 \times t} \quad \text{(3.3)}$$

where:

OD_i	=	OD_{530} of the incubated sample.
OD_u	=	OD_{530} of the unincubated sample.
d	=	Dilution factor of enzyme solution.
t	=	Incubation time in minutes.
OD_F	=	The OD_{530} of a 0.2% w/v fructose solution prepared using 0.5 cm^3 fructose solution, 1.0 cm^3 Sumner reagent and treating as for all other samples. This should equal 0.80 $\pm$0.05 OD_{530}.

3.4.1.3 Practical Aspects of Hostettler's Method

Activities calculated from different incubation times over the 20 minute analysis period were generally linear with time (figure 3.6). Occasionally it proved necessary to dilute the samples so that they fell within the range of the photospectrometer.

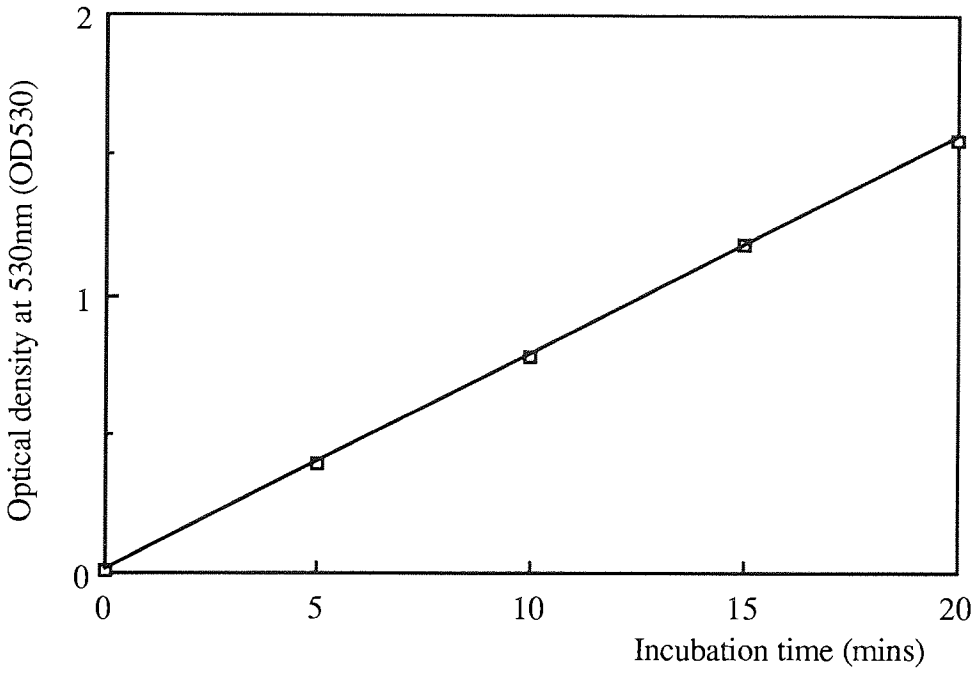

Figure 3.6 OD_{530} Profile During Enzyme Activity Determination.

Ajongwen[75] found that the sucrose solutions used in his initial assays showed aging effects, possibly due to enzyme contamination, resulting in incorrect assay results. He recommended that the sucrose assay solutions should be freshly prepared before assaying. The 0.1 M sodium acetate buffer (pH 5.2) was not prone to contamination and could be prepared in bulk before being used as required in the preparation of the sucrose solutions. To check for contamination, an additional water blank was prepared in the same way as the sucrose blank, except that 0.5 cm^3 of water was used in place of sucrose. The OD_{530} values of the two blank solutions should be the same in the absence of sucrose contamination.

3.5 PROPERTIES OF DEXTRANSUCRASE

The dextransucrase enzyme exhibits maximum activity at pH 5.2, although the enzyme retains at least 90% of its maximum activity in the pH range 4.8 - 5.6 [76] (figure 3.7). The activity decreases markedly outside this range.

The optimum temperature for enzyme activity is 30°C [76] (figure 3.8) but this can lead to a rapid thermal decay in activity. Kobayashi and Matsuda [77] reported a 50% loss in enzyme activity at 30°C in 13.5 minutes. However, the decline in activity is less rapid at lower temperatures. For example, Ajongwen et al[78] have recorded a 40% loss in enzyme activity over a 24 hour period at 20°C. A compromise temperature of 25°C was chosen. Figure 3.8 indicates that at this temperature, the recorded enzyme activity is approximately 90% of the maximum enzyme activity.

3.6 DEXTRANSUCRASE MOLECULAR WEIGHT

The MW of the dextransucrase enzyme is of particular importance in the centrifugal bioreaction-separation studies as it will influence the rate at which the enzyme molecules will sediment. However, the precise MW of the enzyme is unclear.

Ebert and Schenk [79] have measured the MW of a highly purified enzyme preparation by ultracentrifugation, obtaining a value of 280 000. Their sedimentation diagrams indicated that only one substance with a uniform MW was present.

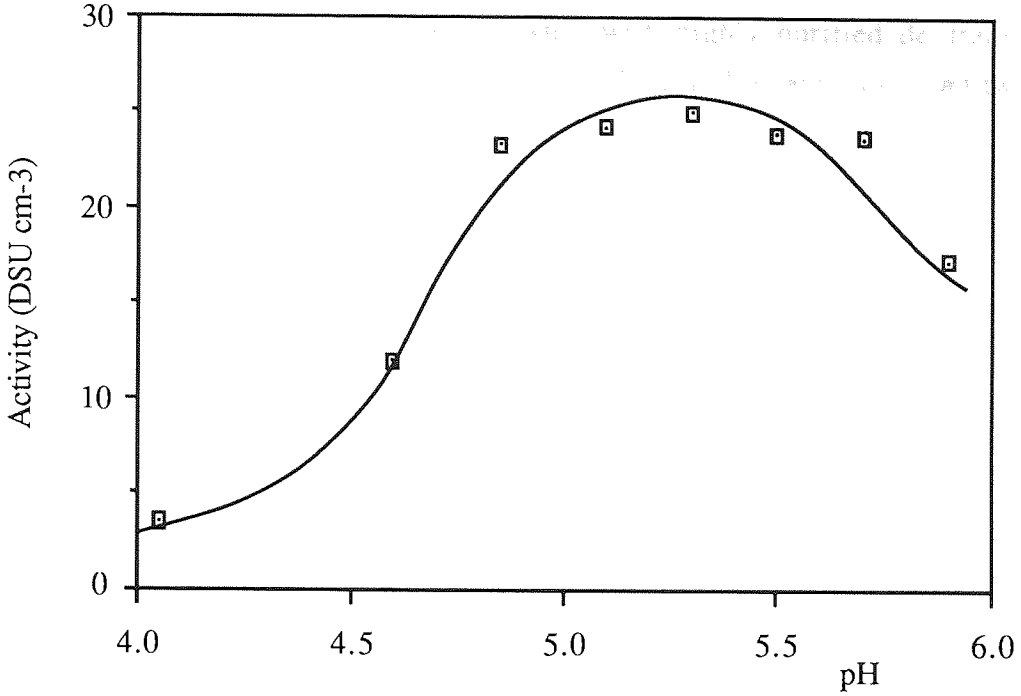

Figure 3.7 Effect of pH on Dextransucrase Activity (76)

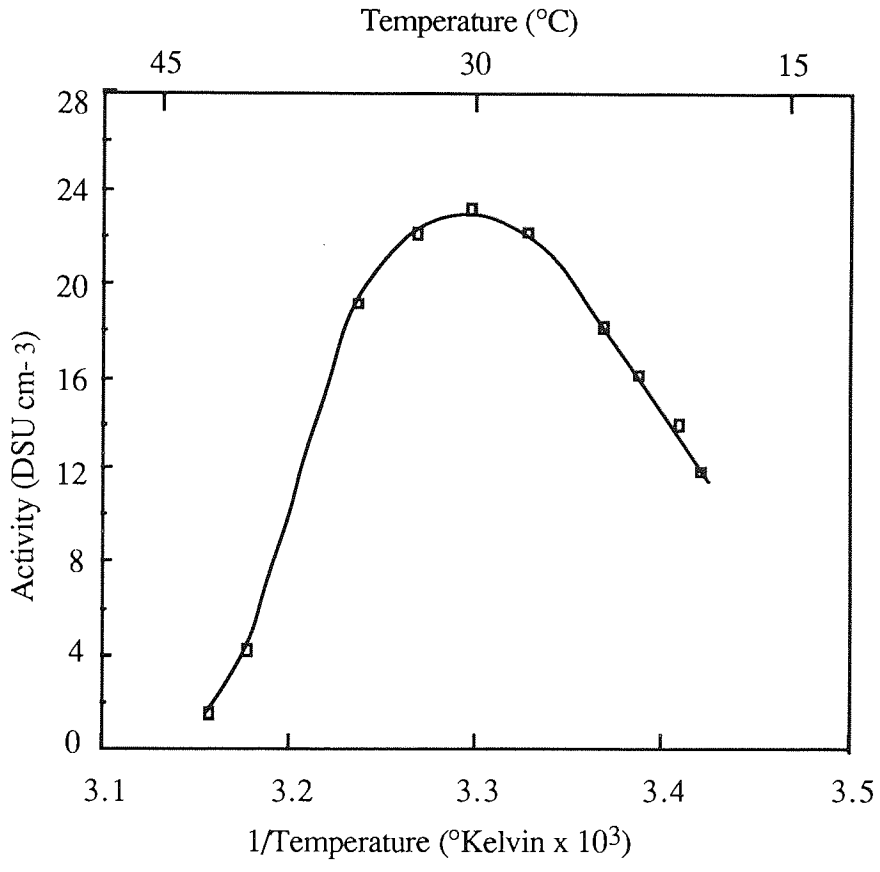

Figure 3.8 Effect of Temperature on Dextransucrase Activity (76)

However, Miller and Robyt [72], also working with highly purified dextransucrase fractions reported that *Leuconostoc mesenteroides* B-512F dextransucrase had two MW forms: 176 000 and 159 000, this data being obtained by SDS gel electrophoresis techniques. The 176 000 MW form prevailed in fresh preparations, while on storage, the 159 000 MW form increased at the expense of the former. These values are in accordance with the value of 171 000 MW reported by Steward and Jackson [80].

However, in this study, the true MW of the enzyme will be masked by the fact that a considerable amount of dextran remains associated with the enzyme molecules even after purification, which will be discussed in Section 3.8. Furthermore, Kobayashi and Matsuda[81] have shown that dextransucrase molecules have a tendency to aggregate. Therefore, it is possible that the enzyme molecules used in this work will be large enzyme-dextran agglomerates with relatively high rates of sedimentation.

3.7 DEXTRANSUCRASE ENZYME PRODUCTION

In this study, the extracellular dextransucrase enzyme was produced using large scale batch fermentation techniques, typically of the order of 800 litres. Barker and Ajongwen[13] reported activities in excess of 440 DSU cm^{-3} when culturing *Leuconostoc mesenteroides* B-512F under nonaerated, fed-batch, pH controlled fermentation conditions with mild agitation. Aerobic fermentations carried out under identical conditions have consistently produced enzyme activities of less than 340 DSU cm^{-3} but with no differences in the final cell concentration of the broth. The enzyme used in this study was produced by Dr J. Ajongwen using the nonaerated fed-batch fermentation technique[13].

3.8 DEXTRANSUCRASE ENZYME PURIFICATION

3.8.1 The Purification Process

Highly purified dextransucrase enzyme was required for the bioreaction-separation studies. The crude fermentation broth contained cells, unused nutrient and considerable quantities of soluble impurities such as dextran, fructose, leucrose, mannitol and other oligosaccharides. Small quantities of levansucrase, invertase and other proteins may also be present. A purified enzyme product will allow meaningful data concerning product formation and dextran MW distribution to be obtained.

Many researchers have attempted to purify the dextransucrase enzyme. A number of these processes have been reviewed by Alsop [3], Barker and Ajongwen [13] Zafar [15] and Ganetsos [17]. Researchers in this laboratory have identified three important criteria for the

successful development of an industrial-scale dextransucrase enzyme purification process[15]:

Scale-up: Most of the reported purification methods are small-scale processes. Although the experiments carried out in this study were small-scale, the proposed scale-up of the process will require larger quantities of purified enzyme. Thus, a method that can easily be scaled-up with little activity losses would be advantageous.

Number of stages: The number of purification stages should be kept to a minimum, because generally, the greater the number of steps, the more expensive and time consuming a process becomes. Furthermore, an increase in the number of stages will increase the possibility of enzyme activity losses.

Degree of purification: Although highly purified enzyme preparations will minimise analytical problems, higher activity losses could again be expected.

Ajongwen et al[78] have proposed a purification process that yields high enzyme purities (over 95%) and recoveries with high throughputs and at relatively low costs. This purification process was successfully employed in this study and is summarised in figure 3.9.

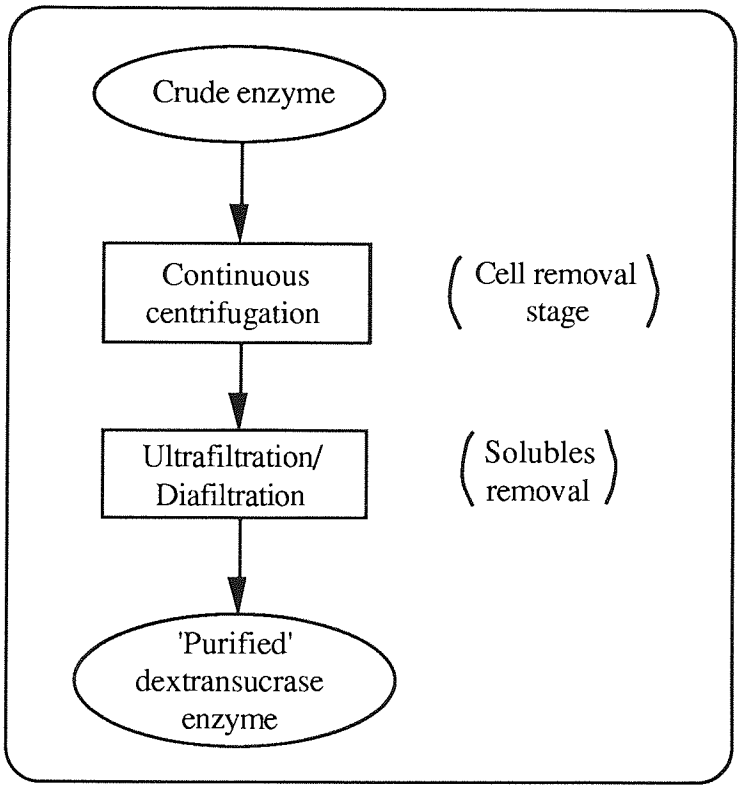

Figure 3.9 The Dextransucrase Enzyme Purification Process

The crude enzyme broth was first centrifuged using a Sharples laboratory T-1 supercentrifuge. This machine has a tubular centrifuge bowl, through which the crude broth was passed. The action of the applied centrifugal field resulted in the sedimentation and deposition of the solids, which were mainly cells, at the bowl wall. The accumulated solids were removed manually at periodic intervals. Most of the extracellular, relatively slowly sedimenting dextransucrase enzyme remained in solution during centrifugation and left the bowl in the 'purified' product stream. The temperature of the process fluid was maintained between 4 and 8°C using a chiller unit to minimise enzyme activity losses.

Ajongwen et al found that cell removal was reduced either by increasing the process fluid throughput or the rotor speed. Enzyme recovery, as expected, increased with throughput due to reduced residence times but decreased with increasing centrifugal force. The degree of enzyme denaturation was low, indicating that the shear created by the centrifugal forces did not greatly damage the enzyme. From these results, it was apparent that high rotor speeds (28 000 to 30 000 rpm) and high throughput rates (100-150 cm^3 min^{-1}) were the optimum conditions for cell removal. These operating conditions resulted in 90% cell removal and only 10% enzyme losses (table 3.2). The low MW impurities were removed by ultrafiltration, carried out at temperatures of between 8 and 12°C to minimise enzyme denaturation. A diafiltration mode of operation was employed with at least four diafiltration stages being used to remove over 95% of the soluble impurities. Of a number of systems tested, Ajongwen et al found that a bank of Millipore Pellicon PTTK 00005 flat sheet cross-flow membranes with a MWCO of 30 000 (total surface area of 1.39 m^2) gave the best results. This module removed nearly 98% of the LMW impurities and nearly 99% of the ions originally present coupled with low enzyme activity losses and high throughputs (figure 3.10).

A disadvantage of this purification process is that it does not result in the removal of any of the dextran material that remains associated with the enzyme molecules. Several researchers have used chemical techniques to achieve dextran removal[82-88] but these processes involved a large number of purification stages and resulted in high costs and low yields.

Relative centrifugal force at rotor wall (g)	Throughput (cm^3/min)	Residence Time (min)	% Cell Removal	% Enzyme Recovery
22 385	80	10.0	91	85.0
155	58	13.7	67	76.5
	100	8.0	45	-
	140	5.7	24	96.7
	220	3.7	12	97.6
780	85	13.7	91	80.3
	100	8.0	75	74.5
	140	5.7	54	88.5
	220	3.7	26	96.8
12 480	58	13.7	97	62.4
	100	8.0	98	-
	140	5.7	96	72.6
	220	3.7	75	95.4

Table 3.2 Cell Removal and Dextransucrase Enzyme Recovery during Centrifugation (78)

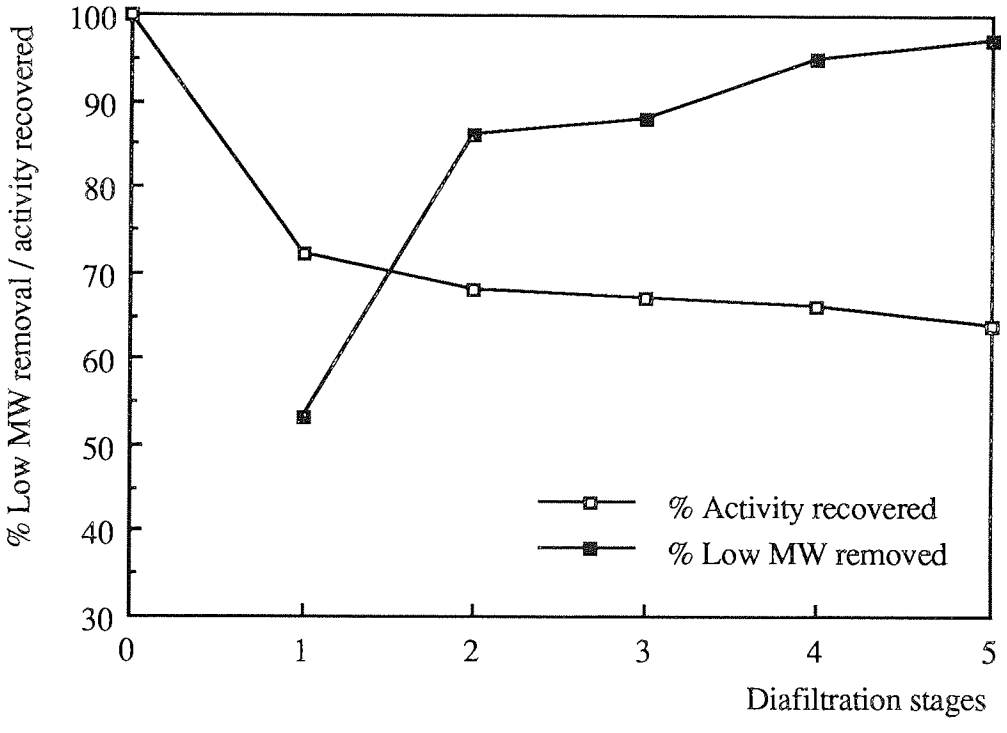

Figure 3.10 Dextransucrase Ultrafiltration Results (78)

3.8.2 Storage and Stability of the Dextransucrase Enzyme.

Due to the thermal instability of the dextransucrase enzyme, it was necessary to store the enzyme at between -12 and -15°C.

Assays on purified enzyme solutions after one week of storage at -15°C have shown activity losses of nearly 10%[78]. Under identical conditions, crude enzyme fractions exhibited no activity losses. Ajongwen et al concluded that the presence of cells and residual dextran in the crude enzyme solutions have a stabilising effect on the enzyme, although there is evidence to suggest that fermentation conditions can also affect enzyme stability and activity [78]. Robyt and Walseth[70] have found that during storage, enzyme stability can be increased by the addition of 0.4 mg cm^{-3} dextran. Ideally, the crude enzyme should be ultrafiltered before storage and when required, the enzyme thawed and centrifuged before use. However, since this procedure will lead to increased membrane fouling, an initial centrifugation was carried out before ultrafiltration and storage. This solution still contained small amounts of cells and dextran which helped stabilise the enzyme and were removed by a second centrifugation prior to enzyme usage.

Since purified enzyme solutions can lose nearly 30% of their activity when stored at 5°C for 24 hours, the enzyme was used as soon as possible after thawing. Enzyme activities were assayed using either of the methods listed in section 3.4 prior to use. Enzyme activity per unit volume could either be increased by ultrafiltration or decreased by the addition of buffer as required.

Analytical problems regarding the presence of enzyme associated dextran were minimal, the reasons being:

(1) The proposed rate zonal centrifugation technique necessitated low enzyme loadings. The effect of associated dextran on dextran MWD will therefore be small.

(2) In MWD studies, the centrifugal bioreaction-separation runs were duplicated in a 'bench' bioreactor using the same enzyme stock solution. Direct MWD comparisons could then be made.

(3) The bulk of the dextransucrase production was carried out at pH 6.7 where enzyme activity, hence dextran synthesis was minimal (figure 3.7). However, the pH was dropped at the end of the fermentation to stabilise the enzyme. This resulted in some dextran synthesis.

(4) The tendency for dextransucrase to agglomerate and the extremely rapid synthesis of HMW dextran as discussed in chapter 2, indicated that, as regards the rate of enzyme sedimentation in centrifugal fields, no great advantage is gained by preparing enzyme solutions completely free of associated dextran.

3.9 DEXTRANSUCRASE ENZYME KINETICS

3.9.1 Introduction

Akintoye[16] has studied the kinetics of the dextransucrase enzyme in this laboratory. He found that the reaction velocity or rate of substrate conversion, V, varied with [S], the substrate concentration. His results, based on a fixed enzyme activity of 25 DSU cm^{-3} are summarised in figure 3.11.

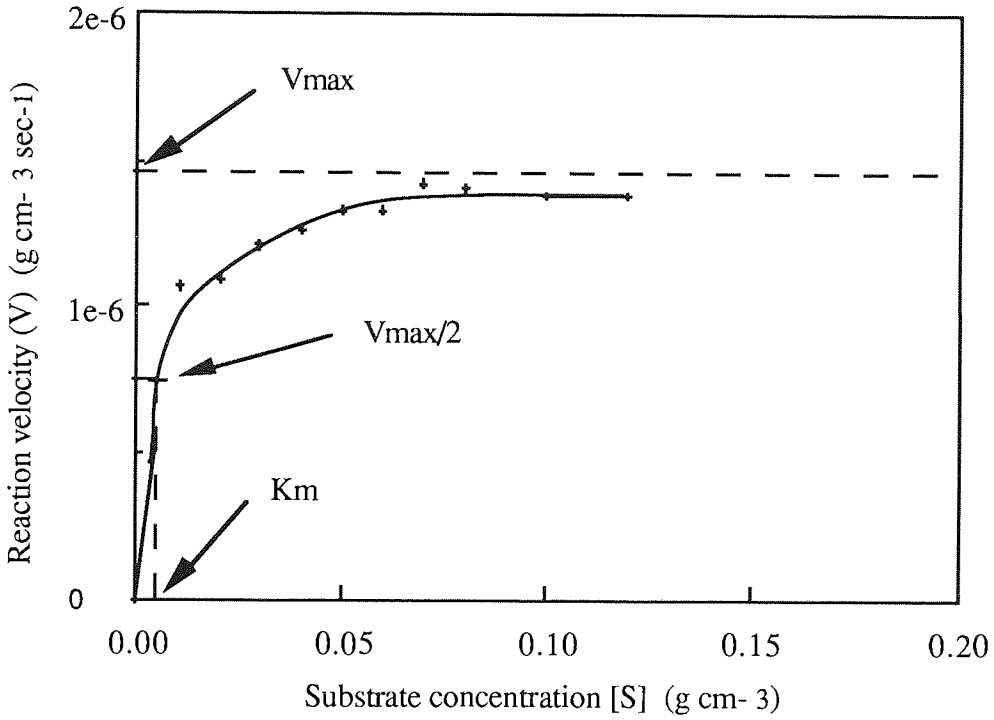

Figure 3.11 A Plot of Reaction Velocity Versus Substrate Concentration for the Dextransucrase Enzyme. (The Vmax and Km Values are Discussed in the Text.)

This graph demonstrates that at sucrose concentrations of less than 2% w/v, V increased linearly with [S], corresponding to a first order reaction. At sucrose concentrations greater than 10% w/v, V was effectively independent of [S] and the reaction can be treated as zero order.

These results fit well into the kinetic model proposed by Michaelis and Menten[89]. A critical feature of this model is the formation of an intermediate complex (ES) during catalysis. The model can be written as:

$$E + S \underset{k2}{\overset{k1}{\rightleftharpoons}} ES \xrightarrow{k3} E + P \qquad (3.4)$$

An enzyme, E, combines with substrate S, to form an ES complex, with a rate constant k_1. The ES complex has two possible fates. It can either dissociate to E and S, with a rate constant k_2, or it can proceed to form product P, with a rate constant k_3. It is assumed that none of the product reverts to the initial substrate, a condition that holds in the initial stage of a reaction before the concentration of product becomes appreciable. Most enzyme data fits this model. The most important relationship that can be derived from this model is the Michaelis-Menten equation, written:

$$V = Vmax \frac{[S]}{[S] + Km} \qquad (3.5)$$

Vmax equals the maximum reaction velocity, attained when all the enzyme sites are saturated with substrate. Km is called the Michaelis constant and is equal to the substrate concentration at which the reaction rate is half of its maximal value.

The dextransucrase Km and Vmax values can be simply derived from V values obtained at different concentrations of [S]. The approximate levels of these values can be read from figure 3.11. Akintoye constructed a Cornish-Bowden plot[90] to accurately calculate these values and obtained a Km value of 6.8×10^{-3} g cm^{-3} and a Vmax value of 1.5×10^{-6} g cm^{-3} sec^{-1}. The Km value was in accordance with other published work [90,92].

It is also possible to transform the Michaelis-Menten equation to yield a linear relationship between V and [S]. This was achieved by taking the reciprocal of both sides of equation 3.5 to give:

$$\frac{1}{V} = \frac{1}{Vmax} + \frac{Km}{Vmax} \times \frac{1}{[S]} \qquad (3.6)$$

A plot of 1/V versus 1/[S] yields a straight line with an intercept of 1/Vmax and a slope equal to Km/Vmax. The corresponding plot using Akintoye's data is shown in figure 3.12.

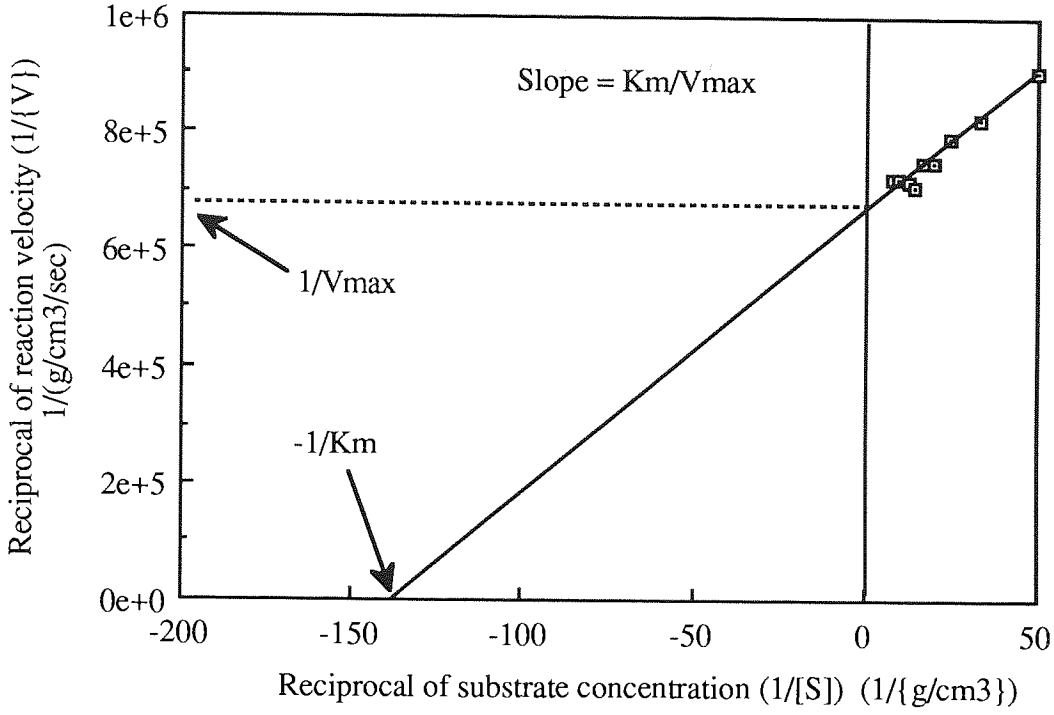

Figure 3.12 A Double Reciprocal Plot of the Dextransucrase Enzyme Kinetic Data

Ignoring the point corresponding to a sucrose concentration of 1% w/v, the graph yielded Km and Vmax values of 7.25 x 10^{-3} g cm^{-3} and 1.48 x 10^{-6} g cm^{-3} sec^{-1} respectively which were in close accordance with Akintoye's results.

3.9.2 The significance of the Km and Vmax Values

The Km value of an enzyme depends of a number of factors, including the substrate and also environmental conditions such as temperature and pH. The Km value has two meanings. Firstly, it is the concentration of substrate at which half the enzyme active sites are filled. The fraction of sites filled, f_{ES}, at any substrate concentration can be calculated from the relationship:

$$f_{ES} = \frac{V}{Vmax} = \frac{[S]}{[S] + Km} \quad \text{(3.7)}$$

Secondly, Km is related to the rate constants of the individual steps in the catalytic scheme given in equation 3.4 The Km value is independent of enzyme concentrations and can be used to identify particular enzymes.

The maximum reaction rate, Vmax, is attained when the condition [S]>> Km is true. Under these conditions, Vmax can be considered proportional to enzyme activity, so that:

$$Vmax = k_3 [E_T] \quad (3.8)$$

$[E_T]$ equals the 'concentration' of enzyme active sites, in a given solution. The kinetic constant k_3 is called the 'turnover number' and is defined as the number of substrate molecules consumed per unit time. Ebert and Schenk[60] have reported the turnover number for the dextransucrase enzyme to be 32 000 min^{-1} (section 2.4.2). For a dextransucrase enzyme solution with an activity of 25 DSU cm^{-3} and hence a Vmax value of 1.5×10^{-6} g cm^{-3} sec^{-1}, $[E_T]$ will equal 2.81×10^{-9} g cm^{-3}.

However, the real significance of equation 3.8 is that Vmax is proportional to enzyme activity. Therefore the Vmax value can be calculated for any given dextransucrase activity. For example, an enzyme activity of 100 DSU cm^{-3} is equivalent to a Vmax value of $(100/25) \times 1.50 \times 10^{-6}$, giving a Vmax value of 6.00×10^{-6}g cm^{-3} sec^{-1} under optimum conditions.

3.9.3 Michaelis-Menten Kinetics and Rate Order

In most of the experiments undertaken in this study, [S] was initially greater than 10% w/v (0.1 g cm^{-3}). Therefore the condition [S]>> Km applied and the enzyme active sites were saturated with substrate. When [S] is greater than 10% w/v , two factors should be noted. Firstly, V effectively equals Vmax. Secondly, V is independent of [S] and the reaction can be assumed zero order. Zero order reactions can be defined by the equation:

$$([S]_0 - [S]_t) = V\Delta t \quad (3.9)$$

where Δt equals reaction time and $[S]_0$ and $[S]_t$ the initial and final substrate concentrations respectively. V can be calculated from equation 3.5 using the appropriate Vmax and [S] values. Therefore, substrate conversion with time can be predicted by using equation 3.9.

When [S] is less than 2% w/v, V can be assumed proportional to [S] and the reaction will be first order and the first order rate equation can be applied:

$$-\text{Ln}\ ([S]_t / [S]_0) = V\Delta t \quad (3.10).$$

4.0 CENTRIFUGATION

4.1 INTRODUCTION

In a gravitational field of force, a particle suspended in a less dense liquid medium will tend to migrate through the medium in a downward direction. For a given medium and fixed external conditions, the rate of this sedimentation depends primarily on the mass of the particle and to a lesser extent, the size and shape of the particle, the medium viscosity and the difference in density between the particle and the surrounding medium.

Centrifuges are capable of accelerating the sedimentation rate of a particle by generating very high gravitational fields. This is achieved by rapidly spinning the particle around a fixed axis. It is customary to indicate the intensity of centrifugation by the 'relative centrifugal field' (R.C.F.) or the 'g' value. This simply represents the accelerating field relative to the earth's gravitational field. Certain sophisticated ultracentrifuges are capable of generating forces of up to 500 000g.

Centrifuges have found considerable uses in the separation and purification of particles in solution. The term 'particle' covers all the materials that may be present in a sample, except the suspending medium. In biological systems these particles may be cells, subcellular organelles or large molecules, while in chemical systems they are usually dissolved macromolecular solutes. Centrifugal separators are also used for the separation and purification of both immiscible liquids and gasses.

Centrifugal separations began finding applications in the process industries about one hundred years ago. The first recorded continuous centrifugal separator was invented in 1877 for the separation of cream from milk[93]. Industrial centrifuges underwent rapid development during the second world war, notably in the field of isotope separation and enrichment. Today, modern centrifuges are used extensively to purify, concentrate and recover oils, fuels, edible proteins, beer, wine, fruit juices and other drinks, industrial and municipal wastes, fertilizers and a wide variety of other materials.

Centrifuge technology is not limited to large scale separators. Laboratory scale centrifuges have been developed in two key areas; analytical ultracentrifugation and preparative (ultra)centrifugation. The former process incorporates an optical system to follow the sedimentation of materials through a homogeneous medium. This allows the characterisation of particle MWs and has given an insight into the size, shape, density and

the basic composition and activity of many macromolecular species. The latter process is capable of completely separating several or all of the components of a sample mixture.

4.2 SEDIMENTATION THEORY

4.2.1 The Sedimentation Coefficient

The rate at which a particle sediments is dependent on its size, shape and density and on the density and viscosity of the surrounding medium. Sedimentation is opposed by a viscous drag or frictional resistance, the magnitude of which is related to the surface area of the particle, so that large or near spherical particles (with small area: mass ratios) will sediment faster than smaller or extended particles. Thus, in a family of particles the largest will generally sediment fastest. The sedimentation rate of a particle is also directly proportional to the difference in density between the particle and surrounding medium and the magnitude of the centrifugal field acting on the particle.

Consider a single particle sedimenting through a medium in a centrifugal cell. The centrifugal force acting on the particle can be defined as:

$$\text{Centrifugal force} = m_{eff}\ \omega^2\ r \quad \text{——} \quad (4.1)$$

where ω equals the angular velocity of the rotor, r is the distance of the particle from the axis of rotation and m_{eff} equals the effective mass of the particle in solution. The angular velocity of the rotor in radians per second can be calculated from the expression:

$$\omega = (2\pi \times \text{rpm}) / 60 \quad \text{——} \quad (4.2)$$

where r.p.m. refers to the number of rotor revolutions per minute. The effective mass of the particle in solutions is equivalent to the true mass of the particle, less the mass of solvent displaced:

$$m_{eff} = m - m\upsilon\rho = m(1 - \upsilon\rho) \quad \text{——} \quad (4.3)$$

The symbol υ refers to the partial specific volume factor of the particle and is defined in section 4.2.3. ρ equals the density of the surrounding solvent. Combining equations 4.1. and 4.3 gives:

$$\text{Centrifugal force} = m(1 - \upsilon\rho)\ \omega^2 r \quad \text{——} \quad (4.4)$$

After a short initial time period, assuming the centrifugal field to be constant, the particle will reach a 'terminal velocity', where the resistance of the medium surrounding the particle is equal to the centrifugal force acting on the particle, thus:

$$m\,(1-\upsilon\rho)\,\omega^2\,r = F \quad \text{——} \quad (4.5)$$

F is the frictional force acting on the particle and is related to the velocity of particle sedimentation, dr/dt, by the expression:

$$F = f\ dr/dt \quad \text{——} \quad (4.6)$$

where f is a constant, known as the frictional coefficient and is related to D, the diffusion coefficient of the particle by the expression:

$$f = k_bT/D \quad \text{——} \quad (4.7)$$

where k_b is the Boltzmann constant and T the temperature in degrees Kelvin. Thus, equation 4.5 may be rewritten:

$$m\,(\,1-\upsilon\rho\,)\,\omega^2\ r = \frac{k_bT}{D}\,\frac{dr}{dt} \quad \text{——} \quad (4.8)$$

Multiplying both sides by Avogadro's number (N), noting that mN will equal particle molecular weight (MW) and that the gas constant R equals k_bN, then equation 4.8 by rearrangement becomes:

$$MW = \frac{RT}{D(1-\upsilon\rho)}\,\frac{dr/dt}{\omega^2 r} \quad \text{——} \quad (4.9)$$

This relationship is called the Svedberg equation [94]. The rate of particle sedimentation in a unit field is commonly called the particle sedimentation coefficient (S) such that:

$$S = \frac{dr/dt}{\omega^2 r} \quad \text{——} \quad (4.10)$$

Equation 4.9 then assumes the form:

$$MW = \frac{RTS}{D(1-\upsilon\rho)} \quad \text{——} \quad (4.11)$$

This equation shows that the mass of a particle is proportional to its sedimentation coefficient S and inversely proportional to its diffusion coefficient D. Thus, particles with low MWs will have small S-values. Knowledge of particle S-values allows the optimum centrifugation conditions to be selected for a desired separation. Equation 4.11 also allows the calculation of particle MWs from experimental data, but requires a knowledge of D and υ for a given particle. These values can be calculated from standard tables or determined experimentally as will be discussed in the following sections.

S-values have units of seconds and are commonly reported in 'Svedberg' units. Since many macromolecules have S-values of the order $\sim 10^{-13}$ sec, 1 Svedberg unit is taken to equal 1×10^{-13} sec.

Integrating equation 4.11 gives:

$$S = \frac{\text{Ln}\,(r_2/r_1)}{\omega^2\,(t_2 - t_1)} \qquad \text{(4.12)}$$

where r_1 and r_2 are the distances from the axis of rotation of the sedimenting particles at times t_1 and t_2 respectively. Therefore, if the distance that a particle sediments during a known interval of time at a given rotor speed is known, then the S-value can be simply determined. Equation 4.12 is often expressed as:

$$r_2 = r_1 e^{S \omega^2 \Delta t} \qquad \text{(4.13)}$$

where Δt equals $t_2 - t_1$.

The relative centrifugal field (RCF) generated during centrifugation can be defined by the equation:

$$\text{RCF} = \omega^2 r / 981 \qquad \text{(4.14)}$$

where r has units of centimetres.

4.2.2 Standardisation of the Sedimentation Coefficient

It is often desirable to compare sedimentation coefficients obtained in different solutions at different temperatures. It is therefore necessary to convert them to the standard state; that of pure water at 20°C, using the following equation[94]:

$$S_{20,w} = S_{OBS}\left(\frac{\eta_{t,solv}}{\eta_{20,w}}\right)\left(\frac{1-\upsilon_{20}\rho_{20,w}}{1-\upsilon_{t}\rho_{t,solv}}\right) \quad \text{——} \quad (4.15)$$

where:

$S_{20,w}$	=	The fully corrected S-value.
S_{OBS}	=	The experimentally observed S-value.
$\eta_{20,w}$	=	The viscosity of water at 20°C.
$\eta_{t,solv}$	=	The viscosity of the surrounding medium at t°C ('medium' refers to the solvent plus added buffers and salts).
υ_{20}	=	The particle specific volume of the solute in the same medium at 20°C.
υ_{t}	=	The particle specific volume of the solute in the same medium at t°C.
$\rho_{20,w}$	=	The density of water at 20°C.
$\rho_{t,solv}$	=	The density of the surrounding medium at t°C.

To standardise a sedimentation coefficient, a knowledge of the partial specific volume factor at 20°C and t°C is required.

4.2.3 The Partial Specific Volume Factor

The partial specific volume is defined as the volume increase resulting from the addition of one kilogram of the solute species to an infinite volume of water. In practical terms it may be regarded as the contribution per kilogram of dissolved material to the total volume of the solution.

McCall [95] has reported a simple method for the calculation of the 'apparent' partial specific volume factor, υ_{app}, which represents the contribution to the volume of 100 kg of solution by 1 kg of the solute using the expression:

$$\upsilon_{app} = \frac{100/\rho - [(100-n)/\rho_o]}{n} \quad \text{——} \quad (4.16)$$

where ρ is the density of solution, ρ_o the density of solvent and n the percentage concentration of solute. Units are in $m^3\ kg^{-1}$ or equivalent. Provided that the solutions are very dilute, υ_{app} may be used in place of υ without serious error [91].

Solutions and solvent densities can be experimentally determined at the required temperature using a pycnometer and waterbath. For proteins, υ_{app} is considered

independent of concentration [91]. Table 4.1 lists the partial specific volume factors of a number of large MW materials. The reciprocal of the partial specific volume factor is equal to the particle density (ρ_D) of a given particulate or molecular species.

Material	Solvent	υ value
Methyl Cellulose	Water	0.72
Starch	Water	0.60
Polystyrene	Chloroform	0.91
Most Proteins	Water	0.745 - 0.750

Table 4.1 The Partial Specific Volume Factors of a Number of High Molecular Weight Materials [94].

4.2.4 Pressure

Considerable pressure is exerted on samples spinning at high speed. At 60 000 r.p.m., the pressure in an ultracentrifuge cell is approximately 250 atmospheres. This will affect sedimentation since both viscosity and density are pressure dependent. However, this effect is slight and need only be considered in very precise work.

4.2.5 The Diffusion Coefficient

Diffusion can be regarded as the transfer of material from a region of higher to lower concentration. The rate of diffusion, dm/dt is proportional to the concentration gradient, dc/dr and the cross-sectional area A through which it occurs:

$$dm/dt \ \alpha \ -A \ dc/dr \quad \text{——} \quad (4.17)$$

The negative sign is because material diffuses in the opposite direction to the concentration gradient. The diffusion coefficient D is a proportionality factor that may be added so that:

$$dm/dt = -DA \ dc/dr \quad \text{——} \quad (4.18)$$

A knowledge of both the mean S and D values of a particle allows the calculation of particle MWs from the Svedberg equation (equation 4.11).

The diffusion coefficient can be calculated from analytical ultracentrifuge data, where the spread of a sedimenting particle species with time can be followed visually. Other optically based systems exist for the measurement of D, such as the use of Tiselius cells to monitor free diffusion. However, these methods are very time consuming. The rate of sample

transfer across porous discs is another common procedure but is prone to mass flow problems. In this study, the D values of several native dextran samples were determined using a dynamic light scattering technique (Chapter 6).

Similarly to S, D can be converted to the standard state, that of pure water at 20°C, by using the equation:

$$D_{20,w} = D_{OBS}\left(\frac{293.2}{T}\right)\left(\frac{\eta_{T,solv}}{\eta_{T,w}}\right) \qquad (4.19)$$

Where $D_{20,w}$ and D_{OBS} are the fully corrected and experimentally determined diffusion coefficients respectively, T equals the absolute temperature of the run in which D_{OBS} was determined and $\eta_{T,solv}$ and $\eta_{T,w}$ equal the viscosities of the sample solution and of water at this temperature.

4.2.6 The Frictional Coefficient

Information concerning the molecular or particle configurations and dimensions of polymer samples in solution can be obtained from a knowledge of the molar frictional coefficient f, defined by equation (4.7) as $f = k_bT/D$. Thus, the frictional coefficient of a particle or molecule can be calculated from a knowledge of the diffusion coefficient. The f value is effectively a combined measure of molecular shape or 'asymmetry' and the degree of solvation or 'hydration' of the polymer in solution. If f_o, the frictional coefficient of an equivalent 'ideal' molecule , that is, a perfectly spherical non-hydrated molecule is known, then the frictional ratio f/f_o may be calculated. By definition, this ratio should be unity if the molecular species in question is spherical and not hydrated. Therefore a value greater than unity indicates a deviation in either particle shape or solvation from the ideal form. f_o can be calculated from the formula:

$$f_o = \eta_t\left(\frac{162\,\pi^2\,MW\,\upsilon_t}{N}\right)^{1/3} \qquad (4.20)$$

Where η_t equals the viscosity of the surrounding medium at t°C and υ_t equals the partial specific volume factor at t°C. The average frictional ratio of several native dextran solutions were evaluated in the course of this work (see chapter 6). f can also be used to estimate particle size. From Stokes law [96], for a spherical particle of radius r_p:

$$f = 6\,\pi\,\eta r_p$$

Thus:

$$k_b T/D = 6 \pi \eta r_p \quad \text{——} \quad (4.21)$$

where η equals the viscosity of the medium in which D was determined. The determination of native dextran particle sizes are also reported in Chapter 6.

4.3 CENTRIFUGE CLASSIFICATION

4.3.1 Introduction

Centrifuges can be classified according to the scheme illustrated in figure 4.1. Industrial settling machines separate materials according to their sedimentation properties and phase density differences, whereas industrial filtering centrifuges use centrifugal fields to force liquid through a filter medium. Laboratory centrifuges have far smaller capacities than industrial centrifuges and are primarily used for research and development purposes. Certain industries, particularly the pharmaceutical industry, use laboratory scale centrifuges for separation and purification purposes.

4.3.2 Laboratory Centrifuges

Laboratory centrifuges may be classified as either preparative or analytical centrifuges.

4.3.2.1 Preparative Centrifuges

This group of centrifuges is classified according to the type of rotor used, namely swinging bucket rotors, fixed angle head rotors, zonal rotors and continuous flow zonal rotors. These rotors are generally made from either aluminium or titanium alloy and have a wide range of sample capacities.

Swinging bucket rotors contain removable tubes that are held in buckets. These rotors are loaded and unloaded in the vertical position. Under an applied centrifugal field, the buckets 'swing out' at a 90° angle so that the direction of sedimentation is approximately parallel with the sides of the tube. The maximum distance of sedimentation is therefore approximately equal to tube length. An example of a swinging bucket rotor is shown in figure 7.1. Swinging bucket rotors are primarily used for small scale separations in density gradients and are particularly useful for sedimentation velocity studies. The use of swinging bucket rotors in this study is reported in chapter 7.

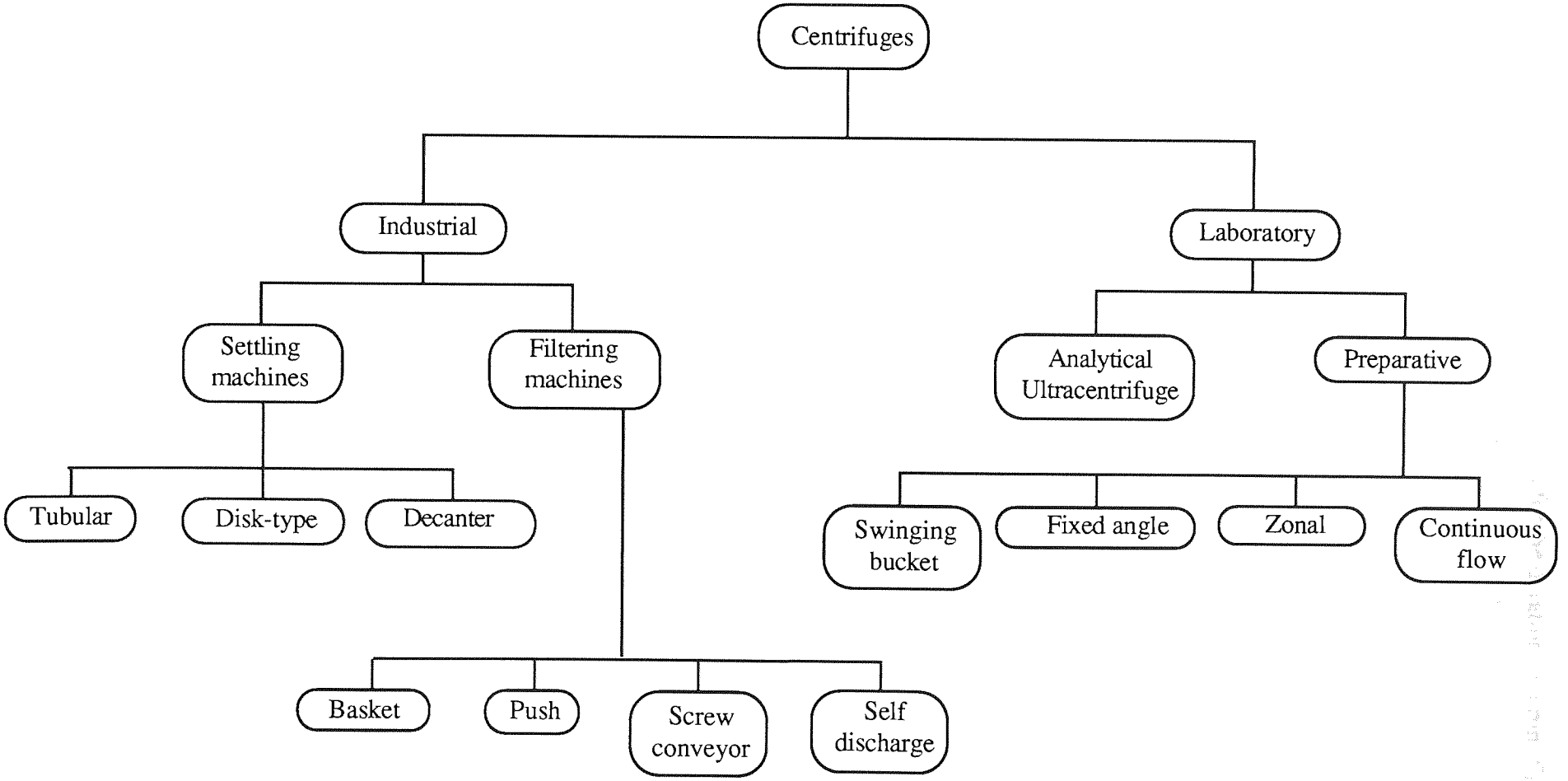

Figure 4.1 Classification Of Centrifuges

Fixed angle head rotors hold tubes at a fixed angle for the duration of a run (figure 4.2) and are generally used for rapid differential or isopycnic centrifugations (discussed in section 4.4). The direction of sedimentation is across the tube, so that the maximum distance of sedimentation is approximately equal to the tube width, hence rapid separations can be achieved. The main advantage of fixed angle head rotors is their solid construction which allows large sample volumes to be spun at high rotational speeds with considerable rotational stability. Generally, the tubes are angled at 35 degrees to the vertical. This has been found to be the most suitable orientation for separating large, slowly diffusing molecules [93]. For smaller, faster diffusing molecules, tubes should be orientated closer to the vertical.

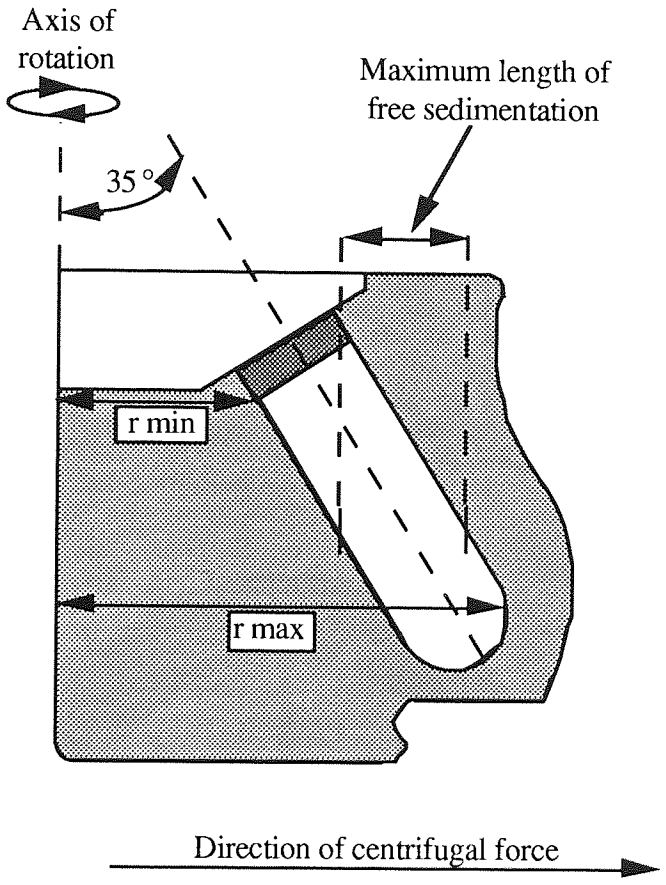

Figure 4.2 An Example of a Fixed Angle Head Rotor

The only practical way to increase the quantity of sample handed in a batch centrifugation system is to increase the capacity of the sample cavity [98]. This has led to the development of zonal rotors, which are essentially large cylindrical or bowl-shaped vessels with capacities of 50-100 times that of a typical swinging-bucket rotor. These rotors have proved highly efficient tools for isolating and purifying a variety of particles [98]. The cylindrical bowl cavity is divided into four equal sector-shaped compartments by vanes attached to the bowl core (figure 4.3). The rotor is enclosed by a removable lid. A

rotating seal assembly allows fluid to be pumped into and out of the cavity 'dynamically' while the rotor is spinning. Reorientation ('Reograd') zonal rotors allow the rotor to be loaded or unloaded while the rotor is at rest. The shape of the rotor core allows the smooth reorientation of the gradient material to a vertical position when the rotor is spun. These rotors are generally used to separate fragile materials which may be damaged by passage through a rotating seal assembly. A Reograd rotor was used in this study, the results being presented in chapter 9. The Reograd operating procedure is outlined in figure 9.2.

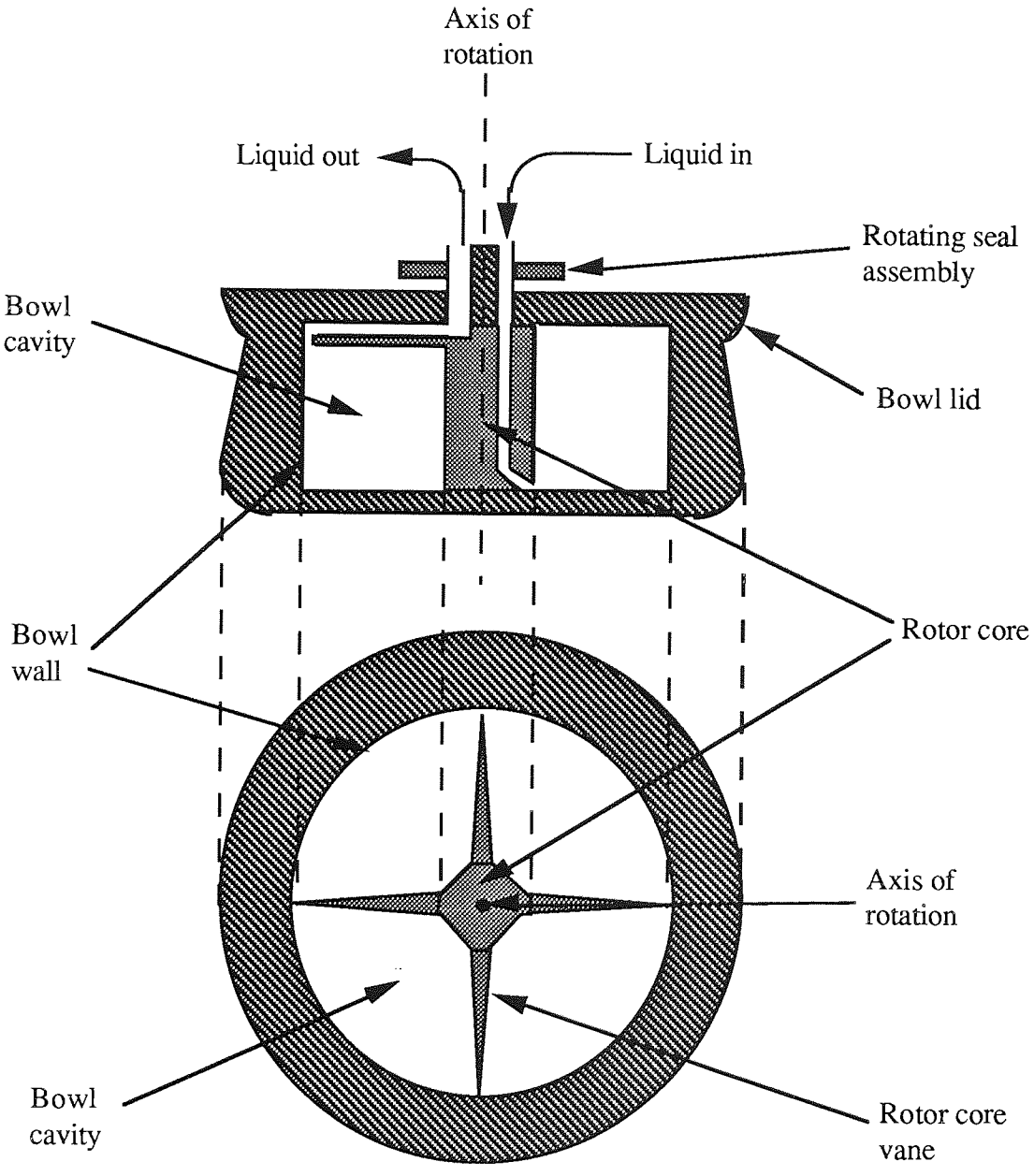

Figure 4.3 Schematic Diagram of a Standard Zonal Rotor

In zonal rotors, material sediments radially towards the rotor wall and therefore, unlike in swinging bucket rotors, there will be no particle-wall collisions [99](figure 4.4).

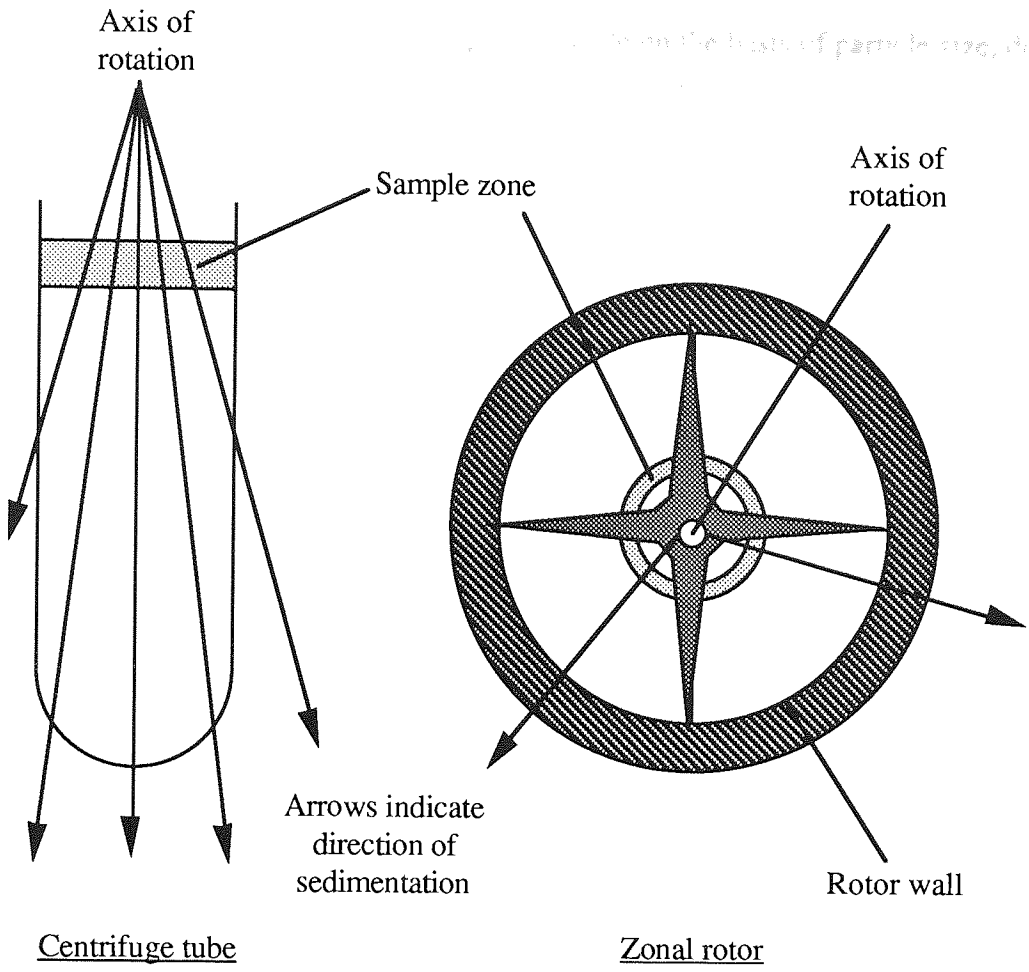

Figure 4.4 Radial Sedimentation in Swinging Bucket and Zonal Rotors

Continuous flow zonal rotors are designed to allow the separation of one or more sample species from large volumes of process fluid [100]. The rotor bowl is similar in shape to a 'batch' zonal rotor, but the core is of a different design and allows different fluid flow patterns in the rotor. The process requires the bowl to be initially partially filled with a dense supporting solution while the bowl is spinning, to form a dense liquid annulus bounded by the bowl wall. Process fluid is then pumped continuously into the vessel so that it runs over the centripetal surface of the more dense solution. The centrifugal separation therefore accounts for two fractions; a sedimenting particle that moves into the rotor cavity and a supernatant fraction that continues to flow through the core and out over the centripetal surface of the supporting solution, before leaving the rotor via the outlet lines (figure 4.5).

Continuous flow processes find particular use in large scale purifications of viruses and subcellular organelles and for harvesting materials such as bacteria [100].

The selection of a rotor for a specific purpose is made on the basis of particle size, density, concentration, volume and the type of separation to be performed.

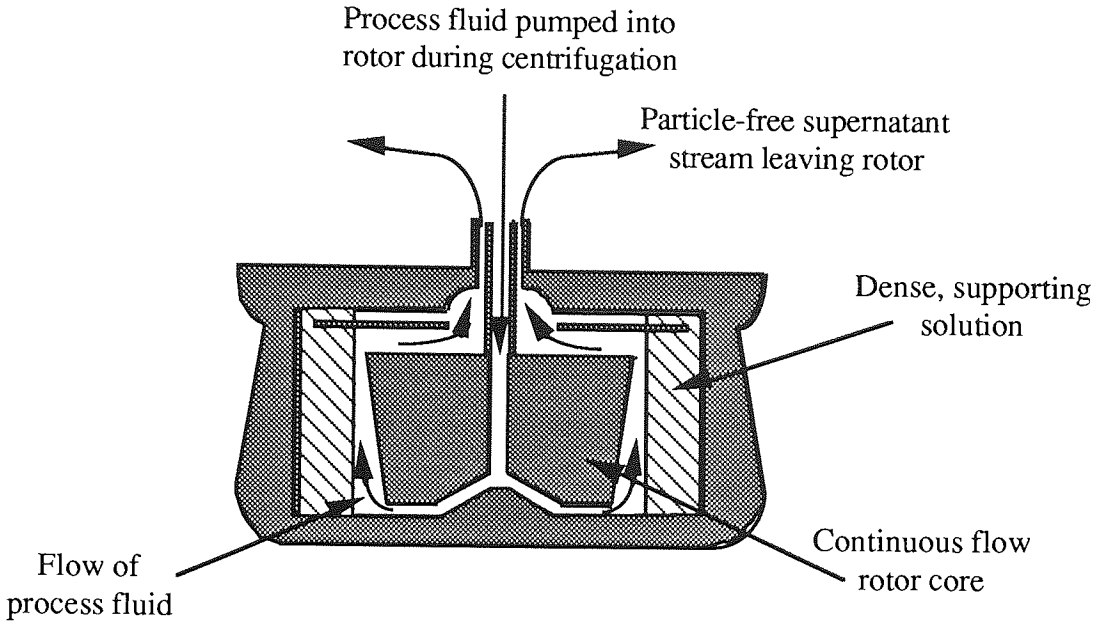

Figure 4.5 Operation of a Continuous Flow Zonal Rotor (100)

4.3.2.2. Analytical Ultracentrifuges

The analytical ultracentrifuge has made a major contribution to the characterisation of mainly biological materials in terms of their molecular properties such as MW, S and D values and buoyant densities. Data from these measurements has also allowed the determination of the 'molecular' size, shape, frictional coefficients, degree of solvation, compressibility and partial specific volume factors of a wide variety of particles (101).

Analytical ultracentrifuges are fitted with sophisticated optical systems that allow the behaviour of samples to be observed during a centrifugal run. Three main types of optical system are available: Ultraviolet absorption, Rayleigh interference and Schlieren optics. The latter system exploits differences in refractive index to visualise samples and yields the most readily understandable data but is the least sensitive system.

The basic design of the rotor has not changed appreciably since the time of Svedberg and co-workers (94). The rotor consists of a rotor body capable of holding sector shaped cells with quartz or sapphire windows. A typical rotor and scanning system is shown in figure 4.6. An Analytical ultracentrifuge was used in this study and the results are reported in chapter 6.

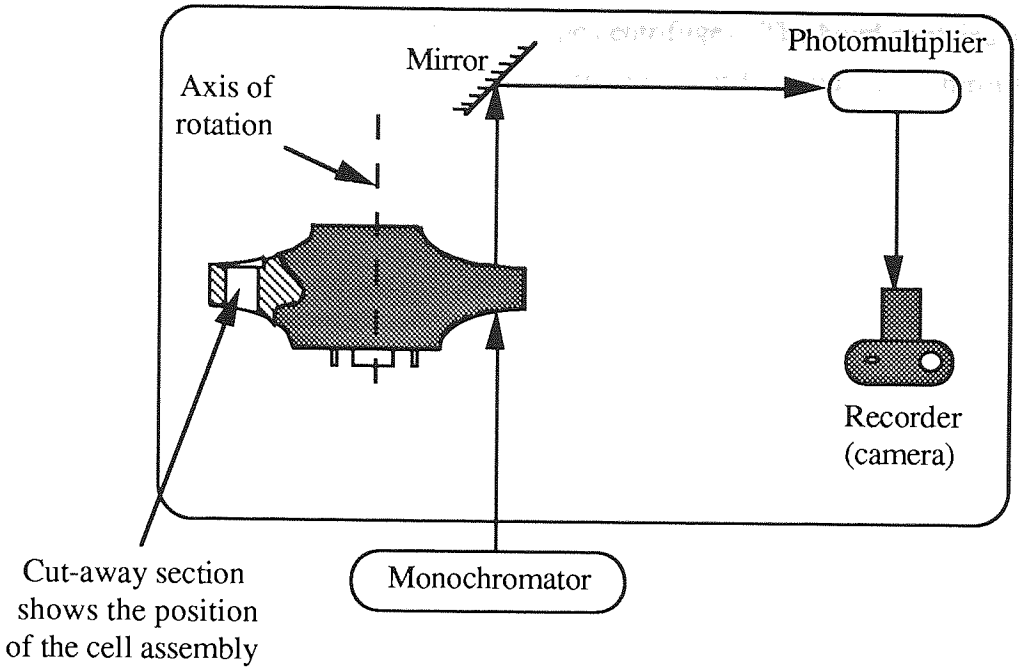

Figure 4.6 A Simplified Diagram of a Typical Analytical Ultracentrifuge Rotor and Scanning System

4.3.3 Industrial Centrifuges

These centrifuges can be classified as either settling or filtering machines. Settling machines include:

(i) High speed, high force separators with manual removal of accumulated solids.

(ii) High speed separators with continuous or periodic discharge of a sludge or slurry.

(iii) Moderate speed separators with continuous discharge of a sludge.

(iv) Slow speed, large diameter separators with intermittent solids removal.

The first category of machine are either of the tubular or disk-type and are primarily used to clarify liquids, concentrate emulsions and separate immiscible liquids such as oil and water. 'Clarification' describes the removal of particulate materials from solutions. This may be done for the purpose of solids recovery or as a liquid purification process. Passage of feed material along the tube length under approximately plug flow conditions will result in the sedimentation of particulate material towards the rotor wall. This will lead to particulate material pelleting at the rotor wall under suitable operating conditions (see figure 8.1). These centrifuges are capable of generating speeds of up to 15 000 r.p.m.(~16 000g), giving throughputs of up to 40 litres per minute, depending on the material to be separated [93]. A laboratory scale centrifuge of this type was used in this study in a preliminary attempt to develop a continuous centrifugal bioreaction-separation process. The results are reported in chapter 8.

Larger throughputs can be achieved using disk-type centrifuges. The bowl contains a stack of cones, called disks, arranged so that the mixture to be clarified must pass through the disk stack before discharge. The resulting stratification of the liquid medium generally reduces the sedimenting distance required before a particle reaches a solid surface and may be considered removed from the process stream. The angle of the cones is sufficiently large so that the aggregated solids will 'slide' radially outwards down the cones before sedimenting freely from the outer edges of the disks to the sloped outer bowl wall for collection. Some machines allow the continuous discharge of accumulated solids during centrifugation via nozzles or valves on the bowl wall. The general fluid flow patterns generated in a disk-type centrifuge during continuous clarification are shown in figure 4.7. Disk-type centrifuges are commonly used to clarify fruit juices, dewater kaolin clay and to purify oil at liquid throughputs of up to 1000 litres per minute [93].

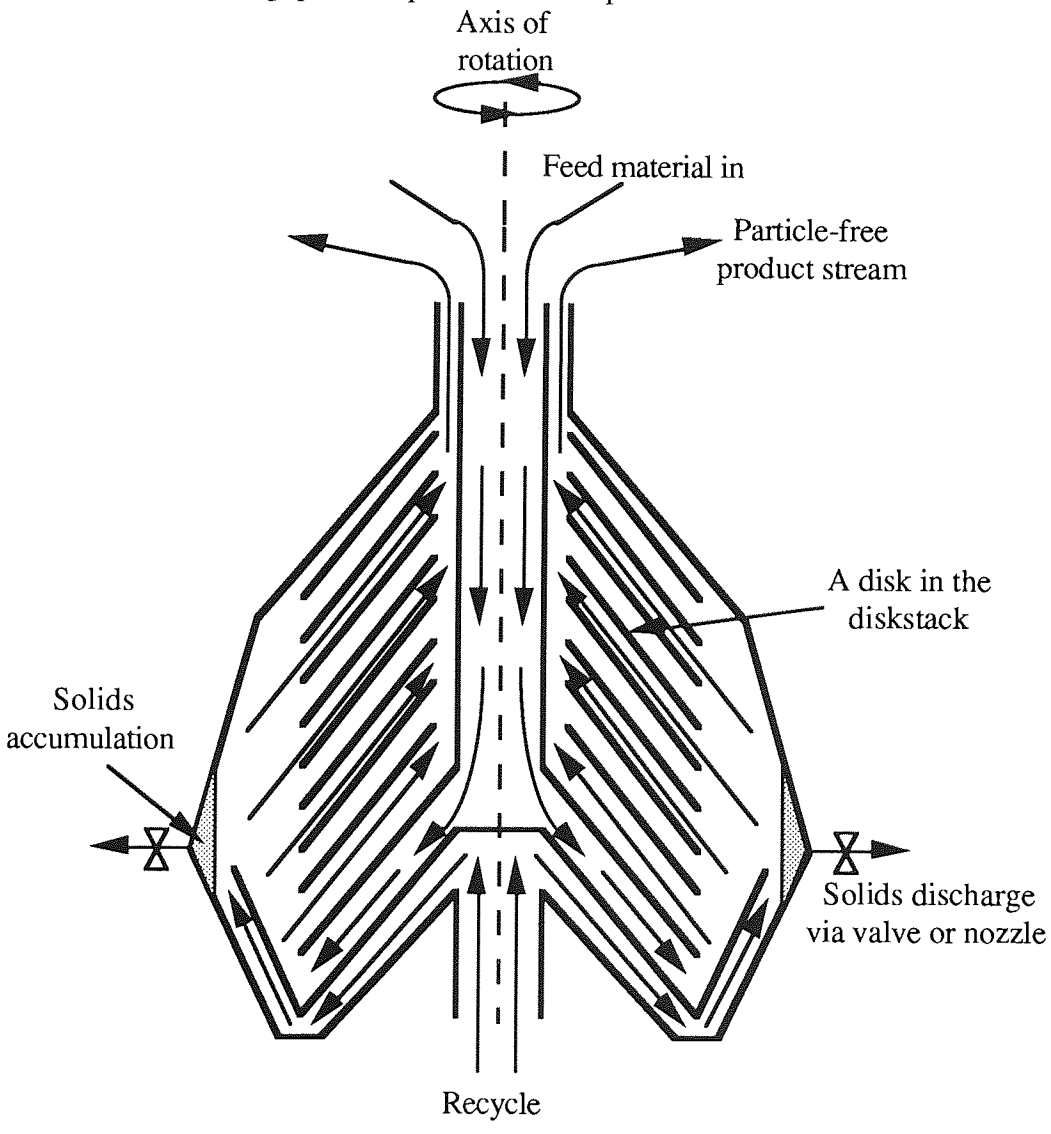

Figure 4.7 Flow Patterns in a Disk-Type Centrifuge. (The arrows indicate the flow of the process stream in the centrifuge bowl.)

Settling centrifuges can be provided with internal conveyors so that both sedimented solid and liquid material are continuously discharged. These 'decanter settling centrifuges' are extensively used to remove solid materials from sewage and industrial wastes (figure 4.8).

Filtering centrifuges contain perforated metal plates or fabric materials through which the process fluid passes. A cake of solid material accumulates on the filter, which can be washed and spun dried if required, during the centrifugation process. The solid material can be unloaded using a knife, although some systems are designed to continuously discharge this material [93].

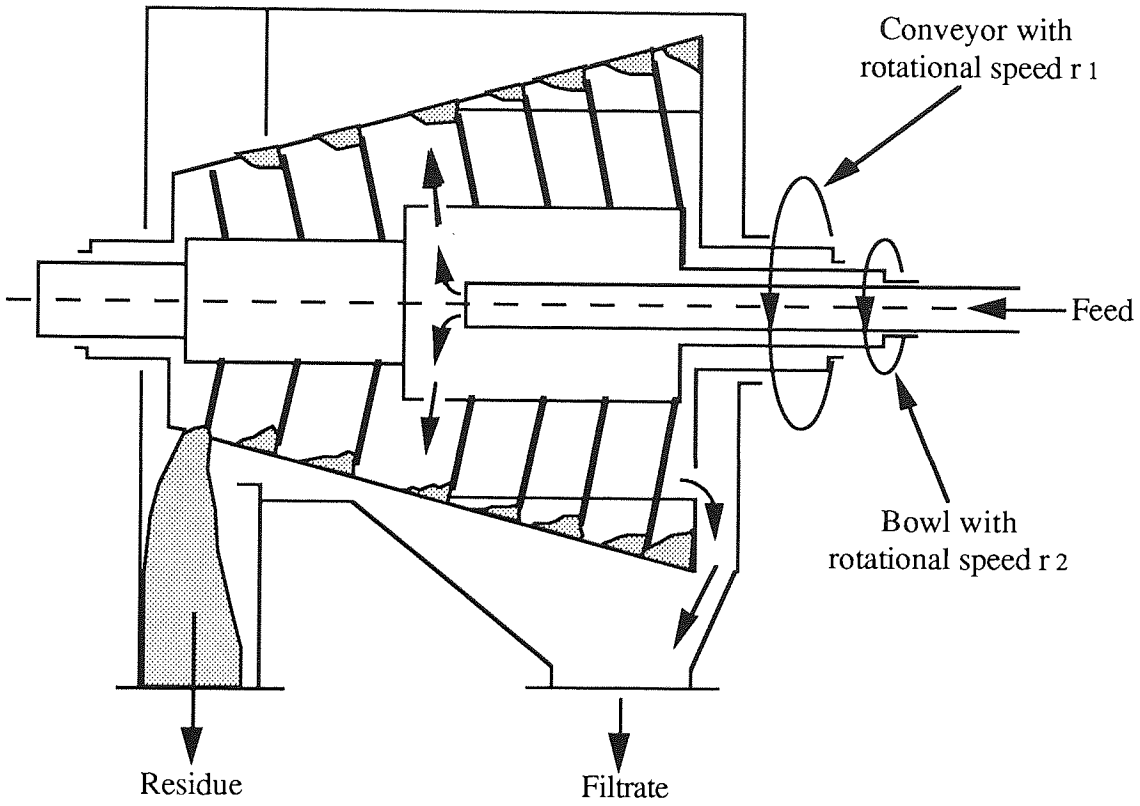

Figure 4.8 Operation of a Decanter Settling Centrifuge

4.4 CENTRIFUGAL SEPARATION TECHNIQUES

Sample purification and separation can be achieved using a wide variety of centrifugal techniques. McCall [95] has categorised these as follows:

1. Normal rate separation.
2. Rate-zonal separation in a density gradient.
3. Isopycnic separation in a preformed gradient.
4. Isopycnic separation in an equilibrium gradient.

5. Sedimentation equilibrium.

The first two categories were used extensively in this work and will be discussed in detail in the following sections.

4.4.1 Normal Rate Separation

Sometimes called pelleting, this is the most common and crudest method of centrifugal separation. When carried out in the analytical ultracentrifuge it is usually termed a 'sedimentation velocity' experiment. In preparative centrifugation, when more than one particle species is present, the term used is 'differential centrifugation'.

The centrifuge tube or bowl is initially filled with a uniform mixture of sample solution. Under the influence of a centrifugal field, two distinct fractions are obtained; a pellet containing sedimented material and a supernatant solution containing unsedimented material. Any particular component in the mixture may end up in the supernatant, the pellet, or distributed in both fractions, depending upon the particle properties and centrifugation conditions. The pellet will contain a mixture of all the sedimented components and will be contaminated with whatever unsedimented material was initially present at the tube base or bowl wall. The only component that will be in a purified form will be the most slowly sedimenting one, but its yield is often very low. The two fractions are separated by decanting the supernatant. The supernatant can be purified further by recentrifuging at higher speeds. The pellet can be recentrifuged after resuspension in a suitable solvent.

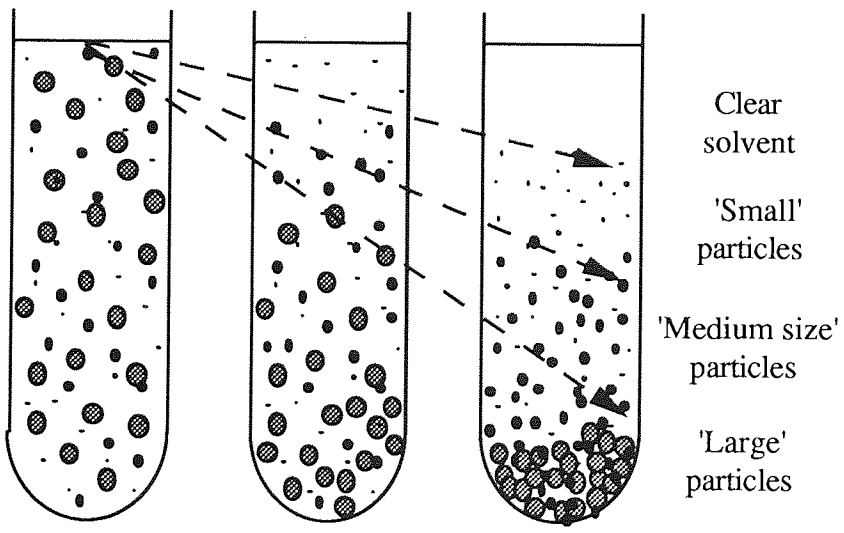

Figure 4.9 Normal Rate 'Differential' Centrifugation

If a single species of particle is centrifuged, the particles will sediment uniformally down the tube or cell. A sharp boundary will then form between the suspension and supporting medium with a plateau region of constant sample concentration on the lower side of the boundary (figure 4.10). The sedimented material will form a highly concentrated pellet. The plateau region will steadily decrease in size as sedimentation proceeds. Back diffusion will reduce the sharpness of the boundary.

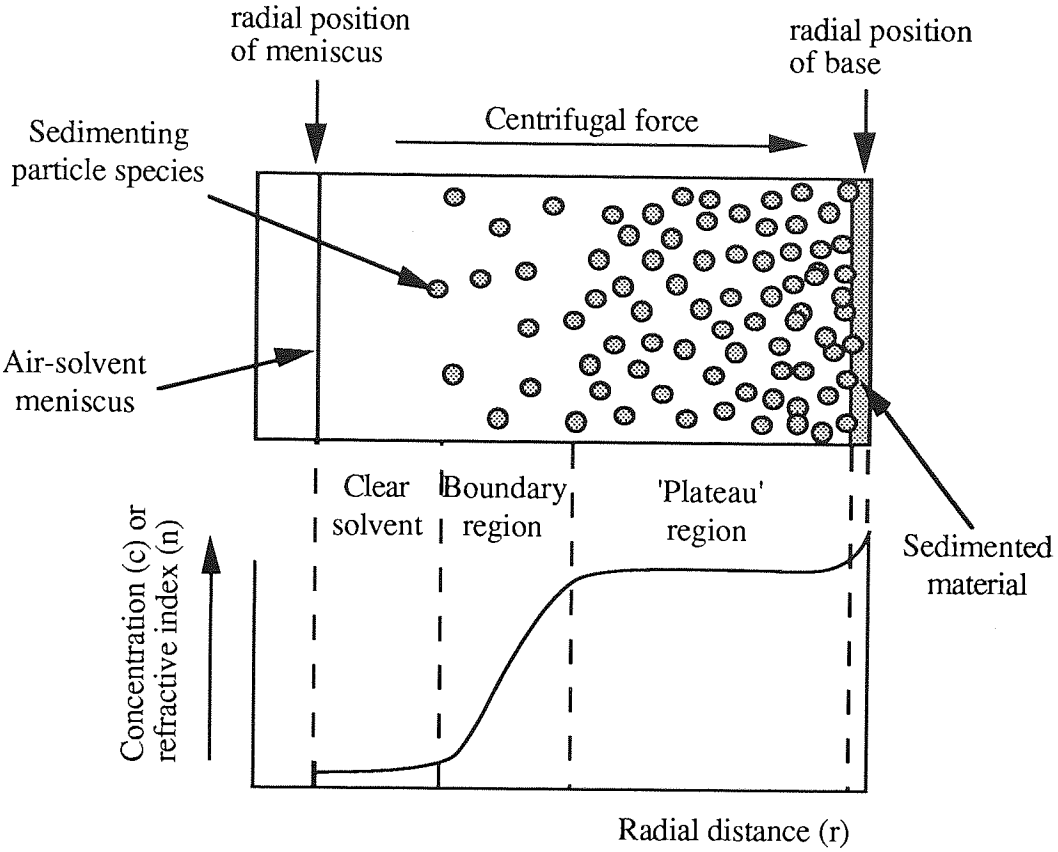

Figure 4.10 The Normal Rate Sedimentation of a Single Particle Species

4.4.1.1 Normal Rate Separations In The Analytical Ultracentrifuge

Normal rate separation studies were performed in an analytical ultracentrifuge in this project and allowed the measurement of various native dextran particle properties. The results are reported in chapter 6.

The analytical ultracentrifuge has a built in optical system so that it is possible to study the shape and movement of the boundary region of a single particle species with time under an applied centrifugal field. When using the Schlieren optical system, particle sedimentation is observed in the form of a concentration gradient (dc/dr) or refractive index gradient (dn/dr) versus radial distance (r) profile. The boundary region is observed as a 'peak' as is discussed in section 6.2.2 and illustrated in figure 6.3. The movement and shape of the

boundary zone yields information concerning particle sedimentation rates as is discussed in the following sections.

4.4.1.2 Calculation of Average Sedimentation Velocities during Normal Rate Centrifugations

By observing the movement of the boundary region with time, an average sedimentation coefficient value S can be calculated for a single sedimenting particle species. When using a Schlieren optical system, this can be achieved by measuring the rate of movement of the boundary peak. Knowledge of the rotor speed then allows calculation of the mean particle S-value according to equation 4.12. The method is complicated by the fact that many particle species are polydisperse and will therefore have a range of S-values. The effect of polydispersity on boundary shape will be discussed in the following section. Often it is sufficient to quote an average S-value.

Many particle species exhibit a decrease in their observed sedimentation rates at higher sample concentrations due to the increasing influence of frictional coefficients. Schachman [102] observed this effect when studying the sedimentation of Tobacco mosaic viruses. His results are summarised in figure 4.11. Sedimentation velocity studies should therefore be conducted at several low concentrations, allowing back-extrapolation of the observed S-values to infinite dilution. It is worth noting that the movement of the boundary is not a measure of the sedimentation rate of the particles in the boundary region, but of the particles in the plateau region ahead of the boundary.

Schachman [102] has reported two equations that have proved useful for extrapolation purposes:

$$S = S_0/(1 + k_s c) \quad \text{—— (4.22)}$$

$$S = S_0(1 - k_s c) \quad \text{—— (4.23)}$$

where S and S_0 are the solute sedimentation coefficient values at solute concentration c and at infinite dilution respectively. k_s is a constant that Rowe [103] has termed the 'concentration dependence coefficient'. It can yield useful information concerning particle size shape and solvation. Eigner et al [104] have determined empirical relationships that link S and S_0 values in several specific cases. These equations only apply at very low sample concentrations.

Because analytical ultracentrifuge cells are sector shaped, a progressive dilution of the sample will occur as sedimentation proceeds. This is known as radial dilution and will affect the sedimentation rates of particles exhibiting concentration dependence effects.

Svedberg and Pedersen [94] showed that this effect could be corrected for by using the following expression:

$$\frac{C_t}{C_0} = \left(\frac{r_1}{r_2}\right)^2 \quad \text{(4.24)}$$

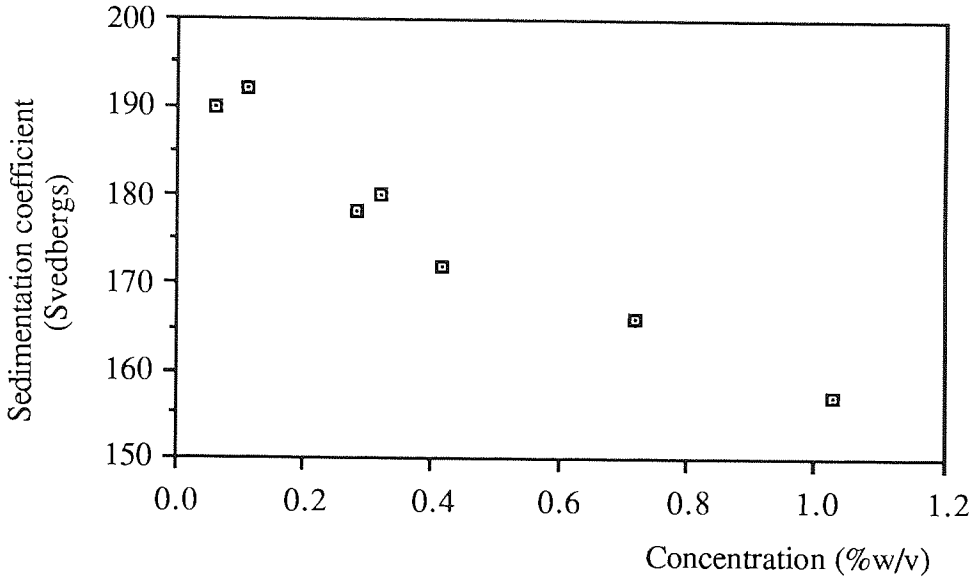

Figure 4.11 Dependence of the Sedimentation Coefficient Values on Sample Concentration for the Tobacco Mosaic Virus [102]

where Co and Ct equal the solute concentration at time zero and time t respectively. r_1 equals the radial distance of the meniscus and r_2 the midpoint of the sedimenting boundary at time t. By using equation 4.13, equation 4.24 can be rewritten in terms of concentration rather than radial distance:

$$Ct = Co\, e^{-2\omega^2 S \Delta t} \quad \text{(4.25)}$$

S-values should also be corrected for density, viscosity and temperature, as was discussed in section 4.2.2.

4.4.1.3 Polydispersity and Boundary Shape

The boundary shape formed by a sedimenting particle species is of considerable importance and allows measurements concerning polymer molecular weight, sedimentation coefficient distributions, size, shape, solvation and particle diffusivity to be made. In general, the shape of a boundary in a sedimentation velocity experiment is controlled by four factors.

First of these is the progressive blurring of the boundary that occurs when a polydisperse material crosses the centrifuge cell. Polydisperse materials such as dextran have a distribution of MWs and hence sedimentation coefficients which results in broader boundary zones. In principle, the observed boundary in a polydisperse system can be considered a composite boundary resulting from the sum of the individual components in solution. Quantitative measurements can be made to estimate polydispersity. Monodisperse materials that have uniform size, shape and density properties and low diffusion coefficients will exhibit sharp boundary zones. A number of researchers [105-111] have studied the effect of polydispersity on boundary shape.

Secondly, there is the distortion of the boundary that occurs due to back diffusion. Back diffusion occurs when solute material in the plateau region of the cell diffuses back down the concentration gradient formed in the boundary region. Svedberg and Pedersen [94] successfully used a Gaussian curve distribution analysis to correct boundary curves for diffusion effects. However, this method can only be applied to monodisperse systems exhibiting a single diffusion coefficient. Fujita [105], Williams et al[106], Gosting [112] and Baldwin [107,113] have all described methods for the correction of diffusion effects.

Opposing these two effects is the so called 'self-sharpening' effect, which is a consequence of the dependence of sedimentation coefficients on concentration. At the trailing or solvent side of the boundary, the concentration is much lower than on the solution side. As a consequence, those molecules falling behind as a result of diffusion find themselves in region of lower concentration and their sedimentation rate increases accordingly until they 'overtake' the boundary [102]. In some cases, this effect is so pronounced that no boundary spreading due to diffusion can be observed. The phenomenon of boundary sharpening has been studied by a number of researchers [105,106,113-116]. Fujita [105], Williams et al [106], Baldwin [113] and Jullander [116] have all proposed methods for the correction of boundary curves for this effect.

Finally, the boundary can be distorted by a phenomenon known as the Johnston-Ogston effect [117]. When a more slowly sedimenting component is sedimenting in the presence of a faster one, the rate of sedimentation of the slower component is decreased due to the increase in total solute concentration in this portion of the tube, resulting in boundary curve distortion. This is termed the Johnston-Ogston effect. Baldwin [118] and Ogston and Woods [119], using polydisperse dextran fractions have reported processes that quantitatively correct for these distortions. The simplest is to carry out the experiment at a series of dilutions of the sample and to determine the apparent relative concentrations of the components at specific points in the boundary region at each dilution. These values are

then graphically extrapolated to zero concentration. Baldwin found that the correction for the boundary shape was significant but not as pronounced as for the boundary sharpening effects. Williams and Saunders [115] have proposed a method that corrects for all concentration dependence distortions in a single step. Schachman[102] has written an excellent review discussing the factors affecting boundary shape in a normal rate centrifugations.

4.4.2 Rate-Zonal Centrifugation

4.4.2.1 Introduction

This technique was used extensively in this study in the development of the centrifugal bioreaction-separation system for the reasons discussed in section 2.3.2.

The rate-zonal centrifugation technique was developed primarily for preparative purposes [120], although the data obtained from such centrifugations also allows the calculation of fairly accurate particle S-values. Separation is dependent upon differences in particle sedimentation rates, which is governed by the size, shape and density of the various particle species and also upon the density and viscosity of the supporting material. Rate-zonal centrifugations are generally used to separate particles ranging in size from macromolecules to cell nucleii and whole cells. In order to minimise convectional mixing, the supporting material must increase in density towards the base of the tube or rotor wall. This will be discussed in greater detail in the following sections.

A suspension of the particles to be separated is applied as a relatively narrow band to the top or 'centripetal end' of the density gradient, into which the particles sediment under the influence of an applied centrifugal field. (Figure 4.12). Particles with similar sedimentation rates will tend to form bands or 'zones' in the gradient. To achieve complete separation, the density of the sample particles must be greater than the gradient density at any point in the tube. The run should be terminated before any of the separated zones reach a position where the gradient density is equal to the particle densities of the sample components. After centrifugation, gradient fractions can be collected for analysis. The similarity between the proposed bioreaction-separation process (figure 2.8) and the conventional rate-zonal process (figure 4.12) should be noted.

The gradient has two main functions. Firstly, it helps minimise convectional mixing and non-ideal sedimentation of the particle species and secondly, the 'shape' of the gradient will dictate the separation achieved between the various sample components.

The maximum sample loading in a rate-zonal centrifugation is generally limited and so a differential centrifugation should be considered where 100% product purity and yield is not required. Rate-zonal separations are best done using swinging-bucket or zonal rotors (121). Both types of rotor were used in this study. Loss of resolution is considerable when using fixed angle-head rotors due to wall effects.

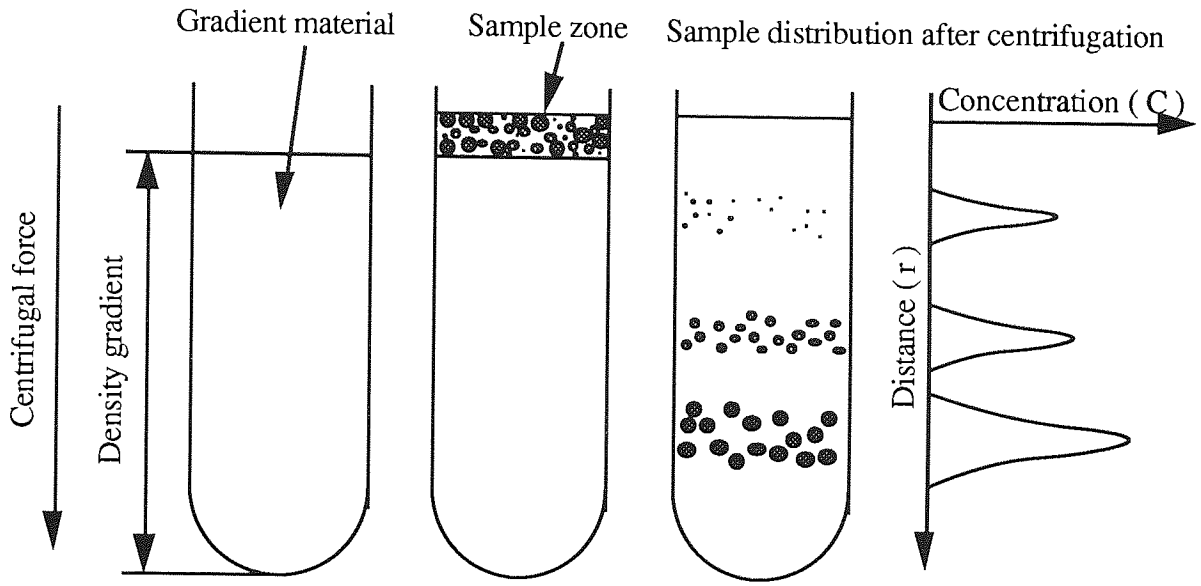

Figure 4.12 The Rate-Zonal Separation Principle. (Explained in text)

4.4.2.2 Gradient Materials

The properties of an 'ideal' gradient solute have been listed by Ridge (122). The material should be inexpensive, readily available, sterilisable and capable of forming high density solutions. It should not be hyperosmotic, hypoosmotic, interfere with the assay technique, absorb UV or visible light, be corrosive, flammable or toxic. Ridge states that the solute should be totally inert towards the sample material, although the requirements of the proposed centrifugal bioreaction-separation process necessitates the use of an interactive gradient material. Simple sugars (sucrose, sorbitol and glycerol), polysaccharides (ficoll, dextran and glycogen), proteins (bovine serum albumin) and deuterium oxide have all been employed as gradient materials.

4.4.2.3 Resolution

The main factors governing the resolution achieved between two or more particle populations in a rate-zonal process lie in the choice of centrifugation conditions. Increasing the applied centrifugal force will shorten run times and minimise diffusion broadening of the bands. Increasing the concentration gradient (slope) of the supporting solution causes band sharpening due to increases in viscous drag. However, excessive band sharpening can lead to zone instability. At intermediate rotor speeds, for example, between 25 000 and

40 000 rpm, optimum separation is achieved using linear sucrose gradients increasing in concentration from 5 to 20% w/w [98]. Resolution can also be decreased by gradient disturbance and applying too much sample to a gradient. Gradient overloading will be discussed in section 4.4.2.5.

4.4.2.4 Gradient Shape and Preparation

The 'shape' of a gradient normally refers to its concentration profile, but concentration does not always have a linear relationship with either density or viscosity. Viscosity is generally more important than density in determining centrifugation time as the particles will be slowed down by the increasing viscous drag as they sediment through a gradient. The density gradient should be steep enough to prevent convection and to maintain the stability of the sedimenting zones during centrifugation. A gradient which needs to be steep at the top to support the sample zone does not need to be so steep further down where the zones have separated from each other. For this reason, 'convex' density gradients are often advocated. However, linear gradients are most commonly used and offer the best resolution of components such as proteins and enzymes [98]. Concave gradients are best used for lipoprotein separation and discontinuous (step) gradients for the separation and purification of whole cells, subcellular organelles and viruses. Noll [123] and McCarty et al [124] have discussed the use of 'isokinetic' gradients, designed so that particle sedimentation rates are independent of column length.

Although most gradient shapes used in zonal rotors are the same as those used in swinging bucket rotors, allowances should be made for the different shape of the zonal rotor bowl. The parallel walls of a centrifuge tube maintain a linear volume/radius relationship with increasing radius, whereas in a bowl shaped zonal rotor cavity the volume/radius relationship is dependent upon the square of the rotor radius (figure 4.13).

Concentration gradients are usually prepared by hand-layering or pumping the gradient material into a centrifuge tube or zonal rotor. The tube loading technique is shown in figure 4.14. The least dense portion of the gradient is loaded first, followed by successively denser fractions, carefully introduced to the tube base, causing displacement of the previously loaded gradient fractions. Standard zonal rotors are loaded while spinning via a 'rotating seal assembly' (called 'dynamic' loading). The loading technique is identical to that used for loading centrifuge tubes. The gradient fractions form liquid annuli at the bowl wall as shown in figure 4.15. The gradient fractions are pumped into the rotor until the lightest portion of the gradient is seen leaving the vessel. Reorientating gradient ('Reograd') rotors, discussed in section 4.3.2.1, can be loaded with gradient material while at rest ('statically').

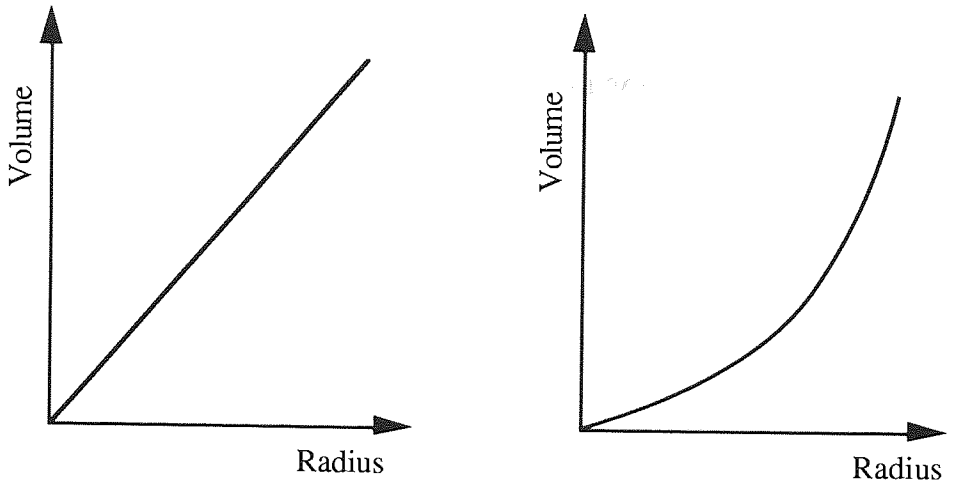

(a) Centrifuge tube (b) Zonal rotor bowl

Figure 4.13 The Volume/Radius Relationship in Centrifuge Tubes and Zonal Rotor Bowls

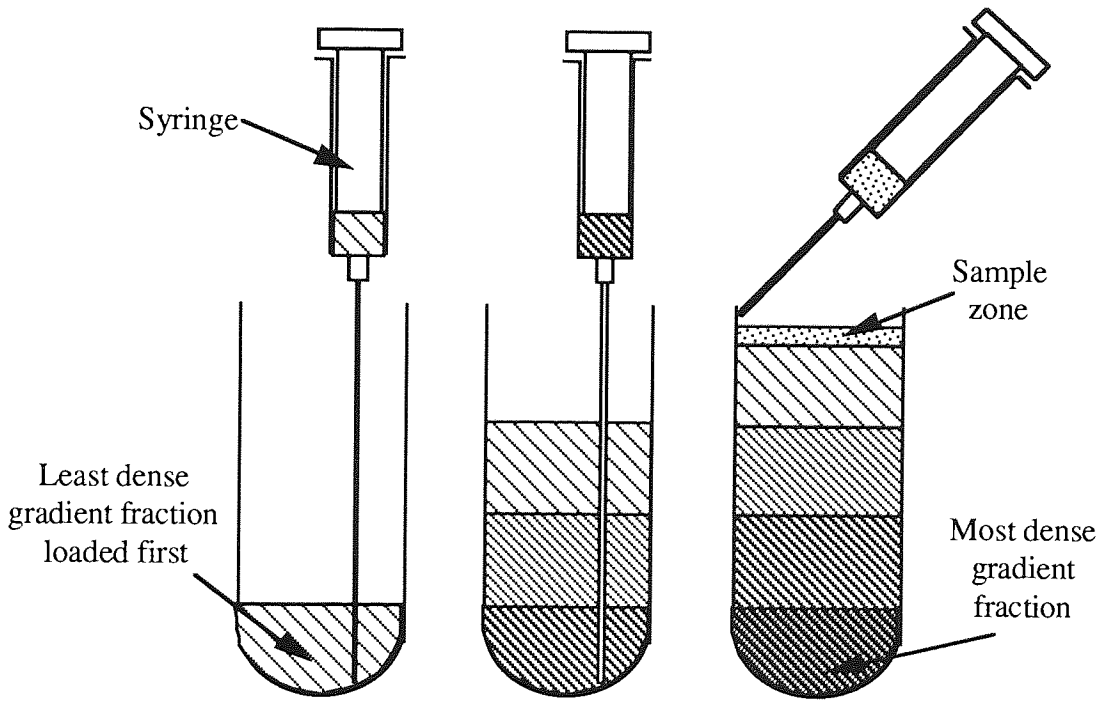

Figure 4.14 Construction of a Gradient and Sample Loading in a Centrifuge Tube. The least dense gradient fraction is loaded first, followed by sucessively denser fractions. The sample is applied as a zone to the top of the gradient.

After loading, the gradient should be left for a number of hours in order to form a 'smooth', continuous density and viscosity gradient. This is achieved by diffusion of the initially sharp gradient fraction boundaries. Schumaker [121] has calculated the time required for smooth gradient formation using the equation :

$$t_D = y^2 / 8D \quad \text{—— (4.26)}$$

where t_D equals the time required for smooth gradient formation, y the distance between the initially sharp boundaries and D, the diffusion coefficient of the gradient solute. Once the gradient has been formed, it will deteriorate due to diffusion. Fortuin [125] has reported that the time that a linear gradient will remain stable can be defined by:

$$t_S = b^2 / 100D \quad \text{—— (4.27)}$$

where t_S equals the time of stability and b is the total gradient length.

Brakke [126] has discussed the technique of manual gradient preparation in detail.

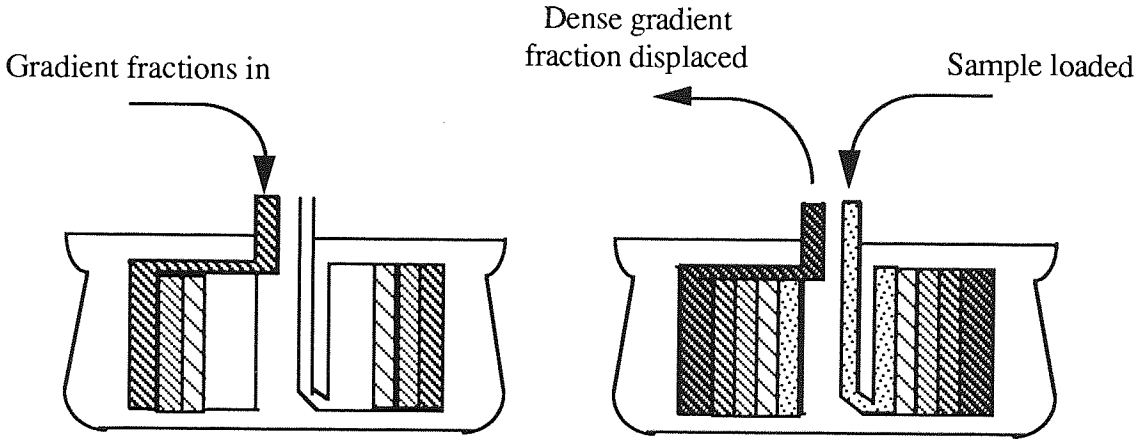

Step 1: Gradient fractions are loaded into the bowl while spinning. The least dense gradient fraction is loaded first, followed by more dense fractions until the bowl is filled.

Step 2: Sample is loaded onto the top of the gradient, causing the displacement of some of the densest gradient material at the rotor wall.

Figure 4.15 Construction of a Gradient and Sample Loading in a Zonal Rotor Bowl Fitted with a Standard Zonal Core

4.4.2.5 Sample Loading and Convection during Zonal Sedimentation

Convection in a rate-zonal centrifugation process may be defined as any form of mass transport by means other than sedimentation and diffusion. The overloading of gradients with sample material can lead to convection effects and the possibility of the sample 'sinking' into the gradient. This is known as 'density inversion'. Therefore, the loading

capacity of the gradient should be determined prior to sample loading. It appears that convective disturbances are present in all zone sedimentation velocity experiments, although conditions may be chosen to minimise them (121).

Schumaker (121) has listed several factors that can cause convective disturbances in rate-zonal centrifugations. The main observations are discussed in this section.

In order to maintain hydrodynamic stability throughout a zone of macromolecules, it is necessary that the total density gradient should increase in the direction of the external field. This density gradient is a function of the concentration gradients of the sample and of the low molecular weight gradient material.

The total density gradient of the solution may be written as $d\rho_T / dr$ and is equal to the overall density gradient of the macromolecule and solute at any point, r, in the liquid column. The total density gradient can be determined using the expression (121):

$$\frac{d\rho_T}{dr} = \frac{dc_s}{dr}(1 - \upsilon_s \rho_w) + \frac{dc_M}{dr}(1 - \upsilon_M \rho_w) \qquad (4.28)$$

Where υ refers to the partial specific volume factor which is assumed constant for practical purposes, ρ equals density and c equals concentration. The subscripts w, s and M refer to water, the low molecular weight solute and the macromolecular material respectively. For hydrodynamic stability, $d\rho_T / dr$ must always be positive and greater than some minimum value, usually written as $d\rho_{min} / dr$.

If a solution of macromolecules is layered onto a more dense solution containing a low molecular weight solute, then the density gradient at the interface will decrease with time, owing to diffusion of both species. If the total density of the gradient falls below the minimum value ($d\rho_{min} / dr$) which is necessary for the maintenance of hydrodynamic stability, then convection will ensue. This condition of hydrodynamic stability may be written:

$$\frac{d\rho_T}{dr} - \frac{d\rho_{min}}{dr} > 0$$

The condition for hydrodynamic stability at the interface between the two solutions has been defined by Schumaker as (121):

$$\frac{1}{2(\pi t)^{0.5}}\left[\frac{c_s(1-\upsilon_s\rho_w)}{Ds^{0.5}} - \frac{c_M(1-\upsilon_M\rho_w)}{D_M^{0.5}}\right] > \frac{d\rho_{min}}{dr} \qquad \text{(4.29)}$$

where t equals the time that the solutions have been in contact. Should the left hand side of this equation be negative, then convection will occur. Therefore, the conclusion can be drawn that a less dense solution cannot necessarily be layered on top of a more dense solution at any finite time with complete boundary stability.

It should be noted in the above equation that the density factors of both solutes are divided by the square roots of their respective diffusion coefficients. The ratio of the square roots of the diffusion coefficients of a typical protein molecule and a sucrose molecule is about 3. Therefore, two solutions containing these solutes may not be layered together without initial convective disturbance unless the density factor due to the sucrose is at least 3 times greater than that due to the protein. In other words, a typical 5% w/w pure protein solution would require a minimum sucrose supporting solution of at least 10% w/w to prevent initial convective disturbances. Clearly, the 'starting' concentration of a gradient is an important factor in preventing convection.

Equation 4.29 also shows that hydrodynamic stability is time dependent. Although initial convection will cause some sample material to sink into the supporting gradient, subsequent diffusion of this material will result in the formation of a smooth sample concentration gradient and hydrodynamic stability will be achieved.

Svensson et al [127] have reported a method for the calculation of the theoretical maximum mass of sample (m) that can be supported by a gradient in a swinging bucket rotor. In equation 4.28, the term $c_s / dr\,(1 - \upsilon_s \rho_w)$ refers to the density gradient due to the low molecular weight solute. If the symbol $d\rho_s / dr$ is used for this term and if $d\rho_T / dr$ is taken as $d\rho_{min} / dr$, which is the condition for maximum loading of the zone, then m can be calculated using the following expression:

$$m = \frac{\frac{d\rho_s}{dr} - \frac{d\rho_{min}}{dr}}{(1-\upsilon_M\rho_w)} \frac{Ah^2}{2} \qquad \text{(4.30)}$$

A equals the cross-sectional area of the tube and h equals the thickness of the sample zone. Thus, it can be seen that 'steeper' gradients can support larger masses of sample without hydrodynamic instability. However, results from this equation did not fit the experimental

data of Brakke [126] who found that much lower sample masses were required in order to maintain hydrodynamic stability. This equation should therefore be treated with caution.

Griffith [98] has reported that gradients in swinging bucket rotors can support most protein samples provided that the ratio between the sample concentration and starting gradient concentration is 1:10. Excessive sample concentrations will result in gradient overloading. Samples are generally hand loaded using a hypodermic syringe. In a zonal rotor, the total sample concentration should be at least 40% less than the starting gradient concentration; or a 6:10 ratio between sample and gradient concentration [98]. Samples are generally loaded by being pumped into the centrifuge bowl (see figure 4.15).

The volume of sample that can be applied to a gradient in a swinging bucket rotor tube is a function of the cross-sectional area of the gradient that is exposed to the sample [98]. Griffith has reported a number of sample volumes suitable for swinging bucket rotors of varying tube diameters. Sample volumes of up to 10% of the total gradient volume can be loaded in zonal rotors with little loss in resolution[98]. Because the recommendations of Griffith were based on experimental data, they were used in preference to theoretical calculations in this study.

Berman [129] and Spragg and Rankin [130] have also discussed the factors affecting the maximum sample capacity of a gradient. Ridge [122] has observed that convectional stability can be increased by dissolving the sample material in a less concentrated portion of the gradient material prior to loading.

Anderson [131] observed in some of his rate-zonal experiments that protein material began to fall in streams from the sample zone into the denser supporting sucrose gradient *without* centrifugation. This phenomenon has been observed by a number of other researchers [132,133] and is termed 'droplet sedimentation'. Brakke [134] believes that this phenomenon is due to diffusion effects. He reasoned that because the protein zone had a lower concentration of gradient material than the gradient immediately below it, the low molecular gradient material diffused into the protein zone more rapidly than the protein material diffused out. The density of the solution at the edges of the protein zone therefore became greater than that of the gradient solution immediately below it and droplets visible to the naked eye began to settle. Apparently, the density of the droplet was constantly being increased by diffusion of sucrose into it and as it settled through the solution, leaving a trail of protein behind it. The formation of these droplets is an extreme form of the density inversion effects described above [121].

Schumaker [121] has described a highly idealised mathematical treatment of this process and concluded that the size and velocity of the droplets is a function of the concentration gradient of the low molecular weight solute. The size of the most rapidly settling drops is independent of macromolecular concentration, but their velocity will be dependent upon concentration. However, under high centrifugal forces, the droplets become so small that they rapidly lose their identity and smooth hydrodynamically stable protein gradients are formed. This is what happens in a typical rate-zonal process. Ridge [122] states that in high centrifugal fields, droplets never achieve a sufficiently large size or high enough density to seriously affect the resolution of a gradient. However the damage may be done before centrifugation is started.

4.4.2.6 Centrifugation, Recovery and Analysis

Centrifugation conditions should be dependent upon particle properties, such as sedimentation coefficient and MW values.

If the rate-zonal process has been carried out in a centrifuge tube, it may be possible to use a syringe to recover the separated sample fractions. Typically however, the separated zones cannot be seen and the tube contents should be carefully collected as fractions prior to analysis.

Tube fractionating systems are generally simple and include; fraction removal using syringes passed through the tube wall; tube slicing techniques using special cutters and most commonly, density displacement techniques. In the latter method, a heavy displacement solution is introduced to the base of the tube causing an ordered displacement of the tube contents. The gradient fractions are collected via a side hole in the centrifuge tube cap as shown in figure 4.16.

Standard zonal rotors are also unloaded using density displacement techniques. The rotor is unloaded dynamically so that the dense fluid forms an increasingly thicker layer at the rotor wall, causing displacement of the less dense gradient material (figure 4.17). The 'Reograd' rotor is unloading statically, air being used as the displacement medium (see figure 9.1).

It is possible to continuously monitor the gradient material as it leaves the centrifuge vessel by using, for example, a UV photometer fitted with a flow cell to determine the exact distribution of the sample materials in the gradient. The gradient fractions are usually collected for further analysis.

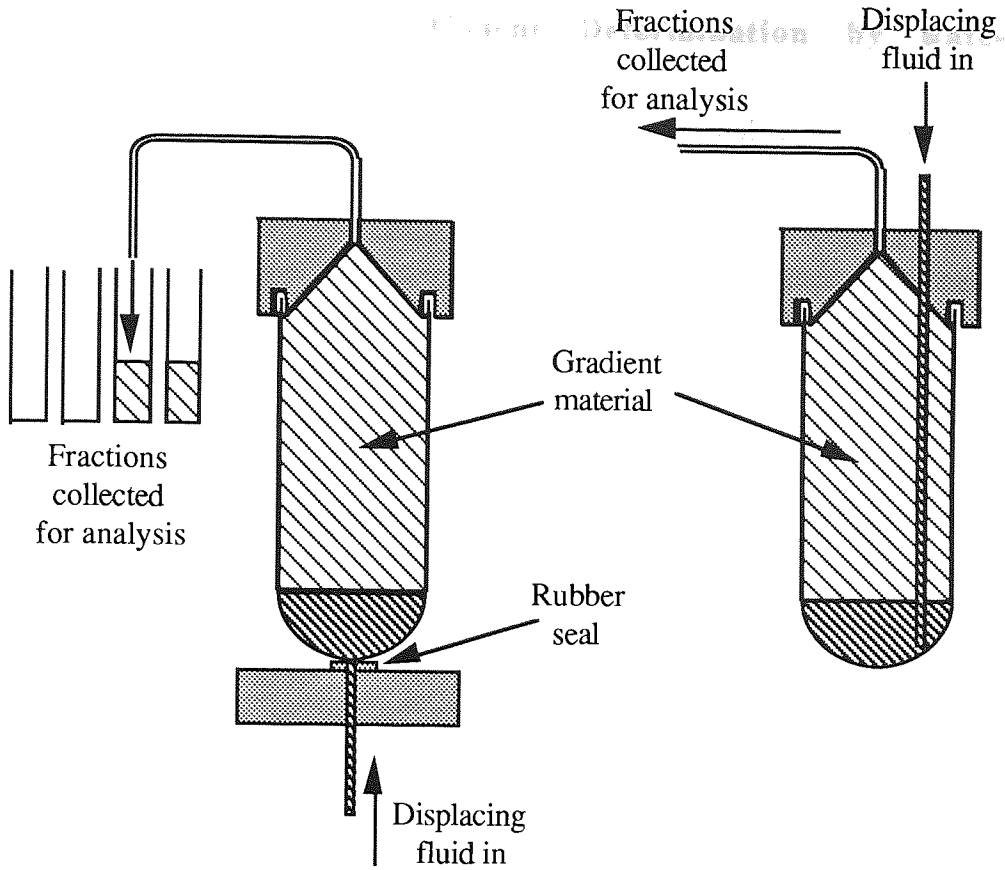

(a) Density displacement via the tube base

(b) Density displacement via the centrifuge cap

Figure 4.16 Gradient Harvesting from Centrifuge Tubes. The displacement medium is applied to the base of the tube causing ordered gradient displacement in both methods.

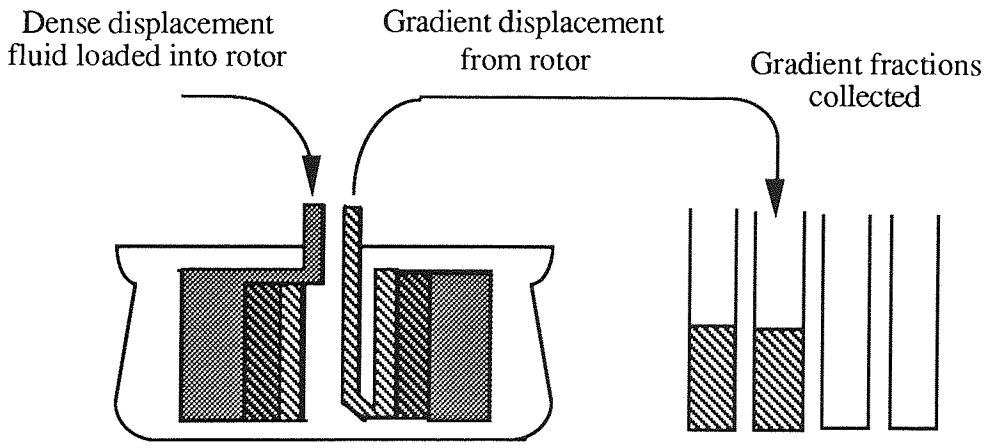

Figure 4.17 The Dynamic Unloading of a Standard Zonal Rotor. The denser displacement medium is displaced via the rotor edge.

4.4.2.7 Sedimentation Coefficient Determination by Rate-zonal Centrifugation

It is possible to determine the sedimentation coefficients of sample zones from a knowledge of run time, rotor speed and band position in a known gradient. A monodisperse particle species should have a single, characteristic sedimentation coefficient value (S-value), hence a well defined sample zone. However, polydisperse materials, such as dextran have a distribution of MWs and hence S-values. Therefore, by determining the distribution of a sample in a gradient after centrifugation, the distribution of the sedimentation coefficients of the various sample components can be determined.

Calculations are complicated by the changing density and viscosity of the gradient media. However, several researchers have offered solutions to this problem [135-137]. Steensgaard et al [135] have proposed a method whereby concentration distributions in density gradients can be converted to equivalent S-values. The method is simple and was used in this study to determine the sedimentation coefficient distribution of native dextran fractions as described in chapter 9 and appendix A8.

This method has many similarities with the normal rate centrifugation method. In the latter process, by using Schlieren optics, the concentration gradient of the boundary region can be viewed as a curve, the shape of which is a function of the sedimentation of particles in the plateau region ahead of that peak (figure 4.10). For a migrating zone, the profile obtained pertains directly to the concentration versus radial distance distribution of the sample. Profiles from the two different techniques are compared in figure 4.18.

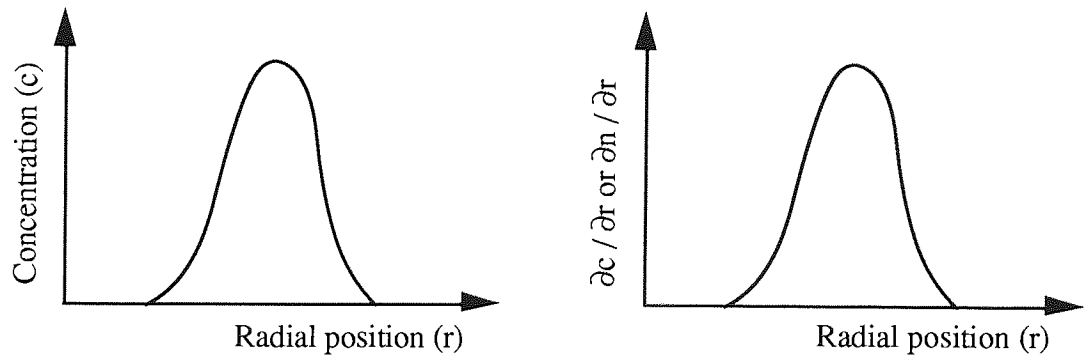

(a) Rate-zonal centrifugation
Concentration versus radial position

(b) Rate normal centrifugation
Concentration gradient versus radial position

Figure 4.18 Comparison of the Zonal and Boundary Centrifugation Methods for Sedimentation Coefficient Determination

The 'boundary' method is more widely used for sedimentation coefficient distribution studies as it is simple to perform, quick, accurate, sensitive and does not require the use of gradients. However, back diffusion, concentration dependency, and the Johnston-Ogston effect can all affect boundary shape (section 4.4.1.3).

The use of markers with known S-values have been used for calibration purposes in rate-zonal sedimentation velocity experiments carried out in fixed angle rotors[138]. Rosenbloom has successfully used radiolabelled bacteriophages as markers [139].

4.4.2.8 Wall Effects

Much early work in rate-zonal centrifugation was concerned with the effect of tube walls on the sedimentation of macromolecules in fixed angle and swinging bucket rotors [140,141]. The subject has been well reviewed by Schumaker [121]. However, wall effects in swinging bucket rotors have been experimentally proven to be negligible and have little or no effect on particle sedimentation velocities during rate-zonal centrifugations [142]. Trautman and Breese [143] believe that the bulk of the material that collides with the sides of the tubes during centrifugation in a swinging bucket rotor results in the formation of circular vortices in which material is moved to the centre of the tube rather than convecting in a radial manner towards the tube base. Brakke [144] favours this possibility which he terms 'cross-tube convection'. If the sedimenting material is 'sticky' as in the case of polystyrene latex, DNA and cell particulates, some losses of material by sticking to the tube wall may occur. The design of zonal rotors prevents convection due to wall effects, as indicated by figure 4.4.

4.4.3 Isopycnic Separation in a Preformed Gradient

This method differs from the rate-zonal method in the fact that the gradient encompasses the whole range of densities of the sample particles. Each particle will sediment to the position in the centrifuge tube at which the gradient density is equal to its own density. The particle will then 'float' at that level. Separation is therefore solely dependent upon particle density and is independent of time.

4.4.4 Isopycnic Separation in an Equilibrium Gradient

This technique is used in analytical ultracentrifuges to observe the position and MW distribution of various sample components in a density gradient. Separation is achieved by exploiting differences in particle densities in an equilibrium gradient. Caesium chloride is generally used as the gradient material.

The centrifuge cell is loaded with a solution of caesium chloride at a suitable concentration, to yield the density range required. The salt solution also contains the sample to be analysed. On spinning, the density gradient is formed by the action of the centrifugal field. The sedimentation rate of the particles is balanced by the particle diffusion rate in the opposite direction due to the concentration gradient induced in the cell. The various sample fractions will then 'float' at a level appropriate to their own particular buoyant density. A period of 2-3 days continuous running is often required to attain this condition [95].

4.4.5 Sedimentation Equilibrium

This technique can be considered an extreme form of differential centrifugation. If a homogeneous solution of a macromolecule is centrifuged in an analytical instrument at a relatively low speed, that is to say, one that will not sediment the material completely, an equilibrium is established where the rate of solute sedimentation will equal the rate of solute back-diffusion down the macromolecular concentration gradient formed in the boundary region. This method is primarily used to study the MW distribution of polydisperse materials in the analytical ultracentrifuge. This technique suffers from the disadvantage that a long period of time is required for the establishment of equilibrium.

4.4.6 Applications of Density Gradient Techniques

Density gradients are used extensively in the separation and purification of a wide variety of biological materials and allows the measurement of sample S-values and buoyant densities. Changes in these measured parameters are used to study the effects of chemical, physical or biological treatment on the sample material. The body of literature concerning the application of gradient techniques is considerable.

Density gradient materials are particularly well suited to the study of viruses [121,144]. For example, viruses have been purified and their purity confirmed; infectivity has been associated with particular physical properties; aggregation, dissociation and serological differences have all been studied and sedimentation coefficients and buoyant densities have been measured.

DNA and RNA have been separated and their sizes estimated from sedimentation coefficient studies. DNA fractions differing only in isotope content have been resolved in density gradients, permitting genetic studies of replication [121,145,146].

Cells and cell particulate fractions such as erythrocytes spermatozoa and bacteria have all been isolated and purified using gradient methods [121,147,148]. Studies on proteins in

density gradients have included sedimentation coefficient measurement and investigations of solvation and molecular interactions [121].

4.5. SEDIMENTATION OF DEXTRAN

Sedimentation has proved one of the most important physical methods for the study of proteins in solution and has also been used extensively in the characterisation of heterogeneous polymeric materials. With the advent of analytical ultracentrifuges, it has proved possible to determine polymer sedimentation coefficient distributions, which in turn can be used to determine the MW distribution of a given polymer species (see section 4.4).

Because of the extensive use of low MW dextran fractions as plasma extenders and blood flow improvers, most dextran sedimentation studies have been carried out on acid hydrolysed dextran fractions rather than the high MW 'native' dextran product. These 'clinical' dextran products must be of a well defined MW and so considerable research has been devoted to the determination of dextran MW distributions, based on sedimentation coefficient distribution data.

Williams and Saunders [115] and Fuhlbrigge et al [149] have studied the sedimenting behaviour of a number of degraded B-512F dextran fractions of between 10 000 and 400 000 MW in an analytical ultracentrifuge. Sedimentation data was obtained by observing the boundary formed during the rate normal centrifugation of the dextran fractions using Schlieren optics. The resultant boundary curves obtained were corrected for diffusion, concentration dependence and Johnston-Ogston effects to yield fully corrected sedimentation coefficient distribution curves. In order to convert this data to give the MW distributions of the hydrolysed dextran fractions, the relationship between the fully corrected sedimentation coefficient, $S_{20,w}$ and MW was required. Further work allowed these researchers to obtain such a relationship for dextrans with MWs of between 10 000 and 400 000:

$$S_{20,w} = 1.32 \times 10^{-15} \, MW^{0.5} \quad \text{—— (4.31)}$$

Exponent values between 0.5 and 0.55 are known to be characteristic of flexible, long chain, highly solvated molecules [115,150].

An exhaustive study on the sedimenting properties of B-512F dextran was conducted by Senti et al [46] using acid hydrolysed dextran fractions with average MWs of between 1.77 $\times 10^3$ and 9.50 $\times 10^6$.

Mean dextran S-values were determined by following the movement of the maximum Schlieren peak ordinate with time and back extrapolating the calculated S-values to infinite dilution. When using mean S-values, diffusion and Johnston-Ogston effects can be assumed negligible [101]. Typical data showing the concentration dependence of the reciprocal of the fully corrected $S_{20,w}$ values for the work of Senti et al is shown in figure 4.19. This data was back-extrapolated to infinite dilution using one of the relationships reported by Schachman [102] (equation 4.22). The slope of each, plot is equal to ks, the concentration dependence coefficient (see section 4.4.1.2).

Figure 4.20 shows a double logarithmic plot of $S_{20,w}$ versus MW for the work of Senti et al. For the MW range $1.77 \times 10^3 - 4 \times 10^5$, the relationship between $S_{20,w}$ and MW can be accurately approximated by the equation:

$$S_{20,w} = 2.45 \times 10^{-15} \, MW^{0.44} \quad (4.32)$$

A considerable discrepancy exists between this relationship and that determined by Williams and Saunders and Fuhlbrigge et al (equation 4.31).

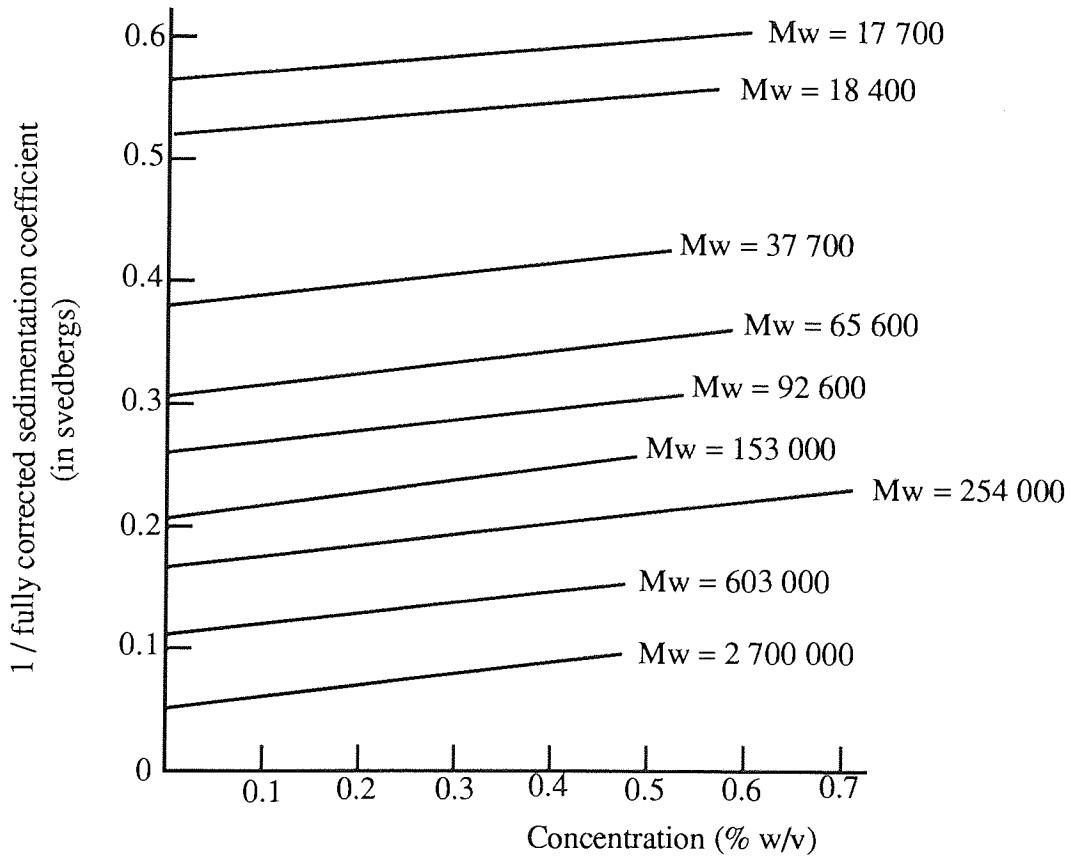

Figure 4.19 A Plot of the Dependence of Various Acid Hydrolysed Dextran Sedimentation Rates on Concentration

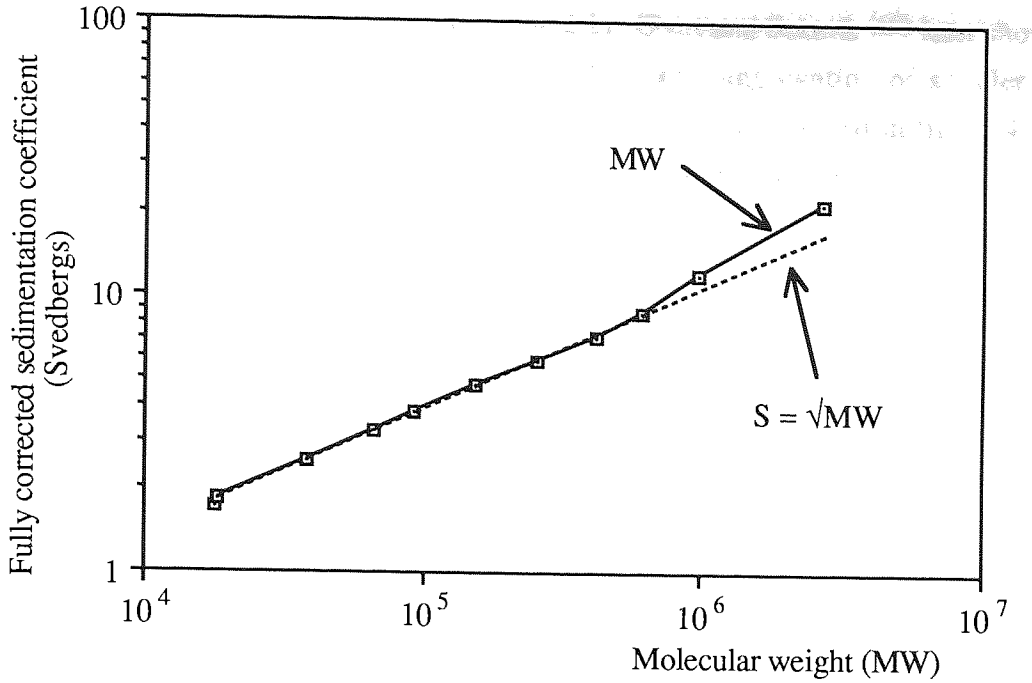

Figure 4.20 A Double Logarithmic Plot of the Corrected Sedimentation Coefficient Values of a Number of Acid Hydrolysed Dextran Fractions Versus Molecular Weight.

An upward curvature of the plot was observed at MWs above 4 x 10^5. Senti et al accounted for this curvature by developing the following relationships at the higher MW values:

Between	4 x 10^5 - 1 x 10^6 MW:	$S_{20,w} = 2.45 \times 10^{-15}$ MW $^{0.53}$
For	MW = 2.7 x 10^6 :	$S_{20,w} = 2.45 \times 10^{-15}$ MW $^{0.64}$

A possible explanation for the upward curvature of the plot is that the dextran molecules are becoming more compact at higher MWs. This may be due to changes in dextran particle structures due to the interaction and stable aggregation of dextran molecules and particles. The sedimenting properties of acid hydrolysed dextran fractions has also been studied by Ogston and Woods [119] and confirmed that dextran particles are highly solvated and nearly spherical. They confirmed the relationship of Fuhlbrigge et al, but observed that it may be affected by different degrees of chain-branching in the sample.

Tsuchiya et al [58] have studied the sedimentation behaviour of a number of native dextran samples taken from batch bioreactors with initial sucrose concentrations varying between 5% and 45% w/v. A bimodal dextran MW distribution was observed, the low modal dextran having MWs of less than 35 000 and the high modal dextran exhibiting MWs of up to 115 million. The latter value is in accordance with the values obtained by Bovey [47]

from light scattering measurements (see table 2.1). Ebert and Schenk [60] later showed that these high 'MW' values were in fact due to the stable aggregation of smaller dextran molecules in solution. The results of Tsuchiya et al are summarised in figure 4.21. The difference in the sedimenting properties of the high and low modal dextran fractions at each sucrose concentration can be readily observed.

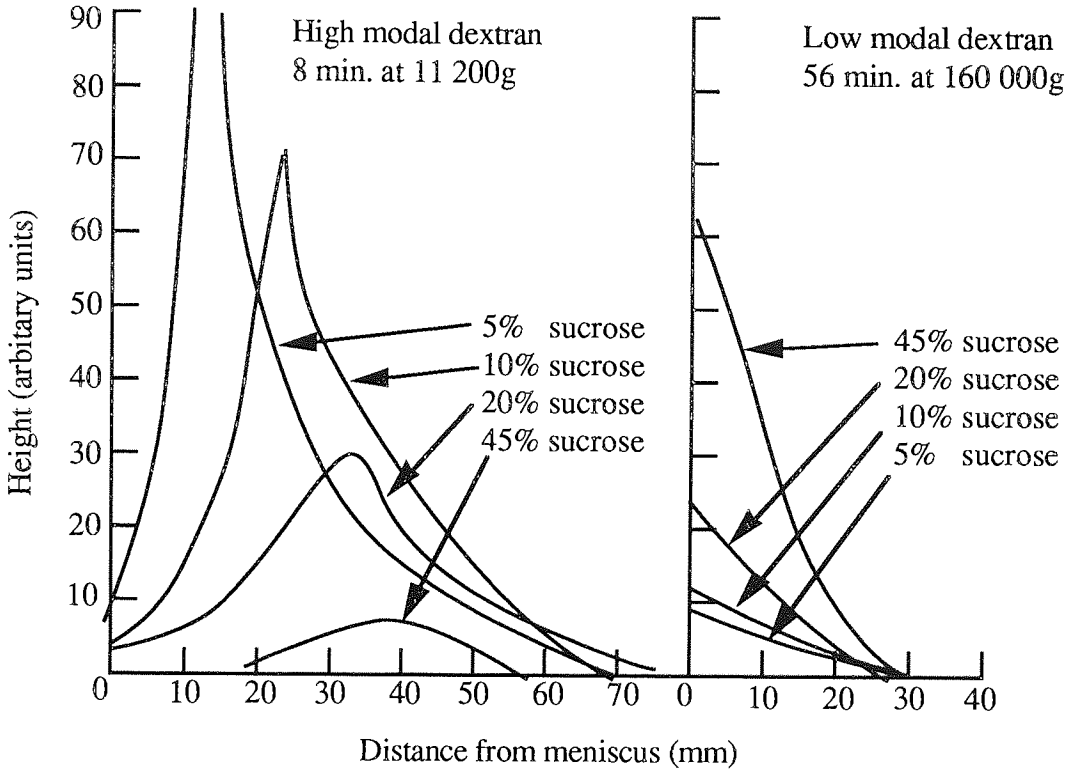

Figure 4.21 The Sedimentation of Native Dextran Fractions Synthesised at Different Sucrose Concentrations [58]

Although all of the native dextran samples were centrifuged at the same high modal dextran concentration, the area under each of the peaks corresponded to the relative concentration of dextran in that sample. The effect of increasing sucrose concentration on high and low modal dextran yields can clearly be seen. At low sucrose concentrations, the majority of the dextran synthesised was of the high modal type. As the sucrose concentration was increased, so the yield of low modal dextran increased and the yields of high modal dextran fell. This is in accordance with the current acceptor theory which has been discussed in chapter 2.

Ultracentrifugation of the high modal dextran fractions at a uniform concentration of 0.14% w/v yielded mean S-values of 380, 480, 504, 471 and 140 Svedbergs at the initial sucrose levels of 5, 10, 20, 30 and 45% w/v respectively. These high sedimentation values are in

accordance with the high native dextran 'MW' values recorded by Bovey [47]. High native dextran sedimentation rates may prove useful in the successful development of the centrifugal bioreactor-separator. The relative sharpness of the high modal native dextran peaks indicated that the sedimentation rate of this material was highly dependent upon concentration (see section 4.4.1.3). Chemical studies on dextran MW distributions have indicated that native dextrans are polydisperse materials [59].

The low modal dextran was also shown to exhibit polydispersity. The fact that some of the low modal material remained at the meniscus during centrifugation is indicative of very low MW material. However, Tsuchiya et al determined that the average MW of the low modal dextran was around 3.5×10^3, although MW values of up to 1×10^5 were recorded. Williams and Saunders [115] have studied the boundary profiles formed during the differential centrifugation of acid hydrolysed dextran fractions. The results, corrected for the effects of diffusion, are summarised in figure 4.22. This figure shows that the shape of the sedimentation coefficient distribution curves, g(S) versus S, are highly dependent on sample concentration. The true distribution curve, g(So) versus So, representing the distribution of the S-values at infinite dilution is labelled as 0% w/w. Extrapolation of the data to infinite dilution was achieved using a procedure similar to that proposed by Jullander [116] which was briefly discussed in section 4.4.1.3.

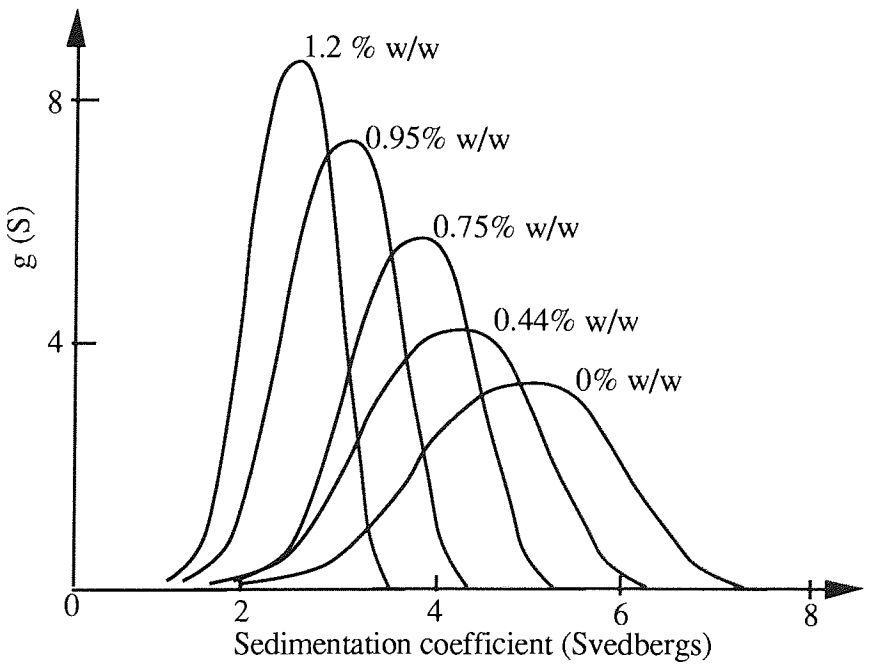

Figure 4.22 The Dependence of Dextran Sedimentation Coefficient Distribution Curves on Concentration

4.6 THE CENTRIFUGATION OF DEXTRAN GELS

In the presence of water, native B-512F dextrans form tacky pastes at high concentrations which are readily dispersed by dilution. The observation of films formed by the evaporation of dilute dextran solutions by electron microscopy have clearly shown networks of microscopic filaments [51,52] as discussed in section 2.4. It is possible that these gel structures will be formed in the proposed centrifugal bioreactor-separator. Therefore the behaviour of gels in centrifugal fields will now be considered.

Svedberg and Pedersen [94] observed that when a centrifugal force is applied to a uniform gel, either no measurable change occurs, or the gel starts to sediment. If the partial pressure of the gel at the base of the cell is below the swelling pressure of the gel, it will remain unchanged. When the partial pressure at the bottom of the cell slightly exceeds the swelling pressure, the gel will be compressed, resulting in some settling. The water that has been squeezed out of the compressed gel at the bottom of the cell can cause the top part of the gel to swell. In some instances, this may result in the gel still continuing to occupy the whole cell. Sedimentation velocities will not be constant, but will decrease as the gel approaches equilibrium conditions where the swelling pressure at all points in the gel is equal to the partial pressure at the same points. The formation of native dextran gel structures will therefore be detrimental to the proposed centrifugal bioreactor-separator.

4.7 DEXTRANSUCRASE ENZYME SEDIMENTATION

No instances concerning the sedimentation of the dextransucrase enzyme were found in the literature. Therefore, the sedimenting properties of the dextransucrase enzyme preparations were studied in this project (chapter 9). Factors affecting the 'MW' of the dextransucrase enzyme used in this study have been discussed in section 3.6.

The sedimentation rate of active dextransucrase enzyme molecules in the centrifugal bioreactor-separator will be primarily dependent upon the MW of the enzyme and the MW of the dextran chain being synthesised. Thus the rate of sedimentation of the dextran-enzyme complex should vary according to the mass of the associated dextran molecules. Using the data of Ebert and Schenk [60], the dextransucrase enzyme, with a turnover number of 32,000 min^{-1} (chapter 2) will take about 12.5 seconds to produce a dextran molecule of around 4 x 10^5 MW before releasing it. Thus, dextran synthesis is extremely rapid and it is possible that the sedimentation rate of the dextran-enzyme complex could be defined by an average value.

However, in this study, relatively high enzyme concentrations were used which could increase the likelihood of dextran particle interactions and the formation of dextran gel structures within the enzyme rich portions of the bioreactor. Given the nature of native dextran structures, this may result in the physical entrapment and the forced, rapid sedimentation of the enzyme molecules with the dextran aggregates. This may benefit the proposed bioreaction-separation process by allowing the rapid sedimentation of the active enzyme molecules away from the fructose rich portions of the centrifuge vessel. This possibility was considered in this work. Native dextrans readily form molecular aggregates in solution, with typical 'MWs' of between 10^7 and 6×10^8 [47]. The relative rates of dextran, dextransucrase enzyme and fructose sedimentation in a centrifugal bioreactor-separator are discussed in section 6.5.

4.8 SUCROSE AND FRUCTOSE SEDIMENTATION

The sedimentation coefficient of sucrose was determined by LaBar and Baldwin [151] to be around 0.276 Svedbergs. Because a freely sedimenting boundary will not be formed during the differential centrifugation of these very small molecules, measurements of the changes in the concentration of material at the meniscus and base of the cell were used to calculate sedimentation coefficients.

No instances of studies on fructose sedimentation were found in the literature. The sedimenting properties of fructose are discussed in section 6.5.

5.0 ANALYSIS

5.1 INTRODUCTION TO ANALYTICAL PROCEDURES

This chapter describes the analytical equipment and procedures used in this study for the analysis of samples collected from the various conventional and centrifugal bioreactor-separator systems studied.

The high pressure liquid chromatography (HPLC) and gel permeation chromatography (GPC) systems employed in this study had similar system set-ups which are summarised in figure 5.1.

5.2 HIGH PRESSURE LIQUID CHROMATOGRAPHY (HPLC)

A 30 cm long by 0.78 cm diameter Aminex HPX-87C column (Biorad UK Ltd., Hemel Hempstead, Herts.) was used to determine the carbohydrate composition and concentration in the samples. These columns have proved satisfactory for the quantification of the saccharides (sucrose, glucose, fructose leucrose and dextran) that may be found in a dextransucrase broth[15,16,22].

The column was packed with an 8% divinylbenzene cross-linked resin in the calcium form. Separation within the column was dictated by the weak bonding that occured between the sample components and the calcium ions on the resin packing. The column was operated at a constant 85°C temperature, with a typical operating pressure of 8 000 kNm^{-2} and was protected using LiChroCART RP-18 precolumns (BDH Ltd., Atherstone, Warwicks., UK).

The eluent used was prepared using distilled and deionised water, containing 0.02% w/v calcium acetate, to maintain the calcium form of the resin. the eluent was degassed by heating to 80°C and prefiltered using a 0.45μm scintered metal filter before being pumped into the analytical columns using a Biorad 1330 model pump (Biorad UK Ltd.) at a flowrate of 0.5 cm^3 min^{-1}.

All samples were filtered using 5.0 μm and 0.45 μm disposable filters (Gelman Sciences, Northampton, UK) to remove particulate impurities and to prolong the life of the main column and guard columns. Samples containing dextransucrase were heat treated in a boiling waterbath for 5 minutes in order to denature the enzyme. Samples were injected automatically using a Talbot ASI-3 autosampler (Talbot Instruments Ltd., Cheshire, UK).

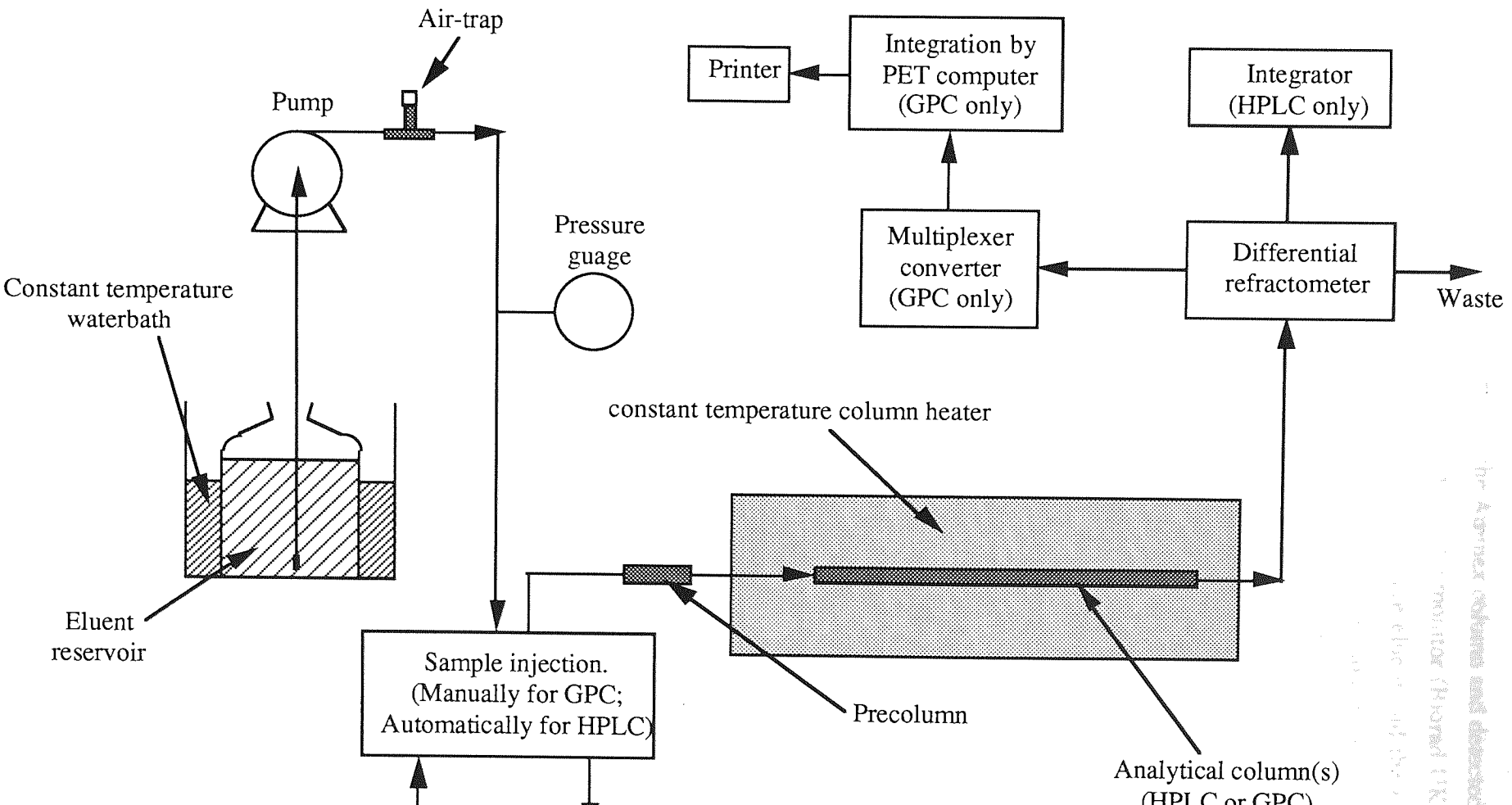

Figure 5.1 Schematic Diagram Of The GPC / HPLC Analytical System

The sample components were resolved in the Aminex column and detected at the column outlet by a Biorad 1750 model refractive index (RI) monitor (Biorad UK Ltd.) The RI monitor measured the differential RI between the pure eluent and the eluent from the column. The RI monitor provided a 1 volt full scale output to a Spectra-Physics type SP 4270 integrator (Spectra-Physics UK Ltd., Herts). The integrator processed the RI data and gave a sample chromatogram where the resolved sample components were identified by their retention times and component concentrations were determined by the areas under the peaks on the chromatograms.

Initially, problems were encountered when quantifying native dextrans when using Hibar LiChrosorb RP-18 precolumns (BDH Ltd., UK). Irreproducible dextran peak areas on the chromatograms and increases in system operating pressure were recorded. From these observations, it was concluded that some of the high MW native dextran material was being absorbed onto the precolumns causing partial blockage of the eluent flow channel, hence resulting in the observed peak area irreproducibility and the pressure increases. Removal of the precolumn was not possible as this would transfer the problem onto the expensive main column. The problem was overcome by sample dilution to between 0.2 and 0.5% w/v native dextran concentration and by using LiChroCART RP-18 precolumns (BDH Ltd., UK), which did not absorb native dextran.

Accurate, sensitive and reproducible native dextran quantification was also achieved by using gel permeation chromatography (GPC), a technique that resolves sample components according to size rather than charge. The GPC columns and precolumns used allowed the free passage of high MW native dextran particles.

5.3 GEL PERMEATION CHROMATOGRAPHY (GPC)

GPC is a chromatographic technique that can separate materials according to size differences. Separation is achieved using columns packed with a gel or some other porous material of variable pore size. A wide range of column packings are commercially available.

5.3.1 The Principle of Gel Permeation Chromatography

The interstitial spaces and pore spaces in the column are completely filled with a flowing eluent stream. The sample material is injected onto the column(s) via the eluent stream and travels through the column via the interstitial regions of the packing. However, some smaller sample molecules may permeate the pores of the packing material and become retarded. The longer these molecules spend in the pores, the longer they remain in the

column. Large molecules are completely excluded from the pores and therefore are eluted first whilst the small molecules which can penetrate the pores are eluted later (Figure 5.2).

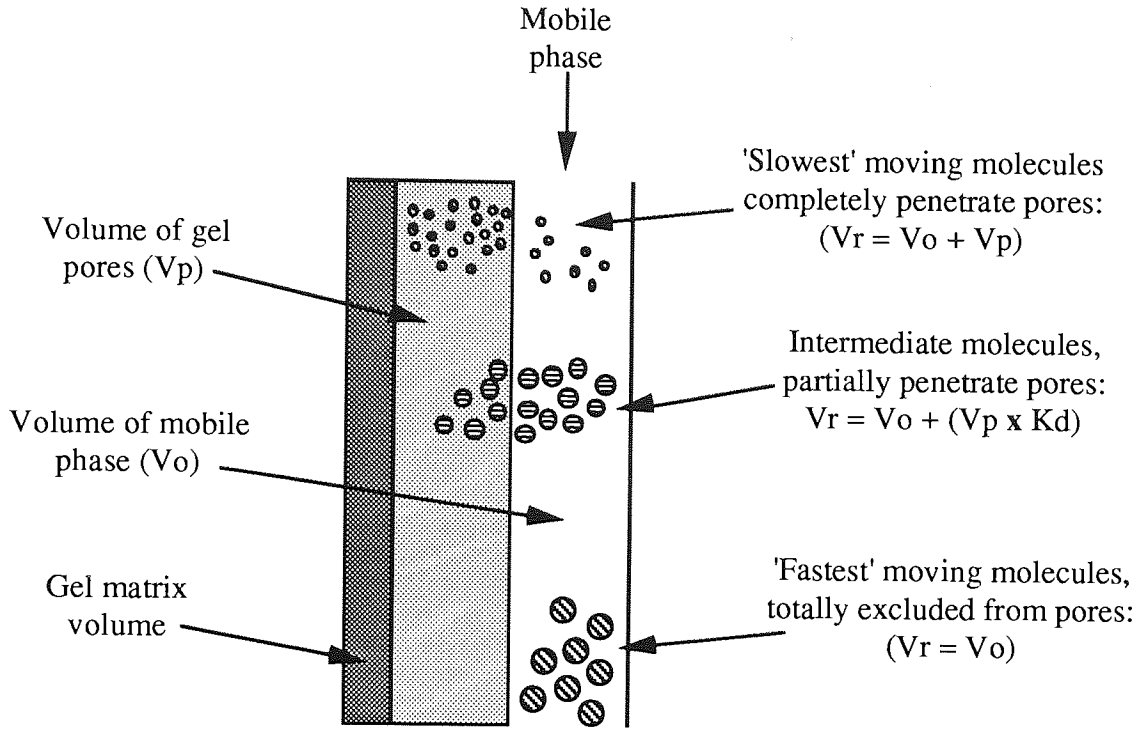

Figure 5.2 The GPC Fractionation Process

A species is eluted at a volume equal to the volume available to it in the column. For large completely excluded molecules, the elution volume Vr equals the void volume Vo and for small molecules which can completely penetrate all pores of the gel it is equal to the total liquid volume Vt, which is equal to the sum of Vo and the internal or 'pore' volume Vp. For molecules of intermediate size, the elution volume is dependent on the pore volume that is 'accessible' to the species and is given by:

$$Vr = Vo + (Kd \times Vp) \quad \text{(5.1)}$$

Where Kd is the distribution coefficient for a sample fraction eluting from the column with an elution volume of Vr. Equation 5.1 may be rewritten as:

$$Kd = \frac{(V_r - V_o)}{V_p} \quad \text{(5.2)}$$

Because GPC separates materials according to size, a number of researchers [152-162] have determined methods of calibrating GPC systems for the determination of sample MWs. GPC is now generally the method of choice for determining the molecular weight distribution (MWD) of polydisperse materials. In this study, GPC was used to assess the MWD of native dextran products formed in conventional bioreactors and rate-zonal bioreactor-separators. The column calibration procedure is discussed in section 5.3.5.

The concentration of native dextran samples was also determined by GPC, the areas under the GPC chromatograms being compared with standard chromatographed dextran fractions of known concentration.

Prior to analysis by GPC, all samples containing native dextran required dialysis to remove low MW contaminants. The dialysis procedure is discussed in section 5.4.

5.3.2 Equipment Description and Analytical Technique

The set-up of the GPC analytical system was similar to that of the HPLC analytical system (figure 5.1).

Initially a 0.2% w/v sodium azide solution was used as the eluent in order to prevent bacterial growth in the columns. However, this eluent was found to give negative peaks in the chromatograph baselines, due to changing azide concentrations in the eluent stream. This problem persisted despite the addition of small quantities of sodium azide to the samples. Therefore, distilled water was used as the eluent and sodium azide solutions were pumped through the GPC columns when not in use. 10 litre volumes of distilled water eluent were thoroughly degassed by being heated at 50°C for at least 48 hours. Dissolved gas was found to significantly alter the retention times of individual sample components within the GPC columns without causing any detectable pressure fluctuations. The eluent was prefiltered using a 0.45μm sintered metal filter and pumped into the system using a Biorad model 1330 pump (Biorad UK Ltd.).

Prior to analysis, the eluent flow rate was slowly stepped up from 0.1 $cm^3\ min^{-1}$ to the operating flowrate of 0.3 $cm^3\ min^{-1}$ over a half hour time period in order to avoid sudden and large pressure increases which can cause column damage. The typical operating pressure of the system was 7 000 kNm^{-2}.

Samples were injected manually via a Rheodyne six-port injection valve (Cotati, California, USA) fitted with a 100 μl sample loop. Sample pretreatment was identical to that employed prior to HPLC analysis.

The GPC columns used in this study are described in section 5.3.3. Stable baselines were maintained by enclosing the columns in a 35°C constant temperature column heater. The columns were left to equilibrate for at least one hour after system start-up.

Sample material was detected at the column outlet using a Waters R401 refractive index monitor (Waters Associates Limited., London, UK.) and measured against a pure eluent reference. The analogue output from the refractometer was transmitted to a multiplexer (Model PCI 1001, CIL Electronics Limited., Sussex, UK) which converted it to a digital signal which was recorded by a PET model CBM 4032 computer (Commodore, UK). The computer was programmed to calculate the MWD and concentration of native dextran samples. Output data was recorded using a Commodore model CBM 4022P printer (Commodore, UK). The raw data obtained after a sample had been chromatographed consisted of an elution profile of detector response versus elution volume or time.

5.3.3 GPC Columns

Hibar prepacked Lichrosopher Diol columns (BDH Ltd., UK) were used in this study. These columns have been found suitable for the analysis of native dextran fractions containing some protein material [22].

The columns were packed with 10 μm spherical hydrophilic support material coated with 1,2-dihydropropoxypropyl chains. The properties of the three columns used are summarised in table 5.1. The columns were joined in series to provide a wide molecular fractionating range.and were protected using precolumns packed with the 1000 Diol material.

Column Position	Packing	Fractionating range (MW)	Dimensions (cm x cm)
1st	1000 Diol	1×10^4 - 2×10^6	25 x 0.4
2nd	500 Diol	4×10^3 - 7×10^5	25 x 0.4
3rd	100 Diol	2×10^2 - 4×10^4	25 x 0.4

Table 5.1 Description of GPC Columns

5.3.4 Monitoring of GPC Column Efficiency

In chromatography, two parameters are widely used to define the efficiency of a column. These are the number of theoretical plates (NTP) and the asymmetry factor (As). If the

peak obtained from a column is approximately gaussian in shape then the NTP can be conveniently expressed as:

$$NTP = 5.54 \left(\frac{Vp}{W_{0.5}} \right)^2 \quad \text{—— (5.3)}$$

Where Vp is the elution volume of the peak and $W_{0.5}$ is the peak width at one half of the peak height, h (figure 5.3a). The NTP value measures the separation potential of a chromatographic system and can be simply determined by using appropriate test solutions. A decrease in the NTP value over a given time period indicates a loss in the separating power of a system.

The asymmetry factor (As) is calculated at one tenth of the peak height h (figure 5.3.b) and is expressed as:

$$As = \left(\frac{b}{a} \right) \quad \text{—— (5.4)}$$

This value is a measure of the resolving power of a column. A deviation of the As value from unity over a given time period indicates a loss in resolution.

Typical NTP and As values recorded on the GPC system used in this project are shown in table 5.2.

Column :	Date	NTP/m	As
LiChrosopher 1000 Diol	06/02/91 (new)	5560	1.55
	08/08/91	4815	1.62
	31/03/92	4274	1.65
Column:	Date	NTP/m	As
LiChrosopher 500 Diol	06/02/91	4713	1.86
	08/08/91	3328	2.45
	31/03/92	3616	2.64
Column	Date	NTP/m	As
LiChrosopher 100 Diol	09/07/91(new)	6404	1.40
	09/08/91	5448	1.38
	31/03/92	4815	1.43

Table 5.2 LiChrosopher Diol Column Efficiency

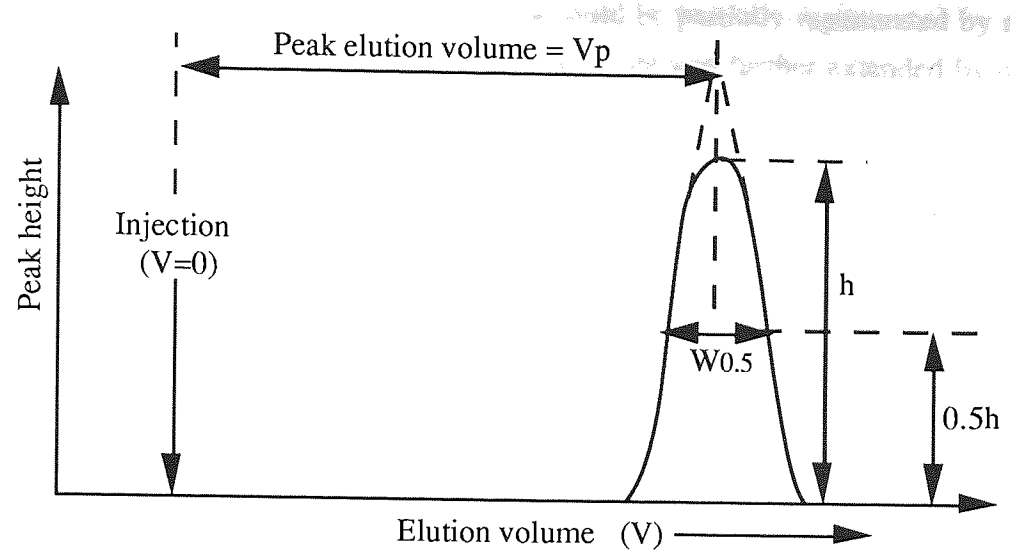

(a)

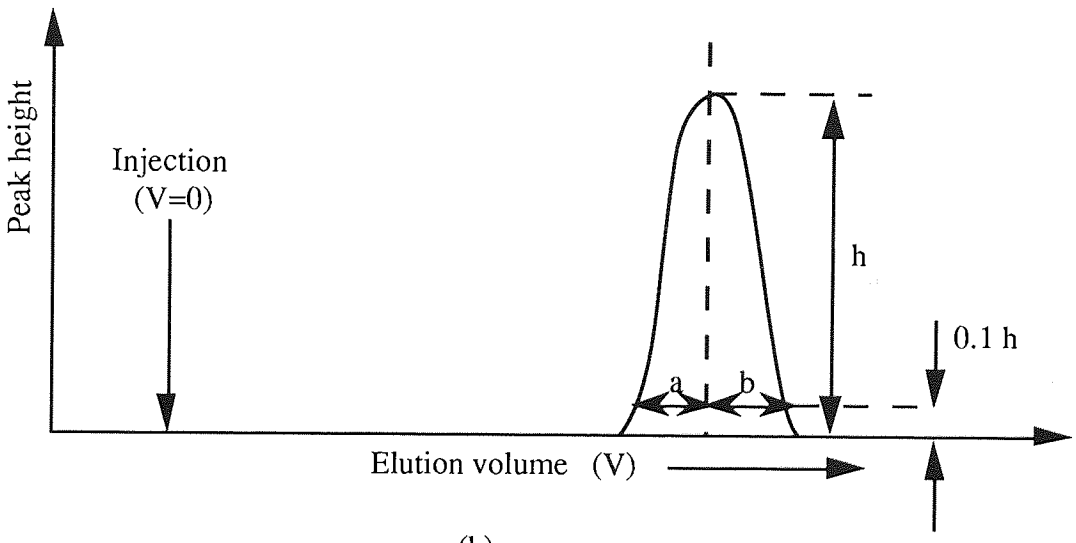

(b)

Figure 5.3. Illustration of the Parameters Required for the Calculation of : (a) the Number of Theoretical Plates and (b) the Asymmetry Factor of a Chromatographic Column

It is difficult to define when losses in column efficiency become 'significant'. Loss of efficiency is dependent on a number of parameters including; number of injections, sample properties, dissolved gas in the eluent and general column care. A 30% decrease in either the NTP or As values from the values calculated for new columns after 10-20 sample injections was considered significant in this study.

Significantly depressed NTP and As values could be partially regenerated by reversing the flow of eluent through the columns. Column life was further extended by observing the following procedures :

(1) Not subjecting the system to excessive pressure or sudden pressure increases as this can cause compaction and damage to the gel packing.

(2) Maintaining an air free system. Air bubbles can damage the columns by forming channels in the packing. Air can enter the system because of poor sample injection techniques and will be present in inadequately degassed eluents.

5.3.5 Determination of Molecular Weight Distributions and Molecular Weight Averages by GPC

5.3.5.1 GPC Data Conversion

Because of the polydisperse nature of polymers, it is not generally possible to characterise a polymer by a single MW value. The MW of a polymer species can only be completely described as a molecular weight distribution (MWD). Such data can be readily obtained by GPC.

A typical elution profile from the GPC system for a polydisperse sample is shown in figure 5.4. The ordinate represents the variable being measured by the detector which is directly proportional to concentration. The abscissa is elution volume, or elution time. The area under the curve represents the amount of sample loaded onto the column and the shaded area represents the amount of sample that has eluted from the column between volume Vr_1 and Vr_2.

The Kd value of this shaded area can be defined by using equation 5.2, so that:

$$Kd = (V_{r\,(average)} - V_o)/V_p \quad \text{—— (5.5)}$$

Thus, the elution volume of any point in an elution profile can be defined in terms of a Kd value.

Calibration of the diol columns was necessary in order to relate the elution volume, through the Kd value, to MW. This was achieved using the method of Nilsson and Nilsson [162] by using the polynomial relationship:

$$(MW)_i = b_5 + \exp [b_4 + b_1(Kd_i) + b_2Kdi)^2 + b_3(Kdi)^3] \quad \text{—— (5.6)}$$

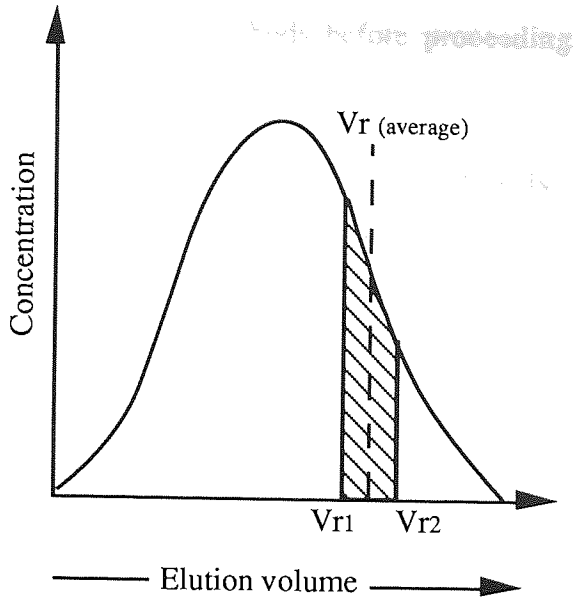

Figure 5.4 A Typical GPC Polymer Chromatogram

The values of the calibration constants b_1 - b_5 were obtained by the following procedure:

(1) The void volume V_0 and the pore volume V_p were determined by chromatographing a native dextran and glucose standard on the Diol System. High MW native dextran material was excluded from the column packing and therefore had an average elution volume equal to V_0. The glucose molecules completely penetrated the column packing, with a resultant average elution volume equal to V_t. The 'pore' volume Vp equals V_t minus V_0.

(2) A series of several Pharmacia standard dextran T-fractions, whose weight average MWs had been measured previously by light scattering techniques, were chromatographed on the GPC system.

(3) The heights, elution volumes and (light scattered) weight average MW values of the T-fraction chromatograms, together with estimated values of the calibration constants b_1-b_5 were entered into the computer calibration program listed in appendix A1. This program was originally written by Vlachogiannis [23] The Hartley's modification of the Gaussian-Newton method [163] was used to calculate the new values of the calibration constants b_1-b_5, which gave the optimum agreement between the actual light scattered weight average MW values of each T-fraction and the calculated values obtained from the GPC elution profiles. Alsop and Vlachogiannis reported that all the calibration standards should have individual weight average MWs obtained by GPC within 90-110% of those

obtained by light scattering methods before proceeding with the analysis of samples by GPC [164].

(4) The calibration was checked at periodic time intervals by analysing standard dextran T-fractions and comparing the weight average MW values with the light scattered values. If the MWD of these fractions changed with time, the system was recalibrated.

The native dextran-glucose standard was the first sample to be run on each day that the GPC system was used to check the Vo and Vt values of the system. Significant changes in these elution volumes were recorded when air had become trapped in the system. This required bleeding air from the system and further degassing of the eluent.

Typical calibration results obtained during this study are shown in table 5.3.

Batch number	Weight average molecular weights		$\frac{GPC}{LS}$ x 100%
	Light Scattering	GPC	
PJ 3636	238 192	239 400	100.5
PH 1078	147 545	145 062	98.3
PG 7427	102 209	103 960	101.7
PF 1601	70 276	70 316	100.1
PB 5227	40 908	40 272	98.4
PE 5382	21 471	21 798	101.5
PA 0094	10 470	10 352	98.9
JD 2985	7 971	7 813	98.0
DK 8868	5 127	5 368	104.7
PD 2335	3 836	3 735	97.4
Glucose	180	180	100.0

Calibration Constants				
b_1	b_2	b_3	b_4	b_5
-8.802	4.745	-3.373	14.459	-948.641

Table 5.3 Typical Diol Column Calibration Data

The resultant calibration curve is shown in figure 5.5. An S-shaped curve was observed which is characteristic of a GPC system. Five regions of the curve can be identified. Above a certain molecular weight (M_x), no fractionation occured (Section a-b), as all the

molecules were excluded from the column packing (Kd=0) and eluted at the void volume V_0. Similarly, below a certain molecular weight (M_y), the molecules were not fractionated (section e-f) as they all completely penetrated the pores (Kd=1) and were eluted at the total liquid volume Vt. Molecules between these two MW limits were fractionated because they penetrated the column packing to varying degrees. A linear region (section c-d) was observed in all of the calibration curves, where the logarithm of the dextran T-fraction MW was directly proportional to elution volume (V_r). In sections b-c and d-e, fractionation was still occurring but the relationship between log MW and V_r was not linear. The system was used to determine MWs in the range of M_x to M_y, which in these studies was typically between 180 and 2 x 10^6 MW.

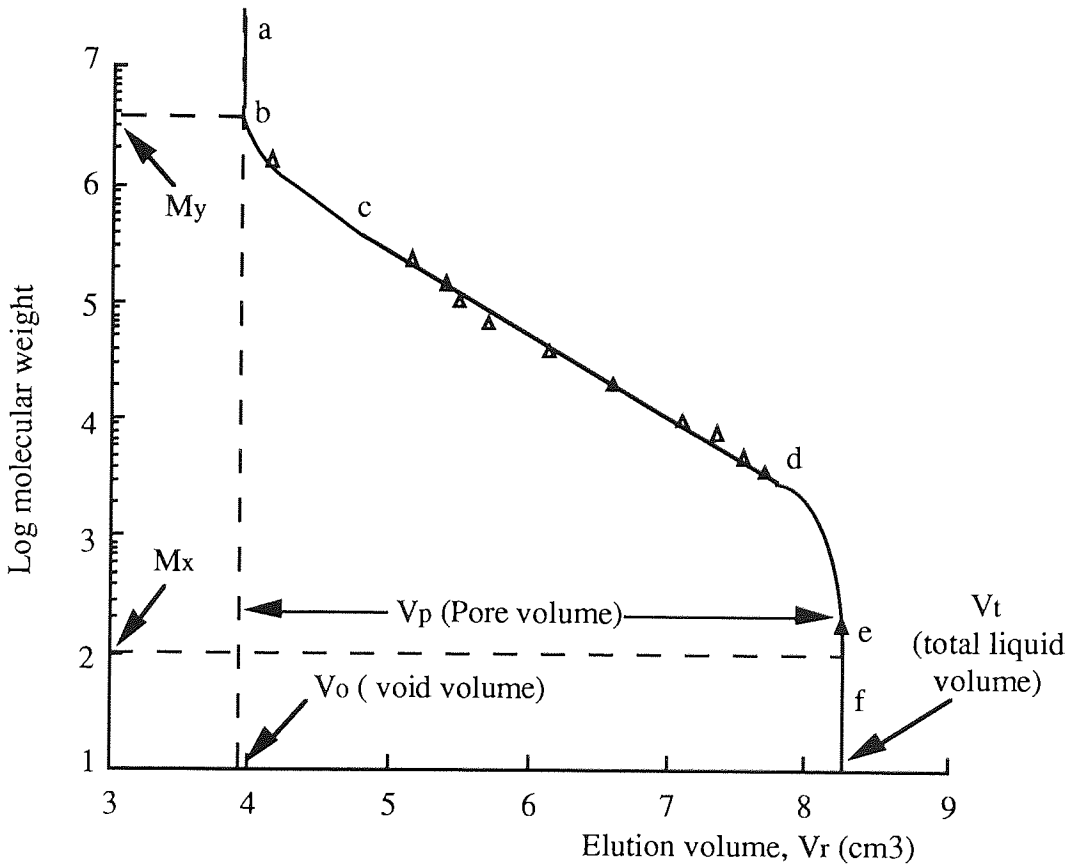

Figure 5.5 A Typical Calibration Curve for a GPC Column

5.3.5.2 Sample Molecular Weight Distribution (MWD) Analysis

To convert the elution time distribution profile of a sample to its equivalent MWD, the following information was required:

(1) 'Peak' heights, which are directly proportional to sample concentration, taken at fixed intervals during the analysis of a sample from the time of injection. Peak height data, recorded at ten second intervals, was stored in the PET computer

memory directly from the refractometer during sample analysis using the data acquisition computer program listed in appendix A2.

(2) The peak elution times of a high MW native dextran peak and a glucose peak, for calculation of V_o, V_t and hence V_p.

(3) The start and finish times of the sample analysis.

(4) The updated calibration constants b_1 - b_5.

This information was then used to calculate the MWD of the sample using the program listed in appendix A3. This program calculated the MW of each discrete sample fraction, *i*, (corresponding to each 10 second time interval) eluting from the column using equations 5.5 and 5.6, thus yielding a complete MWD profile for a given native dextran sample.

Since no single value can adequately characterise the MW of a polydisperse material, various averages were calculated, the commonest being the number-average ($\overline{M}_N$) and weight-average ($\overline{M}_W$) molecular weight. The computer program calculated these values from the chromatographic data using the following equations:

$$\text{Normalised height, } hi = \frac{\text{Chromatogram height } hi'}{\text{Total Chromatogram heights } \sum hi'} \quad \text{—— (5.7)}$$

$$\overline{M}_W = \sum hi \ MWi \ / \ \sum hi \quad \text{—— (5.8)}$$

$$\overline{M}_N = \sum hi \ / \ (\sum hi \ / \ MWi \ ) \quad \text{—— (5.9)}$$

For polydisperse systems, $\overline{M}_W > \overline{M}_N$. 'Polydispersity' is often used to describe the breadth of the MWD of a polydisperse system and was calculated from the chromatographic data using the expression :

$$\text{Polydispersity, } = \overline{M}_W / \overline{M}_N \quad \text{___ (5.10)}$$

A detailed discussion of the above process and an extensive review of a number of other GPC calibration procedures has been reported by Bhambra [152].

5.4 DIALYSIS

The GPC system fractionates samples primarily by size differences. Therefore, when using the system to determine the MWD or concentration of native dextran samples, unwanted material must be removed. Most high MW contaminants had been removed during the enzyme purification and sample prefiltering stages. The commonest low MW contaminants present in the samples analysed were sugars such as sucrose and fructose. These materials were removed by dialysis, a membrane based process that again separates materials according to size. Dialysis has been extensively used for the characterisation of dextran fractions [3,15].

Dialysis membranes with a quoted molecular weight cut off of 1000 (Medicell International Ltd., Liverpool Road, London) were used in this study. Approximately 5cm^3 fractions of sample were clamped within a piece of dialysis tubing and placed in a large volume of deionised water for 36-48 hours. The deionised water was changed at regular intervals to further aid the removal of any low MW contaminants. Dialysis is not an ideal process, the three main drawbacks in this study were:

(1) Although complete sucrose and fructose removal was possible, very low MW dextran material will also diffuse through the membrane. However, due to the bimodal distribution of native dextran, most low MW material appears to have an average MW of around 10,000. The loss of dextran material below 1,000 MW was therefore considered negligible.

(2) When samples are dialysed, there is generally a net inflow of solvent into the system, causing a change in the concentration of the retained material. Therefore, accurate dextran quantification relies on determining the extent of this change in concentration. This was achieved by chromatographing the sample before and after dialysis. By comparing the areas under each profile between two pre-set elution times, the concentration factor and hence the corrected concentration of the dialysed dextran fraction could be determined. This method proved a rather labour intensive process and so HPLC was generally used for native dextran quantification.

(3) All of the samples containing native dextran also contained enzyme, which will affect the overall MWD of the sample. This problem was circumvented by running standard 'bench' control samples in all of the dextran MWD trials undertaken. These control runs had the same enzyme loadings, run times,

temperature and pH as the bioreaction-separation runs, thus allowing direct comparisons to be made (see section 3.8.2).

5.5 THE HAND-HELD REFRACTOMETER

A Bellingham and Stanley hand-held delta refractometer supplied by BDH Ltd. was used to determine the total solids content of the sample solutions prior to loading onto sucrose gradients in the bioreaction-separation studies carried out in the zonal rotor (chapter 9). Accurate solids quantification was essential in order to prevent gradient overloading for the reasons discussed in section 3.8.2. The refractometer was also used to give an estimate of the total solids distribution during the unloading and collection of gradient fractions from the zonal rotor after the completion of the rate-zonal runs.

6.0 MEASUREMENT OF NATIVE DEXTRAN PARTICLE PROPERTIES AND PRELIMINARY BIOREACTION-SEPARATION STUDIES IN THE ANALYTICAL ULTRACENTRIFUGE

6.1 INTRODUCTION

Although hydrolysed dextran sedimentation rates have been reported in the literature[46,58,115,119,149], little work had been reported concerning the sedimentation of native dextran fractions (Section 4.5). The work of Tsuchiya et al [58] on the sedimenting properties of native dextran fractions has been discussed in Section 4.5, but took no account of the effects of dextran concentration on the sedimentation coefficient (S). Therefore it was decided to study the S-values of native dextran samples synthesised in this laboratory at different concentrations using analytical ultracentrifugation.

Knowledge of the fully corrected sedimentation coefficient of the native dextrans allowed the calculation the relative rates of native dextran particle sedimentation in any given centrifugal field. The S-values also proved useful in determining the optimum run parameters required in the bioreaction-separation studies presented in chapters 7-10.

The diffusion coefficient D of the native dextran samples was also measured, using light scattering studies. A knowledge of the S and D coefficients yielded useful information concerning the MW, size and shape of the native dextran particles. This data proved useful for the purposes of modelling the process and helped explain much of the experimental data obtained in the subsequent bioreaction-separation runs.

The analytical ultracentrifuge was also used to study the bioreaction-separation technique (section 6.6).

6.2 ANALYTICAL ULTRACENTRIFUGATION

6.2.1 Ultracentrifuge Design and Operation

Generally, analytical ultracentrifuges are highly sophisticated instruments that employ optical systems that allow the operator to record the behaviour of solute molecules or suspended particles under the influence of an applied centrifugal field (section 4.3.2.2).

The analytical ultracentrifuge used in this study was manufactured by M.S.E Ltd. (Crawley, Sussex, U.K.). Detailed operating instructions and methods of data analysis can be found in the MSE technical publication number 71[165]. Beckman publish a

number of useful guides, including a comprehensive manual of methods for the analytical ultracentrifuge[101]. All the work was carried out at the National Centre for Macromolecular Hydrodynamics, University of Leicester, U.K., under the guidance of Dr Arthur Rowe.

The basic design of the ultracentrifuge rotor has been shown in figure 4.6. A four-place aluminium rotor was used for multi-sample analysis. One of the cell places was fitted with a balance/reference cell. This cell had two slits cut into it at fixed radial distances to allow light through to give reference lines on all of the photographs taken.

Standard single sector cells were used to study the sedimentation properties of the native dextran samples and single sector synthetic boundary overfilling cells were used to study the rate-zonal bioreaction-separation principle. The latter type of cell is commonly used in the study of rate-zonal systems as these cells permit the overlaying of dense supporting solutions with less dense sample solutions while the cell is accelerating in the centrifuge. The two types of cell assembly are shown in figure 6.1.

The cylindrical cell centre-piece is manufactured from epoxy resin and has a sector shaped cavity cut right through it. In addition, the synthetic boundary cell has two small cylindrical cavities cut into it which are connected to the narrow end of the sector shaped cavity by capillary tubes. At each end of the centre-piece is a flat quartz window which forms a seal with the centre-piece by means of a rubber 'O' ring. Each window has a plastic window housing on the outside. All the components are placed, in order, on top of each other as shown in figure 6.1 and are pushed inside the cell housing and clamped tightly with the clamping ring. The hollow sector is filled with sample or material via the filling hole at the narrow end of the sector cavity. The filling hole must be in line with the hole in the housing so that the sector can be filled. This will also ensure that the sector walls are radially aligned, thus minimising wall effects.

A cavity should never be completely filled so that an air-liquid meniscus can be observed during centrifugation. When the synthetic boundary cells are used, the denser liquid is placed in the sector and the sample or lighter liquid is placed in the cylindrical cavities. Both types of cells had nominal capacities of 500 µl. The capacity of each cylindrical cavity in the synthetic boundary cell is 10 µl. All the cavities are closed using the plug and washer fittings. The fitted cells and balance cell should not differ in weight by more than 0.1 grammes and if necessary, balancing rings should be fixed to the balance cell. The cells are then radially aligned in the rotor by means of a locating pin. The cells and rotor can now be spun.

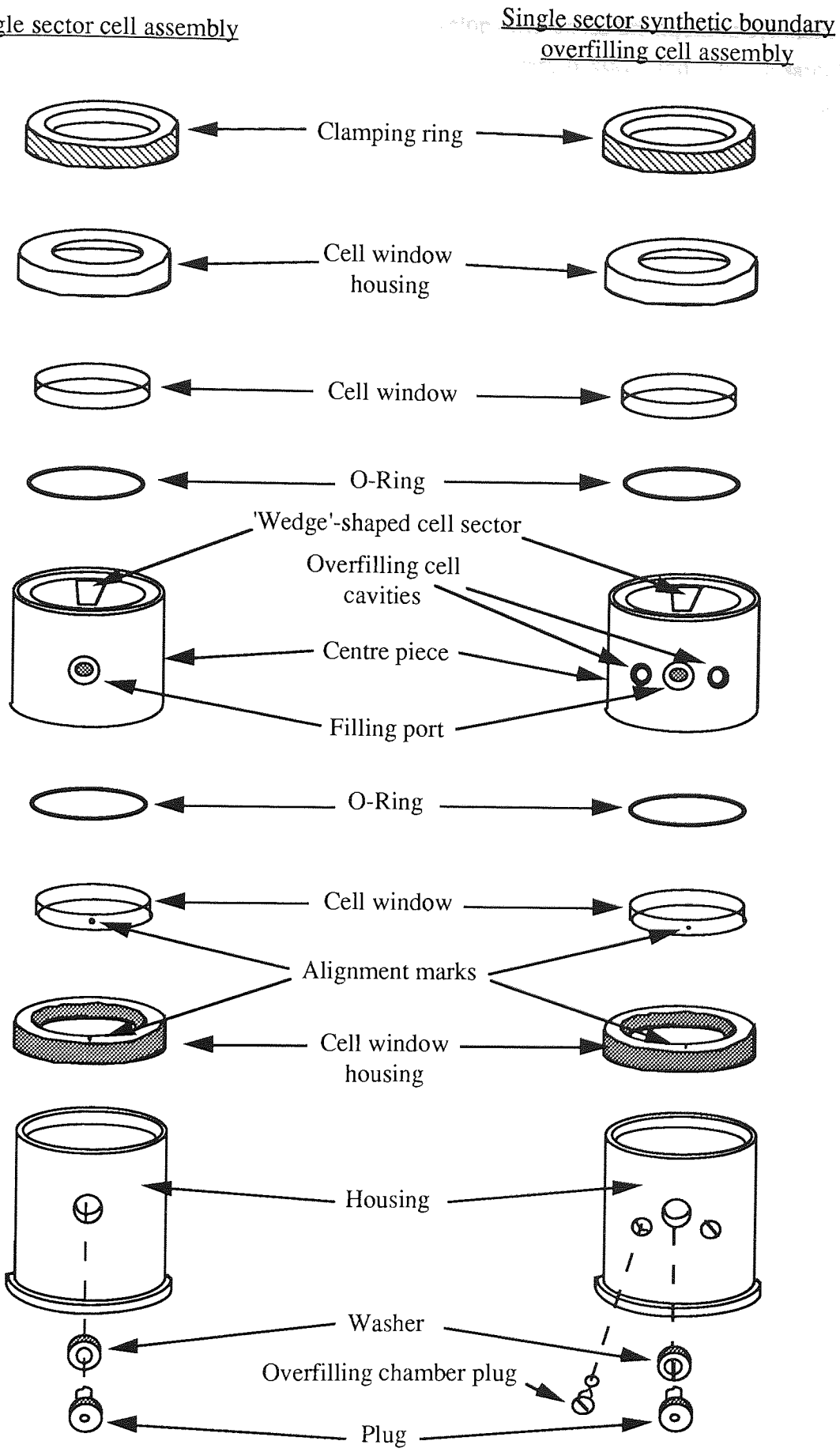

Figure 6.1 Analytical Ultracentrifuge Cell Assemblies

During acceleration, the centrifugal force that develops will cause the liquid in synthetic boundary cell cylindrical cavities to flow along the capillary passage and into the sample sector. This will result in an overlaying of the dense liquid in the sector with the less dense sample solution. Flow of liquid from the cavities starts at approximately 4000-5000 rpm (~1000 - 1600g) and is completed at approximately 15 000 rpm (~14 000g). If rotor speeds of less than 15 000 rpm are required, the rotor speed is decreased immediately after fluid transfer.

A simplified diagram of the optical system is presented in figure 4.6. The progress of the experiment can be observed by means of an eyepiece on the front of the machine and recorded photographically using a camera. The optical system is discussed in more detail in the following section.

Important data concerning the cells used in this study are presented in figure 6.2. It should be noted that the cell sectors subtend an angle of 3° from the axis of rotation in order to minimise wall effects.

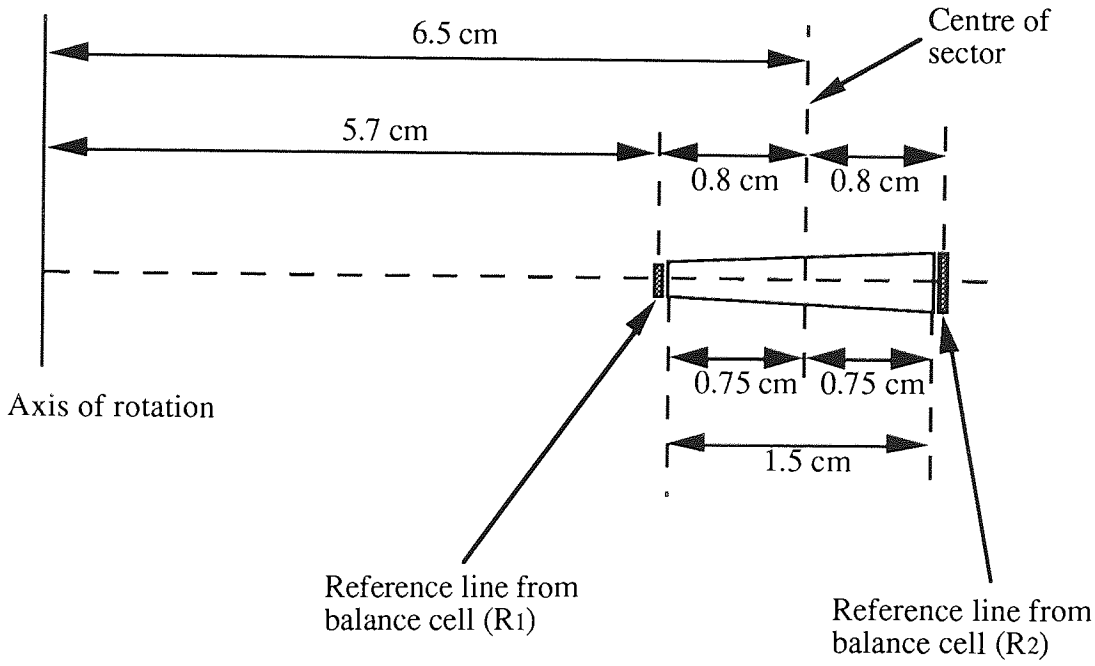

Figure 6.2 MSE Analytical Ultracentrifuge Single Sector Cell Measurements.

6.2.2 The Ultracentrifuge Optical System

The purpose of the optical system is to enable the operator to follow and record the movement of material in the sample cell during centrifugation both quantitatively and qualitatively. The cells are orientated in the rotor to allow light to pass through them while the rotor is in motion.

The MSE Ultracentrifuge has three types of optical system, one method is based on ultraviolet absorption and two, the Schlieren and Rayleigh interference methods are based on the refraction of light. Detailed accounts of these systems are described in the machine's manual [165]. The Schlieren system was used in this study as it gave data that was simple to interpret and was the most suitable system for visualising samples with concentrations in the range of 1-15 mg cm^{-3}. Chervenka [101] has listed the normal working concentration ranges for various ultracentrifuge optical systems.

The Schlieren optical system yields traces that represent the variation of the refractive index gradient $\partial n/\partial r$ with radial distance r. Thus during a normal rate differential centrifugation (see section 4.4.1), the point of maximum gradient indicates the centre of the boundary (figure 4.10). A typical sedimenting boundary and the relationship between the Schlieren peak and concentration of macrospecies in the cell is shown in figure 6.3. It follows that when there is no change in refractive index ($\partial n/\partial r = 0$) then no deviation from the baseline occurs. Since ∂n is proportional to ∂c (the change in concentration), the area under the curve will also be proportional to the concentration c of the sedimenting species.

6.3 DETERMINATION OF NATIVE DEXTRAN SEDIMENTATION COEFFICIENTS BY ANALYTICAL ULTRACENTRIFUGATION

Dextran sedimentation rates were determined using the normal rate differential centrifugation technique (section 4.4.1). Native dextran fractions were initially uniformally distributed throughout the ultracentrifuge cells. Under the applied centrifugal field, the material sedimented, forming an upper clear solvent region, separated from a lower region, containing sedimented dextran by a boundary zone (see figure 4.10). Sedimentation rates were determined by observing the movement of the boundary zone with time, using Schlieren optics (figure 6.3).

6.3.1 Experimental Details

Because many molecules exhibit sedimentation rates that are dependent upon concentration, native dextran samples of different concentrations were analysed. Native dextran fractions were prepared by reacting 16 cm^3 of a 5% w/w sucrose solution, at pH 5.2 and 25°C with 4 cm^3 of dextransucrase enzyme with an activity of 10 DSU cm^{-3}. After complete reaction, the enzyme was denatured by heating for five minutes in a boiling waterbath and the sample was dialysed. Analysis by GPC and HPLC showed the retained material to be dextran of a very high 'molecular' weight. Dextran was quantified by GPC, before being appropriately diluted with potassium chloride solution to give 0.5,

1.0 and 1.5% w/w native dextran concentrations in 0.1 molar potassium chloride. The salt was added to suppress the effect of charged groups on the particles.

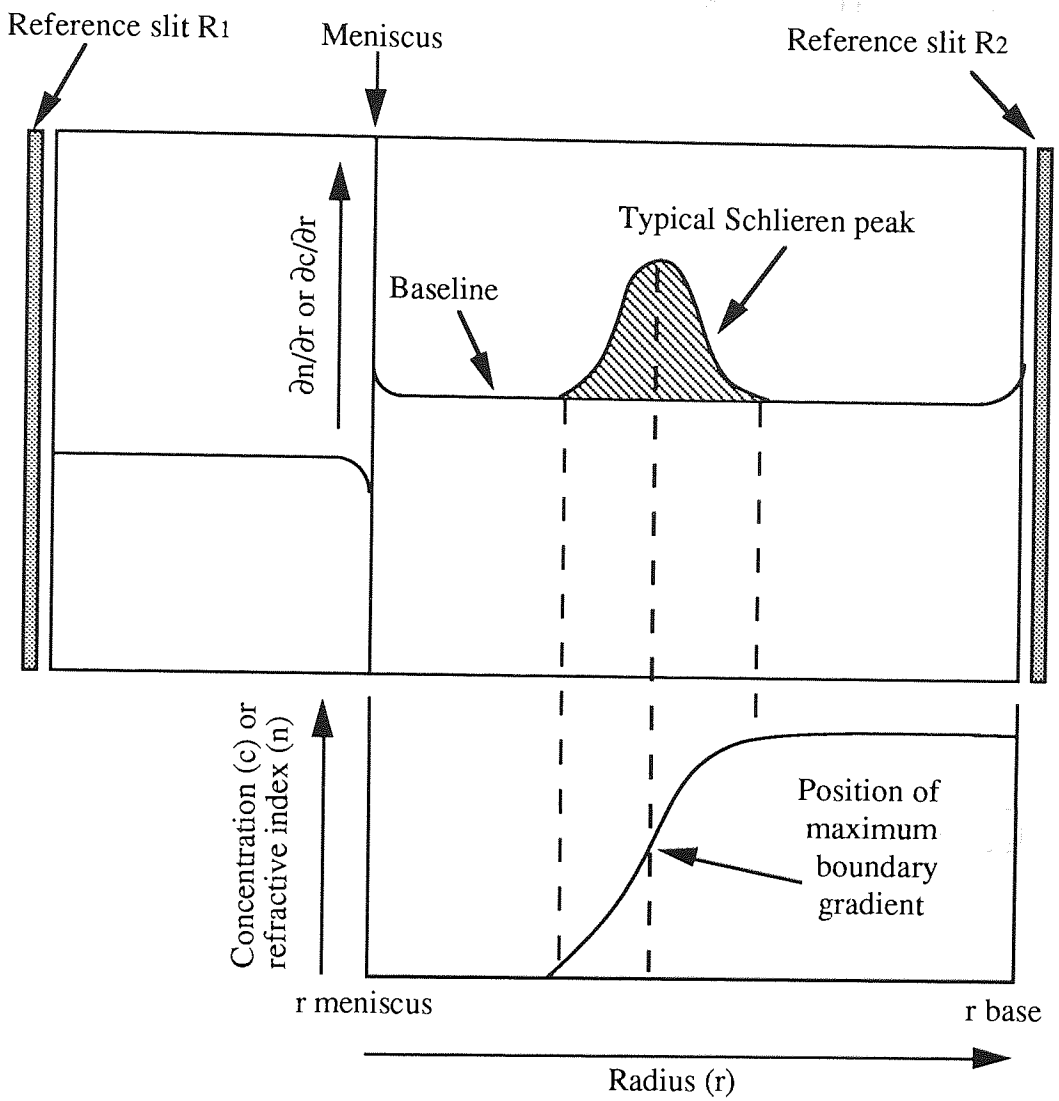

Figure 6.3 Schlieren Trace of a Typical Sedimenting Boundary

Three 500µl capacity standard single sector cells were then assembled and loaded with 300µl of each dextran solution and balanced against the reference cell as described in section 6.2.1. The cells were aligned in the rotor pockets by means of the locating pins and the rotor fitted to the centrifuge spindle. The cooling chamber and rotor guard were then fitted into place. The rotor had been allowed to equilibriate at the operating temperature of 25°C prior to the run. The system maintained a constant bowl and rotor temperature using a water cooling system.

The run time, rotor speed and Schlieren optical system were then selected and the run started. The rotor was accelerated to 10 000 rpm (equivalent to an average 7 300g) and

the system left to stabilise for several minutes. The observed Schlieren traces were recorded photographically at ten minute intervals. The run was halted when significant sedimentation had been observed in each of the three cells. The cells were then immediately removed and cleaned according to the instructions given in the manual. Extreme care was taken to avoid scratching the quartz cell windows and epoxy resin centre-piece.

6.3.2 Analysis of the Schlieren Traces

Typical Schlieren traces taken during the run are shown in figure 6.4. All three cells containing the native dextran samples are recorded side by side on the same photograph. Most of the third cell cannot be seen in figure 6.4(a), but can clearly be seen in figure 6.4(b). The trace on the left of each photograph records the sedimentation of the 0.5% w/w native dextran sample and the central and right hand side traces record the sedimenting properties of the 1.0 and 1.5% w/w samples respectively. The data obtained from these photographs was used to determine a number of factors pertaining to the native dextran studied, such as the average sedimentation coefficient at infinite dilution and the degree of sample polydispersity.

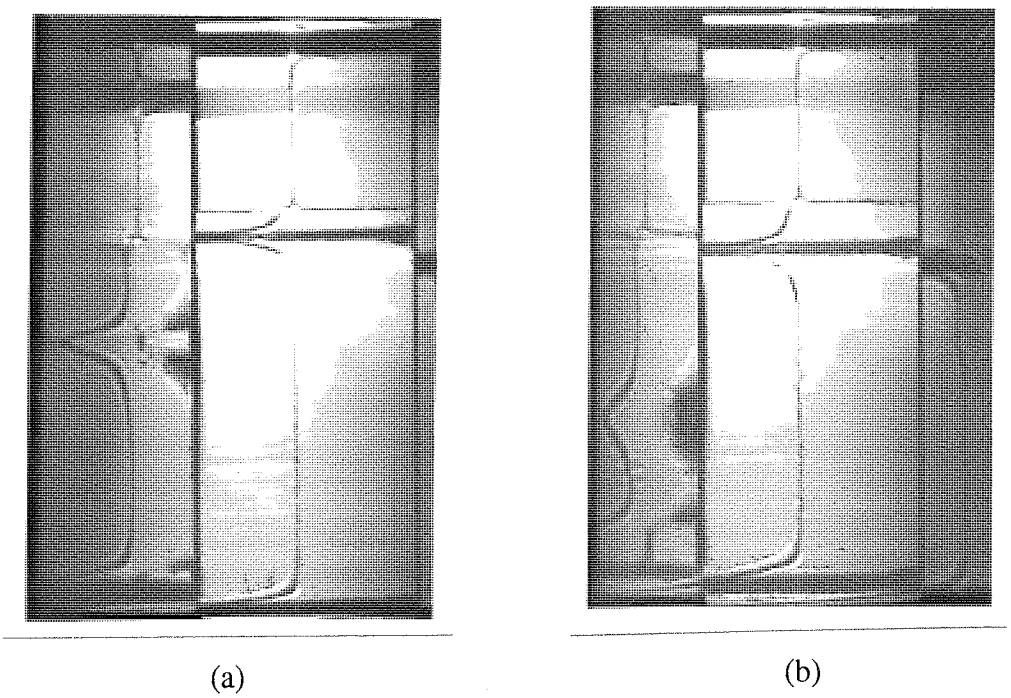

(a) (b)

Figure 6.4 Typical Schlieren Traces Taken During the Analytical Ultracentrifuge Runs at (a) 30 and (b) 60 Minutes After the First Photograph was Taken.

6.3.2.1 Determination of the Average Sedimentation Coefficient

The average sedimentation coefficient, S, can be sufficiently accurately determined by observing the rate of movement of the maximum peak ordinate in the Schlieren traces

(101). Errors due to temperature and rotor speed fluctuations were assumed negligible. Similarly, the change in the partial specific volume of the solute with pressure in the cell can also be assumed negligible with little losses in accuracy (101). To calculate S from the photographic data, the following measurements were made:

1. $R_1 \rightarrow R_2$: R_1R_2 represents the distance between reference points R_1 and R_2 on each photographic print and was found to equal 129.5 mm in all cases. The actual distance between the points is 16 mm (figure 6.2), giving a magnification factor of 8.094. Therefore, in order to replace the photographic distances with the true distances, all measured values should be divided by the magnification factor. However, this was not necessary as these values cancelled out during calculations.

2. $m(O \rightarrow R_1)$: OR_1 represents the distance from the centre of rotation O, to the centre of the upper reference band R_1 which equalled 57.009149 mm. This included an allowance for rotor stretch, which at 10 000 rpm equals 9.147×10^{-3} mm for this particular rotor. mOR_1 was the distance OR_1 in magnified units, which equaled 461.4177mm.

3. $R_1 \rightarrow M$: R_1M represents the distance from R_1 to the air/liquid meniscus, M.

4. Determination of R_1P and $mOR_1 + R_1P$: R_1P represents distance between R_1 and the position of the maximum ordinate of the peak (P) on each photograph. By adding mOR_1 to R_1P, the distance of the moving peak from the axis of rotation at a given time is obtained in magnified units and is referred to as r.

Equation 4.12 can be written:

$$S = \frac{1}{\omega^2} \times \frac{\text{Ln } r_2 - \text{Ln } r_1}{t_2 - t_1} \qquad \text{— (6.1)}$$

Where r_2 and r_1 equal the radial distances of P from the axis of rotation at times t_2 and t_1 respectively. $1/\omega^2$ is constant for a given rotor speed and can be calculated from equation 4.2, giving a value of 9.1189×10^{-7} radians^2 sec^{-2} at a rotor speed of 10 000 rpm. Therefore, a plot of the natural logarithm of the maximum peak ordinate in magnified units (Ln r) versus time should yield a linear relationship, proportional to the average sedimentation coefficient of the sedimenting dextran sample. The distances R_1P and Ln r for the three dextran concentrations studied at time t after the first photograph was taken are shown in tables 6.1 (a), (b) and (c). Plots of Ln r versus time for each dextran concentration are shown in Figure 6.5.

Time from first photograph (t) (seconds)	Distance R_1P in magnified units (mm)	Ln r (Ln[R_1P+mOR_1])
0	49.50	6.236
600	53.50	6.244
1200	58.50	6.254
1800	64.50	6.265
2400	70.50	6.276
3000	76.50	6.282
3600	82.75	6.299
4200	88.50	6.310

Table (a)

Time from first photograph (t) (seconds)	Distance R_1P in magnified units (mm)	Ln r (Ln[R_1P+mOR_1])
0	39.00	6.215
600	40.00	6.217
1200	41.50	6.220
1800	43.00	6.223
2400	44.50	6.226
3000	45.50	6.228
3600	47.00	6.231
4200	48.50	6.234
4800	50.00	6.237
5400	51.00	6.239
6000	52.50	6.242
6600	54.00	6.245
7200	55.50	6.248
7800	57.50	6.252
8400	59.00	6.255
9000	60.50	6.258

Table (b)

Time from first photograph (t) (seconds)	Distance R_1P in magnified units (mm)	Ln r (Ln[R_1P+mOR_1])
0	48.00	6.233
600	48.00	6.233
1200	48.00	6.233
1800	49.00	6.235
2400	49.50	6.236
3000	50.00	6.237
3600	50.75	6.239
4200	51.00	6.239
4800	51.50	6.240
5400	52.00	6.241
6000	52.75	6.243
6600	53.50	6.244
7200	54.50	6.246
7800	55.25	6.247
8400	55.75	6.248
9000	56.00	6.249

Table (c)

Table 6.1 Optical Ultracentrifugation of Native Dextran Fractions. (a) 0.5% w/w (b) 1.0% w/w (c) 1.5 %w/w native dextran concentrations.

Careful examination of Figure 6.5 shows that dextran sedimentation with time is slightly less pronounced in the first few minutes of the run. This was because the sedimenting particles were being accelerated by the applied centrifugal force towards their characteristic terminal velocities, which was dictated by the properties of the dextran particles, the surrounding medium and the applied centrifugal field.

Ignoring these initial points, particle sedimentation appeared approximately linear with time. The lines of best fit for these sets of data were found by using the method of least squares, from which the true gradients of the slopes were found. Substitution of each gradient into equation 6.1 yielded a mean S-value for each of the three dextran samples studied. The results are presented in table 6.2

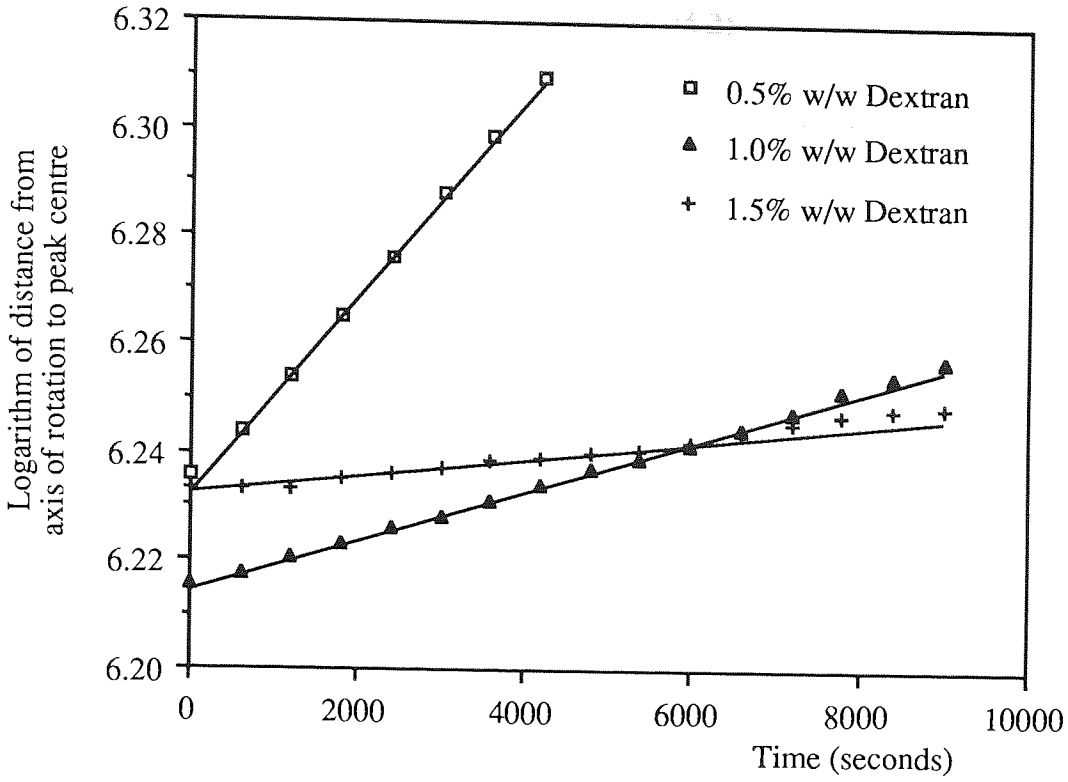

Figure 6.5 Logarithm of Peak Centroid Position Versus Time

Dextran Concentration ($g\ cm^{-3}$)	Average Sedimentation Coefficient (Svedbergs)
0.005	163.70
0.010	42.29
0.015	17.25

Table 6.2 Average Sedimentation Coefficients Calculated by the Method of Least Squares

These results show that S is highly dependant upon concentration. Many particle species exhibit a decrease in their observed sedimentation rates at higher sample concentrations due to the increasing influence of frictional effects.

It is usual in concentration dependent systems to extrapolate the sedimentation data obtained at finite concentrations to infinite dilution (zero concentration) where solution properties approach thermodynamic ideality and are independent of concentration (section 4.4.1.2). The observed sedimentation coefficients recorded in table 6.2 were back extrapolated to infinite dilution using equation 4.23 which links the experimentally determined sedimentation coefficient Sc, obtained at sample concentration c with S_o, the sedimentation coefficient at infinite dilution by the expression:

$$S_c = S_o\ (1 - k_s c) \quad \text{—— (6.2)}$$

where k_s is the concentration dependence coefficient at limiting low concentrations. Using the data in table 6.2, equation 6.2 can be rewritten as:

$$163.710 = S_o\ (1 - 0.005\ k_s) \quad \text{—— (6.3 (a))}$$
$$42.257 = S_o\ (1 - 0.010\ k_s) \quad \text{—— (6.3 (b))}$$
$$17.250 = S_o\ (1 - 0.015\ k_s) \quad \text{—— (6.3 (c))}$$

Equations 6.3. (a) and 6.3. (b) were solved simultaneously giving a k_s value of 85.17. Similarly, equations 6.3 (b) and (c) and 6.3 (a) and (c) were solved simultaneously to give k_s values of 54.21 and 61.81 respectively. Substitution of the k_s value obtained from equation 6.3 (a) and (b) into the same two equations yielded an S_o value of 285.13 Svedbergs. Using the same procedure for equations 6.3 (b) and (c) and 6.3 (a) and (c), S_o values of 92.35 and 236.86 Svedbergs respectively were found.

These widely differing S_o values highlighted the problems associated with back extrapolating S-values at finite concentrations to infinite dilution. However, because equation 6.2 only holds true at limiting low macromolecular concentrations, back-extrapolation of the more dilute dextran solutions should yield a more accurate S-value, in this case 285.13 Svedbergs, than if all three dextran solutions are considered (figure 6.6).

Study of more dilute dextran solutions would enable a more accurate So value to be determined.

6.3.2.2 Sedimentation Coefficient Correction and the Partial Specific Volume Factor

The observed sedimentation coefficients were converted to the standard state, that of pure water at 20°C, by the manner described in section 4.2.2. Equation 4.15 shows that the fully corrected sedimentation coefficient is given by:

$$S_{20,w} = S_{OBS} \left(\frac{\eta_{t,solv}}{\eta_{20,w}} \right) \left(\frac{1-\upsilon_{20}\rho_{20,w}}{1-\upsilon_t \rho_{t,solv}} \right)$$

The symbols have been defined in section 4.2.2. The supporting medium in the centrifuge cells was a weak potassium chloride buffer. For the purposes of calculation, this medium was assumed to have the same properties as water. The runs were conducted at 25°C. Thus $\eta_{20,w}$ and $\eta_{t,solv}$ equal the viscosities of water at 20°C and 25°C

respectively and $\rho_{20,w}$ and $\rho_{t,solv}$ equal the densities of water at 20°C and 25°C respectively.

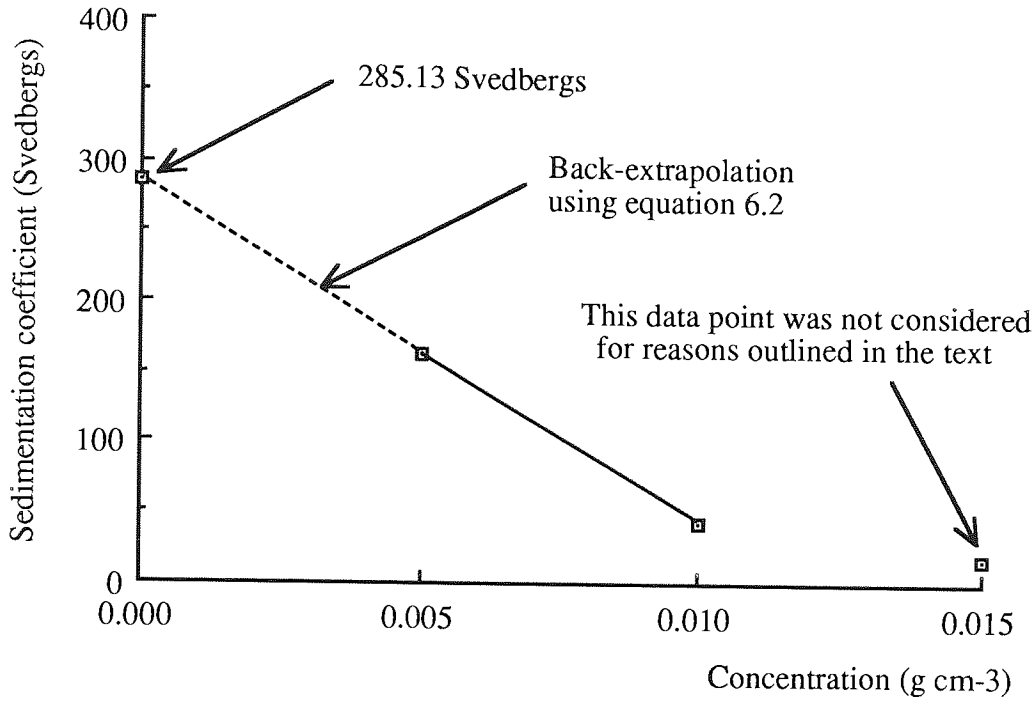

Figure 6.6 Back-Extrapolation of Sedimentation Coefficient Data to Infinite Dilution using the Equation of Schachman [102]

The partial specific volume factors, υ_{20} and υ_{25} (υ_t) were determined in the laboratory using the method outlined by McCall (see section 4.2.3). Density measurements using a pycnometer and constant temperature water baths gave an average υ_{app20} and υ_{app25} values for 1% w/w native dextran solutions of 0.628 $cm^3\ g^{-1}$ and 0.631 $cm^3\ g^{-1}$ respectively. These values compare favourably with υ_{20} values calculated using standard data tables [166], giving mean υ_{app} values of 0.635 $cm^3\ g^{-1}$. A υ value of 0.625 $cm^3\ g^{-1}$ is widely quoted in the literature for polysaccharides [94].

Equation 4.15 can therefore be rewritten:

$$S_{20,w} = S_{OBS} \times \frac{0.8704}{1.002} \times \frac{(1-[0.628 \times 0.99823])}{(1-[0.631 \times 0.99707])} = 0.894\ S_{OBS}$$

The fully corrected S-values obtained for the native dextrans studied could then be calculated. The results are listed in table 6.3

Dextran Solution (% w/w)	Observed S-value (Svedbergs)	Fully corrected S-value ($S_{20,w}$) (Svedbergs)
0	~285.000	~254.80
0.5	163.710	146.36
1.0	42.287	37.81
1.5	17.250	15.42

Table 6.3 Fully Corrected Sedimentation Coefficients

It can be seen that the standard state sedimentation coefficient values were about 10% less than the observed values.

6.3.2.3 Radial Dilution Effects

Because of the sector shape of the analytical ultracentrifuge cells, a progressive dilution of the sample will occur as sedimentation proceeds, which will effect the sedimentation rates of particles with concentration dependence effects. Radial dilution has been discussed in Section 4.4.1.2.

A close examination of Figure 6.5 shows that at longer time intervals, the experimental points tended to lie very slightly above the lines, particularly in the cases of the 1.0% and 1.5% w/w dextran samples. It was concluded that this was due to radial dilution effects.

Consider the rate of sedimentation of the 1% w/w dextran sample. The distance from the axis of rotation to the meniscus ($mOR_1 + R_1M$) was 461.4177 + 38 mm = 499.417 mm in magnified units. After 9000 seconds, the distance from the axis of rotation to the maximum peak ordinate ($mOR_1 + R_1P$) was 461.4177 + 60.5mm = 521.9177 mm. Substitution of these values into equation 4.24 gives an actual sample concentration of 0.956% w/w due to radial dilution.

Table 6.2 shows that native dextran particles exhibited concentration dependence effects and will therefore be affected by radial dilution effects. Because these rate increases were very low and because only very limited data was known concerning the relationship between dextran sedimentation rate and concentration, the radial dilution effect was considered negligible when calculating the fully corrected mean sedimentation coefficient values.

6.3.2.4 Dextran Polydispersity

The boundary shapes formed during the sedimentation of the 0.5% w/w dextran solution at 600 second time intervals is shown in figure 6.7. It can be observed that the boundary broadens progressively with time of sedimentation which is characteristic of a polydisperse material.

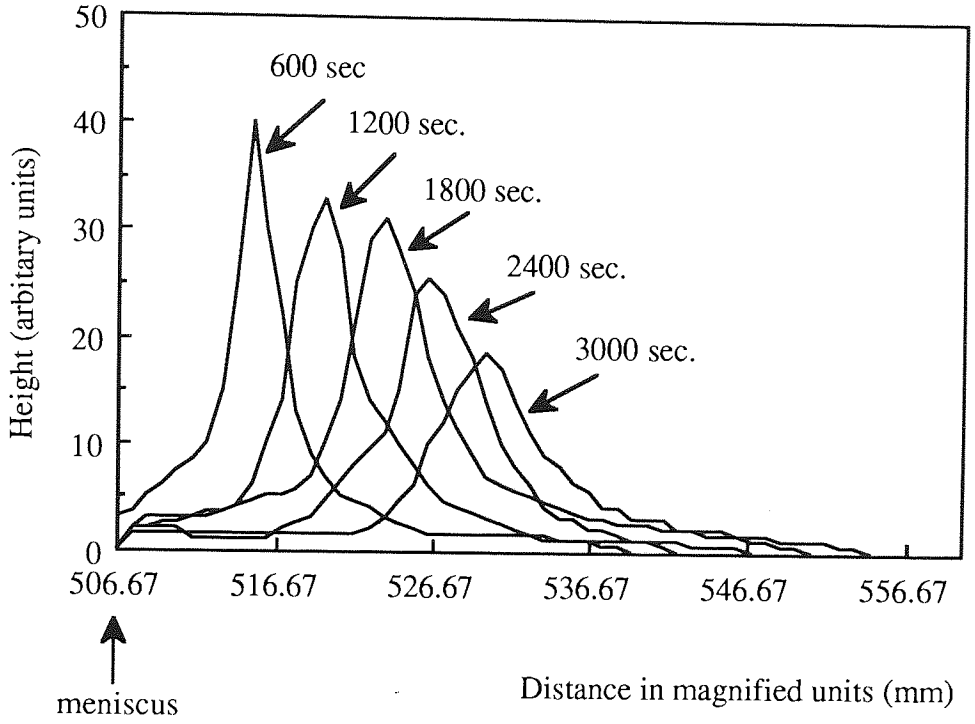

Figure 6.7 The Boundary Shapes Formed during the Sedimentation of the 0.5% w/w Native Dextran Fraction at 600 Second Time Intervals

Although the native dextrans were polydisperse, the distinctive Schlieren peaks indicate that the majority of the sedimenting dextran particles lie close to an average characteristic sedimentation value. This observation was in accordance with Tsuchiya et al[58] (Section 4.5). Tsuchiya's results have been summarised in figure 4.21.

For a given run time and rotor speed, any radial position in the ultracentrifuge cell can be converted to an equivalent sedimentation coefficient. In section 6.3.2 the mean sedimentation coefficient of the native dextran fractions were calculated by observing the rate of movement of the peak centroid. Thus, only a knowledge of rotor speed, peak position and the time intervals between photographs was required. However, when assigning a sedimentation coefficient to a given radial position, the effective total time of centrifugation from 'zero' time, assuming a constant rotor speed of 10 000 rpm, to when

the photograph of interest was taken must first be calculated. This was done for the 0.5% w/w native dextran fraction by the following procedure:

The mean S-value of the 0.5% w/w dextran fraction was calculated to be 163.71 Svedbergs (table 6.2). The Ln r value of the peak at the time that, for example, the third photograph was taken was 6.254 (table 6.1(a)). The Ln r value of the peak at time zero was equal to the radial position of the meniscus, which was 6.229. Substituting these values into equation 6.1 and assuming a rotor speed of 10 000 rpm, gave an effective centrifugation time of 1422 seconds. Thus the effective time of centrifugation from time zero to when the third photograph was taken, assuming a constant rotor speed of 10 000 rpm was 1422 seconds. The equivalent sedimentation coefficient of any radial position in the cell at the time the third photograph was taken was then calculated using the following procedure:

Consider, for example, a radial position, which in magnified units is 530 mm from the axis of rotation, then:

$\text{Ln } r_2 = \text{Ln (530)}$	=	6.273
$\text{Ln } r_1 = \text{Ln (meniscus)}$	=	6.229
Δt = effective time of centrifugation	=	1422 seconds
$1/\omega^2$	=	9.12×10^{-7}

substitution of this data into equation 6.1 gave an S-value of 280.18 Svedbergs. Thus the radial position on the third photograph corresponding to 530mm from the axis of rotation in magnified units had an equivalent S-value of 280.18 Svedbergs. This example deals specifically for the third photograph taken, but can simply applied to any photograph provided that sufficient data is available. Thus, any of the boundary profiles shown in figure 6.7 can be plotted against equivalent sedimentation coefficient rather than radial position. This is shown for the third photograph taken during the sedimentation of the 0.5% w/w native dextran sample in figure 6.8.

By applying Simpsons rule, it was concluded that over 80% of the dextran sample had a sedimentation coefficient of between 100 and 250 Svedbergs, with an average value of around 165 Svedbergs. However, extreme care should be taken when studying distribution data from sedimentation profiles, because several factors can affect boundary shape. These factors have been discussed in section 4.4.1.3. Table 6.2 shows that the sedimentation rate of native dextran is highly dependent upon concentration. This can lead to significant boundary sharpening effects which can greatly alter the apparent sedimentation coefficient distribution profile shown in figure 6.8. Several researchers

(112-119) have reported methods of correcting for concentration and diffusion effects, but these methods are complex and were considered to be outside the scope of this study. However, given the extreme dependence of native dextran sedimentation rates on sample concentration, it must be concluded that native dextran is considerably more polydisperse than figure 6.8 suggests.

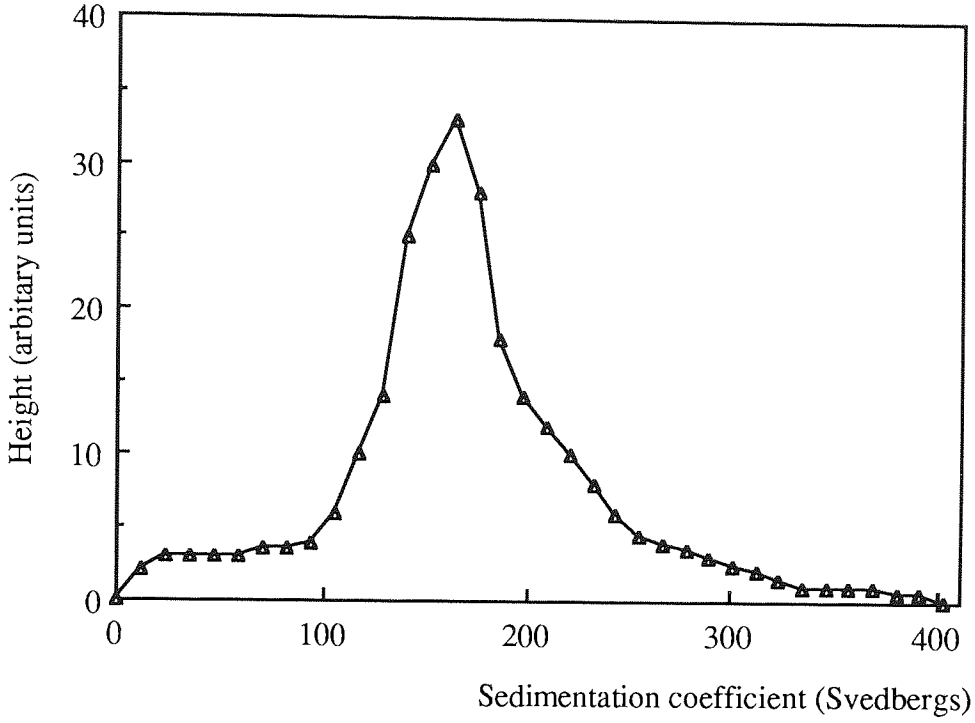

Figure 6.8 The Approximate Sedimentation Coefficient Distribution of the Native Dextran Sample using Boundary Profiles

6.3.2.5 Dextran Gel Structure

The electron microscopic observation of films formed by the evaporation of dilute solutions of dextrans indicate the presence of networks of microscopic filaments (Section 2.4.1). It is evident from the sedimentation studies that even relatively low dextran concentrations can result in large decreases in sedimentation rate (see figures 6.4 and 6.6). If this data is extrapolated to higher dextran concentrations, it is evident that a point will be reached where the dextran sedimentation rate will effectively equal zero and the dextran material will exhibit the classic behaviour of an incompressible gel in a centrifugal field. The data suggests that this could occur at dextran concentrations as low as 1.5% w/w These network structures can be readily dispersed by dilution, presumably to give the high MW particle structures observed by Bovey (47).

The fact that dextran solutions appear to form relatively slow sedimenting gel-like structures at relatively low dextran concentrations may have important implications

regarding the sedimentation behaviour of native dextran in the proposed centrifugal bioreaction-separation process. Gel-like dextran complexes may lead to the entrapment and forced sedimentation of enzyme molecules and possibly even fructose molecules. These possibilities were considered in this study.

6.4 USES OF THE SEDIMENTATION COEFFICIENT

Knowledge of particle sedimentation coefficients allow a number of useful calculations concerning native dextran particle properties to be made. For example, from equation 4.10, sedimentation coefficient data allows the calculation of particle sedimentation velocities under a given centrifugal field. This allows optimum centrifugation conditions to be determined. Furthermore, with a knowledge of the diffusion coefficient D, particle 'molecular weights' can be calculated using the Svedberg equation (equation 4.11).

6.4.1 Diffusion Coefficient Measurements

The diffusion coefficient of several native dextran fractions were measured using a model 801 molecular size detector (Oros Instruments Ltd., Slough, UK). This machine used a dynamic light scattering (DLS) technique whereby a beam of monochromatic light was passed through the sample and the fluctuations in light intensity analysed. The output from the DLS system gave the diffusion coefficient, D, of the particles in solution. Native dextran solutions of the required concentrations were prepared according to the method described in section 6.3.1. Samples were not dialysed because low molecular weight impurities will not affect measurements. All the samples were centrifuged at low speeds (1300 rpm) prior to analysis to remove high MW impurities such as dust particles. Measurements were made at the ambient temperature of the laboratory (22.7°C). The viscosity of the surrounding medium was assumed to be equal to that of pure water, allowing the calculation of the fully corrected $D_{20,w}$ value for each native dextran fraction studied using equation 4.19. The results are listed in table 6.4.

It can be observed that native dextran diffusion coefficients are not concentration dependent over the concentration range 0.1 - 1.5% w/w dextran.

6.4.2 The Molecular Weight of Native Dextran

Calculations were based on the fully corrected sedimentation coefficients determined in the preceeding sections and summarised in table 6.3.

Native Dextran Concentration (% w/w)	Observed Mean Diffusion Coefficient ($x10^8$ cm^2/sec)	Standard Deviation ($x 10^8$)	Fully Corrected Diffusion Coeff. ($x10^8$ cm^2/sec)
0.1	1.423	1.833	1.410
0.3	1.535	2.254	1.522
0.5	1.425	1.288	1.413
1.0	1.429	1.347	1.417
1.5	1.450	1.650	1.438
Mean	1.459	1.771	1.447

Table 6.4 Mean Diffusion Coefficients of Native Dextran Solutions

The density of the surrounding medium was taken as equal to that of pure water at 20°C and the υ_{20} value was taken as 0.628 cm^3 g^{-1} (section 6.3.2.2). At 20°C, the absolute temperature is 293.15°K. Using this data the 'molecular weights' of the dextran particles were calculated from the Svedberg equation, the results being presented in table 6.5.

Native Dextran Concentration (% w/w)	Corrected Sedimentation Coefficient (Svedbergs)	Mean Diffusion Coefficient ($x10^8$ cm^2 sec^{-1})	Molecular weight ($x10^{-6}$)
Infinite dilution	~ 254.80	1.447	114.81
0.5	146.36	1.410	67.52
1.0	37.81	1.417	17.39
1.5	15.42	1.438	6.99

Table 6.5 Native Dextran Molecular Weight Determinations

Similarly to the observed sedimentation coefficients, the apparent 'molecular weights' of the native dextrans were found to be highly concentration dependent. An estimate of the true mean 'MW' of the particles can be obtained at infinite dilution, where particle interactions which cause the observed concentration dependent effects are effectively zero. Table 6.5 indicates this value to be in the order of 114.8 x 10^6 daltons and is in close accordance with values determined by Tsuchiya et al [58] and Bovey [47], (section 4.5), which is evidence of the aggregation of dextran molecules in solution to form high MW dextran particles.

As has been previously discussed the term 'molecular weight' is a misnomer when considering high MW dextrans. These particles have been shown to consist of aggregates

of native dextran molecules with molecular weights varying between 3×10^5 and 5×10^5 (see section 4.5).

6.4.3. Calculation of the Frictional Ratio

D can be used to determine the frictional ratio f/fo, by using equations 4.20 and 4.21. The frictional ratio is a measure of the asymmetry and hydration of a particle in solution and has been discussed in section 4.2.6.

Taking the average molecular weight (MW) of the native dextran particles to equal the observed molecular weight at infinite dilution (table 6.5) and η to be the viscosity of water at 20°C, then fo can be calculated for native dextran. f can simply be calculated using the mean diffusion coefficient listed in table 6.4. f was found to equal 2.773×10^{-6} g sec^{-1} and fo to equal 5.775×10^{-7} g sec^{-1}. Thus the native dextran studied had a frictional ratio of 4.802. This value indicates that native dextran particles are highly hydrated and/or asymmetric.

6.4.4 Native Dextran Particle Sizes

From Stokes' law, for a spherical particle of radius r_p (section 4.2.6):

$$f = 6\pi\eta r_p$$

where η equals the viscosity of the medium in which the diffusion coefficient was determined.

Using Stokes' equation, a native dextran particle with an 'f' value of 2.773×10^{-6} g sec^{-1} will have a radius of 1.468×10^{-5} cm (1468 Å). An equivalent spherical non-hydrated 'ideal' particle having an 'fo' value of 5.775×10^{-7} g sec^{-1},will give an equivalent radius of 305.8 Å. Thus, native dextran particles have radii around 5 times larger than equivalent 'ideal' particles. Assuming the particles to be spherical, an average native dextran particle will occupy a volume around 125 times greater than the equivalent 'ideal' particles.

Therefore, the idea of a native dextran particle as a large, highly solvated asymmetric aggregation of smaller molecules can be drawn. Sedimentation studies indicate that at higher concentrations, considerable interactions occur between these particles. Electron microscopy studies have indicated the present of gel networks in even relatively dilute dextran solutions (Section 2.4.1).

Using equation 4.21, the mean particle radii were also determined using the diffusion coefficient data reported in table 6.6. The results, expressed in Angstroms are summarised in table 6.6.

Mean particle radii were found to be around 1500 Å and are independent of dextran concentration between 0.5 and 1.5% w/w. The low standard deviation values indicate that the native dextran particles studies had a relatively small range of particle sizes. This observation is supported by the relatively 'sharp' boundary regions observed during the differential sedimentation of dextran (figure 6.8). However boundary profiles can be significantly 'sharpened' due to concentration effects [102,114-116].

Native Dextran Concentration (% w/w)	Mean Particle Radius (Angstroms)	Standard Deviation
0.1	1501.3	176.2
0.3	1427.6	201.7
0.5	1531.8	137.7
1.0	1548.0	126.4
1.5	1542.3	158.4
Mean	1505.1	166.4

Table 6.6 Mean Particle Radii of Native Dextran Particles using Stokes' Law

The mean particle radius of 1500 Å is considerably larger than the values of 800 Å recorded by Bovey [47] using light scattering measurements (Section 2.4.3). However, by using the relationship observed by Senti et al [46] between dextran MW and radius (equation 2.1), then for a native dextran particle weight of 115 x 10^6 (determined from the S and D coefficient measurements) a radius of 1930 Å was found. This is closer to the values presented in the above table.

6.5 DEXTRAN, DEXTRANSUCRASE ENZYME AND FRUCTOSE SEDIMENTATION RATES

Some of the values quoted in this section are based on estimated data. The aim of this section is to give an approximate indication of the relative rates of sedimentation of the various particle species.

The mean sedimentation and diffusion coefficients, S and D, of the native dextran samples studied in this work are presented in table 6.7. The S and D values of a fructose molecule were considered to be of the same order as sucrose, which have been

determined experimentally to be 0.28 Svedbergs and 4.6 x 10^{-6} cm^2 sec^{-1} respectively (121,151).

At present, the exact MW of the dextransucrase enzyme molecule is uncertain due to the presence of enzyme associated dextran (section 3.8.1). However, the MW value of 171 000 reported by Jackson and Steward (80) is in accordance with the work of Miller and Robyt (72). Enzymes of this MW size have diameters typically of the order of 100Å, giving a D value of around 5 x 10^{-7} cm^2 sec^{-1}. Assuming a υ value of 0.750 cm^3 g^{-1}, which is characteristic of proteins (94) and a MW of 171 000, then S was calculated from the Svedberg equation and is presented in table 6.7.

Substance	Mean diffusion coefficient in water at 25°C (cm^2 sec^{-1})	Mean, fully corrected sedimentation coefficient in water at 25°C (Svedbergs)
Native dextran	~ 1.46 x 10^{-8}	~285.00
Fructose	~460 x 10^{-8}	~0.28
Dextransucrase enzyme	~50 x 10^{-8}	~8.62

Table 6.7 The Experimentally Determined or Estimated Sedimentation and Diffusion Coefficients Values of Native Dextran, Fructose and Dextransucrase Enzyme.

Table 6.7 indicates that native dextran particles have mean sedimentation rates over 30 times greater than the dextransucrase enzyme molecules and sedimentation rates around 1000 times greater than the fructose molecules. Enzyme S-values are over 30 times greater than fructose S-values.

However, the S-value of active enzyme molecules will also be dependent upon associated dextran material and the dextran synthesized by enzyme action. Furthermore, the formation of dextran network structures may result in the physical entrapment and forced sedimentation of enzyme molecules. Thus, in reality, the effective S-value of the enzyme may be substantially higher than the value recorded in table 6.7 and may even be comparable with that of the native dextran particles. This factor was considered in the bioreaction-separation runs.

The rate of sedimentation of these particles in a given centrifugal field can be calculated using equation 4.10

$$S\omega^2 r = dr/dt \quad \text{—— (4.10)}$$

where S equals the particle sedimentation coefficient, $\omega^2 r$ equals the accelerating force of the centrifugal field and dr/dt equals the rate of particle sedimentation.

For a particle exactly 10 cm from the axis of rotation in a centrifuge cell spinning at 20 000 rpm, the accelerating force $\omega^2 r$ will equal 4.386×10^7 cm sec^{-2}. Therefore, by using the S-values in table 6.7, the rate of particle or molecule sedimentation in this field can be calculated. The results, expressed in units of cm sec^{-1} and Ångstroms sec^{-1} are shown in table 6.8.

Assuming that the diameter of an acceptor fructose molecule is the same as that of a glucose molecule, which has been reported to have a radius of around 5Å (166), then table 6.8 indicates that an enzyme molecule will sediment a distance of between 750 and 25 000 fructose molecule diameters per second, depending upon the extent of the interaction between the enzyme molecule and native dextran particles. Noting that a dextransucrase enzyme molecule will produce around 32 000 fructose molecules per minute (section 2.4.2), which is equivalent to around 500 fructose molecules per second when saturated with substrate, then it would appear that sedimentation rates of this order should result is substantial removal of the acceptor fructose molecules from the vicinity of the enzyme's nucleophyllic sites. It is expected that this will lead to a decrease in dextran chain termination and an increase in high MW dextran product.

Substance	Rate of sedimentation	
	cm sec^{-1}	Ångstroms sec^{-1}
Native dextran	1250.00×10^{-6}	125 000
Fructose	1.18×10^{-6}	118
Enzyme	37.81×10^{-6}	3781

Table 6.8 Rates of Native Dextran, Fructose and Dextransucrase Enzyme Sedimentation in cm sec^{-1} and Ångstroms sec^{-1}

6.6 CONCLUSIONS

Studies in an analytical ultracentrifuge showed that the rate of native dextran sedimentation to be highly dependent on concentration. The sedimentation coefficient of dextran was nearly ten times higher when the concentration of native dextran was decreased from 1.5 % to 0.5% w/w in a normal rate centrifugation. It was concluded that dextran particle interactions greatly affected the rate of dextran sedimentation in a normal rate centrifugation. Extrapolation of this data to higher dextran concentrations indicated

that a point would be reached, where the dextran sedimentation rate would effectively equal zero and the dextran material would exhibit the classic behaviour of an incompressible gel in a centrifugal field. This could occur at native dextran concentrations of the order of 1.5% w/w.

Back extrapolation of sedimentation coefficient data yielded a dextran sedimentation coefficient of 285 Svedbergs at infinite dilution. This corresponded to a fully 'corrected' standard state ($S_{20,w}$) value of 254 Svedbergs. This was indicative of dextran molecules aggregating to form stable particulate structures.

The shape of the sedimenting boundary was seen to progressively increase in width with time indicating that the sedimenting dextran material was polydisperse. However, the true polydispersity of the system was masked by the fact that the peak was distorted due to concentration and Johnston-Ogston effects and to a lesser extent, diffusion effects.

Light scattering measurements indicated that native dextran particles had fully corrected diffusion coefficients in the order of 1.4×10^8 cm^2 sec^{-1}. This allowed the MW of native dextran fractions to be calculated using Svedberg's equation, giving a value of 115×10^6 daltons which is in accordance with data in the literature. 'Molecular' weight is a misnomer as native dextran fractions appear to form molecular aggregates even in dilute aqueous solutions.

Frictional ratio calculations indicated that the native dextran particles were highly asymmetric and/or hydrated. Frictional coefficients were also used to calculate native dextran particle sizes, giving mean values of around 1.5×10^3 Ångstroms.

Preliminary calculations based on estimated data and data from the literature suggested that native dextran particles sediment up to 1000 times faster than fructose molecules under identical conditions.

6.7 BIOREACTION-SEPARATION STUDIES IN THE ANALYTICAL ULTRACENTRIFUGE

6.7.1 Introduction

In addition to the native dextran sedimentation velocity experiments undertaken, the rate-zonal bioreaction-separation process discussed in section 2.3.2 was also studied using the analytical ultracentrifuge.

6.7.2 Experimental Details

Three single sector synthetic boundary overfilling cells were loaded with 290µl volumes of appropriately buffered and concentrated sucrose solutions at pH 5.2 and the cells assembled. 10µl volumes of purified dextransucrase enzyme were then placed in the two overfilling cavities of each cell and the cavities were plugged. The cells were balanced before centrifugation.

The action of the applied centrifugal field on the synthetic boundary cell resulted in the overlaying of the sucrose solution by the enzyme. The Schlieren traces were recorded photographically at ten minute intervals during the run.

The sucrose concentration and enzyme activities used in each run are summarised in table 6.9. A rotor speed of 10 000 rpm was used in all the runs.

Enzyme Loading (DSU cm^{-3})	Concentration sucrose (% w/v)		
	10%	15%	20%
65	Run 1		
130		Run 2a	Run 2b
260	Run 3a	Run 3b	
600	Run 4a		Run 4b

Table 6.9 Experimental Details of the Analytical Ultracentrifuge Rate-Zonal Runs.

Due to the very small capacity of the ultracentrifuge cells (300 µl), the construction of sucrose gradients, which are important in rate-zonal centrifugation for the minimisation of conventional mixing was not attempted.

6.7.3 Results

6.7.3.1 Overlaying of Substrate Solution with Enzyme.

In many of the runs, it appeared that there was either no transfer, or incomplete transfer of enzyme solution from the overfilling cavities, via the capillary tubes into the cells. This was believed to be due to the transfer of sucrose solution into the capillary tubes by capillary action during cell assembly. Thus, when the enzyme solution contacted the sucrose solution, some polymerisation occurred, resulting in tube blockage by the gelatinous native dextran product. Despite very careful cell assembly, this problem persisted. In the runs where enzyme transfer did occur, the capillary tube blockage problem appeared to result in some runs receiving smaller volumes of enzyme than others. Therefore direct comparison between runs should be treated with caution.

Analysis of the resultant Schlieren traces showed that initially, successful transfer of the enzyme solution resulted in the formation of a sharp interface between the two solutions due to density differences. In runs 1, 4a and 4b, the interface remained sharp, but in runs 2a, 2b, 3a and 3b, the interface became progressively more diffuse with time. This was shown by the continuous broadening of the Schlieren peak and finally resulting in the complete annihilation of the peak, indicating that complete mixing between the two solutions had occurred (figure 6.9). It appeared that this observation was not dependent on either substrate concentration or enzyme activity. A combination of the differences in enzyme activity, enzyme solution, solids concentration and the variability in enzyme transfer due to capillary tube blockage may be the cause of the differences of interface behaviour. The inability of the sucrose solution to support the enzyme solution was indicative of 'gradient' overloading. The factors that cause overloading have been discussed in section 4.4.2.5.

The possibility that overloading had occurred was also supported by the fact that the enzyme solution constituted at most, about 6% of the total cell contents (20µl in 310µl). However, even allowing for the sector shape of the cells, the initial volume occupied by the overlay solution, as indicated by the dark upper band observed at the beginning of each run (figure 6.9), was generally in excess of 20% of the total solution volume. This suggested that the enzyme solution was 'sinking' into the sucrose solution due to density inversion effects. The extremely small capacity of the ultracentrifuge cells hindered the construction of sucrose gradients in the cells which would help minimise mixing between the solutions by convection. The use of sucrose gradients may improve the hydrodynamic stability of the enzyme zone when layered onto the supporting sucrose solution.

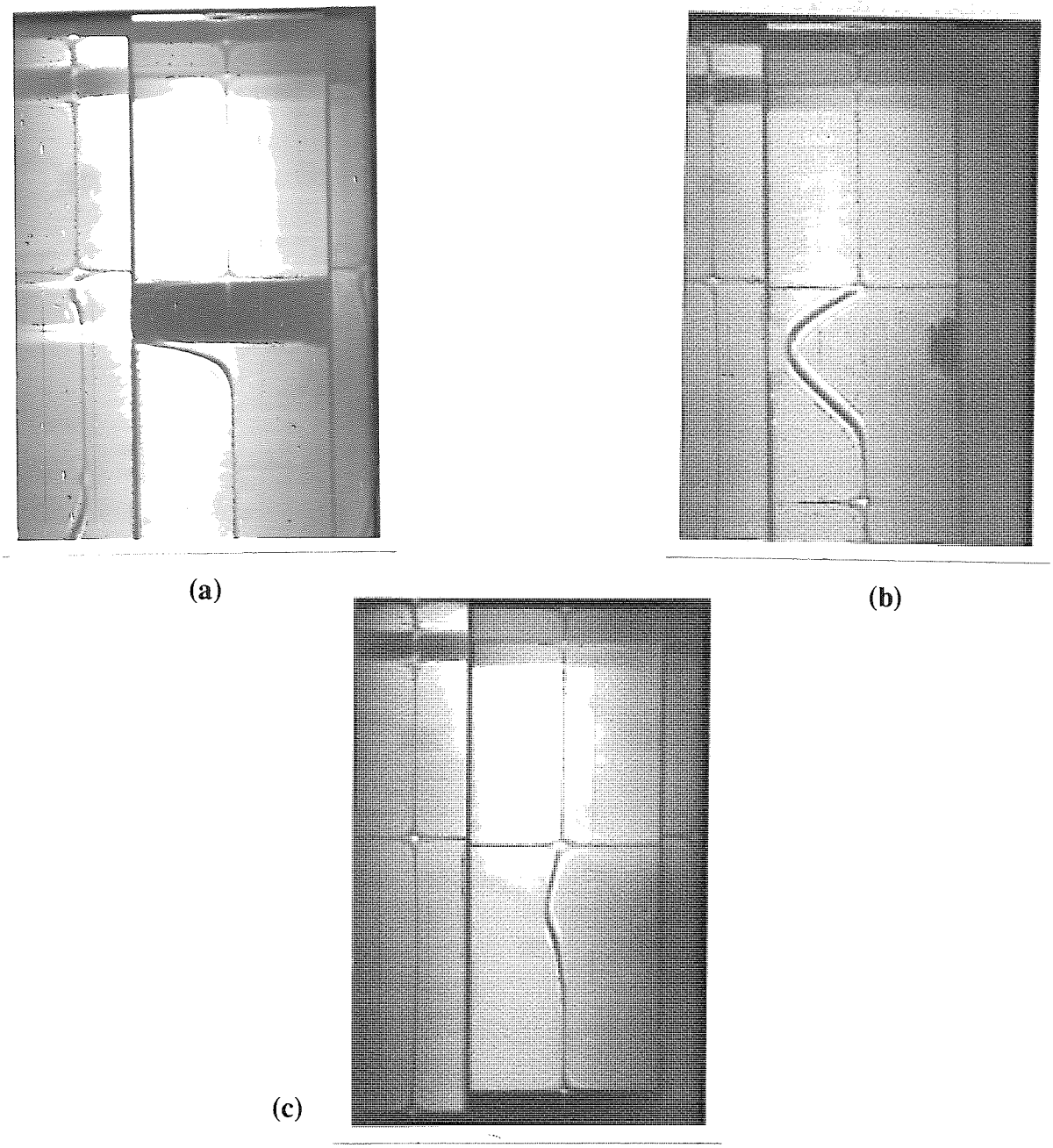

Figure 6.9 Overloading of Substrate Solutions with Enzyme. Photographs (a)was taken at the start of the run and photographs (b) and (c) were taken at 50 and 160 minutes after the first photograph was taken and show the progressive loss of the interface between the enzyme solution and sucrose substrate with time during run 2a.

6.7.3.2 Build-Up of the Gel Layer

The presence of a dark band at the base of the cells that increased in thickness with time, indicated that material was migrating through the substrate solution and accumulating at the cell base. Analysis of this material showed it to be mainly gelatinous dextran polymer. The build up of this gel fraction was monitored by measuring the thickness of the gel layer in the photographs with time. Typical plots are shown in figure 6.10 for runs 2a and 4a.

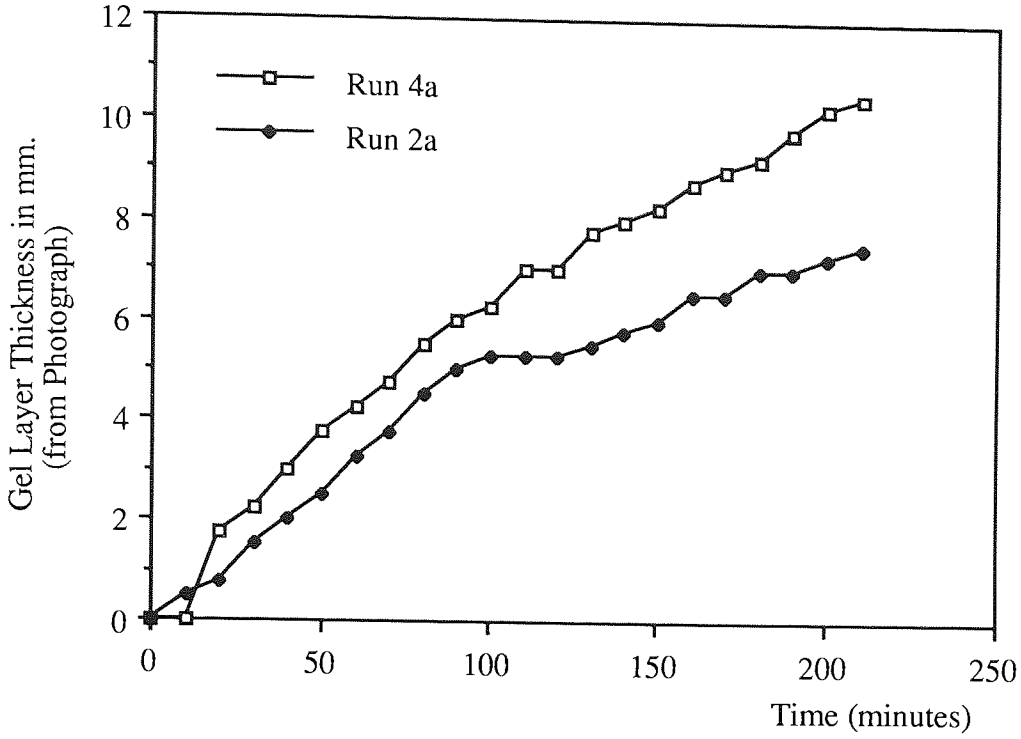

Figure 6.10 Gel Layer Build-Up

After a short period, all runs showed an approximately linear increase in gel layer thickness with time although some runs showed a marked decrease in the rate of gel layer build-up as centrifugation proceeded. This latter observation could have been due to the bulk of the sedimenting dextran material reaching the base of the tube within the duration of the centrifugation.

The data shows that the dextran material formed migrated to the tube bases under the applied centrifugal field. The continuous build up of this layer, coupled with the fact that no distinctive Schlieren peaks were seen along the length of the ultracentrifuge cells, indicated that no obvious dextran or dextran-enzyme rich zones were sedimenting through the supporting sucrose solution. This was a disappointing observation, although it was realised that non-ideal sedimentation was occuring due to the absence of stabilising sucrose viscosity and density gradients.

It was possible to calculate the sedimentation coefficients of the migrating material from data concerning the gel layer build-up with time in a manner similar to that employed for the calculation of native dextran sedimentation coefficients (see section 6.3.2).

Firstly, the distance from the axis of rotation, O to the reference point R_1, and hence mOR_1 was calculated. Secondly, R_1M, the distance from R_1 to the initial centre of the

dark band of overlay solution (M) was measured. Thirdly, R_1B, the distance from R_1 to the top of the thickening gel layer was measured.

From this data, Ln r, which equalled $Ln(mOR_1 + R_1B) - Ln(R_1M)$ was calculated and substituted into equation 6.1. Time t was taken as the number of seconds from the start of centrifugation, which approximated to the point at which the rotor reached 10 000 rpm and the first photograph taken. Monitoring the build-up of the gel layer allowed the sedimentation coefficients of the most rapidly sedimenting dextran-rich material to be determined. The results for each run are listed in table 6.10. These results cannot be considered very accurate due to the possibility of sample overloading, but do indicate that the values are of the same order as those recorded for the native dextran fractions examined in section 6.3. It appeared that increases in enzyme activity resulted in an increase in the maximum S-value. This could be due to enzyme overloading and/or dextran particle interactions.

Run Number	Maximum S-value (Svedbergs)
1	92.37
2a	377.59
2b	298.07
3a	383.42
3b	483.67
4a	569.54
4b	409.11

Table 6.10 Maximum Recorded Sedimentation Coefficient Values for the Analytical Ultracentrifuge Bioreaction-Separation Studies.

This set of experiments did not yield any quantitative data, because gel layer thickness cannot be equated to the quantity of gel material. Furthermore, the gel layer will become more 'compact' under the influence of the applied centrifugal field. Therefore the true effects of enzyme activity and substrate concentration on dextran and enzyme sedimentation could not assessed.

6.7.4 CONCLUSIONS

The data in table 6.10 is evidence that dextran sedimentation is relatively rapid at rotor speeds of 10 000 rpm (~7 300g). This rapid rate of dextran formation and sedimentation appeared promising. The successful development of a rate-zonal dextran bioreactor-

separator will be dependent on high dextran recoveries per unit time. The fact that dextran migrates at a rapid rate to the rotor wall will enhance those recoveries.

Unfortunately, however, no evidence of the rate zonal sedimentation of dextran-enzyme complexes, as shown, ideally in figure 2.8 was observed. If rate-zonal sedimentation was occurring, then large increase in gel layer thickness would be seen at the time when the sedimenting zone of dextran and enzyme reached the tube base. Furthermore, characteristic Schlieren traces would also be observed. However, no such observation were recorded. This led to the conclusion that dextran and/or the dextran-enzyme complexes were not sedimenting as a band through the sucrose solution. Although these results were disappointing, it was concluded that the analytical ultracentrifuge was not the ideal method for the analysis of the rate-zonal process for the reasons summarised below:

(1) Sucrose gradients could not be constructed in the ultracentrifuge cells. Density and viscosity gradients have been shown to minimise mixing by convection and will therefore increase the possibility of the band-like sedimentation of dextran and enzyme.

(2) The factors affecting the overloading of the sucrose solutions could not be adequately assessed using this method.

(3) There were problems associated with enzyme loading due to capillary tube blockage.

(4) The method did not yield quantitative data. The distribution of dextran, fructose and enzyme in the cells could not be differentiated. Furthermore, the sedimented dextran material cannot be quantified on the basis of the gel layer thickness.

The results indicate that dextran and enzyme sedimentation may be relatively rapid due to the formation of relatively high 'MW' gel structures. Thus the build-up of material at the base of the tubes may not be solely due to the continued sedimentation of material, but rather is due to the continued synthesis of dextran by enzyme molecules associated with the high MW dextran complexes that have already sedimented to the tube base. For these reasons it was realised that a more quantitative assessment of the bioreaction-separation process was required. Such work is reported in the following chapters.

7.0 BATCH BIOREACTION-SEPARATION STUDIES IN AN MSE SUPERSPEED 50 ULTRACENTRIFUGE

7.1 INTRODUCTION

Initial experimentation was focussed on determining the feasibility of the rate-zonal centrifugation technique, described in section 2.3.2, as a potential simultaneous bioreaction-separation process. Preliminary experimentation was undertaken to yield information concerning the distribution of the substrate, enzyme and reaction products after centrifugation. Also, product separation, rates of enzyme and product sedimentation, enzyme and product accumulation at the base of the tube and enzyme efficiencies were studied. The effects of four factor variables, run time, rotor speed, enzyme activity and substrate concentration were studied. These results are reported in section 7.4. In addition to these studies, a further set of trials were carried out in order to determine if the proposed rate-zonal bioreaction-separation process altered the molecular weight distribution (MWD) of the native dextran biosynthesised. These results are reported in section 7.5.

7.2 THE MSE SUPERSPEED 5O ULTRACENTRIFUGE

All trials were conducted on an M.S.E. Superspeed (SS) 50 ultracentrifuge. Operating instructions for this machine can be found in the M.S.E. technical publication number 24 (167).

A 3 x 20 cm^3 swinging bucket rotor was used (figure 7.1). At the minimum tube radius of 6.88 cm from the axis of rotation, the rotor generates an R.C.F. of 30 500g when revolving at 20 000 rpm. This corresponds by a maximum R.C.F. of 57 000g at the tube base.

Because a partial vacuum was generated in the centrifuge cavity during centrifugation, all the tubes were sealed within the rotor using bucket caps. The rotor itself was prewarmed to 25°C, the optimum temperature for dextransucrase enzyme activity and stability, prior to experimentation. This temperature was maintained during the trials using a temperature sensitive arm that was fitted into the rotor core prior to centrifugation. Usually, it is recommended in order to minimise mixing that the rotor should be allowed to coast to a halt without using the braking system. However, these studies required the rapid termination of enzyme activity at the end of a trial and this necessitated rapid rotor deceleration.

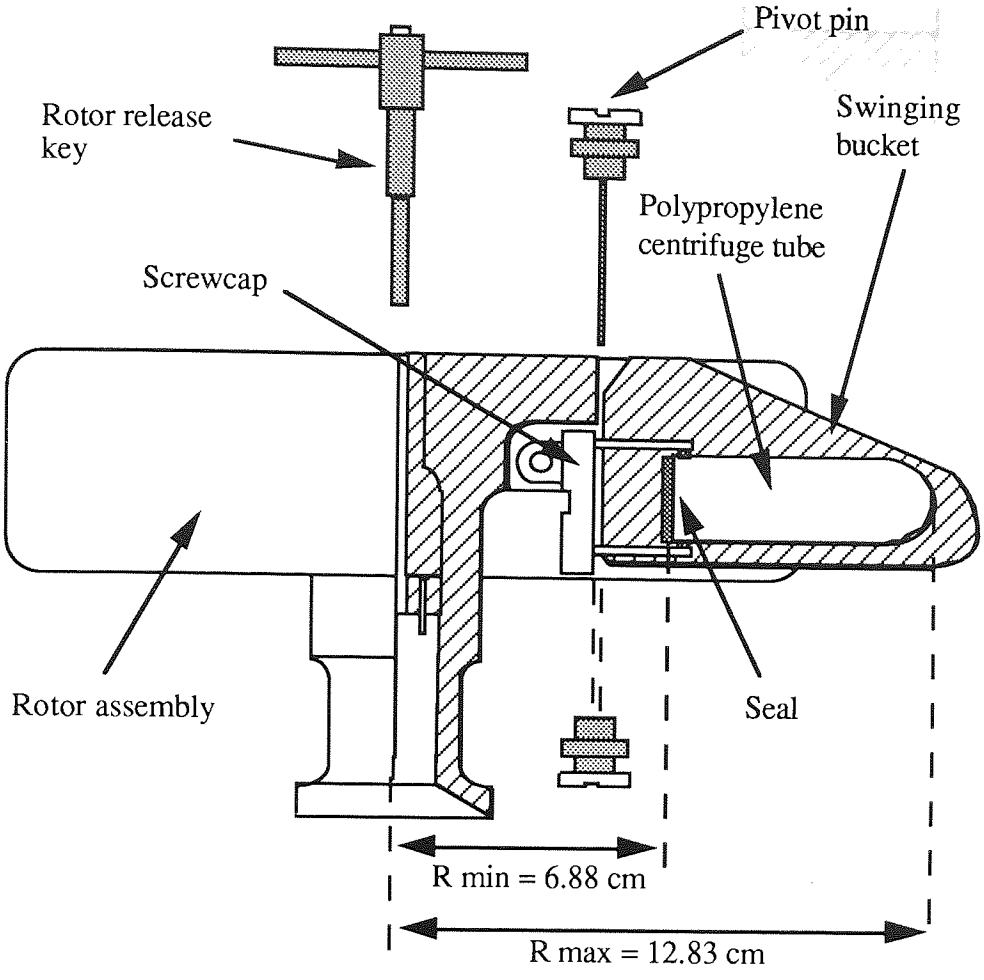

Figure 7.1 The MSE 3 x 20 cm^3 Swinging Bucket Rotor Assembly

7.3 PRACTICAL ASPECTS OF THE RATE-ZONAL CENTRIFUGATION TECHNIQUE

7.3.1 Minimisation of Convection

The use of density and viscosity gradients in rate-zonal separations has been discussed in section 4.4.2. The primary purpose of the gradients is to prevent convectional mixing and non-ideal sedimentation of the sedimenting zones of material due to hydrodynamic instability. Mixing by convection will have a negative effect on the proposed bioreaction-separation system by causing the dextransucrase enzyme molecules to sediment as a broad, poorly defined zone rather than as a more, well defined narrower band. This may result in poor separation of fructose molecules from enzyme rich zones of the bioreactor during dextran synthesis. A thin, well defined zone of enzyme material should result in a more instantaneous separation of the fructose and enzyme molecules and hence a minimisation of the acceptor reaction (figure 7.2).

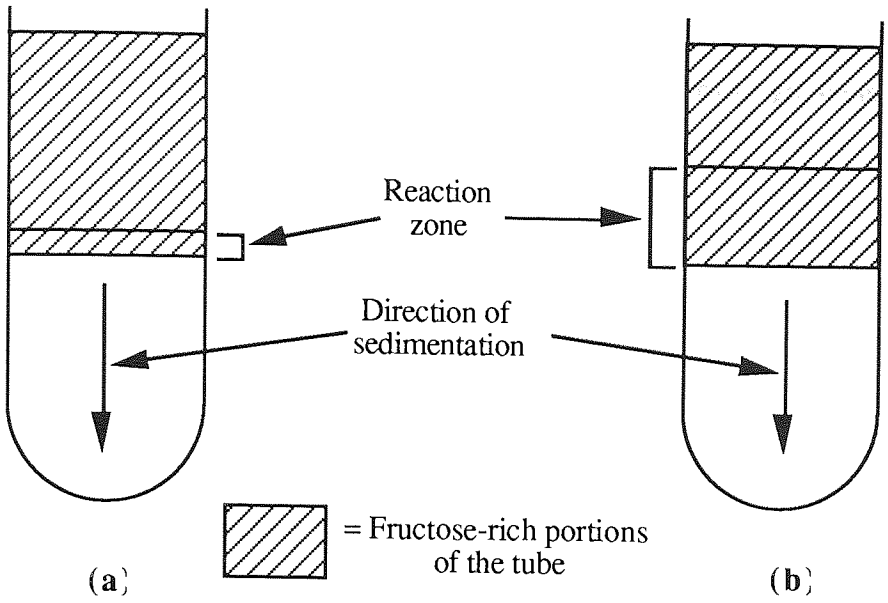

Figure 7.2 Broadness of Reaction Zone. (a) A thin reaction zone will give improved enzyme-fructose separation. (b) A broad reaction zone will give poorer separation.

However, the use of gradients will result in analysis problems. Consider, for example, a linear 5-20% w/w sucrose gradient in a centrifuge tube that was been overlaid with enzyme and centrifuged. As the dextransucrase enzyme sediments towards the tube base, it will pass through low, intermediate and high sucrose concentrations, where the levels of acceptor activity will vary accordingly. Thus accurate comparisons between the molecular weight distribution (MWD) of the polymer product from the rate-zonal bioreactor with a completely mixed conventional reactor cannot be made. However, Cohen et al [28] successfully used very 'shallow' density and viscosity gradients to minimise convectional mixing in their rate-zonal experiments using active enzyme.

A compromise was reached by conducting two sets of experiments. The first set were carried out to determine the distribution of the reaction products in the tube after a rate-zonal centrifugation of the dextransucrase enzyme through a shallow sucrose gradient. These experiments are reported in section 7.4. The second set of experiments were primarily concerned with the MWD of the polymer product and were carried out using 'flat' sucrose density and viscosity gradients, where a single concentration of sucrose was present throughout the gradient. These experiments are reported in section 7.5 and allowed direct comparisons between the MWD of the dextran product from the rate-zonal bioreactor and an equivalent, well mixed conventional batch reactor. Unavoidably, this will result in some zone mixing due to convection.

7.3.2 Gradient Loading Capacities

Factors governing the loading of samples onto density and viscosity gradients have been reviewed in section 4.4.2.5.

The theoretical maximum volumetric loading of sample onto a given gradient in an MSE 20 cm^3 centrifuge tube was based on the recommendation of Griffith[98]. The centrifuge tubes had a diameter of 2.3 cm corresponding to a maximum sample volume of between 0.5 and 1.0 cm^3. 0.6 cm^3 volumetric loadings were used in these experiments.

The theoretical mass of sample that a gradient can support has been determined by Svensson et al [127] (equation 4.30). This equation was not used in this study because the theoretical values obtained did not agree with the thorough and extensive experimental studies carried out by Brakke [128]. Therefore, in this study, the recommendations of Griffith [98] were followed. This required that the ratio between sample concentration (% w/w) and starting gradient concentration (% w/w) be 1:10 in swinging bucket rotors. Optimisation of sample loadings was studied in greater detail in chapter 9, where the design of the JCF-Z zonal rotor allowed a more quantitative assessment of gradient loading capacities.

7.4 BATCH BIOREACTION-SEPARATION STUDIES ON THE MSE SS 50 ULTRACENTRIFUGE

7.4.1 Introduction

The experiment described in this section was designed to determine the effects of a number of factors on the distribution of the two dextransucrase enzyme reaction products. The term factor refers to any variable experimental parameter such as rotor speed or run time.

The amount of experimental work required to assess a given number of factors can be minimised by factorial experimentation. A factorial experiment is designed so that the effect of changing any one factor can be assessed independently of any other factor. This is achieved by deciding upon a set of values, or levels, for each of the factors to be studied and carrying out one or more trials of the process at each of the possible combinations of the levels of the factors. The principles of factorial experimentation are given in Appendix A4.

The effects of four factors were studied, each at two levels, giving a total of 2^4 (=16) different sets of experimental conditions. The combination of the factor levels for a given trial is termed the treatment combination.

Each trial was evaluated by determining the distribution of the reaction products within the batch tube. Many independent sets of data can be obtained from this type of experiment, for example, the mass of dextran that pellets at the base of a tube, or the mass of fructose remaining in solution. Each such set of data is called a response.

For a given set of response values, the effect of a particular factor combination was assessed by determining the change in the response values caused by a change in that factor level. For example, when a factor is examined at two levels only, the effect is simply the difference between the average response value of all the trials carried out at the first level of the factor and that of all the trials carried out at the second level. This will result in all the factor combinations having an effect value, as is shown in the method described in appendix A4. The 'effect' of a factor is a measure of the change in the response value caused by that factor. Therefore, the importance of a change in the factor level on bioreactor performance can readily be assessed. In this study, the variance between the trials carried out at the different factor levels was required, and was calculated in a similar manner to the effect values as described in appendix A4. Variance is defined as the mean value of the squares of the deviations of a set of observations from their mean value. These values were statistically evaluated for significance by applying the variance ratio test (F-test) which will be discussed in this chapter.

7.4.2. Choice of Factors and Factor Variables

It is usual to denote a factor by a capital letter, while the factor levels are represented by a numbered subscript. The chosen factor and factor levels were:

A:	Rotor speed (r.p.m.)	A1 = 10 000	A2 = 20 000
B:	Run time (hours)	B1 = 1.5	B2 = 3.0
C:	Sucrose gradient (% w/w)	C1 = 8-12	C2 = 18-22
D:	Enzyme activity (DSU cm^{-3})	D1 = 60	D2 = 100

Thus each of the 16 treatment combinations can be represented using the above notation.

The levels of factor C show that shallow sucrose gradients were chosen. Gradient C1 had a starting concentration of 8% w/w, increasing linearly to a 12% w/w concentration at the tube base. Gradient C2 had a starting concentration of 18% w/w, increasing through to 22% w/w. The mean gradient concentrations were therefore 10% w/w and 20% w/w. Thus, changes in the distribution of product material due to changes in sucrose density and viscosity and the effects of the acceptor reaction could be determined.

Rotor speeds and run times were chosen after initial trials had been carried out using a modified form of equation 4.12:

$$\text{Ln}\,(r_2/r_1) = S\,\omega^2\,t \quad \text{—— (7.1)}$$

where r_2 = 12.83 cm, the radial position of the tube base rand r_1 = 7.43 cm, the average radial position of the meniscus in a centrifuge tube loaded with 20 cm^3 of material and t, the run time. The sedimentation coefficient (S) of the native dextran synthesised in a trial was taken as 250 Svedbergs based on the measurements made in chapter 6. These values allowed appropriate run times and rotor speeds to be selected using the above equation.

Each treatment combination was tested once only and in a random order, to eliminate any underlying time dependent trends. The order in which the experimental trials were performed is shown in table 7.1. Thus it can be seen that the first trial performed had a rotor speed of 20 000 rpm, a run time of 1.5 hours, an 8-12%w/w sucrose gradient and the dextransucrase enzyme used had an activity of 100 DSU cm^{-3}.

		A_1		A_2	
		B_1	B_2	B_1	B_2
C_1	D_1	6	12	3	9
	D_2	2	8	1	5
C_2	D_1	14	16	11	10
	D_2	4	7	15	13

Table 7.1 Experimental Programme

7.4.3 Experimental Details

The sucrose gradients were prepared by hand layering appropriately concentrated fractions of sucrose into preweighed centrifuge tubes. For the construction of the linear 8-12% w/w sucrose gradient, 8%, 10% and 12% w/w sucrose solutions were prepared in 0.1 molar acetate buffer at pH 5.2. A 10 cm^3 syringe, fitted with a long needle was used to place 6.5 cm^3 of the 8% w/w solution at the bottom of the tube. The syringe and needle were then carefully removed from the tube and filled with 6.5 cm^3 of the 10% w/w solution which was then gently injected into the bottom of the centrifuge tube, keeping the tip of the needle at the tube base (see figure 4.14). This process was repeated for the 12% w/w solution. If required, the tubes were balanced to within 0.1 g by adding or removing small volumes of the gradient material. Based on the recommendations of Griffith[98], the centrifuge tubes were left for 2 hours in a 25°C waterbath in order to form a smooth and continuous density

and viscosity gradient at the optimum temperature for enzyme activity and stability (section 3.5). Gradient formation has been discussed in more detail in section 4.4.2.4. An identical loading procedure was used to construct the 18-22% w/w sucrose gradients.

The total solids content of the enzyme solution to be loaded onto the gradient was determined using HPLC in order to ensure that the gradients were not being overloaded with sample (section 4.4.2.5). The enzyme was then warmed to 25°C and applied to the sucrose gradient using a 1 cm^3 syringe, fitted with a needle. The blunt tip of the needle was placed at a 45° angle to the tube wall, approximately 3 mm above the meniscus. A 0.6 cm^3 volume of enzyme was injected slowly and allowed to run down the side of the tube onto the sucrose gradient.

The tubes were then capped and loaded into the rotor, prewarmed to 25°C, as quickly as possible with the minimum of disturbance. The rotor temperature sensing device was then fitted and the rotor accelerated up to the required speed and spun for exactly 90 or 180 minutes before being decelerated to rest. The tubes were then carefully removed from the rotor and uncapped. The non-pelleted solution, henceforth referred to as the 'solution fraction' was removed from the tube using a pasteur pipette, care being taken not to disturb the pelleted material at the base of each tube.

Each solution fraction was thoroughly mixed before being placed in a boiling water bath for 5 minutes to denature the enzyme. The bases of each centrifuge tube were similarly immersed in the water bath to destroy enzyme activity within the pelleted fractions. The mass of each solution fraction was then determined by weighing. The masses of the remaining pelleted fractions were found by reweighing the centrifuge tubes. As native B-512F dextran gels are readily soluble in water, known quantities of water were then added to the centrifuge tubes and the tubes thoroughly shaken to recover all of the pelleted material. Sample analysis was achieved using the procedures detailed in chapter 5.

The quoted run times refer to the time that the tube contents were exposed to the maximum rotor speed, whereas in reality the time that the enzyme spent in contact with the substrate included the duration of enzyme loading, rotor acceleration and deceleration and fraction recovery. With practice, the time between the initial enzyme loading and final sample heat treatment was reduced to approximately 15 minutes longer than the quoted run times. This factor was taken into account when calculating such values as enzyme efficiency.

7.4.4 Results and Statistical Analysis

The masses of the solution and pellet fractions and the concentrations of the individual components in these fractions for each of the treatment combinations studied are presented in table 7.2 These results can be used to calculate several sets of responses that will allow the performance of the bioreactor-separator to be evaluated. A number of important sets of response values are listed in table 7.3. Many other sets of response values exist.

Response (1) measures enzyme 'efficiency', calculated by expressing the total mass of fructose detected on a trial as a percentage of the fructose detected in an equivalent, well mixed bench bioreactor. Responses (2) and (3) record the masses of dextran and fructose found in the pelleted and solution fractions respectively, response (4) measures the dextran to fructose mass ratio in the solution fraction and responses (5) and (6) record the percentage of the total mass of the dextran and fructose found in the pelleted fraction at the end of each trial.

Davies[168] has outlined a systematic tabular method for the calculation of the variance or mean square values for each factor and each interaction. This method is reported in appendix A4.

In this experiment, no trials were repeated and no prior estimate of the experimental error was available. Therefore it was necessary to estimate the error variance from the higher order interactions so that the significance of the variance values of a particular treatment combination could be assessed. The method used to estimate the error variance and the justification for using the higher order interactions to calculate the error variance is again detailed in appendix A4.

Knowledge of the error variance for a given set of response values allows the error variance ratio, called the F-ratio, to be calculated for each treatment combination. The F-ratio is simply the observed variance value of a treatment combination response value, divided by the error variance calculated for that particular set of responses. Again, details of the F-test are provided in appendix A4. Using F-tables, a standard F-value can then be obtained, which corresponds to the number of degrees of freedom used to calculate both the variance and error variance values based on a particular level of significance, which in this case, was set at 10%. As either positive or negative changes in the observed F-values were of interest, a double-sided test was appropriate, giving a standard F-value of 6.61. The level of significance must be stipulated at the start of a trial and then adhered to.

Treatment Combination	Mass of solution fraction (g)	Mass of gel (g)	% w/w 'gel' fraction			% w/w 'solution' fraction		
			Dextran	Sucrose	Fructose	Dextran	Sucrose	Fructose
A1B1C1D1	17.63	2.19	0.64	8.54	0.00	0.06	9.62	0.17
A2B1C1D1	18.32	1.52	1.00	7.07	0.25	0.04	9.76	0.18
A1B2C1D1	18.14	1.42	2.15	7.21	0.43	0.11	9.55	0.31
A2B2C1D1	18.00	1.95	2.55	5.92	0.84	0.00	9.48	0.22
A1B1C2D1	19.57	0.34	1.44	9.74	0.00	0.08	19.76	0.13
A2B1C2D1	19.25	0.68	1.31	8.78	0.60	0.06	19.88	0.14
A1B2C2D1	18.68	1.00	1.71	13.17	0.91	0.15	19.90	0.27
A2B2C2D1	17.56	2.32	1.69	7.21	0.83	0.04	20.79	0.22
A1B1C1D2	18.16	1.37	2.18	8.51	0.83	0.11	9.67	0.23
A2B1C1D2	18.13	1.56	2.78	8.70	1.15	0.00	9.21	0.19
A1B2C1D2	16.76	3.16	2.67	7.93	1.20	0.00	9.23	0.37
A2B2C1D2	15.85	3.49	2.70	9.23	1.73	0.00	8.73	0.25
A1B1C2D2	17.47	2.41	1.03	16.45	0.42	0.09	19.51	0.23
A2B1C2D2	18.42	1.55	2.25	14.23	1.09	0.07	19.82	0.20
A1B2C2D2	17.02	2.77	2.39	10.69	0.86	0.09	19.93	0.46
A2B2C2D2	16.35	3.41	2.23	8.83	1.22	0.08	20.21	0.35

Table 7.2 Experimental Results from the M.S.E. SS 50 Bioreaction-Separation Studies. Factorial Experiment

Treatment combination	Mass of Dextran in solution (mg)	Mass of Fructose in gel (mg)	Response 1 Percent enzyme activity	Response 2 Mass of Dextran in gel (mg)	Response 3 Mass of Fructose in solution (mg)	Response 4 Ratio of Fruc to Dex. in solution	Response 5 Percent Dextran in gel	Response 6 Percent Fructose in gel
A1B1C1D1	10.55	0.00	83.96	14.10	30.67	0.34	57.20	0.00
A2B1C1D1	6.56	3.74	98.93	15.24	32.40	0.20	69.91	10.35
A1B2C1D1	20.27	6.06	105.87	30.52	56.87	0.36	60.09	9.63
A2B2C1D1	0.00	16.40	93.81	49.79	39.36	0.00	100.00	29.41
A1B1C2D1	16.13	0.00	71.09	4.91	25.97	0.62	23.34	0.00
A2B1C2D1	12.45	4.09	82.86	8.90	26.18	0.48	41.69	13.51
A1B2C2D1	28.13	9.09	98.91	17.07	49.70	0.57	37.77	15.46
A2B2C2D1	7.55	19.21	97.61	39.29	38.81	0.19	83.88	33.11
A1B1C1D2	20.88	11.38	94.98	29.81	42.38	0.49	58.81	21.17
A2B1C1D2	0.00	17.99	93.30	43.30	34.82	0.00	100.00	34.07
A1B2C1D2	0.00	38.01	97.86	84.39	62.82	0.00	100.00	37.70
A2B2C1D2	0.00	60.53	96.74	94.39	39.15	0.00	100.00	60.72
A1B1C2D2	16.54	10.06	89.26	24.91	40.46	0.41	60.09	19.91
A2B1C2D2	13.03	16.97	95.80	34.80	37.25	0.35	72.76	31.30
A1B2C2D2	16.11	23.81	99.80	66.27	79.02	0.20	80.44	23.15
A2B2C2D2	13.83	41.58	96.67	75.94	58.03	0.24	84.59	41.74

Table 7.3 Some Selected Sets of Response Values Calculated from Table 7.2

Thus the F-value ratio obtained for any treatment combination for any given response can be assessed for significance at the 10% level by comparison with this standard F-value. For example; if an observed F-value was less than 6.61, then there was a greater than 10% chance that the observed variance was due to random variation. If greater than 6.61, then the observed F-value was significant. Discretion must be observed for F-values close to 6.61.

7.4.5 Discussion of Statistical Results

Most sedimentation theory is based on the fact that the sedimenting particle can be defined by a single sedimentation coefficient. In other words, there should be no change in particle properties during centrifugation. However, in the proposed bioreaction-separation process, dextran synthesis will result in the formation of particles that will increase in size and mass with time. The analytical ultracentrifugation studies (chapter 6) indicated that native dextran particles have mean sedimentation coefficients in the order of 250 Svedbergs at infinite dilution. Light scattering studies have shown that the formation of high MW native dextran particles to be extremely rapid (Section 2.4) due to molecular aggregation. Based on these observations, the assumption was made that the time taken to synthesise the high MW dextran particles with average $S_{20,w}$ values of 250 Svedbergs was relatively short compared with the time of centrifugation and was assumed negligible.

7.4.5.1 Effect of Rotor Speed

Table 7.4 lists the F-values obtained by increasing the rotor speed from 10 000 to 20 000 rpm for the sets of responses shown in table 7.3.

Response (Number)	F-Value
Efficiency of enzyme usage (1)	(+) 0.10
Mass of pelleted dextran (2)	(+) 20.73
Mass of fructose in solution fraction (3)	(-) 29.45
Rates of dextran to fructose in solution (4)	(-) 6.84
Percent pelleted dextran (5)	(+) 9.91
Percent pelleted fructose (6)	(+) 56.85

Table 7.4 The Effects of Increasing Rotor Speed.

Equation 4.1 shows that the centrifugal force acting on a particle at a radial position r in a centrifuge field is dependant on the effective mass of the particle and the square of the angular velocity of the rotor. Thus, when rotor speed only is increased, the centrifugal force acting on the particle will be increased. This will result in increased sedimentation

velocities. Native dextran particles have relatively high masses and thus will sediment rapidly towards the tube bases during centrifugation. Increases in rotor speed should therefore lead to increased masses of pelleted dextran. The F-values of responses (2) and (5) in table 7.4 show this to be the case. However, this was accompanied by a significant increase in pelleted fructose (response (6)). This was believed to be due to the following reasons:

Firstly, it appeared that some, or all of the rapidly sedimenting high MW dextran material that pelleted at the tube bases remained associated with the enzyme molecules, thus forcing these molecules to sediment with the native dextran particle aggregates, resulting in some enzyme activity in the gel fractions. Subsequent analysis in the zonal rotor (chapter 9) confirmed the presence of elevated levels of enzyme activity in the pelleted dextran rich fractions recovered from the system. Secondly, native dextrans are highly solvated particles, as was discussed in section 6.4.3. Therefore the physical 'entrapment' and forced sedimentation of fructose molecules within the highly solvated dextran particles may be occurring. This is know as 'entrainment'. Again, subsequent analysis in a zonal rotor (chapter 9) has confirmed this observation.

Increasing rotor speeds led to improved separation of dextran from fructose as reflected by the significant decreases in the dextran : fructose ratios in the solution fractions.

7.4.5.2 Effect of Run Time

Sedimentation theory treats run time and rotor speed as interchangeable factors. However, when biosynthesis as well as sedimentation is occurring, there will be changes in the system with run time due to the continuous formation of reaction products. Increased run times will result in increases in the masses of dextran and fructose synthesised in a trial. This is shown by the large positive F-values recorded for responses (2) and (3) in table 7.5.

Response (Number)	F-Value
Efficiency of enzyme usage (1)	(+) 2.99
Mass of pelleted dextran (2)	(+) 204.59
Mass of fructose in solution fraction (3)	(+) 103.65
Rates of dextran to fructose in solution (4)	(-) 5.20
Percent pelleted dextran (5)	(+) 8.58
Percent pelleted fructose (6)	(+) 51.14

Table 7.5 The Effects of Increasing Run Time

Equation 4.10 shows that the distance that a particle sediments in a given medium is dependent on the square of the angular velocity of the rotor and the run time. Thus when run time alone is increased, the particles will sediment a greater distance. This explains the significant increases observed in the percentages of pelleted dextran. However, increased levels of pelleted fructose were also noted. This was believed to be due to greater quantities of enzyme and fructose material reaching the tube bases due to entrapment within the highly solvated native dextran material, which was reaching the tube bases in larger quantities due to the longer run times. An increase in run time, like rotor speed, resulted in improved dextran and fructose separation in solution shown by a significant decrease in the dextran to fructose ratios. Again, this was linked to the increased levels of dextran sedimentation to the tube bases.

7.4.5.3 Effect of Gradient Concentration

The frictional resistance acting on a sedimenting particle is dependant upon the density and viscosity of the surrounding medium. An increase in average sucrose gradient concentrations from 10% to 20% w/w resulted in an increase in density from 1.0366 to 1.0790 g cm^{-3} and viscosity from 0.01179 to 0.01697 poise at 25°C [166]. The contribution to the medium by the native dextran material was not considered at this stage. Substitution of these values into equation 4.15 showed that the observed sedimentation coefficient in the average 20% w/w sucrose gradient was only 64% of the observed sedimentation coefficient in the average 10% w/w gradient, assuming no other complicating factors. Furthermore, the increased synthesis of low MW dextran at the expense of high MW dextran in the 20% w/w solution due to increased acceptor action will result in a mean decrease in native dextran sedimentation rates which may decrease the levels of pelleted dextran further. A significant decrease in pelleted dextran levels were noted at higher gradient concentrations as shown by the negative F-values for responses (2) and (5) in table 7.6. As expected, this led to a significant increase in the ratio of dextran to fructose found in the solution fractions at the higher substrate concentrations.

Response (Number)	F-Value
Efficiency of enzyme usage (1)	(-) 0.56
Mass of pelleted dextran (2)	(-) 20.63
Mass of fructose in solution fraction (3)	(+) 1.26
Rates of dextran to fructose in solution (4)	(+) 8.06
Percent pelleted dextran (5)	(-) 8.42
Percent pelleted fructose (6)	(-) 2.17

Table 7.6 The Effects of Increasing Substrate Concentration.

7.4.5.4 Effect of Enzyme Activity

Increases in enzyme concentration will result in greater quantities of dextran and fructose being synthesised. This was reflected by the significant positive F-values shown in table 7.7. However, there was no significant change in the proportion of dextran and fructose in solution.

Response (Number)	F-Value
Efficiency of enzyme usage (1)	(+) 0.49
Mass of pelleted dextran (2)	(+) 193.56
Mass of fructose in solution fraction (3)	(+) 38.78
Rates of dextran to fructose in solution (4)	(-) 3.32
Percent pelleted dextran (5)	(+) 10.80
Percent pelleted fructose (6)	(+) 88.06

Table 7.7 The Effects of Increasing Enzyme Activity.

7.4.5.5 Significant Interactions

The significant interactions found for the six responses that were considered in this experiment are summarised in table 7.8. The most significant interaction was recorded for response (2) between factors B and D, giving an F-value of (+)35.59. In other words, increases in both run time and enzyme activity further enhanced the mass of dextran found in the pelleted fractions. Increases in run time and enzyme activity alone were shown to increase the mass of pelleted dextran, as was indicated by the equivalent F-values in tables 7.5 and 7.7.

Treatment combination	Response number			
	(2)	(3)	(4)	(5)
A1 B2 C2 D1	(-)7.72		(+)7.24	(-)6.92
A1 B2 C1 D2	(+)35.59	(+)7.31		
A2 B1 C2 D1				(-)24.59

Table 7.8 Significant Interactions

Table 7.5 shows that, as expected, an increase in rotor speed alone led to a significant increase in the proportion of pelleted dextran whereas table 7.7 shows that an increase in sucrose viscosity and density led to a significant decrease in the proportion of pelleted dextran, which was expected. However, table 7.8 shows that these two factors interacted

negatively to yield a significant reduction in the proportion of the total dextran synthesised that was found in the pelleted fraction.

The remaining interactions recorded in table 7.8 were only just significant at the 10% level.

7.4.5.6 Enzyme Efficiency

The F-values for response (1) in tables 7.4 to 7.7 indicated that changes in the factor levels had no effect on enzyme efficiency. However, there F-values are only a relative measure of the enzyme efficiency between the different trials. Therefore, the masses of fructose synthesised in each of the trials were compared with the fructose synthesised in equivalent well mixed bench bioreactors. The results are shown in table 7.9.

Treatment combination	Mass (mg) Fructose Detected		Difference (Centrifugal minus static Bioreactor results)
	Static Bioreactor	Centrifugal Bioreactor	
$A_1 B_1 C_1 D_1$	36.53	30.67	-5.86
$A_2 B_1 C_1 D_1$	36.53	36.14	-0.39
$A_1 B_2 C_1 D_1$	59.44	62.93	3.49
$A_2 B_2 C_1 D_1$	59.44	55.76	-3.68
$A_1 B_1 C_2 D_1$	36.53	25.97	-10.56
$A_2 B_1 C_2 D_1$	36.53	30.27	-6.26
$A_1 B_2 C_2 D_1$	59.44	58.79	-0.65
$A_2 B_2 C_2 D_1$	59.44	58.02	-1.42
$A_1 B_1 C_1 D_2$	56.60	53.76	-2.84
$A_2 B_1 C_1 D_2$	56.60	52.81	-3.79
$A_1 B_2 C_1 D_2$	103.04	100.83	-2.21
$A_2 B_2 C_1 D_2$	103.04	99.68	-3.36
$A_1 B_1 C_2 D_2$	56.60	50.52	-6.08
$A_2 B_1 C_2 D_2$	56.60	54.22	-2.38
$A_1 B_2 C_2 D_2$	103.04	102.83	-0.21
$A_2 B_2 C_2 D_2$	103.04	99.61	-3.43

Table 7.9 Enzyme Efficiency

Significant differences between the static and centrifugal bioreactor data were assessed using a simple t-test as follows:

Mean difference $(\bar{x})$ of the two sets of data = -3.1019

Standard deviation (σ_{n-1}) of the differences = 3.188

Number of observations (n) = 16

Standard error of the mean ($\sigma_{n-1} / \sqrt{n}$) = 0.797

't' = mean / standard error of mean = -3.892

Number of degrees of freedom (n-1) = 15

The mean difference was negative, suggesting that the enzyme activity was lowered in a centrifugal field. Reference to a t-table showed that the appropriate 1% significance point was 2.60. The value of t was therefore significant at the 1% level and it was concluded that there was a 99% probability that the recorded enzyme activity was lower in the centrifugal bioreactor. Decreases in enzyme activity could be caused by a number of factors, such as:

(i) Deformation/denaturation caused by the high centrifugal forces and pressures, although Cohen et al [28] did not report any such problems (section 2.3.1).

(ii) Experimental error, such as fluctuating centrifuge cavity temperatures and incomplete recovery of the solution fractions and pelleted material.

(iii) Pelleted enzyme molecules may be 'cut off' from the supply of substrate during longer centrifugations or at higher rotor speeds due to the subsequent sedimentation and deposition of native dextran and enzyme molecules at the tube bases. Parts and Elbing[29] noted this phenomenon when studying the polymerisation of acrylonitrile (section 2.3.1).

At present, it would be difficult to conclude which , if any, of these factors is the most likely cause. It was expected that the zonal rotor studies would allow a more detailed examination of enzyme efficiency.

7.4.6 Quantitative Data

Although factorial experiments are invaluable methods for the evaluation of the effect of a given variable factor or factor combination on the performance of a system, the results obtained from such a study are only relative measurements. Equally useful observations can be made by examining the quantitative data obtained under the reported experimental conditions. Therefore the quantitative data reported in tables 7.2 and 7.3 is discussed in this section.

Firstly, consideration of the effects of the increasing density and viscosity of the sucrose solution on particle sedimentation will be considered. The average sedimentation coefficient of a band of sedimenting particles under standard conditions (in water at 20°C) can be defined by integrating equation 4.10 with respect to time and distance to give:

$$S_{20,w} = \int_{t_1}^{t_2} \frac{1}{\omega^2} dt \quad x \quad \int_{r_1}^{r_2} \frac{1}{r} dr \quad \text{___ (7.1)}$$

where r_1 and r_2 equal the radial positions of the particle zone at time t_1 and t_2 respectively.

In the case when a zone of particles is sedimenting through a gradient of increasing density and viscosity, equation 7.1 can be expressed as [135]:

$$S_{20,w} = \int_{t_1}^{t_2} \frac{1}{\omega^2} dt \quad x \quad \int_{r_1}^{r_2} \frac{(\rho_D - \rho_{20,w})}{\eta_{20,w}} \quad x \quad \frac{\eta_{SOLV,r}}{\rho_D - \rho_{SOLV,r}} \quad \frac{1}{r} dr$$

which for a run time of t simplifies to:

$$S_{20,w} = \frac{1}{\omega^2 t} \quad x \quad \frac{(\rho_D - \rho_{20,w})}{\eta_{20,w}} \quad x \quad \int_{r_1}^{r_2} \frac{\eta_{SOLV,r}}{\rho_D - \rho_{SOLV,r}} \quad \frac{1}{r} dr \quad \text{_____(7.2)}$$

where $\rho_{20,w}$, ρ_D and $\rho_{SOLV,r}$ are the densities of water at 20°C, the particle, and the gradient material at the operating temperature and radial position r respectively. The symbols $\eta_{20,w}$ and $\eta_{SOLV,r}$ equal the viscosities of water at 20°C and the gradient material at the operating temperature at radial position r.

Griffith[98] has compiled a table of values that allow the evaluation of equation 7.2 for different linear sucrose gradients at several specific particle densities and temperatures, whereby the above equation is written as:

$$S_{20,w} = \frac{1}{\omega^2 t} (IZ_2 - IZ_1) \times 10^{13} / 3600 = \frac{1}{\omega^2 t} \times k \quad (7.3)$$

where IZ_1 and IZ_2 equal integral values obtained from standard tables corresponding to the minimum (IZ_1) and maximum (IZ_2) concentrations of the sucrose gradient. In the following discussion, $[IZ_2 - IZ_1] \times 10^{13} / 3600$ has been abbreviated to k,with units of hours. $S_{20,w}$ and t are expressed in Svedbergs and hours respectively. Therefore $k/\omega^2 t$ will also have units of Svedbergs. The integral values take into account the initial and final radial positions of the sedimenting particle zone.

In the particular case when a band of particles sediment from the meniscus to the base of the tube (called pelleting), r_1 will equal r_{min}, the radial position of the meniscus and r_2 will equal r_{max}, the radial position of the tube base. Average r_{min}, and r_{max}, values of 7.43 and 12.88 cm were recorded for the loaded centrifuge tubes used in this study.

Assuming dextran particle densities of 1.6 g cm^{-3}, based on partial specific volume factor measurements (section 6.3.2.2), approximate integral values were obtained from standard tables for the two density gradients studied in this experiment. The results are shown in table 7.10.

Sucrose Gradient (% w/w)	Maximum sucrose conc. (Z_2) (% w/w)	Minimum sucrose conc. (Z_1) (% w/w)	IZ_2 Value	IZ_1 Value	IZ_2-IZ_1
8-12	12	8	2.580	1.391	1.189
18-22	22	18	4.257	3.657	0.600

Table 7.10 Gradient Integral Values

The $k/\omega^2 t$ term in equation 7.3 can now be evaluated for the different treatment combinations used in this study, as shown in table 7.11. Enzyme activity (factor D) will have no effect on the calculation of the k value. The $k/\omega^2 t$ value represents the minimum $S_{20,w}$ value, in Svedbergs, that a particle requires in order to be pelleted for a given treatment combination. Thus, for treatment combinations $A_2 B_2 C_2 D_1$ or $A_2 B_2 C_2 D_2$, only particles with $S_{20,w}$ values in excess of 126.6 Svedbergs will be pelleted.

Plots of the percentage of sedimented dextran versus $k/\omega^2 t$ are presented in figure 7.3. These plots show that the percentage of pelleted dextran increased markedly at low $k/\omega^2 t$ values, indicating that high rotor speeds and run times improve dextran sedimentation. In the less concentrated sucrose gradient, 100 percent dextran sedimentation was recorded at

k/ω^2t values of 250 Svedbergs. This indicates that the material in the pellet had $S_{20,w}$ values of at least 250 Svedbergs, which is in accordance with the $S_{20,w}$ values obtained in the presynthesised dextran sedimentation studies. This would indicate that the synthesis of high molecular weight particles occurs in a very short time period.

Treatment Combination	k value (hours)	Rotor speed (rpm)	Run Time (hours)	k/ω^2t (Svedbergs)
A_1 B_1 C_1 D1&D2	5.26×10^9	10 000	1.5	2008.5
A_2 B_1 C_1 D1&D2	5.26×10^9	20 000	1.5	502.1
A_1 B_2 C_1 D1&D2	5.26×10^9	10 000	3.0	1004.3
A_2 B_2 C_1 D1&D2	5.26×10^9	20 000	3.0	251.1
A_1 B_1 C_2 D1&D2	1.67×10^9	10 000	1.5	1012.7
A_2 B_1 C_2 D1&D2	1.67×10^9	20 000	1.5	253.2
A_1 B_2 C_2 D1&D2	1.67×10^9	10 000	3.0	506.4
A_2 B_2 C_2 D1&D2	1.67×10^9	20 000	3.0	126.6

Table 7.11 k/ω^2t Values (Factor D does not affect the k values)

Figure 7.3 also shows the effect of gradient concentration on dextran pelleting. At k/ω^2t values of 250 Svedbergs, only 40% of the total dextran produced had sedimented to the base of the tube in the 18-22% w/w gradient, compared with complete dextran removal in the less concentrated gradient. This decrease in dextran sedimentation was believed to be due to increased density and viscosity effects and increased acceptor activity. It was observed in section 7.4.5.3 that the observed sedimentation coefficient of a particle in a mean 20% w/w sucrose solution is 64% of its observed value in a mean 10% w/w solution under fixed external conditions. Furthermore, the work of Alsop[3] has shown that increasing sucrose concentrations results in large increases in low MW dextran (table 3.1).

Figure 7.3 also shows that at a k/ω^2t value of 1000 Svedbergs, which is equivalent to an $S_{20,w}$ value of 1000 Svedbergs, 60% of the dextran synthesised had pelleted in the 10% w/w sucrose gradient, compared with only 20% in the 20% w/w sucrose gradient. This indicated that dextran particles with $S_{20,w}$ values far in excess of the value of 250 Svedbergs, determined by analytical ultracentrifugation (chapter 6) had been synthesised. However, these apparently high sedimentation rates may be due to non-ideal sedimentation caused by gradient overloading and the hydrodynamic instability of the sedimenting material. These possibilities were studied more effectively using a zonal rotor, the results being reported in chapter 9. Svensson et al [127] have shown that the maximum mass of material a gradient can support is a function of the starting concentration of the gradient

(section 4.4.2.5). The fact that the very high rates of dextran sedimentation were more pronounced in the less concentrated gradient suggested that gradient overloading had occurred.

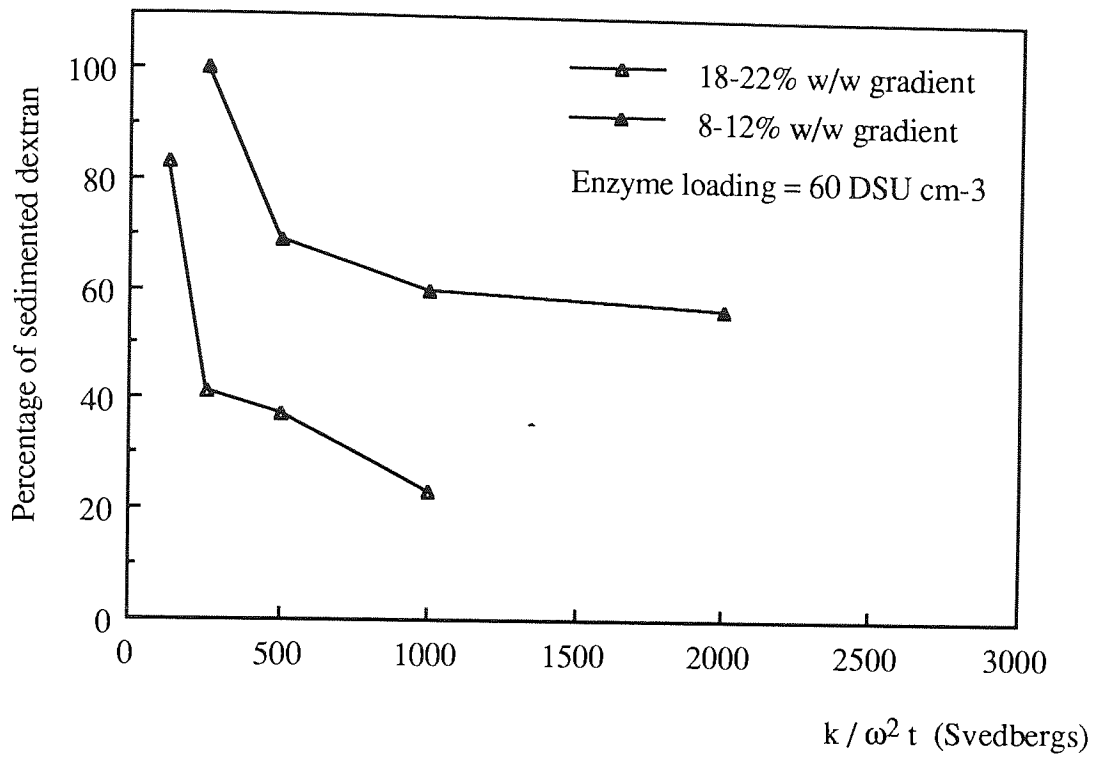

Figure 7.3 Plot of the Percentage of Sedimented Dextran versus k / ω^2 t

A plot of the percentage of pelleted fructose versus k/ω^2t is presented in figure 7.4. At a k/ω^2t value of 250 Svedbergs, 60% of the fructose produced was found in the pellet at the higher enzyme concentration, compared with only 30% at the lower enzyme concentration. As expected, pelleted fructose levels fell as the k/ω^2t value increased. It would therefore appear that enzyme concentration had a market effect on the distribution of the product materials. This may be due to an increase in particle interactions at the higher enzyme concentration, supported by the fact that the rate at which dextran particles sediment is highly dependent upon concentration, as was shown in table 6.2. Increases in particle interactions may lead to increased fructose and enzyme entrainment, which could be the cause of the observed increases in pelleted fructose levels.

A plot of the ratio of dextran to fructose (D:F) found in the pelleted fraction versus k/ω^2 t is presented in figure 7.5. This graph shows that higher D:F ratios were found in the pellet at higher k/ω^2 t values, suggesting that shorter run times and slower rotor speeds improve the quality of the sedimented dextran product. The low D:F ratios obtained at low k/ω^2 t values indicated that there was some enzyme activity at the bases of the tubes, caused by

increases in run times and rotor speeds. Poorer ratios were noted at higher enzyme activities, particle interactions again being considered the likely cause. The effect of particle interaction was subsequently studied more effectively using a zonal rotor (chapter 9).

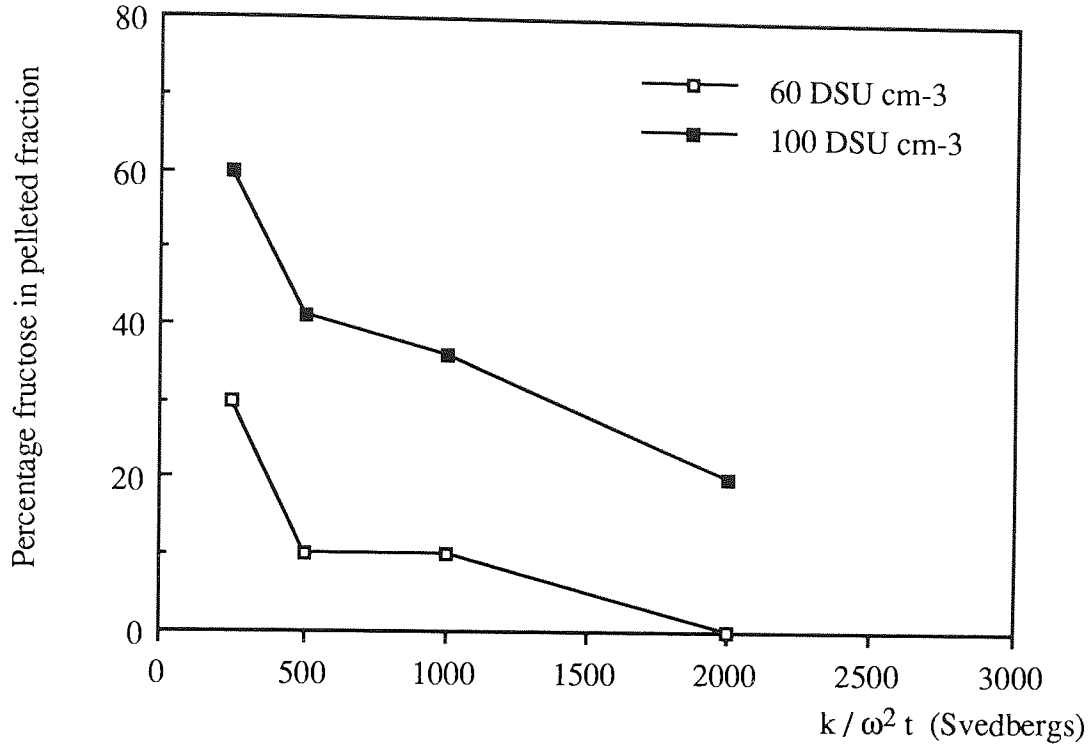

Figure 7.4 Plot of the Percentage of Pelleted Fructose Versus $k/\omega^2 t$

Bovey[47] has shown that at low substrate concentrations, native dextran particles typically have 'MWs' of between $3\text{-}5 \times 10^5$ and readily aggregate to form particle structures (section 2.4). Analytical ultracentrifuge studies have shown that these particles to be highly solvated and as a result may physically 'entrap' smaller particles within their structure. The presence of high levels of fructose in the pelleted zones indicated that both fructose and enzyme molecules were entrapped within the rapidly sedimenting native dextran particles. Thus, it is probable that rapidly sedimenting dextran-enzyme complexes were formed during the runs. Again, the zonal rotor proved a more effective tool in studying these phenomena.

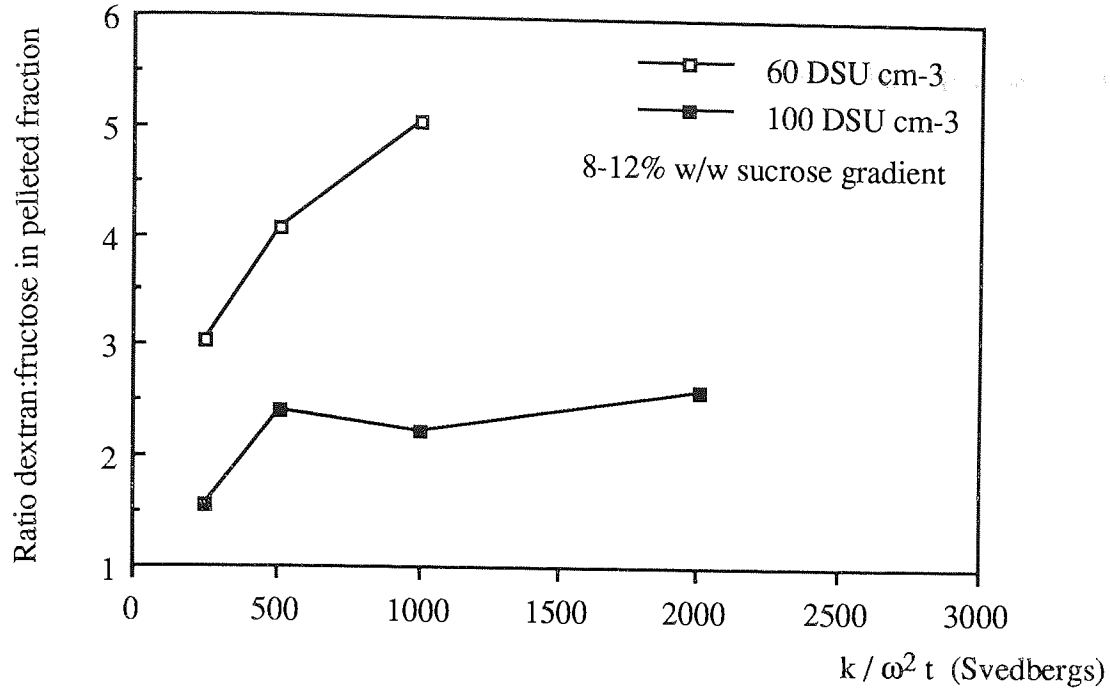

Figure 7.5 Plot of the Ratio of Dextran to Fructose Found in the Pelleted Fractions Versus k / ω^2 t

7.4.7 CONCLUSIONS

Increases in rotor speed improved dextran sedimentation to the tube base per unit time, but also resulted in significant increases in the amounts of fructose found at the tube bases. At lower rotor speeds, active enzyme molecules spend a longer time in solution which improves substrate conversion.

Longer run times led to small but significant increases in the percentages of pelleted dextran, which was accompanied by large increases in the percentages of pelleted fructose.

Increased sucrose concentrations reduced the amounts and proportions of dextran found in the pelleted fractions, but resulted in significant improvements in the ratio of dextran to fructose found in these fractions. Density and viscosity effects and the acceptor reaction are all increased at higher sucrose concentrations. The extremely high rates of dextran sedimentation in the less concentrated gradient suggested that gradient overloading had occurred. High bioreactor substrate levels are important for economic reasons, as discussed in chapter 2. The rate-zonal technique is expected to improve the yields of high MW dextran in concentrated sucrose solutions. Molecular weight distribution (MWD) studies of dextran fractions recovered from the centrifugal bioreactor are presented in the following section.

As expected, increased enzyme activities led to greater yields of product. It appeared that enzyme activity had a marked effect on the distribution of the product materials, which was believed be due to increased dextran particle interactions.

Very high rates of sedimentation were noted in many trials which was believed to be due to non-ideal sedimentation which can be caused by gradient overloading and the hydrodynamic instability of the sedimenting material. The purchase of a zonal rotor subsequently allowed a more accurate investigation of the factors that affect the proposal rate-zonal bioreaction-separation process to be undertaken (see chapter 9).

The high levels of fructose in the pelleted zones was believed to be due to enzyme and fructose entrainment by the highly solvated dextran particles. Again, subsequent evaluation using a zonal rotor proved this observation to be correct.

A longer term aim of this study was to develop semi-continuous and continuous centrifugal bioreaction-separation processes. This led to the evaluation of a Sharples T-1 laboratory supercentrifuge as a continuous bioreactor-separator, which is discussed in chapter 8.

7.5 DEXTRAN MOLECULAR WEIGHT DISTRIBUTION

7.5.1 Introduction

In addition to the dextransucrase product distribution experiment presented in the previous section, a further set of trials were carried out in order to determine if the proposed centrifugal bioreaction-separation process altered the molecular weight distribution (MWD) of the native dextrans biosynthesised during centrifugation.

It was envisaged that by using the rate-zonal process, biosynthesis of dextran and fructose would occur, coupled with the simultaneous removal of the fructose by-product from the active enzyme-rich portion of the centrifuge tube (see figure 2.8). It was expected that this would lead to an increase in the yield of high MW dextran by minimising the acceptor reaction. In an industrial process, this high MW product would then be broken down under controlled hydrolytic conditions to yield the clinical dextran product.

To test this hypothesis, a series of runs were carried out using the centrifugal bioreaction-separation technique. The MWD of the dextran products were then characterised by GPC (chapter 5) and compared with the dextran product from an equivalent well mixed conventional batch bioreactor. This was done by employing identical run times, substrate concentrations, enzyme stock solutions and enzyme volumetric loadings for both the bench and centrifugal bioreactors. The enzyme used was purified by centrifugation and diafiltration (section 3.8), but this still resulted in the presence of enzyme associated dextran in the purified preparations which interfered with the MWD studies. To eliminate this problem, equal volumes of enzyme, from the same stock solution were used in both the centrifugal and batch bioreactors. Any changes in dextran MWD could then be directly observed.

7.5.2 The Conventional Batch Bioreactor

The conventional batch bioreactor consisted of a beaker containing the sucrose substrate, to which a 0.6 cm^3 volume of the dextransucrase enzyme with an activity of 60 DSU cm^{-3} was added. The sucrose solution was prepared from a 25% w/w sucrose stock solution in a 0.1M acetate buffer, at pH 5.2. The reaction mixtures were left for 1.5 hours in a 25°C water bath before being heat treated to halt the reaction. Five different sucrose concentrations were studied, the reaction conditions being summarised in table 7.12.

Initial sucrose concentration (% w/w)	Mass of 25% w/w sucrose stock solution (g)	Mass of 0.1M acetate buffer, pH5.2 (g)	Total mass, buffer and stock solutions (g)	Volume enzyme (cm^3)
2.0	1.6	17.8	19.4	0.6
5.0	4.0	15.4	19.4	0.6
10.0	8.0	11.4	19.4	0.6
15.0	12.0	7.4	19.4	0.6
20.0	16.0	3.4	19.4	0.6

Table 7.12 Reaction Conditions for the Conventional Batch Bioreactor Experiments.

After heat treatment, the samples were dialysed and diluted as necessary before analysis by GPC. The trials were conducted in duplicate. A summary of the MWD of the dextran fractions obtained from the conventional batch bioreactor for the five sucrose concentrations studied in this experiment is presented in Table 7.13.

The values in this table show that increases in sucrose concentration from 2% to 20% w/w resulted in significant increases in lower MW dextran yields. This was expected because higher sucrose concentrations give rise to higher fructose concentrations in the locality of the enzyme active sites. Fructose molecules have the ability to displace growing dextran chains from enzyme molecules, resulting in the release of lower MW dextran (section 3.2.2). Table 7.13 shows that there was a very significant increase in dextran below 98 000 MW when sucrose concentrations were raised from 10% to 20% w/w. At a sucrose concentration of 20% w/w, between 30 and 40% of the total dextran produced was below 12 000 MW. This material would be unusable in the production of clinical grade dextran.

The rise in the levels of 'intermediate' dextran, that is, dextran with MWs of between 12 000 and 98 000, increased markedly at sucrose concentrations greater than 10% w/w. This data is illustrated graphically in figure 7.6.

Run Number	Inital Sucrose Concen-tration (%w/w)	% Dextran in Each Molecular Weight Range							
		179 -12 788	12 788 -39 950	39 950 -60 425	60 425 -83 957	83 957 -99 001	99 001 -126 961	126 961 -150 094	>150 094
1	2	-	0.12	0.46	0.63	0.36	0.70	0.56	97.17
2		0.20	0.76	0.54	0.68	0.39	0.74	0.59	96.10
3	5	0.69	2.92	1.43	1.36	0.78	1.31	0.98	90.53
4		0.53	1.50	1.38	1.28	0.72	1.30	1.09	92.20
5	10	7.73	0.77	0.50	0.60	0.34	0.63	0.51	88.92
6		6.82	1.56	0.65	0.54	0.31	0.46	0.79	88.87
7	15	25.84	2.66	0.53	0.73	0.22	0.39	0.27	60.69
8		20.17	2.34	1.88	1.67	1.54	1.32	1.17	69.91
9	20	30.61	8.86	1.98	1.36	0.68	1.01	0.72	54.78
10		38.42	5.97	1.35	0.77	0.82	0.56	0.90	51.21

Table 7.13 Dextran Molecular Weight Distributions at Different Sucrose Concentrations from the Conventional Batch Bioreactor.

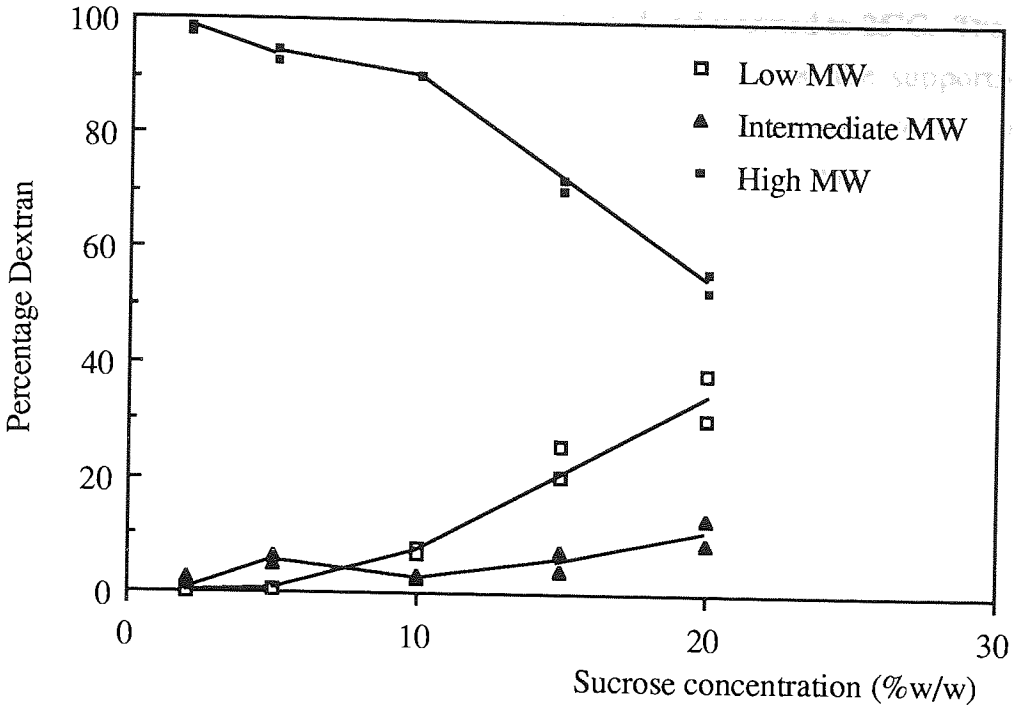

Figure 7.6 Changes in Dextran Molecular Weight with Sucrose Concentration in a Conventional 'Static' Bioreactor

7.5.3 The Centrifugal Bioreactor-Separator

Trials were carried out on the centrifugal bioreactor-separator using the rate-zonal centrifugation principle. Meaningful comparison between the MWD of the dextran products from the batch and centrifugal bioreactors can only be made if the substrate concentration is the same in both systems. Therefore, the use of sucrose gradients to prevent convection in the rate-zonal process was not possible, because the enzyme would sediment through increasingly concentrated sucrose solutions. This would, in turn, affect the acceptor reaction. Therefore, in the MWD studies, a constant sucrose concentration was used, giving 'flat' sucrose density and viscosity gradients. Unfortunately, this will result in some convectional mixing and an increase in hydrodynamic instability and non-ideal sedimentation.

A 25% w/w sucrose stock solution in a 0.1M acetate buffer at pH 5.2 was prepared and appropriately diluted to give 10, 15 and 20% w/w sucrose solutions using 0.1M acetate buffer at pH 5.2. 19.4 grammes of each solution were then added to 20 cm^3 capacity swinging-bucket rotor centrifuge tubes. The tubes were balanced by adding or removing small volumes of the sucrose solutions as required before being placed in a 25°C water-bath to reach the desired operating temperature.

Meanwhile, the enzyme stock solution was defrosted and warmed to 25°C. The total solids content of the enzyme was checked by HPLC to ensure that the supporting sucrose solutions were not being overloaded. The enzyme stock solution had a solids concentration of 0.3% w/w Enzyme volumes of 0.6 cm^3 were then added to each centrifuge tube The tubes were capped, placed in the rotor and accelerated to 10 000 rpm according to the method given in section 7.4.3. Upon reaching the operating speed of 10 000 rpm, the tubes were spun for exactly one hour before being rapidly decelerated to rest.

The overall MWD of the dextran produced in each trial was determined by thoroughly mixing and heat treating the centrifuge tube contents prior to dialysis and characterisation by GPC. The samples were heat treated exactly 1.5 hours after the enzyme had been loaded.

Six separate experiments, two at each sucrose concentration, were carried out, the conditions for these experiments being given in table 7.14. A summary of the results is given in table 7.15. Comparisons between the molecular weights of the dextran produced from the two reactors are presented graphically in figures 7.7 to 7.9

Run number	Initial sucrose concentration (% w/w)	Mass of sucrose solution (g)	Volume of enzyme solution (cm^3)	Rotor speed (rpm)	Run time (hours)	Run time at operating speed (hours)
1,2	10	19.4	0.6	10 000	1.5	1.0
3,4	15	19.4	0.6	10 000	1.5	1.0
5,6	20	19.4	0.6	10 000	1.5	1.0

Table 7.14 Reaction Conditions for the Centrifugal Bioreactor-Separator Experiments

7.5.4 Conclusions

From the results, the following conclusions were made:

(1) The centrifugal bioreactor produced up to three times less low MW dextran (<12 788 MW) than the conventional batch bioreactor at all three sucrose concentrations. At an initial sucrose concentration of 20% w/w, only 14% of the dextran produced was below 12 000 MW compared with 34% in the conventional bioreactor. This was believed to be due to a minimisation of the acceptor reaction caused by the partial removal of fructose from enzyme rich portions of the tube.

Run Number	Inital Sucrose Concen-tration (%w/w)	% Dextran in Each Molecular Weight Range							
		179 -12 788	12 788 -39 950	39 950 -60 425	60 425 -83 957	83 957 -99 001	99 001 -126 961	126 961 -150 094	>150 094
1	10	2.56	1.71	0.52	0.67	1.02	1.13	2.28	90.11
2	10	0.45	1.06	0.72	0.85	1.00	1.05	2.03	92.84
3	15	7.11	6.09	5.35	3.28	2.70	3.50	5.41	66.56
4	15	7.32	4.88	3.19	2.24	1.78	1.73	4.29	74.57
5	20	13.42	6.51	6.54	4.13	3.23	2.46	2.40	59.51
6	20	14.27	8.82	5.19	3.33	2.54	1.96	2.81	61.08

Table 7.15 Dextran Molecular Weight Distributions at Different Sucrose Concentrations from the Centrifugal Bioreactor-Separator.

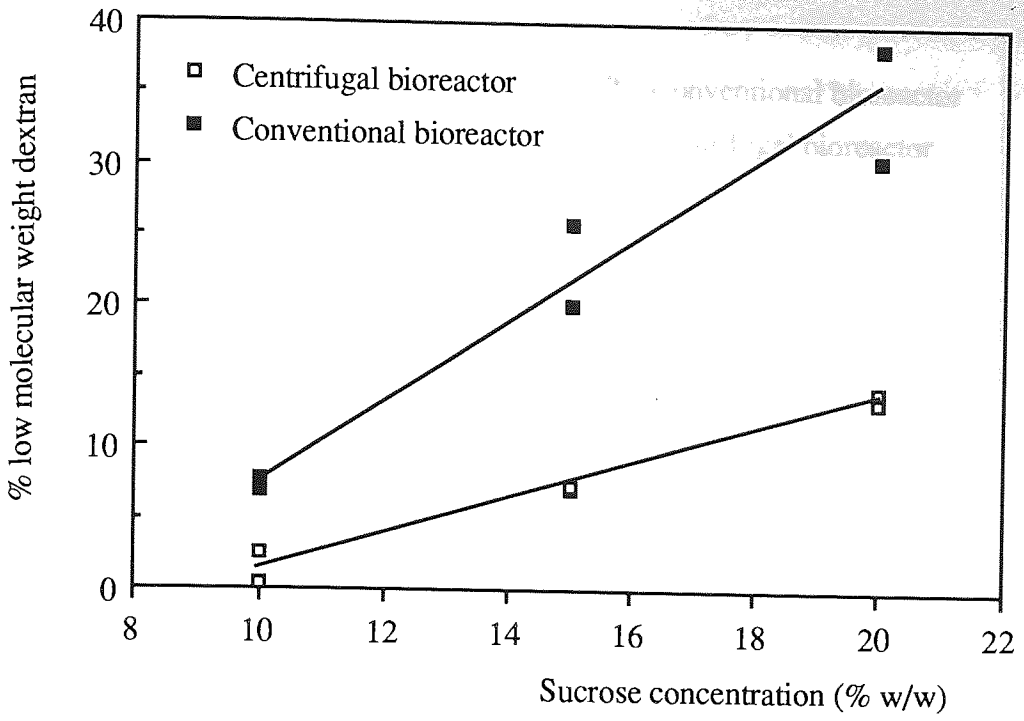

Figure 7.7 Comparison of the Percentages of Dextran Below 12 000 MW found in the Conventional and Centrifugal Bioreactors

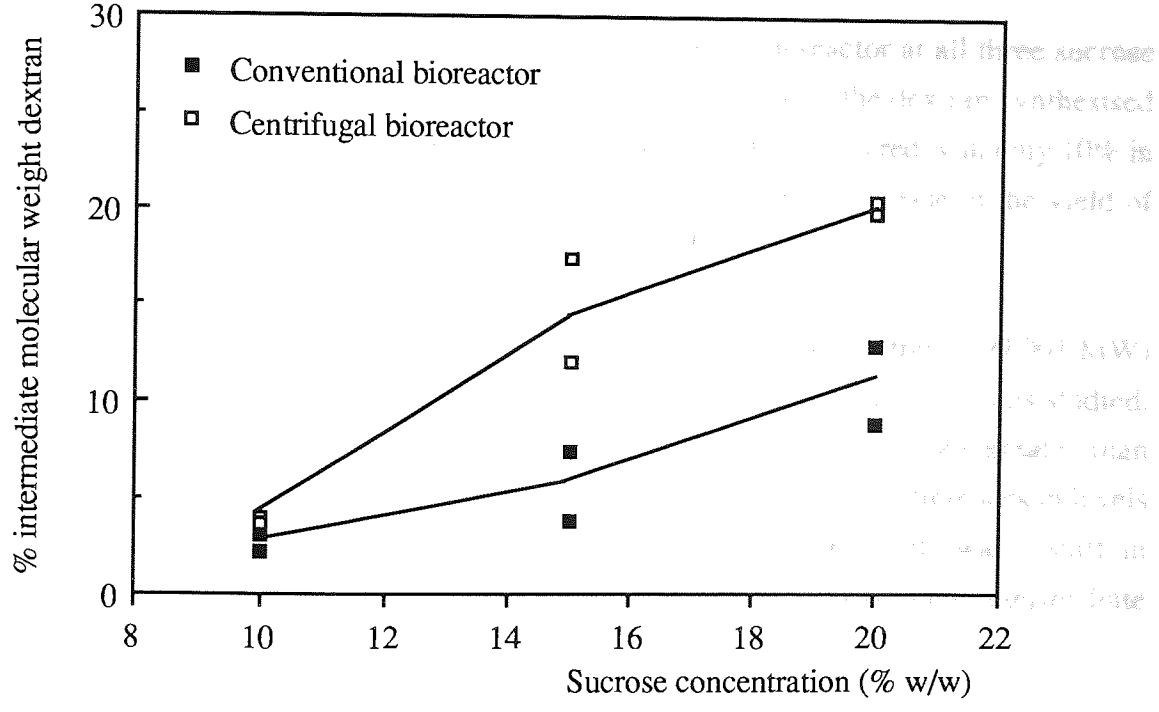

Figure 7.8 Comparison of the Percentages of Dextran Between 12000 and 98 000 MW found in the Conventional and Centrifugal Bioreactors

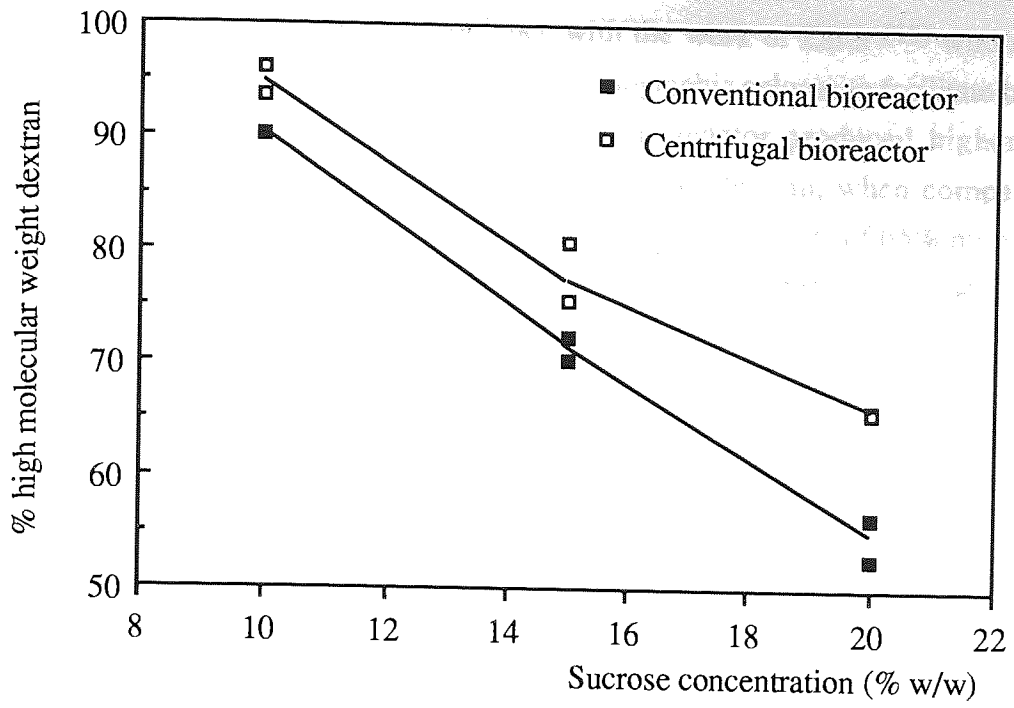

Figure 7.9 Comparison of the Percentages of Dextran Above 98 000 MW found in the Conventional and Centrifugal Bioreactors

(2) The centrifugal bioreactor produced higher levels of intermediate MW dextran (12 788 - 99 001 MW) than the conventional batch bioreactor at all three sucrose concentrations. At 20% w/w sucrose levels, up to 20% of the dextran synthesised was of an intermediate MW in the centrifugal bioreactor compared with only 10% in the conventional batch system. This represented a 100% increase in the yield of clinical range dextran.

(3) The centrifugal bioreactor produced 6-10% more high MW dextran (<99 001 MW) than the conventional batch bioreactor at the three sucrose concentrations studied. However, it is interesting to note that when the levels of dextran greater than 150 000 MW from the two reactors were compared, only small differences in levels were observed (figure 7.10). It was therefore concluded that there was a 'shift' in the dextran MWD from the low MW region of below 12 000 to the intermediate MW region of between 12 000 and 150 000.

(4) The bioreaction-separation process resulted in an increase in the levels of clinical range dextran. Clinical range dextran levels may be further improved by the addition of acceptor molecules to sucrose gradient solutions. This has already been suggested by Monsan and Lopez [91].

These results are found to be in accordance with the work of Zafar [15] who studied the dextransucrase reaction using a large scale chromatographic column to facilitate bioreaction-separation. He found that the chromatographic reactor produced higher levels of intermediate MW dextran at the expense of low MW dextran, when compared with a conventional batch system (figure 7.11). Furthermore, an average of 65% more high MW dextran was produced in the chromatographic reactor when compared with the conventional system at initial sucrose concentrations of 20% w/w.

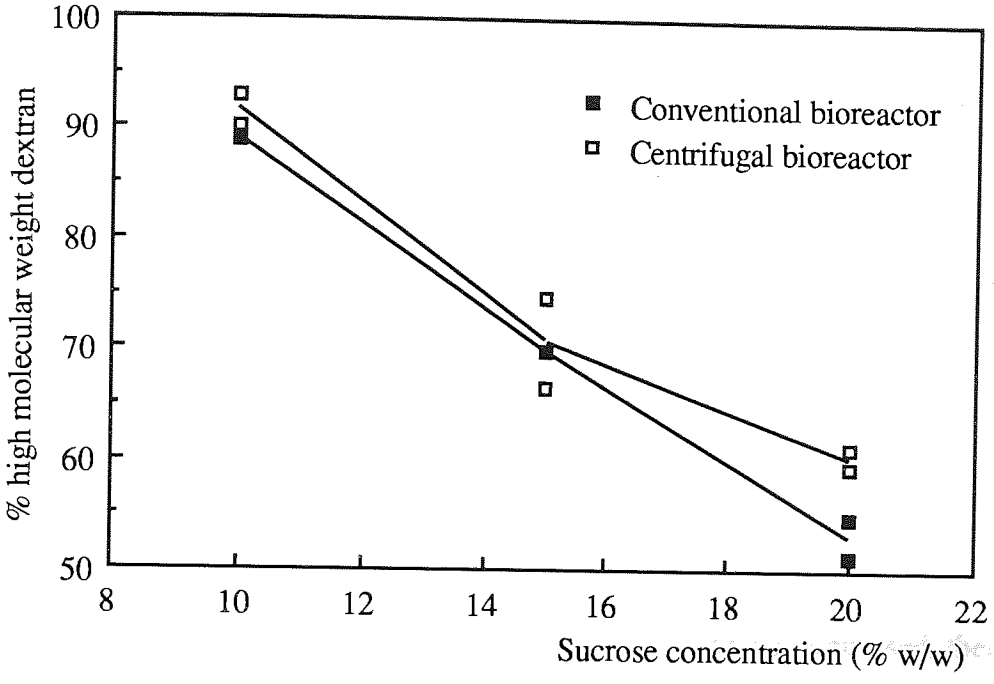

Figure 7.10 Comparison of the Percentages of Dextran above 150 000 MW found in the Conventional and Centrifugal Bioreactors

7.5.5 Future Work

This research has demonstrated for the first time that dextran can be manufactured in a centrifugal bioreactor-separator with improved yields of clinical and high molecular weight dextran as compared with a conventional batch bioreactor. However, there is a need to investigate the following points:

(1) Effect of enzyme volume; larger enzyme volumes may contribute to zone broadening effects, but can help increase dextran yields per unit time.

(2) Effect of enzyme activity; high enzyme activities will result in higher dextran concentrations in the bioreactor and hence will increase the likelihood of molecular interactions and 'entrainment' (section 7.4.5.1) which may affect the acceptor reaction.

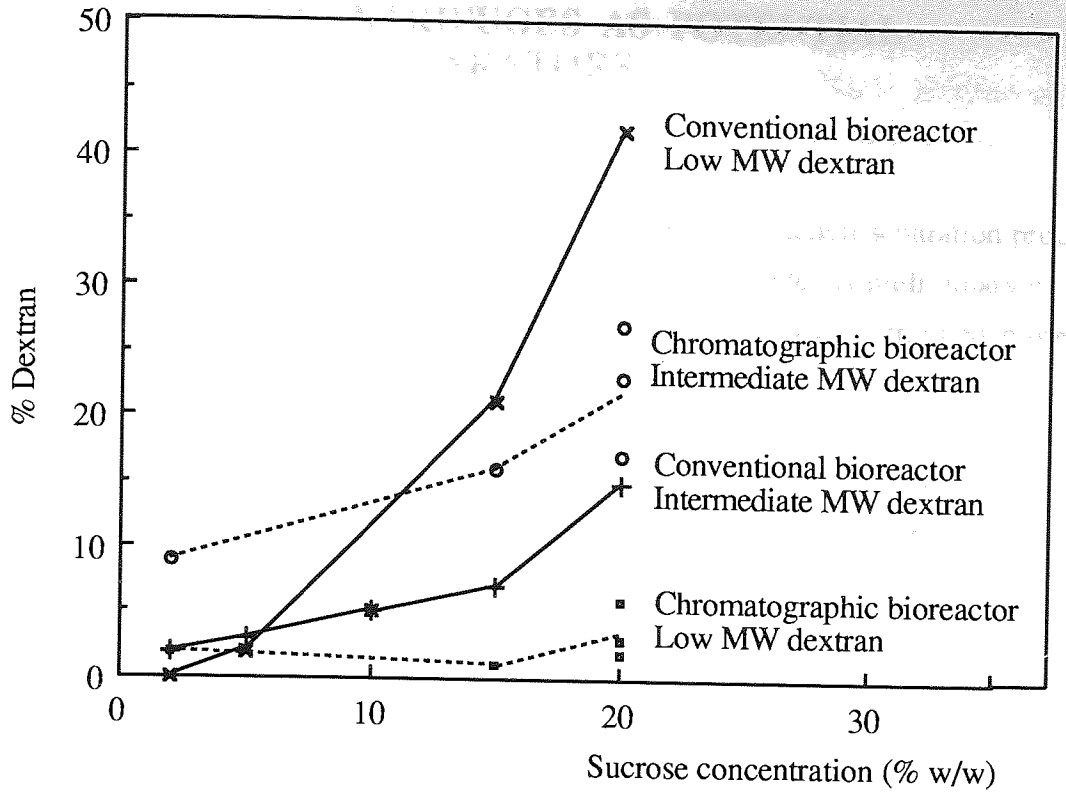

Figure 7.11 Comparison of the Dextran Molecular Weight Distribution in a Conventional Batch Bioreactor and a Chromatographic Bioreactor-Separator [15].

(3) Effect of rotor speed; Provided that entrainment can be minimised, then high rotor speeds will encourage the rapid removal of fructose from reaction zones in the bioreactor, but will result in faster rates of enzyme sedimentation. This will result in a decrease in sucrose conversion along the length of the tubes.

(4) The use of sucrose gradients; in this work, sucrose gradients were not used so that direct comparisons between the centrifugal and conventional batch bioreactors could be made. However, even 'shallow' density and viscosity gradients can help prevent convection and non-ideal sedimentation.

The effects of some of these factors were investigated using a zonal rotor, the results being presented in chapter 9.

8.0 TUBULAR CENTRIFUGES AS POTENTIAL BIOREACTOR-SEPARATORS

8.1 INTRODUCTION

A principle aim of this study was to develop a combined bioreaction-separation process that could be operated in either continuous or semi-continuous mode. A preliminary evaluation of the use of the rate-zonal centrifugation technique to achieve combined bioreaction-separation in batch systems has been assessed in chapters 6 and 7.

In this project a Sharples T-1 laboratory Supercentrifuge was used to study the continuous centrifugation principle. This machine is an example of a laboratory tubular settling centrifuge (see section 4.3.3).

The performance characteristics of the machine were initially assessed by calibrating the system using native dextran-fructose broths. The data obtained from this study allowed the process parameters that gave the highest throughputs of broth and maximum amounts of dextran removal from the broths to be determined. This data was used to predict the efficiency of the separation process on a number of different types of industrial centrifuge. The native dextran - fructose broth studies are presented in section 8.5.

The unique design of the tubular centrifuge lends itself to the possibility of being used as a continuous bioreactor-separator system as is described in section 8.3. Central to this process is the formation and maintenance of two distinct liquid zones in the tubular bowl. Studies on the flow patterns generated in the vessel during centrifugation are reported in section 8.6.

8.2 THE SHARPLES T-1 BENCH SUPERCENTRIFUGE

This machine is an example of a laboratory scale tubular setting centrifuge and was supplied by Pennwalt Sharples Limited (Camberley, Surrey, UK). The rotor, or bowl, is a hollow cylinder through which the process fluid is passed. Centrifugal force is generated by rapidly rotating the bowl about its long axis. The bowl is suspended from an overhead motor by means of a spindle and ball bearing assembly. The lower end of the bowl fits into a guide bushing which allows restricted movement, so that the bowl can freely rotate about its own axis. The process fluid is fed under pressure via a nozzle so that it 'jets' into the bowl. Tubular setting centrifuges can either be operated as clarifiers or as liquid-liquid separators.

Clarification describes the process whereby high 'molecular weight' particulate solids are removed from a process stream. Ideally, the solids will form a pellet at the rotor wall under an applied centrifugal field. Typical applications include the harvesting of bacteria and the recovery of finely divided metal particles. The clarification process is shown in figure 8.1. The liquid in the vessel is assumed to follow the plug flow model. The centrifuge must be halted at periodic intervals for the removal of accumulated material from the bowl wall.

The continuous liquid-liquid centrifugal separation process is capable of continuously separating and discharging two liquids of differing specific gravities. The heavier liquid fraction forms a cylindrical annulus bound by the inside wall of the bowl, above which 'floats' the cylindrical layer of the lighter liquid. When the liquids to be separated are fed into the bowl, they either sink or float to positions in the liquid layers that equal their own specific gravities and are separated. Centrifugal liquid-liquid separations are usually performed between immiscible liquids, such as the recovery of oil from water. The liquid-liquid separation process is shown in figure 8.2. Ring dams with different internal diameters are attached to the outlet and of the bowl in order to increase or decrease the thickness of the denser and lighter liquid layers as required.

8.3 BIOREACTION AND SEPARATION IN TUBULAR CENTRIFUGES

The proposed bioreaction-separation principle in a tubular centrifuge is shown in figure 8.3. In this proposal, the centrifuge would be operated as a continuous liquid-liquid separator, as described in the previous section. It was envisaged that the final process would incorporate two inlet ports, one to continuously introduce the denser sucrose solution and one to continuously introduce a thin layer of enzyme onto the surface of the sucrose solution. It was expected that density differences between the two solutions would be sufficient to maintain a distinct interface between the solutions (section 4.4.2.5). Under the effects of the applied centrifugal field, the enzyme molecules would sediment into the solution and bioreaction and separation would be achieved in the manner described in section 2.3.2. Assuming plug flow in both the flowing streams, it was envisaged that the enzyme molecules would progressively sediment through the denser solution to the bowl wall as the two solutions progressively moved along the length of the rotor. With the correct choice of process parameters, this would result in a supernatant phase, corresponding to the solution that originally held the enzyme molecules and a fructose rich phase. Dextran rich material would accumulate at the rotor wall. If the bowl is divided into a number of elements, as shown in figure 8.3, the similarities between this process and the bioreaction-separation principle shown in figure 2.8 can clearly be seen.

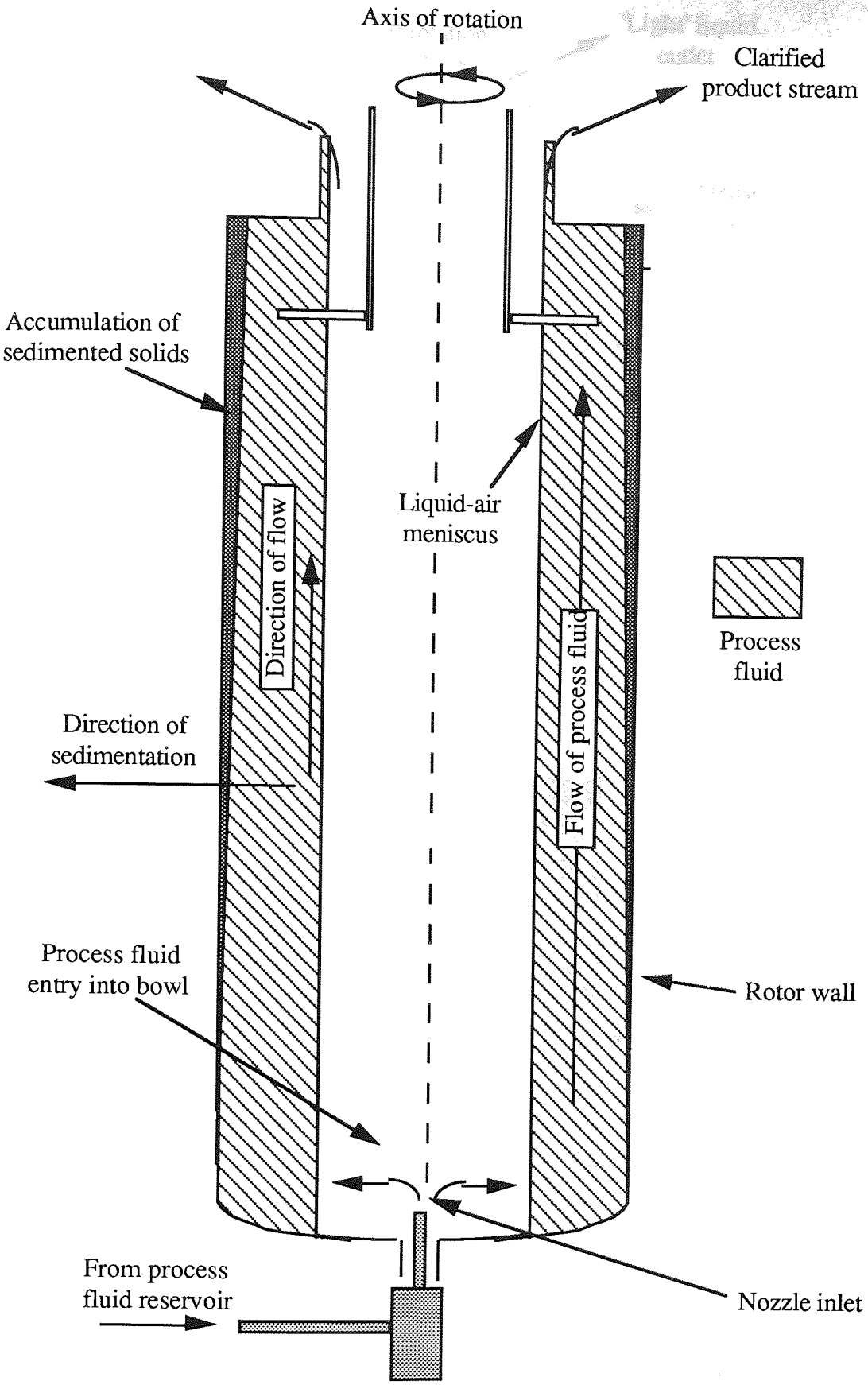

Figure 8.1 A Cross Section of the Tubular Centrifuge Rotor Showing the Clarification Principle and Fluid Flow Patterns

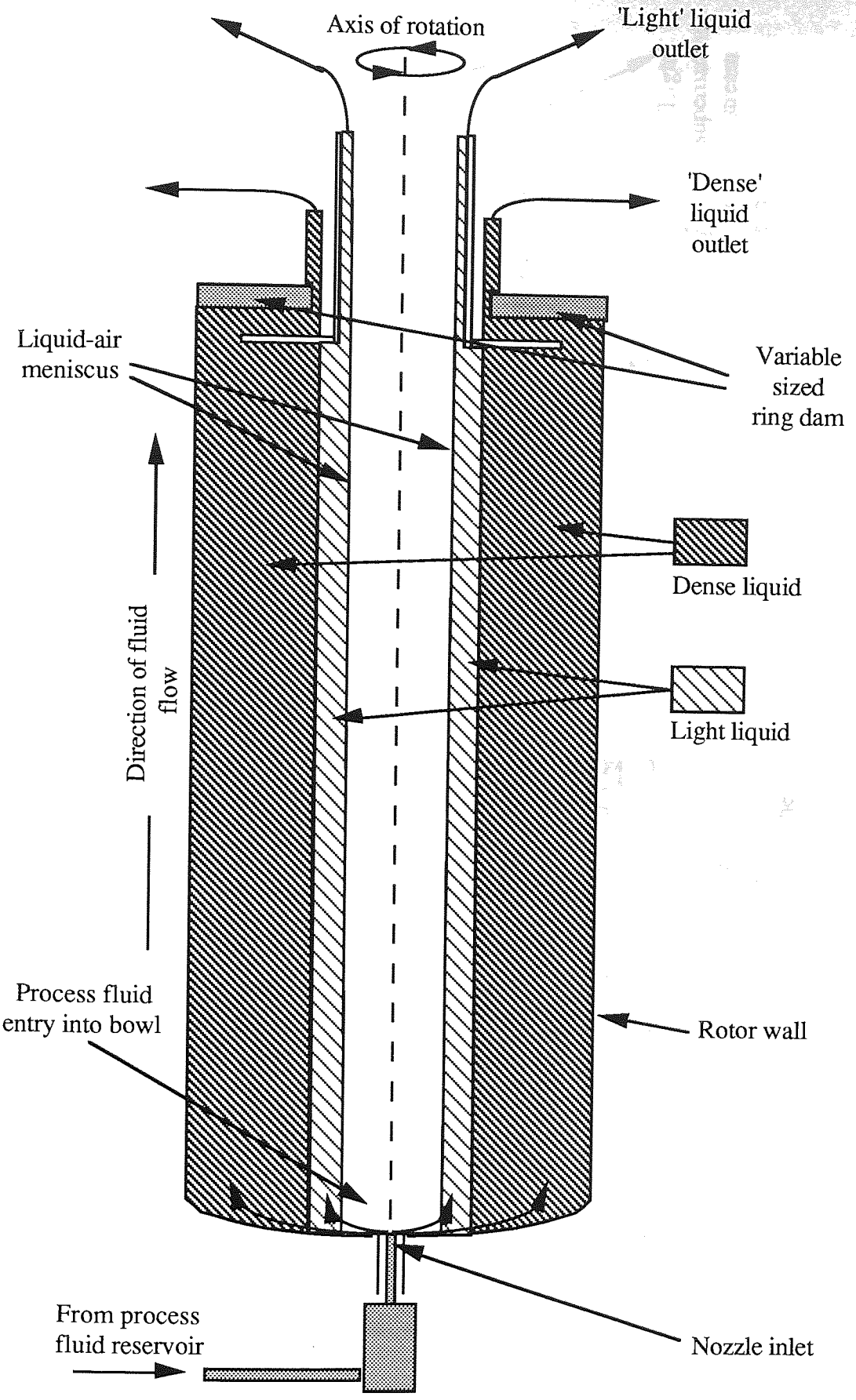

Figure 8.2 A Cross Section of the Tubular Setting Centrifuge Showing the Liquid-Liquid Separation Principle and Fluid Flow Patterns

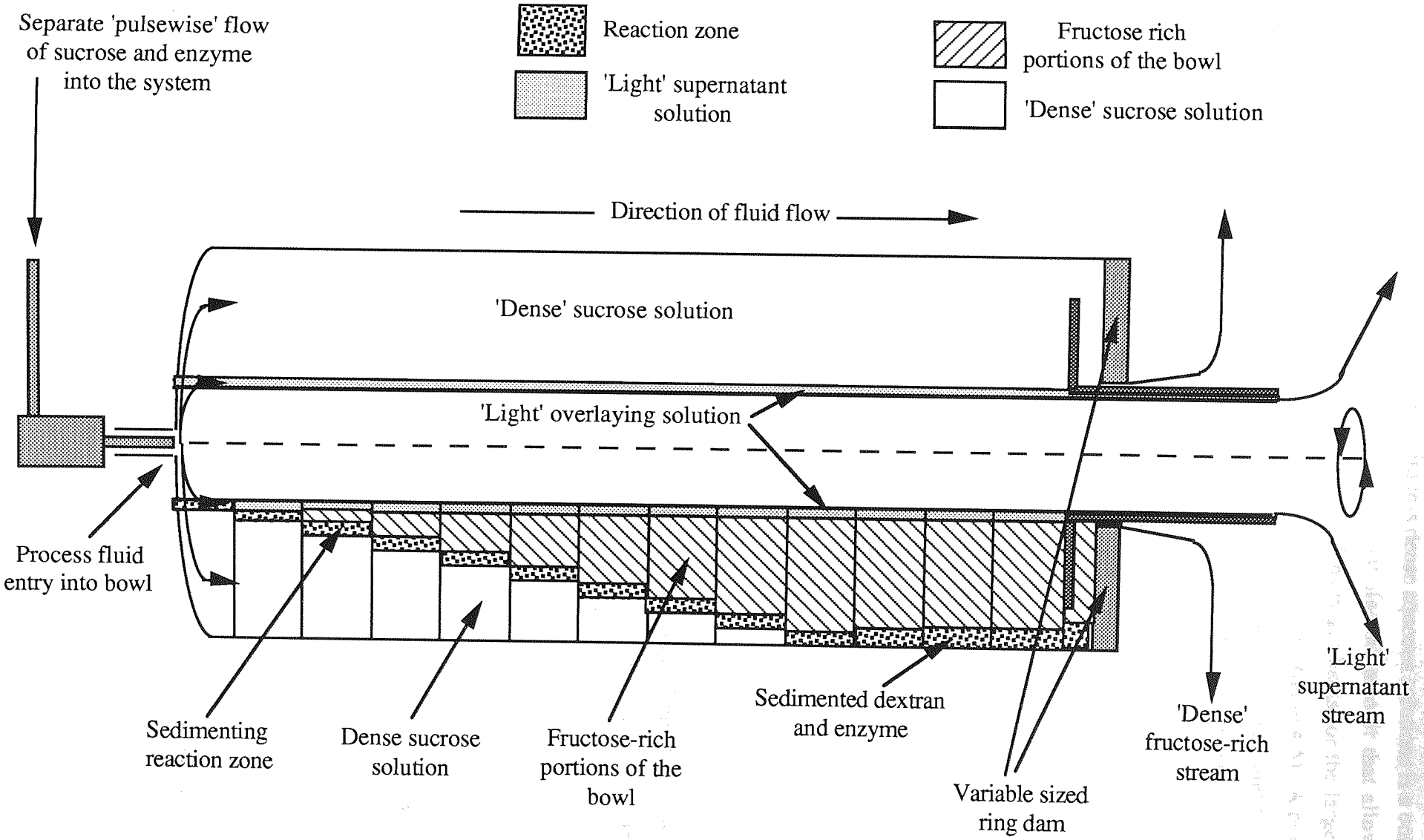

Figure 8.3: The Proposed, Highly Idealised, Bioreaction-Separation Process in a Tubular Settling Centrifuge.

The overlaying of dense aqueous solutions with less dense aqueous solutions is a common practice in centrifugation. For example, Beckman manufacture a rotor that allows the continuous passage of aqueous process streams over density gradients for the large scale separation of biological materials by rate-zonal centrifugation (see figure 4.5). A potential problem with this process would be the construction of continuous density and viscosity gradients within the bowl, which would be required to minimise convectional mixing and hence the acceptor reaction. However, the use of gradients may not be necessary in the development of a purely combined bioreaction-separation process if the constraints of the acceptor reaction are not considered.

8.4 SEDIMENTATION IN TUBULAR CENTRIFUGES

8.4.1 Sedimentation Theory

The theory of particle sedimentation in tubular centrifuges is discussed in this section. The radial sedimentation of particles in centrifugal fields has been reviewed in chapter 4. However, in a tubular centrifuge, account must also be taken of the axial flow of the liquid in the bowl. The following discussion is based on a normal rate separation (clarification) process, but can equally be applied to the rate-zonal process as will be described in section 8.5.2.

Consider a cylinder with end caps, rotating about its axis as shown in figure 8.4. The flow is assumed uniform and streamlined in the axial direction. Residence time distribution studies, to be presented in section 8.6 have indicated that the flow of solution through the bowl is a reasonable approximation to the plug flow model. Upon entering the bowl, the liquid phase is assumed to have an angular velocity identical to that of the rotating cylinder. If the particles in the feed solution are assumed to be uniformally distributed, can be characterised by a single sedimentation coefficient and are of a sufficiently low concentration so that interparticle interactions can be assumed negligible, than from equation 4.10:

$$\partial r/\partial t = S\omega^2 r \quad \text{—} \quad (8.1)$$

where r equals the radial position of any given particle (P) and t expresses the time that the particle has been subjected to the applied centrifugal field. The axial velocity of the particle is assumed identical to that of the continuous phase flowing through the cylinder, so that:

$$\frac{\partial z}{\partial t} = \frac{Q_o}{\pi (r_o^2 - r_i^2)} = \frac{Q_o l}{V} \quad \text{—} \quad (8.2)$$

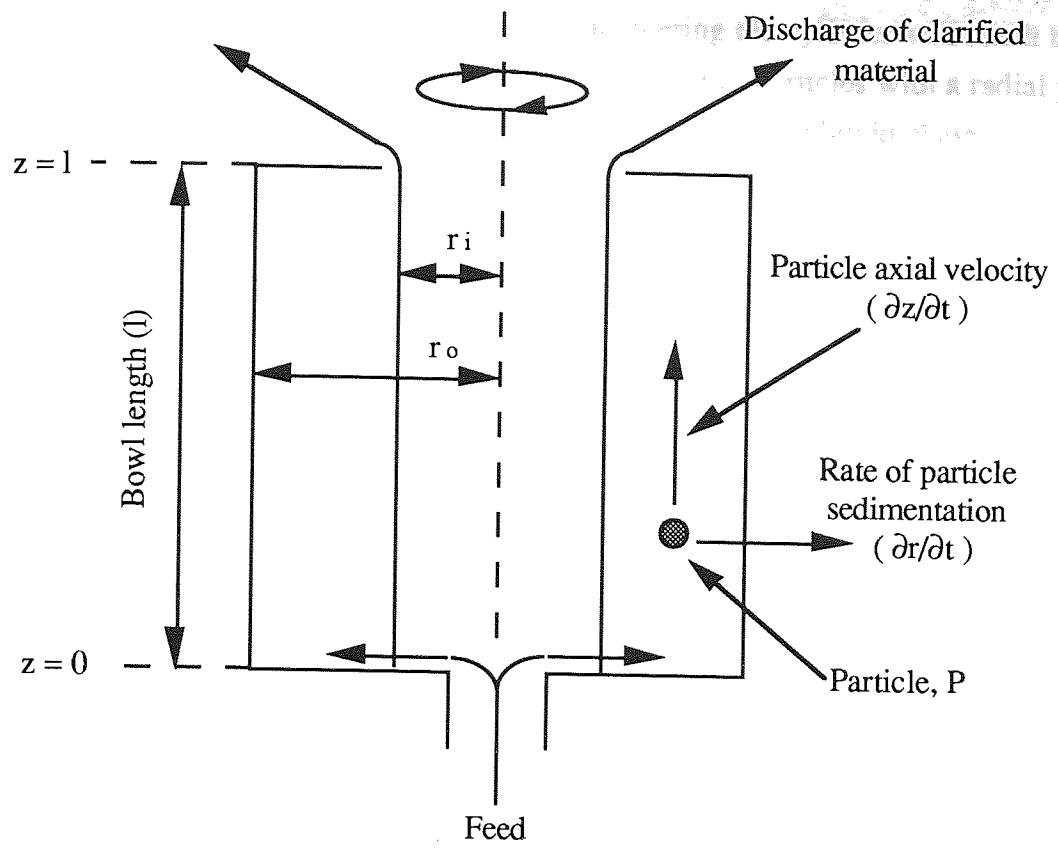

Figure 8.4 Sedimentation in a Tubular Centrifuge. (The symbols have been defined in the text.)

where z equals the distance along the axis of the cylinder measured from the point of particle entry into the centrifuge bowl, t is again the time interval that the particle has been subjected to the centrifugal acceleration, Q_o is the volumetric flow rate of the continuous phase, r_o and r_i are the radii of the inner cylinder wall and free surface of the liquid layer in the cylinder respectively, l is the length of the settling zone and V is the volume of the cylinder which is occupied by the continuous phase. Dividing equation 8.1 by 8.2 gives:

$$\frac{\partial r}{\partial z} = \frac{S\omega^2 r\, V}{Q_o l} \quad \text{—— (8.3)}$$

Integration of equation 8.3 between the limits $r = r_o$ at $z = l$ and $r = r$ at $z = 0$ determines the smallest radius, r, at which sedimentation of a particle with sedimentation coefficient S may start in order that it may just reach the cylinder wall after covering the full length (l) of the bowl. Thus:

$$\text{Ln}\left(\frac{r_o}{r}\right) \quad \frac{S\omega^2\, V}{Q_o} \quad \text{—— (8.4)}$$

Particles located at a radius greater than r when entering the cylinder will reach the rotor wall and will therefore be separated from the feedstream. Particles with a radial position less than r will not reach the wall and will leave the system in the liquid phase.

8.4.2 The Capacity Factor

If r is chosen such that the annular area confined between radii ro and r equals the area between r and ri, then:

$$\pi (r_o^2 - r^2) = \pi (r^2 - r_i^2) \quad \text{—— (8.5)}$$

Since a uniform initial distribution of particles is assumed, then there are initially as many particles in the outer annular area as in the inner annular area. If this condition is applied to equation 8.4, then 50% of the particles present in the suspension will sediment to the rotor wall and 50% will escape. This condition is referred to as the 50% cut off point. Rearranging equation 8.5 gives:

$$r = [(r_o^2 + r_i^2) / 2]^{0.5} \quad \text{— (8.6)}$$

Substituting into equation 8.4 gives:

$$Q_o = S \left(\frac{w^2 V}{ß} \right) \quad \text{— (8.7)}$$

where:

$$\beta = \text{Ln} \frac{r_o}{\left[\left(\frac{r_o 2 + r_i 2}{2} \right)^{0.5} \right]} \quad \text{——— (8.8)}$$

It is usual when defining the capacity factor of a centrifuge to express the settling velocity of the particle in a ' 1 g' gravitational field. In such cases, the 'acceleration' factor $\omega^2 r$ (see equation 4.1) will equal 1 g. Therefore, from equation 4.10, under earth gravity:

$$S = (dr/dt) / g \quad \text{—— (8.9)}$$

Expressing the settling velocity (dr/dt) at 1 g as υ_G, then equation 8.9 can be rewritten:

$$S = \upsilon_G / g \quad \text{—— (8.10)}$$

and equation 8.7 will become:

$$Q_o = \upsilon_G \left(\frac{\omega^2 V}{\beta g} \right) \quad \text{——} \quad (8.11)$$

It can be observed that the right hand side of equations 8.11 can be divided into two groups, the first group pertaining to settling properties of the particle and the second group pertaining to the centrifuge itself. This equation is usually written in the form:

$$Q_o = 2\upsilon_G \left(\frac{1}{2} \frac{\omega^2 V}{\beta g} \right) = 2\upsilon_G \Sigma_T \quad \text{——} \quad (8.12)$$

where

$$\Sigma_T = \left(\frac{1}{2} \frac{\omega^2 V}{\beta g} \right) \quad \text{——} \quad (8.13)$$

The Σ_T factor represents the theoretical 'capacity factor' for a given centrifuge and has units of area. This factor is often approximated by the following relationship [169].

$$\Sigma_T = 2\pi l \frac{\omega^2}{g} (0.75\, r_o^2 + 0.25\, r_i^2) \quad \text{——} \quad (8.14)$$

The capacity factor represents the area of a gravity settling tank that would be required to give an equivalent separating performance as a given centrifuge with an angular velocity of ω radians per second, assuming a constant υ_G value for both processes. In some cases the particle υ_G value may differ greatly between centrifugal and gravity systems due to particle disaggregation caused by the vigorous agitation and high shear forces that liquids are subjected to during acceleration on entering a centrifuge.

Similar derivations can be used to obtain capacity factor equations for different types of centrifugal separators, such as disk-type and bottle centrifuges [169]. The capacity factors of a number of commonly used centrifuges are shown in table 8.1

Centrifuge	Diameter ($2 \times r_o$) (cm)	Maximum speed (rpm)	Capacity factor ($\times 10^{-6}$ cm^2)	Recommended Scale-up Factors
Laboratory #(1)	4.45	23 000	2.84	1
Industrial # (1)	10.48	15 000	25.08	9
Industrial # (2)	12.70	15 000	39.02	14

Table 8.1 Scale-up Data for Tubular Settling Centrifuges[170].

8.4.3 Application of the Capacity Factor Concept.

Capacity factors are commonly used to predict the separating performance of different sized centrifuges. In order to do this, some further assumptions must be made [169]:

(1) No changes in particle size, shape or weight during centrifugation.

(2) Fresh feed is assumed to be uniformally introduced into the full space available for its flow. This condition requires that the feed material immediately occupies the full liquid layer thickness between the free surface and the rotor wall.

(3) The displacement of the flow pattern of the feed material by the sedimented material at the rotor wall is negligible.

(4) Remixing at the interface between the feed and sedimented material is assumed negligible.

Few of these assumptions are fully satisfied in practice and it is therefore not surprising that attempts to predict the theoretical separating performance of a centrifuge solely on the basis of the capacity factor concept have given disappointing results when compared with experimental data [169]. However, theoretically, the capacity factor concept does allow performance comparisons between geometrically and hydrodynamically similar centrifuges operating on the same feed material. Equation 8.12 shows that the sedimentation performance of two similar centrifuges treating the same suspension will be the same if the quantity Q_o/Σ_T has the same value for each. Thus for two similar centrifuges A and B, operating on the same feed material, equation 8.12 may be written:

$$Q_A / \Sigma_A = Q_B / \Sigma_B \quad \text{(8.15)}$$

Lavanchy and Keith [169] have published experimental data for the separation of a slurry in two similar centrifuge types at two different rotor speeds (figure 8.5). The experimental results closely supported the theoretical approach. The performance characteristic appears to be linear when plotted on logarithmic scales, this is indicative of a log normal size distribution of a particle species in suspension.

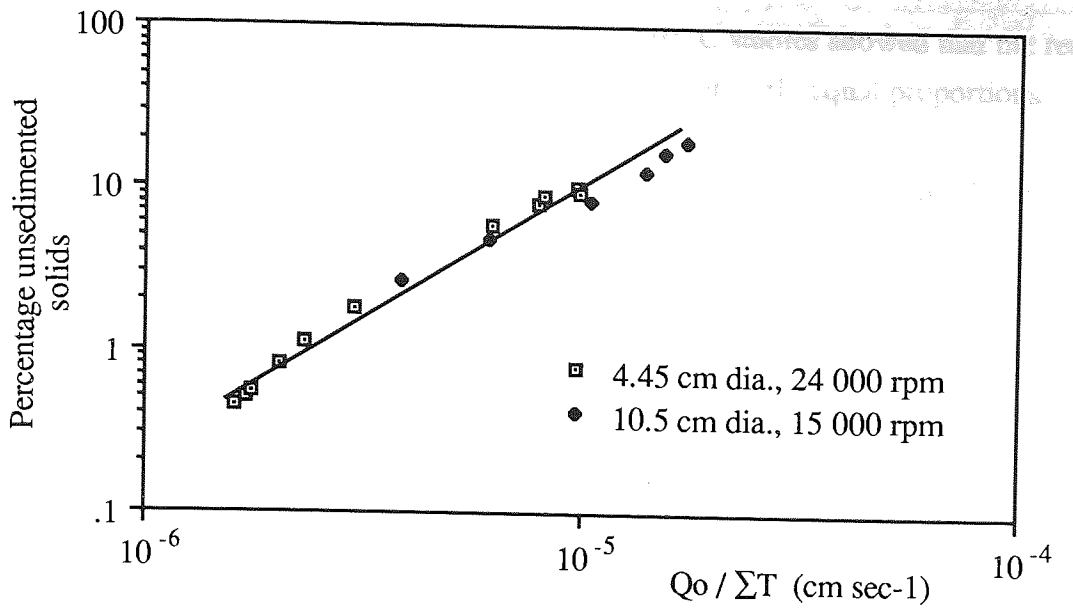

Figure 8.5 Sedimentation Performance Versus Qo/Σ_T on two Different Tubular Centrifuges [169].

8.5 SEPARATION OF NATIVE DEXTRAN AND FRUCTOSE BROTHS

8.5.1 Practical Considerations

The aim of the experimental work was to determine the suitability of using tubular settling centrifuges as combined bioreactor-separators for the production of dextran. The performance characteristics of the system were initially assessed by calibrating the system using native dextran fructose broths. This was achieved by determining the percentage of unsedimented high 'molecular weight' dextran material in the effluent stream at different Qo/Σ_T values. The degree of dextran-fructose separation was also studied.

The volumetric capacity of the spinning centrifuge bowl was measured using distilled water and was found to be 250.38 cm^3. The density of the water used was taken as 1 g cm^{-3} and the internal diameter and length of the bowl were taken as 4.45 cm and 19.95 cm respectively. This allowed the radius of the free liquid surface r_i to be calculated when the bowl was fully loaded, giving a value of 0.966 cm.

Dextran and fructose rich broths were prepared in the usual manner by adding purified dextransucrase enzyme to approximately concentrated sucrose solutions in 0.1 M sodium acetate buffers at a pH of 5.2 and at 25°C. The initial sucrose concentrations varied from between 1 and 10% w/w. After complete reaction had occurred, which was checked by HPLC, the broths were frozen in two litre volumes. The broths were defrosted as required

and allowed to reach room temperature before use. HPLC studies showed that the reaction broths consisted of mainly dextran and fructose in approximately equal proportions.

At the start of each run, the centrifuge bowl was accelerated to the required speed and a charge of broth was pumped into the bowl at a high flowrate, typically 50 cm^3 min^{-1}, until the broth was observed leaving the outlet ports at the top of the bowl. The broth flowrate was then adjusted to the required rate by measuring the effluent flowrate. A time period was then required for the system to approach a steady state. This was necessary because not all of the initial broth charge will have remained in the system for the required mean residence time before leaving the bowl. Only when all of the initial charge has been displaced from the bowl by the broth entering the system (according to the assumptions listed in section 8.4.1) will the difference in concentration between dextran in the effluent and feed stream be a true measure of the degree of clarification.

Residence time distribution (RTD) studies, presented in Section 8.6 for a single flowing liquid in the Sharples T-1 centrifuge indicated that material can remain in the system up to three times longer than the calculated mean residence time (RT). In this study, low flowrates were required, giving maximum mean RTs of around one hour. Therefore a three hour time period would be recommended for complete removal of the initial broth charge prior to any measurements. However, a second consideration is that as material accumulates at the rotor wall, the bowl radius, r_0, will decrease and will thus alter the capacity factor of the centrifuge. The longer the duration of a run, the greater the change in capacity factor, so measurements should be taken as close to the start of a run as possible. To minimise these conflicting problems, a compromise was sought. The same RTD studies showed that, generally, around 95% of a material will have left the system after two mean RTs. Furthermore, the relatively low dextran broth concentrations resulted in relatively low rates of accumulation. The effluent sample was collected over a 30 minute period commencing exactly two mean RTs after the initial bowl loading. The average effluent flow rate was determined over the same time period.

The dextran and fructose concentrations of the effluent were quantified by GPC and HPLC and were expressed as percentages of the initial feed concentrations. The operating conditions used in these runs are listed in table 8.2.

Run Number	Initial Sucrose Concentration (% w/w)	Effluent Flowrate in $cm^3\ min^{-1}$	Effluent Flowrate in $cm^3\ sec^{-1}$	Rotation Speed (rpm)
2	1	7.33	0.12	21 800
8	1	4.11	0.07	22 600
9	1	4.31	0.07	23 100
12	1	4.50	0.08	37 800
13	1	3.40	0.06	38 200
14	1	6.27	0.10	37 800
19	1	3.64	0.06	13 600
22	1	7.17	0.12	22 700
6	2	4.15	0.07	38 900
11	2	3.54	0.06	24 500
15	2	7.00	0.12	22 200
16	2	3.70	0.06	22 800
18	2	6.17	0.10	23 100
23	2	3.42	0.06	38 400
7	3	3.58	0.06	22 800
20	3	3.61	0.06	39 100
21	3	6.24	0.10	38 600
1	5	4.17	0.07	38 200
3	10	3.84	0.06	39 120

Table 8.2 Operating Conditions for the Native Dextran and Fructose Broth Separation Studies

8.5.2 Results and Discussion

The β factor was calculated for the Sharples T-1 centrifuge using equation 8.13. If r_o is assumed unchanged at 2.22 cm, then β is equal to 0.260. Similarly, the volumetric capacity of the bowl was assumed unchanged at 250.38 cm^2. Taking g to be 981 cm sec^{-2}, the capacity factor of the centrifuge was found to equal 0.49 ω^2. The capacity and Q_o/Σ_T factors and percentages of unsedimented dextran for each of the runs listed in table 8.2 are presented in table 8.3.

This table shows that at higher total broth concentrations, very low levels of dextran sedimentation were recorded. This was believed to be due to concentration and viscosity effects. Analytical ultracentrifuge studies (chapter 6) showed that an increase in dextran concentration from 0.5% to 1.5% w/w led to a tenfold decrease in sedimentation rate. The 5% and 10% w/w broths in this study behaved similarly and appeared to have the classic

properties of a gel in a centrifugal field as defined by Svedberg and Pedersen [94] (section 4.6).

The data in table 8.3 was used to construct plots of the percentage of unsedimented dextran versus Q_o/Σ_T values. Logarithmic plots indicated an approximately linear relationship between these two factors for the 1, 2 and 3% w/w broth concentrations as shown in figure 8.6, although further data points would be valuable in confirming these observations.

Run Number	Rotor Speed Squared(ω^2) ($x10^{-6}$ sec^{-2})	Capacity Factor (Σ_T) ($x10^{-6}$ cm^2)	Q_o/Σ_T ($x10^8$ cm sec^{-1})	Percentage Unsedimented Dextran (%)
2	5.23	2.54	4.80	56.05
8	5.59	2.72	2.52	51.53
9	5.82	2.83	2.53	48.59
12	15.66	7.63	0.98	19.12
13	15.95	7.76	0.73	24.12
14	15.65	7.62	1.37	22.81
19	2.03	9.90	6.13	70.70
22	5.64	2.75	4.35	64.46
6	16.62	8.09	0.86	42.99
11	6.60	3.21	1.84	81.32
15	5.38	2.62	4.46	88.35
16	5.68	2.76	2.23	85.44
18	5.84	2.84	3.62	67.72
23	16.19	7.88	0.72	40.57
7	5.68	2.77	2.15	84.22
20	16.71	8.21	0.73	76.12
21	16.28	9.01	1.30	81.40
1	16.00	7.78	0.90	94.78
3	16.78	8.16	0.79	91.30

Table 8.3 Experimental Capacity Factors, Q_o/Σ_T Values and Percentages of Unsedimented Dextran

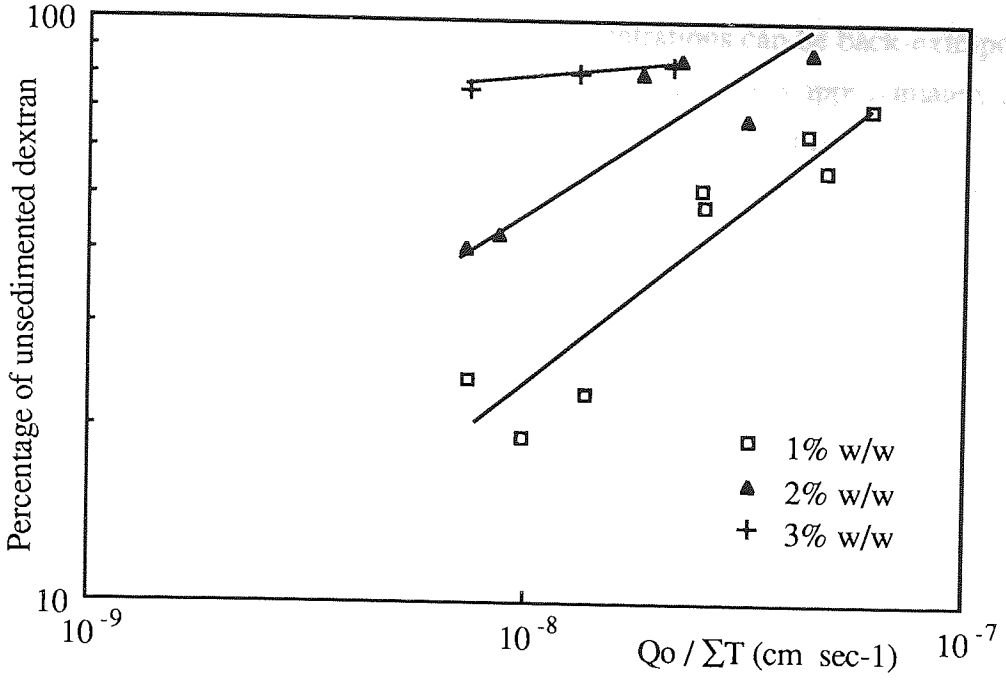

Figure 8.6 A Plot of the Percentage of Unsedimented Dextran Versus Q_o/Σ_T for Native Dextran and Fructose Broths

The difference in the percentage of unsedimented dextran between the 1, 2 and 3% w/w broths at different Q_o/Σ_T levels can clearly be seen. The highest level of sedimentation for a given Q_o/Σ_T value was achieved at the lowest broth concentration. For example, at a Q_o/Σ_T value of 1.0×10^8 cm sec^{-1}, 75% of the dextran in a 1% w/w broth sedimented to the rotor wall, compared with only 20% in a 3% w/w broth. This was believed to be due to concentration and viscosity effects. The low level of sedimentation recorded for the 3% w/w broth solution (containing around 1.5% w/w native dextran) was comparable with the analytical ultracentrifuge data (chapter 6) which showed that the sedimentation rate of a 1.5% w/w native dextran sample was about ten times less than that of a 0.5% w/w dextran.

However, calibration of the system using native dextran and fructose solutions had been successfully achieved. If the plots shown in figure 8.6 are assumed to be linear, then this allows prediction of the process parameters required for a given degree of dextran sedimentation to be determined on the Sharples T-1 centrifuge. For example, to achieve a 50% removal of dextran from a 1% w/w reaction broth, a Q_o/Σ_T value of 3.6×10^{-8} cm sec^{-1} was required. A Sharples T-1 centrifuge bowl, rotating at 38 000 rpm has a capacity factor of 8×10^6 cm^2. Thus to achieve the required level of sedimentation, a flowrate of 17.3 cm^3 min^{-1} is required.

Figure 8.6 also indicates that the three broth concentrations can be back-extrapolated to a point where no measurable dextran sedimentation occurs. This is approximately equivalent to a Q_o/Σ_T value of 10 x 10^{-8} cm sec^{-1} for the three broth concentrations. Thus for a Sharples T-1 centrifuge with a capacity factor of 8 x 10^6 cm^2, flowrates in excess of 50 cm^3 min^{-1} will result in no measurable dextran sedimentation.

The lowest Q_o/Σ_T values studied in this work were around 0.7 x 10^{-8} cm sec^{-1}. Lower Q_o/Σ_T values could be obtained by using centrifuges with higher maximum capacity factors and by lowering flowrates. An estimate of the machines performance at lower Q_o/Σ_T values can be found by assuming a linear relationship between the log percentage of unsedimented dextran and log Q_o/Σ_T and extrapolating the plots to lower Qo/Σ_T values. For the 1, 2 and 3% w/w broths, approximately 94%, 82% and 38% dextran sedimentation respectively was achieved at a Q_o/Σ_T value of 0.1 x 10^{-8} cm sec^{-1}. This corresponds to a feed flowrate of 0.5 cm^{-3} min^{-1}, assuming a capacity factor of 8 x 10^6 cm^2. This low flowrate indicates that alternative centrifuge systems with significantly higher capacity factors are required to achieve high levels of dextran sedimentation per unit time.

The above calibration process was based on a normal rate separation technique (section 4.4.1). In order to apply the findings to a rate-zonal bioreaction-separation in a tubular settling centrifuge, the following points should be considered. Firstly, the rate of synthesis of the dextran particles. Light scattering studies have shown this to be very rapid [47,60] and for the purpose of calculation, this has been assumed negligible when compared with mean native dextran sedimentation rates (Chapter 6). Secondly, the sedimentation of a dextran particle in a rate-zonal centrifugation will effectively be from the liquid meniscus to the rotor wall. Thus, to recover all of the sedimenting zone of dextran, all of the zone must reach the rotor wall before the process fluid exits the system. This is equivalent to a normal rate separation in a tubular centrifuge where 100% dextran sedimentation is achieved. In the above discussion, it was noted that a tubular centrifuge with a capacity factor of 8 x 10^6 cm^2 required a flow rate of 0.5 cm^3 min^{-1} for the removal of 94% dextran in a 1% w/w feed stream. This would be a prohibitively low flow rate of process fluid in an industrial rate-zonal process, but many centrifuges with far higher capacity factors are commercially available. Furthermore, the concentration effects will be lower than in normal rate centrifugation, which will lead to significantly higher dextran sedimentation rates. The complete removal of dextran from the process fluid would yield a fructose rich product stream which has a high commercial value.

8.5.3 Dextran-Fructose Separation in the Tubular Centrifuge

Because of the very low MW of fructose, it was expected that there should be almost no fructose sedimentation and pelleting during the passage of the dextransucrase feed broths through the centrifuge vessel. This presumption was tested by measuring the fructose concentration of the feed and eluent streams for the 1% and 2% w/w feed broths.

By dividing the fructose concentration of the effluent stream by that of the feed stream, the percentage of pelleted fructose could be calculated for each run. These values are presented in table 8.4. From this data, the ratio of sedimented dextran to sedimented fructose could be calculated, the values also being presented in table 8.5.

Run No.	Broth Concentration	% Sedimented Fructose	Ratio of Sedimented Dextran to Fructose
2	1% w/w	8.57	5.13:1
8		6.86	7.07:1
9		10.60	4.85:1
12		9.26	8.73:1
13		7.79	9.74:1
14		7.41	10.42:1
19		6.99	4.19:1
22		9.19	3.85:1
6	2% w/w	7.29	7.82:1
11		5.26	3.55:1
5		3.61	3.23:1
16		3.10	4.69:1
18		8.41	3.84:1
23		6.97	8.52:1

Table 8.4 Native Dextran-Fructose Separation Results

These values show that the presence of dextran in the feed broths caused significant fructose sedimentation. For example, an average of over 9% of the fructose in the feed streams was pelleted in the 1% w/w feed broth runs, whereas in theory, this value should be close to zero. This was believed to be because the rapidly sedimenting high MW dextran aggregates had physically entrapped some of the fructose molecules within their highly solvated structure. This process, known as entrainment, was studied more effectively using the zonal-rotor system as described in chapter 9.

A plot of the percentage of sedimented fructose versus sedimented dextran is shown in figure 8.7. This plot suggests that the levels of fructose in the pelleted fractions was dependent upon pelleted dextran levels. High levels of dextran sedimentation resulted in increased levels of fructose sedimentation.

Figure 8.8 shows the effect of sedimented dextran levels on the ratio of sedimented dextran to sedimented fructose. High levels of pelleted dextran corresponded to high dextran : fructose ratios in the pellet. In other words, the separation of dextran from fructose in the bowl was improved when greater amounts of dextran pelleted at the rotor wall. This was an unexpected observation and may be due to the back diffusion of fructose molecules from the pelleted gel layer at the rotor wall back into the process stream.

These results show that the centrifugal process is a promising method for the separation of dextran from fructose. Even under conditions where 80% of the dextran in a feed stream is removed by pelleting, a decrease of only around 10% of the fructose material initially present in the feedstream was recorded. This contaminating fructose material could easily be removed in the acid hydrolysis stage of the clinical dextran production process.

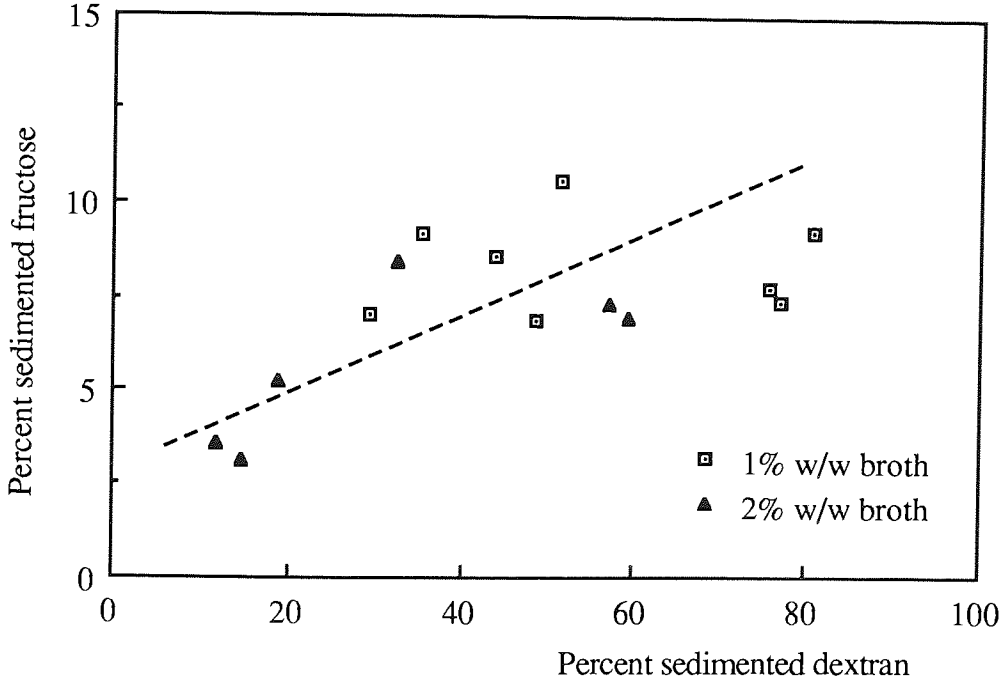

Figure 8.7 A Plot of the Percentage of Sedimented Fructose Versus the Percentage of Sedimented Dextran in the Tubular Centrifuge

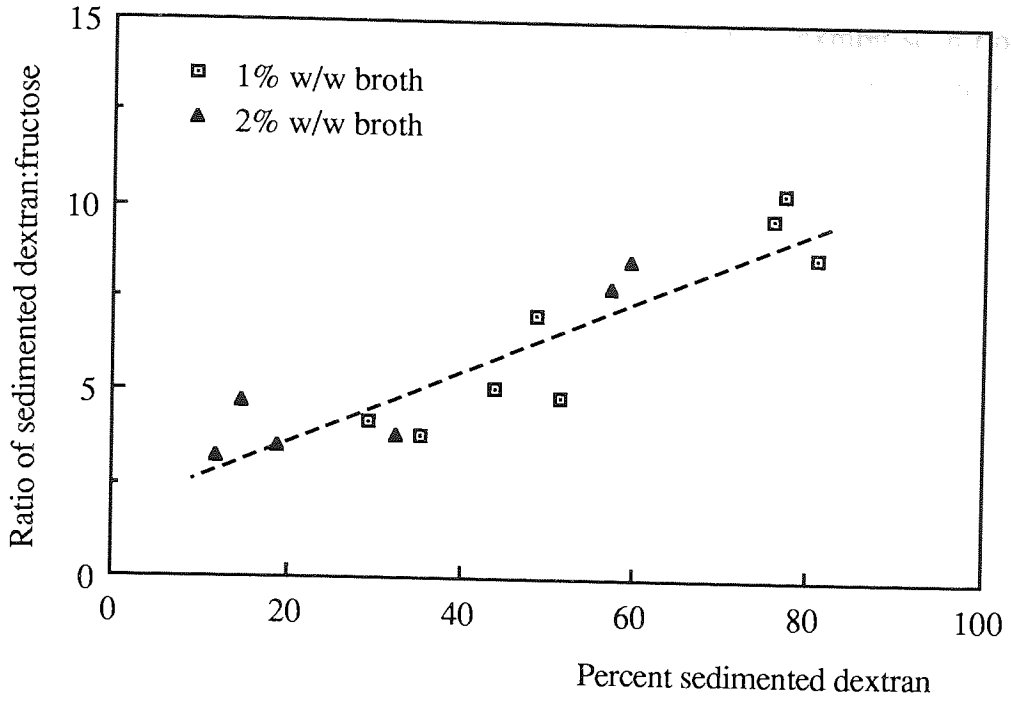

Figure 8.8 A Plot of the Ratio of Sedimented Dextran : Fructose Versus the Percentage of Sedimented Dextran in the Tubular Centrifuge

8.5.4 Prediction of Industrial Centrifuge Performance

The data obtained on the laboratory scale tubular centrifuge can be used to predict the performance of industrial scale centrifuges. The aim of this section is to predict the throughputs of process fluid required to achieve close to 100% dextran sedimentation, which would be the level, of dextran sedimentation required for a successful continuous rate-zonal separation process as described in section 8.5.2.

The maximum capacity factor of the Sharples T-1 bench centrifuge was calculated to be 8×10^6 cm^2. The maximum capacity factors of two industrial scale tubular centrifuges have been listed in table 8.5. As discussed in the previous section, the flow rate required for 94% recovery of a 1% w/w native dextran-fructose broth was 0.5 cm^3 min^{-1} on the Sharples laboratory centrifuge. The Q_o/Σ_T value for this separation was therefore equal to 0.1×10^{-8} cm sec^{-1}. By using equation 8.15 it was possible to predict the throughputs necessary to give the same degree of separation on the industrial scale machines. The results are shown in table 8.5.

The predicted flowrates reported in table 8.5 were disappointingly low. Higher throughputs could be achieved by using separators with much larger capacity factors. Such systems must allow sucrose solutions to be overlaid with dextransucrase enzyme in order to develop a successful continuous bioreaction-separation process. Disk-type centrifuges

have far higher capacities than tubular centrifuges but do not exhibit such flow patterns. No instances of larger capacity tubular centrifuges were found in the literature. Beckman manufacture a rotor that is capable of continuous rate-zonal centrifugation (section 4.3.2.1). The use of this rotor in the centrifugal bioreaction-separation process will be discussed in chapter 9.

Centrifuge	Capacity Factor ($x10^{-6}$ cm^2)	Qo/Σ_T Value ($x10^8$ cm sec^{-1})	Flow rate (cm^3 min^{-1})
Sharples Lab.	8.00 (max)	0.10	0.50
Industrial # 1	25.08	0.10	1.50
Industrial # 2	39.02	0.10	2.44

Table 8.5 Tubular Industrial Centrifuge Performance

Although the dextran product has a high commercial value, it is clear that the above process will not be commercially viable due to the very low predicted throughputs. It is likely that these throughputs would be significantly improved in a rate-zonal process because of less pronounced concentration effects. However, the technique of rate-zonal bioreaction-separation is a potentially useful process and has been shown to improve the yield of commercially important dextran product (chapter 7).

The process may be more ideally suited for the smaller scale production of a higher cost product. A number of alternative products were found in the literature that may benefit from the process. For example, the polysaccharides pullulan and xanthan are produced by batch and continuous fermentation methods similar to those employed for dextran synthesis, sucrose being the optimum carbohydrate source. Usable product yields are decreased at high sucrose concentrations indicating that acceptor molecules affect the reaction. Both polysaccharides enjoy wide ranging uses and show considerable potential in medical and pharmaceutical fields and in the food industry. This technique may also improve the yields of hyaluronic acid and levan. At present, pharmaceutical grade hyaluronic acid is produced by fermentation. A key requirement of the process is to separate the cells from the product without rupturing them, as this may result in the release of inflammatory agents. This problem could be overcome by using cell-free enzyme preparations, as is the case in the proposed dextran production process. The particular viscous properties of hyaluronic acid have been commercially exploited in the field of medicine. Levan appears to have few commercial uses at present.

It was decided to continue to study the combined bioreaction-separation process in the tubular settling centrifuge because a prime objective of the study was to investigate the centrifugal bioreaction-separation principle.

The possible use of tubular settling centrifuges in the development of a solvent free clinical dextran production process has been discussed in appendix A5.

8.5.5 CONCLUSIONS

Studies on the sedimentation behaviour of presynthesised native dextran and fructose broths indicated that very low sample feedrates would be required to achieve high recoveries of native dextran material if the machine were operated as a rate-zonal bioreactor-separator. Scale-up factors were used to predict the equivalent flowrates required for an identical separation on an existing industrial scale tubular centrifuge. Although prohibitively low values were found, it should be noted that concentration effects will be lower in rate-zonal than in normal rate centrifugations, which will lead to significantly higher rates of native dextran sedimentation. It was concluded that the process would be more ideally suited for the smaller scale production of a higher cost product.

8.6 RESIDENCE TIME STUDIES ON THE SHARPLES T-1 TUBULAR CENTRIFUGE

Despite the poor predicted performance of the tubular centrifuge as a continuous bioreactor-separator, which was reported in the previous section, it was decided to study the flow patterns of the process streams in the rotating bowl. The main reason for this study was that the proposed use of tubular centrifuges as continuous rate-zonal bioreactor-separators was a novel process with no parallels in the literature. The success of this operation was expected to lead to the consideration of alternative catalytic processes that would benefit from the proposed continuous bioreaction-separation process and would be a valuable contribution to the body of centrifuge literature.

8.6.1 Stimulus - Response Experiments

The continuous bioreaction-separation process proposed in section 8.3 made two assumptions. Firstly that both process fluids exhibited plug flow in the system, that is, every element of the liquid fraction remains in the bowl for the same period of time and secondly, there was no significant mixing between the two solutions. The design of the system, particularly the nozzle inlet and the exit ports and the rapid spinning of the bowl may significantly affect fluid flow. Other factors such as fluid channelling, diffusion, stagnant regions and swirls and eddies will further affect liquid flow. The aim of the work presented in this section was to test these assumptions. This was achieved by carrying out a number of stimulus-response experiments.

The degree of plug flow in the system was assessed by studying the flow of a single solution through the vessel. This experiment is described in section 8.6.2. Results from this work proved useful for a second study, designed to assess the extent of the mixing that occurred between sucrose and dextransucrase enzyme solutions in the centrifuge bowl. These results are presented in section 8.6.3.

Stimulus-response experiments enable the residence time distribution (RTD) of a fluid within a system to be measured by disturbing the system and measuring the response to this stimulus. In the following experiments, the stimulus was a tracer material injected into the fluid entering the vessel. The response was a time record of the tracer leaving the vessel, usually called a C-curve. It is convenient to represent the RTD in such a way that the area under the C-curve, usually termed 'E', equals unity. This is called normalising the distribution and is achieved by dividing the total measured concentration (C) of the tracer material by A, the area under the concentration-time curve [171] so that :

$$E = \int_0^\infty C\,dt = \int_0^\infty \frac{C}{A_C}\,dt = 1 \quad \text{where } A_C = \int_0^\infty C\,dt \quad \text{___} \quad (8.16)$$

Figure 8.9 shows a typical C-curve and its properties

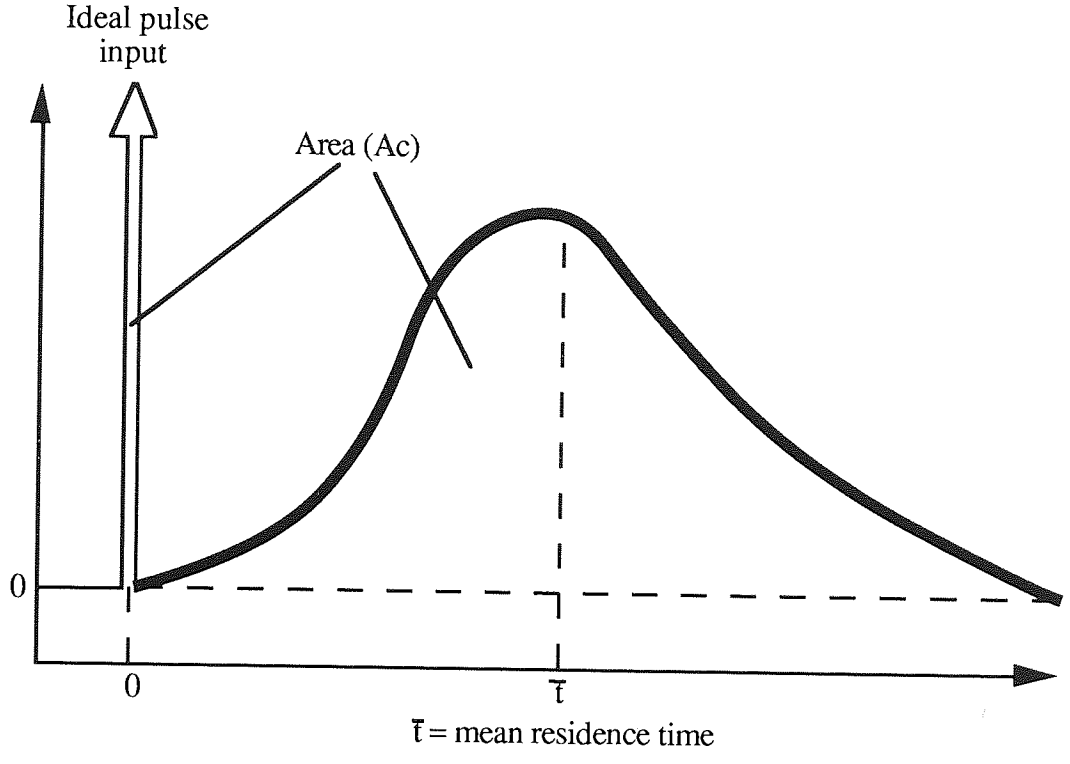

Figure 8.9 Typical C-Curve in Response to an Upstream Input Signal

The C-curve records directly when the molecules from the tracer input leave the bowl. In other words, the C-curve represents the exit age distribution and hence the RTD of the fluid in the system. It is common to compare distribution curve data by determining the theoretical mean residence time ($\bar{t}$) of the fluid in the system. For the steady state flow of a constant density fluid [171]:

$$\bar{t} = V / Q_0 \quad \text{___} \quad (8.17)$$

where V is the vessel volume and Q_0 the fluid flow rate.

8.6.2 Liquid Flow in a Tubular Centrifuge Operated in Clarification Mode

Stimulus-response experiments were carried out to determine the C-curve response of a single liquid passing through the tubular centrifuge bowl for the reasons discussed in section 8.6.1. A schematic representation of the apparatus used is shown in figure 8.10.

8.6.2.1 Experimental Details

The effect of two variable factors, flow rate (factor A) and rotor speed (factor B) on the C-curve response were studied in this experiment. A factorial experimental design was followed as described in section 7.4 and appendix A4. The treatment combinations and corresponding factor levels used in this experiment are listed in table 8.6. Each treatment combination was tested in duplicate.

Treatment Combination	Liquid Flowrate ($cm^3\ min^{-1}$)	Rotor Speed (rpm)
A1B1	5.5	10 000
A2B1	11.0	30 000
A1B2	5.5	10 000
A2B2	11.0	30 000

Table 8.6 Experimental Conditions : Single Liquid Flow in a Tubular Centrifuge

Distilled, deionised water was used as the liquid stream. A 5 cm^3 pulse of a 10% w/w potassium chloride solution served as the tracer input. It was assumed that this material would not disturb the flow patterns in the bowl and was detected on leaving the bowl by an Aqua Scientific conductivity meter, model Alpha 800. The meter response was found to be linear with potassium chloride concentration (figure 8.11).

The liquid stream entering the vessel was maintained at a constant 25°C. The centrifuge casing was enclosed in a water jacket in an attempt to maintain a constant rotor temperature in order to minimise mixing due to convection. However, a constant temperature proved difficult to maintain due to the heat generated by the centrifuge motor and rotor friction effects.

Mixing outside the system was minimised by locating the tracer input port as close as possible to the rotor inlet nozzle. Similarly the conductivity meter probe was situated as close as possible to the centrifuge outlet port. A chart recorder was used to collect the data from the conductivity meter. The trials were conducted in a random order.

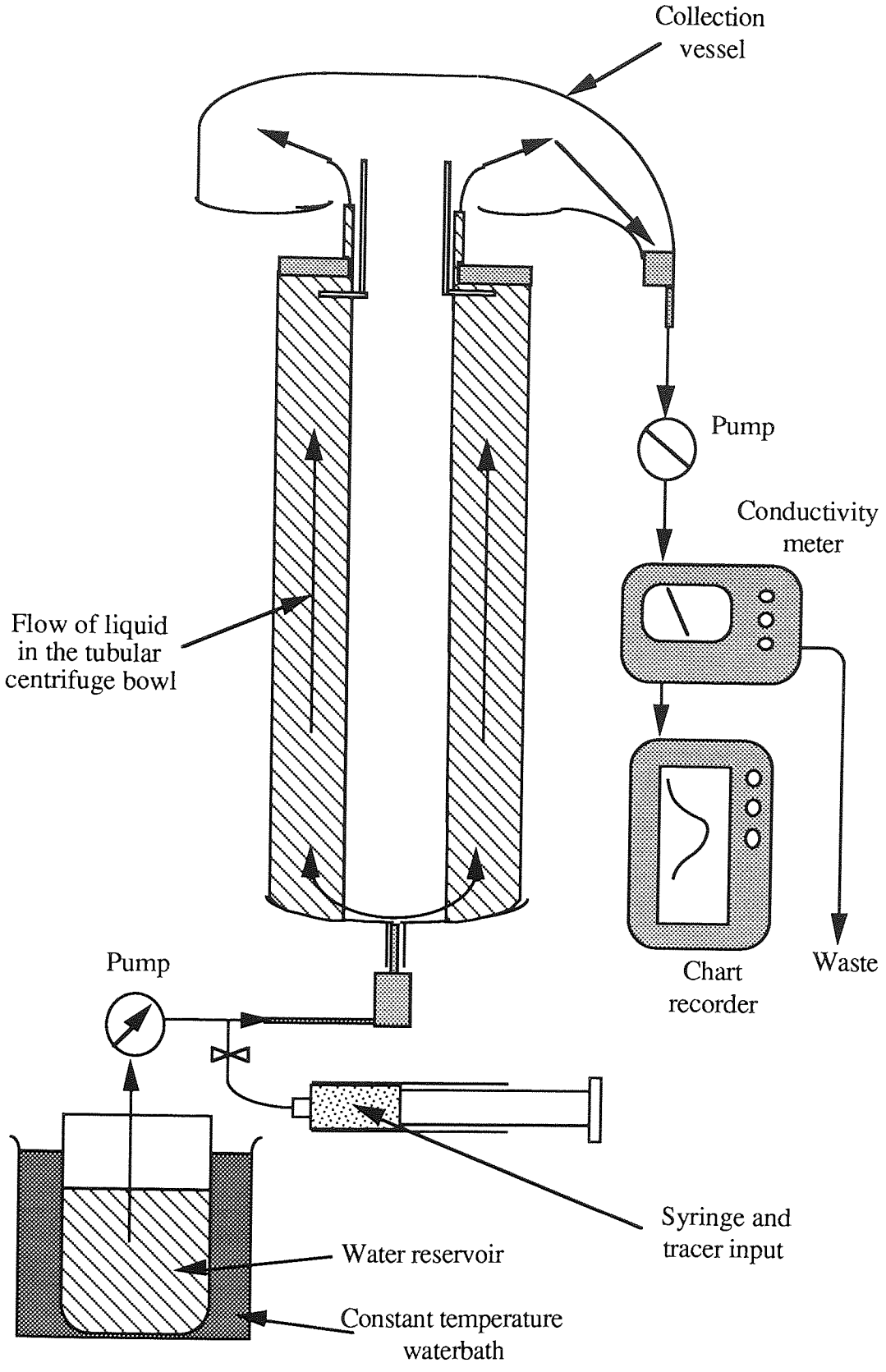

Figure 8.10 Equipment Set-up for the Single Liquid Flow Studies in the Tubular Centrifuge

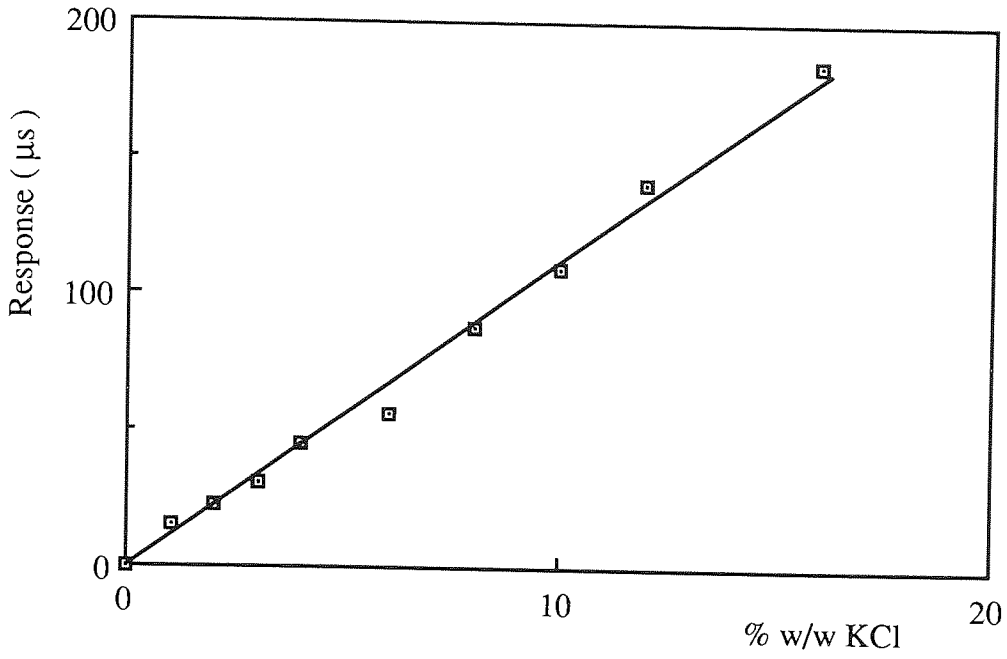

Figure 8.11 Calibration Curve for the Alpha-800 Conductivity Meter

8.6.2.2 Treatment of Results

The distribution curves (C-curves) obtained from the stimulus response experiments were characterised numerically by measuring the curve height, which was proportional to the tracer material concentration, at uniform time intervals as shown in figure 8.12. This figure shows that the area (A_c) under the C-curves can be approximated using the following expression:

$$A_c = \Sigma\, C_z\, \Delta t \quad \text{—} \quad (8.18)$$

Where C_z equals the concentration of tracer material leaving the vessel at time t_z. The normalised concentration of tracer material leaving the centrifuge bowl with time was calculated by dividing each of the discretised concentration readings (C_z) by A_c for each discretised value of t (equation 8.16), thus giving the C-curve data in the normalised form

The mean residence time (RT) of the centrifuge bowl for a particular set of experimental conditions was determined by locating the peak centroid of the normalised C-curve using the expression (171):

$$\bar{t} = \frac{\Sigma\, t_i\, C_i\, \Delta t}{\Sigma\, C_i\, \Delta t} \quad \text{—} \quad (8.19)$$

where C_i and t_i represent the concentration and time of the normalised C-curve at point i. Another important descriptive quantity used to describe a C-curve is the spread of distribution, usually measured by the variance σ^2, which can be defined in discrete form as:

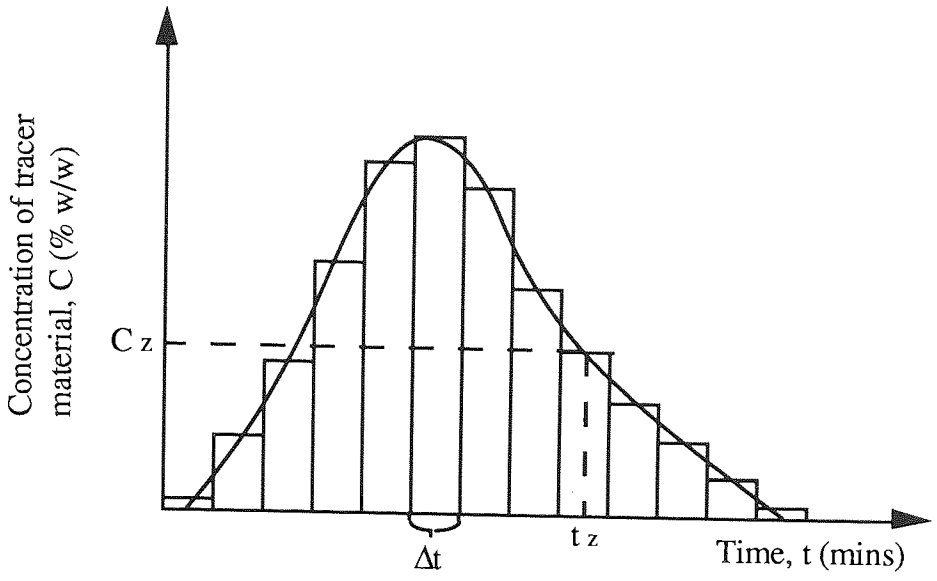

Figure 8.12 Numerical Characterisation of a C-curve

$$\sigma^2 = \frac{\sum t_i^2 C_i \Delta t_i}{\sum C_i \Delta t_i} - \bar{t}^2 \qquad (8.20)$$

Large σ^2 values indicate that considerable mixing is occurring within the vessel. A third commonly used parameter for representing non-ideal flow is the tanks-in-series model which expresses C-curve data as the number of identical stirred vessels that would have to be placed in series to achieve an identical C-curve shape. This number is calculated using the expression:

$$\sigma^2 / \bar{t}^2 = 1/N \qquad (8.21)$$

where N represents the theoretical number of vessels required to duplicate the C-curve shape. The expression $\sigma^2 / \bar{t}^2$ is commonly written as σ^2_{θ} and is dimensionless. When N tends to infinity, mixing is decreased and the system approaches the plug flow model. As N tends to 1, mixing within the vessel increases and when N equals 1, the system behaves as a perfectly mixed vessel. Figure 8.13 shows that as N tends to infinity, so the shape of the C-curve tends to that of a normal distribution. Tanks-in-series data was used in this study to describe the extent of mixing within the centrifuge bowl.

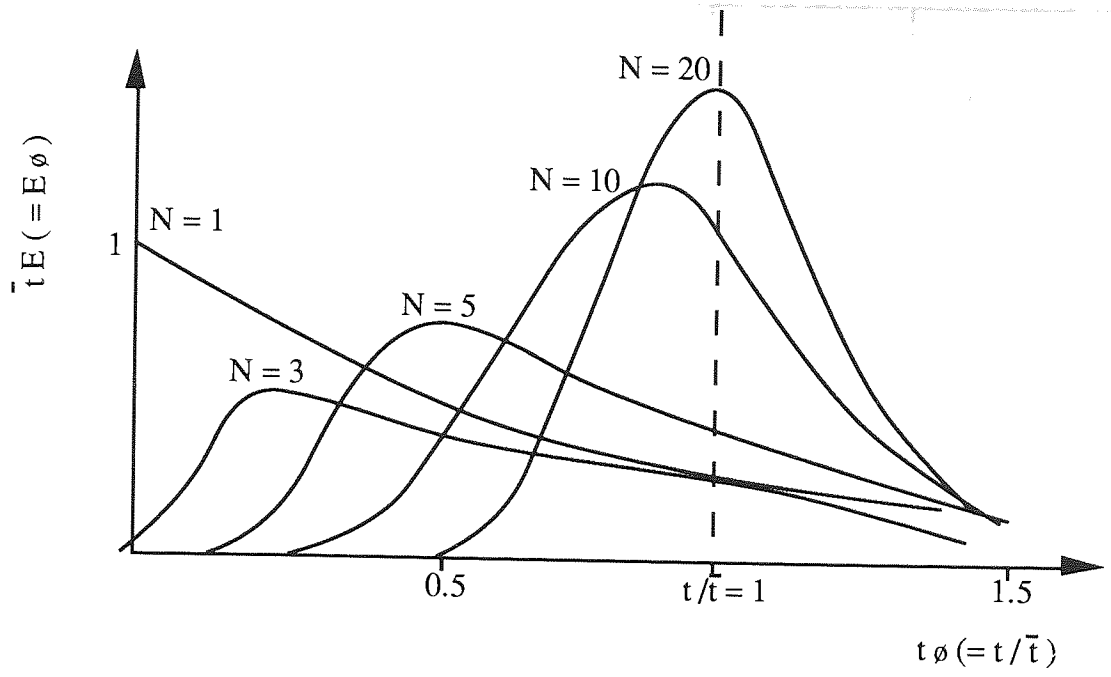

Figure 8.13 Comparing C-curve Distribution Profiles with the Tanks-in-Series Model.

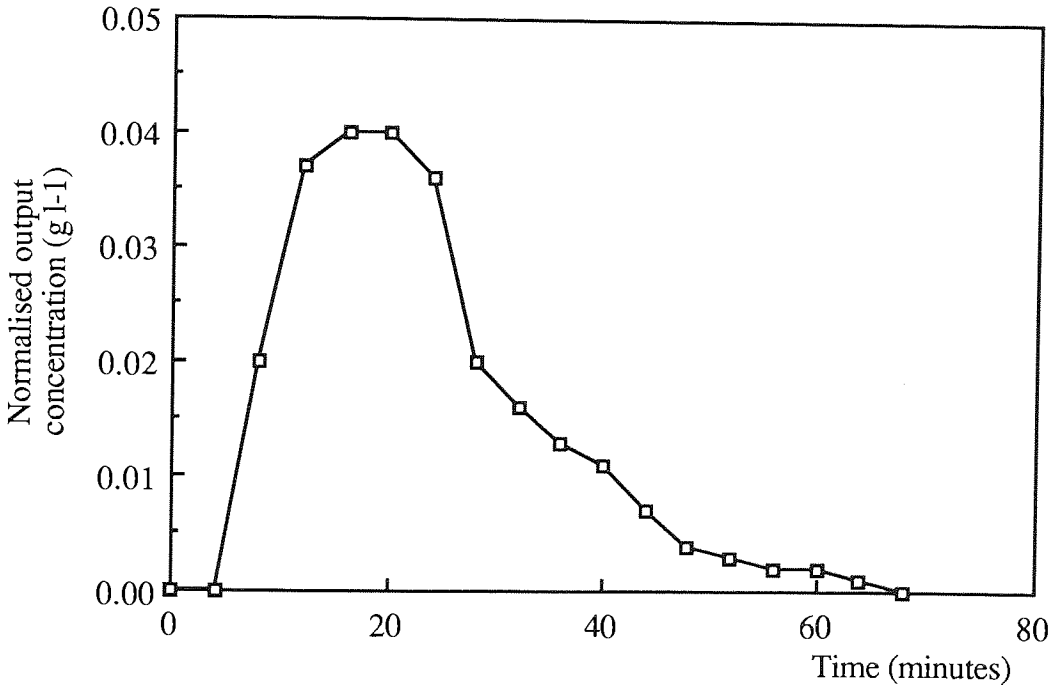

Figure 8.14 Normalised C-curve for Trial Combination 2 (Table 8.7).

Time (t_i) (mins)	Tracer Concentration (C_i) ($g\ l^{-1}$)	Normalised Output Concentration $E_i = C_i/A$	$t_i \times E_i$	$(t_i)^2 \times E_i$
0	0	0	0	0
4	0	0	0	0
8	3.58	0.020	0.158	1.264
12	6.68	0.037	0.441	5.292
16	7.33	0.040	0.645	10.320
20	7.33	0.040	0.806	16.120
24	6.52	0.036	0.860	20.640
28	3.58	0.020	0.552	15.456
32	2.93	0.016	0.516	16.512
36	2.28	0.013	0.452	16.272
40	1.96	0.011	0.430	17.200
44	1.30	0.007	0.315	13.860
48	0.65	0.004	0.172	8.256
52	0.49	0.003	0.140	7.280
56	0.33	0.002	0.100	5.600
60	0.33	0.002	0.108	6.580
64	0.16	0.001	0.057	3.648
68	0	0	0	0
Sum Σ	$\Sigma C_i =$ 45.46	$\Sigma E_i =$ 0.250	$\Sigma t_i E_i =$ 5.753	$\Sigma t_i^2 E_i =$ 164.200

Δt = 4 minutes

$A_c = (\Sigma C_i)\,\Delta t = 45.46 \times 4 = 181.82$

$\bar{t} = (\Sigma t_i E_i)\,\Delta t = 5.753 \times 4 = 23.011$

$$\sigma^2 = \left[\frac{(\Sigma t_i^2 E_i)}{\Sigma E_i}\right] - \Sigma \bar{t}^2 = \left[\frac{164.2}{0.25}\right] - (23.011)^2 = 127.423$$

$$\sigma_\theta^2 = \sigma^2 / \bar{t}^2 = (127.423)^2 / (23.011)^2 = 0.241$$

$N = 1/\sigma_\theta^2 = 1 / 0.241 = 4.16$

Table 8.7 Treatment of C -Curve Data for Trial Combination 2.

The tanks-in-series values for each of the trials performed in this study were calculated from the C-curves obtained for each of the treatment combinations listed in table 8.6. C-curve data from trial combination 2 (table 8.6) is shown in table 8.7 as an example of the treatment of the distribution curve data. The normalised distribution of the C-curve from this trial is presented in discrete form in the first two columns of this table. The normalised C-curve is shown in figure 8.14. The calculations in this table show that for trial combination 2, the centrifuge vessel approximates 4.16 identical stirred tanks-in-series.

8.6.2.3 Results and Discussion

TANKS-IN-SERIES DATA

The tanks-in-series values obtained for all the replicated trials are presented in table 8.8 and typically show that the flow of liquid in the tubular bowl was equivalent to approximately four identically stirred tanks-in-series. The experiment was designed so that the experimental results could be assessed factorially, using a similar method to that described for the bioreaction-separation studies performed on the MSE centrifuge described in section 7.4 and appendix A4. The factorial assessment of the data reported in table 8.8 is described in Appendix A6. It was found that changes in liquid flow rate from 5.5 to 11.0 $cm^3\ min^{-1}$ and rotor speeds from 10 000 to 20 000 rpm had no significant effect on the mixing that occurs in a Sharples T-1 Supercentrifuge bowl, at the 10% level of significance (see appendix A6).

Trial Number	Tanks-in-series Values		
	Run 1	Run 2	Mean
A1B1	3.36	4.02	3.69
A2B1	4.16	4.35	4.26
A1B2	3.45	3.86	3.66
A2B2	4.38	4.09	4.24

Table 8.8 Tanks-in-Series Values: Single Liquid Flow Studies

MEAN RESIDENCE TIME DATA

The observed mean RT data, henceforth referred to as $\bar{t}_a$, obtained from this experiment is presented in table 8.9. This table also records the theoretical mean RT values of each treatment combination, henceforth referred to as $\bar{t}$, calculated using equation 8.17.

Treatment Combination	Theoretical Mean RT $(\bar{t})$ (minutes)	Observed Mean RT $(\bar{t}_a)$ (minutes)	
		Run 1	Run 2
A1B1	45.45	41.84	38.60
A2B1	22.73	23.01	22.53
A1B2	45.45	39.28	41.78
A2B2	22.73	23.47	22.73

Table 8.9 Residence Time Data: Single Liquid Flow Studies

This data was used to determine whether changes in flow rate and rotor speed caused any significant changes in observed mean RT values $(\bar{t}_a)$. The deviation of a $\bar{t}_a$ value from the equivalent theoretical mean RT value $(\bar{t})$ was measured by dividing $\bar{t}_a$ by $\bar{t}$. $\bar{t}$ represents the theoretical retention time that a molecule would spend in an ideal system. Therefore:

when	$\bar{t}_a / \bar{t} = 1$	Ideal liquid flow
and when	$\bar{t}_a / \bar{t} \neq 1$	Non-ideal liquid flow

The greater the deviation of $\bar{t}_a / \bar{t}$ from unity, the greater the extent of non-ideal flow in the system. The $\bar{t}_a / \bar{t}$ values are recorded in table 8.10 and were tested for significance in a similar manner to the tanks-in-series values (see appendix A6).

Treatment Combination	$\bar{t}_a / \bar{t}$ values	
	Run 1	Run 2
A1B1	0.921	0.849
A2B1	1.012	0.991
A1B2	0.864	0.919
A2B2	1.032	0.973

Table 8.10 Deviation of the Observed RT Values from the Theoretical RT Values: Single Liquid Flow Studies.

It was found that increases in liquid flowrate from 5.5 to 11.0 $cm^3\ min^{-1}$ and rotor speeds from 10 000 to 20 000 rpm had no significant effect on the deviance of the observed RTs from their equivalent theoretical RTs at the 10% level of significance (see appendix A6).

8.6.2.4 Conclusions

Throughput and rotor speed will have a significant bearing on determining the economic viability of any combined centrifugal bioreaction-separation system. Higher flowrates and

rotor speeds have been shown to have no significant effect on system mixing or the creation of stagnant regions which is a promising observation.

Under the experimental conditions studied, the centrifuge bowl was shown to approximate four stirred tanks-in-series. This represents a reasonable approximation to plug flow for the purposes of calculation.

8.6.3 Liquid Flow in a Tubular Centrifuge Operated in Liquid-Liquid Separation Mode

The aim of the following set of experiments was to obtain data concerning the non-ideal flow and mixing that occurred between a heat treated dextransucrase enzyme stock solution and sucrose solutions in the spinning Sharples T-1 tubular centrifuge bowl for the reasons discussed in section 8.6.1.

8.6.3.1 Experimental Design

Stimulus-response experiments were again used to obtain RTD data, which was used to assess the non-ideal flow and the mixing that occurred between the two miscible liquids in the bowl. Because of the design of the centrifuge inlet, it was not possible to continuously introduce two separate liquid streams into the bowl simultaneously. However, because of the considerable problems involved in characterising non-ideal flow and mixing between two flowing liquids, the sucrose solution was first loaded into the bowl and held within the bowl as a stationary solution before a continuous stream of enzyme stock solution was passed through the bowl, over the surface of the sucrose solution. Analysis of the material eluting from the bowl would yield information concerning the state of mixing between the 'mobile' enzyme solution and 'stationary' sucrose solution. The enzyme solution originally had an activity of 262 DSU cm^{-3} but was heat treated to remove all enzyme activity in order to minimise non-ideal mixing effects and simplify data assessment. If mixing proved minimal in this system, then active enzyme studies would be undertaken. A schematic diagram of the apparatus used is shown in figure 8.15. A ring dam with a sufficiently small internal diameter was required to prevent sucrose loss from the system during enzyme flow as shown in figure 8.3.

The effects of three variable factors on liquid-liquid mixing were studied. Again, a factorial experimental design was followed, as described in appendices A4 and A6. The chosen factors and their corresponding levels were:

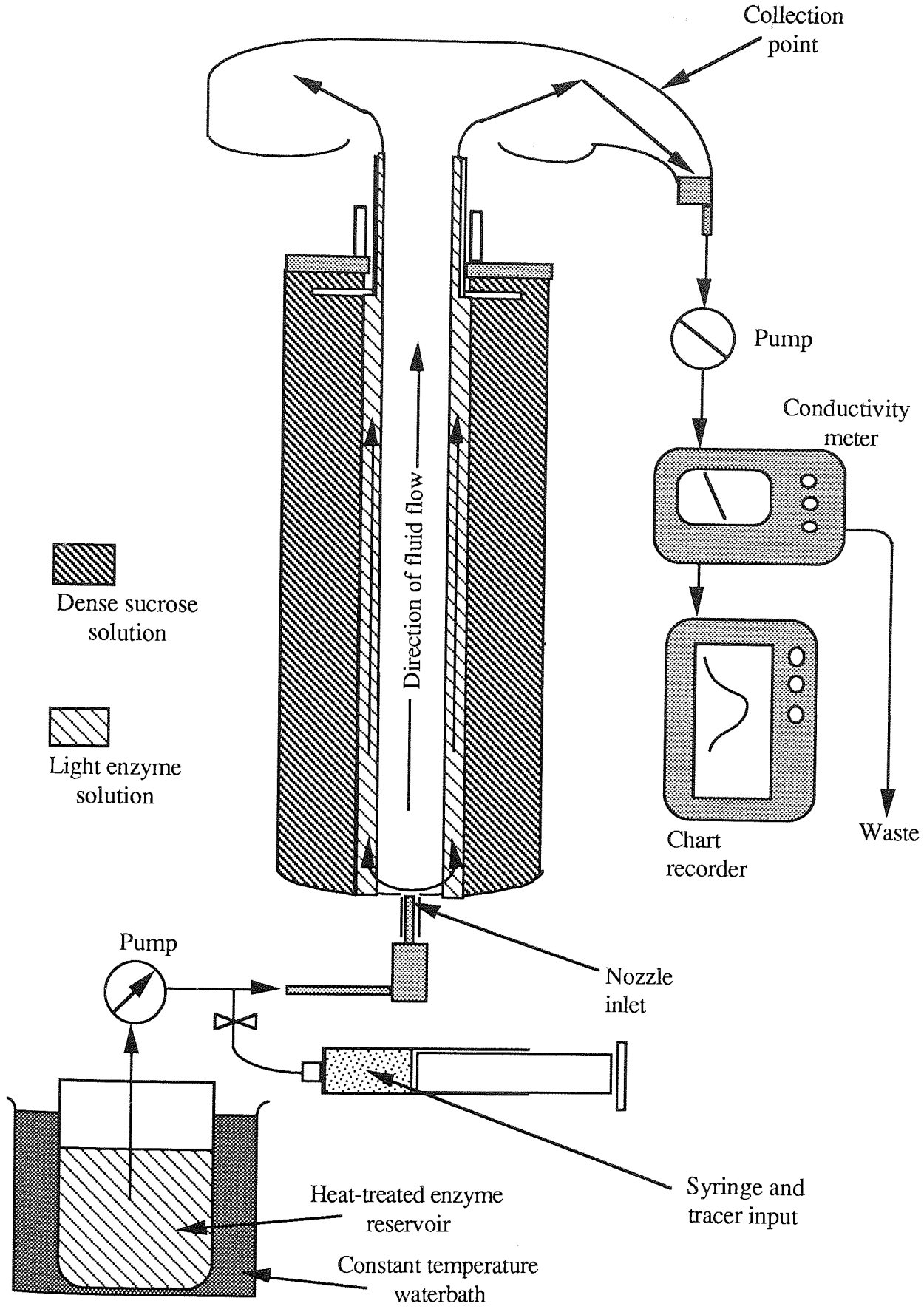

Figure 8.15 Equipment Set-up for the Liquid-Liquid Flow Studies in the Tubular Centrifuge

A	Enzyme flowrate	A_1	4.0 cm^3 min^{-1}
		A_2	8.0 cm^3 min^{-1}
B	Sucrose concentration	B_1	10.0 % w/w
		B_2	20.0 % w/w
C	Sucrose volume : Enzyme volume	C_1	215 cm^3 : 35 cm^3
		C_2	200 cm^3 : 50 cm^3

The rotor was held constant at a speed of 10 000 rpm. Low flowrates were chosen to ensure that the residence times of the flowing enzyme solutions were not too short. Short residence times may result in the presence of dextran in the fructose rich product stream in the proposed bioreactor-separator. High sucrose concentrations were chosen so that the correspondingly high liquid densities and viscosities would, at least initially, support the lower density enzyme solution without density inversion effects. The construction of stable sucrose gradients is not a practical option in flowing process streams. Small enzyme volumes were required so that the enzyme solutions would initially form a thin zones on the surface of the sucrose solutions.

8.6.3.2 Experimental Details

The centrifuge chamber was allowed to equilibrate to 25°C at a constant rotor speed of 10 000 rpm. The bowl was then loaded with the required volume of sucrose solution at 25°C using a 50 cm^3 syringe located close to the nozzle inlet. The heat treated enzyme solution was then continuously pumped into the bowl using a peristaltic pump, at the required flowrate. Exactly 10 minutes after the initial enzyme input, a 4.0 cm^3 pulse of enzyme stock solution, containing 10% w/v potassium chloride was carefully injected via the nozzle inlet. The tracer material was detected on leaving the system using the Aqua conductivity meter and the RTD curve was recorded on a chart recorder. All trials were conducted in a random order and in duplicate.

8.6.3.3 Treatment of Results

The extent of mixing between the two liquids was assessed from RT data by making the following observations: If the two solutions were completely mixed on entering the bowl, then the theoretical mean RT of the system would be defined by equation 8.17. However, in the situation when the sucrose formed a 'stationary' zone beneath the mobile enzyme solution, if total mixing were not to occur, the 'stationary' fluid would act as a 'dead space' within the vessel. Dead spaces are defined as regions within the vessels that contain

liquids with RTs in excess of five times the mean RT (171). A dead space in a vessel can be considered as a volume of liquid, V_d, related to the observed mean RT, $\bar{t}_a$, by (171):

$$\bar{t}_a = (V_e - V_d) / Q_o \quad \text{(8.22)}$$

Where V_e equals the theoretical volume occupied by the enzyme solution in the vessel and Q_o equals the flow rate of the enzyme solution. If V_d is small, then $\bar{t}_a$ will approximately equal the theoretical mean RT ($\bar{t}$)of the enzyme solution in the vessel (equation 8.17).

The residence time data was then treated in a similar manner to that described in section 8.6.2. The deviation of a $\bar{t}_a$ value from the equivalent theoretical mean RT value ($\bar{t}$) was measured by dividing $\bar{t}_a$ by $\bar{t}$. $\bar{t}$ represents the theoretical retention time that an enzyme molecule would spend in the system if no mixing were to occur between the two liquids during enzyme passage through the bowl. Therefore:

when	$\bar{t}_a / \bar{t} = 1$	no mixing is occurring
and when	$\bar{t}_a / \bar{t} > 1$	mixing is occurring.

The greater the deviation of $\bar{t}_a / \bar{t}$ from unity, the greater the extent of mixing between the two solutions.

8.6.3.4 Results and Discussion

The observed mean retention times $\bar{t}_a$ are recorded in table 8.11. The $\bar{t}_a / \bar{t}$ values are recorded in table 8.12.

Trial No.	Treatment Combination	Residence Time ($\bar{t}_a$) (mins)		Mean Value	Theoretical Mean Residence Time (mins)
		Run 1	Run 2		
1	A1 B1 C1	23.87	22.78	23.33	8.75
2	A2 B1 C1	17.99	16.92	17.46	4.38
3	A1 B2 C1	13.34	15.11	14.23	8.75
4	A2 B2 C1	8.22	10.72	9.47	4.38
5	A1 B1 C2	19.57	20.59	20.08	12.50
6	A2 B1 C2	16.12	17.86	16.99	6.25
7	A1 B2 C2	16.35	17.80	17.08	12.50
8	A2 B2 C2	10.10	14.68	12.39	6.25

Table 8.11 Residence Time Data: Liquid-Liquid Mixing Studies.

Trial No.	$\bar{t}_a / \bar{t}$ Values		Mean
	Run 1	Run 2	
1	2.73	2.60	2.67
2	4.11	3.86	3.99
3	1.53	1.73	1.63
4	1.88	2.45	2.16
5	1.57	1.65	1.61
6	2.58	2.86	2.18
7	1.31	1.42	1.37
8	1.62	2.35	1.98

Table 8.12 Deviation of the Observed RT Values from the Theoretical RT Values: Liquid-Liquid Mixing Studies.

The effects of each variable factor on the $\bar{t}_a / \bar{t}$ values were assessed factorially according to the method described in appendix A6. The significant t-values are listed in table 8.13. A t-value of 6.13 was required for significance at the 10% level.

Effect	t-value
Main Effect A	+ 7.03
Main Effect B	- 7.53

Table 8.13 Significant t-values: Liquid-Liquid Mixing Studies.

All the $\bar{t}_a / \bar{t}$ values in table 8.12 are larger than the theoretical mean RT value. In one case, the $\bar{t}_a$ value was over 4 times larger. This indicated that considerable mixing had occurred between the two liquids and that the enzyme molecules were spending up to four times longer in the vessel than would be expected if no mixing were occuring. The most favourable factor combination was noted for trial number 7, which corresponded to the lower enzyme flowrate and higher sucrose concentration. The mean $\bar{t}_a$ value was only about one third larger than the theoretical mean RT value had no mixing occurred. The t-values from the factorial analysis confirmed statistically that increases in enzyme flowrate from 4 to 8 cm^3 min^{-1} led to a significant increase in liquid-liquid mixing, whereas increases in sucrose concentration from 10% to 20% w/w led to the opposite effect. Thus, in order to minimise liquid-liquid mixing, low enzyme flowrates and sucrose solutions of high density and viscosity are recommended. The volume of the enzyme overlay had no significant effect on the degree of liquid mixing at the 10% level.

8.6.3.5 Conclusions and Recommendations

The poor correlation between the observed mean RT values and theoretical mean RT values indicated that considerable mixing had occurred between the two solutions and therefore the system did not show potential as a continuous combined rate-zonal bioreaction-separation system. The liquid-liquid separation principle is a well proven technique for the separation of two immiscible solutions [172], but was shown to give poor results when both liquids were in the aqueous form. Therefore, further analysis of the tubular centrifuge system was not considered.

The design of the centrifuge nozzle inlet was such that the flowing solution was forced through a narrow aperture, causing it to leave the inlet with a distribution of velocities. It is therefore possible that the inlet is increasing the degree of turbulence within the system which may contribute to system mixing. Thus, redesign of the nozzle inlet is indicated. The inlet could simply be redesigned to allow the flow of two separate liquid streams into the bowl with a minimum of turbulence. A possible design is shown in figure 8.16.

The main problem of the proposed system was perceived to be the mixing that occurred between the two aqueous liquid streams. Ideally, an immiscible solvent within which either the sucrose or enzyme solution could be dissolved, while not affecting the dextransucrase reaction would solve this problem, although the author does not know of such a material.

It is recommended that the proposed bioreaction-separation process be investigated in other centrifuge systems with different rotor designs. This was done using a JCF-Z zonal rotor fitted with a reorienting gradient core and is reported in the next chapter.

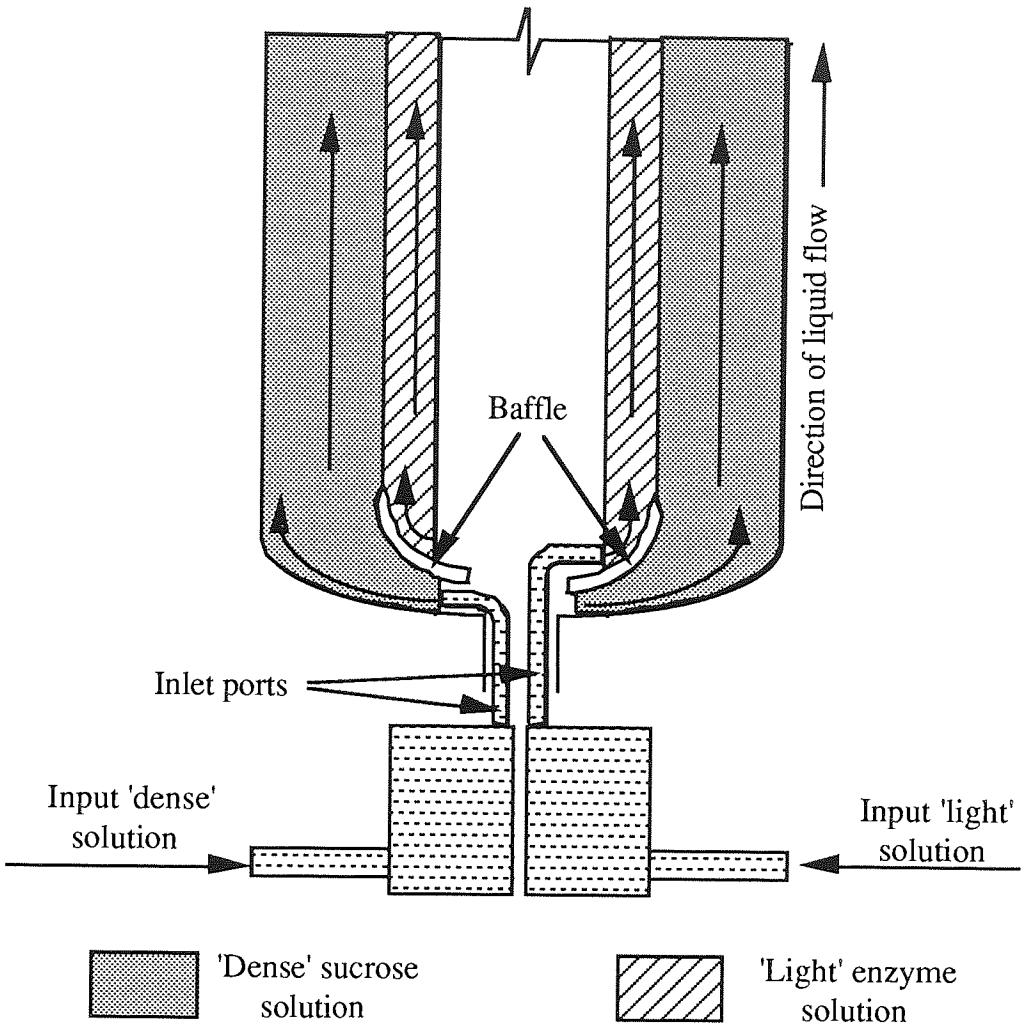

Figure 8.16 Possible Redesign of the Inlet Nozzle in the Tubular Centrifuge

9.0 BIOREACTION-SEPARATION STUDIES IN ZONAL ROTORS

9.1 RATE-ZONAL SEPARATIONS IN ZONAL CENTRIFUGE ROTORS

Zonal rotors represent the only practical way to significantly increase the quantity of sample handled in zonal separations. The design of these rotors has been reviewed in section 4.3.2.1. Zonal rotor cores allow reproducible loading and harvesting of gradient and sample materials. Although such systems were primarily developed for preparative purposes, the data obtained from such centrifugations should prove invaluable in the study of the proposed bioreaction-separation technique.

The bioreaction-separation principle in a *standard* zonal centrifuge is shown in figure 9.1. This figure can be compared with figure 2.8 which illustrates the principle in a centrifuge tube.

9.1.1 The J2-MC Centrifuge and the JCF-Z Zonal Rotor

A model J2-MC centrifuge containing a JCF-Z zonal rotor fitted with a Reograd rotor core was used in this study. This equipment was purchased from Beckman Instruments Limited (High Wycombe, Bucks., U.K.) towards the end of this research with SERC funding.

The centrifuge was fitted with a thermistor to monitor chamber temperature. A microprocessor was used to calculate the chamber temperature that was required to maintain a constant rotor temperature by using a set of compensation values unique to the JCF-Z rotor. Rotor speeds were controlled to within 20 rpm of the selected speeds. A vacuum pump was used to reduce the chamber pressure to below 0.5 atmospheres to minimise friction effects during the runs. The machine had a controlled acceleration / deceleration facility that was required for the smooth reorientation of the gradient when using the Reograd rotor core.

9.1.2 The Reorienting ('Reograd') Zonal Rotor Core

Beckman Instruments Ltd. manufacture a number of different zonal rotors and zonal rotor cores. A Beckman JCF-Z zonal rotor fitted with a reorientating gradient, referred to as a 'Reograd' core was used in this study and the operating principle of this equipment is shown in figure 9.2. As the name suggests, the reorientating gradient core allows the bowl contents to be reorientated under the influence of an applied centrifugal field. The advantage of the Reograd rotor core over other rotor core designs for the the study of the bioreaction-separation principle is discussed in the next section.

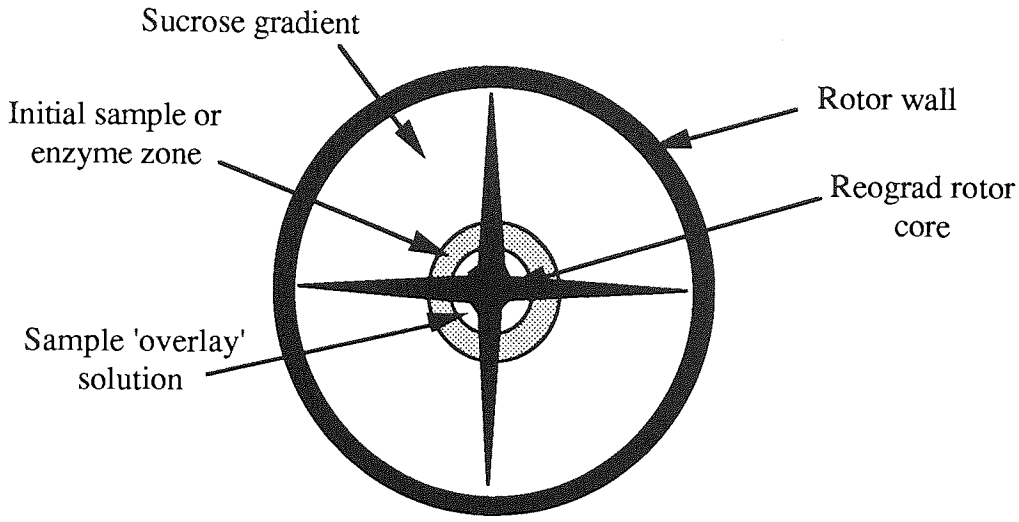

(1) The dextransucrase enzyme initially forms a circular reaction zone on top of the sucrose gradient in the zonal rotor.

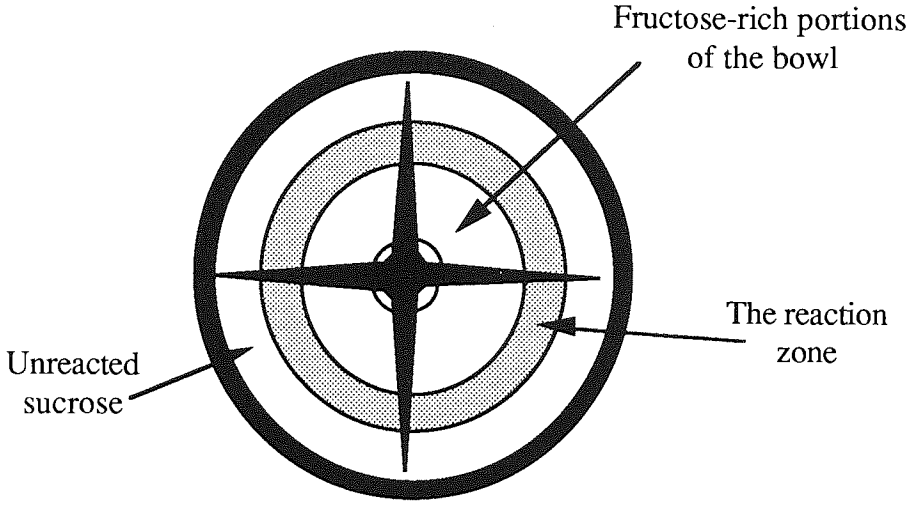

(2) The reaction zone sediments radially through the sucrose gradient under the applied centrifugal field. Enzyme and dextran are separated from fructose rich portions of the bowl as the reaction proceeds.

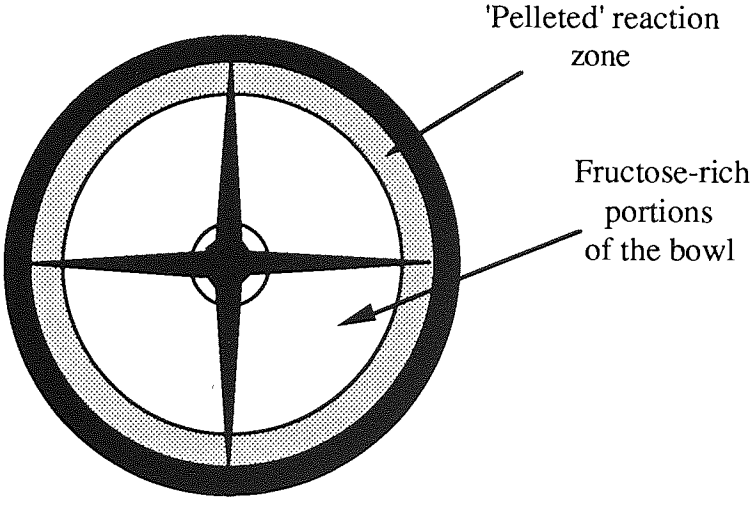

(3) The run is halted when the reaction zone reaches the bowl wall. The fructose rich solution and dextran rich gel can be removed from the rotor for sample analysis.

Figure 9.1 Bioreaction-Separation Principle using a Standard Zonal Core

The gradient is introduced into the base of the rotor via passages cut into the Reograd rotor core. The gradients are constructed in a manner analogous to that used to prepare gradients in centrifuge tubes (section 7.4.3). The least dense gradient fraction is loaded into the rotor first, where it forms a layer at the base of the bowl. As successively denser gradient fractions are fed into the rotor, the less dense fractions are gradually pushed to the top of the rotor cavity (figure 9.2.a). Loading continues until the required gradient fractions fill the rotor bowl. The gradient is then left for a number of hours to form a smooth 'continuous ' gradient due to diffusion. The sample material can then be loaded into the rotor via the gradient outlet port so that it forms a zone above the least concentrated end of the gradient (figure 9.2 b). This results in the loss of a small quantity of the dense end of the gradient from the rotor. When the rotor is spun, the shape of the 'Reograd' core facilitates smooth reorientation of the gradient to the vertical position (figures 9.2.c and d). Rate-zonal bioreaction and separation will then occur under the applied centrifugal field. During rotor deceleration the layers reorientate back to the horizontal position (figure 9.2.e). The rotor contents are displaced by air pressure, the most dense part of the gradient being unloaded first (figure 9.2f).

Photographs of the JCF-Z zonal rotor and the Reograd rotor core used in this study are presented in figure 9.3. The left hand side of the photograph shows the Reograd rotor core and rotor core base fitted into the JCF-Z zonal rotor. The transfer tube, pictured in the centre of the photograph, screws into the shaft of the rotor lid, pictured on the right side of the photograph and has an inlet and outlet port to allow the ordered loading and unloading of the rotor. Passages are cut diagonally through the vanes of the rotor core to allow process fluids to be introduced to the base of the rotor, close to the rotor wall. The centre of the rotor core has four grooves cut into it. When the lid is screwed onto the rotor, the four grooves effectively become passages that allow the flow of process fluids into and out of the vessel via the transfer tube assembly. The inner cylinder of the core has a radius of 2.6cm and the rotor wall has a radius of 8.9cm. The total capacity of the bowl is 1750 cm^3.

The special design of the rotor core and fluid passages allows the relative order and distribution of material in the rotor at the conclusion of the high speed run to be retained in the effluent stream of the rotor. Typically, 10-30 equal fractions of the rotor volume can be collected during the unloading procedure. The collected fractions may be analysed to determine the concentration of materials, the specific biological activity or some other property required for a given experiment. This will yield information concerning the distribution of material in the rotor at the end of a centrifugal run.

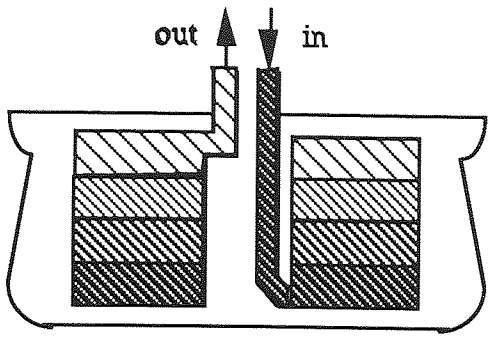

(a) Gradient fractions are loaded until the bowl is filled

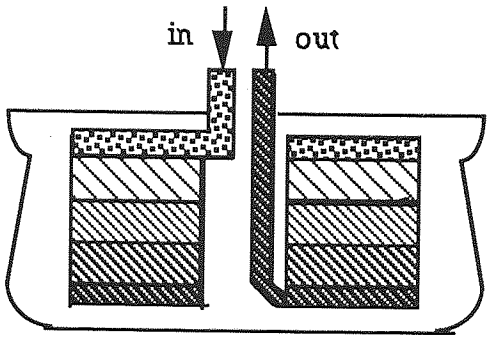

(b) The sample is loaded causing some gradient displacement from the bowl

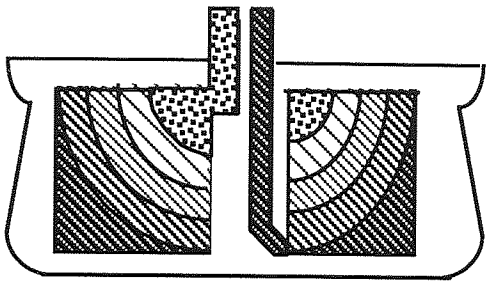

(c) The gradient is reorientated under the influence of an applied centrifugal field.

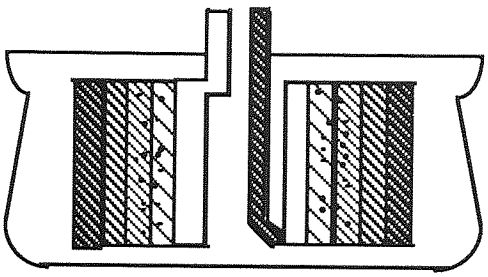

(d) Sample sedimentation occurs radially towards the rotor wall.

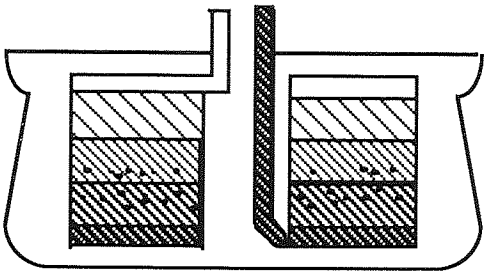

(e) The gradient reorientates back to the horizontal position after rotor deceleration

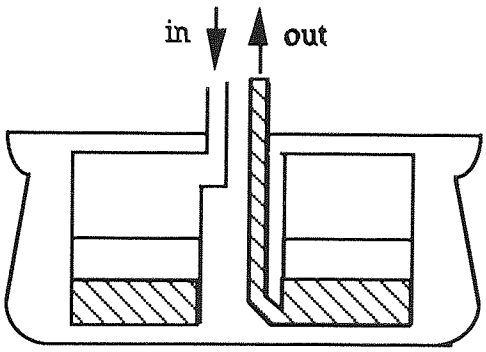

(f) The rotor contents are displaced from the bowl by air pressure

Figure 9.2 Operating Principle of the Beckman Reorienting ('Reograd') Rotor Core

Knowing the volume of each gradient fraction and the dimensions of the rotor bowl cavity and rotor core, then the exact position that each gradient fraction occupied in the bowl during centrifugation can be calculated from simple geometrical formulae. An example calculation is presented in Appendix A7.

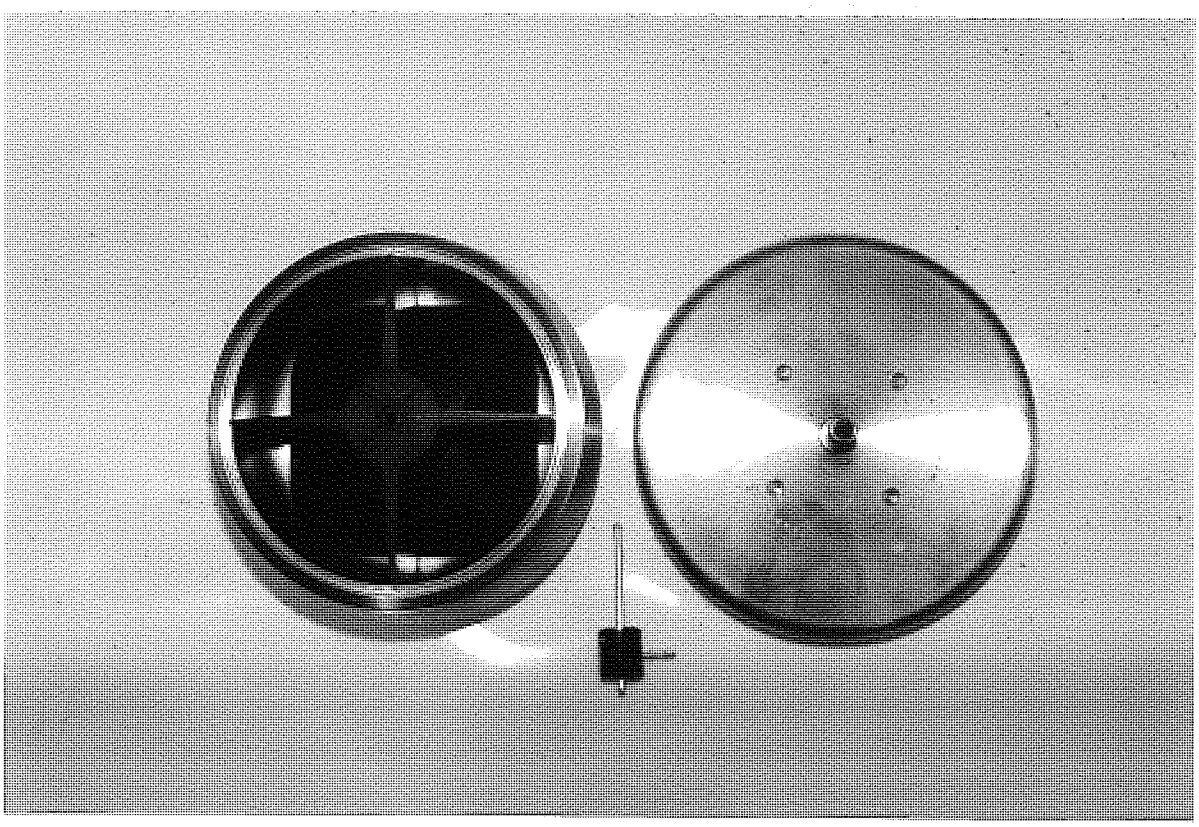

Figure 9.3 Photograph of the Beckman JCF-Z Zonal Rotor and Reograd Rotor Core.

The similarity between this system and the rate-zonal centrifugation technique in centrifuge tubes can be readily observed by comparing figures 9.1 and 4.12. Because the unloading technique yields a number of gradient fractions with no appreciable loss in sample resolution, the Reograd zonal rotor can be used to determine the optimum conditions for the operation of the proposed bioreaction-separation system. For example, the density and viscosity profile of the supporting gradient solution will affect the distribution of the enzyme and reaction products within the bowl (Section 4.4.2.4). A gradient shape that helps maintain the enzyme as a distinct band in the sucrose gradient will enhance the separation of the bulk of the enzyme molecules from the fructose rich portions of the tube which is important for minimising the acceptor reaction. By determining the enzyme activities of each of the gradient fractions collected after a rate-zonal bioreaction-separation, the effect of gradient 'shape' on the enzyme and fructose distributions can be studied and the optimum gradient shape determined. Using similar procedures, optimum run times and rotor speeds can be selected.

Only low levels of substrate conversion to product were achieved in the batch studies on the MSE SS 50 centrifuge (Chapter 7). In order to maximise sucrose conversion and hence

improve the yield of dextran product per unit time from the bioreactor, high activity and large volume enzyme loadings are indicated. However, this may result in non-ideal sedimentation due to gradient overloading and density inversion effects (Section 4.4.2.5). By studying the distributions of the various materials after centrifugation, it will be possible to determine which combination of factors cause sample overloading[120]. The aim of this set of experiments can therefore be summarised as evaluating the principles of the centrifugal bioreaction-separation technique and process optimisation.

9.1.3 Alternative Rotor Core Designs

In addition to the Reograd rotor core, Beckman manufacture two other rotor cores that fit the JCF-Z zonal rotor. These are the standard zonal core and the B-29 zonal core. Both cores allow loading and unloading of the rotor during centrifugation via a rotating seal assembly so that no gradient or sample reorientation occurs (figure 9.3).

Both cores require liquid to displace the gradient material from the rotor bowl. The standard core requires a more dense solution of the same gradient material to displace the bowl contents. Because sucrose acts as both the gradient material and enzyme substrate and because dextran and enzyme will sediment to the rotor wall during centrifugation, the addition of highly concentrated sucrose solutions at the rotor wall cannot be recommended.

The B-29 core uses water as the displacement liquid, introduced at the rotor centre so that the bowl contents are collected via the rotor edge. However, it was considered that the flow of gradient material via the rotor edge would lead to disruption and mixing of the sedimented material at the rotor wall.

By using a Reograd rotor,which uses air as the displacement medium, the anticipated problems associated with the liquid displacement techniques would not be encountered.

9.2. PRACTICAL ASPECTS OF THE LOADING AND UNLOADING OF ZONAL ROTORS

9.2.1 Loading of Sucrose Gradients

The Reograd core was fitted into the JCF-Z rotor and the rotor lid screwed firmly into place. The rotor was then left to equilibrate in a 25°C waterbath, so that the lid shaft protruded above the level of the water in the bath.

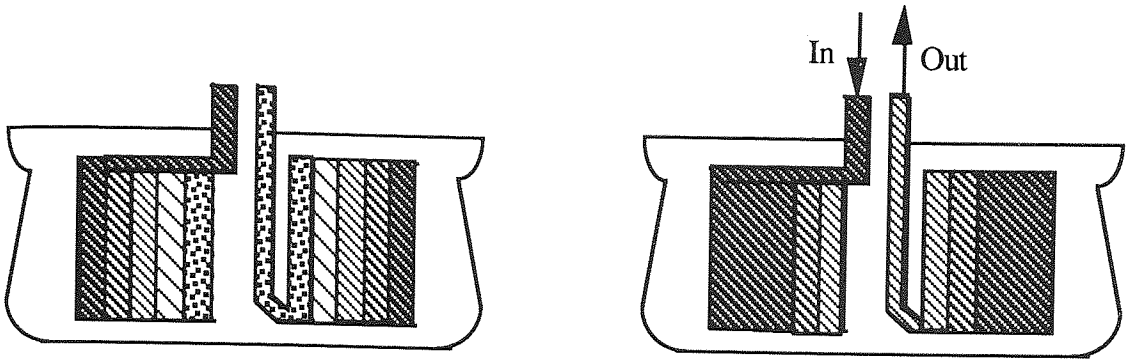

(a) The Gradient and sample are loaded at rotor speeds of 2000 rpm. The particles are separated under the applied centrifugal field.

(b) Contents are unloaded by introducing a dense solution at the rotor edge, displacing the bowl contents via the centre of the rotor.

Figure 9.4 (a) The Standard Zonal Core

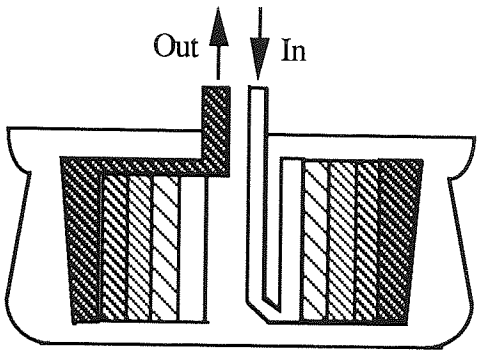

The bowl contents are unloaded using a less dense solution at the centre of the rotor, resulting in the displacement of the material via the edge of the rotor.

Figure 9.4 (b) The B-29 Zonal Rotor Core

Figure 9.4 Operating Principles of the Beckman Standard Zonal Core and the Beckman B-29 Zonal Core

Three to four appropriately concentrated sucrose solutions were prepared in 0.1 molar sodium acetate solutions at pH 5.2 and were left to equilibrate in the 25°C waterbath. The least concentrated sucrose solution was then loaded into the rotor via the transfer tube inlet, so that it formed a layer at the base of the bowl. This process was repeated using the successively denser sucrose solutions until the lightest gradient fraction was seen leaving the bowl via the exit port. Maximum gradient loading rates of 30-50 cm^3 min^{-1} were used in order to minimise mixing between the gradient layers[98]. The successive sucrose solutions typically varied in concentration by 5 or 10% w/w. For example, the preparation

of a 5-20% w/w gradient required sucrose solutions with concentrations of 5, 10, 15 and 20% w/w.

The layering technique used to construct the gradients resulted in the formation of discontinuous 'step' gradients. Using equation 4.26, the time period required for the layers to diffuse and form continuous, smooth gradients was calculated. Generally, time periods in excess of 19 hours were required. Therefore, the filled rotors were left overnight in the 25°C waterbath. Beckman manufacture gradient forming machines that can form continuous gradients of any shape in zonal rotors in a few minutes.

Unlike in swinging bucket rotors where the volumetric capacity of a tube is proportional to its length, the volumetric capacity of a bowl-shaped zonal rotor is proportional to the square of the bowl radius (section 4.4.2.4). The volume-radius relationship for the JCF-Z rotor containing the Reograd core is shown in the figure 9.5.

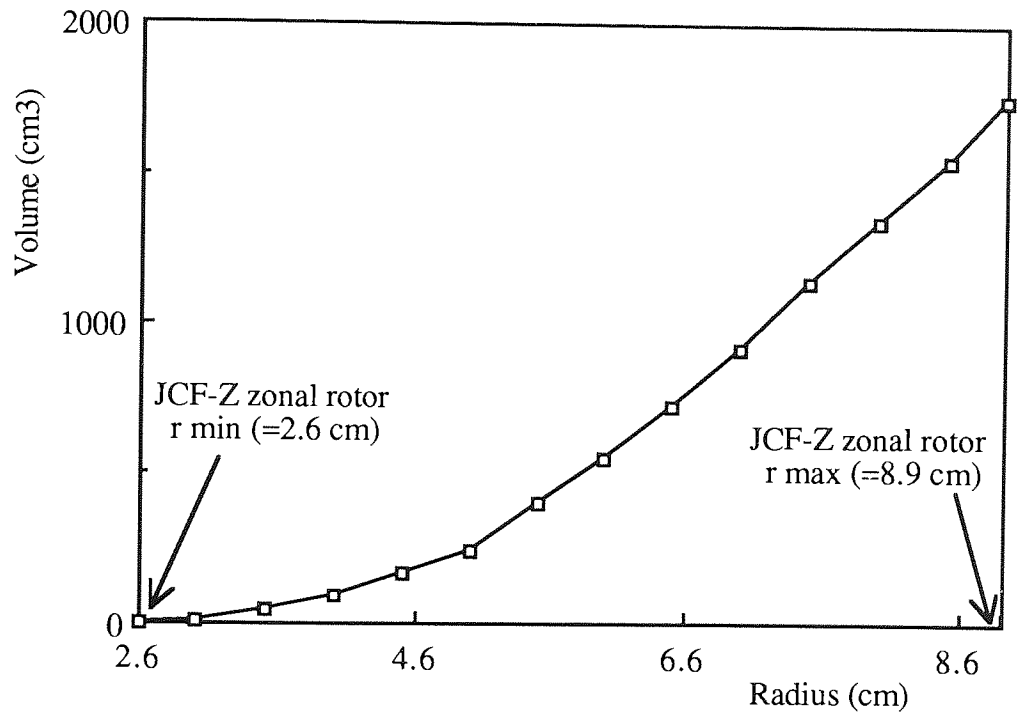

Figure 9.5 The Volume Versus Radius Relationship for the Beckman JCF-Z Zonal Rotor Fitted with the Reograd Core[173].

This figure can be used to calculate the volumes of each gradient fraction required to construct density and viscosity gradients of any chosen shape. For example, consider the construction of a sucrose gradient that is linear with respect to rotor radius. If four sucrose solutions are used in the construction, then for calculation purposes, the rotor must be split up into four equal radial sections as shown in figure 9.6. Knowing the minimum and maximum radii of rotation in the bowl, 2.6 cm and 8.9 cm respectively, the radial positions

of points r_1, r_2 and r_3 can be calculated. These radial values can then be used to determine the values of sucrose solution required for gradient construction from Figure 9.5. The gradient volumes required for the construction of a 5 -20% w/w linear sucrose gradient is given in table 9.1. The initial 'shapes' of the several gradients used in this study were all calculated using the above technique.

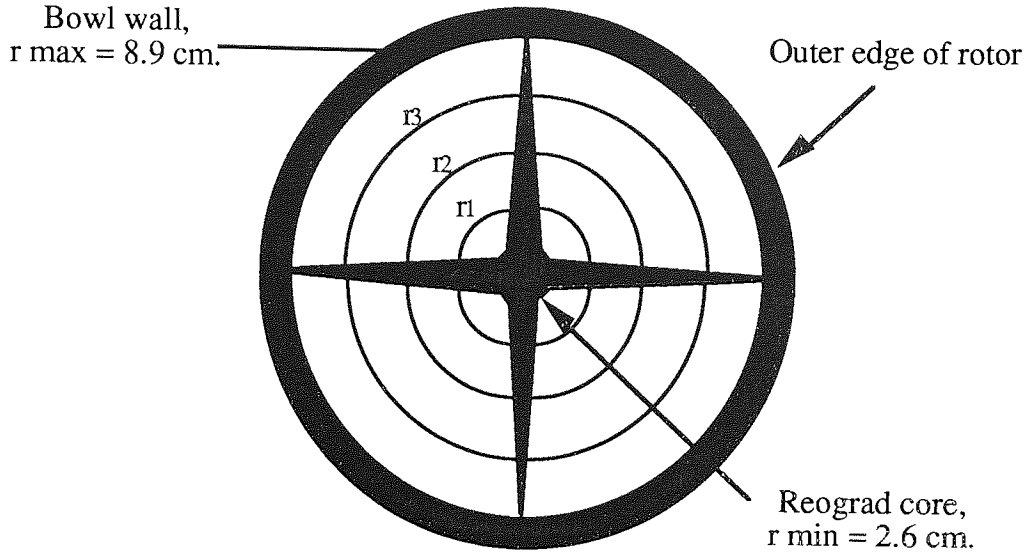

Figure 9.6 The Radial Measurements Required for the Construction of a 'Linear' Sucrose Gradient.

Sucrose Concentration (% w/w)	Required Radial Position (cm)	Equipment Gradient Volume (cm^3)
5	2.600 - 4.175	100
10	4.175 - 5.750	380
15	5.750 - 7.325	550
20	7.325 - 8.900	720

Table 9.1 The Solution Volumes Required for the Preparation of a Linear 5-20% w/w Gradient in a JCF-Z Zonal Rotor Fitted with a Reograd Core

9.2.2 Sample Concentration

Before being loaded onto a gradient, the total solids concentration of the enzyme sample was determined using a Bellingham and Stanley refractometer, supplied by BDH Limited, Warwicks., U.K. The use of hand-held refractometers to measure sample solids concentrations prior to rate-zonal centrifugations is an established technique[98]. The sample solids concentration was always at least 40% less than the starting gradient concentration, in order to prevent gradient overloading (Section 4.2.2.5). Griffith[98] has

reported that this maximum loading guideline is in reasonable agreement with investigators formulae for gradient loading capacities in zonal rotors. When necessary, the enzyme was diluted using a 0.1 molar sodium acetate solution at pH 5.5 before being left in a waterbath to equilibrate at 25°C.

It has been recommended that the sample solutions used in a rate-zonal centrifugation should contain a small amount of the gradient material, the added viscosity of this material helping to reduce sample diffusion into the gradient (122). The additional material does not affect the recommended sample loading concentration. For example, an 8% w.w solution, containing 6% w/w sample and 2% w/w sucrose should be supported by a gradient with a starting concentration of 10% w/w sucrose. Therefore, in several runs, a small precalculated volume of a buffered 50% w/w sucrose solution was added to the dextransucrase enzyme immediately prior to loading. The enzyme was then layered onto the top of the gradient using a hypodermic syringe via the transfer tube outlet as shown in figure 9.2.(b). The addition of sucrose to active enzyme solutions resulted in some enzymic reaction during sample loading.

9.2.3 Sample Volume

The determination of the optimum volume of enzyme that should be applied to a given sucrose gradient was a leading objective of this experimental work. Although large volumes of enzyme will allow increased conversion of substrate to product, this may result in poor separation of the reaction products. Furthermore, 'thin' enzyme zones should result in a more instantaneous removal of the fructose molecules from the enzyme rich portions of the bioreactor, which may help minimise the acceptor reaction. Griffith(98) has recommended a maximum sample loading equal to 10% of the gradient volume in a zonal centrifuge, which is about 160 cm^3 in the JCF-Z rotor fitted with a Reograd core. Maximum sample loading rates of 25 cm^3 min^{-1} were used in order to minimise mixing between the sample and gradient during loading.

9.2.4 Overlaying Samples

It is usual when conducting rate-zonal centrifugations in zonal rotors to overlay sample zones with less dense 'overlay' solutions, in order to displace the sample away from the rotor core and into regions of higher centrifugal fields(122). 0.1 molar sodium acetate solutions at pH 5.2 were employed in these studies, introduced into the rotor via the transfer tube outlet using loading rates of 15-25 cm^3/min. Some trials were carried out without an overlay in order to minimise back-diffusion of sample material into the overlay.

9.2.5 Centrifugation

After loading, the transfer tube was removed from the rotor lid shaft and the rotor was capped. The rotor was then carefully removed from the waterbath and placed on the greased centrifuge spindle.

Run parameters such as run time, rotor temperature, rotor speed and acceleration / deceleration rates had been previously stored in the machine's memory. Slow initial acceleration rates were required to help prevent mixing of the bowl contents at the start of a run. The rotor was rapidly decelerated to 500 rpm at the end of each run before being slowly decelerated to rest, again to help minimise mixing in the vessel. Typical acceleration and deceleration rates are shown in Figure 9.7.

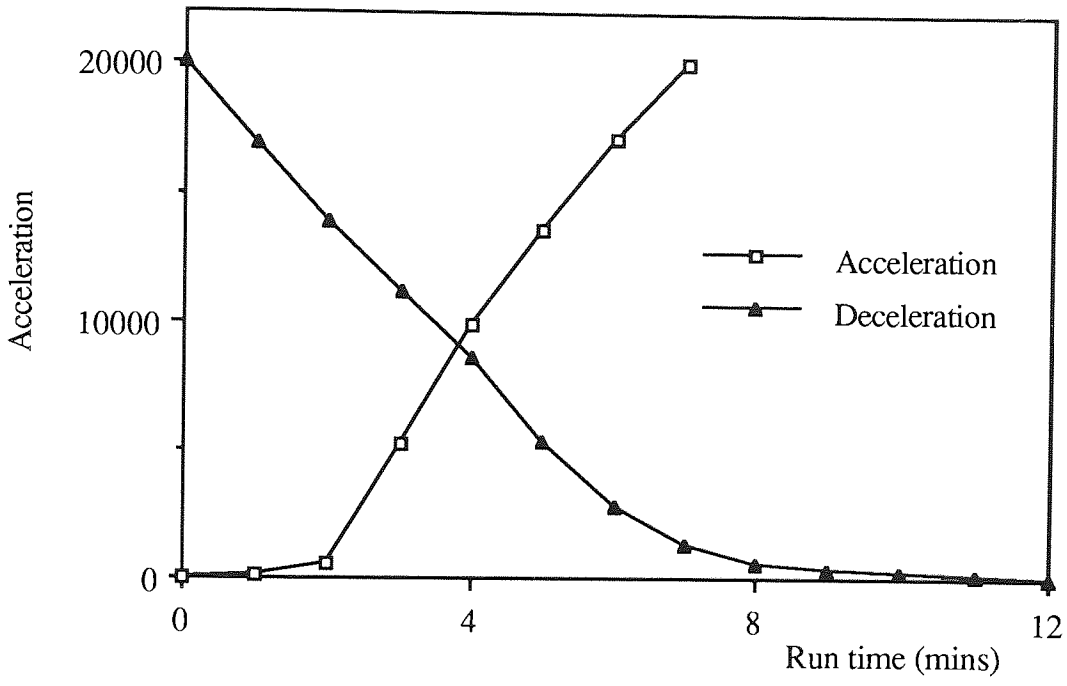

Figure 9.7 Typical Acceleration and Deceleration Rates of a Beckman JCF-Z Zonal Rotor in a J2-MC Centrifuge

9.2.6 Gradient Unloading and Sample Recovery

Initially, the rotor contents were unloaded by air displacement (figure 9.2f). However, in trials where an appreciable build up of gelatinous dextran rich material at the rotor wall had occurred, the removal of the supporting gradient by the introduction of air into the vessel resulted in the collapse of gel material from the rotor wall and subsequent mixing with the remaining gradient material. This led to the development of a novel gradient harvesting technique, whereby water, rather than air was used as the displacement medium (figure 9.8). The water supported the sedimented material at the rotor wall during gradient

harvesting and prevented it from collapsing into and mixing with the liquid contents of the rotor.

Typically, 20 to 30 equal fractions of rotor volume, corresponding to 60-90 cm^3 fraction volumes were collected during unloading. The samples were unloaded at flowrates of up to 50 cm^3/min. Typically it took around 40 minutes to harvest the liquid contents from the rotor at the end of a run. By measuring the exact volume of each gradient fraction and knowing the dimensions of the rotor bowl cavity and rotor core, then the exact position that each gradient fraction occupied in the bowl during centrifugation can be calculated as described in Appendix A7.

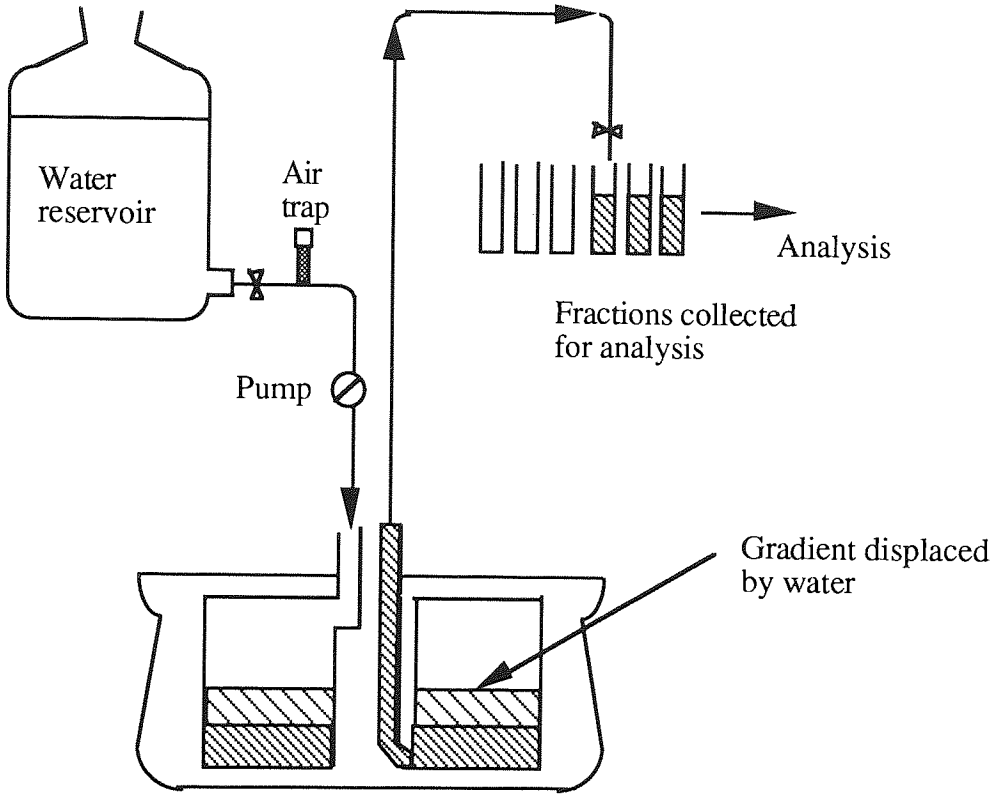

Figure 9.8 Gradient Harvesting by Water Displacement.

9.2.7 Sample Analysis

After harvesting, each gradient fraction was assayed to determine the concentrations of sucrose, fructose, other low MW sugars and dextran present. Enzyme assays were performed on the gradient fractions in order to determine the distribution of enzyme activity in the bioreactor at the end of each run. The experimental procedure was designed to yield information concerning the distribution of the various saccharides and the enzyme activity in the bioreactor at the end of each bioreaction-separation run. The assay procedure is outlined in Figure 9.9.

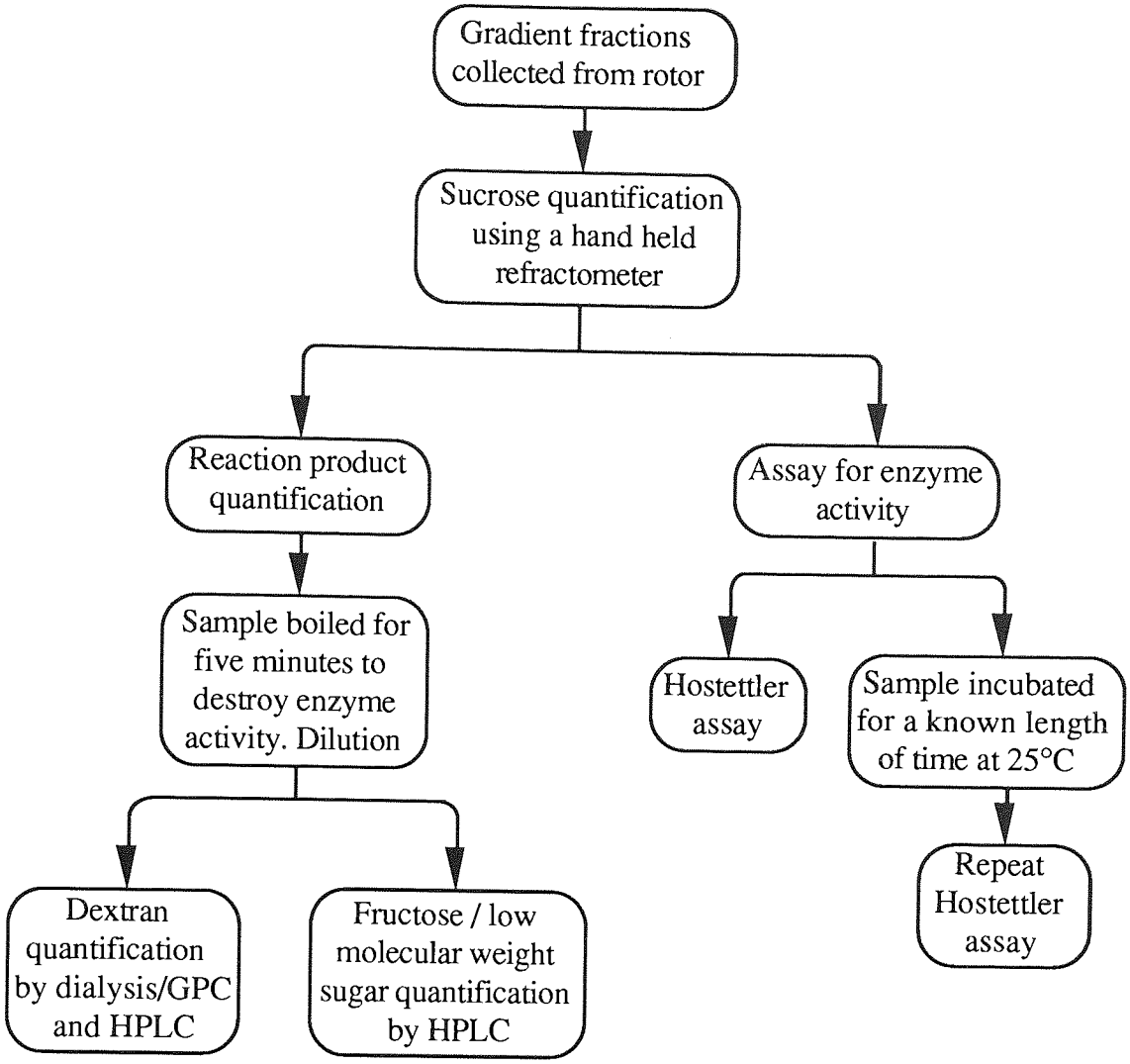

Figure 9.9 Sample Analysis Procedure.

During sample unloading, the approximate solids concentration of each fraction was determined using the hand-held refractometer. After gradient unloading had been completed, a small portion of each fraction was heat treated and the dextran, fructose and other low MW sugar levels were determined by the GPC/dialysis and HPLC techniques as described in chapter 5.

The remaining non-heat treated fractions were then tested for enzyme activity as follows : A 0.5 cm^3 portion of each fraction was added to a 4.5 cm^3 portion of a 5% w/v sucrose solution at pH 5.2 and 25°C, shaken and a 0.5 cm^3 fraction removed and assayed by Hostettler's method (section 3.4.1.2) to determine its reducing sugar content. The remaining solutions were then incubated in a waterbath at 25°C for a known period of time before 0.5 cm^3 fractions were similarly treated. The analytical procedure was designed so that all of the 10-30 fractions were initially assayed for reducing sugar content within 30 minutes of the completion of the unloading procedure. The fractions were re-assayed in the same order as they were originally assayed, after being incubated for a specific time

interval. Therefore, the time interval between the original assay and the re-assay was the same for each fraction. The dextransucrase enzyme activity of a given gradient fraction could then be calculated using equation 3.3.

The molecular weight distribution (MWD) of the dextran materials collected from the bioreactor were not determined because the use of sucrose gradients caused analytical problems for the reasons discussed in section 7.3.1.

The sample fractions collected for HPLC analysis were heat treated as soon as possible after run termination. Therefore, the saccharide concentration and enzyme activity profiles obtained in these runs represent the distribution of the reaction materials at this time. The enzymic reaction will continue to occur after the termination of centrifugation and will therefore represent the concentration and activity profiles at the time of heat treatment or enzyme assay. This effect will be less important in the longer duration runs.

9.3 RESULTS

9.3.1 Introduction

The data and run conditions for all the bioreaction-separation runs undertaken using the JCF-Z rotor fitted with the Reograd core are summarised in tables 9.6 to 9.16. The saccharide concentrations and enzyme activity versus radial distance profiles are shown in figures 9.14 to 9.24. The run conditions used in all the bioreaction-separation trials are summarised in table 9.17.

A number of preliminary runs were conducted prior to the bioreaction-separation trials. The first set of runs were effectively a 'calibration' of the system, using presynthesised native dextran and fructose mixtures. Two such runs, numbers 3 and 4, are reported here (see tables 9.2 and 9.3 and figures 9.10 and 9.11). A second set of trials were conducted in order to study the sedimenting properties of heat treated enzyme fractions during a rate-zonal separation. These results are reported in tables 9.4 and 9.5 and figures 9.12 and 9.13).

Steensgaard et al[120] have reported a method that allows the influence of the increasing density and viscosity of the supporting gradient medium on particle sedimentation to be simply treated in physical terms. The procedure is reported in appendix A8. Essentially this method calculates the equivalent sedimentation coefficient value (S-value) that a particle would require in order to sediment to the centre of a given gradient fraction under the stated centrifugation conditions, while taking account of the increasing density and viscosity of the surrounding medium. This method proved very useful for calculating the S-value in the

preliminary rate-zonal separation trials involving the presynthesised native dextran-fructose mixtures and heat-treated enzyme samples (sections 9.3.2 and 9.3.3). The calculated sedimentation coefficient value corresponding to the radial position of each gradient fraction recovered from the bioreactor for these runs is shown in tables 9.2 to 9.5. However, in the special case of the rate-zonal bioreaction-separation process, this method had two serious drawbacks. Firstly, the sucrose gradient concentrations and hence the gradient densities and viscosities changed as the dextransucrase reaction proceeded and secondly, there was the problem of substantial changes in bioreactor viscosity due to the native dextran formed. Therefore, the sedimentation coefficient calculations reported in tables 9.6 to 9.16 should be treated with caution. For this reason the concentration / activity profiles of the presynthesised native dextran-fructose mixtures and heat-treated enzyme runs are plotted against sedimentation coefficient (figures 9.10 to 9.13) and the bioreaction-separation profiles are plotted against radial position in the bioreactor (figures 9.14 to 9.24).

A useful method of assessing bioreactor performance involved comparing the quantity and degree of separation of the native dextran product that had accumulated as a 'gel' layer at the rotor wall. Such data for all of the bioreaction-separation runs is summarised in table 9.18. In this table, the mass of dextran sedimenting to the rotor wall per hour was calculated by dividing the total mass of dextran recovered from the rotor wall at the end of a run by the total run time. The percentage of dextran at the rotor wall represented the amount of dextran recovered from the rotor wall as a percentage of the total dextran recovered from the bioreactor at the end of a trial. The mass of dextran divided by the mass of fructose found in the 'gel' fraction at the rotor wall at the end of a trial was recorded in table 9.18 in the 'dextran:fructose ratio in gel' column. The maximum S-value required for a particle to migrate from the centre of the initial sample zone to the rotor wall under the stated run conditions, calculated as described in appendix A8, is listed in column 5. This value is only very approximate in the bioreaction-separation runs because of the changing densities and viscosities of the supporting 'gradient' medium due to sucrose consumption and dextran formation. The final mean dextran concentrations, expressed as %w/v, were calculated by dividing the mass of dextran recorded at the termination of each trial by the total bowl volume (1750 cm^3). The percentage of sucrose consumed in a trial was calculated from the amount of sucrose initially loaded into the bioreactor and the amount of dextran and fructose recovered from the vessel.

In run number 17, the JCF-Z rotor fitted with the Reograd core was loaded with sample and the bowl contents unloaded via a rotating seal assembly while the rotor was spinning at 2000 rpm ('dynamic' loading/unloading). This run was carried out in order to determine if gradient reorientation had a significant effect on the distribution of the dextransucrase enzyme and reaction products at the end of a trial. A 'flat' 20% w/w sucrose gradient was

used in run 20 to help assess the effect of gradient shape on bioreactor performance. Run number 21 used a 'repeat' injection technique where 35 cm^3 fractions of enzyme solution were injected at ninety minute time intervals throughout the duration of the run. Five injections were made in all. This was done in an attempt to minimise viscosity effects in the bioreactor. A detailed breakdown of the mass balances of these trials are recorded in appendix A9.

Sample number	Radial position (cm)	Ln Radius	Sucrose conc. (%w/w)	Equiv. Sedim value	S 20,w value (Sved)	Percent Fructose	Percent Dextran
28	3.50	Vi = 1.24	5.00	1.35	0.00	48.50	11.94
27	3.85	1.35	7.40	1.49	47.26	9.88	1.66
26	4.16	1.43	10.10	1.64	85.62	5.11	1.06
25	4.46	1.49	11.60	1.74	120.84	3.47	2.97
24	4.74	1.56	12.60	1.82	153.33	2.58	6.31
23	5.00	1.61	13.20	1.89	183.60	4.95	9.47
22	5.25	1.66	13.90	1.95	211.47	10.35	14.76
21	5.48	1.70	14.60	1.99	237.45	11.44	22.92
20	5.71	1.74	15.20	2.06	262.35	0.73	3.65
19	5.93	1.78	16.00	2.14	286.07	0.00	4.49
18	6.14	1.82	16.70	2.20	308.70	0.00	5.12
17	6.35	1.85	17.50	2.29	330.76	0.00	4.68
16	6.54	1.88	18.20	2.38	352.25	0.00	3.79
15	6.74	1.91	19.00	2.48	373.48	0.00	2.43
14	6.92	1.93	19.60	2.55	394.00	0.00	2.03
13	7.10	1.96	20.10	2.61	413.97	0.00	1.18
12	7.28	1.98	20.60	2.69	433.39	0.00	0.00
11	7.45	2.01	21.30	2.79	452.62	0.00	0.00
10	7.62	2.03	22.00	2.91	471.82	0.00	0.00
9	7.78	2.05	22.80	3.04	491.10	0.00	0.00
8	7.94	2.07	23.30	3.13	509.95	0.00	0.00
7	8.10	2.09	24.00	3.27	528.93	0.00	0.00
6	8.26	2.11	24.30	3.32	547.54	0.00	0.00
5	8.41	2.13	24.60	3.37	565.73	0.00	0.00
4	8.56	2.15	24.70	3.40	583.47	0.00	0.00
3	8.70	2.16	25.00	3.47	600.85	0.00	0.00
2	8.85	2.18	25.00	3.47	617.74	1.97	0.00
1	8.90	2.19	25.00	3.47	623.62	1.02	1.54

Sample volume (cm 3):	50
Overlay volume (cm 3):	100
Corresponding initial radial position (cm)	3.45
Ln (initial radial position)	1.24
Run time (mins):	120
Acceleration & Deceleration time (mins):	7 & 18.67
Rotor speed (rpm):	20 000
Corresponding force-time integral:	3E+10
Sucrose gradient (% w/w)	5 - 25

Table 9.2: Experimental Data from the Presynthesised Native Dextran and Fructose Rate-Zonal Centrifugation Studies. Run 3

Sample number	Radial position (cm)	Ln Radius	Sucrose conc. (%w/w)	Equiv. Sedim value	S 20,w value (Sved)	Percent Fructose	Percent Dextran
28	3.50	Vi = 1.25	4.70	1.35	0.00	59.56	13.10
27	3.86	1.35	7.00	1.46	41.09	1.25	1.93
26	4.17	1.43	9.60	1.57	77.87	1.31	3.16
25	4.47	1.50	11.20	1.72	113.09	0.46	4.65
24	4.75	1.56	12.00	1.78	145.01	3.33	8.59
23	5.02	1.61	12.80	1.83	174.34	6.93	7.90
22	5.27	1.66	13.40	1.91	201.69	14.15	13.94
21	5.50	1.71	14.00	1.95	227.21	7.85	18.67
20	5.73	1.75	14.70	2.01	251.35	0.00	4.64
19	5.95	1.78	15.40	2.08	274.44	0.00	5.28
18	6.16	1.82	16.20	2.16	296.62	0.00	4.84
17	6.37	1.85	17.20	2.25	318.48	0.00	3.32
16	6.57	1.88	18.00	2.36	339.91	0.00	2.71
15	6.76	1.91	18.70	2.43	360.47	0.00	2.06
14	6.95	1.94	19.40	2.54	380.97	0.00	1.40
13	7.13	1.96	20.00	2.61	400.84	0.00	1.25
12	7.30	1.99	20.40	2.67	419.95	0.00	0.00
11	7.48	2.01	21.00	2.76	439.02	0.00	0.00
10	7.64	2.03	21.60	2.84	457.79	0.00	0.00
9	7.81	2.06	22.40	2.97	476.52	0.00	0.00
8	7.97	2.08	23.20	3.10	495.42	0.00	0.00
7	8.13	2.10	23.70	3.17	513.93	0.00	0.00
6	8.29	2.11	24.20	3.30	532.50	0.00	0.00
5	8.44	2.13	24.40	3.34	550.46	0.00	0.00
4	8.59	2.15	24.60	3.38	568.12	0.00	0.00
3	8.74	2.17	24.80	3.41	585.46	0.00	0.00
2	8.88	2.18	24.80	3.41	601.97	0.00	0.00
1	8.90	2.19	23.80	3.17	603.73	2.78	0.00

Sample volume (cm 3):	50
Overlay volume (cm 3):	100
Corresponding initial radial position (cm)	3.49
Ln (initial radial position)	1.25
Run time (mins):	120
Acceleration & Deceleration time (mins):	7 & 18.67
Rotor speed (rpm):	20 000
Corresponding force-time integral:	3E+10
Sucrose gradient (% w/w)	5 - 25

Table 9.3: Experimental Data from the Presynthesised Native Dextran and Fructose Rate-Zonal Studies. Run 4.

Sample Number	Radial Position (cm)	Ln Radius	Sucrose Conc. (%w/w)	Equiv. Sedim Value	Solids Conc. (%w/w)	S 20, w Value Svedbergs
-	3.12	Vi = 1.14	8.00	1.16	1.36	0.00
19	3.25	1.18	8.60	1.18	1.15	38.29
18	3.79	1.33	10.40	1.27	0.98	197.81
17	4.26	1.45	12.00	1.36	0.82	328.15
16	4.69	1.55	13.00	1.42	0.36	438.07
15	5.08	1.63	14.00	1.48	0.22	534.39
14	5.44	1.69	15.00	1.55	0.11	621.13
13	5.78	1.75	15.80	1.61	0.07	700.45
12	6.10	1.81	17.00	1.69	0.04	774.88
11	6.41	1.86	18.00	1.77	0.02	845.29
10	6.70	1.90	19.00	1.86	0.00	912.62
9	6.97	1.94	19.90	1.96	0.00	977.60
8	7.24	1.98	20.90	2.06	0.00	1040.82
7	7.50	2.02	22.00	2.17	0.00	1102.74
6	7.75	2.05	23.00	2.29	0.00	1163.79
5	7.99	2.08	23.60	2.34	0.00	1222.48
4	8.23	2.11	24.20	2.44	0.00	1280.09
3	8.46	2.13	24.40	2.46	0.00	1334.92
2	8.68	2.16	24.60	2.47	0.26	1387.15
1	8.89	2.19	24.80	2.49	0.76	1437.29

Sample Volume (cm3)	55 cm3 heat treated enzyme
Overlay Volume (cm3)	45 cm3 buffer solution
Approximate solids content (% w/w)	9.1
Run time (mins)	180
Accel./Decel (mins)	2 / 17.25
Rotor speed (rpm)	10 000
Corresponding force-time integral	1.23E+10
Mass of sample loaded (g)	5.01
Mass of sample detected (g)	4.88
Sucrose gradient (% w/w)	10 - 25

Table 9.4: Experimental Data from the Heat Treated Dextran-sucrase Enzyme Rate-Zonal Centrifugation Studies. Run 10.

Sample Number	Radial Position (cm)	Ln Radius	Sucrose Conc. (%w/w)	Equiv. Sedim Value	Solids Conc. (%w/w)	S 20, w Value Svedbergs
-	3.21	Vi = 1.17	7.70	1.29	0.63	0.00
18	3.54	1.26	8.90	1.37	0.58	20.37
17	4.06	1.40	10.40	1.45	0.49	49.88
16	4.51	1.51	12.00	1.55	0.33	74.72
15	4.93	1.59	13.50	1.72	0.19	97.36
14	5.31	1.67	14.10	1.69	0.18	116.31
13	5.67	1.73	15.60	1.82	0.13	134.03
12	6.00	1.79	16.30	1.88	0.11	150.30
11	6.32	1.84	17.90	2.02	0.09	165.94
10	6.62	1.89	18.80	2.12	0.11	180.79
9	6.91	1.93	19.60	2.21	0.13	194.98
8	7.19	1.97	20.40	2.28	0.08	208.48
7	7.45	2.01	21.20	2.41	0.04	221.67
6	7.71	2.04	22.10	2.52	0.01	234.54
5	7.96	2.07	22.60	2.58	0.00	246.86
4	8.20	2.10	23.30	2.68	0.00	258.92
3	8.44	2.13	23.60	2.72	0.00	270.46
2	8.67	2.16	23.70	2.73	0.00	281.43
1	8.89	2.18	24.10	2.82	0.09	292.16
wall	8.90	2.19	23.60	2.72	2.21	292.70

Sample Volume (cm3)	70 cm3 heat treated enzyme
Overlay Volume (cm3)	50 cm3 buffer solution
Approximate solids content (% w/w)	3.2
Run time (mins)	1006
Accel./Decel (mins)	2 / 17.25
Rotor speed (rpm)	10 000
Corresponding force-time integral	6.66E+10
Mass of sample loaded (g)	2.24
Mass of sample detected (g)	2.81
Sucrose gradient (% w/w)	10 - 25

Table 9.5: Experimental Data from the Heat Treated Dextran-sucrase Enzyme Rate-Zonal Centrifugation Studies. Run 11.

Sample number	Radial position (cm)	Ln Radius	Mean Sucrose Conc	Equiv. Sedim value	S 20,w value Svedbergs	Percent Fructose	Percent Dextran
26	3.36	1.24	6.30	1.10	0.00	9.89	8.44
25	3.71	1.31	6.90	1.12	18.47	4.59	3.43
24	4.03	1.39	7.70	1.13	41.36	4.58	3.72
23	4.32	1.46	8.20	1.18	61.89	4.85	3.43
22	4.60	1.53	9.00	1.21	80.35	4.21	3.14
21	4.86	1.58	9.60	1.23	97.09	4.52	3.00
20	5.11	1.63	10.40	1.28	112.69	3.71	2.72
19	5.35	1.68	11.10	1.32	127.38	3.06	2.43
18	5.57	1.72	11.80	1.35	141.15	3.49	2.57
17	5.79	1.76	12.60	1.39	154.24	2.87	2.00
16	6.00	1.79	13.40	1.44	166.87	3.54	1.86
15	6.20	1.82	14.50	1.51	179.20	2.92	1.86
14	6.40	1.86	14.90	1.53	190.89	3.46	1.86
13	6.59	1.89	15.50	1.58	202.26	3.23	2.43
12	6.77	1.91	15.90	1.60	213.16	2.95	2.14
11	6.95	1.94	16.60	1.70	224.16	3.80	2.29
10	7.13	1.96	17.00	1.69	234.53	5.06	2.43
9	7.30	1.99	17.30	1.71	244.54	5.59	2.00
8	7.46	2.01	17.60	1.74	254.23	5.01	1.72
7	7.63	2.03	18.10	1.78	263.72	3.38	3.86
6	7.79	2.05	18.20	1.79	272.89	2.43	4.43
5	7.95	2.07	18.20	1.79	281.70	1.76	3.43
4	8.10	2.09	18.20	1.79	290.17	1.35	3.14
3	8.25	2.11	18.40	1.81	298.41	1.08	2.43
2	8.40	2.13	18.30	1.80	306.29	0.78	2.00
1	8.54	2.15	19.50	1.89	314.31	0.65	3.86
gel	8.90	2.19	17.70	1.75	331.89	7.25	23.38

Enzyme activity (DSU cm-3)	150	
Sample solids concentration (% w/w)	3	
Initial enzyme pulse (cm3)	50	(+ 2.4%w/w
Overlay volume (cm3)	100	sucrose)
Corresponding initial radial position (cm)	3.47	
Ln (initial radial position)	1.24	
Run time (mins)	150	
Acceleration/Deceleration time (mins)	7 / 6	
Rotor speed (rpm)	20000	
Corresponding force time integral	2.5E-11	
Sucrose gradient (%w/w)	5 - 20	

Table 9.6: Experimental Data from the JCF-Z Zonal Rotor Bioreaction-Separation Studies. Run Number 6.

Sample number	Radial position (cm)	Ln Radius	Mean Sucrose Conc	Equiv. Sedim value	S 20,w value Svedbergs	Percent Fructose	Percent Dextran
24	3.27	1.24	6.00	1.08	0.00	7.20	3.16
23	3.68	1.30	6.70	1.10	26.29	4.88	1.91
22	4.05	1.40	7.50	1.14	70.19	4.35	1.64
21	4.39	1.48	8.30	1.18	108.23	4.04	1.64
20	4.71	1.55	9.00	1.21	141.86	2.50	0.55
19	5.00	1.61	9.60	1.23	171.99	3.83	1.37
18	5.28	1.66	10.30	1.27	199.69	4.05	1.09
17	5.54	1.71	10.90	1.30	225.19	3.24	1.09
16	5.80	1.76	11.60	1.33	249.08	3.77	1.37
15	6.04	1.80	12.30	1.38	271.71	3.68	0.82
14	6.27	1.84	13.20	1.43	293.44	3.37	1.09
13	6.49	1.87	14.40	1.50	314.61	3.12	1.64
12	6.71	1.90	14.90	1.54	334.90	2.94	1.64
11	6.92	1.93	15.80	1.58	354.46	3.06	2.19
10	7.12	1.96	16.10	1.62	373.30	3.67	3.28
9	7.32	1.99	16.80	1.66	391.62	3.74	3.01
8	7.52	2.02	17.40	1.71	409.52	3.37	3.83
7	7.70	2.04	17.70	1.74	426.79	4.18	4.38
6	7.89	2.07	17.90	1.77	443.53	3.83	4.92
5	8.07	2.09	18.20	1.82	459.95	4.30	6.56
4	8.24	2.11	18.20	1.82	475.67	4.48	6.02
3	8.41	2.13	18.30	1.83	490.86	4.72	6.02
2	8.58	2.15	18.40	1.85	505.57	4.58	6.29
1	8.75	2.17	18.40	1.85	519.72	4.21	8.48
gel	8.90	2.19	18.00	1.77	532.04	4.99	26.23

Enzyme activity (DSU cm-3)	50	
Sample solids concentration (% w/w)	1.8	
Initial enzyme pulse (cm3)	50	(+ 2%w/w
Overlay volume (cm3)	100	sucrose)
Corresponding initial radial position (cm)	3.47	
Ln (initial radial position)	1.24	
Run time (mins)	90	
Acceleration/Deceleration time (mins)	7 / 6.5	
Rotor speed (rpm)	20000	
Corresponding force time integral	4E+11	
Sucrose gradient (%w/w)	5 - 20	

Table 9.7: Experimental Data From the JCF-Z Zonal Rotor Bioreaction-Separation Studies. Run Number 7.

Sample number	Radial position (cm)	Ln Radius	Mean Sucrose Conc	Equiv. Sedim value	S 20,w value (Sved.)	Percent Fructose	Percent Dextran
25	3.28	1.24	7.80	1.15	0.00	11.08	5.39
24	3.68	1.30	8.60	1.18	115.39	4.16	2.38
23	4.05	1.40	11.00	1.31	320.51	5.81	2.96
22	4.39	1.48	12.00	1.36	499.69	7.43	4.07
21	4.71	1.55	12.70	1.39	657.38	9.35	6.20
20	5.00	1.61	13.00	1.42	798.67	9.64	5.18
19	5.28	1.66	13.60	1.44	926.94	6.25	4.72
18	5.54	1.71	14.40	1.51	1047.93	5.33	3.61
17	5.80	1.76	14.90	1.54	1160.16	0.83	0.00
16	6.04	1.80	15.40	1.58	1265.82	0.49	0.00
15	6.27	1.84	16.00	1.62	1365.96	3.20	1.11
14	6.49	1.87	16.60	1.66	1461.31	2.85	1.29
13	6.71	1.90	17.00	1.69	1552.38	3.35	1.57
12	6.92	1.93	17.80	1.76	1641.50	2.95	1.29
11	7.13	1.96	18.30	1.80	1727.01	3.48	1.94
10	7.32	1.99	18.60	1.82	1809.00	2.87	1.76
9	7.52	2.02	19.00	1.86	1888.34	2.64	2.03
8	7.70	2.04	19.20	1.88	1964.36	3.43	2.59
7	7.89	2.07	19.60	1.91	2037.97	1.55	1.94
6	8.07	2.09	19.60	1.91	2108.27	1.20	3.88
5	8.24	2.11	19.60	1.91	2175.54	1.37	4.90
4	8.41	2.13	19.60	1.91	2240.03	1.71	5.92
3	8.58	2.15	19.70	1.92	2302.46	1.97	7.77
2	8.75	2.17	19.60	1.91	2362.04	2.31	12.58
1	8.91	2.19	19.10	1.86	2418.18	3.77	11.47
gel	8.94	2.19	17.70	1.74	2427.07	0.99	3.44

Enzyme activity (DSU cm-3)	220
Sample solids concentration (% w/w)	4.4
Initial enzyme pulse (cm3)	50
Overlay volume (cm3)	100
Corresponding initial radial position (cm)	3.47
Ln (initial radial position)	1.24
Run time (mins)	90
Acceleration/Deceleration time (mins)	4 / 4
Rotor speed (rpm)	10000
Corresponding force time integral	1.6E+10
Sucrose gradient (%w/w)	10 - 25

Table 9.8: Experimental Data from the JCF-Z Zonal Rotor Bioreaction-Separation Studies. Run Number 8

Sample number	Radial position (cm)	Ln Radius	'Mean' Sucrose conc. (%w/w)	Equiv. Sedim value	S 20,w value (Sved)	Percent Fructose	Percent Dextran
-	2.83	Vi = 1.04	9.21	1.08	0.00	0.00	0.00
19	2.90	1.07	9.21	1.08	5.08	1.75	1.13
18	3.51	1.26	10.44	1.08	38.30	11.08	10.25
17	4.02	1.39	13.69	1.21	69.44	11.17	9.07
16	4.48	1.50	16.36	1.36	96.77	11.28	8.81
15	4.90	1.59	20.06	1.70	124.81	10.45	6.25
14	5.28	1.66	23.10	2.06	153.79	8.05	6.01
13	5.64	1.73	26.00	2.53	184.65	6.33	4.39
12	5.97	1.79	28.06	2.91	216.09	6.14	4.27
11	6.29	1.84	30.34	3.48	249.75	5.34	3.20
10	6.59	1.89	31.86	3.83	283.37	4.33	3.26
9	6.88	1.93	32.79	3.78	313.69	4.17	3.12
8	7.16	1.97	34.56	4.67	348.17	3.42	4.13
7	7.42	2.00	34.61	4.26	377.31	3.27	3.99
6	7.68	2.04	37.39	5.83	414.49	2.14	4.67
5	7.93	2.07	40.05	8.08	462.69	1.93	6.07
4	8.17	2.10	42.11	10.55	521.85	2.19	4.63
3	8.41	2.13	42.56	10.55	577.65	1.67	4.97
2	8.63	2.16	43.00	10.55	630.46	1.74	4.39
1	8.86	2.18	43.11	9.43	675.28	2.85	5.68
Gel	8.90	2.19	41.52	7.02	681.48	0.69	1.74

Enzyme activity (DSU cm-3)	800
Sample solids concentration (%w/w)	9
Sucrose gradient (%w/w)	15-30
Initial enzyme pulse (cm3):	60
Overlay volume (cm3):	0
Corresponding initial radial position (cm)	2.84
Ln (initial radial position)	1.04
Run time (mins):	200
Acceleration & Deceleration time (mins):	5 & 5
Rotor speed (rpm):	20 000
Corresponding force-time integral:	5.4E+10

Table 9.9: Experimental Data from the JCF-Z Zonal Rotor Bioreaction-Separation Studies. Run Number 13.

Sample number	Radial position (cm)	Ln Radius	'Mean' Sucrose conc. (%w/w)	Equiv. Sedim value	S 20,w value (Sved)	Percent Fructose	Percent Dextran
-	2.77	Vi = 1.02	0.00	0.00	0.00	0.00	0.00
19	3.01	1.10	8.93	1.62	84.15	5.39	7.42
18	3.57	1.27	10.49	1.77	182.35	9.34	9.95
17	4.06	1.40	12.24	1.94	330.05	8.85	8.07
16	4.50	1.50	13.55	2.07	455.36	10.22	8.13
15	4.89	1.59	16.13	2.24	568.04	7.61	5.73
14	5.26	1.66	17.59	2.48	674.94	7.31	4.88
13	5.60	1.72	19.30	2.90	784.09	6.66	4.74
12	5.93	1.78	20.98	3.27	893.22	7.15	5.22
11	6.23	1.83	22.80	3.51	998.52	6.40	5.21
10	6.52	1.88	25.32	4.21	1113.27	3.39	6.03
9	6.80	1.92	27.28	4.46	1224.57	6.09	3.72
8	7.07	1.96	29.45	5.13	1342.86	2.62	3.05
7	7.33	1.99	30.84	5.95	1470.05	2.26	4.76
6	7.58	2.03	32.43	6.95	1608.79	2.50	3.40
5	7.82	2.06	34.26	7.64	1751.65	2.51	2.82
4	8.06	2.09	36.36	9.06	1911.06	2.40	2.15
3	8.29	2.11	37.84	9.78	2073.49	1.73	3.15
2	8.51	2.14	38.48	8.21	2202.71	1.30	1.98
1	8.73	2.17	39.74	9.06	2345.44	2.35	3.79
Gel	8.90	2.19	38.91	8.21	2436.57	3.93	5.79

Enzyme activity (DSU cm-3)	400	
Sample solids concentration (%w/w)	5.7	
Sucrose gradient (%w/w)	15-45	
Initial enzyme pulse (cm^3):	40	(+2% w/w
Overlay volume (cm^3):	0	sucrose)
Corresponding initial radial position (cm)	2.75	
Ln (initial radial position)	1.01	
Run time (mins):	1020	
Acceleration & Deceleration time (mins):	1 & 1.5	
Rotor speed (rpm):	5 000	
Corresponding force-time integral:	1.7E+10	

Table 9.10: Experimental Data from thev JCF-Z Zonal Rotor Bioreaction-Separation Studies. Run Number 15.

Sample number	Radial position (cm)	Ln Radius	'Mean' Sucrose conc. (%w/w)	Equiv. Sedim value	S 20,w value (Sved)	Percent Fructose	Percent Dextran
-	2.77	Vi = 1.02	0.00	0.00	0.00	0.00	0.00
18	2.90	1.07	6.41	1.25	38.51	2.28	2.28
17	3.51	1.26	7.48	1.30	186.99	5.29	5.32
16	4.03	1.39	7.43	1.30	294.05	5.61	5.28
15	4.50	1.50	7.80	1.31	378.29	4.32	4.00
14	4.91	1.59	8.54	1.34	449.46	5.68	5.65
13	5.30	1.67	9.17	1.39	511.82	5.97	6.14
12	5.66	1.73	9.73	1.40	566.65	5.46	5.67
11	6.00	1.79	10.93	1.49	617.96	6.11	6.65
10	6.31	1.84	11.90	1.55	665.99	4.57	4.83
9	6.62	1.89	12.98	1.61	711.20	5.36	6.00
8	6.91	1.93	13.42	1.65	753.32	5.03	5.56
7	7.19	1.97	14.27	1.71	793.64	5.35	5.91
6	7.46	2.01	14.16	1.70	830.86	4.73	4.33
5	7.72	2.04	15.31	1.78	867.15	5.11	5.19
4	7.97	2.08	16.10	1.84	902.27	5.18	5.23
3	8.21	2.11	16.63	1.89	936.03	5.25	5.39
2	8.45	2.13	16.95	1.93	968.59	5.08	5.07
1	8.68	2.16	17.65	1.98	1000.24	4.97	4.53
Gel	8.90	2.19	15.86	1.81	1027.67	8.67	11.46

Enzyme activity (DSU cm-3)	400
Sample solids concentration (%w/w)	5.7
Sucrose gradient (%w/w)	10 - 25
Initial enzyme pulse (cm3):	40
Overlay volume (cm3):	0
Corresponding initial radial position (cm)	2.77
Ln (initial radial position)	1.02
Run time (mins):	1020
Acceleration & Deceleration time (mins):	1 & 1.5
Rotor speed (rpm):	5 000
Corresponding force-time integral:	1.7E+10

Table 9.11: Experimental Data from the JCF-Z Zonal Rotor Bioreaction-Separation Studies. Run Number 16.

Sample number	Radial position (cm)	Ln Radius	'Mean' Sucrose conc. (%w/w)	Equiv. Sedim value	S 20,w value (Sved)	Percent Fructose	Percent Dextran
-	2.64	Vi = 0.97	15.12	1.77	0.00	0.00	0.00
14	3.27	1.18	15.12	1.77	70.74	10.22	8.82
13	3.82	1.34	16.60	1.89	125.92	10.26	8.89
12	4.31	1.46	17.83	1.99	170.28	7.63	8.04
11	4.74	1.56	19.11	2.12	208.44	7.81	9.12
10	5.14	1.64	20.05	2.23	241.99	5.63	6.24
9	5.51	1.71	20.51	2.27	271.39	4.66	5.57
8	5.86	1.77	21.75	2.42	298.97	4.29	4.93
7	6.18	1.82	22.41	2.52	324.56	3.25	5.46
6	6.49	1.87	23.93	2.76	349.83	4.09	4.21
5	6.79	1.92	24.56	2.83	373.39	4.34	3.98
4	7.07	1.96	25.75	3.01	396.45	3.35	3.36
3	7.34	1.99	26.54	3.16	418.77	4.15	3.54
2	7.61	2.03	26.64	3.18	439.66	4.41	1.85
1	8.70	2.16	28.76	3.64	530.95	18.90	0.05
'Wall'	8.90	2.19	25.75	3.01	543.73	6.92	20.71

Enzyme activity (DSU cm-3)	800
Sample solids concentration (% w/w)	9
Initial enzyme pulse (cm3):	10
Overlay volume (cm3):	0
Corresponding initial radial position (cm)	2.64
Ln (initial radial position)	0.97
Run time (mins):	200
Acceleration & Deceleration time (mins):	5 & 5
Rotor speed (rpm):	20000
Sucrose gradient (%w/w)	15-30
Corresponding force-time integral:	5.4E+10

Table 9.12: Experimental Data from the JCF-Z Zonal Rotor Bioreaction-Separation Studies. Run Number 17.

Sample number	Radial position (cm)	Ln Radius	'Mean' Sucrose conc. (%w/w)	Equiv. Sedim value	S 20,w value (Sved)	Percent Fructose	Percent Dextran
-	2.68	Vi = 0.99	0.00	0.00	0.00	0.00	0.00
16	3.27	1.18	15.54	1.80	134.02	9.49	3.86
15	3.82	1.34	16.56	1.87	243.71	8.85	3.58
14	4.31	1.46	18.47	2.06	335.47	8.12	2.85
13	4.74	1.56	19.55	2.16	413.05	8.69	2.96
12	5.14	1.64	21.08	2.35	483.77	7.31	3.47
11	5.51	1.71	21.76	2.41	546.29	7.76	4.03
10	5.86	1.77	23.07	2.60	605.60	6.12	3.75
9	6.18	1.82	24.04	2.75	661.47	6.00	4.36
8	6.49	1.87	24.38	2.76	712.09	5.24	4.86
7	6.79	1.92	25.41	2.97	761.69	4.36	4.58
6	7.07	1.96	26.21	3.11	809.29	4.35	5.28
5	7.34	1.99	27.17	3.30	855.93	4.77	5.59
4	7.61	2.03	27.20	3.30	899.28	4.36	6.33
3	7.86	2.06	28.06	3.48	942.01	5.06	6.04
2	8.11	2.09	28.46	3.58	983.27	4.63	6.62
1	8.60	2.15	27.70	3.13	1052.31	7.65	12.58
'Wall'	8.90	2.19	27.78	3.11	1091.59	15.59	26.70

Enzyme activity (DSU cm-3)	400
Sample solids concentration (% w/w)	6.6
Sucrose gradient (%w/w)	15-30
Initial enzyme pulse (cm 3):	20
Overlay volume (cm 3):	0
Corresponding initial radial position (cm)	2.68
Ln (initial radial position)	0.99
Run time (mins):	400
Acceleration & Deceleration time (mins):	4 & 4
Rotor speed (rpm):	10 000
Corresponding force-time integral:	2.7E+10

Table 9.13: Experimental Data from the JCF-Z Zonal Rotor Bioreaction-Separation Studies. Run Number 18.

Sample number	Radial position (cm)	Ln (Radius)	'Mean' Sucrose conc. (%w/w)	Equiv. Sedim value	S 20,w value (Sved)	Percent Fructose	Percent Dextran
-	2.60	Vi = 1.12	7.50	1.30	0.00	0.00	0.00
15	3.35	1.21	8.39	1.35	46.62	3.82	1.99
14	3.96	1.38	9.12	1.39	134.39	4.90	3.11
13	4.49	1.50	9.75	1.40	200.82	5.03	3.54
12	4.96	1.60	10.31	1.45	255.56	5.02	4.08
11	5.40	1.69	10.83	1.48	302.07	5.68	4.42
10	5.80	1.76	11.30	1.51	342.74	6.67	3.83
9	6.17	1.82	11.75	1.51	378.44	6.88	3.44
8	6.52	1.88	12.17	1.56	411.07	7.74	4.50
7	6.86	1.93	12.57	1.58	440.89	8.00	6.61
6	7.17	1.97	12.95	1.61	468.56	6.99	5.73
5	7.48	2.01	13.31	1.65	494.51	7.26	6.41
4	7.77	2.05	13.66	1.66	518.59	7.48	7.59
3	8.05	2.09	13.99	1.69	541.31	7.36	8.03
2	8.33	2.12	14.32	1.71	562.76	7.68	9.60
1	8.59	2.15	14.63	1.72	583.04	8.39	8.78
'Wall'	8.90	2.19	15.00	1.76	606.48	9.81	12.83

Enzyme activity (DSU cm-3)	400
Sample solids concentration (%w/w)	6.6
Sucrose gradient (% w/w)	15-25
Initial enzyme pulse (cm 3):	125
Overlay volume (cm 3):	0
Corresponding initial radial position (cm)	3.06
Ln (initial radial position)	1.12
Run time (mins):	400
Acceleration & Deceleration time (mins):	4 & 4
Rotor speed (rpm):	10 000
Corresponding force-time integral:	3.2E+10

Table 9.14: Experimental Data from the JCF-Z Zonal Rotor Bioreaction-Separation Studies. Run Number 19.

Sample number	Radial position (cm)	Ln (Radius)	'Mean' Sucrose conc. (%w/w)	Equiv. Sedim value	S 20,w value (Sved)	Percent Fructose	Percent Dextran
-	3.06	Vi = 1.11	7.50	1.30	0.00	0.00	0.00
15	3.39	1.22	7.50	1.30	51.28	5.77	5.52
14	4.03	1.39	7.50	1.30	136.14	5.47	5.67
13	4.59	1.52	7.50	1.30	199.06	6.09	5.26
12	5.08	1.63	7.50	1.30	249.10	5.78	5.73
11	5.53	1.71	7.50	1.30	290.64	6.53	6.80
10	5.94	1.78	7.50	1.30	326.15	7.24	6.68
9	6.33	1.85	7.50	1.30	357.17	7.56	7.73
8	6.70	1.90	7.50	1.30	384.70	6.87	6.49
7	7.04	1.95	7.50	1.30	409.45	6.64	6.74
6	7.37	2.00	7.50	1.30	431.94	6.91	6.89
5	7.69	2.04	7.50	1.30	452.53	6.94	6.55
4	7.99	2.08	7.50	1.30	471.53	6.49	6.17
3	8.29	2.11	7.50	1.30	489.16	6.59	6.19
2	8.57	2.15	7.50	1.30	505.61	7.07	6.82
1	8.71	2.16	7.50	1.30	513.77	3.55	3.33
wall	8.90	2.19	7.50	1.30	524.29	4.50	7.43

Enzyme activity (DSU cm-3)	400
Sample solids concentration (% w/w)	7.4
Initial enzyme pulse (cm3):	125
Overlay volume (cm3):	0
Corresponding initial radial position (cm)	3.06
Ln (initial radial position)	1.11
Run time (mins):	400
Acceleration & Deceleration time (mins):	4 & 4
Rotor speed (rpm):	10 000
Corresponding force-time integral:	2.6E+10
Sucrose gradient (% w/w)	15% 'flat' gradient

Table 9.15: Experimental Data from the JCF-Z Zonal Rotor Bioreaction-Separation Studies. Run Number 20.

Sample number	Radial position (cm)	Ln (Radius)	'Mean' Sucrose conc. (%w/w)	Equiv. Sedim value	S 20,w value (Sved)	Percent Fructose	Percent Dextran
-	3.22	Vi = 1.17	-	-	0.00	0.00	0.00
17	3.25	1.18	10.51	1.45	4.06	3.41	3.44
16	3.79	1.33	11.60	1.51	73.38	4.20	3.07
15	4.26	1.45	12.33	1.57	58.04	4.43	3.31
14	4.69	1.55	12.87	1.60	105.82	4.42	3.23
13	5.08	1.63	13.61	1.66	147.50	5.12	2.97
12	5.44	1.69	14.38	1.72	184.79	4.32	2.96
11	5.78	1.75	15.10	1.77	218.46	4.65	3.43
10	6.10	1.81	16.05	1.84	249.75	4.85	3.64
9	6.41	1.86	16.63	1.88	278.53	4.98	3.98
8	6.70	1.90	17.69	1.98	306.21	4.95	3.98
7	6.97	1.94	18.23	2.05	332.48	5.09	3.89
6	7.24	1.98	18.74	2.06	356.98	5.11	4.30
5	7.50	2.02	19.34	2.14	380.61	5.15	5.19
4	7.75	2.05	19.80	2.19	403.18	5.78	5.55
3	7.99	2.08	20.68	2.31	425.55	5.39	5.42
2	8.23	2.11	20.52	2.31	446.63	5.05	5.47
1	8.37	2.12	20.73	2.31	458.88	3.43	3.82
wall	8.90	2.19	16.88	1.58	489.56	19.66	32.35

Enzyme activity (DSU cm-3)	270
Sample solids concentration (% w/w)	3.9
Initial enzyme pulse (cm3):	5 x 35
Overlay volume (cm3):	0
Corresponding initial radial position (cm)	3.22
Ln (initial radial position)	1.17
Run time (mins):	480
Acceleration & Deceleration time (mins):	4 & 4
Rotor speed (rpm):	10 000
Corresponding force-time integral:	3.2E+10
Sucrose gradient (% w/w)	15-25%

Table 9.16: Experimental Data from the JCF-Z Zonal Rotor Bioreaction-Separation Studies. Run Number 21.

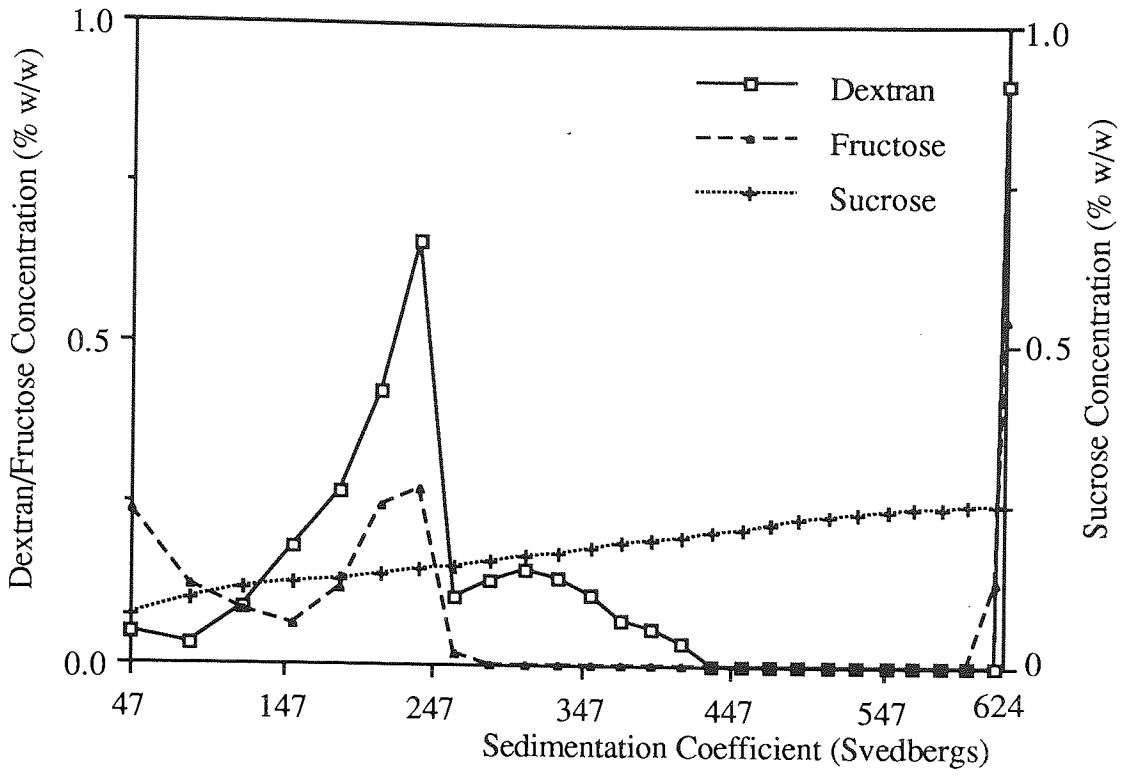

Figure 9.10 Plots of Concentration Versus Sedimentation Coefficient: Presynthesised Native Dextran and Fructose Mixture, Run 3

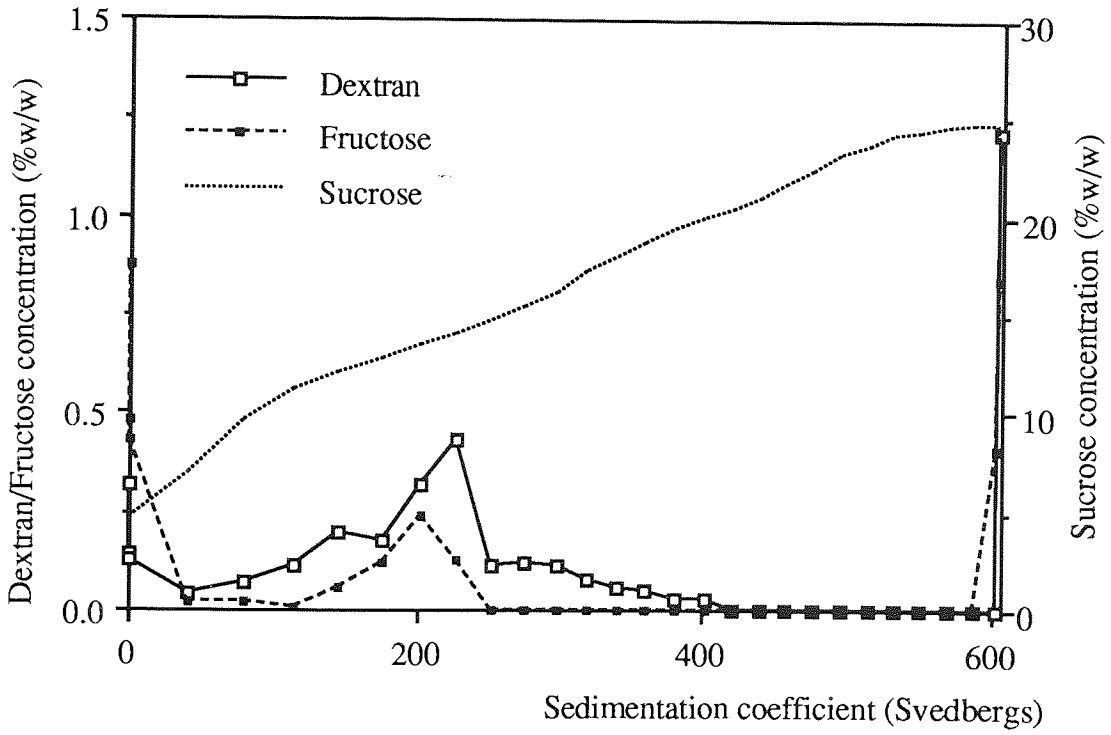

Figure 9.11 Plots of Concentration Versus Sedimentation Coefficient: Presynthesised Native Dextran and Fructose Mixture, Run 4

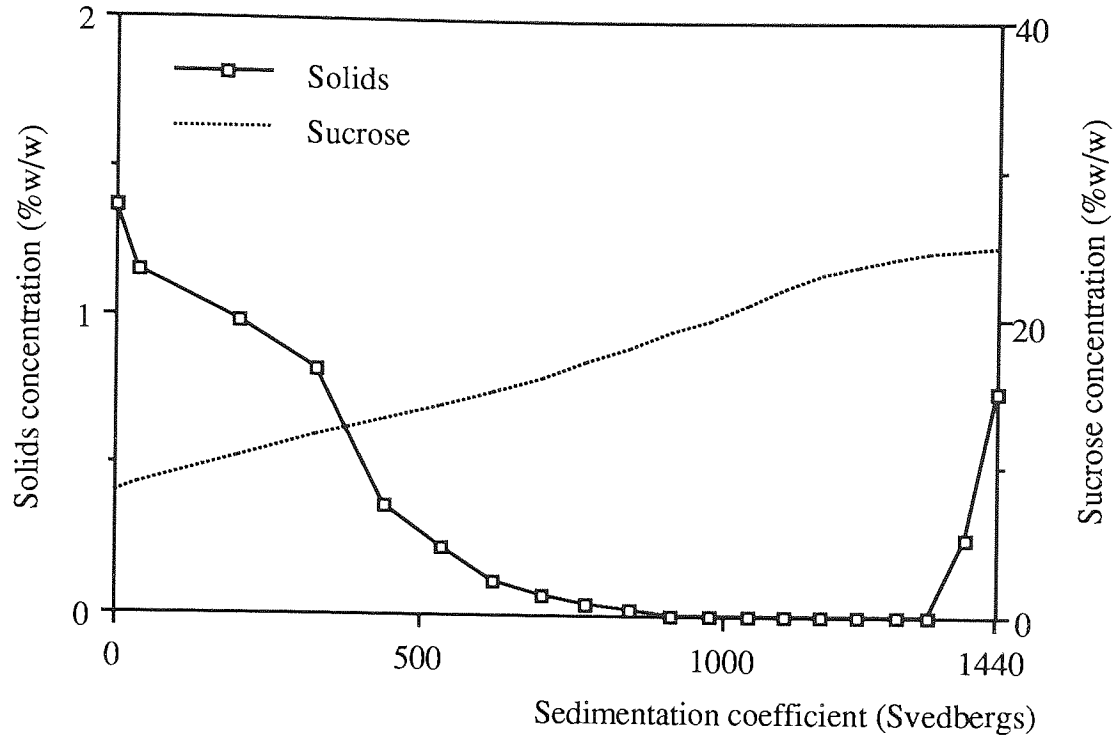

Figure 9.12 Plots of Sample and Sucrose Concentration Versus Sedimentation Profile: Heat Treated Enzyme Run Number 10

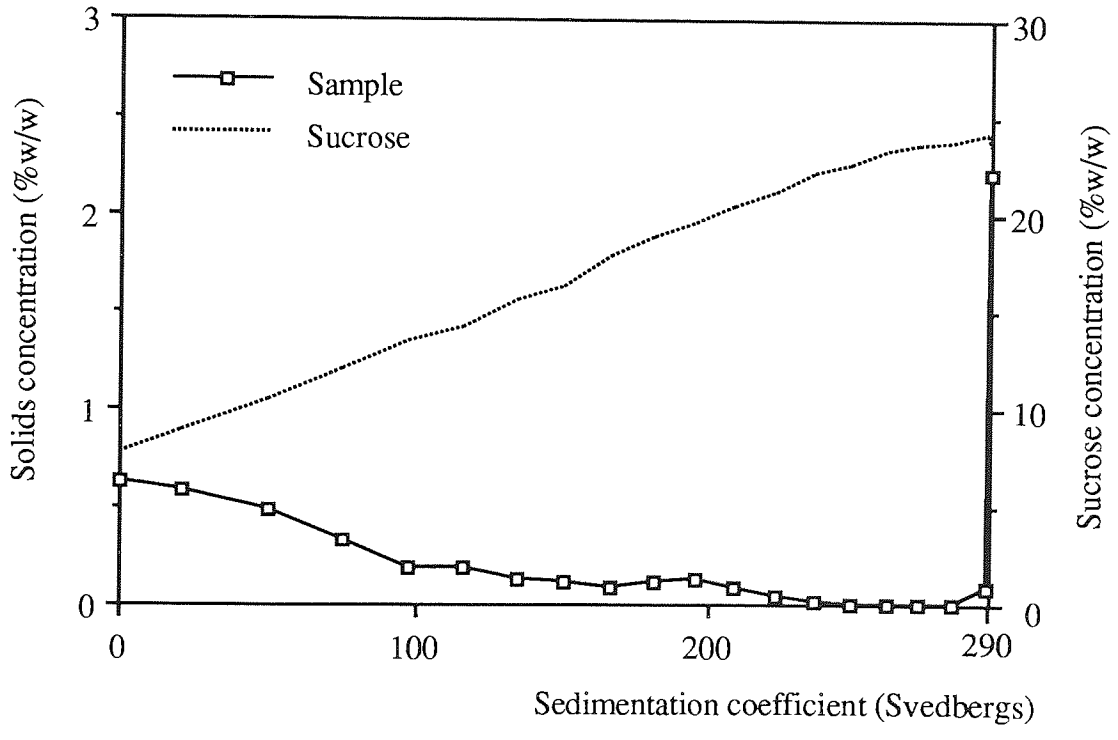

Figure 9.13 Plots of Sample and Sucrose Concentration Versus Sedimentation Profile: Heat Treated Enzyme Run Number 11

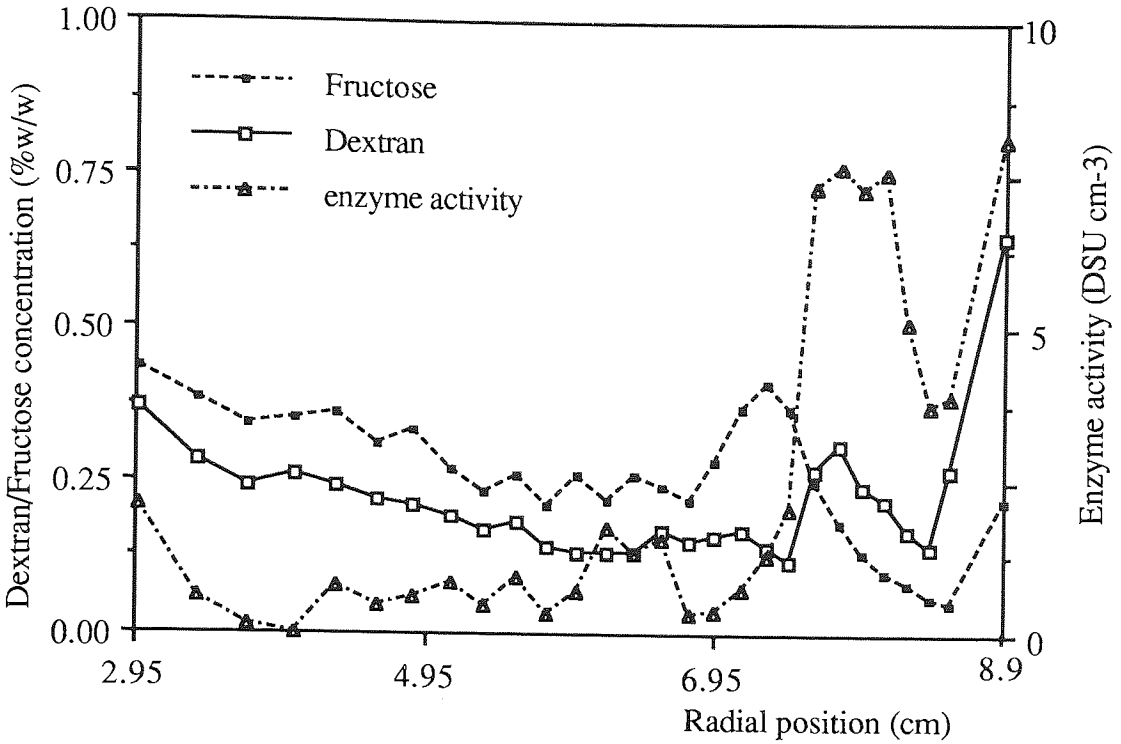

Figure 9.14 Plots of Dextran and Fructose Concentration and Enzyme Activity Versus Radial Position: Bioreaction-Separation Run Number 6

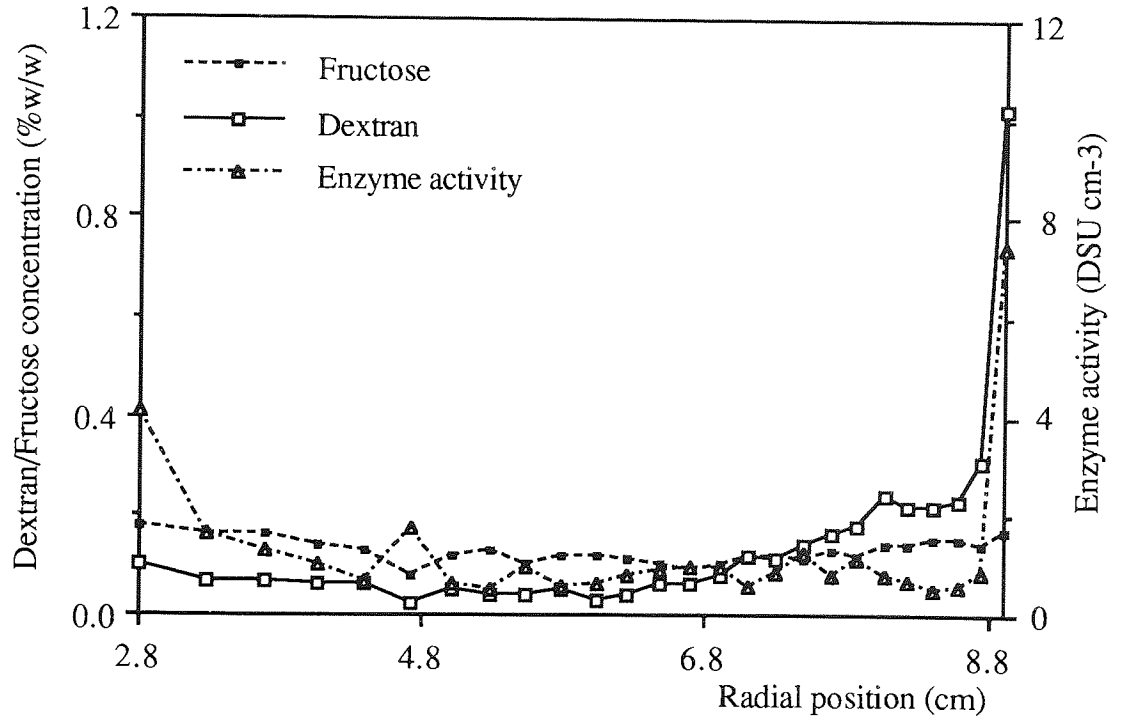

Figure 9.15 Plots of Dextran and Fructose Concentration and Enzyme Activity Versus Radial Position: Bioreaction-Separation Run Number 7

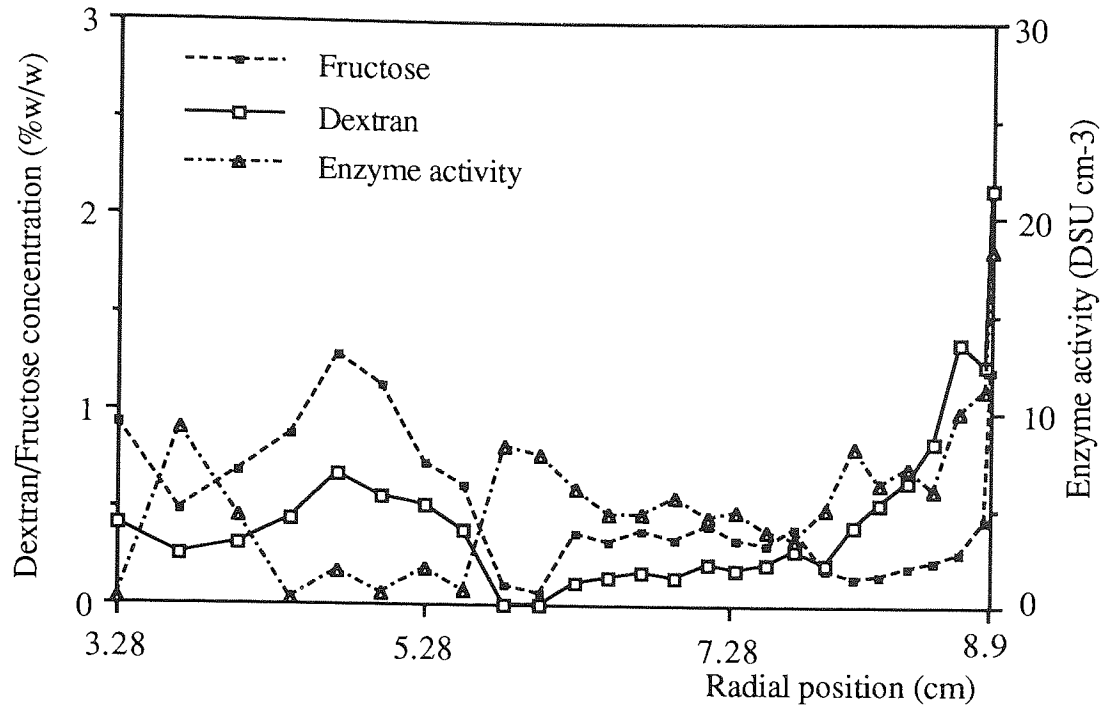

Figure 9.16 Plots of Dextran and Fructose Concentration and Enzyme Activity Versus Radial Position: Bioreaction-Separation Run Number 8

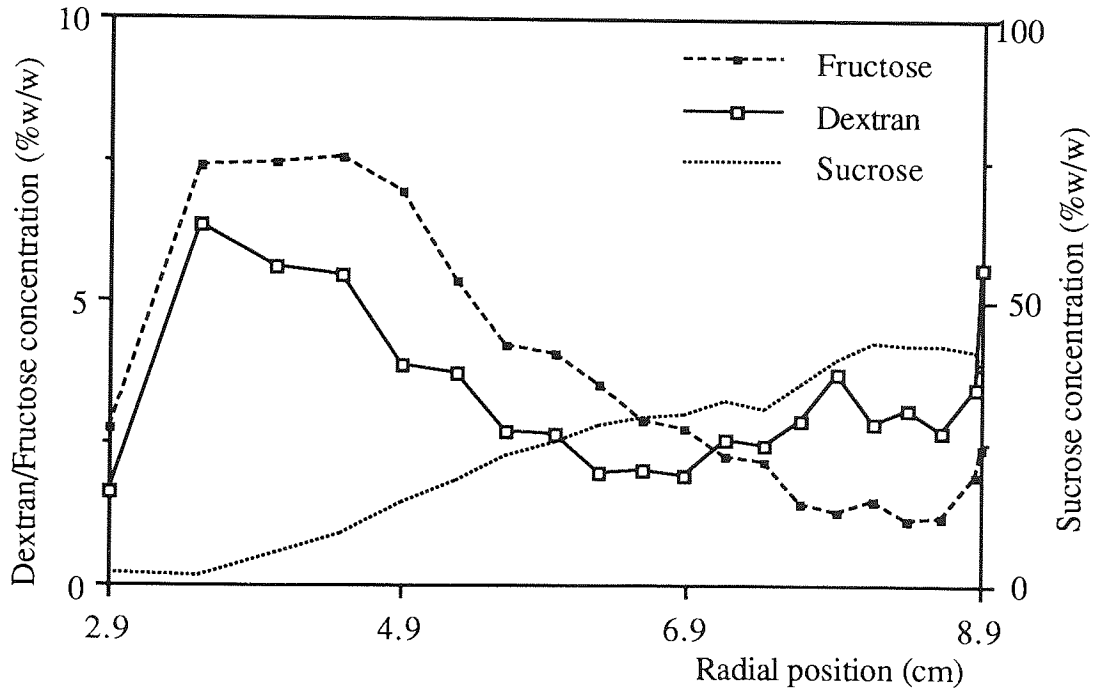

Figure 9.17 Plots of Dextran, Fructose and Sucrose Concentration Versus Radial Position: Bioreaction-Separation Run Number 13

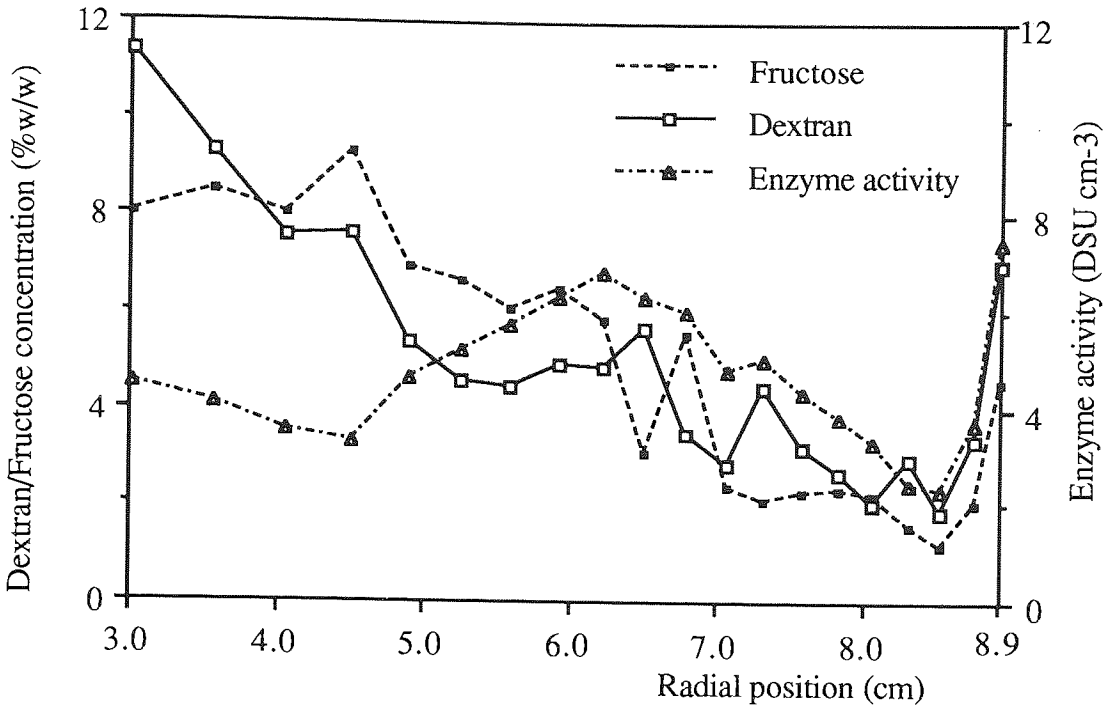

Figure 9.18 Plots of Dextran and Fructose Concentration and Enzyme Activity Versus Radial Position: Bioreaction-Separation Run Number 15

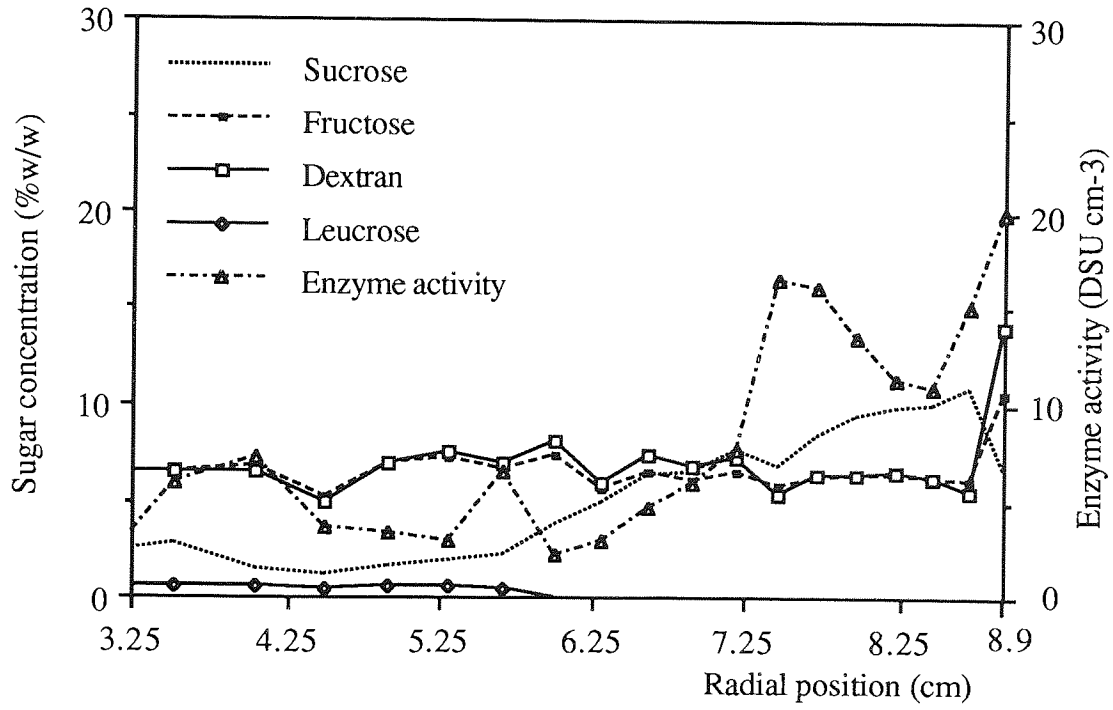

Figure 9.19 Plots of Dextran, Fructose, Sucrose and Leucrose Concentration and Enzyme Activity Versus Radial Position: Bioreaction-Separation Run Number 16

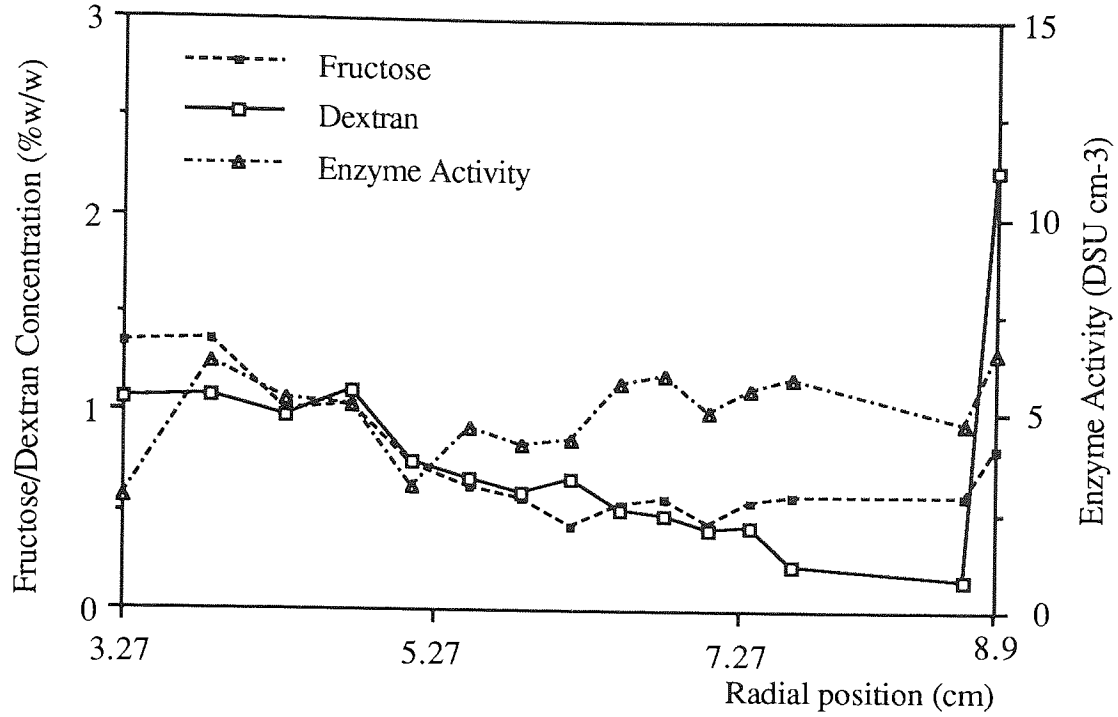

Figure 9.20 Plots of Dextran and Fructose Concentration and Enzyme Activity Versus Radial Position: Bioreaction-Separation Run Number 17

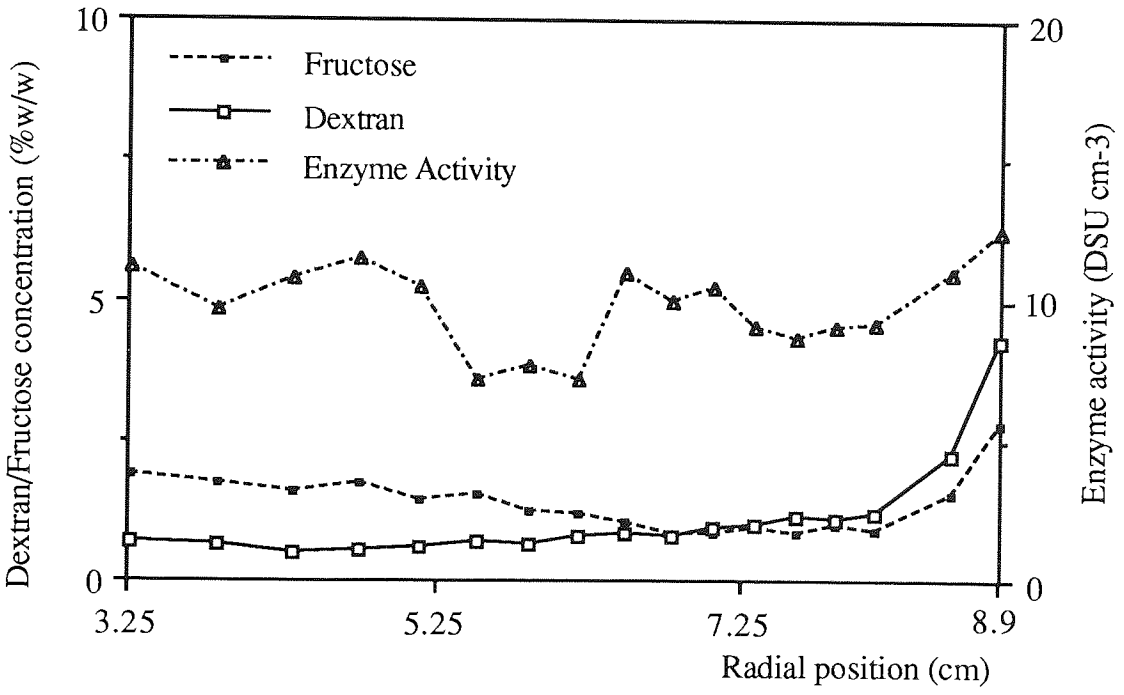

Figure 9.21 Plots of Dextran and Fructose Concentration and Enzyme Activity Versus Radial Position: Bioreaction-Separation Run Number 18

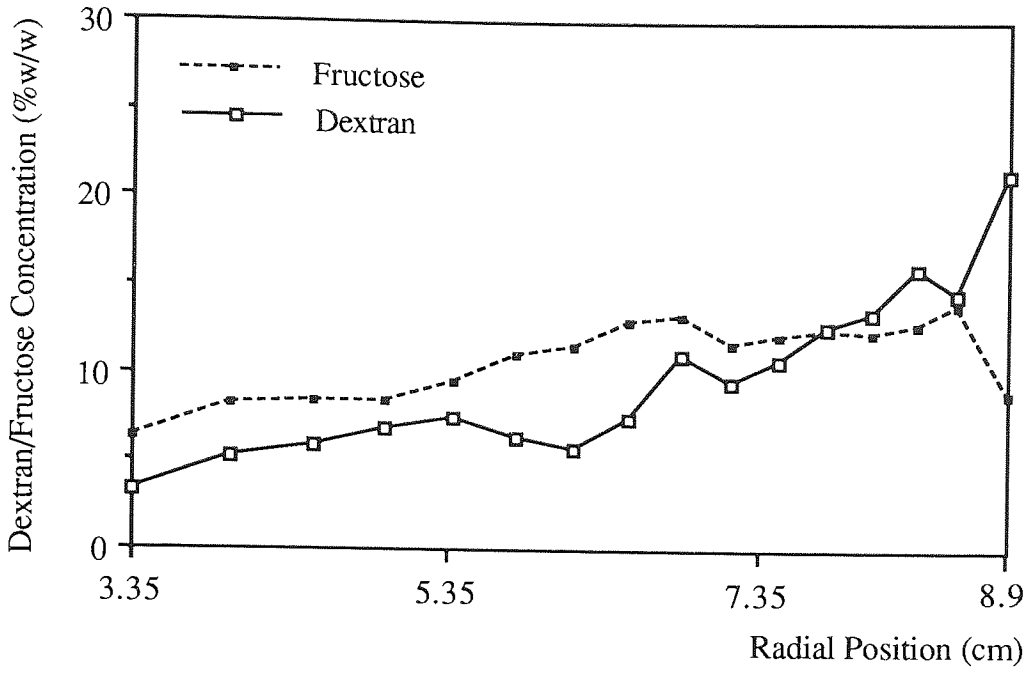

Figure 9.22 Plots of Dextran and Fructose Concentration Versus Radial Position: Bioreaction-Separation Run Number 19

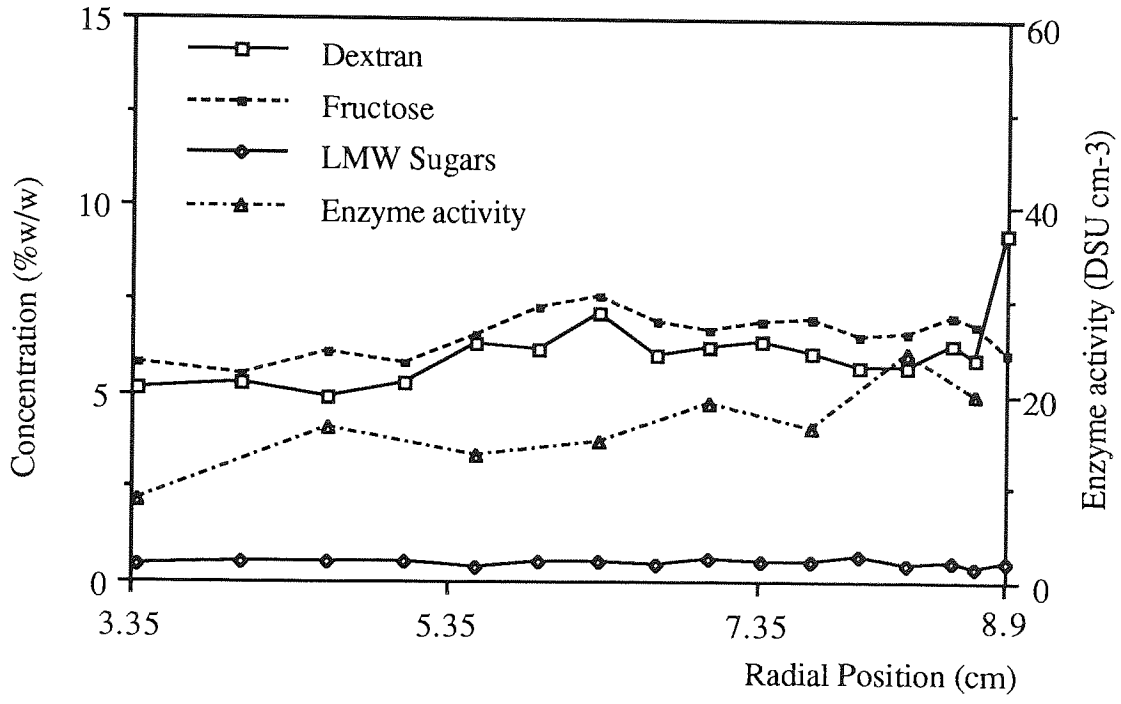

Figure 9.23 Plots of Dextran, Fructose and Low MW Sugar Concentration and Enzyme Activity Versus Radial Position: Bioreaction-Separation Run Number 20

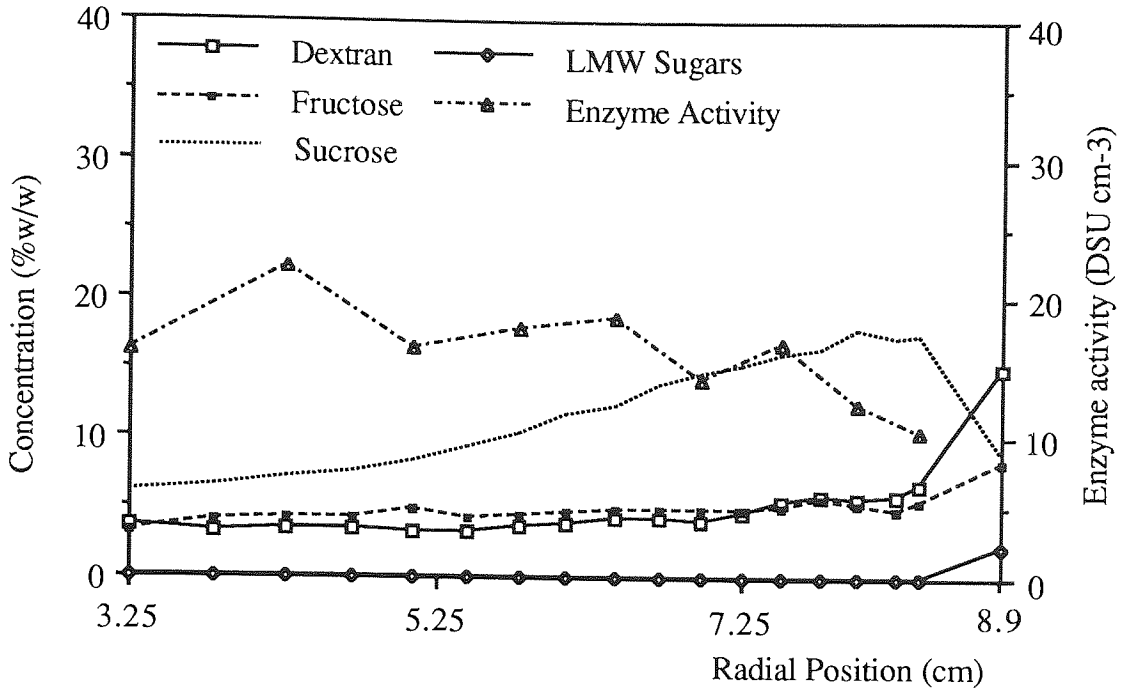

Figure 9.24 Plots of Dextran, Fructose, Sucrose and Low MW Sugar Concentration and Enzyme Activity Versus Radial Position: Bioreaction-Separation Run Number 21

Run No.	Enzyme Solids Conc. (w/w)	Enzyme activity (DSU cm^{-3})	Enzyme volume (cm^3)	Sucrose gradient (% w/w)	Rotor Speed (rpm)	Run time (minutes)
6	3.0	150	50	5-20	20 000	150
7	1.8	50	50	5-20	20 000	90
8	4.4	220	50	10-25	10 000	90
13	9.0	800	60	15-45	20 000	200
15	5.7	400	40	15-45	5 000	1020
16	5.7	400	40	10-25	5 000	1020
17	9.0	800	10	15-30	20 000	200
18	6.6	400	20	15-30	10 000	400
19	6.6	400	125	15-25	10 000	400
20	7.4	400	125	15-15	10 000	400
21	3.9	270	5x35	15-25	10 000	400

Table 9.17 Summary of the Run Conditions for the Zonal Rotor Bioreaction-Separation Studies

Run No.	Mass of dextran sedimenting to rotor wall per hour (g)	% dextran at rotor wall	Dextran: Fructose Ratio in gel	Maximum S-value (Svedbergs)	Final mean dextran conc. (% w/v)	Sucrose consumption (%)
6	0.39	23.38	3.05	331.9	0.24	4.6
7	0.44	26.23	5.25	532.0	0.14	1.9
8	0.17	3.44	3.25	2427.1	0.43	5.4
13	0.30	1.74	2.52	681.5	3.32	21.5
15	0.29	5.79	1.47	2436.6	4.81	29.0
16	0.78	10.97	1.27	1027.7	6.93	72.2
17	0.71	20.71	3.00	543.7	0.65	5.7
18	0.68	26.70	1.71	1091.6	0.97	8.5
19	3.04	14.53	1.46	606.5	8.07	100.0
20	1.19	7.43	1.65	524.3	6.08	100.0
21	4.68	32.35	1.65	489.6	5.51	49.1

Table 9.18 Zonal Rotor Bioreaction-Separation Studies: Summary of Experimental Data.

9.3.2 The Rate Zonal Sedimentation of Presynthesised Native Dextran and Fructose Mixtures.

Initial calibration of the system was carried out by studying the rate-zonal separation of presynthesised native dextran and fructose mixtures. The samples were prepared in a conventional 'bench' dextransucrase bioreactor, initially containing 200 cm^3 of 6% w/w sucrose solution with an enzyme activity of 10 DSU cm^{-3} at 25°C. HPLC analysis of the fully reacted, heat treated bioreactor product showed it to consist of material corresponding to high MW dextran and fructose at concentrations of approximately 3% w/w each.

Simple rate-zonal centrifugations using this stock solution were performed using the JCF-Z zonal rotor and Reograd core. Two of these runs are reported here and the run conditions are summarised in table 9.19. Detailed data relating to these runs are given in tables 9.2 and 9.3 and the concentration versus sedimentation coefficient profiles, calculated according to the method described in appendix A8 are shown in figures 9.10 and 9.11.

	Run 3	Run 4
Dilution of stock solution	None	1:2
Sample volume (cm^3)	50	50
Overlay volume (cm^3)	100	100
Run time (minutes)	120	120
Rotor speed (rpm)	20 000	20 000
Gradient profile (% w/w)	10-25	10-25

Table 9.19 Run Conditions for the Calibration Trials.

The results from these trials allow a number of important conclusions to be drawn which are summarised below:

(1) The native dextran samples were synthesised at relatively low sucrose concentrations where the acceptor reaction was minimal. The bulk of the dextran material formed was therefore of a high 'MW'. The relative 'sharpness' of the sedimentation coefficient distribution profiles indicated that the sedimenting dextran species had similar sedimentation coefficients and hence were behaving more as particles with similar physical properties rather than large gel network structures. At the end of both runs, the bulk of the native dextran material was found in a zone corresponding to around 25% of the entire bowl volume (~ 450 cm^3). Thus the initially more concentrated native dextran samples had been diluted by a factor of around nine times (50 cm^3 in 450 cm^3) giving mean concentrations of around 0.15 - 0.3% w/w native dextran. It appeared that this sample dilution encouraged the native dextran material to sediment as the more discrete agglomerations of native dextran molecules observed by Bovey[47], rather than as the extensively cross-linked gel-like structures that native dextrans readily form in more concentrated solutions[49-53]. This is clearly shown by comparing the sedimenting properties of the 0.5 and 1.5% w/w native dextran samples in the analytical ultracentrifuge studies (chapter 6). Bovey[47] who reported that stable high MW dextran aggregates were formed during dextran synthesis at low substrate and enzyme concentrations.

(2) These results compare favourably with the analytical ultracentrifugation results reported in chapter 6, as can be seen by comparing figures 9.10 and 6.7. The maximum ordinate of the native dextran peaks observed in the zonal rotor trials corresponded to standardised sedimentation coefficient values (S-values) of 237 and 227 Svedbergs for runs 3 and 4 respectively. Table 6.3 shows that, at infinite dilution, using the normal rate separation technique, the native dextran sample had an $S_{20,w}$ value of around 255 Svedbergs. The similarity of these results indicates the validity of the calibration procedure.

Few conclusions regarding the sedimentation coefficient and MW distributions of the native dextran sample was drawn from the analytical ultracentrifuge studies due to the distortion of the observed Schlieren peaks by concentration, Johnston-Ogston and back-diffusion effects[112-119]. Such effects were minimised using the rate zonal technique due to the relatively small quantities of sample used[174]. In run 3, 57% of the native dextran material had S-values in the range of 153-262 Svedbergs (see table 9.2). Using Svedberg's equation (equation 4.11), it can be calculated that 57% of the native dextran material had 'molecular weights' of between 72.2 x 10^6 and 123.7 x 10^6. In run 4, around 54% of the native dextran material had a similar range of S-values. This is in accordance with the data of Arond and Franks [59].

(3) Gradient overloading would have been indicated in these runs if the mean S-value of the dextran material in run 3, where a greater sample loading was used, was significantly greater than the equivalent S-value in run 4. This was not the case as figures 9.10 and 9.11 indicate. The similarities of these profiles indicate that the rate zonal technique in the Reograd rotor was highly reproducible.

(4) Around 2% of the total amount of solids initially loaded onto the sucrose gradient were recovered from the rotor wall at the end of each of the runs by washing from the wall using water. This material yielded HPLC chromatograms consistent with the dextran and fructose materials. It was probable that a significant proportion of the material corresponding to the 'dextran' peak was of a very high 'molecular weight' such as cell fragments not removed during the enzyme purification process.

(5) A potentially important phenomenon was also observed during these runs. In theory, the fructose molecules, because of their very low S-values should not sediment appreciably during the runs and should therefore remain in the vicinity of the zone initially occupied by the sample. While this was approximately true for about 60% of the loaded fructose, around 25% of the total fructose loaded was detected as a zone at the same radial position in the rotor as the bulk of the dextran material. This fructose material was therefore 'forced' to sediment with the migrating dextran material by being entrapped within its structure. Considering the structural properties and high degree of solvation of native dextran particles, this was expected. These results explained the similar observations recorded in the bioreaction-separation studies that were carried out in batch tubes on the MSE SS 50 centrifuge (sections 7.4.5 and 7.4.6).

Fructose entrapment may have important consequences for the combined bioreaction-separation process. If fructose molecules can be entrapped by native dextran particles, then similarly it must be expected that enzyme molecules will likewise be entrapped. Thus the

simultaneous synthesis and separation of fructose molecules from the enzyme molecules will be hindered.

9.3.3 The Rate Zonal Sedimentation of Heat Treated Dextransucrase Enzyme Fractions

Preliminary study of the combined bioreaction-separation process using the Reograd rotor had indicated the possibility that the gradients were being overloaded. Gradient overloading results in the non-ideal sedimentation effects discussed in section 4.4.2.5 and also results in poorer product separation and a loss in system resolution. In the proposed bioreaction-separation process, this would decrease the likelihood of the formation of enzyme or dextran-enzyme rich zones in the bioreactor and hence would have a detrimental effect on bioreactor performance by decreasing the likelihood of simultaneous bioreaction and separation.

Gradient overloading was studied and evaluated by observing the sedimenting properties of heat treated dextransucrase enzyme fractions. Two runs were carried out, the run conditions are shown in Table 9.20. Detailed data relating to these runs is given in tables 9.4 and 9.5 and the concentration versus S-values profiles are shown in figures 9.11 and 9.12.

	Run 10	Run 11
Total sample solids concentration (% w/w)	9.0	3.2
Sample volume (cm^3)	55	70
Overlay volume (cm^3)	45	50
Run time (minutes)	180	1006
Rotor speed (rpm)	10 000	10 000
Gradient profile (% w/w)	10-25	10-25

Table 9.20 Run Conditions for the Heat Treated Enzyme Trials.

The concentration profile from the second heat-treated enzyme rate-zonal centrifugation trial (run 11 in the above table) is shown in figure 9.13. A broad range of S-values were recorded at the end of the run, indicating that a broad range of particle 'molecular' weights were present in the heat treated enzyme solution.

While a significant proportion of this material was dextransucrase enzyme, it should be remembered that the enzyme purification process, pictured in figure 3.9, separated materials according to size. Therefore, 'intermediate' sized materials, such as cell fragments, other proteins, native dextran particles and other impurities will remain in

solution and will contribute to the sedimentation coefficient concentration profile observed in figure 9.13. Although this material will not affect the dextransucrase reaction, it will limit the quantity of enzyme that can be loaded onto a gradient due to hydrodynamic instability and density inversion effects (section 4.4.2.5). However, results from the bioreaction-separation trials reported in the next section indicated that low enzyme loadings improved bioreactor performance, thereby minimising gradient overloading problems.

Experimental data from the presynthesised native dextran and fructose sedimentation studies reported in the previous section showed that a significant proportion of the fructose material sedimented with the high MW dextran material by being physically entrapped in the highly solvated native dextran particle structures. Therefore it was considered highly likely that a significant proportion of the dextransucrase enzyme molecules in the bioreactor also remained associated with the native dextran particles or gel-structures even after the dextran chains were released from the active sites of the enzyme. This observation was supported by the fact that a small peak, corresponding to around 15% of the total solids material detected in the heat treated enzyme run 11 exhibited a distribution of S-values that would be consistent with such high MW dextran-enzyme complexes. It was also a possibility that a proportion of the enzyme molecules in the solution were not associated with the dextran particles.

The effect of gradient overloading could be readily observed between the two trials. In run 11, where a solution containing 3.2% w/w solids was loaded onto a 10-25% w/w gradient, only around 10% of the material had S-values of less than 240 Svedbergs. Conversely, in run 10, where a heat treated enzyme solution containing 9% w/w solids was loaded onto the same gradient, around 35% of the material had S-values in excess of 240 Svedbergs. Clearly the loading capacity of the gradient had been exceeded in run 10, resulting in some non-ideal sedimentation. Consequently, falsely high S-values were recorded. To help minimise gradient overloading problems in the bioreaction-separation runs, the recommendation of Griffith[98] were followed. These have been discussed in section 4.4.2.5. According to Griffiths' guidelines, sample concentrations in excess of 6% w/w will cause gradient overloading when layered onto a gradient with a starting concentration of 10% w/w.

In both runs, around 3% of the total solids detected were recovered by washing from the rotor wall. This material was presumed to be very high 'MW' material, such as cell fragments that were not removed during the enzyme purification process.

9.3.4 Results from the Rate-Zonal Bioreaction-Separation Trials

Data from the bioreaction-separation trials are reported in tables 9.6 to 9.16 and figures 9.14 to 9.24. A detailed breakdown of the mass balances of these trials are recorded in appendix A9. The run conditions of these trials are reported in table 9.17 and key data from the runs are summarised in table 9.18 as described in section 9.3.1.

9.3.4.1 Gradient Overloading

It was immediately apparent on studying the saccharide concentrations and enzyme activity versus radial distance profiles that extremely high rates of particle sedimentation were being achieved in the bioreaction-separation runs. For example, in run 8, 50% of all of the dextran synthesised had S-values in excess of 2000 Svedbergs. These values were around ten times higher than the S-values recorded for the presynthesised dextran fractions obtained using the rate-zonal method (section 9.3.2). Initially, it was believed that these high values were due to non-ideal sedimentation caused by gradient overloading and density inversion effects.

Non-ideal sedimentation in a rate-zonal centrifugation process may be defined as any form of mass transport by means other than sedimentation or diffusion. This subject has been discussed in section 4.4.2.5. Generally, non-ideal sedimentation in a rate-zonal process is caused by density inversion effects.

Although the recommendations of Griffith[98] were used to prevent density inversion, the equation of Schumaker [121] (equation 4.29) indicates that some density inversion is inevitable in a rate-zonal centrifugation process. Taking the diffusion coefficient (D) of a dextransucrase enzyme molecule and a sucrose molecule to be 5×10^{-7} cm^2 sec^{-1} and 0.46×10^{-5} cm^2 sec^{-1} respectively, then it can be calculated from equation 4.29 that the density increment due to the enzyme solution should be around 3 times less than the density of the supporting sucrose solution for initial layering stability, otherwise droplet sedimentation would occur. However, if the assumption is made that the enzyme molecules remain associated, physically or chemically, with native dextran particles during the enzyme purification process, which is supported by a number of experimental observations [64,91,175] and the further assumption is made that enzyme and high 'molecular weight' native dextran complexes are rapidly formed at the initial enzyme-sucrose interface, then the enzyme molecules will effectively have mean D values similar to those of the associated dextran particles, which are typically of the order of 1.4×10^{-8} cm^2 sec^{-1} (section 6.4.1). Calculations using equation 4.29 show that the density increment due to such dextran-enzyme solutions should be around 18 times less than the starting density of the supporting sucrose gradients in order to prevent non-ideal sedimentation. Subsequent density measurements of a number of the enzyme stock solutions showed that

some density inversion would have occurred in all of the runs. Although several of the experiments indicated that some gradient overloading may be occurring, conclusive results were not obtained due to complicating factors such as changes in system viscosity.

Comparison of runs 8 and 16, which both had identical initial gradients to the heat treated enzyme runs 10 and 11 (see section 9.3.3), allowed some useful conclusions to be drawn. Gradient loading details for these trials are summarised below in table 9.21

Run Number	Sample Solids Concentration (%w/w)	Sucrose Gradient (% w/w)
8	4.4	10-25
16	5.7	10-25
10 (Heat treated)	9.1	10-25
11 (Heat treated)	3.2	10-25

Table 9.21 Run Conditions in the Gradient Overloading Studies

Comparison of the heat treated enzyme runs 10 and 11 showed that increases in sample solids concentration from 3.2 to 9.1% w/w on a 10-25% w/w sucrose gradient resulted in significant increases in the observed S-values. This was due to gradient overloading However in the bioreaction-separation runs 8 and 16, the observed S-values of the native dextran samples on the same gradients were very different, even though relatively low sample solids concentrations were used when compared with run 10. Very broad native dextran S-value profiles were obtained that could not be adequately explained by gradient overloading alone. It would therefore appear that other factors were affecting the particle sedimentation rates in the bioreaction-separation runs. Two possible explanations are discussed below.

Newbrun et al [51] and Ingelman et al [52] showed that in even relatively dilute solutions, dextran molecules can combine to form network structures (section 2.4.1). Presumably such structures will have a wide variety of size, shape, aggregation, 'particle' weight and hence sedimenting properties. These rapidly forming network structures could be the main cause of the broad range and extremely high S-values observed in these studies. Assuming this reasoning to be correct, then it is apparent that during synthesis the dextran particles have different sedimenting properties to presynthesised dextrans as can be seen by observing the differences between figures 9.14 and 9.10. This may be due to changes in the intermolecular and interparticle bonding that occurs between stable dextran aggregates. The sedimenting properties of native dextran fractions had been studied in this project using the analytical ultracentrifuge yielding mean sedimentation coefficients of 250 Svedbergs at

infinite dilution. Bovey[47] found by light scattering measurements that dextran particle sizes continued to change after complete substrate conversion. However, he found that this actually led to an increase in particle sizes. Dextran particle structures and sizes is a complex subject that has been reviewed in section 2.4.

A second explanation of the high observed S-values concerns the 'active' nature of the sedimenting enzyme molecules. It is possible that the consumption and hence removal of sucrose gradient material at the active sites of the enzyme molecules will cause localised hydrodynamic instability in the gradient which could result in the dextran-enzyme complexes sedimenting at higher rates than their sedimentation properties alone would dictate. Brakke[134] reported that '*a zone is (hydrodynamically) stable as soon as a smooth sucrose concentration gradient is re-established ..... at the lower boundary of the zone*'. As this can never truly occur in the presence of active dextransucrase enzyme in a sucrose gradient, some convection will always occur.

9.3.4.2 Droplet Sedimentation

Droplet sedimentation, which has been discussed in section 4.2.2.5., is an extreme form of the 'turnover' effect. Because sucrose molecules will diffuse into the enzyme layer more rapidly than the enzyme molecules will diffuse into the sucrose gradient, a more dense solution will be formed at the interface between the enzyme zone and the sucrose gradient. Brakke[128] noted in his experiments that under conditions of 1-g (earth gravity), droplets visible to the naked eye rapidly sedimented from the sample zone to the base of the tube, leaving behind a trail of protein due to this effect. According to Schumaker[121], droplet sedimentation should not be a serious problem during centrifugation as high centrifugal forces decrease the size of the droplets, which then rapidly loose their identity due to diffusion. This results in the formation of smooth sample gradients in the vicinity of the initial interface between the sample and supporting gradient solutions.

In these studies, a 'static' sample loading technique at 1-g was used (figure 9.2), which increased the likelihood of droplet sedimentation. Run 17 however, was loading dynamically, thus giving conditions where droplet sedimentation should be minimised. This run yielded similar profiles and S-value distributions as other comparable statically loaded runs, indicating that droplet sedimentation alone could not account for the high S-value observed in the bioreaction-separation runs. However, in future runs it would be judicious to eliminate the possibility of droplet sedimentation completely by using the dynamic loading process.

9.3.4.3 Gradient Loading / Unloading

The smooth sucrose concentration profiles obtained at the end of the bioreaction-separation runs where low sucrose consumption was recorded, showed that successful reorientation of the gradient had occurred, which indicated that gradient mixing during reorientation was minimal. However, in order to verify this, run 17 was conducted without gradient reorientation. The Reograd rotor core was used in this run, but a rotating seal assembly was fitted to the bowl, allowing the dynamic loading and unloading of the various solutions without reorientation of the bowl contents (see figure 9.4a). Water was still used as the displacement medium. Study of the concentration / activity profiles indicated that no significant changes in bioreactor performance could be attributed to this change in experimental technique.

The addition of small, precalculated amounts of sucrose to the enzyme samples immediately prior to injection, for the reasons discussed in section 9.2.2, was done in trials 3,4, 6-8, 13 and 15. However, addition of this material had no detectable effect on the saccharide concentration and enzyme activity distribution profiles obtained from these runs.

Overlay solutions were used in trials 6-8 for the reasons discussed in section 9.2.4. Again, no significant changes in the concentration and activity distributions from these runs could be attributed to the use of overlay solutions. The method of Steensgaard et al[120] for the calculations of S-values (appendix A8) took account of overlay sample volume.

Details concerning sucrose stabiliser concentrations and overlay volumes have been reported, where relevant, in tables 9.6 to 9.16.

9.3.4.4 The Presence of Dextran Enzyme Zones in the Bioreactor

It had been envisaged that the rate-zonal technique, coupled with the use of positive density and viscosity gradients, would result in the maintenance and sedimentation of dextran-enzyme zones as shown, ideally, in figure 2.8. Run number 6 showed some evidence of an enzyme-dextran zone near to the centrifugal (rotor wall) end of the bioreactor (figure 9.14). This zone accounted for only 19.3% of the total dextran formed and more significantly, 48.5% of the total enzyme activity recovered from the bioreactor. This run was characterised by a low bioreactor medium viscosity. However, similar zones were not observed in any of the other run profiles obtained. In run 7, characterised by very low bioreactor medium viscosities, relatively 'flat' concentration and activity profiles were obtained (figure 9.15).

These profiles helped to explain the data obtained in the analytical ultracentrifuge bioreaction-separation runs reported in section 6.7. Figure 6.10 showed that the thickness

of the gel layer increased with time in the ultracentrifuge cells, but the rate of gel layer build-up decreased as the runs proceeded. The broad distribution of dextran in the JCF-Z rotor bioreaction-separation studies showed that a gradual build-up of the gel layer with time would be expected. The observed decrease in gel layer build-up in figure 6.10 was probably due to increases in medium viscosity causing a decrease in particle sedimentation rates. This will be discussed in more detail in the next section.

9.3.4.5 Bioreactor Medium Viscosity

The concentration of native dextran synthesised during a run had a very significant effect on the overall viscosity of the reaction medium in the bioreactor. Viscosity studies undertaken in this department by Mr Paul Tack on native dextran-fructose broths produced by the action of the dextransucrase enzyme on several sucrose solutions are summarised in table 9.22.

Initial sucrose concentration in reaction mixture (%w/w)	Viscosity at 25°C mPas (cP)
0	~0.9
1	5
2	11
3	28
5	183
10	785
15	983
20	1137

Table 9.22 Dextransucrase Broth Viscosity Measurements

This data suggests that the viscosity due to native dextran is appreciable, even at low dextran concentrations. For example a 1% w/w broth, which will contain approximately 0.5% w/w native dextran, has a viscosity comparable with that of a 40% w/w sucrose solution.

Although centrifugation theory states that it is the density and viscosity of the *surrounding medium* that dictates the rate of sedimentation of a particle species, the assumption is made that the sedimenting particles do not interact with each other[94]. However, due to the tendency for native dextran molecules to form extensive network structures even at low concentrations (section 2.4), then the high viscosity values of the native dextrans in solution will have a significant effect on particle sedimentation rates and medium viscosity.

The effect of concentration on native dextran sedimentation rates had already been studies in this project using an analytical ultracentrifuge (section 6.3). The results indicated that increases in dextran concentration from 0.5 to 1.5% w/w resulted in nearly a ten fold decrease in S-values from 163.7 to 17.3 Svedbergs. Extrapolation of this data above 1.5% w/w indicated that a point would be reached where the dextran sedimentation rate effectively equalled zero and the native dextran material would exhibit the classic behaviour of a gel in a centrifugal field (section 4.6). These results indicated that in order to maintain high rates of dextran sedimentation in the JCF-Z bioreactor, the concentration of native dextran in solution should not be allowed to increase above a critical value which could be as low as 1% w/w native dextran. However, it should be noted that the analytical ultracentrifuge data was obtained from a normal rate centrifugation where the native dextran material was initially distributed throughout the whole of the centrifuge cell. This was not the case in the rate-zonal bioreaction-separation process. Figures 9.14 to 9.24 indicate that native dextran concentrations vary with radial position in the bioreactor in these runs which will influence the localised native dextran sedimentation rates.

Column 4 in table 9.18 conclusively shows that the degree of dextran-fructose separation was dependent upon dextran concentration and hence viscosity. For example, in runs 6,7,8 and 17, all of which had final mean dextran concentrations of below 0.7% w/w, the ratio of dextran to fructose (D:F) in the gel fractions were all greater than 3:1 and in the case of run 7, which corresponded to the lowest final mean dextran concentration, this ratio rose to 5.25:1. Runs 16, 19 and 20, which all had final mean dextran concentrations of above 6% w/w, all the D:F ratios were below 1.7:1.

The concentration and activity profiles of runs 6 and 8 showed that there were significant increases in dextran concentration towards the centrifugal (rotor wall) end of the bioreactor (figures 9.14 and 9.16). These runs corresponded to low enzyme activities and system viscosities. 67.1% and 65.5% of the total dextran synthesised was found in the lower half of the gradients in runs 6 and 8 respectively, compared with only 41.3% and 40.6% of the total amount of fructose synthesised. These values can be compared with runs 15 and 17 where 51.1% and 48.1% of the total dextran synthesised was found in the lower half of the gradients compared with 44.6% and 53.7% of the total fructose synthesised. Clearly, poorer separation was being achieved in the latter runs.

However, some separation was achieved at higher native dextran concentrations. For example, 32.2% of the dextran material synthesised in run 13 had apparent S-values in excess of 400 Svedbergs compared with only 13.2% of the total fructose detected (see table 9.9). However, such runs tended to yield poor dextran : fructose ratios in the recovered gel fractions (2.52:1).

The trials corresponding to low final mean dextran concentrations resulted in higher percentages of the total dextran produced being found at the rotor wall. For example, in runs 6,7,17 and 18, which had average final mean dextran concentrations of between 0.14 and 0.97% w/w, an average of 24.3% of the total dextran synthesised in each run was recovered from the rotor wall (column 3 table 9.18). These values can be compared with the 'high viscosity' runs (13,15,16,19 and 20), which had mean final dextran concentrations of between 3.3 and 8.1% w/w and an average native dextran recovery from the rotor wall of 8.1%.

However, although low viscosities improved dextran sedimentation to the rotor wall, the yields were correspondingly lower. Dextran sedimentation to the rotor wall per hour is reported in column 2, table 9.18. These values show that the 'low viscosity' runs (6,7,17 and 18) had mean recoveries of dextran from the rotor wall of 0.56 grammes per hour, whereas the 'high viscosity' runs (13,15,16,19 and 20) had mean yields of 1.12 grammes per hour.

The highest dextran yield per unit time was recorded in run 21. In this run, 35 cm^3 pulses of enzyme solution were injected into the bowl at 90 minute intervals throughout the duration of the run. By introducing smaller pulses of enzyme into the vessel, the dextran material formed should sediment more rapidly to the rotor wall due to the relatively low medium viscosity and hence result in higher dextran recoveries. Higher dextran throughputs should be achieved by injection of the additional pulses of enzyme throughout the run. As expected, high dextran recoveries from the rotor wall of 4.68 grammes per hour were recorded in this run, despite the high final dextran concentration in the reactor. Therefore, the repeat injection method significantly improved the separating performance of the process, but suffered from the fact that there will be a build-up of acceptor fructose molecules in the bowl which will interfere with the synthesis of long chain dextran molecules during the passage of sedimenting enzyme material from the subsequent injections of enzyme.

However, based on the existing results, no truly distinctive enzyme reaction zones were recorded in any of the trials (see section 9.3.4.4), indicating that true simultaneous bioreaction-separation, as envisaged in figure 2.8 cannot be achieved. Therefore as there was no truly simultaneous bioreaction-separation occurring, the use of repeated pulse injections becomes more attractive. Although the benefits of higher dextran yields per unit time by minimisation of the acceptor reaction will be lost, this may well be compensated for by the integration of the bioreaction-separation processes into a single unit operation.

A relatively poor D:F ratio was recorded in the repeat injection run (1.65:1), but this should be improved by decreasing the enzyme activity of the pulse injections. This would minimise viscosity effects by decreasing the overall concentration of the native dextran material which would allow the material to sediment more rapidly to the rotor wall. This in turn would allow more frequent enzyme injections to be made. Low enzyme activities were shown to improve the separating performance of the bioreactor (section 9.3.4.7). It is expected that by increasing the frequency of enzyme injection, high rates of dextran synthesis can be achieved without sacrificing the separating power of the system.

Ultimately it is envisaged that the process would achieve full potential by continuously passing an enzyme solution of low activity over a sucrose gradient in a continuous flow zonal rotor (see figure 4.5). When an acceptable amount of sucrose conversion had been achieved, the non-sedimented fructose-rich gradient material would be displaced from the rotor by pumping air into the bowl. Methods for the displacement of the pelleted dextran-rich material at the rotor wall have yet to be studied, but it is envisaged that 'jetting' warm water into the bowl will readily disperse the gelatinous dextran pellet, as B-512F dextran gels are readily soluble in water [53]. Smooth sucrose gradients could rapidly be reloaded into the bowl using a gradient forming machine, displacing the less dense aqueous dextran solution from the bowl and the enzyme flow restarted. Gradient forming machines are commercially available[98]. A rotating seal can be used to allow the dynamic loading and unloading of the bowl contents at speeds of 2000 rpm. This method although applied to the synthesis of dextran, could be equally applicable for the synthesis of other high value macromolecular products.

9.3.4.6 Sucrose Conversion

Run 19 represented a special case where complete sucrose conversion was achieved. This run clearly showed the problems that can occur due to high bioreactor viscosities. In all of the bioreaction-separation runs, it appeared that enzyme molecules sedimented to all points in the bioreactor when the effects of viscosity were minimal. As the viscosity increased in run 19, so the sedimentation rates of the enzyme and dextran molecules were arrested while bioreaction continued. This resulted in complete substrate conversion but no significant dextran / enzyme migration and product separation as indicated by figure 9.22. This was reflected by the very low dextran to fructose ratio in the gel layer recovered from the rotor wall of 1.46:1 and a relatively poor dextran recovery from the rotor wall of 14.4%. Clearly, viscosity must be minimised to achieve good product separation and enhance bioreaction-separation.

9.3.4.7 The Effect of Enzyme Activity, Pulse Size and Run Time on Bioreactor Performance.

Enzyme activity, pulse size and run time will all influence the total amount of native dextran synthesised during the process and therefore will directly influence the rate of viscosity build-up in the system. Viscosity effects in the bioreactor have been discussed in section 9.3.4.5.

In run 8, which had a relatively low enzyme loading activity of 220 DSU cm^{-3}, 85.4% of the enzyme detected compared with only 41.6% of the total fructose detected was found in the lower half of the gradient. In run 17, which had a comparable final native dextran concentration to run 8, but with a higher enzyme activity loading of 800 DSU cm^{-3}, only 48.1% of the enzyme activity was located in the lower half of the gradient compared with 53.7% of the total fructose material, despite the fact that longer run times and higher rotor speeds were used in this run. These results indicated that low enzyme activities improved product separation.

Brakke[128] showed that the volume of sample applied to a gradient in a rate-zonal centrifugation had no significant effect on the final sample distribution in his studies. However, in these studies, sample volume, like enzyme activity, will influence the rate of viscosity build-up in the bioreactor. The effect of enzyme injection volume on bioreactor performance in these studies was assessed by comparing data from runs 18 and 19. A 20 cm^3 x 400 DSU cm^{-3} enzyme charge was injected in run 18, compared with 125 cm^3 x 400 DSU cm^{-3} charge in run 19. All the other run conditions were identical. In run 18, 86.7% of the total dextran synthesised and 68.1% of the total fructose synthesised was found in the lower half of the gradient, compared with 82% and 74.4% dextran and fructose respectively in run 19, indicating that lower injection volumes slightly improved product separation. Furthermore, a significant improvement in the proportion of pelleted dextran was observed when using the lower injection volume. Again this could be attributed to a decrease in overall native dextran concentrations and hence viscosities.

The effect of run time on bioreactor performance was difficult to access. However, longer run times will result in increases in dextran concentration and hence system viscosities, which has been shown to influence the separating power of the system. Longer run times will also improve dextran recoveries from the rotor wall. Provided that viscosity effects are minimised in the bioreactor, such as by using low enzyme activities and pulse sizes, then dextran recoveries from the rotor wall should increase with run time. In runs 15 and 16, which had the longest run times of 1020 minutes, relatively low dextran recoveries of 0.14 and 0.78 g hr^{-1} were recorded. Again, the determining factor was bioreactor viscosity. In the repeat injection run, viscosity build-up in the bioreactor was partially controlled and

greatly improved dextran recoveries of 4.68 g hr^{-1} were obtained. By using this method, high dextran recoveries were achieved using short run times.

It should also be noted that decreases in acceptor activity, hence improved yields of high 'MW' dextran were achieved using the rate-zonal process in swinging bucket rotors (section 7.5). Relatively low enzyme activities of 60 DSU cm^{-3} were used in these runs.

9.3.4.8 The Effect of Rotor Speed

The effect of increasing rotor speed on bioreactor performance in the bioreaction-separation runs carried out in swinging bucket rotors (chapter 7), was to increase the quantity of pelleted dextran. However, those runs had relatively low final viscosities because lower enzyme activities, volumetric loadings and run times were used. In the bioreaction-separation runs in JCF-Z rotor, the effects of rotor speed was masked by the high viscosity of the bioreactor medium. By minimising viscosity effects, the effect of rotor speed on bioreactor performance could be more adequately studied and assessed.

The very high S-values recorded in these trials indicated that under conditions of low viscosity, high dextran recoveries could be obtained at very low rotor speeds. Appreciable dextran sedimentation rates were observed in runs 15 and 16 where rotor speeds of only 5 000 rpm were used.

9.3.4.9 Enzyme-Fructose Separation

Combined enzyme-fructose separation is an important requirement of the combined centrifugal bioreaction-separation process for the reasons discussed in section 2.3.2. Concentration and activity profile data suggested that enzyme-fructose separation was enhanced when viscosity effects were low. For example, the profile from run 8 which had a final mean native dextran concentration of 0.43% w/w (figure 9.16) showed that the bulk of the enzyme activity was concentrated towards the centrifugal (rotor wall) end of the bioreactor, whereas the fructose concentration was very much higher at the centripetal (inlet) end. Table A9.3 indicates that 85.4% of the total enzyme activity detected, compared with only 41.6% of the total fructose mass detected was found in the lower half of the gradient at the end of the run. Similarly run 6, which again corresponded to a relatively low loaded enzyme activity of 150 DSU cm^{-3}, 78% of the enzyme activity detected was found between the radial position 7.63 and 8.90 cm, compared with only 21.8% of the total fructose detected (table A9.1). However, in the trials that had higher final native dextran concentrations, enzyme fructose separation was much poorer. In run 15 for example, which had a relative high final native dextran concentration of 4.8% w/w, 51.1% of the enzyme activity was located in the lower half of the gradient compared with

44.6% of the total fructose material. Similar values were noted in the other high viscosity runs.

It appeared that enzyme activity was also an important factor in enzyme-fructose separation. Enzyme activity effects have been discussed in section 9.3.4.7.

9.3.4.10 Effects of Gradient Shape

The equation of Svensson et al[127] (equation 4.30) relates the theoretical sample loading capacity of a gradient to two factors. Firstly is the 'steepness' of the density gradient. Effectively, the steeper the gradient, the greater the mass of material it can support without hydrodynamic instability. Secondly, the density of the sample zone that can be applied to a gradient without serious convectional mixing is a function of the density of the gradient material immediately below the sample zone (section 4.4.2.5). Brakke[128] showed experimentally that the amount of sample that a given gradient can support without convectional mixing was only a small fraction of the theoretical value calculated using equation 4.30.

Initially it has been expected that the use of steep gradients would both help prevent convective disturbances and improve system resolution, resulting in the formation of sedimenting enzyme rich 'reaction zones' within the bioreactor. It was expected that this would result in higher yields of the commercially important dextran product by minimisation of the acceptor reaction. This method had been shown to work in swinging bucket rotors (see section 7.5), resulting in significant increases in 'intermediate' MW dextran even in the absence of a stabilising gradient (table 7.15). However in those particular runs, small volumetric loadings of enzyme solution with relatively low activities and total solids concentrations were used, coupled with short run times. Analysis of the activity profiles in the Reograd bioreaction-separation runs showed little evidence of distinctive enzyme bands in any of the trials (section 9.3.4.4).

The effect of gradient shape on product distribution could clearly be seen by comparing runs 15 and 16. Both trials were performed under identical experimental conditions, except that a 15-45% w/w sucrose gradient was used in run 15, compared with a 10-25% w/w gradient in run 16. Figure 9.18 and 9.19 clearly show that a greater proportion of dextran mass and enzyme activity was found towards the rotor wall in the less steep gradient. Quantitatively, in run 15, 39.6% of all the enzyme activity was detected in the final third of the gradient, compared with 76.6% in run 16. Similarly, 34.6% and 58.7% of all the dextran synthesised in runs 15 and 16 respectively were recorded in the same region of the bioreactor. Clearly, less steep, hence less dense and viscous sucrose gradients encouraged dextran sedimentation. However, as bioreaction proceeded in the runs, the increasing

viscosity effects due to increases in native dextran concentrations affected sedimentation behaviour in the bioreactor to a greater extent than the original sucrose gradient shape.

Although less steep gradients appeared to improve the dextran sedimentation rates, dextran-fructose separation was slightly poorer. In the less steep gradient, 54.7% of the total fructose and 58.7% of the total dextran synthesised, was found in the final third of the gradient compared with 22.3% and 34.6% of the total fructose and dextran respectively in the steeper gradient. Combining low enzyme activity pulses with shallow gradients should result in improved dextran sedimentation coupled with good dextran-fructose separation.

Although steep sucrose gradients improved the process by contributing to the minimisation of non-ideal sedimentation, the presence of highly concentrated sucrose solutions adjacent to the rotor wall, where bioreaction, but not separation occurs will be detrimental to bioreactor performance. The continued enzyme conversion of sucrose to product at this point will result in the formation of high concentrations of acceptor molecules which will interfere with dextran synthesis, yielding higher quantities of the unwanted low MW dextran material at the rotor wall.

The fact that low system viscosities improve bioreactor performance (section 9.3.4.5), then the use of enzyme samples with high activities, hence higher solids concentrations, which will increase the possibility of gradient overloading, will not be necessary. Dilute enzyme solutions will require less concentrated 'starting' gradient concentrations and less steep density gradients to minimise convectional mixing and thus will minimise the problems associated with acceptor activity at the rotor wall.

Run 20 was carried out using a 'flat' gradient profile in order to determine how the absence of a density and viscosity gradient affected the distribution of the reaction materials. 100% sucrose conversion was achieved in this trial, but poor product separation was observed, indicating that mixing by convection had occurred.

9.3.4.11 Evidence of Enzyme Entrainment

In all of the bioreaction-separation profiles, the distribution of the active enzyme material indicated that the enzyme molecules had a broad range of high S-values, in fact, far higher than theory would predict (see section 6.5). While non-ideal sedimentation effects may partially account for this observation (section 9.3.4.1), it appeared that the enzyme molecules became physically associated and hence sedimented with the native dextran particles formed during the bioreaction-separation process. This was expected considering the structure and highly solvated nature of the dextran particle aggregates (section 2.4) and

explained the observed distribution of the enzyme molecules in the bioreactor at the end of the runs. The possibility of enzyme entrainment was supported by two observations:

(1) High dextran concentrations at the rotor wall were accompanied by high enzyme activities.

(2) The entrainment and 'forced' sedimentation of molecules by native dextran particles was clearly demonstrated in the JCF-Z rotor calibration runs (section 9.3.2).

On the one hand, the rate of fructose removal from the vicinity of enzyme active sites will be increased due to the entrainment of the enzyme molecules by native dextran, which should aid the bioreaction-separation process. On the other hand, fructose entrainment will result in higher localised levels of acceptor molecules within the native dextran structures which will have a detrimental effect on high MW dextran formation.

9.4 Conclusions

9.4.1 The Rate Zonal Sedimentation of Presynthesised Native Dextran and Fructose Mixtures

Presynthesised dextran fractions were found to have relatively narrow ranges of S-values, which was indicative of the material having discrete particle structures rather than gel network structures. The maximum ordinates of the observed peaks corresponded to S-values of between 227 and 237 Svedbergs, which compared well with analytical ultracentrifuge measurements of 285 Svedbergs (chapter 6) Typically, up to 60% of the total native dextran detected had S-values in the region of 150 to 260 Svedbergs, corresponding to 'molecular weight' values of 70×10^6 to 125×10^6.

A significant proportion of the fructose molecules detected had similar S-values to those of the native dextran material. It appeared that the highly solvated nature of the native dextran particles had resulted in the physical 'entrapment' of these fructose molecules within the dextran structure, resulting in the forced sedimentation of the fructose material. This could have a negative effect on the proposed bioreaction-separation process by hindering the removal of acceptor molecules from reaction zones in the bioreactor.

9.4.2 The Rate Zonal Sedimentation of Heat-Treated Dextransucrase Enzyme Fractions

Very broad ranges of sample S-values were observed in these runs, indicating that broad ranges of particle MWs were present in the sample fractions. This was believed to be due

to 'intermediate' sized particles not removed during the enzyme purification process. These materials could contribute to gradient overloading.

Sample solids concentrations of 9% w/w resulted in the overloading of 10-25% w/w sucrose gradients which was observed as a significant increase in the observed S-values. The recommendations of Griffiths [98] were used in this study as a guideline in order to prevent gradient overloading.

9.4.3 Bioreaction-Separation Results

All the data from the bioreaction-separation runs indicated that very high rates of particle sedimentation were being achieved. Subsequent calculations showed that these high values will have partly been due to density inversion effects. In order to prevent density inversion, the density increment due to the enzyme sample should be a factor of 3-18 times less than the density increment of the supporting sucrose solution. Comparison of the the bioreaction-separation runs with the heat treated enzyme runs showed that density inversion alone could not account for the very high S-values recorded. It therefore appeared that other factors affected particle sedimentation. Two possibilities were considered. Firstly, the dextran particles formed very high molecular weight network structures with correspondingly high S-values. Secondly, the enzymic conversion of the sucrose gradient materials to product at the active sites of the enzymes prevented the formation of smooth sucrose concentration gradients in the vicinity of the enzyme molecules, which could result in significant hydrodynamic instability and non-ideal sedimentation.

Because the enzyme samples were loaded statically, there was a risk that non-ideal sedimentation of the enzyme molecules could occur due to droplet sedimentation. Although the experimental data indicated that droplet sedimentation did not have a significant effect on product distribution in the bioreactor, it is recommended that in future, all samples should be loaded dynamically to eliminate the possibility of droplet sedimentation altogether.

Mixing in the gradient during reorientation appeared to be minimal. The use of overlay solutions and the addition of sucrose gradient material to enzyme samples immediately prior to injection in order to minimise density inversion effects had no detectable effect on bioreactor performance.

Viscosity studies on presynthesised native dextran and fructose broths showed that native dextrans form remarkably viscous solutions even at low macromolecular concentrations. These high viscosities were found to greatly affect bioreactor performance.

Because of viscosity effects, dextran-fructose separation was found to be highly dependent upon dextran concentration. Lower final mean dextran concentrations in the bioreactor resulted in significant increases in the mean dextran:fructose ratios found in the gel layer. This observation was supported by the distributions of dextran and fructose recovered from the bioreactor. Furthermore, in the lower viscosity runs, higher percentages of dextran were found at the rotor wall.

Although dextran-fructose separation and dextran sedimentation was improved at lower viscosities, the dextran yields were correspondingly lower. The highest dextran yield per hour was recorded in the repeat injection run. The repeat injection technique was designed to minimise viscosity effects in the bioreactor but suffered from the fact that there will be a build-up of acceptor molecules in the bowl which will inhibit dextran chain growth and high MW dextran formation. Although the benefits of higher dextran yields per unit time by minimisation of the acceptor reaction will be lost by using the repeat injection technique, this may be compensated for by the integration of the bioreaction-separation process into a single unit operation. Poor dextran:fructose ratios were recorded in the gel fractions in the repeat injection run. but this should be improved by decreasing the activity of the enzyme injections.

Enzyme activity, volume and run time are all factors that will influence the rate of viscosity build-up in the bioreactor. Low enzyme activities were shown to improve the separation of enzyme molecules and dextran material from regions of higher fructose concentrations. Decreasing the volume of the enzyme charge injected into the bioreactor appeared to slightly improve product separation, and led to an increase in the percentage of dextran synthesised in the reaction that was found at the rotor wall. Presumably this was due to a decrease in viscosity effects. The effect of run time on bioreactor performance proved difficult to assess. However, longer run times should increase dextran recoveries from the rotor wall, but will result in overall increases in dextran concentration in the bioreactor and hence very significant increases in system viscosities. Therefore, viscosity must be minimised in order for longer run times to be of benefit in this process. Similarly, higher rotor speeds should also increase dextran recoveries from the rotor wall, but will have little effect in highly viscous systems. Like run time, viscosity in the bioreactor must be minimised in order for optimum rotor speeds to be selected. Appreciable amounts of dextran sedimentation was observed at rotor speeds as low as 5000 rpm.

There was very little evidence to suggest that the rate zonal technique, coupled with the use of positive density and viscosity gradients resulted in the sedimentation of distinctive dextran-enzyme zones, indicating that simultaneous bioreaction and separation was limited in this system. Minimisation of the acceptor reaction is dependent upon the removal of

acceptor molecules from regions of high enzyme activity in the bioreactor and this was occuring in many of the runs.

The use of steep gradients should help minimise the possibility of convective disturbances within the bioreactor and improve the resolving power of the system, thus encouraging the formation of distinctive 'reaction zones' within the bioreactor. However, little evidence of distinct reaction zones was observed. Less steep gradients resulted in higher proportions of native dextran and enzyme activities being found in the lower portions of the gradient and at the rotor wall. However, as bioreaction proceeded, the increasing viscosity effects caused by native dextran synthesis had a far greater effect on sedimentation behaviour than the shape of the sucrose viscosity gradient. Dextran-fructose separation was poorer in the less steep gradients, but this could be improved by using lower activity enzyme charges into the bioreactor. The use of enzyme solutions with low activities hence low solids concentrations in order to minimise viscosity effects, will allow less steep gradients to be used if required.

The activity profiles strongly indicated that significant proportions of the enzyme molecules had become physically entrapped within the highly solvated native dextran structures and were forced to sediment at the relatively high sedimentation rates of these structures. This possibility was supported by the fact that fructose entrainment by native dextran aggregates had been observed in the JCF-Z rotor calibration runs. Enzyme and fructose entrainment will affect the simultaneous synthesis and removal of fructose molecules from regions of high enzyme activity within the bioreactor. The experimental data strongly suggested that entrainment would be minimised by using low activity enzyme solutions.

9.5 SYSTEM SCALE-UP CONSIDERATIONS

This section is merely intended to give a very approximate indication of the potential dextran recoveries that could be achieved in a scaled-up version of this process.

In the above bioreaction-separation runs, it was noted that a dextran recovery of 4.68 g hr^{-1} was achieved from the rotor wall using the repeat injection method. Although this method will suffer from the fact that there will be a build up of acceptor molecules in the reactor which will inhibit dextran chain growth, this may be compensated for by the integration of the bioreaction-separation process into a single unit operation. This process may achieve full potential by continuously passing a very dilute enzyme solution over a sucrose gradient in a continuous flow zonal rotor with periodic recoveries of the fructose-rich supernatant solutions and dextran rich gel fractions. By determining the optimum conditions for

minimising viscosity build-up in the bioreactor, considerable improvements to this recovery rate should be possible.

By using this method and with process optimisation, it is estimated that it would be possible to achieve a five fold increase in dextran recovery per unit time, giving a dextran yield of 25 g hr^{-1}. Assuming that this machine could be operated as a semi-continuous system with 10% down time, then it is predicted that a J2-MC centrifuge fitted with a JCF-Z rotor would be capable of producing up to 200 kilograms of high molecular weight dextran per year.

From centrifuge theory, it is possible to represent the separating power of a given centrifugal separator, rotating at a given rotor speed, by a theoretical capacity factor (Σ_T). The capacity factor concept has been discussed in section 8.4. Σ_T has the dimensions of area and represents the area of a gravity settling tank having a separation performance equivalent to the rotor in question and can be calculated using equation 8.13:

$$\Sigma_T = \frac{\omega^2 V}{2 ß g}$$

where the symbols have been described in section 8.4.2. Taking the minimum and maximum rotor radii of the JCF-Z zonal rotor fitted with the Reograd core to be 2.6 and 8.9 cm respectively and taking the rotor capacity to be 1750 cm^3, then the capacity factor of the vessel rotating at 10 000 rpm was calculated to equal 3.2 x 10^6 cm^2.

Capacity factors are extensively used to predict the performance of larger scale centrifugal separators: consider an industrial scale tubular centrifuge, commercially available machines have maximum internal rotor radii of up to 12.7 cm, rotor lengths of up to 76.2 cm and are capable of rotating at speeds of 15 000 rpm [170]. If a zonal separator could be built to similar specifications and there appears to be no reasons why this could not be achieved, then by assuming maximum and minimum bowl internal radii of 15.0 and 5.0 cm respectively and a bowl height of 30 cm (giving a total bowl volume of 18.85 litres), then such a machine would have a capacity factor of around 80.7 x 10^6 cm^2. Therefore a scale-up factor of around 25 times that of the laboratory machine could be expected. On such a machine, dextran recoveries of up to 25 x 200 kg , or around 5 tonnes of usable dextran per year may be possible. Clinical grade dextran has a high retail cost of around £30 000 per tonne. It is again stressed that this is only a very approximate attempt at system scale-up. Process optimisation with a view to improving the recoveries of native dextran from the bioreactor is ongoing as part of an SERC sponsored project.

10 PRELIMINARY MODELLING OF THE RATE-ZONAL BIOREACTION-SEPARATION PROCESS

10.1 INTRODUCTION

The fundamental equation describing mass transport in a centrifugal field was first derived by Lamm [41] and is commonly known as the differential equation of the ultracentrifuge. Cann [42] has discussed the derivation of this equation. Exact solutions of this equation have been derived, but are of such complexity as to be virtually useless for computational purposes [42]. Archibald [176] has reported an approximate solution of the differential equation from which numerical solutions can be achieved. Dishon and co-workers [177,178] have also described numerical solutions of the basic transport equation.

A number of workers have addressed the problem of mass transport and chemical reaction in centrifugal fields. Interestingly, the mass balance equations that have been developed are equally applicable to both centrifugal and electrophoretic systems. Most of the work in this field has concentrated on systems exhibiting reversible macromolecular isomerisation in normal rate as opposed to rate-zonal centrifugations. Such systems are relatively simple to model because each species of isomer can be characterised by a single sedimentation coefficient and the rate of interconversion can be characterised by a single specific value. The analytical solution of the differential equations describing the transport of reversibly reacting systems has proved an extremely difficult mathematical problem, even when the differential equations were linear. Gilbert and Jenkins [33,36], in a series of papers, simplified the problem by assuming negligible diffusion and rectilinear sedimentation. The equations have been solved using similarity transformations [42]. Field and Ogston [179] were the first workers to include the effect of diffusion on the shape of reaction boundaries in reversibly interacting systems and used a numerical integration procedure to solve the differential equations. Goad [180] has reported a FORTRAN program to simulate the transport and interaction of a reversibly interacting monomer:polymer system. An alternative approach has been reported by Dishon et al. [177].

The rate-zonal transport of reversibly reacting systems in centrifugal fields was studied by Bethune and Kegeles [181,182] who obtained data concerning the distribution patterns of reversible dimerising and trimerising systems and bimolecular complexing systems in centrifugal and electrophoretic systems. Again the differential equations were solved numerically. Cohen et al[28] have studied the behaviour of the enzyme glutamic

hydrogenase in centrifugal fields using the rate-zonal centrifugation technique as described in section 2.3. They assumed that the reaction was non-reversible and that the enzyme kinetics could be described by the Michaelis-Menten equation. They developed the differential equations describing the transport and bioreaction of the reaction species by application of the thermodynamics of irreversible processes. This approach has also been discussed by Fujita [183]. A FORTRAN program was written and the equations were solved using numerical procedures. Good agreement was obtained between the simulation data and experimental data.

In this study, the centrifugal bioreaction-separation process was modelled using the kinetic approach. Due to the non-linearity of the reaction term, the equations were solved numerically using finite difference methods. It should be noted that there are many similarities between the rate-zonal centrifugal bioreaction-separation process and the batch combined chromatographic bioreactor-separators that have been studied over a number of years by Barker and co-workers in this laboratory [4-9.15,16]. Both systems involve the mass transport of active enzyme-substrate zones through the bioreactor. Similarities between the model developed in this chapter and that developed by Zafar [15] who studied the dextransucrase bioreaction-separation process on a batch chromatographic column are interesting to observe.

10.2 INITIAL ASSUMPTIONS

The following initial assumptions were made in this preliminary study of the centrifugal bioreaction-separation process:

(1) Initially, molecular diffusion was neglected in the model development. However, the use of finite difference analysis methods to solve the differential equation led to a solution that introduced a 'numerical diffusion' factor into the model which can be controlled and used to simulate the real diffusion that occurs in the system.

(2) Each sedimenting particle species can be defined by a single mean sedimentation coefficient value (S-value). Light scattering studies of Bovey [47] indicated that at low sucrose and enzyme concentrations, the dextran particles formed were of a broadly similar particle weight. This has been discussed in more detail in section 2.4.2.

(3) The centrifugal force is independent of the radial distance from the axis of rotation.

(4) The density and viscosity of the bioreactor medium remain constant.

(5) The enzymic reaction follows Michaelis-Menten kinetics.

(6) At all sucrose concentrations, 1g of sucrose form 0.526g of fructose and 0.474g of dextran.

(7) Sedimentation is rectilinear

Some of the assumptions are inaccurate. For example, sucrose concentration gradients were required to minimise non-ideal sedimentation in the bioreactor. Furthermore, the viscosity of the bioreactor medium changed greatly during a typical run due to the increasing concentration of native dextran. However, the model development presented in this chapter was intended only as a preliminary study of the process and is in need of further future development.

10.3 MODELLING OF THE PROCESS

10.3.1 The Material Balance Equation

Consider the conversion of sucrose to dextran and fructose by the enzyme dextransucrase across a thin, sector-shaped slice or element of a zonal centrifuge bowl under the influence of random translational diffusion and an applied centrifugal force (figure 10.1).

In figure 10.1, the symbol 'a' refers to the 'height' of the slice; ø equals the angle subtended by the sector; øar is the surface area of the element at a radial distance r from the axis of rotation and ∂r equals the thickness of the slice in the direction of the centrifugal field. A material balance across this slice will take the form:

Accumulation of material	=	Net influx of material due to sedimentation and diffusion	—	Destruction or disappearance of material due to chemical reaction

First, the net change of material in the slice due to sedimentation and diffusion will be considered.

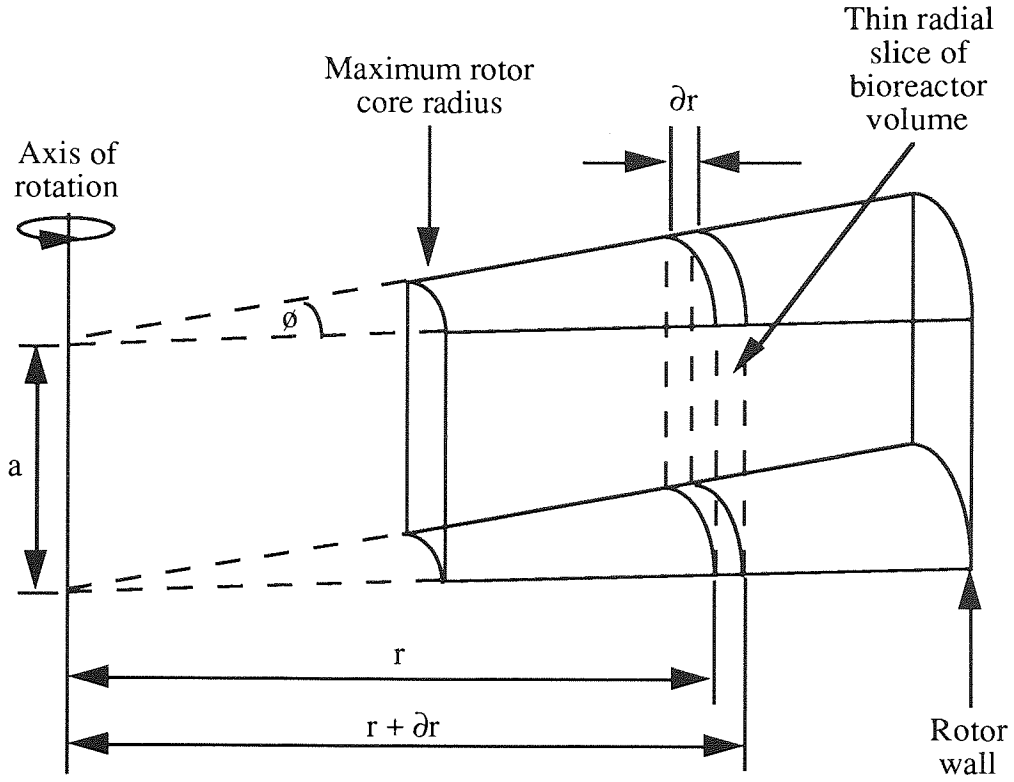

Figure 10.1 Schematic Diagram Showing a Sector Shaped Segment of a Zonal Centrifuge Bowl Containing a Thin Radial Slice of Bioreactor Volume. (The symbols are defined in the text).

The amount of a particular material entering the slice across its surface at position r in a differential time unit of dt due to diffusion is given by Fick's first law as:

$$-D\text{ø}ar(\partial C/\partial r)dt \qquad \text{\_\_\_\_\_(10.1)}$$

Where D equals the diffusion coefficient of the material and $\partial C/\partial r$ equals the concentration gradient of the material across the slice. During the same time interval, the amount of that material leaving the slice by diffusion at position r + dr will be:

$$-\left(D+\frac{\partial D}{\partial r}dr\right)\text{ø}a(r+dr)\left(\frac{\partial C}{\partial r}+\frac{\partial^2 C}{\partial r^2}dr\right)dt$$

$$=-D\text{ø}ar\frac{\partial C}{\partial r}dt-\left[\frac{\partial}{\partial r}\left(rD\frac{\partial C}{\partial r}\right)\right]\text{ø}a\,dr\,dt \qquad \text{\_\_\_\_\_(10.2)}$$

The amount of a particular material that accumulates in the slice due to diffusion is given by the difference between equations 10.1 and 10.2 which equals:

$$\left[\frac{\partial}{\partial r}\left(rD\frac{\partial C}{\partial r}\right)\right]\phi a\, dr\, dt \qquad \text{_____(10.3)}$$

The amount of the material simultaneously entering the slice through the surface at r due to sedimentation is given by the product of the concentration of the material, rate of sedimentation of the material , area of the surface and the time interval. From equation 4.10 it can be observed that the rate at which a particle sediments in a centrifugal field is given by the expression $S\omega^2 r$, so that the amount entering the slice will be:

$$C(\phi ar)\,(S\omega^2 r)\,dt = C\phi aS\omega^2 r^2\,dt \qquad \text{_____(10.4)}$$

The amount leaving through the surface at r + dr will be:

$$\left(C+\frac{\partial C}{\partial r}dr\right)\phi a(r+dr)\left(S+\frac{\partial S}{\partial r}dr\right)\omega^2(r+dr)dt$$

$$= C\phi aS\omega^2 r^2\,dt + \left[\frac{\partial}{\partial r}(C\,S\omega^2 r^2)\right]\phi a\, dr\, dt \qquad \text{_____(10.5)}$$

The accumulation in the slice due to sedimentation will be the difference between equations 10.4 and 10.5:

$$-\left[\frac{\partial}{\partial r}(CS\omega^2 r^2)\right]\phi a\, dr\, dt \qquad \text{_____(10.6)}$$

The total accumulation in the slice due to diffusion and sedimentation, $(\partial C/\partial t)\phi ar\, dr\, dt$, is equal to the sum of equations 10.3 and 10.6:

$$\frac{\partial C}{\partial t}\phi ar\, dr\, dt = \left[\frac{\partial}{\partial r}\left(rD\frac{\partial C}{\partial r}\right)\right]\phi a\, dr\, dt - \left[\frac{\partial}{\partial r}(CS\omega^2 r^2)\right]\phi a\, dr\, dt$$

which can be rewritten;

$$\frac{\partial C}{\partial t} = \frac{1}{r}\frac{\partial}{\partial r}\left[\left(D\frac{\partial C}{\partial r} - C\,S\omega^2 r\right)r\right] \qquad \text{_____(10.7)}$$

and which is the differential equation for combined diffusion and sedimentation. This expression is also known as the Lamm equation. Several investigators have attempted to solve this equation. Faxen [184] first gave an approximate solution to this equation and

more recently exact solutions have been obtained, but are of such complexity as to be virtually useless for computational purposes [42].

Since the solution of this equation presents formidable mathematical problems, many of the investigations into the sedimentation of reacting systems assume rectilinear rather than radial sedimentation [33-36,42,176], so that effectively the flux area is assumed constant. Rectilinear sedimentation in the bioreactor is shown in figure 10.2. Given this approximation, equation 10.7 becomes:

$$\frac{\partial C}{\partial t} = D\frac{\partial^2 C}{\partial r^2} - S\omega^2\frac{\partial (C\,r)}{\partial r} \qquad \text{(10.8)}$$

Equation 10.8 takes a similar form to the material balance equations across a differential section of an electrophoresis gel[42] and also an ideal liquid chromatographic column[185].

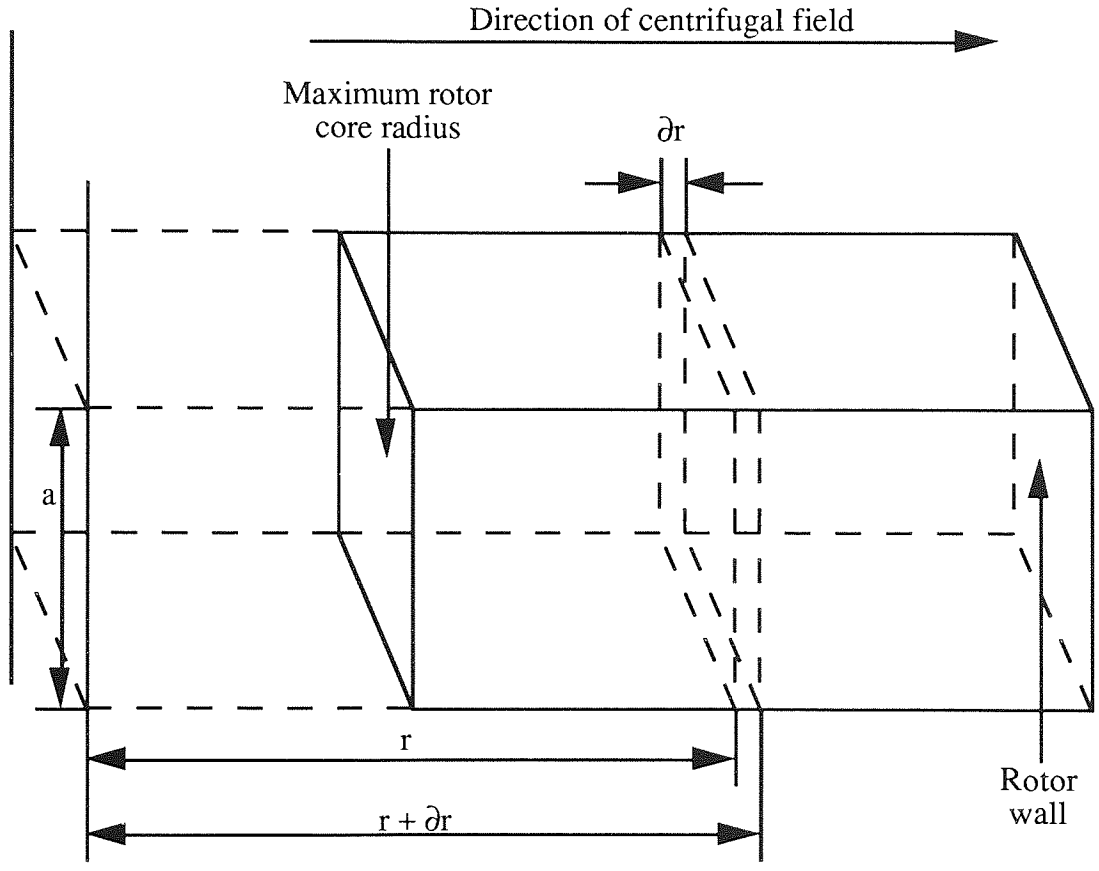

Figure 10.2 Rectilinear Sedimentation in a Zonal Centrifuge Bowl

The change in the quantity of material in the slice due to the biochemical reaction can be determined from Michaelis-Menten kinetics (see chapter 3). The rate of substrate consumption is given by the Michaelis-Menten equation (equation 3.5):

$$V\ (\text{reaction rate}) = \frac{C\,V_{max}}{C + K_M} \qquad \text{(10.9)}$$

where C equals the concentration of the reactant at any given time. Combining equations 10.8 and 10.9 gives the combined bioreaction, sedimentation and diffusion equation. Noting that reactant material, in this case sucrose, was consumed during the enzymic reaction, then this equation can be written for sucrose as:

$$\frac{\partial C}{\partial t} = D_C \frac{\partial^2 C}{\partial r^2} - S_C \omega^2 \frac{\partial (C\,r)}{\partial r} - \frac{C\,V_{max}}{C + K_M} \qquad \text{(10.10)}$$

where D_C and S_C equal the diffusion and sedimentation coefficients of sucrose. Noting that stoichiometrically 1.000 gramme of sucrose will be consumed by the dextransucrase enzyme to yield 0.474 grammes of dextran and 0.526 grammes of fructose product, then similar equations can be written to describe dextran (D) and fructose (F) behaviour in the bioreactor:

for dextran:

$$\frac{\partial D}{\partial t} = D_D \frac{\partial^2 D}{\partial r^2} - S_D \omega^2 \frac{\partial (D\,r)}{\partial r} + 0.474 \frac{C\,V_{max}}{C + K_M} \qquad \text{(10.11)}$$

for fructose:

$$\frac{\partial F}{\partial t} = D_F \frac{\partial^2 F}{\partial r^2} - S_F \omega^2 \frac{\partial (F\,r)}{\partial r} + 0.526 \frac{C\,V_{max}}{C + K_M} \qquad \text{(10.12)}$$

The subscripts D and F refer to dextran and fructose respectively. Equation 10.10 can be converted to a dimensionless form by introducing the following variables:

$$C' = \frac{C}{C_0}\ ,\quad l = \frac{r}{R}\quad \text{and}\quad \Theta_C = S_C \omega^2 t$$

where C_0 equals the initial concentration of the sucrose reactant and R equals the maximum centrifuge bowl radius. By substitution and rearrangement, equation 10.10 assumes the form:

$$\frac{1}{S_C\omega^2}\frac{\partial C'C_0}{\partial t}=\left(\frac{D_C}{S_C\omega^2}\frac{\partial^2(C'C_0)}{\partial(lR)^2}\right)-\frac{\partial(C'C_0lR)}{\partial(lR)}-\left(\frac{1}{S_C\omega^2}\frac{C'C_0V_{max}}{C'C_0+K_M}\right)$$

Which can be simplified to give:

$$\frac{\partial C'}{\partial\Theta_C}=\left(\frac{D_C}{S_C\omega^2R^2}\frac{\partial^2C'}{\partial l^2}\right)-\frac{\partial(C'l)}{\partial l}-\left(\frac{1}{S_C\omega^2}\frac{C'V_{max}}{C'C_0+K_M}\right) \qquad (10.13)$$

Similar dimensionless equations can be written for dextran and fructose:

for dextran:

$$\frac{\partial D'}{\partial\Theta_D}=\left(\frac{D_D}{S_D\omega^2R^2}\frac{\partial^2D'}{\partial l^2}\right)-\frac{\partial(D'l)}{\partial l}+0.474\left(\frac{1}{S_D\omega^2}\frac{C'V_{max}}{C'C_0+K_M}\right) \qquad (10.14)$$

for fructose:

$$\frac{\partial F'}{\partial\Theta_F}=\left(\frac{D_F}{S_F\omega^2R^2}\frac{\partial^2F'}{\partial l^2}\right)-\frac{\partial(F'l)}{\partial l}+0.526\left(\frac{1}{S_F\omega^2}\frac{C'V_{max}}{C'C_0+K_M}\right) \qquad (10.15)$$

It can be seen that the introduction of the dimensionless terms results in three different Θ variables. By taking the Θ factor to equal Θ_D (the dextran Θ term), which is defined by the expression:

$$\Theta_D = S_D\omega^2 t$$

then equations 10.13 to 10.15 can all be written with respect to Θ_D. Consequently, the Θ variable now refers to the sedimenting behaviour of dextran rather than sucrose. However, because these three equations have been linked to the mean sedimentation rate of dextran, the equations must take account of the differing sedimentation coefficients of the three particle species. This can be done by expressing the sedimentation coefficient of each particle species to that of dextran, so that the rate of sedimentation will be linked to S_C / S_D for sucrose, S_D / S_D (=1) for dextran and S_F / S_D for fructose. Equation 10.13 will then assume the form:

$$\frac{\partial C'}{\partial \Theta_C}\left(\frac{S_C}{S_D}\right) = \left[\left(\frac{S_C}{S_D}\right)\left(\frac{D_C}{S_C \omega^2 R^2}\frac{\partial^2 C'}{\partial l^2}\right)\right] - \left(\frac{S_C}{S_D}\right)\frac{\partial (C'1)}{\partial l}$$

$$- \left(\frac{S_C}{S_D}\right)\left(\frac{1}{S_C \omega^2}\frac{C' V_{max}}{C' C_0 + K_M}\right)$$

which can be simplified to give:

$$\frac{\partial C'}{\partial \Theta_D} = \left(\frac{S_C}{S_D}\right)\left(\frac{1}{Pe}\frac{\partial^2 C'}{\partial l^2}\right) - \left(\frac{S_C}{S_D}\right)\frac{\partial (C'1)}{\partial l} - \left(\frac{1}{S_D \omega^2}\frac{C' V_{max}}{C' C_0 + K_M}\right) \qquad (10.16)$$

Similar equations can be derived for dextran and fructose:

for dextran:

$$\frac{\partial D'}{\partial \Theta_D} = \left(\frac{S_D}{S_D}\right)\left(\frac{1}{Pe}\frac{\partial^2 D'}{\partial l^2}\right) - \left(\frac{S_D}{S_D}\right)\frac{\partial (D'1)}{\partial l} + 0.474\left(\frac{1}{S_D \omega^2}\frac{C' V_{max}}{C' C_0 + K_M}\right) \qquad (10.17)$$

for fructose:

$$\frac{\partial F'}{\partial \Theta_D} = \left(\frac{S_F}{S_D}\right)\left(\frac{1}{Pe}\frac{\partial^2 F'}{\partial l^2}\right) - \left(\frac{S_F}{S_D}\right)\frac{\partial (F'1)}{\partial l} + 0.526\left(\frac{1}{S_D \omega^2}\frac{C' V_{max}}{C' C_0 + K_M}\right) \qquad (10.18)$$

where 1/Pe equals:

$$\frac{1}{Pe} = \frac{D}{S_D \omega^2 R^2}$$

The diffusion coefficient, D, will be dependent on the particle being considered. The Pe term is an example of a Peclet number and as the above equation indicates, is used to compare the sedimentation and diffusion properties of a particle or molecule. As an approximate guide, the expression D/R, which is effectively the 'diffusion velocity' of a given particle, has SI units of m/sec and gives the distance that a particle with a diffusion coefficient D will migrate in a given time due to diffusion. The expression $S_D\ \omega^2 R$ in the above equation is effectively the 'sedimentation velocity' of a given particle and also has SI units of m/sec. This term serves to indicate the distance that a dextran particle with a mean S-value equal to S_D will migrate in a centrifugal field over the same time period.

Large Peclet numbers indicate that particle movement is due primarily to sedimentation rather than diffusion.

The mean diffusion and sedimentation coefficients of a native dextran sample were measured in this project as discussed in section 6.5. Mean $S_{20,w}$ and D values of 285 Svedbergs and 1.46×10^{-8} cm^2 sec^{-1} respectively at infinite dilution were obtained. A typical native dextran particle at a radial distance of 7cm from the axis of rotation in the JCF-Z zonal rotor, rotating at an average speed of 10 000 rpm will have a Peclet number in the order of 10^5. Thus it can be concluded, that in the case of dextran, the rate of particle sedimentation is about 10^5 times greater than any particle movement due to diffusion. Therefore, the rate of dextran sedimentation when compared with diffusion can be assumed negligible and so the diffusion term in equation 10.17 can be neglected.

In the case of sucrose and fructose, with diffusion coefficients in the order of 5×10^{-6} cm^2 sec^{-1}, taking the same dextran S-value, Peclet numbers of around 1.3×10^2 were found. Again, in such cases, the rate of sucrose and fructose diffusion when compared with dextran sedimentation can be considered negligible. This observation can be explained by considering the rate of sucrose sedimentation during a typical bioreaction-separation run in the JCF-Z zonal rotor. A typical run time would be in the order of 2 hours (chapter 9), in which time the high 'molecular' weight dextran material would have sedimented to the rotor wall. In this time, a typical sucrose molecule would have diffused across approximately 3.6×10^{-2} cm of the cell length. Thus diffusion can be assumed negligible in the case of sucrose and fructose and the diffusion terms in equations 10.16 and 10.18 can be assumed negligible. In the case of negligible diffusion, equation 10.16 simplifies to:

$$\frac{\partial C'}{\partial \Theta_D} = -\left(\frac{S_C}{S_D}\right)\frac{\partial (C'1)}{\partial 1} - \left(\frac{1}{S_D \omega^2}\,\frac{C'\,V_{max}}{C'\,C_0 + K_M}\right) \qquad \text{(10.19)}$$

Similar equations can be derived for fructose and dextran. The above equation can be further simplified by assuming that the centrifugal force acting on any given particle is independent of the radial distance of the particle from the axis of rotation. This is a crude approximation but was justified by the fact that the modeling of this system was only intended to be a preliminary study of the process. Using this approximation, equation 10.19 takes the form:

$$\frac{\partial C'}{\partial \Theta_D} = -\bar{l}\,\frac{S_C}{S_D}\frac{\partial C'}{\partial l} - \left(\frac{1}{S_D^2\omega^2}\,\frac{C'\,V_{max}}{C'\,C_0 + K_M}\right) \qquad \text{(10.20)}$$

where

$$\bar{l} = \frac{R + r_{(meniscus)}}{2R} = 0.646$$

The Reaction term in the above equation can also be written in terms of dimensionless variables:

$$\left(\frac{1}{S_D^2\,\omega^2}\,\frac{C'\,V_{max}}{C'\,C_0 + K_M}\right) = \frac{V_{max}}{C_0 S_D^2\omega^2}\,\frac{C'}{\frac{K_M}{C_0}} = \frac{R\,C'}{(K + C')} \qquad \text{(10.21)}$$

where:

$$\frac{V_{max}}{C_0 S_D^2\omega^2} = R \quad \text{and} \quad \frac{K_M}{C_0} = K \qquad \text{(10.22)}$$

So that equation 10.20 now assumes the form:

$$\frac{\partial C'}{\partial \Theta_D} = -0.646\left(\frac{S_C}{S_D}\right)\frac{\partial C'}{\partial l} - \frac{R\,C'}{(K + C')} \qquad \text{(10.23)}$$

Similarly for dextran:

$$\frac{\partial D'}{\partial \Theta_D} = -0.646\left(\frac{S_D}{S_D}\right)\frac{\partial D'}{\partial l} + 0.474\,\frac{R\,C'}{(K + C')} \qquad \text{(10.24)}$$

and fructose:

$$\frac{\partial F'}{\partial \Theta_D} = -0.646\left(\frac{S_F}{S_D}\right)\frac{\partial F'}{\partial l} + 0.526\,\frac{R\,C'}{(K + C')} \qquad \text{(10.25)}$$

The R and K terms are dimensionless variables and can be used to estimate the run conditions and enzyme activities required to achieve a given degree of conversion.

Equations 10.23-10.25 were derived making the assumption that enzyme material was uniformally distributed throughout the bioreactor. Clearly this was not the case in the rate-zonal bioreaction-separation process as the enzyme was initially introduced as a distinct zone onto the supporting sucrose substrate at the start of a run. The true

magnitude of the reaction term in equations 10.23 to 10.25 is therefore dependent on the enzyme 'concentration' (activity) at any given position and time in the bioreactor. However because this was only a preliminary attempt at modelling the centrifugal bioreaction-separation process, the model was simplified by making the assumption that the enzyme solution was initially uniformally distributed throughout the bioreactor and the sucrose substrate was introduced as a zone onto the enzyme solution. The advantage of this assumption was that the reaction term can be assumed independent of enzyme concentration, thereby considerably simplify the modelling process. The process was therefore viewed as a sedimenting band of sucrose moving through a constant density and viscosity enzyme solution with a sedimentation rate equal to that of an enzyme molecule entrapped in a highly solvated dextran particle. In this model, the enzyme molecules themselves were assumed to have a negligible rate of sedimentation. In order for this simplification to be valid, then the sucrose molecules must be assumed to have the same sedimenting properties as the entrapped enzyme molecules in the real system. Therefore, for modelling purposes, S_C was taken to equal S_D. This assumption is discussed in more detail in section 10.4.

10.3.2 Solution of the Mass Balance Equation

Despite the simplifications made, the analytical solution to equations 10.23 to 10.25 cannot be easily determined due to the non-linearity of the reaction term. Zafar and Barker [4] using similar mathematical relationships to model bioreaction and separation in chromatographic systems successfully solved their equations using numerical methods where the reactor was treated as a number of discrete mixed cells. The theory of numerical methods has been well documented in the literature; therefore the techniques used in this work are only briefly described below. Czok and Guiochon [186] have written an excellent review concerning the numerical solution of mass balance equations in chromatographic systems.

Using the finite difference method, the change in substrate concentration in the bioreactor due to bioreaction and sedimentation is calculated in a stepwise manner at discrete fractions of l and Θ_D. Thus the differential terms in equation 10.23 assume the form:

$$\frac{\partial C'}{\partial l} = \frac{\Delta C'}{\Delta l} \quad \text{and} \quad \frac{\partial C'}{\partial \Theta_D} = \frac{\Delta C'}{\Delta \Theta_D}$$

Where Δl, $\Delta\Theta_D$ and $\Delta C'$ represent discretised fractions of l, Θ_D and C'. Effectively by discretising l and Θ_D, a grid of Δl versus $\Delta\Theta_D$ can be constructed as shown in figure 10.3.

Each cell in the grid has dimensions of Δl versus $\Delta\Theta_D$. In order to calculate $C'(l_{i-1}, \Theta_j)$, which denotes the concentration in the l^{th} radial slice of the bioreactor after the Θ_D^{th} time interval, the C' value averaged over Δl and$\Delta\Theta_D$ must be calculated for every incremental value of l and Θ_D. Thus every value in the grid must be determined.

The vertical columns of the grid represent the concentration profiles in the bioreactor in the plane of the centrifugal field at a given value of Θ_D; the horizontal rows show how concentration changes with respect to Θ_D over one thin slice of bioreactor. Thus, the first column ($\Theta_D = 0$) describes the initial injection profile and the last column will describe the concentration profile at the termination of a run. When a zone of material sediments through the bioreactor, the corresponding concentrations are propagated through the grid from the point of injection to the rotor wall and from the time of injection to the time of run termination. This 'grid propagation' method will be explained shortly.

		$\Delta\Theta_D$ values			
		$\Theta_D = 0$			$\Theta_D = \Theta$
		j	j + 1	.....	j + n
l = 0	i - 1	$C'(l_{i-1}, \Theta_j)$	$C'(l_{i-1}, \Theta_{j+1})$	.....	$C'(l_{i-1}, \Theta_{j+n})$
	i	$C'(l_i, \Theta_j)$	$C'(l_i, \Theta_{j+1})$		
Δl	i + 1	$C'(l_{i+1}, \Theta_j)$			
values	...	...			
	...	...			
l = l	i + m	$C'(l_{i+m}, \Theta_j)$			

Figure 10.3 A Grid of Concentration Values at Discretised Fractions of l and Θ_D

It can be seen from figure 10.3 that the differential quotients with respect to l and Θ_D can be expressed in terms of finite difference quotients. The derivative with respect to Θ_D is converted into a forward type difference equation, whereas the derivative for distance is replaced by the backwards type, so that for sucrose:

$$\frac{\partial C'}{\partial \Theta_D} = \frac{C'(l_i, \Theta_{j+1}) - C'(l_i, \Theta_j)}{\Delta \Theta_D} \qquad (10.26)$$

$$\frac{\partial C'}{\partial l} = \frac{C'(l_i, \Theta_j) - C'(l_{i-1}, \Theta_j)}{\Delta l} \qquad (10.27)$$

Using the same notation, the reaction term becomes:

$$\frac{R\,C'}{(K + C')} = \frac{R\,C'\,(l_i, \Theta_j)}{\left(K + C'\,(l_i, \Theta_j)\right)} \qquad (10.28)$$

The differential quotients in equation 10.23 can be expressed in terms of other points on the grid with certain limitations if so desired, but will result in an identical solution to the differential equation. Czok and Guiochon [186] have discussed the use of different combinations of other finite difference quotients. Substituting equations (10.26) - (10.28) into equations 10.23 yields:

$$\frac{C'\,(l_i, \Theta_{j+1}) - C'\,(l_i, \Theta_j)}{\Delta\Theta_D} = -\,0.646\left(\frac{S_C}{S_D}\right)\frac{C'\,(l_i, \Theta_j) - C'\,(l_{i-1}, \Theta_j)}{\Delta l} - \frac{R\,C'\,(l_i, \Theta_j)}{\left(K + C'\,(l_i, \Theta_j)\right)}$$

which can be rearranged to give:

$$C'\,(l_i, \Theta_{j+1}) = C'\,(l_i, \Theta_j) - \beta_C\left[C'\,(l_i, \Theta_j) - C'\,(l_{i-1}, \Theta_j)\right] - \Delta\Theta\,\frac{R\,C'\,(l_i, \Theta_j)}{\left(K + C'\,(l_i, \Theta_j)\right)} \qquad (10.29)$$

where:

$$\beta_C = 0.646\,\frac{S_C}{S_D}\,\frac{\Delta l}{\Delta\Theta}$$

Similarly for dextran:

$$D'\,(l_i, \Theta_{j+1}) = D'\,(l_i, \Theta_j) - \beta_D\left[D'\,(l_i, \Theta_j) - D'\,(l_{i-1}, \Theta_j)\right] + 0.474\,\Delta\Theta\,\frac{R\,C'\,(l_i, \Theta_j)}{\left(K + C'\,(l_i, \Theta_j)\right)} \qquad (10.30)$$

and for fructose:

$$F'(l_i, \Theta_{j+1}) = F'(l_i, \Theta_j) - \beta_F \left[F'(l_i, \Theta_j) - (F'\ l_{i-1}, \Theta_j) \right] + 0.526\ \Delta\Theta \frac{R\,C'(l_i, \Theta_j)}{\left(K + C'(l_i, \Theta_j)\right)} \quad (10.31)$$

In order to evaluate equations 10.29 to 10.31, the initial and boundary conditions of the system are required. The initial conditions were:

$$C'(0,\Theta) = 0, \qquad D'(0,\Theta) = 0, \qquad F'(0,\Theta) = 0,$$

The boundary conditions used were identical to those used by Zafar [15] in his modelling of a dextransucrase chromatographic bioreactor-separator. At time zero, C' will be equal to zero everywhere, except at the point of injection where it is equal to unity in the injection volume. The model assumes that the sucrose pulse entering the reactor contains enzyme whose activity is the same as that in the bioreactor, for the reasons discussed in section 10.3.1. In practice the pulse was an enzyme solution that did not contain any sucrose. The following boundary conditions therefore apply:

C' = the concentration of sucrose in the injection volume at zero time (pulse),
C' = 0 at all other points in the bioreactor at zero time,
$D'(1,0) = 0, \qquad F'(1,0) = 0,$

The initial and boundary conditions for sucrose on the grid are shown in figure 10.4. The grid concentration values can be determined by evaluating equation 10.29. This was done as follows:

(1) It can be seen from figure 10.4 that:

$$C'(l_{i-1}, \Theta_j) = 0, \qquad C'(l_i, \Theta_j) = \text{pulse}$$

Substitution of these values into equation 10.29 gives the value of C' at (l_i, Θ_{j+1}).

(2) Using the grid propagation method, the newly calculated C' (l_i, Θ_{j+1}) value becomes the 'new' C' (l_i, Θ_j) value for calculation purposes. The 'new' C' (l_{i-1}, Θ_j) is therefore the previous C' (l_{i-1}, Θ_{j+1}) value shown in table 10.4. These values are fed into equation 10.29 to give the next C' (l_i, Θ_{j+1}) value.

(3) This C' (l_i, Θ_{j+1}) value becomes the 'new' C' (l_i, Θ_j) value. C' (l_{i-1}, Θ_{j+1}) becomes the new C' (l_{i-1}, Θ_j) value.

(4) Steps (2) to (3) are repeated until row i-1 on the grid is completed. This process is then repeated for each subsequent grid row until the whole grid is completed. The final column then yields the concentration profile at the termination of the run. The finite difference equations for dextran and fructose (equations 10.30 and 10.31) are evaluated on separate grids in a similar manner, using the correct values of $C'(l_i, \Theta_j)$ as required.

		$\Delta\Theta_D$ values			
		$\Theta_D = 0$			$\Theta_D = \Theta$
		j	j + 1	.....	j + n
l = 0	i - 1	0	0	.....	0
	i	pulse			
Δl	i + x	pulse			
values	i + y	0			
	...	0			
	...	0			
l = 1	i + z	0			

Figure 10.4 The Initial and Boundary Conditions of the Sucrose Substrate on the Grid

10.3.3 Computer Program

A FORTRAN computer program was written to perform the above calculations. The concentrations of sucrose, enzyme and dextran in each grid cell were calculated as described above and stored in two dimensional arrays. The final column of figures in each of these arrays provided the simulation data required. Typical input data is shown in table 10.1. A copy of the program is presented in appendix A10.

S_C and S_D (sec)	250.00×10^{-13}
S_F (sec)	0.46×10^{-13}
Km ($g\ cm^{-3}$)	6.8×10^{-3}
Vmax ($g\ cm^{-3}\ sec^{-1}$)	1.5×10^{-6}
ω^2 (sec^{-2})	4.39×10^{6}
C_o ($g\ cm^{-3}$)	0.2
Sample volume (cm^3)	50
Run time (sec)	variable
Δl and $\Delta\Theta_D$	variable

Table 10.1 Typical Input Values for the Simulation Program

10.3.4 Selection of Δl and $\Delta\Theta_D$

Due to the approximations made in the finite difference analysis methods, errors are unavoidable. The magnitude of these errors are dependent upon the incremental values chosen and have been shown to influence band broadening in chromatographic simulations in much the same way as molecular diffusion does in real systems [186]. In the derivation of the mass balance equation, molecular and particle diffusion was assumed negligible. By controlling the so called 'numerical diffusion' that is inherent in finite difference methods, it should be possible to simulate the band broadening that occurs due to molecular or particle diffusion in the plane of the centrifugal field in the centrifugal bioreactor in much the same manner as the axial diffusion that occurs in chromatographic systems.

The procedure consists of adjusting the magnitude of the Δl and $\Delta\Theta_D$ values so that the numerical diffusion created equals the dispersion due to molecular diffusion. Czok and Guiochon [186] have reviewed a number of mathematical relationships that can be used to determine the appropriate grid spacing that will produce the desired amount of zone broadening in chromatographic systems. At present, such relationships have not been elucidated for the centrifugal system. However it is expected that the ratio of the incremental values will be linked to the rate of zone movement through the bioreactor.

10.3.5 Simulation Results

Analysis of the simulation data is ongoing as part of an SERC sponsored project. The program has been run sucessfully to yield characteristic sucrose, fructose and dextran concentration versus distance profiles. At present, the initial simulation results obtained from the program are being compared with actual experimental data obtained from the bioreaction-separation runs reported in chapter 9. It is intended to compare the model simulations with the experimental data obtained during the bioreaction and rate-zonal sedimentation of some of the more 'ideal' enzymic systems that have been reported in the literature. Cohen et al for example, have studied the sedimentation of the glutamic dehydrogenase enzyme and the synthesis and sedimentation of the reaction products formed during a rate zonal centrifugation using an analytical ultracentrifuge [28]. This reaction is not seriously affected by complicating factors such as increases in medium viscosity with run time and concentration effects. Furthermore, the enzyme and reaction products can be accurately characterised by a relatively narrow range of S-values. Furthermore, it will also be of interest to compare the native dextran concentration distribution profiles reported in chapter 6 (see figure 6.4) with data from the model simulation. In such cases, the reaction term will equal zero.

10.4 Future Work

In addition to the elucidation of the optimum Δl and $\Delta\Theta_D$ values, the following points will be considered:

(1) In section 10.3.1, the assumption was made that enzyme material was uniformally distributed throughout the bioreactor. The advantage of this approach was that the reaction term could be assumed to remain independent of enzyme activity throughout the process. However, in the real system it was the enzyme that was initially introduced as a distinct zone onto the supporting sucrose substrate at the start of a run. The true magnitude of the reaction term in equations 10.23 to 10.25 is therefore dependent on the enzyme 'concentration' (activity) at any given position and time in the bioreactor. To take account of this factor, equation 10.23 should be rewritten as:

$$\frac{\partial C'}{\partial \Theta_D} = -0.646 \left(\frac{S_C}{S_D}\right) \frac{\partial C'}{\partial l} - E' \frac{R\,C'}{(K + C')} \qquad \text{(10.32)}$$

where E' equals the dimensionless enzyme concentration. The value of E' at any given position and time in the bioreactor can be described in a similar manner as C', so that:

$$\frac{\partial E'}{\partial \Theta_D} = -0.646 \left(\frac{S_E}{S_D}\right) \frac{\partial E'}{\partial l} \qquad \text{(10.33)}$$

The reaction term in the above equation will equal zero because enzyme is neither synthesised nor consumed during the process. The enzyme molecules would be assumed to have the same mean S-values as the native dextran particles as indicated by experimental data, so that $S_E = S_D$. The sucrose molecules will have an S-value of around 0.276 Svedbergs as determined by LaBar and Baldwin [151].

The initial conditions in this process would be:

$$C'(0,\Theta) = 0, \qquad D'(0,\Theta) = 0, \qquad F'(0,\Theta) = 0, \qquad E'(0,\Theta) = 0$$

The boundary conditions would be similar to those used for elution chromatography [15,187]. At time zero E' will be equal to zero everywhere, except at the point of injection where it is equal to unity in the injection volume. The model would assume that the enzyme pulse entering the reactor contained sucrose with a concentration equal to that in the bioreactor, although in practice the pulse does not contain any sucrose. The following boundary conditions would therefore apply:

C' (1,0) = pulse C', D' (1,0) = 0, F' (1,0) = 0,

E' = pulse E', in the portion of the bioreactor occupied by the enzyme and E' = 0 in the remainder of the vessel at zero time.

Equation 10.32 and 10.33 could then be written in the finite difference form and equation 10.33 solved numerically to yield an E' (l_i, Θ_{j+1}) value which would then be substituted into the finite difference form of equation 10.32 and the corresponding C' (l_i, Θ_{j+1}) value determined. This process would be repeated using the grid propagation method discussed in section 10.3.2 to yield the solution to equations 10.32 and 10.33. Similar equations could be written and solved for dextran and fructose.

The following points should also be considered in the future development of the model:

(2) In the preliminary development of this model, the assumption was made that the centrifugal force was the same at all points in the bioreactor. However, centrifugal force is directly proportional to the radial distance from the axis of rotation and hence is related to the magnitude of the l term. It is intended to develop the program to take account of this factor.

(3) Experimental studies have shown that even relatively low native dextran concentrations result in large increases in system viscosity (for example, see table 9.22). This factor must be considered in order to successfully relate the experimental data to the simulation results. The effect of native dextran concentration on S-values was studied in the analytical centrifuge (chapter 6) and a concentration dependence coefficient was calculated over the native dextran concentration range of 0-1.5% w/w. Schachman [102] has reported two equations (equations 4.22 and 4.23) that relates sample concentrations and concentration dependence coefficients to sample sedimentation coefficients in rate normal centrifugations. It is intended to determine similar relationships between native dextran concentration and sedimentation coefficients in the centrifugal bioreactor, with the eventual aim of improving the model.

(4) The rate-zonal process required the use of sucrose gradients in order to minimise hydrodynamic stability. However, in the model development it was assumed that an enzyme solution with a uniform density and viscosity was distributed throughout the bioreactor. After the modifications discussed in point (1) above have been applied, the effect of the increasing gradient density and viscosity could be incorporated into the model. Provided that the initial sucrose concentration versus radial distance profiles were

known then sucrose concentration like centrifugal force could also be directly related to the l term and the program adjusted accordingly.

(5) The use of dextransucrase Vmax and Km values from the literature.

10.5 Further Suggestions

The model developed in this chapter was intended as a preliminary study of the centrifugal bioreaction-separation principle. Although the biochemical conversion of sucrose to fructose and dextran polymer was considered, the model is equally applicable to any enzymic process that follows the Michaelis-Menten model.

One of the main assumptions made in this work was that the native dextran particles could be adequately defined by a single S-value. This assumption, although crude, was based on the light scattering studies of Bovey [47], which indicated that high MW dextran particles had broadly similar particle sizes during synthesis. However, these studies were carried out at very low enzyme and sucrose concentrations. It was apparent from the experimental results obtained that considerable particle interactions had occurred, which resulted in a significant increase in dextran particle polydispersity. This was primarily due to the structure of native dextran and the high dextran concentrations recorded in this study. Given the experimental data obtained, it was felt that more data concerning the formation of native dextran particles and the mechanism of molecular association is required in order to relate experimental and simulation data successfully. Native dextran particle formation, as discussed in chapter 2, is a highly complex process. It is possible that this model could predict system performance at very low dextran concentrations and hence very low system viscosities,

It was concluded that the model would be more ideally suited to the study of biochemical reactions involving substrates and products that can truly be defined by a single S-value or narrow range of S-values and where only small changes in the overall system viscosity and in the degree particle interaction occurs throughout the course of the reaction.

11.0 CONCLUSIONS AND RECOMMENDATIONS

11.1 CONCLUSIONS

The main conclusions from this project are summarised below:

Analytical Ultracentrifuge studies

(1) Studies in an analytical ultracentrifuge showed that the rate of native dextran sedimentation was highly dependent on concentration. The sedimentation coefficient of dextran increased from 17 to 163 Svedbergs when the concentration of native dextran was decreased from 1.5 % to 0.5% w/w in a rate normal centrifugation. It was concluded that dextran particle interactions greatly affected the rate of dextran sedimentation. Extrapolation of this data above 1.5% w/w indicated that a point was reached where the dextran sedimentation rate effectively equalled zero and the native dextran material exhibited the classic behaviour of an incompressible gel in a centrifugal field. This occurred at native dextran concentrations of around 1.6% w/w.

Batch Bioreaction-Separation Studies in the MSE Superspeed 50 Ultracentrifuge Fitted with a 3 x 20 cm^3 Swinging Bucket Rotor

(2) Increases in rotor speed from 10 000 to 20 000 rpm (~10 000g to 40 000g average) significantly improved dextran sedimentation to the tube base per unit time, in some cases by over 100%, but also resulted in significant increases in fructose found at the tube base, typically by 60-100%. Increases in run times from 1.5 to 3 hours led to an average 40% increase in the percentage of dextran recovered from the pelleted fraction. However, this was accompanied by increases in the percentage of pelleted fructose typically by between 15 and 200%. Increases in mean sucrose concentrations from 10% w/w to 20% w/w reduced the proportion of dextran found in the pellets by an average 30%, but resulted in significant improvements in the ratio of dextran to fructose found in the pelleted fractions. It appeared that enzyme activity had a marked effect on the distribution of the product materials,. This phenomenon was studied more effectively in the JCF-Z zonal rotor studies. The high levels of fructose in the pelleted zones was believed to be due to enzyme and fructose entrainment by the large dextran particles. This was subsequently proven using the zonal rotor.

(3) The centrifugal bioreactor produced up to three times less low MW dextran (<12 788 MW) and up to 100% more 'clinical range' dextran (12788 - 99 001 MW) than a conventional batch bioreactor at initial sucrose concentrations of 10, 15 and 20%w/w. Increased proportions of high molecular weight dextran of between 6 and 10% were also recorded in the centrifugal bioreactor at the three initial sucrose concentrations studied.

However, when the percentages of dextran greater than 150 000 MW from the two reactors were compared, only small differences in dextran levels were observed. It was concluded that there was a 'shift' in dextran MWD from the low MW region to an intermediate MW region of between 12 000 and 150 000 MW.

This research has therefore demonstrated for the first time that dextran can be manufactured in a centrifugal bioreactor-separator with improved yields of clinical and high molecular weight dextran as compared with a conventional batch reactor. Furthermore, the integration of the bioreaction and separation steps could also reduce the capital and processing costs.

Studies in the Sharples T1 Laboratory Supercentrifuge

(4) Studies on the sedimentation behaviour of presynthesised native dextran and fructose broths indicated that feedrates of around 2.5 cm^3 min^{-1} would be required to achieve high recoveries of native dextran material using industrial scale tubular centrifuges operated as rate-zonal bioreactor-separators. It was concluded that the process was more ideally suited for the smaller scale production of a higher value product.

(5) Despite the poor predicted performance of the tubular centrifuge, the flow patterns of the process streams in the rotating bowl were studied. If the flow patterns indicated that fluid mixing in the bowl was minimal then alternative catalytic processes were to be considered. The mixing behaviour of a single fluid in the centrifuge bowl was shown to approximate four stirred tanks-in-series. Increases in process fluid flowrate from 4 to 8 cm^3 min^{-1} and rotor speeds from 10 000 to 30 000 rpm had no significant effect on mixing in the bowl. A second experiment was undertaken to determine the extent of non ideal flow and the mixing that occurred between a 'stationary' sucrose solution overlaid by a flowing stream of heat treated dextransucrase enzyme. The results showed that substantial mixing occurred between the two solutions in the vessel. A redesign of the nozzle inlet to help to minimise mixing in the system was discussed. The extent of mixing indicated that the process was far from ideal for the successful development of a continuous bioreaction-separation process.

Studies in the JCF-Z Zonal Rotor fitted with the Reograd Zonal Rotor Core

(6) The rate-zonal centrifugation of presynthesised native dextran and fructose mixtures indicated that the native dextran material had relatively narrow ranges of sedimentation coefficient values (S-values). This was indicative of the material having discrete particle structures rather than gel network structures. The maximum ordinates of

the observed peaks corresponded to S-values of between 227 and 237 Svedbergs, which compared well with analytical ultracentrifuge measurements of 285 Svedbergs (chapter 6). Typically, up to 60% of the total native dextran detected had S-values in the region of 150 to 260 Svedbergs, corresponding to 'molecular weight' values of 70 x 10^6 to 125 x 10^6.

(7) These same studies showed that up to 25% of the fructose molecules detected had similar S-values to those of the native dextran material. It appeared that the highly solvated nature of the native dextran particles resulted in the physical 'entrapment' of these fructose molecules within the dextran structure, resulting in the forced sedimentation of the fructose material. Entrapment may have a negative effect on bioreactor performance by hindering the removal of acceptor molecules from reaction zones in the bioreactor. The use of ethanol fractionation to recover the clinical dextran product at a later stage in the manufacturing process will remove any residual entrained fructose.

(8) The Rate-zonal centrifugation of heat treated dextransucrase enzyme fractions showed that this material had a broad ranges of S-values and hence a broad range of particle MWs. This was believed to be due to 'intermediate' sized particles not removed during the enzyme purification process. These materials contribute to gradient overloading.

(9) All the data from the bioreaction-separation runs indicated that very high rates of particle sedimentation were being achieved. Subsequent calculations showed that these high values will have partly been due to density inversion effects. In order to prevent density inversion, the density increment due to the enzyme sample must be a factor of 3-18 times less than the density increment of the supporting sucrose solution. Comparison of the the bioreaction-separation runs with the heat treated enzyme runs showed that density inversion alone could not account for the very high S-values recorded. It therefore appeared that other factors affected particle separation. Two reasons were considered. Firstly, the dextran particles formed very high 'molecular weight' network structures with correspondingly high S-values. Secondly, the enzymic conversion of the sucrose gradient material to product at the active sites of the enzymes prevents the formation of smooth sucrose concentration gradients in the vicinity of the enzyme molecules, which will inevitably result in some hydrodynamic instability and non-ideal sedimentation.

(10) Mixing in the gradient during reorientation appeared to be minimal.

(11) Viscosity studies on presynthesised native-dextran and fructose broths showed that native dextrans formed remarkably viscous solutions even at low macromolecular concentrations. Broths containing 0.5% w/w native dextran had viscosities of around 5 mPas which is equivalent to the viscosity of a 40% w/w sucrose solution and rose to over 1000 mPas for 10% w/w broths. Because of viscosity effects, dextran-fructose separation was found to be highly dependent upon dextran concentration. When the average final mean dextran concentration was below 0.7% w/w, the average dextran versus fructose ratios in the gel layers was above 3:1, whereas when the average final mean dextran concentration was above 6% w/w, the mean ratio decreased to under 1.7:1. Furthermore at average native dextran concentrations of 0.5% w/w, 24% of all the dextran synthesised in a run was found at the rotor wall compared with only 8% at dextran concentrations of 5.8% w/w.

(12) Although dextran-fructose separation and dextran sedimentation was improved at lower viscosities, the dextran yields were correspondingly lower. The highest dextran yield per hour was recorded using the repeat injection technique. This technique was designed to minimise viscosity effects in the bioreactor but suffered from the fact that there will be a build up of acceptor molecules in the bowl which will inhibit dextran chain growth. Although the benefits of higher dextran yields per unit time by minimisation of the acceptor reaction will be lost, this may be compensated for by the integration of the bioreaction-separation process into a single unit operation. Experimental data has indicated that the poor dextran:fructose ratios recorded in the gel fractions in the repeat injection run will be improved by decreasing the activity of the enzyme injections.

(13) Enzyme activity, volume and run time are all factors that will influence viscosity in the bioreactor. Low enzyme activities were shown to improve the separation of enzyme molecules and dextran from regions of higher fructose concentrations. Decreasing the volume of the enzyme charge injected into the bioreactor appeared to slightly improve product separation, and led to an increase in the percentage of dextran synthesised in the reaction that was found at the rotor wall. The effect of run time on bioreactor performance proved difficult to assess. Longer run times had been shown to significantly improve dextran recoveries in the studies carried out on the MSE centrifuge, but will result in viscosity increases. Viscosity must be minimised in order for longer run times to be of benefit in this process. Similarly, higher rotor speeds were also shown to increase dextran recoveries in the MSE trials, but like run time, viscosity in the bioreactor must be minimised in order for optimum rotor speeds to be selected. Appreciable amounts of dextran sedimentation was observed at rotor speeds as low as 5000 rpm.

(14) The use of steep gradients has been shown to minimise the possibility of convective disturbances within the bioreactor and improve the resolving power of the system, which will in theory encourage the formation of distinctive 'reaction zones' within the bioreactor. However, little evidence of band formation was observed in any of the trials, indicating that simultaneous bioreaction and separation was limited in this system. However, minimisation of the acceptor reaction is dependent upon the removal of acceptor molecules from the regions of high enzyme activity and this was occuring in many of the runs. Less steep gradients resulted in higher proportions of native dextran and enzyme activities being found in the lower portions of the gradient and at the rotor wall. However, as bioreaction proceeded, the increasing viscosity effects caused by native dextran synthesis had a far greater effect on sedimentation behaviour than sucrose gradient shape. The experimental data suggested that the poorer dextran-fructose separation obtained when using the less steep gradients will be improved by using lower activity enzyme charges.

(15) The activity profiles strongly indicated that significant proportions of the enzyme molecules had become physically entrapped within the highly solvated native dextran structures and were forced to sediment at the high sedimentation rates of these structures. This possibility was supported by the fact that fructose entrainment in native dextran had been observed in the JCF-Z rotor calibration runs. Enzyme and fructose entrainment will have an effect the simultaneous synthesis and removal of fructose molecules from regions of high enzyme activity within the bioreactor. The experimental data however, indicated that entrainment will be minimised by using low enzyme activities. Furthermore, the use of ethanol fractionation to recover the clinical dextran product at a later stage in the process will also result in the removal of any entrained fructose.

Modelling of the Process

(16) A preliminary attempt at modelling the rate-zonal bioreaction-separation process was attempted. A set of non-linear equations that describe the combined bioreaction and sedimentation of the reaction components were derived and subsequently solved using the finite difference analysis method. The equations were converted into a dimensionless form and a FORTRAN computer program was written to simulate the process. At present, the initial simulation results obtained from the program are being compared with actual experimental data obtained from the bioreaction-separation runs reported in chapter 9. It is also intended to compare the model simulations with the experimental data of more 'ideal' enzyme systems that have been reported in the literature. This work is ongoing as part of an SERC sponsored project.

11.2 RECOMMENDATIONS FOR FUTURE WORK

The following recommendations are made for future work:

(1) The investigation of the process should be continued using the JCF-Z zonal rotor system. The unique design of this equipment will allow further process optimisation to be made.

(2) Determination of the optimum conditions for minimising viscosity build-up in the bioreactor and hence improving native dextran yields should be made. The repeat injection method should be studied further as it has proved a promising method of minimising viscosity build-up in the bioreactor while significantly improving the yields of dextran rich material at the rotor wall. Although this method suffered from the fact that there will be a build up of acceptor molecules in the bowl which will inhibit dextran chain growth, this may be compensated for by the integration of the bioreaction-separation process into a single unit operation. This process may achieve full potential by continuously passing a very dilute enzyme solution over a sucrose gradient in a continuous flow zonal rotor with periodic recoveries of the fructose-rich supernatant solutions and dextran rich gel fractions.

(3) The use of low enzyme activities and less steep sucrose gradients is recommended to maximise dextran recoveries at the rotor wall. Low enzyme activities will minimise density inversion effects and improve dextran-fructose separation.

(4) Methods for the displacement of the pelleted dextran rich material at the rotor wall must be studied. It is envisaged that 'jetting' warm water into the bowl will readily disperse the gelatinous dextran pellets as B-512F dextran gels are readily soluble in water.

(5) In future runs, the rotor should be loaded dynamically in order to eliminate the possibility of droplet sedimentation.

(6) The MW distribution of dextran fractions recovered from the JCF-Z zonal rotor must be assessed to determine if the combined bioreaction-separation process improves the dextran yields in the JCF-Z rotor. MW distribution studies will be complicated by the presence of sucrose concentration gradients.

(7) The study of alternative enzymic processes using the proposed bioreaction-separation process should be considered. For example, the polysaccharides pullulan and

xanthan are produced by batch and continuous fermentation methods similar to those employed for dextran synthesis, sucrose being the optimum carbohydrate source. The proportion of usable product is decreased at higher sucrose concentrations indicating increased acceptor activity. Both polysaccharides enjoy wide ranging uses and show considerable potential in medical and pharmaceutical fields and in the food industry. 1-2% xanthan solutions can be pumped into oil wells as a means of enhancing oil recoveries.

This technique may also improve the yields of hyaluronic acid and levan. At present, pharmaceutical grade hyaluronic acid is produced by fermentation. A key requirement of the process is to separate the cells from the product without rupturing them, as this may result in the release of inflammatory agents. This problem could be overcome by using cell-free enzyme preparations, as is the case in the proposed dextran production process. The particular viscous properties of hyaluronic acid have been commercially exploited in the field of medicine. Levan appears to have few commercial uses at present.

(8) There is still a need to investigate the various factors that may affect dextran MW distribution in the centrifugal bioreactor. The effect of enzyme pulse size and activity, rotor speed, run time and sucrose gradient shape on dextran MW distribution must all be determined.

(9) Modelling of the process should be continued and improved. Selection of the appropriate input values for the computer program is a priority. The effects of particle polydispersity, gradient shape, viscosity effects and the non-linearity of the centrifugal field term should be considered. Alternative enzyme systems should be considered.

(10) A techno-economic comparison of the proposed process with the existing industrial dextran production process should also be performed.

(11) It would be interesting to determine if the use of ethanol would enhance the bioreaction-separation process by increasing the rate of native dextran sedimentation. Preliminary study of the process would involve a number of 'bench' studies. However, a flame proof centrifuge would be required for this work.

REFERENCES

1 Thoren L, Dextran as a Plasma Substitute, Blood Substitutes and Plasma Expanders. Progress in Clinical and Biological Research, 19, Ed. Liss AR, 265-282, (1978).

2 Nilsson K, Soderlund G, Clinical Dextrans. Specifications and Quality of Preparations on the Market. Acta Pharmaceuticals Suec, 15, 434-454, (1978).

3 Alsop RM, Industrial Production of Dextrans, Progress in Industrial Microbiology, Ed Bushell ME, Elsevier Press, 18, 1-45, (1983).

4 Zafar I, Barker PE, An Experimental and Computational Study of a Biochemical Polymerisation Reaction in a Chromatographic Reactor Separator. Chem. Eng. Sci., 43(9), 2369-2375, (1988).

5 Barker PE, Zafar I, Alsop RM, Production of Dextran and Fructose in a Chromatographic Reactor-Separator in *Separations for Biotechnology*, Ed.Verral MS and Hudson MJ, Publ. Ellis Horwood, Series in Biochemistry and Biotechnology, Ch. 9, 127, (1987).

6 Barker PE, Zafar I, Alsop RM, A Novel Method for the Production of Dextran and Fructose. Int. Conf. on Bioreactors and Biotransformations, Gleneagles, Scotland. Publ. Elsevier Scientific Press, (1987).

7 Barker PE, Ganetsos G, The Biosynthesis of Macromolecules usingChromatographic Biochemical Reactor-Separators in *Bioreactors, Downstream Processing, Vol. 2*, ACHEMA 88, Frankfurt, June 5-11 1988, DECHEMA Biotechnology Conferences, , 91-95, (1988).

8 Barker PE, Ganetsos G, Ajongwen NJ, Akintoye A, Continuous Chromatographic Bioreaction -Separation in *Separations for Biotechnology Vol. 2*, Ed Pyle DL, Elsevier Applied Science Publishers, 549-557, (1990).

9 Barker PE, Ganetsos G, Biochemical Reaction and Separation in Chromatographic Columns, in *Adsorption Science and Technology,* NATO ASI Series E, 158, 491, (1988).

10 Scheibler C, Ver. Rubenzucker. Ind., 24, 309, (1874).

11 Jeanes A, in *Encyclopaedia of Polymer Science and Technology,* Ed.Conrad J, Publ. John Wiley and Sons Inc., New York, Vol 4, 805-829, (1968).

12 Tsuchiya HM, Koepsell HJ, Corman J, Bryant G, Bogard MO, Feger VH, Jackson RW, The Effects of Certain Cultural Factors on the Production of Dextransucrase by *Leuconostoc mesenteroides*, J. Bact., 64, 521-526, (1952).

13 Barker PE, Ajongwen NJ, The Production of the Enzyme Dextransucrase using Nonaerated Fermentation Techniques, Biotech. Bioeng., 37, 703-707, (1991).

14 Hehre EJ, Studies on the Enzymatic Synthesis of Dextran from Sucrose, J. Biol. Chem., 163, 221, (1946).

15 Zafar I, Biosynthesis and Separation of Dextran-Fructose Mixtures in a Chromatographic Reactor, PhD Thesis, Aston University, (1986).

16 Akintoye A, Continuous Chromatographic Biochemical Reaction-Separation, PhD Thesis, Aston University, (1990).

17 Ganetsos G, The Chromatographic Separation of Carbohydrate Mixtures, PhD Thesis, Aston University, (1986).

18 Barker PE, Alsop RM, Vlachogiannis GJ, Fractionation, Purification and Concentration of Dextran Solutions by Ultrafiltration, J. Membr. Sci., 21, 79-91, (1984).

19 Barker PE, Poland K, Till A, The Development of a Diafiltration Cascade System for the Fractionation of a Dextran Hydrolysate, Chem. Eng Res. Des., 67(3), 261-266, (1989).

20 Alsop RM, Barker PE, Vlachogiannis GJ, Efficient Production of Clinical Dextran from Dextran Hydrolysate, The Chemical Engineer, 399, 24-27, (1984).

21 Poland KR, The Fractionation of Dextran Polymer by Ultrafiltration to Yield Clinical Products. PhD Thesis, Aston University, (1986).

22 Till A, The Production of Clinical Dextran using Membrane Processes. PhD Thesis, Aston University, (1988).

23 Vlachogiannis GJ, Dextran Polymer Fractionation by Production Scale Chromatography and Ultrafiltration. PhD Thesis, Aston University, (1982).

24 Barker PE, Ganetsos G, Ajongwen NJ, A Novel Approach to Clinical Dextran Production. *In press.*

25 Vanninen E, Doty T, The Properties, Manufacture and Use of Fructose as an Industrial Raw Material, in Sugar Science and Technology, Eds. Birch GG, Parker KJ, Applied Science Publishers Ltd., London, 311-324, (1979).

26 Green LF, The Balance of Natural and Synthetic Sweetners in Food in *Sweetness and Sweetners,* Eds. Birch GG, Green LF, Coulson CB, Applied Science Publishers Ltd., London, 7-20, (1971).

27 Barker SA, Proc. High fructose syrups - New sweetners in the food industry, Biochem., 10, 39-45, (1975).

28 Cohen R, Giraud B, Messiah A, Theory and Practice of the Analytical Centrifugation of an Active Substrate-Enzyme Complex, Biopolymers, 5, 203-225, (1967).

29 Parts AG, Elbing E, The Polymerisation of Acrylonitrile in Centrifugal Fields. Paper Presented at American Chemical Society Meeting, Philadelphia, Polym. Prepr., 16, 211-216, (1975).

30 Carenza M, Tavan M, Palma G, Radiation Induced Bulk Polymerisation of Vinyl Chloride under Centrifugation, J. Polym. Sci., 17, 2087-2091, (1979).

31 Gilbert GA, Sedimentation and Electrophoresis of Interacting Substances I. Ideal Boundary Shape for a Single Substance Aggregating Reversibly, Proc. Roy. Soc. (London), A250, 377-388, (1959).

32 Gilbert GA, Reversible Aggregation, in *Ultracentrifugal Analysis in Theory and Experiment*, Ed. Williams JW, Academic Press, New York, 73, (1963).

33 Gilbert GA, Jenkins RCLl, Boundary Problems in the Sedimentation and Electrophoresis of Comple Systems in Rapid Reverse Equilibrium, Nature, 177, 853-854, (1956).

34 Gilbert GA, Jenkins RCLl, Sedimentation and Electrophoresis of Interacting Substances II. Asymptotic Shape for two Substances Interacting Reversibly, Proc. Roy. Soc., A253, 420-437, (1959).

35 Svensson, The Behaviour of Weak Electrolytes in Moving Boundary Systems (1), Acta Chem. Scand., 2, 841-855, (1948).

36 Nichols JC, Dismukes EB, Alberty RA, Weak Electrolytes in Moving Boundary Systems Analogous to the Electrophoresis of Two Proteins, J. Am. Chem. Soc., 80, 2610-2615, (1958).

37 Kegeles G, Rao MSN, Ultracentrifugation of Chemically Reacting Systems, J. Am. Chem. Soc., 80, 5721, (1958).

38 Kegeles G, Rhodes L, Bethune JL, Sedimentation Behaviour of Chemically Reacting Systems, Proc. Natl. Acad. Sci., 58, 45, (1967).

39 Rao MSN, Kegeles G, An Ultracentrifuge Study of the Polymerisation of α-chymotrypsin, J. Am. Chem. Soc., 80, 5724, (1958).

40 Adams ET, Fujita H, Sedimentation Equilibrium in Reacting Systems, in *Ultracentrifugal Analysis in Theory and Experiment*, Ed. Williams JW, Academic Press, New York, 119, (1963).

41 Lamm O, Zur Theorie und Methodik der Ultrazentrifugierung, Z. Physik. Chem. (Liepzig), A143, 177, (1929).

42 Cann JR, Interacting Macromolecules. The Theory and Practice of their Electrophoresis, Ultracentrifugation and Chromatography, Publ. Academic Press Inc., London, (1970).

43 Gilbert W, Muller-Hill B, Isolation of the Lac Repressor, Proc. Natl. Acad. Sci. U.S., 56, 1891-1898, (1966).

44 Gilbert W, Muller-Hill B, The Lac Operator is DNA, Proc. Natl. Acad. Sci. U.S., 58, 2415-2421, (1967).

45 Lindberg B, Lunderstrom H, 6-Deoxy-6-p-tolylsulphonyl-D-glucopyranosides, Acta Chem. Scand., 20, 2423-2426, (1966).

46 Senti FR, Hellman NN, Ludwig NH, Babcock GE, Tobin R, Glass CA, Lamberts BL, Viscosity, Sedimentation and Light Scattering Properties of Fractions of an Acid-Hydrolysed Dextran, J. Polym. Sci., 17, 527-546, (1955).

47 Bovey FA, Enzyme Polymerisation I, Molecular Weight and Branching During the Formation of Dextran, J. Polym. Sci., 35, 167-183, (1959).

48 Robyt JF, Dextran in *Encyclopaedia of Polymer Science and Engineering Vol. 4*, Ed. Kroschwitz JI, Publ. John Wiley and Sons Inc., New York, 752-767, (1986).

49 Rees DA, Structure, Conformation and Mechanism in the Formation of Polysaccharide Gels and Networks, Advan. Carbohyd. Chem. Biochem., 24, 267-332, (1969).

50 Miller RL, in *Encyclopaedia of Polymer Science and Technology, Vol. 4*, Ed. Conrad J, Publ. John Wiley and Sons Inc., New York, 449-528, (1966).

51 Newbrun E, Lacy R, Christie TM, The morphology and size of the extracellular polysaccharides from oral Streptococci, Arch. Oral. Biol., 16, 863872, (1971).

52 Ingelman B, Siegbagn K, Dextran and Levan Molecules Studied with the Electron Microscope, Nature, 154, 237-238, (1944).

53 Sidebotham RL, Dextrans, Adv. Carbohydr. Chem. Biochem., 30, 371-444, (1974).

54 Jeanes A, Schieltz NC, Wilham CA, Molecular Associations in Dextran and in Branched Amylaceous Carbohydrates, J. Biol Chem., 176, 617-627, (1948).

55 Taylor NW, Zobel HF, Hellman NN, Senti FR, Effect of Structure and Crystallinity on Water Sorption of Dextrans, J. Phys Chem., 63, 599-603, (1959).

56 Taylor NW, Cluskey JE, Senti FR, Water Sorption by dextrans and Wheatstarch at High Humidities, J. Phys. Chem., 65, 1810-1816, (1959).

57 Rees DA, Scott WE, Polysaccharide Conformation. Part 6, J. Chem. Soc. (B), 469-479, (1971).

58 Tsuchiya HM, Hellman NN, Koepsell HJ, Corman J, Stringer CS, Rogovin SP, Bogard MO, Bryant G, Feger VH, Hoffman CA, Senti FR, Jackson RW, Factors affecting Molecular Weight of Enzymatically Synthesised Dextran, , J. Am. Chem. Soc., 77, 2412-2419, (1955).

59 Arond LH Franks HP, Molecular Weight, Molecular Weight Distribution and Molecular Size of a Native Dextran, Journal J. Phys. Chem, 58, 953-957, (1954).

60 Ebert KH, Schenk G, Mechanisms of Biopolymer Growth: The Formation of Dextran and Levan, Advan. Enzymol., 30, 179-219, (1968)

61 Launer HF, Tomimatsu Y, Reaction of Sodium Chlorite with various polysaccharides, Anal. Chem., 31, 1569-1574, (1959).

62 Atkinson B, Mavituna F, Biochemical Engineering and Biotechnology Handbook, MacMillan Publishers Ltd., Surrey, (1983).

63 Koepsell HJ, Tsuchiya HM, Hellman NN, A Kinetic Study of Dextransucrase, J. Am. Chem. Soc., 80, 6620, (1958).

64 Robyt JF, Walseth TF, The Mechanism of Acceptor Reaction of *Leuconostoc mesenteroides* B-512F Dextransucrase, Carbohyd. Res., 61, 433-445, (1978).

65 Koepsell HJ, Tsuchiya HM, Hellman NN, Kazenko A, Hoffman CA, Sharpe ES, Jackson RW, Enzymic Synthesis of Dextran: Acceptor Specificity and Chain Initiation, J. Biol. Chem., 200, 793, (1952).

66 Robyt JF, Eklund SH, Stereochemistry involved in the Mechanism of Action of Dextransucrase in the Synthesis of Dextran and the Formation of Acceptor Products, Bioorganic Chem., 11, 115-132, (1982).

67 Cote GL, Robyt JF, The formation of α-D-(1-3) branch linkages by an exocellular glucansucrase from *Leuconostoc mesenteroides* NRRL B-742, Carbohyd. Res., 119, 141-156, (1983).

68 Robyt JF, Taniguchi H, The Mechanism of Dextransucrase Action: Biosynthesis of Branch Linkages by Acceptor Reactions with Dextran, Arch. Biochem. Biophys., 174, 129-135, (1976).

69 Cote GL, Robyt JF, The formation of α-D-(1-3) branch linkages by a D-glucansucrase from *Streptococcus mutans* 6715 producing a soluble D-glucan, Carbohyd. Res., 127, 95-107, (1984).

70 Robyt JF, Walseth TF, Production, Purification and Properties of Dextransucrase from *Leuconostoc mesenteroides*, Carbohyd. Res., 68, 95-111, (1979).

71 Robyt JF, Kimble BK, Walseth TF, The Mechanism of Dextransucrase Action : Direction of Dextran Biosynthesis, Arch. Biochem. Biophys, 165, 634-640, (1974).

72 Miller AW, Robyt JF, Activation and Inhibition of Dextransucrase by Calcium, Biochim. Biophys. Acta., 880, 32-39, (1986).

73 Robyt JF, Martin PJ, Machanism of synthesis of D-glucans by D-glucosyltransferases from *Streptococcus mutans* 6715, Carbohyd. Res., 113, 301-315, (1983).

74 Hostettler F, Bovel E, Deuel H, Uber Die Reduktion Der 3,5 - Denitrosalicylsaure Durch Zucker, Helvetica Chimica Acta., 34, 2132-2139, (1951).

75 Ajongwen-Numfor NJ, The Production of the Enzyme Dextransucrase by Batch and Continuous Fermentation Techniques, PhD Thesis, Aston University, (1988).

76 Kaboli H, Reilly PJ, Immobilisation and Properties of *Leuconostoc mesenteroides* Dextransucrase, Biotech. Bioeng., 22, 1055-1069, (1980).

77 Kobayashi M, Matsuda K, Characterisation of the Multiple Forms and Mass Components of Dextransucrase from *Leuconostoc mesenteroides* NRRL B-512F, Biochim Biophys. Acta., 614, 46-62, (1980).

78 Ajongwen JN, Akintoye A, Barker PE, Ganetsos G, Shieh MT, Large Scale Purification of *Leuconostoc mesenteroides* NRRL B-512F Dextransucrase for use in the Biosynthesis of Dextran by Batch and Continuous Chromatography. *In Press.*

79 Ebert KH, Schenk G, Reindarstellung und Charakterisierung von Dextransaccharase aus Leuconostoc mesenteroides B-512F, Zeitschrift fur Naturforsch., 17(b), 732-738, (1962).

80 Steward GSAB, Jackson CC, Personal Communication to Barker PE.

81 Kobayashi M, Matsuda K, The Dextransucrase Isoenzymes of *Leuconostoc mesenteroides NRRL* B-512F, Biochim Biophys. Acta., 370, 441-449, (1974).

82 Hehre EJ, Studies on the Enzymatic Synthesis of Dextran from Sucrose, J. Biol. Chem., 163, 221, (1946).

83 Lawford GR, Klingerman A, William T, Dextran Biosynthesis and Dextransucrase Production by Continuous Culture of *Leuconostoc mesenteroides*, Biotech. Bioeng., 21, 1121-1131, (1979).

84 Kobayashi M, Mihara K, Matsuda K, Dextransucrase from *Leuconostoc mesenteroides* NRRL B-512F: characterisation of the enzyme bound to sephadex gel, Agric. Biol Chem., 50(3), 551-556, (1986).

85 Lopez A, Monsan P, Dextran Synthesis by Immobilised Dextransucrase, Biochimie, 62, 323-329, (1980).

86 Kroner KH, Hustedt H, Kula MR, Evaluation of Crude Dextran as a Phase Forming Polymer for the Extraction of Enzymes in Aqueous Two Phase Systems in Large Scale, Biotech. Bioeng., 24, 1015-1045, (1982).

87 Kula M-R, Extraction and Purification of Enzymes Using Aqueous Two Phase Systems, Applied Biochem. and Bioeng., 2, 71-94, (1979).

88 Miller AW, Eklund SH, Robyt JF, Milligram to gram scale purification and characterisation of dextransucrase from *Leuconostoc mesenteroides* NRRL B-512F, Carbohyd. Res., 147, 119-133, (1986).

89 Michaelis L, Menten ML, Biochem. Z., 49, 333, (1913).

90 Cornish-Bowden H, *Fundamentals of Enzyme Kinetics*, Publ. Butterworth and Co., London, (1979).

91 Monsan P, Lopez A, On the Production of Dextran by Free and Immobilised Dextransucrase, Biotech Bioeng., 23, 2027-2037, (1981).

92 Martinez-Espindolar JP, Lopez Mungwa CA, On the Kinetics of Dextransucrase and Dextran Synthesis in Batch Reactors, Biotech. Letters, 7, 483-486, (1985)

93 Hsu-Wen H, *Separations by Centrifugal Phenomena* in Techniques of Chemistry, Vol.16, Ed. Perry ES, Publ. John Wiley and Sons Inc.,New York, (1981).

94 Svedberg T, Pedersen KO, *The Ultracentrifuge*, Publ. Oxford University Press, (1940).

95 McCall JS, Potter BJ, *Ultracentrifugation,* Publ. Bailliere Tindall, London (1973).

96 Stokes GG, On the Effect of the Internal Friction of Fluids on the Motion Pendulum, Trans. Cam. Phil. Soc., 9, 8, (1851).

97 Anderson NG, The Development of Zonal Centrifuges, in *Natl. Cancer Inst. Monogr. 21*, 9-39, (1966).

98 Griffith OM, in *Techniques of Preparative, Zonal and Continuous Flow Ultracentrifugation,* 5th Edition, Publication Number DS-468G, Beckman Instruments Ltd., Spinco Division, Palo Alto, California, USA, (1986).

99 Graham JM, in New Techniques in Biophysics and Cell Biology,Ed. Pain RH, Smith BJ, John Wiley and Sons Inc., London, (1975).

100 Continuous Flow Centrifugation, Beckman Applications Data Number DS-595B, Beckman Instruments Ltd., Spinco Division, Palo Alto, California, USA, (1990).

101 Chervenka CH, *A Manual of Methods for the Analytical Ultracentrifuge*. Library of Congress Number 72-81833, Beckman Instruments Ltd., Spinco Division, Palo Alto, California, USA, (1973).

102 Schachman HK, *The Ultracentrifuge in Biochemistry*, The Academic Press, New York, (1959).

103 Rowe AJ, Techniques for Determining Molecular Weight, Part 1. BS106 - Suppliment in *Techniques in Protein and Biochemistry,* Techniques in the Life Sciences, Elsevier Scientific Publishers Ireland Ltd., (1984).

104 Eigner J, Schildkraut C, Doty P, Concentration Effects in the Hydrodynamic Properties of Deoxyribonucleic Acid, Biochim. Biophys. Acta., 55, 13-21, (1962).

105 Fujita H, Effects of Concentration Dependence of the Sedimentation Coefficient in Velocity Ultracentrifugation, J. Chem. Phys., 24, 1084, (1956).

106 Williams JW, Baldwin RL, Saunders WM, Squire PG, Boundary Spreading in Sedimentation-Velocity Experiments. I. The Enzymic Degredation of Serum Globulins, J. Am. Chem. Soc., 74, 1542-1547, (1952).

107 Baldwin RL, Boundary Spreading in Sedimentation-Velocity Experiments (4). Measurement of the Standard Deviation of a Sedimentation Coefficient Distribution: Application to Bovine Albumin and ß-Lactoglobulin, Biochem. J., 65, 490, (1957).

108 Baldwin RL, Van Holde KE, Sedimentation of High Polymers, Adv. Polym. Sci., 1, 451-511, (1960).

109 Baldwin RL, Williams JW, Boundary Spreading in Sedimentation Velocity Experiments (1), J. Am. Chem. Soc., 72, 4325, (1950).

110 Williams JW, Sedimentation Analysis and some Related Problems, J. Polym. Sci., 12, 351-378, (1954).

111 Wales M, Rehfeld SJ, Molecular Weight Distribution by Velocity Ultracentrifugation, J. Polym. Sci., 62, 179-196, (1962).

112 Gosting LJ, Solution of Boundary Spreading Equations for Electrophoresis and the Velocity Ultracentrifuge, J. Am. Chem. Soc.,74, 1548-1552, (1952).

113 Baldwin RL, Boundary Spreading in sedimentation Velocity Experiments (3), Effects of Diffusion on the Measurement of Heterogeneity when Concentration Dependence is Absent, J. Phys. Chem., 58, 1081-1086, (1954).

114 Peacocke AR, Schachman HK, Studies on the Sedimenting Behaviour of Thymus Deoxypentose Nucleic Acid with Reference to it's Homogeneity, size and shape, Biochim. et Biophys. Acta, 15, 198-210, (1954).

115 Williams JW, Saunders WM, Size Distribution Analysis in Plasma Extender Systems. II. Dextran, J. Phys Chem., 58, 854-859, (1954).

116 Jullander I, Concentration Dependence of Sedimentation Constant for Nitrocellulose J. Polym. Sci., 3, 631-634, (1948).

117 Johnston JP, Ogston AG, A Boundary Anomality found in the Ultracentrifugal Sedimentation of Mixtures, Trans. Faraday Soc. 42, 789-799, (1946).

118 Baldwin RL, Boundary Spreading in Sedimentation Velocity Experiments (2). The Correction of Sedimentation Coefficient Distributions for the Dependence of Sedimentation Coefficient on Concentration, J. Am. Chem. Soc., 76, 402-407, (1954).

119 Ogston AG, Woods EF, The Sedimentation of Some Fractions of Degraded Dextran, Trans. Faraday Soc., 50, 635-643, (1954).

120 Steensgaard J, Moller NPH, Funding L, Rate Zonal Centrifugation: Quantitative Aspects in *Centrifugal Separations in Molecular and Cell Biology*, Eds. Birnie GD, Rickwood D, Butterworth and Co.,London, (1978).

121 Schumaker VN, Zone Centrifugation, Advan. Biol. Med. Phys., 11, 245-339, (1967).

122 Ridge D, Practical Aspects of Rate-Zonal Centrifugation in *Centrifugal Separations in Molecular and Cell Biology*, , Eds. Birnie GD, Rickwood D, Butterworth and Co.,London, (1978).

123 Noll H, Characterisation of Macromolecules by Constant Velocity Centrifugation, Nature, 215, 360-363, (1967).

124 McCarty KS, Vollmar RT, McCarty KS, Improved Computer Program Data for the Resolution and Fractionation of Macromolecules by Isokinetic Sucrose Density gradient sedimentation, Anal. Biochem., 61,165-183, (1974).

125 Fortuin JMH, Theory and Application of Two Supplimentary Methods for Constructing Density Gradient Columns, J. Polym. Sci., 44, 505-515, (1960).

126 Brakke MK, Estimation of Sedimentation Constants of Viruses by Density gradient Centrifugation, Virology, 6, 96-114, (1958).

127 Svensson H, Hagdahl L, Lerner K-D, Zone Electrophoresis in a Density Gradient. Stability Conditions and Separation of Serum Proteins, Science Tools, 4, 1-10, (1957).

128 Brakke MK, Nonideal Sedimentation and the Capacity of Sucrose Gradient Columns for Virus in Density Gradient Centrifugation, Arch. Biochem. Biophys., 107, 388-403, (1964).

129 Berman AS, Theory of Centrifugation : Miscellaneous Studies in *Natl. Cancer Inst. Monogr.*,*21*, 41-76, (1966).

130 Spragg SP, Rankin CT, The Capacity of Zones in Density Gradient Centrifugation, Biochim. Biophys. Acta., 141, 164-173, (1967).

131 Anderson NG, Studies on Isolated Cell Components 8. High Resolution Gradient Differential Centrifugation, Exptl. Cell. Res., 9, 446-459, (1955).

132 Wilbur KM, Anderson NG, Studies on Isolated Cell Components 1. Nuclear Isolation by Differential Centrifugation, Exptl. Cell. Res., 2, 47-57, (1951).

133 Hogeboom GH, in *Methods in Enzymology,* Eds. Colowick SP, Kaplan NO, Vol. I, Academic Press, New York, (1955).

134 Brakke MK, Zone Electrophoresis of Dyes, Proteins and Viruses in Density Gradient Columns of Sucrose Solutions, Arch. Biochem. Biophys., 55, 175-190, (1955).

135 Bishop BS, Digital Computation of Sedimentation Coefficients in Zonal Centrifuges, in *Natl. Cancer Inst. Monogr.* 21, 175-190, (1966).

136 Martin RG, Ames BN, A Method for Determining the Sedimentation Behaviour of Enzymes: Applications to Protein Mixtures, J. Biol. Chem., 236, 1372-1379, (1961).

137 Hinton RH, Computational Approaches in the Analysis of Zonal Separations, in *Separations with Zonal Rotors,* Section Z-5, Ed. E Reid, Univ. Surrey Press, Guildford, UK, (1971).

138 Carlwood PA, Applications of Radioactively Labelled Marker Proteins in Density Gradient Ultracentrifugation, Anal. Biochem., 5, 226-245, (1963).

139 Rosenbloom J, Cox E, Sedimentation Coefficient of T-even Bacteriophage DNA, Biopolymers, 4, 747-757, (1966).

140 Pickels EG, Sedimentation in the angle centrifuge, J. Gen. Phys., 26, 341-365, (1943).

141 de Duve C, Berthet J, Beaufay H, Gradient Centrifugation of Cell Particles: Theory and Applications, Progr. Biophys. Chem., 9, 326-369, (1959).

142 Brakke MK, Wall Effects during Density Gradient Centrifugation of Southern Bean Mosaic Virus, Arch. Biochem. Biophys., 93, 214-219, (1961).

143 Trautman R, Breese SS, Moving Boundary Theory Applied to Preparative Ultracentrifugation, J. Phys. Chem., 63, 1592-1603, (1959).

144 Brakke MK, Density Gradient Centrifugation and it's Applications to Plant Viruses, Advan. Virus Res., 7, 193-224, (1964).

145 Vinograd J, in *Methods in Enzymology* Vol 6, Ed. Colowick SP, Kaplan NO, Publ. Academic Press, New York, 854-870, (1963).

146 Flamm WG, Birnstiel ML, Walker PMB, in *Subcellular Components: Preparation and Fractionation,* 2nd Ed, Ed. Birnie GD, Publ. Butterworths, and Co., London, 279-310, (1972).

147 de Duve C, Tissue Fractionation Past and Present, J. Cell Biol., 50, 20D-55D, (1971).

148 Sykes J, in *Methods in Microbiology,* Vol 5B, Ed. Norris JR, Ribbons DW, Publ. Academic Press, New York, 55-207, (1971).

149 Fuhlbrigge, Haltner, Saunders, Van Holde, Williams, Williams, *Interim Report*, University of Wisconsin, Nov. 30, (1951).

150 Richards EG, The Hydrodynamic Properties of Large Molecules in Solution, in *An Introduction to Physical Properties of Large Molecules in Solution,* Cambridge University Press, 154-197, (1980).

151 LaBar FE, Baldwin RL, The Sedimentation Coefficient of Sucrose, J. Am. Chem. Soc., 85, 3105-3108, (1963).

152 Bhambra KS, The Fractionation of Dextran using Ethanol, PhD Thesis, Aston University, (1985).

153 Yau WW, Kirkland JJ, Bly DD, Modern Size Exclusion Liquid Chromatography, Publ. John Wiley and Sons, Inc., New York, (1979).

154 Hatt BW, Polymer Molecular Weight Distribution by Gel Permeation Chromatography, in *Developments in Chromatography - 1*, Ed. Knapman CEH, Applied Science Publishers, Essex, 157-199, (1979).

155 Grabistic Z, Rempp R, Benoit H, A Universal Calibration for Gel Permeation Chromatography, J. Polym. Sci., Part B, 5, 753-759, (1967).

156 Frank FC, Ward IM, Williams T, Calibration Procedure for Gel Permeation Chromatography, J. Polym. Sci., 6, A2, 1357-1369, (1968).

157 McCracken FL, Calibration of GPC columns using Polydisperse Polymer Standards, J. App. Polym. Sci., 21, 191-198, (1977).

158 Hester RD, Mitchell PH, A New Universal Calibration Method, J. Polym. Sci., Polym. Chem. Ed., 18, 1727-1738, (1980).

159 Balke ST, Hamielec AE, Gel Permeation Chromatography Calibration Curve from Polydisperse Standards, Ind. Eng. Prod. Res. Dev., 8, 54-57, (1969).

160 Cervenka A, Bates TW, Characterisation of Polydispersed Branched Polymer by means of Gel Permeation Chromatography , J. Chromatog., 53, 85-93, (1970).

161 Chaplin RP, Chang W, Accurate Calibration of GPC by use of Broad Molecular Weight Distribution Standards, J. Macromol. Sci. Chem., A14, 257-263, (1980).

162 Nilsson G, Nilsson K, Molecular Weight Distribution Determination of Clinical Dextran by GPC, J. Chromatog., 101, 137-153, (1974).

163 Hartley HO, The Modified Gauss-Newton Method for Fitting Non Linear Regression Functions by Least Squares, Technometrics, 3, 269-280, (1961).

164 Alsop RM, Vlachogiannis GJ, Determination of the Molecular Weight of Clinical Dextran by Gel Permeation Chromatography on TSK-PW Type Columns, J. Chromatog., 246, 227-240, (1982).

165 MSE Technical Publication No. 71, The MSE Analytical Ultracentrifuge Mk.2, Measuring and Scientific Equipment Ltd., Crawley, Sussex, UK.

166 The Handbook of Chemistry and Physics, 53rd Ed., Ed. Weast RC, Publ. CRC Press, A Division of the Chemical Rubber Company, Ohio, USA (1972).

167 MSE Technical Publication No. 24, The MSE The MSE Superspeed 50 Ultracentrifuge, Measuring and Scientific Equipment Ltd., Crawley, Sussex, UK.

168 Davies OL, *Design and Analysis of Industrial Experiments*, 2nd. Ed., Publ. Oliver and Boyd, Tweeddale Court, Edinburgh, UK, (1956).

169 Lavanchy AC, Keith FW, Centrifugal Separation, Reprint Number 1013, Alfa-Laval Sharples Ltd., Camberley, Surrey, UK.

170 Perry RH, Chilton C, Section 19, Chemical Engineers Handbook, 5th. Ed., Publ. McGraw-Hill, (1963).

171 Levenspiel O, Nonideal Flow, in *Chemical Reaction Engineering*, 2nd. Ed., Publ. John Wiley and Sons Inc., New York (1972).

172 Lavanchy AC, Keith FW, Centrifugal Separation, in the *Encyclopaedia of Chemical Technology*, Kirk Othmer, Volume 5, 3rd Ed., John Wiley and Sons Inc., (1979).

173 Beckman JCF-Z Zonal and Continuous Flow Rotor Instruction Manual, Publication JCFZ-IM-4, November 1980, Publ. Spinco Division of Beckman Instruments Inc., Palo Alto, California, USA.

174 Vinograd J, Bruner R, Kent R, Weigle J, Band Centrifugation of Macromolecules and Viruses in Self Generating Density Gradients, Proc. Natl. Acad. Sci., 49, 902-910, (1963).

175 Lopez A, Monsan P, Dextran Synthesis by Immobilised Dextran Sucrase, Biochimie, 62, 323-329, (1980).

176 Archibald WJ, An Approximate Solution of the Differential Equation of the Ultracentrifuge, Journal of Applied Physics, 18, 362-367, (1947).

177 Dishon M, Weiss GH, Yphantis DA, Numerical Solution of the Lamm Equation. I. Numerical Procedure, Biopolymers, 4, 449-455, (1966).

178 Dishon M, Weiss GH, Yphantis DA, Numerical Solution of the Lamm Equation. III. Velocity Ultracentrifugation. Biopolymers, 5, 697-713, (1967).

179 Field EO, Ogston AG, Boundary Spreading in the Migration of a solute in Rapid Dissociation Equilibrium. Theory and its Application to the Case of Human Haemoglobin. Biochem. J., 60, 661-665, (1955).

180 Goad WB, in *Interacting Macromolecules. The Theory and Practice of their Electrophoresis, Ultracentrifugation and Chromatography*, Ed. Cann JR, Publ. Academic Press Inc., London, (1970).

181 Bethune JL, Kegeles G, Countercurrent Distribution of Chemically Reacting Systems. I. Polymerisation. J. Phys. Chem., 65, 433-438, (1961).

182 Bethune JL, Kegeles G, Countercurrent Distribution of Chemically Reacting Systems. II. Reactions of the Type A + B = C. J. Phys. Chem., 65, 1755-1760, (1961).

183 Fujita H, in *Mathematical Theory of Sedimentation Analysis*, Publ. Academic Press, New York, (1962).

184 Faxen H, Arkiv. Mat. Astron. Fysik, 21B, No. 3, (1929).

185 Guiochon G, Golshan-Shirazi S, Jaulmes A, Computer Simulation of a Large Concentration Band in Liquid Chromatography, Anal. Chem., 60, 1856-1866, (1988).

186 Czok M, Guiochon G, The Physical Sence of Simulation Models of Liquid Chromatography: Propagation Through a Grid or Solution of the Mass Balance Equation ?, Anal. Chem., 62, 189-200, (1990).

187 Golshan-Shirazi S, Guiochon G, Comparison of the Various Kinetic Models of the Non-Linear Chromatography, J. Chromatog., 603, 1-11, (1992).

188 Bartlett MS, Properties of Sufficiency and Statistical Tests, Proc. Royal Soc. A, 160, 268, (1937).

189 Nair KR, The Distribution of the Extreme Deviates from the Sample Mean and its Studentised Form, Biometrika, 35, 118, (1948).

190 Coulson JM, Richardson JF, in *Chemical Engineering* Vol 2, 4th. Ed., Pergamon International Library, Pergamon Press, Oxford, (1991).

APPENDICES

APPENDIX A1

Computer Program for the Calibration of the Gel Permeation Chromatography Columns

```
C     THIS PROGRAM CARRIES OUT THE CALIBRATION OF GEL-PERMEATION
C     CHROMATOGRAPHIC COLUMNS USING "BROAD" FRACTIONS OF KNOWN
C     WEIGHT AVERAGE MOLECULAR WEIGHTS.
C
      IMPLICIT DOUBLE PRECISION (A-H,O-Y)
      DOUBLE PRECISION M1,M2,KD,Z
      DIMENSION NY(32),M1(32),M2(32),
     CY(32,60),KD(32,60),SUM(32,5),
     CB(5),C(5),RO(5),R1(5),R2(5),
     CXMAT(25),Q(4),ZZ(4)
      READ (1,102) (B(K),K=1,5)
      READ (1,105) NNI
      WRITE (2,200)
      WRITE (2,255)
      WRITE (2,265) (K,B(K),K=1,5)
      WRITE (2,210)
      NP=0
      T=10000.0
      B(4)=B(4)-DLOG(T)
      B(5)=B(5)/T
      DO 30 I=1,11
      READ (1,110) M1(I),P,VO,VT,VE,VDE,DIFF,VM,YM,SD
      NY(I)=P
      READ (1,120) (Y(I,J),J=1,NY(I))
      WRITE(2,557)(Y(I,J),J=1,NY(I))
  557 FORMAT(84F0.0)
      M1(I)=M1(I)/T
      VP=VT-VO
      SY=0.0
      IF (DIFF.NE.0.0) YG=-1/(2*SD**2)
      DO 25 J=1,NY(I)
      IF (DIFF.EQ.0.0) GOTO 20
      IF (VE.EQ.VM) GOTO 20
      YA=YG*(VE-VM)**2
      YE=DLOG(Y(I,J)/YM)
      YE=YM*EXP(YA*YE/(YA-YE))
      IF (YE.LT.Y(I,J)) Y(I,J)=YE
   20 SY=SY+Y(I,J)
      KD(I,J)=(VE-VO)/VP
      VE=VE+VDE
      WRITE(2,765)SY,KD(I,J),VE
  765 FORMAT(3F20.6)
   25 CONTINUE
      DO 28 J=1,NY(I)
      Y(I,J)=Y(I,J)/SY
      WRITE(2,876)Y(I,J)
  876 FORMAT(F10.5)
   28 CONTINUE
      NP=NP+1
   30 CONTINUE
C
C     ITERATION PHASE
C
   32 IF (NNI.EQ.0) GOTO 85
```

```
    DO 34 K=1,3
 34 ZZ(K)=K*1Ø.ØE1Ø
    DO 8Ø NI=1,NNI
    DO 4Ø I=1,NP
    M2(I)=Ø.Ø
    DO 35 K=2,5
 35 SUM(I,K)=Ø.Ø
    SUM(I,1)=1.Ø
    DO 4Ø J=1,NY(I)
    Z=DEXP(B(4)+B(1)*KD(I,J)+B(2)*KD(I,J)**2+B(3)*KD(I,J)**3)
    M2(I)=M2(I)+(B(5)+Z)*Y(I,J)
    SUM(I,2)=SUM(I,2)+Y(I,J)*Z
    SUM(I,3)=SUM(I,3)+Y(I,J)*Z*KD(I,J)
    SUM(I,4)=SUM(I,4)+Y(I,J)*Z*KD(I,J)**2
    SUM(I,5)=SUM(I,5)+Y(I,J)*Z*KD(I,J)**3
 4Ø CONTINUE
    DO 45 K=1,5
    RO(K)=Ø.Ø
    DO 45 I=1,NP
 45 RO(K)=RO(K)+(M1(I)-M2(I))/M1(I)**2*SUM(I,K)
    JK=Ø
    DO 5Ø K=1,5
    DO 5Ø J=1,5
    JK=JK+1
    XMAT(JK)=Ø.Ø
    DO 5Ø I=1,NP
    XMAT(JK)=XMAT(JK)+SUM(I,K)*SUM(I,J)/M1(I)**2
 5Ø CONTINUE
    CALL MATINV (XMAT)
    JK=Ø
    DO 55 K=1,5
    R1(K)=Ø.Ø
    DO 55 J=1,5
    JK=JK+1
    R1(K)=R1(K)+RO(J)*XMAT(JK)
 55 CONTINUE
    R2(5)=R1(1)
    R2(4)=R1(2)
    R2(1)=R1(3)
    R2(2)=R1(4)
    R2(3)=R1(5)
    DO 7Ø N=1,3
    Q(N)=Ø.Ø
    DO 6Ø K=1,5
    IF (N.EQ.1) C(K)=B(K)
    IF (N.EQ.2) C(K)=B(K)+Ø.5*R2(K)
 6Ø IF (N.EQ.3) C(K)=B(K)+R2(K)
    DO 7Ø I=1,NP
    M2(I)=Ø.Ø
    DO 65 J=1,NY(I)
    Z=DEXP(C(4)+C(1)*KD(I,J)+C(2)*KD(I,J)**2+C(3)*KD(I,J)**3)
 65 M2(I)=M2(I)+(C(5)+Z)*Y(I,J)
    Q(N)=Q(N)+((M1(I)-M2(I))/M1(I))**2
 7Ø CONTINUE
```

```
   72 NII1=NI-1
      WRITE (2,25Ø) NII1,B(1),B(2),B(3),B(4),B(5),Q(1)
      Q(4)=Ø.5+Ø.25*(Q(1)-Q(3))/(Q(3)-2.Ø*Q(2)+Q(1))
      DO 75 K=1,5
   75 B(K)=B(K)+Q(4)*R2(K)
      DO 77 KK=2,4
      K=6-KK
   77 ZZ(K)=ZZ(K-1)
      ZZ(1)=SNGL(Q(1))
      IF (ZZ(4).NE.ZZ(3)) GOTO 8Ø
      IF (ZZ(3).NE.ZZ(2)) GOTO 8Ø
      IF (ZZ(2).NE.ZZ(1)) GOTO 8Ø
      NI=NI+1
      GOTO 85
   8Ø CONTINUE
C
C     FINAL RESULTS OUTPUT
C
   85 Q(1)=Ø.Ø
      DO 95 I=1,NP
      M2(I)=Ø.Ø
      DO 9Ø J=1,NY(I)
      Z=EXP(B(4)+B(1)*KD(I,J)+B(2)*KD(I,J)**2+B(3)*KD(I,J)**3)
   9Ø M2(I)=M2(I)+(B(5)+Z)*Y(I,J)
   95 Q(1)=Q(1)+((M1(I)-M2(I))/M1(I))**2
      NII1=NI-1
      WRITE (2,25Ø) NII1,B(1),B(2),B(3),B(4),B(5),Q(1)
      B(4)=B(4)+DLOG(T)
      B(5)=B(5)*T
   98 WRITE (2,26Ø)
      WRITE (2,265) (K,B(K),K=1,5)
      WRITE (2,27Ø)
      WRITE (2,275)
      DO 3 I=1,NP
      M1(I)=M1(I)*T
      M2(I)=M2(I)*T
    3 CONTINUE
      WRITE (2,28Ø) (M1(I),M2(I),I=1,NP)
      STOP
C
C     FORMAT STATEMENTS
C
  1Ø2 FORMAT (5FØ.Ø)
  1Ø5 FORMAT (I3)
  11Ø FORMAT (12FØ.Ø)
  12Ø FORMAT (14ØFØ.Ø)
  2ØØ FORMAT (' GPC CALIBRATION PROGRAM')
  21Ø FORMAT(//11X,'B1',8X,'B2',8X,'B3',8X,'B4',
     C8X,'B5',9X,'RES SS'/)
  25Ø FORMAT(I3,3X,5F1Ø.5,D15.6)
  255 FORMAT (//'     INITIAL VALUES OF CALIBRATION CONSTANTS :-')
  26Ø FORMAT (//'     FINAL VALUES OF CALIBRATION CONSTANTS :-')
  265 FORMAT (12X,'B',I1,'=',F11.3)
  27Ø FORMAT (//' COMPARISON OF MOLECULAR WEIGHTS:-')
```

```
275 FORMAT (11X, 'MW(LS)',4X,'MW(GPC)')
280 FORMAT (7X,F10.0,1X,F10.0)
    END
    SUBROUTINE MATINV (A)
C   MATRIX INVERSION ROUTINE
    DOUBLE PRECISION A,R,AA,AH
    DIMENSION A(25),L(5),M(5)
    R=1.0
    N=5
    NK=-N
    DO 80 K=1,N
    NK=NK+N
    L(K)=K
    M(K)=K
    KK=NK+K
    AA=A(KK)
    DO 20 J=K,N
    IJ=N*(J-1)
    DO 20 I=K,N
    II=IJ+I
    IF (DABS(AA).GE.DABS(A(II))) GOTO 20
    AA=A(II)
    L(K)=I
    M(K)=J
 20 CONTINUE
    J=L(K)
    IF (J.LE.K) GOTO 35
    KI=K-N
    DO 30 I=1,N
    KI=KI+N
    JI=KI-K+J
    AH=-A(KI)
    A(KI)=A(JI)
 30 A(JI)=AH
 35 I=M(K)
    IF (I.LE.K) GOTO 45
    JJ=N*(I-1)
    DO 40 J=1,N
    JN=NK+J
    JI=JJ+J
    AH=-A(JN)
    A(JN)=A(JI)
 40 A(JI)=AH
 45 IF (AA.NE.0.0) GOTO 50
    R=0.0
    GOTO 150
 50 DO 55 I=1,N
    IF (I.EQ.K) GOTO 55
    IK=NK+I
    A(IK)=A(IK)/(-AA)
 55 CONTINUE
    DO 65 I=1,N
    IK=NK+I
    AH=A(IK)
```

```
      IJ=I-N
      DO 65 J=1,N
      IJ=IJ+N
      IF (I.EQ.K)GOTO 65
      IF (J.EQ.K)GOTO 65
      KJ=IJ-I+K
      A(IJ)=AH*A(KJ)+A(IJ)
   65 CONTINUE
      KJ=K-N
      DO 75 J=1,N
      KJ=KJ+N
      IF (J.EQ.K) GOTO 75
      A(KJ)=A(KJ)/AA
   75 CONTINUE
      R=R*AA
      A(KK)=1.Ø/AA
   8Ø CONTINUE
      K=N
  1ØØ K=K-1
      IF (K.LE.Ø.Ø) GOTO 15Ø
      I=L(K)
      IF (I.LE.K) GOTO 12Ø
      KK=N*(K-1)
      II=N*(I-1)
      DO 11Ø J=1,N
      JK=KK+J
      JI=II+J
      AH=A(JK)
      A(JK)=-A(JI)
      A(JI)=AH
  11Ø CONTINUE
  12Ø J=M(K)
      IF (J.LE.K) GOTO 1ØØ
      KN=K-N
      DO 13Ø I=1,N
      KN=KN+N
      JN=KN-K+J
      AH=A(KN)
      A(KN)=-A(JN)
      A(JN)=AH
  13Ø CONTINUE
      GOTO 1ØØ
  15Ø RETURN
      END
      FINISH
****
```

APPENDIX A2

Data Aquisition Program for the Gel Permeation Chromatography Columns

```
10   DIM A(400),Z(5)
6000 I=1:T1=TI:Y=1
6010 GO SUB 7000
6020 E=TI-T1
6030 IF E<120 THEN 6020
6040 IF Y=5 THEN 6090
6050 Y=Y+1:T1=TI
6060 GO TO 6010
6090 T1=TI
6100 A(I)=Z(I)+Z(2)+Z(3)+Z(4)+Z(5))/5
6105 PRINT"READING";I/6;"=";A(I),A(I)/4
6510 IF I<360 THEN 6750
6550 FOR Q=156 TO I
6560 OPEN 1,4,1
6570 OPEN 2,4,2
6580 F$="9999.99     S9999.99        S9999.99"
6590 PRINT#2,F$
6600 PRINT#1,Q/6,A(Q),A(Q)/4
6610 CLOSE1:CLOSE2
6620 NEXT Q
6650 END
6750 Y=1.0:I=I+1
6760 GO TO 6010
7000 OPEN 1,9,1
7010 GET#1,J$,K$
7020 IF K$="" THEN K=-224:GO TO 7040
7030 K=ASC(K$)-224
7040 IF K<0 THEN D=(K+32)*-1
7050 IF K>=0 THEN D=K
7060 D=D*256
7070 IF J$="" THEN J=0:GO TO 7090
7080 J=ASC(J$)
7090 IF K<0 THEN J=J*-1
7100 Z(Y)=J+D
7105 PRINT Z(Y),Z(Y)/4
7110 CLOSE1
7120 RETURN
```

APPENDIX A3

Computer Program for Calculating the Average Molecular Weights and Molecular Weight Distributions from GPC Data

```
5 REM PROGRAM TO CALCULATE THE MOL
10 REM WEIGHT DISTRIBUTION OF A DEXTRAN SAMPLE
12 REM
15 REM     BY A.TILL 1986
17 REM     MODIFIED BY S.J.SETFORD 1990
20 DIM A(400),Z(5),B(170),VIN(170),
   S(170),S5(170),MAX(2),AMIN(170)
40 X=0.0
60 PRINT "RUN A VO-VT....YES OR NO"
80 INPUT ANS$
100 IF ANS$="YES" THEN X=1:GOTO 320
120 PRINT "THEN INPUT TO AND TT"
140 INPUT MAX(1),MAX(2)
150 X=2.0
160 PRINT "INPUT THE FLOW RATE"
180 INPUT RATE
200 PRINT "TYPE IN THE BATCH NO"
220 INPUT KR$
240 PRINT "TYPE IN DATE"
260 INPUT KP$
280 PRINT "READY TO START TYPE....GO"
300 INPUT NUM$
320 I=1:T1=TI:Y=1
340 GOSUB 1570
360 E=TI-T1
380 IF E<120 THEN 360
400 IF Y=5 THEN 460
420 Y=Y+1:T1=TI
440 GOTO 340
460 T1=TI
480 A(I)=(Z(1)+Z(2)+Z(3)+Z(4)+Z(5))/5
500 PRINT "READING AT";I/6;"MINS =";A(I)/4
520 IF I>=210 THEN 580
540 Y=1.0:I=I+1
560 GOTO 340
580 IF X=1.0 THEN GOSUB 1380
600 IF X=0.0 THEN 150
610 GOSUB 3140
620 GOSUB 2140:GOSUB 2520
640 OPEN1,4
660 OPEN2,4,1
680 OPEN3,4,2
700 F$="999  9.999  9999999  9999.99  99.99  99.99"
720 PRINT#3,F$
740 PRINT#1,CHR$(1)"BATCH NUMBER:";KR$
760 PRINT#1:PRINT#1
780 PRINT#1,CHR$(1)"DATE OF ANALYSIS:";KP$
800 PRINT#1:PRINT#1
820 PRINT#1,"FLOWRATE=";RATE;"ML/MIN"
840 PRINT#1,"     VO=";MAX(1)
860 PRINT#1,"     VT=";MAX(2)
880 PRINT#1,"     VS=";BEGIN
900 PRINT#1,"     VF=";FINISH
920 PRINT#1
```

```
940 PRINT#1,"WEIGHT AVERAGE MOL WT="AAAW
960 PRINT#1,"NUMBER AVERAGE MOL WT="AVMN
1000 PRINT#1,"            MW/MN RATIO="SPR
1020 PRINT#1:PRINT#1:PRINT#1
1040 HD$="POINT"+"       "+"KD VALUE"+"       "
1060 GH$="MOL WEIGHT"+"      "
1080 FH$="HEIGHT"+"       "+" WT FRAC "+"     CUMM%"
1100 EH$=HD$+GH$+FH$
1120 PRINT#1,EH$
1140 FOR I=NMAX TO 1 STEP -1
1160 PRINT#2,I,VIN(I),AMIN(I),B(I),S(I),S5(I)
1180 NEXT I
1200 PRINT#1:PRINT#1:PRINT#1
1220 PRINT#1,"ASTON GPC CONSTANTS"
1240 PRINT#1,"         B1=";B1
1260 PRINT#1,"         B2=";B2
1280 PRINT#1,"         B3=";B3
1300 PRINT#1,"         B4=";B4
1320 PRINT#1,"         B5=";B5
1340 CLOSE 1:CLOSE 2:CLOSE 3
1345 GOSUB 3300
1355 GOTO 200
1360 END
1380 REM  TO FIND TO AND TT TIMES
1400 Z=1.0
1420 FOR I=30 TO 210
1440 IF A(I)<200 THEN 1500
1460 IF A(I)>=A(I-1) THEN MAX(2)=I/6:GO TO 1500
1480 Z=2.0
1500 NEXT I
1510 PRINT "   "
1520 PRINT "TO=";MAX(1);"TT=";MAX(2)
1530 PRINT "   "
1535 GOTO 3140
1540 X=0.0
1560 RETURN
1570 REM HEIGHTS FROM REFRACTOMETER
1580 OPEN1,9,15
1600 GET#1,J$,K$
1620 IF K$="" THEN K=-224:GOTO 1660
1640 K=ASC(K$)-224
1660 IF K<0 THEN D=(K+32)*-1
1680 IF K>=0 THEN D=K
1700 D=D*256
1720 IF J$="" THEN J=0:GOTO 1760
1740 J=ASC(J$)
1760 IF K<0 THEN J=J*-1
1780 Z(Y)=J+D
1800 PRINT Z(Y),Z(Y)/4
1820 CLOSE 1
1840 RETURN
2130 REM CALC OF ELUTION VOLUMES
2140 VIE=RATE*BEGIN
2160 VFE=RATE*FINISH
2180 VI=(VIE-(RATE*MAX(1)))/(RATE*(MAX(2)-MAX(1)))
2200 VF=(VFE-(RATE*MAX(1)))/(RATE*(MAX(2)-MAX(1)))
2220 VH=(VF-VI)/(NMAX-1)
```

```
2240 RETURN
2520 REM CALC OF MWD
2540 B1=-8.971:B2=5.122:B3=-3.637:B4=14.481:B5=-911.858
2560 S1=0.0:S2=0.0:S3=0.0
2580 FOR I=1 TO NMAX
2600 VIN(I)=VI+VH*(I-1)
2620 IF VIN(I)>1.0 THEN 2680
2640 IF VIN(I)<0.0 THEN 2720
2660 AMIN(I)=B5+EXP(B4+B1*VIN(I)+B2*(VIN(I)↑2)
     +B3*(VIN(I)↑3)):GOTO 2740
2680 AMIN(I)=B5+EXP(B4+B1+B2+B3)
2700 GOTO 2740
2720 AMIN(I)=B5+EXP(B4)
2740 S1=S1+B(I):S2=S2+(AMIN(I)*B(I))
2760 S3=S3+(B(I)/AMIN(I)):NEXT I
2780 AAAW=S2/S1
2800 AVMN=S1/S3
2820 SPR=AAAW/AVMN
2840 PRINT "WEIGHT AVERAGE MOL WT=";AAAM
2860 PRINT "NUMBER AVERAGE MOL WT=";AVMN
2880 PRINT "              MW/MN RATIO";SPR
2900 S4=0.0
2920 FOR I=1 TO NMAX:S4=S4+B(I):NEXT I
2940 FOR I=1 TO NMAX:S(I)=B(I)*100/S4:NEXT I
2960 S5(NMAX+1)=0.0
2980 FOR I=NMAX TO 1 STEP -1
3000 S5(I)=S5(I+1)+S(I)
3020 NEXT I
3040 RETURN
3140 FOR I=30 TO 210
3160 OPEN 1,4,1
3180 OPEN 2,4,2
3200 F$="9999.99     $9999.99      $9999.99"
3220 PRINT#2,F$
3240 PRINT#1,I/6,A(I),A(I)/4
3260 CLOSE1:CLOSE2
3280 NEXT I
3290 IF X=1.0 GOTO 1540
3300 PRINT " IF DATA IS GOOD, TYPE Y"
3320 PRINT " ELSE TYPE ANY OTHER"
3340 PRINT " LETTER"
3360 INPUT ROP$
3380 IF ROP$="Y" THEN 3640
3400 REM
3420 PRINT "TYPE IN THE START AND FINISH TIMES"
3440 INPUT AB,BC
3445 PRINT "INPUT BASELINE"
3450 INPUT SJS
3460 NMAX=0.0:SAP=0.0
3535 IF A(BC)<0.0 THEN A(BC)=0.0
3540 FOR I=AB TO BC
3550 NMAX=NMAX+1
3560 IF 78>=I THEN B(NMAX)=(A(I)-A(48))/4:GOTO 3600
3580 B(NMAX)=(A(I)-SJS)/4
3600 NEXT I
3620 BEGIN=AB/6:FINISH=BC/6
3630 GOTO 620
3640 RETURN
```

APPENDIX A4

The Statistical Analysis Of The Experimental Data Reported In Section 7.4

This appendix has been written to explain the statistical treatment of the response values reported in table 7.3. The first stage of the analysis procedure is to determine the mean square (or variance) value corresponding to each treatment combination.

Davies [168] has outlined a systematic tabular method for the calculation of the effect and mean square values for experiments following the factorial procedure. The treatment combinations and response values are listed in a 'standard order', as shown in the first two columns in table A 4.1. As an example, the previously calculated values for response (2), the mass of dextran detected in the pelleted fraction, are listed here. The first entry in column (1) is the sum of the first two response values (14.10 +15.24), the second entry equals the sum of the second pair (30.52+49.79) and so on until the top half of column (1) is complete. The values in the lower half of column (1) are calculated by subtracting the first value in each of the same pairs from the second. Column (2) is derived in a similar way, by summing and differencing the successive pairs of values listed in column (1). Columns (3) and (4) are derived from the preceding column in a similar manner.

Treatment combination	Mass of dextran in pellet (mg) (response 2)	(1)	(2)	(3)	(4)	Effect value col (4)/16	Mean square (variance)
A1B1C1D1	14.10	29.34	109.65	179.82	633.63	-	-
A2B1C1D1	15.24	80.31	70.17	453.81	89.67	11.21	502.54
A1B2C1D1	30.52	13.81	251.89	46.62	281.69	35.21	4959.33
A2B2C1D1	49.79	56.36	201.92	43.05	32.65	4.08	66.63
A1B1C2D1	4.91	73.11	20.41	93.52	-89.45	-11.18	500.08
A2B1C2D1	8.90	178.78	26.21	188.17	1.87	0.23	0.22
A1B2C2D1	17.07	59.71	23.49	36.36	-31.59	-3.95	62.37
A2B2C2D1	39.29	142.21	19.56	-3.71	3.37	0.42	0.71
A1B1C1D2	29.81	1.14	50.97	-39.48	273.99	34.25	4691.91
A2B1C1D2	43.30	19.27	42.55	-49.97	-3.57	-0.45	0.80
A1B2C1D2	84.39	3.99	105.67	5.80	94.65	11.83	559.91
A2B2C1D2	94.39	22.22	82.50	-3.93	-40.07	-6.82	100.35
A1B1C2D2	24.91	13.49	18.13	-8.42	-10.49	-1.31	6.88
A2B1C2D2	34.80	10.00	18.23	-23.17	-9.73	-1.22	5.92
A1B2C2D2	66.27	9.89	-3.49	0.10	-14.75	-1.84	13.60
A2B2C2D2	75.94	9.67	-0.22	3.27	3.17	0.40	0.63

Table A 4.1 Calculation of Effect and Mean Square Data for Response (2); the Mass of Dextran Detected in the Pelleted Fraction

The effect value was calculated by dividing each of the values in column (4) by the number of treatment combinations carried out at each factor level, in this case 8. The use of the effect values in the statistical analysis of experimental data is discussed in more detail in appendix A6. In this study, the mean square values were required and were calculated by squaring each of the entries in column (4) and dividing by the number of treatment combinations, in this case 16.

Estimate of Error Variation

In this experiment, no trials were repeated and no prior estimate of error was available. Therefore it was necessary to estimate the error variance (V) from the higher order interactions so that the significance of the mean square value of a particular treatment

combination could be assessed. The practice may be justified because usually, higher order effects of this level are non-existent or at least negligible. On this assumption, the mean square values corresponding to the higher order interactions can be added together and divided by the total of their degrees of freedom to give an estimate of the error variance (V). Calculation of the estimated error variance for the data shown in table A 4.1 is presented in table A 4.2.

Interaction	Mean square (Variance)
ABC	0.71
ABD	100.35
ACD	5.92
BCD	13.60
ABCD	0.63
Total	121.21

Number of degrees of freedom (ϕ_2) = 5
Estimate of error variance (V) = 121.21/5 = 24.24

Table A 4.2 Calculation of Estimate of Error Variance

The danger in such assumptions is that one or more of the mean square values may appear considerably larger than the rest, for example, interaction ABD in table A 4.1. This can lead the observer to the conclusion that the value should be ignored to obtain a more accurate estimate of error variance. Fortunately, it is possible to test the hypothesis that a given set of mean square values are in fact estimates of the same variance by using the method proposed by Bartlett (188).

Bartlett proposed that the criterion measuring the divergence (M) of a group of mean square values, based on one degree of freedom, can be calculated using the expression:

$$M = \phi \text{ Ln } V - \sum \text{Ln } V_i \qquad \text{(A 4.1)}$$

where ϕ equals the total number of degrees of freedom, V is the error variance value and V_i, an individual mean square value.

For the data presented in table A 4.1, the calculations were as follows:

Interaction	Mean square	Ln (Mean square)
ABC	0.71	-0.34
ABC	100.35	4.61
ACD	5.92	1.78
BCD	13.60	2.61
ABCD	0.63	-0.47
	121.21	8.19 = $\sum$ Ln V_i

ϕ = 5
V = 24.24
Ln V = 3.19
ϕ Ln V = 15.94

Thus: $M = \phi \text{ Ln } V - \sum \text{Ln } V_i$ = 7.75

The importance of M is then assessed by applying a significance test. This type of test adopts a procedure to determine whether a quantity which is subject to random variation differs from a postulated figure by an amount greater than that attributable to random variation alone. This is achieved by making an assumption, called 'the null hypothesis',

that only random variation is occuring. If the observed value of the quantity, in this case M, has only a small probability (termed α) of being attained or exceeded if the null hypothesis were true, then it is concluded that the hypothesis is untrue. α is called the level of significance and the conclusion is usually expressed in the form "a statistical test indicates a significant departure from the given null hypothesis at the 100% α level' (for example, at the 10% level).

Thus by knowing M and stipulating a value of α, by reference to the correct table, it is possible to determine whether the divergence of the higher-order mean square values are small enough to be ignored of not. Such a table has been compiled by Nair [189]. For the case when each mean square value has one degree of freedom and the total number of degrees of freedom is 5, the M value, when α is set at 0.05 is 12.00. Because the calculated M value is less than 12.00, then there is a greater than 5% chance that the observed divergence of the mean square values in table A4.2 is due to random variation. In other words, there is no evidence of significant variation between the five mean values at the 5% level. Thus these values can be used to obtain an estimate of the error variance for response (2) in this factorial experiment.

The divergence of the mean square values of the higher order interactions can be similarly assessed for the other responses of interest. The calculated M values are shown in table A 4.3 and show that there is no evidence of significant error variation.

Response (number)	M value
Enzyme efficiency (1)	9.88
Mass of dextran in pellet (2)	7.75
Mass of fructose in solution (3)	8.10
Ratio dextran:fructose in solution (4)	1.97
Proportion of pelleted dextran (5)	2.79
Proportion of pelleted fructose (6)	8.62

Table A 4.3 Response M Values for Assessment of Error Variation

The Variance Ratio Test For Significance (The 'F' test)

Having ascertained that the higher order mean square values can be used to give a reasonable estimate of the error variance, the mean square (variance) values listed in table A 4.1 can be used to test for significance. Again, a significance test is used, an appropriate test being the F test, which compares the estimate of the error variance. If the observed deviation is significantly greater than the error can account for, then the cause of the deviation is significant. For example, an increase in rotor speed may increase the mass of pelleted dextran. The average mass of pelleted dextran at the lower speed is subtracted from the average at the higher speed, squared and divided by the number of treatment combinations, to give the required variance. This value is then compared with the variance due to the error to give an 'F' value:

$$F = \frac{\text{Mean square value}}{\text{Error variance}}$$

The F values for each treatment combination listed in table A 4.1 are given in table A 4.4.

The method used to calculate the values in table A 4.1 ensures that each treatment combination corresponds to a particular effect. For example, combination A2B1C1D2 corresponds to the effect of increasing rotor speed whilst keeping the remaining factors constant. Thus the effect of rotor speed has an F-value. The combination A2B1C1D2

corresponds to the effect of increasing both rotor speed and enzyme activity and the resulting F-value of 0.03 is a measure of the interaction between these two factors.

Treatment combination	mean square (variance)	F-value
A1B1C1D1	-	-
A2B1C1D1	502.54	(+)20.73
A1B2C1D1	4959.33	(+)204.59
A2B2C1D1	66.63	(+)2.75
A1B1C2D1	500.08	(-)20.63
A2B1C2D1	0.22	(+)0.01
A1B2C2D1	62.37	(-)2.57
A2B2C2D1	0.71	(+)0.03
A1B1C1D2	4691.91	(+)193.56
A2B1C1D2	0.80	(-)0.03
A1B2C1D2	559.91	(+)23.10
A2B2C1D2	100.35	(-)4.14
A1B1C2D2	6.88	(-)0.28
A2B1C2D2	5.92	(-)0.24
A1B2C2D2	13.60	(+)0.56
A2B2C2D2	0.63	(-)0.03

Table A 4.4 The F-Values Calculated from the Mean Square Values of Response (2)

The F-value above which there is a greater than 100% α chance that the observed variance is not consistent with random variation is calculated from an F-table. This F-value was found using the following information:

(1) The observed variance values were based on one degree of freedom ($\phi = 1$).
(2) The error variance was calculated using five degrees of freedom ($\phi = 5$).
(3) The level of significance was set at $\alpha = 0.10$ (10% level). This level was stipulated before the statistical analysis and was then adhered to. It is generally sufficient to indicate significance.
(4) A significant departure in either direction from the expected value of the quantity of the null hypothesis was of interest. Therefore a double-sided test was appropriate.

This data gave an F-value of 6.61. In other words, if an F-value of less than 6.61 is recorded, then there is a greater than 10% chance that the observed variance is due to random variation. If greater than 6.61, then the observed F-value was significant. Discretion must be exercised for F-values close to 6.61.

As an example, consider Table A 4.4. This table shows that a change in sucrose concentration (factor C) results in an F-value of 20.63. The corresponding effect value shown in column (4) in table A 4.1 is negative, indicating that the response value decreases as the factor level increases. Thus there is a greater than 90% chance that an increase in sucrose concentration decreases the mass of pelleted dextran. An increase in rotor speed (factor A) significantly increases the mass of pelleted dextran. However, the interactive effect of sucrose concentration and rotor speed (factors A and C) gives an F-value of (+) 0.01 indicating that this effect is not significant.

Calculation of the F-values for response (1) and responses (3) to (6) are given in tables A 4.5 to 4.9. and the significant F-values are discussed in section 7.4.5.

Treatment combination	Enzyme 'effici-ency' (%) (1)	(1)	(2)	(3)	(4)	Mean square (variance)	F-value
A1B1C1D1	83.96	182.89	382.57	733.04	1497.5	140147.28	-
A2B1C1D1	98.93	199.68	350.47	764.41	13.99	12.23	0.10
A1B2C1D1	105.87	153.95	382.88	13.38	77.09	371.42	2.99
A2B2C1D1	93.81	196.52	381.53	0.61	-49.21	151.35	(-)1.22
A1B1C2D1	71.09	188.28	2.91	59.36	-33.45	69.93	(-)0.56
A2B1C2D1	82.86	194.60	10.47	17.73	13.77	11.85	0.10
A1B2C2D1	98.91	185.06	-2.80	-40.10	30.87	59.55	0.48
A2B2C2D1	97.61	196.47	3.41	-9.11	3.73	0.87	0.01
A1B1C1D2	94.98	14.97	16.79	-32.10	31.37	61.50	0.49
A2B1C1D2	93.30	-12.06	42.57	-1.35	-12.77	10.19	(-)0.08
A1B2C1D2	97.86	11.77	6.32	7.56	-41.63	108.32	(-)0.87
A2B2C1D2	96.74	-1.30	11.41	6.21	30.99	60.02	0.48
A1B1C2D2	89.26	-1.68	-27.03	25.78	30.75	59.09	0.48
A2B1C2D2	95.80	-1.12	-13.07	5.09	-1.35	0.11	(-)0.00
A1B2C2D2	99.80	6.54	0.56	13.96	-20.69	26.75	(-)0.22
A2B2C2D2	96.67	-3.13	-9.67	-10.23	-24.19	36.57	(-)0.29

Table A 4.5 Calculation Of F-Values For Enzyme 'Efficiency' Data (Response 1)

Treatment combination	Mass of fructose in solution (3)	(1)	(2)	(3)	(4)	Mean square (variance)	F-value
A1B1C1D1	30.67	63.07	159.30	299.96	733.91	33663.76	-
A2B1C1D1	32.40	96.23	140.66	433.94	-78.03	380.63	(-)26.96
A1B2C1D1	56.87	52.15	219.18	-26.46	179.68	2017.70	142.89
A2B2C1D1	39.36	88.51`	214.77	-51.57	-46.39	134.53	(-)9.52
A1B1C2D1	25.97	84.19	-15.77	69.52	-23.04	33.20	(-)2.35
A2B1C2D1	26.18	134.99	-10.68	110.15	8.27	4.27	0.30
A1B2C2D1	49.70	77.71	-27.37	-30.34	11.74	8.61	0.61
A2B2C2D1	38.80	137.06	-24.20	-16.05	-11.36	8.08	(-)0.57
A1B1C1D2	49.37	1.73	33.16	-18.64	133.98	1121.99	79.45
A2B1C1D2	34.82	-17.51	36.36	-4.40	-25.11	39.43	(-)2.79
A1B2C1D2	73.90	0.21	50.81	5.09	40.63	103.18	7.31
A2B2C1D2	61.08	-10.89	59.35	3.17	14.28	12.76	0.90
A1B1C2D2	40.46	-14.55	-19.23	3.20	14.23	12.66	0.90
A2B1C2D2	37.24	-12.82	-11.10	8.54	-1.92	0.23	(-)0.02
A1B2C2D2	79.02	-3.21	1.73	8.14	5.34	1.78	0.13
A2B2C2D2	58.03	-20.99	-17.78	-19.50	-27.64	47.75	(-)3.38

Table A 4.6 Calculation Of F-Values For The Mass Of Fructose Found In The Solution Fraction (Response 3)

Treatment combination	Dextran to fructose ratio (4)	(1)	(2)	(3)	(4)	Mean square (variance)	F-value
A1B1C1D1	0.68	0.88	1.24	2.58	4.99	1.56	-
A2B1C1D1	0.20	0.36	1.34	2.41	-2.04	0.26	(-)91.83
A1B2C1D1	0.36	0.76	1.21	-1.17	-1.57	0.16	(-)54.45
A2B2C1D1	0.00	0.58	1.20	-0.87	0.37	0.01	2.94
A1B1C2D1	0.46	0.88	-0.83	-0.70	0.10	0.00	0.20
A2B1C2D1	0.30	0.33	-0.34	-0.86	1.31	0.11	37.58
A1B2C2D1	0.38	0.76	-0.84	0.08	0.57	0.02	7.24
A2B2C2D1	0.19	0.44	-0.02	0.28	-0.24	0.00	(-)1.36
A1B1C1D2	0.70	-0.47	-0.52	0.10	-0.16	0.00	(-)0.60
A2B1C1D2	0.18	-0.36	-0.18	-0.01	0.30	0.00	2.01
A1B2C1D2	0.33	-0.15	-0.55	0.49	-0.17	0.00	(-)0.57
A2B2C1D2	0.00	-0.19	-0.31	0.82	0.20	0.00	0.87
A1B1C2D2	0.41	-0.52	0.11	0.34	-0.11	0.00	(-)0.29
A2B1C2D2	0.35	-0.33	-0.03	0.24	0.34	0.01	2.47
A1B2C2D2	0.20	-0.06	0.19	-0.15	-0.10	0.00	(-)0.23
A2B2C2D2	0.24	0.03	0.09	-0.09	0.05	0.00	0.07

Table A 4.7 Calculation Of F-Values For The Ratio Of Dextran to Fructose Found In The Solution Fraction (Response 4)

Treatment combination	Total mass dextran in pellet (5)	(1)	(2)	(3)	(4)	Mean square (variance)	F-value
A1B1C1D1	15.74	85.65	245.74	493.42	1079.6	72855.45	-
A2B1C1D1	69.91	160.09	247.68	586.25	238.77	3563.19	107.46
A1B2C1D1	60.09	106.03	288.37	139.54	196.21	2406.15	72.57
A2B2C1D1	100.00	141.65	297.88	99.23	-40.77	103.89	(-)3.13
A1B1C2D1	43.34	117.20	94.08	110.06	11.45	8.19	0.25
A2B1C2D1	62.69	171.17	45.46	86.15	-114.2	815.24	(-)24.59
A1B2C2D1	57.77	132.85	82.41	-7.50	-60.61	229.60	(-)6.92
A2B2C2D1	83.88	165.03	16.82	-33.27	37.25	86.72	2.62
A1B1C1D2	31.81	54.17	74.44	1.94	92.83	538.59	16.24
A2B1C1D2	85.39	39.91	35.62	9.51	-40.31	101.56	(-)3.06
A1B2C1D2	71.17	19.35	53.97	-48.62	-23.91	35.73	(-)1.08
A2B2C1D2	100.00	26.11	32.18	-65.59	-25.77	41.51	(-)1.25
A1B1C2D2	60.09	53.58	-14.26	-38.82	7.57	3.58	0.11
A2B1C2D2	72.76	28.83	6.76	-21.79	-16.97	18.00	(-)0.54
A1B2C2D2	80.44	12.67	-24.75	21.02	17.03	18.13	0.55
A2B2C2D2	84.59	4.15	-8.52	16.23	-4.79	1.43	(-)0.04

Table A 4.8 Calculation Of F-Values For The Percentage Of Dextran Produced During The Run, Found In The Pelleted Fraction (Response 5)

Treatment combination	Percent fructose in pellet (6)	(1)	(2)	(3)	(4)	Mean square (variance)	F-value
A1B1C1D1	0.00	10.35	49.39	111.47	335.23	7023.70	-
A2B1C1D1	10.35	39.04	62.08	223.76	129.19	1043.13	49.46
A1B2C1D1	9.63	13.51	107.66	61.29	100.61	632.65	30.00
A2B2C1D1	29.41	48.57	116.10	67.90	6.89	2.97	0.14
A1B1C2D1	0.00	42.24	30.13	63.75	21.13	27.90	1.32
A2B1C2D1	13.51	65.42	31.16	36.86	-6.91	2.98	(-)0.14
A1B2C2D1	15.46	51.21	37.92	13.57	-3.13	0.61	(-)0.03
A2B2C2D1	33.11	64.89	29.98	-6.68	15.79	15.58	0.74
A1B1C1D2	8.17	10.35	28.69	12.69	112.29	788.07	37.36
A2B1C1D2	34.07	19.78	35.06	8.44	6.61	2.73	0.13
A1B2C1D2	26.70	13.51	23.18	1.03	-26.89	45.19	(-)2.14
A2B2C1D2	38.72	17.65	13.68	-7.94	-20.25	25.63	(-)1.22
A1B1C2D2	19.91	25.90	9.43	6.37	-4.25	1.13	(-)0.05
A2B1C2D2	31.30	12.02	4.14	-9.50	-8.97	5.03	(-)0.24
A1B2C2D2	23.15	11.39	-13.88	-5.29	-15.87	15.74	(-)0.75
A2B2C2D2	41.74	18.59	7.20	21.08	26.37	43.46	2.06

Table A 4.9 Calculation Of F-Values For The Percentage Of Fructose Produced During The Run, Found In The Pelleted Fraction (Response 6)

APPENDIX 5

THE USE OF CONTINUOUS CENTRIFUGATION IN THE DEVELOPMENT OF A SOLVENT FREE CLINICAL DEXTRAN PRODUCTION PROCESS

Barker and co-workers have studied alternative methods of industrial dextran production in recent years [4-9,15,16,18-23] and have proposed an alternative clinical dextran production process [24] which has been outlined in figure 2.3.

In Barkers' process it was envisaged that the dextran rich product stream from the bioreactor-separator (SCCR-S) unit would be broken down under controlled hydrolytic conditions to produce dextrans of lower molecular weight, typically below 2×10^6 daltons. The dextran material would then be fractionated on a semi-continuous chromatographic refiner (SCCR) unit. Dextran rich product streams from the SCCR-S unit have typically been found to be between 1 and 2% w/v [24]. Studies on the SCCR unit have shown that dextran solutions of up to 20% w/v can be successfully fractionated using this process. In order to maximise the throughputs of dextran hydrolysate through the SCCR unit and hence reduce the operating costs of the proposed clinical dextran process, concentration of the dextran rich product stream from the SCCR-S unit would be required. This could be achieved using a continuous centrifugation system.

Samples of material removed from the rotor walls in the clarification studies reported in section 8.5 had dextran concentrations of up to 10% w/w.

The aim of this appendix is to predict the theoretical throughputs of process fluid and maximum dextran recoveries that can be achieved on a number of commercially available industrial separators, based on the experimental data reported in section 8.5.

Equation 8.15 shows that the sedimentation performance of two similar centrifuges treating the same suspension will be the same if the quantity Q_o/Σ_T has the same value for each. In practice it is possible to compare dissimilar centrifuge types by including an efficiency factor 'e' which takes into account the different levels of turbulence and remixing that exist between different centrifuges, even when operating on the same feed material. Consider two dissimilar centrifuges A and B with efficiencies of e_A and e_B, operating on the same feed. For equal performance:

$$Q_{oA}/e_A \Sigma_A = Q_{oB}/e_B \Sigma_B \quad \text{(A5.1)}$$

Perry [170] has listed the recommended efficiency factors for three types of centrifuge. These are: e = 100% for 'bottle' (bucket) centrifuges, e = 80% for tubular centrifuges and e = 55% for disk-type centrifuges. Disk-type centrifuges have a nozzle or valve facility to allow the continuous or periodic discharge of solids while the bowl is still spinning (see section 4.3.3).

Perry has also listed the capacity factors of a number of commonly used centrifuges. The scale-up data for the laboratory and the largest reported tubular and disk-type centrifuges are listed in table A5.1.

Centrifuge Type	Capacity Factor ($x10^6$ cm^2)	Recommended Scale-up Factor
Laboratory tubular	2.97	1
Industrial tubular	39.02	13
Laboratory Disk-type	10.22	1
Industrial Disk-type	975.45	73

Table A5.1 Scale-up Data for Sedimentation Centrifuges (170)

Consider the situation where 75% of the dextran present in a 1% w/w feed solution is removed by centrifugation on the Sharples T-1 laboratory tubular centrifuge. Assuming that a linear relationship exists between the percentage of unsedimented dextran and the Q_o/Σ_T values as indicated by the experimental data reported in section 8.5, then from figure 8.6 , the corresponding Q_o/Σ_T value, which is equivalent to a 75% removal of dextran from a 1% w/w broth feedstream, was found to be 1×10^{-8} cm sec^{-1}. Using equation 8.13, the Sharples T-1 centrifuge at a rotor speed of 23 000 rpm was calculated to have a capacity factory equal to 2.97×10^6 cm^2. Therefore:

$$1 \times 10^{-8} = Q_o / 2.97 \times 10^6 \quad \text{—— (A5.2)}$$

giving a Q_o value of 1.78 cm^3 min^{-1}. In other words, a Sharples T-1 centrifuge with a rotor speed of 23 000 rpm will require a flowrate of 1.78 cm^3 min^{-1} to remove 75% of the dextran from a 1% w/w reaction broth.

Now consider an industrial tubular centrifuge with a maximum capacity factor of 39.02×10^6 cm^2 (table A5.1). For an equivalent separation, that is, a 75% removal of dextran from a 1% w/w dextransucrase broth, the Q_o/Σ_T value must be maintained at 1×10^{-8} cm sec^{-1}, which corresponds to a process fluid flowrate of 23.4 cm^3 min^{-1}.

The industrial disk-type centrifuge (table A5.1) has a theoretical maximum capacity factor of 975.45×10^6 cm^2. Perry (170) however, states that the practical maximum capacity factor is approximately 746.06×10^6 cm^2, which is the product of the capacity factor of the laboratory disk-type centrifuge (10.22×10^6 cm^2) and the recommended scale-up factor of 73. The flowrate required to maintain a Q_o/Σ_T value of 1×10^8 cm sec^{-1} in this centrifuge can be predicted from equation A5.1, assuming efficiency factors of 80% and 55% for the tubular and disk-type centrifuges, so that:

$$Q_{oB} / (55 \times 746.06 \times 10^6) = 1 \times 10^{-8} / 80$$

Therefore the flowrate required to remove 75% of the dextran from a 1% w/w reaction broth in an industrial scale disk-type centrifuge is 307.7 cm^3 min^{-1}. Clearly, industrial disk-type centrifuges allow the highest throughputs of process fluid for a given degree of separation.

Further Q_o/Σ_T values taken from figure 8.6 over a range of unsedimented dextran values for the 1%, 2% and 3% w/w broths are presented in table A5.2. These values can be used to calculate the flowrates required for a given separation for all 3 broth concentrations for the different centrifuge types in the same manner as described above. The calculated flowrates are presented in table A5.3.

Percentage Dextran Removal (%)	Total Broth Concentration (% w/w)		
	1	2	3
5	-	-	7.00
10	-	-	4.60
15	-	-	2.20
20	-	3.60	1.10
25	6.00	3.00	-
30	5.00	2.70	-
35	4.40	2.20	-
40	4.00	1.80	-
45	3.40	1.80	-
50	3.00	1.15	-
75	1.00	-	-

Table A5.2 Q_O/Σ_T Values at Different Levels of Dextran Sedimentation and Broth Concentrations. Units: $1x10^8$ Cm Sec^{-1}

Type of Centrifuge	% Dextran Removal						
	75	50	45	40	35	30	25
Lab. tubular	1.8	5.4	6.1	7.1	7.8	8.9	10.7
Ind. tubular	23.4	70.2	79.6	93.6	103.0	117.1	140.5
Lab. Disk-type	4.2	12.6	14.3	16.9	18.5	21.1	25.3
Ind. Disk-type	307.07	923.2	1046.2	1230.9	1354.0	1438.6	1846.3

(a) 1% w/w broth

Type of Centrifuge	% Dextran Removal						
	50	45	40	35	30	25	20
Lab. tubular	2.1	2.5	3.2	3.9	4.8	5.4	6.4
Ind. tubular	26.9	32.8	42.1	51.5	63.2	70.2	84.3
Lab. Disk-type	4.8	5.9	7.6	9.3	11.4	12.6	15.2
Ind. Disk-type	353.9	430.8	553.9	677.0	830.8	923.2	1107.8

(b) 2% w/w broth

Type of Centrifuge	% Dextran Removal			
	20	15	10	5
Lab. tubular	2.0	3.9	8.2	12.5
Ind. tubular	25.8	51.5	107.7	163.9
Lab. Disk-type	4.6	9.3	19.4	29.5
Ind. Disk-type	338.5	676.9	1415.5	2154.0

(c) 3% w/w broth

Table A5.3 Maximum Flowrates for Different Levels of Dextran Removal on Different Sedimentation Machines in Units of cm^3 min^{-1}.

These projected flowrates can be used to estimate the maximum amounts of dextran that can be collected from a particular separator over a given time period. Values were

calculated in units of kilogrammes per year and the results are presented in tables A5.4 (a), (b) and (c).

Type of Centrifuge	% Dextran Removal						
	75	50	45	40	35	30	25
Lab. tubular	3.3	6.7	6.8	7.1	6.8	6.7	6.7
Ind. tubular	43.8	87.5	89.3	93.4	89.9	87.5	87.5
Lab. Disk-type	7.9	15.8	16.1	16.8	16.2	15.8	15.8
Ind. Disk-type	575.4	1150.7	1173.8	1227.5	1181.4	1150.7	1150.7

(a) 1% w/w broth

Type of Centrifuge	% Dextran Removal						
	50	45	40	35	30	25	20
Lab. tubular	5.1	5.6	6.4	6.8	7.2	6.7	6.4
Ind. tubular	67.1	73.5	84.0	89.9	94.6	87.5	84.0
Lab. Disk-type	12.1	13.2	15.1	16.2	17.0	15.8	15.1
Ind. Disk-type	382.2	966.6	1104.7	1181.4	1242.8	1150.7	1104.7

(b) 2% w/w broth

Type of Centrifuge	% Dextran Removal			
	20	15	10	5
Lab. tubular	2.9	4.4	6.1	4.7
Ind. tubular	38.5	57.8	80.5	61.3
Lab. Disk-type	6.9	10.4	14.5	11.0
Ind. Disk-type	506.3	759.5	1058.7	805.5

(c) 3% w/w broth

Table A5.4 Projected Maximum Amounts of Dextran Separated on Different Centrifugal Machines in Units of Kg Year^{-1}

A typical calculation is as follows:

The industrial disk-type centrifuge requires a flowrate of 830.8 cm^3 min^{-1} to remove 30% of the dextran from a 2% w/w feed broth (table A8.5(b)). Assuming that the dextransucrase enzyme converts 1 unit mass. of sucrose to yield 0.474 mass units of dextran, then the amount of dextran separated per minute will therefore be:

$$830.8 \times 0.474 \times (2/100) \times (30/100) = 2.363 \text{ g min}^{-1}$$

which in kilogrammes per year is:

$$2.363 \times 60 \times 24 \times 365.325/1000 = 1247.7 \text{ kg year}^{-1}.$$

The values take no account of 'down time' which would be required for maintenance purposes and for the manual recovery of accumulated material, although many disk-type centrifuges can be unloaded dynamically. The highest projected yields of dextran were obtained on the separator with the highest capacity factor. The data in table A5.4 indicates that there are optimum conditions for maximum dextran removal from feed solutions. For example, when processing a 2% w/w broth, maximum dextran removal is

achieved by aiming for a 30% removal of dextran. This value reflects the concentration of dextran in the feed, the volumetric throughput of the feed and the percentage of dextran removal. The industrial disk-type centrifuge gives the highest yields. Plots of the yields at different levels of dextran removal for this centrifuge are presented in figure A5.1. The highest recoveries were recorded for the 2% w/w feed broth, although the true optimum may be slightly higher or lower than this value.

A plot of yield versus Q_o/Σ_T will indicate the optimum volumetric throughput of broth required to achieve maximum dextran recovery on a particular separator. The percentage of dextran removal achieved at a particular feed broth concentration can be equated to a specific Q_o/Σ_T value using table A5.2. The plot for the industrial disk-type machine is presented in figure A5.2. Maximum dextran recovery was achieved for the 2% w/w broth at a Q_o/Σ_T value of 2.7×10^{-8} cm sec^{-1}. This was found to correspond to a flowrate of 1.21 litres per minute.

CONCLUSIONS

The projected process fluid throughputs and dextran recoveries were poor, even when considering the high capacity factors of the disk-type centrifuges. The maximum recorded dextran recoveries were of the order of 1.243 tonnes per year at process fluid throughputs of 1.21 litres per minute. The present UK market for dextran is about 100 tonnes per year. Therefore, approximately 88 industrial scale disk-type centrifuges would be required to recover this quantity of dextran, assuming 10% 'down times'. This number of machines is probably prohibitively high when considering the equipment costs and the energy intensity of the process. Furthermore, the conditions required for optimum dextran removal result in a large proportion of dextran in the process fluid remaining unsedimented as shown in table A5.4. A system of fluid recycle could be employed to counteract this.

Alternative less energy intensive methods of sample concentration that can be operated on an industrial scale do exist. Ultrafiltration is widely used to concentrate and separate process fluids [190]. However, the viscous nature of the HMW native dextran product may result in severe concentration polarisation and membrane fouling effects.

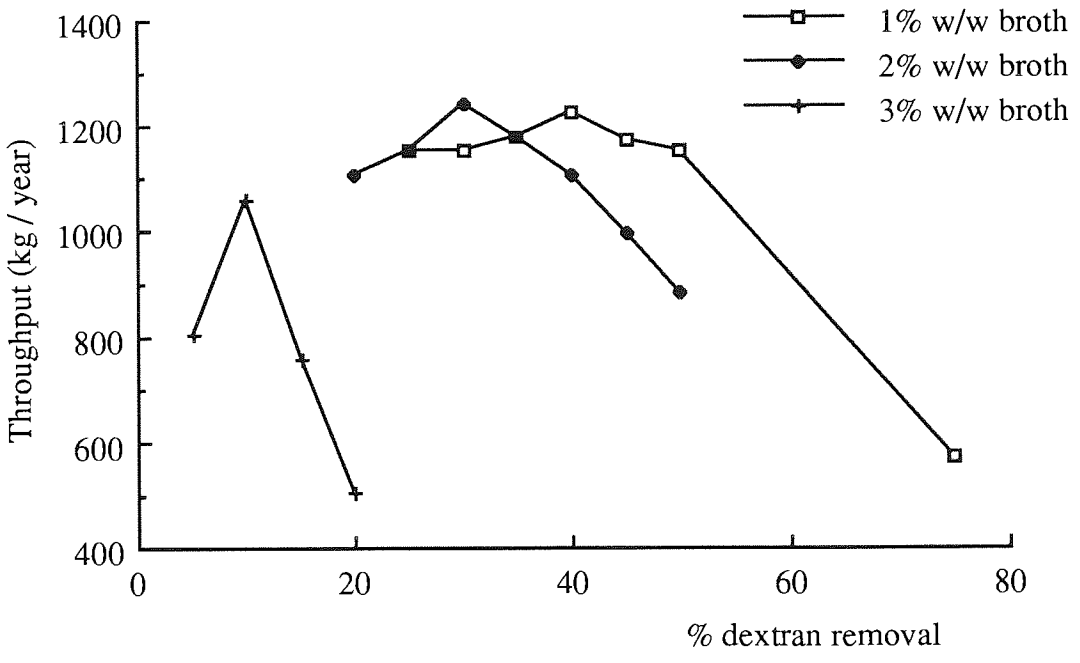

Figure A5.1 Projected Dextran Recovery Versus Level of Dextran Removal from Feed Broths in an Industrial Centrifuge

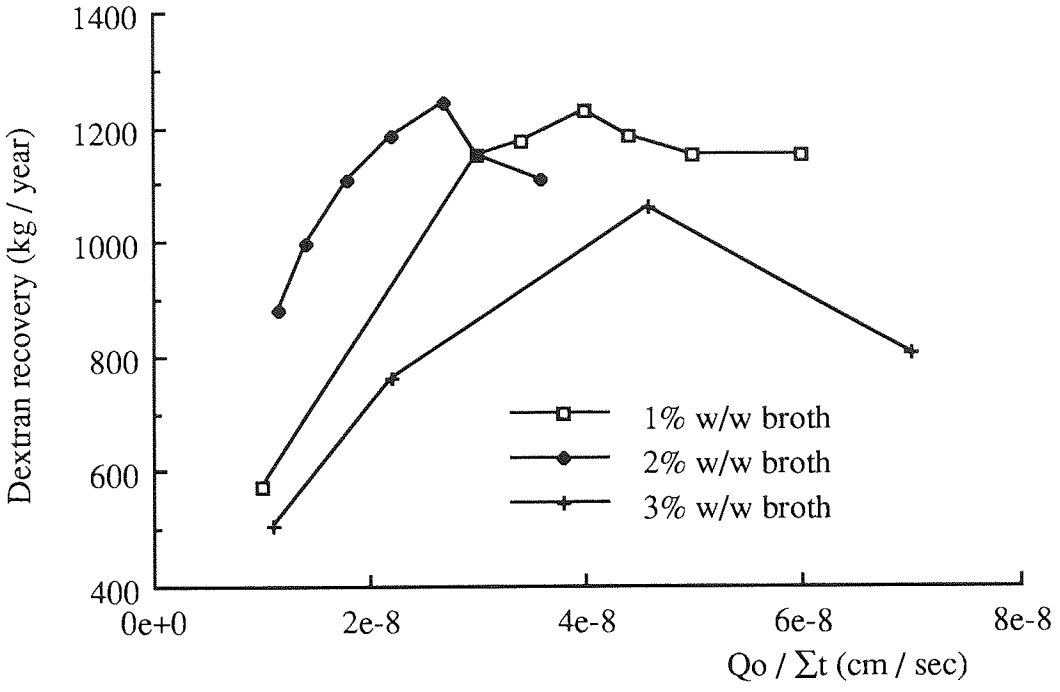

Figure A5.2 Projected Dextran Recovery Versus Q_o/Σ_T Values in an Industrial Centrifuge

APPENDIX A6

The Statistical Analysis of the Experimental Data Reported in Section 8.6

In appendix A4, the application of a factorial statistical analysis procedure to determine the significance of a number of variable factors on the performance of a batch centrifugal bioreactor-separator was discussed. The main and interactive effects and mean square values of a number of different sets of responses were calculated using a systematic tabular method reported by Davies [168]. Because none of the trials were repeated, an estimate of error variance of the experiment was calculated from the mean square values corresponding to the higher order interactions. This practice may be justified on the grounds that, often, higher order effects of this kind are non-existent, or at least negligible. This hypothesis was tested using Bartlett's criterion (see appendix A4). The significance of the main and interactive mean square values for each response were then determined using the variance ratio (or 'F') test.

The experimental data presented in tables 8.8, 8.10 and 8.12 was also assessed factorially in a manner similar to that reported in appendix A4. However certain modifications were made. Because the treatment combinations reported in tables 8.10 to 8.13 were replicated, it was first necessary to modify the method used to calculate the effect and mean square values of each set of response values. Such a modification has been reported by Davies [168] . The first step is to calculate, for each treatment combination, the sum of the replicate observations. These sums are then arranged in a standard order and the columns of the sums and differences of pairs are obtained in the usual way. Because in this case there are two replicate observations, the effect and mean square values obtained in this way have to be divided by 2. The relevant calculations for the response values reported in table 8.8 are presented below in table A6.1.

Treatment combination	Tanks in series values			(1)	(2)	Effect =col(2)/2x2	Mean square value =col(2)^2/4x2
	1	2	sum				
A1B1	3.36	4.02	7.38	15.89	31.67	7.92	125.37
A2B1	4.16	4.35	8.51	15.78	2.29	0.57	0.66
A1B2	3.45	3.86	7.31	1.13	-0.11	-0.03	0.00
A2B2	4.38	4.09	8.47	1.16	0.03	0.01	0.00

Table A6.1 Calculation of the Effect and Mean Square Values for the Data Presented in Table 8.8

The effect value, is merely the average response value recorded at the first factor level subtracted from the average response value recorded at the second factor level.

Unlike the factorial experiment described in appendix A4 where an estimate of the error variation was calculated from the mean square values of the higher interactions, a measurement of the error variation in these studies was obtained by repeating one of the trials in each set of experiments a further 3 times. The trial chosen was the one where all the factors were at the lower level (corresponding to treatment combination A1B1 in all cases). The results from the replicated trials for the experiments reported in section 8.6 are listed in table A6.2.

The estimate of the error variation was determined by calculating the standard error (SE) for each set of replicated response values. The SE was calculated using the following expression:

$$SE = \frac{SD}{\sqrt{n}}$$

Where SD equals the standard deviation and n, the number of degrees of freedom for each set of replicated trial responses, which in these cases was 3. Using this equation, the standard errors of the tanks-in-series and retention time data presented in table A6.2 were calculated and are shown in table A6.3.

Response	Table number	Trial number			
		1	2	3	4
Tanks-in-series values	Table 8.8	3.36	4.02	3.57	3.85
Residence time data	Table 8.10	0.92	0.85	0.84	0.79
Residence time data	Table 8.12	2.73	2.60	2.36	2.88

Table A6.2 Replicated Trial Response Values for the Factorial Experiments Conducted in Section 8.6

Response	Table number	SE
Tanks-in-series values	8.8	0.169
Retention time data	8.10	0.031
Retention time data	8.12	0.127

Table A6.3 The Standard Errors of the Replicated Trials

These standard error values were then used to test the main and interactive effects of the factorial experiments reported in section 8.6 for significance using the so called 't'-test

Unlike the 'F'-test, which tests the probability of finding a deviation as extreme or more extreme than the observed deviation by comparing the mean square value of a given factor or factor combination with the estimated error variance (see appendix A4), The t-test tests for significance by comparing the effect value of a particular factor or factor combination with its standard error (SE), such that:

$$'t' = \frac{\text{Effect}}{\text{Standard error}}$$

The effect and SE values for the data reported in table 8.8 are shown in tables A6.1 and A6.3. The corresponding t-values are shown in table A6.4

Treatment combination	Effect value	Standard error	t-value
A1B1	-	-	-
A2B1	0.57	0.169	3.39
A1B2	-0.03	0.169	-0.16
A2B2	0.01	0.169	0.04

Table A6.4 Calculation of the t-values for the Response Data Presented in Table 8.8

The method reported by Davies ensures that each treatment combination corresponds to a particular effect. Thus it can be seen from table A6.4, an increase in flow rate alone from 5.5 to 11.0 cm^3/min. gives a t-value of 3.39.

The t-test, like the F-test is a test of significance. The theory behind significance tests has been discussed in appendix A4. As with the F-test, by stipulating a level of significance (α) and by reference to a t-table, the significance of the above t-values can be assessed. At the 10% level ($\alpha = 0.1$), for a double sided test with one degree of freedom, the t-table yields a t-value of 6.31. In other words, if the effect t-value is less than 6.31, then there is a greater than 10% chance that the observed deviation for the effect is in fact caused by

random variation. In statistical experiments, such a probability is sufficient to maintain there is no significant departure from the hypothesis that the observed deviation was due to random variation only. If the effect t-value is greater than 6.31, then the observed deviation is not consistent with random variation and the particular effect is said to be significant.

For example, consider the tanks-in-series response to changes in liquid flow rate in the clarification mode studies. From table A6.4, the t-value for the effect of flow rate is 3.39. The t-value is positive, indicating that the response increases as flow rate increases. Thus there is a greater than 90% chance that an increase in flow rate from 5.5 to 11.0 cm^3/min. has no significant effect on the internal mixing of the liquid in the centrifuge bowl. Similarly table A6.4 indicates that an increase in rotor speed from 10 000 to 30 000 rpm. also has no significant effect on the tanks-in-series values. There were no significant interactive effects recorded between the two factors.

Tables A6.5 and A6.6 show the calculation of the effect and t-values for the data reported in tables 8.10 and 8.12.

Treatment combination	ta / t values			(1)	(2)	Effect =col(2)/2x2	t-value
	1	2	sum				
A1B1	0.921	0.849	1.770	3.773	7.561	-	-
A2B1	1.012	0.991	2.003	3.788	0.455	0.114	3.68
A1B2	0.864	0.919	1.783	0.233	0.015	0.004	0.12
A2B2	1.032	0.973	2.005	0.222	-0.011	-0.003	-0.09

Table A6.5 Calculation of the Effect and t-values for the Data Presented in Table 8.10

Treatment combination	ta / t values			(1)	(2)	(3)	Effect	t-value
	1	2	sum				col(2)/2x2	
A1B1C1	2.73	2.60	5.33	13.30	20.89	36.25	-	-
A2B1C1	4.11	3.86	7.97	7.59	15.36	7.17	0.896	7.03
A1B2C1	1.53	1.73	3.26	8.66	3.71	-7.67	-0.959	-7.53
A2B2C1	1.88	2.45	4.33	6.70	3.46	-2.55	-0.319	-2.50
A1B1C2	1.57	1.65	3.22	2.64	-5.71	-5.53	-0.691	-5.42
A2B1C2	2.58	2.86	5.44	1.07	-1.96	-0.25	-0.03	-0.24
A1B2C2	1.31	1.42	2.73	2.22	-1.57	3.95	0.494	3.88
A2B2C2	1.62	2.35	3.97	1.24	-0.98	0.59	0.074	0.58

Table A6.6 Calculation of the Effect and t-values for the Data Presented in Table 8.12

The t-values in table A6.5 show that increases in flow rate from 5.5 to 11.0 cm^3 min^{-1} and increases in rotor speed from 10 000 to 30 000 rpm had no significant effect on the retention time values in the clarification mode studies.

The t-values in table A6.6 confirmed statistically that increases in enzyme flowrate from 4 to 8 cm^3 min^{-1} led to a significant increase in liquid-liquid mixing, whereas increases in sucrose concentration from 10% to 20% w/w led to the opposite effect. The significance of these values is discussed in more detail in section 8.6. The theory behind the significance test has been discussed in more detail in appendix A4.

APPENDIX 7

Calculation of Gradient Fraction Radial Position

Consider the situation when a series of 20 gradient fractions were unloaded from the rotor: The volume of each gradient fraction in the series was measured as it was collected from the rotor and written down in order, as shown in column B, table A 7.1.

Fraction number (column A)	Volume (cm^3) (column B)	Accumulated volume (cm^3) (column C)	Maximum radial position (cm) (column D)	Average radial position (cm) (column D)
Rotor wall	0	0	2.60	-
20	78	78	3.16	2.88
19	88	166	3.69	3.43
18	88	254	4.16	3.93
17	88	342	4.57	4.37
16	88	430	4.96	4.77
15	88	518	5.31	5.14
14	88	606	5.64	5.47
13	88	694	5.96	5.80
12	88	782	6.26	6.11
11	88	870	6.54	6.40
10	88	958	6.81	6.68
9	88	1046	7.08	6.95
8	88	1134	7.33	7.23
7	88	1222	7.57	7.45
6	88	1310	7.91	7.74
5	88	1398	8.04	7.98
4	88	1486	8.26	8.15
3	88	1574	8.48	8.37
2	88	1662	8.69	8.59
1	88	1750	8.90	8.80

Table A 7.1 Calculation of Gradient Fraction Radial Position

From these values the corresponding accumulated fraction volume was calculated and written in column C. The Reograd central core had a radius, r, of 2.6 cm and a height, h, of 7.69 cm which allowed the volume, V of the central core to be calculated from the equation $\pi r^2 h = V$, giving a volume of 163.3 cm^3. The volume of fraction number 20, which was the last gradient fraction harvested from the bowl and hence the fraction closest to the central core during centrifugation was 78 cm^3. The maximum radial position (r_{20}) of the fraction was calculated from the equation $\pi r_{20}^2 h = V$ where:

$$V = 163.3 + 78 = 241.3 \text{ cm}^3$$

Thus r_{20} was found to be 3.16 cm. Therefore fraction number 20 had a minimum radial position equivalent to the inner core radius (2.6 cm) and a maximum radial position of 3.16 cm, which was recorded in column D.

The radial position that fraction number 19 occupied during centrifugation can be calculated in a similar manner, where V will equal 241.3 + 88 cm^3 (column C), giving a maximum radial position of 3.69 cm. This process was repeated for the remaining fractions and the results recorded in column D. The average radial position of a gradient fraction can simply be calculated from the data in column D and is shown in column E. For example, the mean radial position of fraction number 20 is (2.60 + 3.16)/2 = 2.88 cm. This process is applicable to any number of gradient fractions.

APPENDIX 8

The Calculation of Sedimentation Coefficients in Density and Viscosity Gradients

The sedimentation of particles in density and viscosity gradients has been discussed in section 7.4.6. Equation 7.2 showed that the influence of density and viscosity of the surrounding medium on particle sedimentation can easily be treated in physical terms. This equation can be rewritten:

$$S_{20,w} = \frac{1}{C_1} \times \frac{\rho_D - \rho_{20,w}}{\eta_{20,w}} \times \int_{r_1}^{r_2} \frac{\eta_{SOLV,r}}{\rho_D - \rho_{SOLV,r}} \frac{1}{r} dr \qquad \text{(A8.1)}$$

where C_1, the force time integral equals:

$$C_1 = \int_0^t \frac{1}{\omega^2} dt \qquad \text{(A8.2)}$$

The other symbols have been described in section 7.4.6. In all of the bioreaction-separation studies undertaken in chapter 9, a series of fractions were recovered from the bioreactor, each representing a small radial step within the rotor. By determining the density and viscosity of each fraction, an approximate solution to the integral term in equation A8.1 can be achieved.

Steensgaard et al [120] have shown that these calculations can be simplified by use of the 'Sedim' function, which for any given gradient fraction (k) can be defined as:

$$Sedim_k = \frac{\rho_D - \rho_{20,w}}{\eta_{20,w}} \times \frac{\eta_{SOLV,r,k}}{\rho_D - \rho_{SOLV,r,k}} \qquad \text{(A8.3)}$$

Using the Sedim function, equation A8.1 can be approximated by:

$$S20,w = \frac{1}{C_1} \times [\, Sedim_j \times (Ln\, r_j - Ln\, r_i) + \sum_{k=j}^{r-1} Sedim_{k+1} \times (Ln\, r_{k+1} - Ln\, r_k) \qquad \text{(A8.4)}$$

where i equals the initial sample mass centre at the start of centrifugation, j the gradient fraction that contained the initial sample mass centre and r, the final gradient fraction. This is illustrated in figure A8.1.

The force time integral, C_1, can be evaluated by using the following expression:

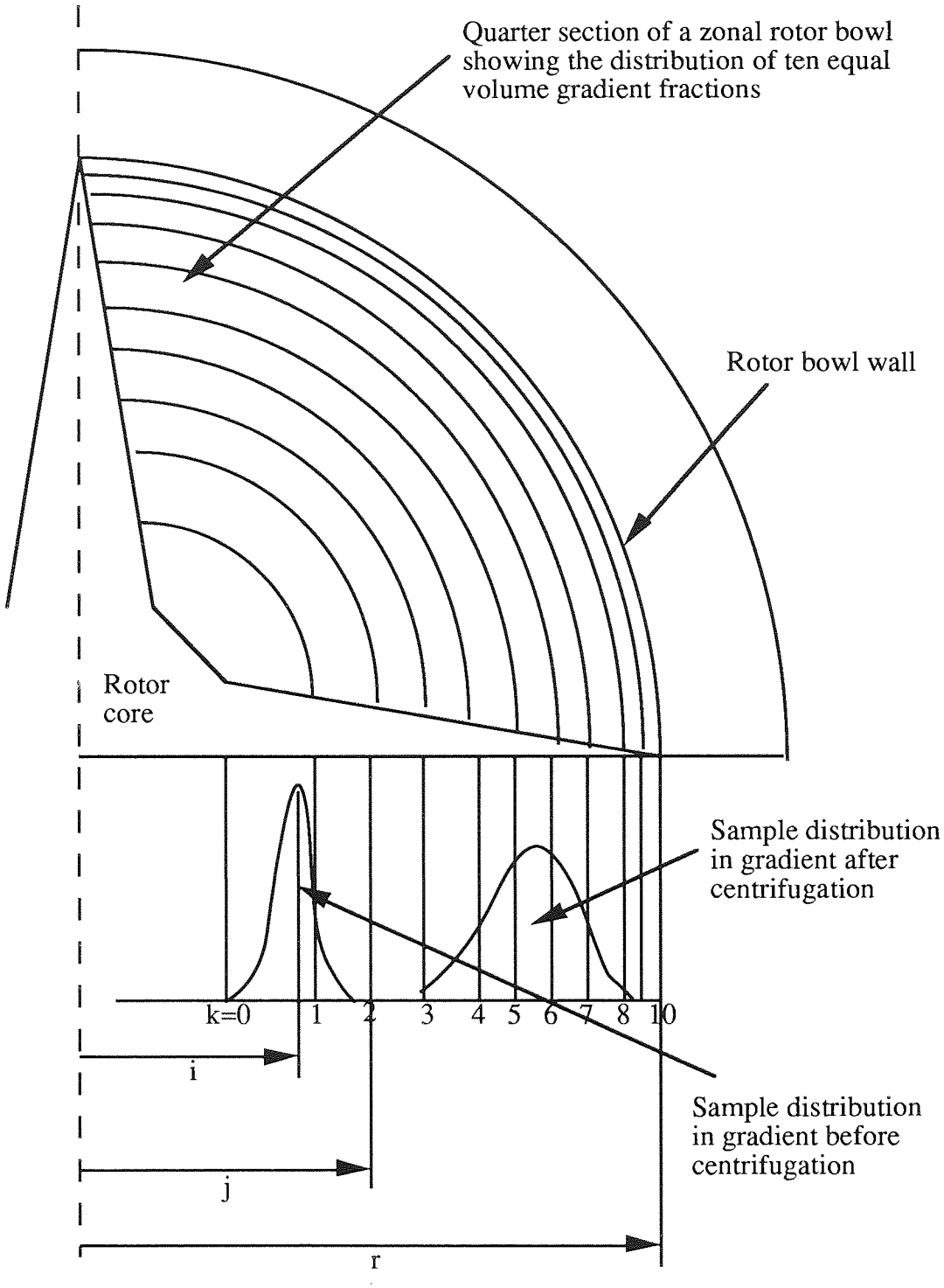

Figure A8.1 A Quarter Section of a Zonal Rotor and Core Showing the Initial and Final Sample Distributions During a Typical Rate-Zonal Centrifugation. (i Equals the Initial Mass Centre, r Equals the final Sample Radial Position, j Equals the Fraction Containing the Initial Mass Centre and k Equals the Fraction Numbers. From Birnie [120].)

$$C_1 = \int_0^t \omega^2 \, dt = \left(\frac{2\pi \times rpm}{60} \right)^2 \times \left(P + \left[\frac{A + D}{3} \right] \right) \qquad \text{(A8.5)}$$

where P equals the run time in minutes at the chosen rotor speed and A and D, the time in minutes for rotor acceleration and deceleration respectively. The low initial acceleration and deceleration rates required for smooth gradient reorientation in the bioreaction-separation runs were ignored in the calculations as figure 9.7 showed that these values would have a minimal effect on the total value of the force time integral.

In order to demonstrate how the $S_{20,w}$ values of a sedimenting particle can be calculated by this method, one of the presynthesised native dextran-fructose rate-zonal centrifugations reported in section 9.3.2 is considered in the following discussion. The sample was prepared from the products of a heat-treated dextransucrase-sucrose reaction broth. This run was a simple rate-zonal separation and not a combined bioreaction-separation process which would use an active enzyme solution as the 'sample' material. The data from this run enabled the system to be calibrated and yielded information concerning the separation of native dextran and fructose in centrifugal fields. The run conditions are shown in table A8.1.

Sample	6.4% w/w Dextransucrase Broth with 2% w/w Sucrose 'Stabiliser'
Sample volume	50 cm^3
Overlay volume	100 cm^3
Sucrose gradient	Linear 10% - 25% w/w
Rotor Speed	20 000 rpm
Run time	120 mins
Gradient fractions collected	30 mins
Acceleration time	7 mins
Deceleration time	18.67 mins
Temperature	25°C

Table A8.1 Preliminary Rate-Zonal Separation Run Conditions

The force-time integral was calculated from equation A8.5 and was found to equal 3.383 x 10^{10}. This run represented a special case where the rotor was allowed to decelerate to rest with no brake as rapid rotor deceleration was not required.

Data from the collected gradient fractions is shown in table A8.2 . The volume of each gradient fraction is written in column B and the equivalent radial position, calculated according to the method reported in appendix A7, is recorded in column C. The concentration of dextran and fructose in each fraction are recorded in columns D and E. The sucrose concentration in each fraction is noted in column F.

The particle density of dextran (ρ_D) was taken as 1.6g cm^{-3} which is standard for all polysaccharide species [94]. Knowing the sucrose concentration of each gradient fraction (column F, table A8.3), the density and viscosity of the fractions at 25°C were determined from standard tables [93]. This allowed the Sedim value, defined in equation A8.4 to be calculated for each gradient fraction. The calculated Sedim values are shown in column G, table A8.4.

The volume, V_i, corresponding to the sample mass centre at the beginning of the run was taken as the sum of the overlay volume and half of the sample volume which in this case was 125 cm^3. The logarithm of the corresponding rotor radius was calculated according to the procedure listed in appendix A7 and was used as the starting point of the calculation procedure. The logarithms of the rotor radii listed in column C, table A8.3 for the fractions inside the range of interest were written in Column H.

Fraction Number	Volume (cm^3)	Radial Position (cm)	Concentration (% w/w)		
			Dextran	Fructose	Sucrose
A	B	C	D	E	F
30	10.1	2.68	0.16	0.43	5.3
29	61.8	3.12	0.14	0.50	4.3
28	61.3	3.50	0.18	0.58	4.0
27	61.1	3.85	0.05	0.24	7.4
26	61.4	4.16	0.03	0.12	10.1
25	61.4	4.46	0.09	0.08	11.6
24	61.6	4.74	0.18	0.06	12.6
23	62.1	5.00	0.27	0.12	13.2
22	61.4	5.25	0.42	0.25	13.9
21	61.4	5.48	0.66	0.27	14.6
20	62.1	5.71	0.10	0.02	15.2
19	61.5	5.93	0.13	0.00	16.0
18	61.4	6.14	0.15		16.7
17	61.3	6.35	0.13		17.5
16	61.4	6.54	0.11		18.2
15	61.6	6.74	0.07		19.0
14	61.3	6.92	0.06		19.6
13	61.4	7.10	0.03		20.1
12	61.1	7.28	0.00		20.6
11	61.1	7.45			21.3
10	61.2	7.62			22.0
9	61.5	7.78			22.8
8	60.9	7.94			23.3
7	61.1	8.10			24.0
6	61.3	8.26			24.3
5	61.2	8.41			24.6
4	61.4	8.56			24.7
3	61.1	8.70			25.0
2	61.3	8.85			25.0
1	21.9	9.80			25.0
Wall	3.0	8.90			25.0

Table A8.3 Gradient Fraction Data from the Preliminary Rate-Zonal Separation Run Number 3

The calculations required to determine the $S_{20,w}$ distribution of the sedimenting species are presented in table A8.4.

The differences between the values at each successive step in column H were entered in Column I, representing the dr/r term in equation A8.1. The product of the Sedim values (column G) and Ln(radius) difference values (column I) were entered in column J and the accumulated total of these values in Column K. The equivalent fully corrected sedimentation coefficients of the fractions of interest were then calculated by dividing the values in column K with the previously calculated force time integral and are recorded in Column L.

This method takes account of the increasing density and viscosity of the supporting sucrose gradient and proved very useful in the preliminary rate-zonal separation trials using presynthesised native dextran-fructose mixtures and heat-treated enzyme samples as reported in sections 9.3.2 and 9.3.3. However, in the special case of the rate-zonal bioreaction-separation process, this system had two serious drawbacks.

Firstly, the sucrose gradient concentrations and hence the sucrose densities and viscosities changed as the dextransucrase reaction proceeded. To counter this, the S-value calculations took account of the 'mean' sucrose concentration of each gradient fraction, calculated using the initial and final sucrose concentrations of the fraction. Secondly, there was the problem of dextran viscosity, which had a very significant effect on the overall viscosity of the reaction medium and hence the particle S-values. No satisfactory method of accounting for these viscosity changes was found in this work. For these reasons the sedimentation coefficient calculations reported in tables 9.6 to 9.16 should be treated with caution.

Fraction Number A	Sedim Value G	Ln (Radius) H	Ln (Radius) difference I	Sedim x difference J	Σ Sedim x difference K	S20,w x10^{-13} Sec L
30	1.36					
29	1.33					
28	1.35	Vi=1.24	-			0
27	1.49	1.35	0.108	0.160	0.160	47
26	1.64	1.43	0.079	0.130	0.290	85
25	1.74	1.49	0.068	0.119	0.409	121
24	1.82	1.56	0.060	0.110	0.519	153
23	1.89	1.61	0.054	0.102	0.621	184
22	1.95	1.66	0.048	0.094	0.715	211
21	1.99	1.70	0.044	0.088	0.803	237
20	2.06	1.74	0.041	0.084	0.888	262
19	2.14	1.78	0.038	0.080	0.969	286
18	2.20	1.82	0.035	0.077	1.044	309
17	2.29	1.85	0.033	0.075	1.120	331
16	2.38	1.88	0.031	0.073	1.181	352
15	2.48	1.91	0.029	0.072	1.264	373
14	2.55	1.93	0.027	0.069	1.333	394
13	2.61	1.96	0.026	0.069	1.401	414
12	2.69	1.98	0.024	0.066	1.466	433
11	2.79	2.01	0.023	0.065	1.531	453
10	2.91	2.03	0.022	0.065	1.596	472
9	3.04	2.05	0.021	0.065	1.661	491
8	3.13	2.07	0.020	0.064	1.725	510
7	3.27	2.09	0.020	0.064	1.790	529
6	3.32	2.11	0.019	0.063	1.853	548
5	3.37	2.13	0.018	0.062	1.914	566
4	3.40	2.15	0.018	0.060	1.974	583
3	3.47	2.16	0.017	0.059	2.033	601
2	3.47	2.18	0.016	0.057	2.090	618
1	3.47	2.19	0.006	0.020	2.110	624
Wall	3.47	2.19	0.000	0.000	0.000	624

Table A8.4 Calculation of the $S_{20,w}$ Values for the Preliminary Rate-Zonal Separation Run

Sample number	Sample volume (cm 3)	Radial position (cm)	Enzyme activity (DSU/cm 3)	Concentration (%w/w)				Mass balance (grammes)				Total DSU detected (DSU)
				Sucrose	Fructose	Dextran	Other Saccharides	Sucrose	Fructose	Dextran	Other Saccharides	
27	50.00	2.97	2.09	5.90	0.43	0.37	-	2.95	0.21	0.19	-	104.71
26	59.00	3.36	0.59	6.30	0.38	0.28	-	3.72	0.22	0.17	-	34.77
25	59.00	3.70	0.14	6.90	0.34	0.24	-	4.07	0.20	0.14	-	8.18
24	59.00	4.02	0.01	7.70	0.34	0.26	-	4.54	0.20	0.15	-	0.00
23	59.00	4.31	0.77	8.20	0.36	0.24	-	4.84	0.21	0.14	-	45.41
22	59.00	4.59	0.46	9.00	0.31	0.22	-	5.31	0.18	0.13	-	27.00
21	59.00	4.85	0.58	9.60	0.33	0.21	-	5.66	0.20	0.12	-	34.37
20	59.00	5.09	0.83	10.40	0.27	0.19	-	6.14	0.16	0.11	-	49.09
19	59.00	5.33	0.44	11.10	0.23	0.17	-	6.55	0.13	0.10	-	26.18
18	59.00	5.55	0.91	11.80	0.26	0.18	-	6.96	0.15	0.11	-	53.59
17	59.00	5.77	0.33	12.60	0.21	0.14	-	7.43	0.13	0.08	-	19.23
16	59.00	5.97	0.66	13.40	0.26	0.13	-	7.91	0.15	0.08	-	38.87
15	59.00	6.18	1.72	14.50	0.22	0.13	-	8.56	0.13	0.08	-	101.46
14	59.00	6.37	1.30	14.90	0.26	0.13	-	8.79	0.15	0.08	-	76.50
13	59.00	6.56	1.55	15.50	0.24	0.17	-	9.15	0.14	0.10	-	91.64
12	59.00	6.74	0.33	15.90	0.22	0.15	-	9.38	0.13	0.09	-	19.23
11	59.00	6.92	0.37	16.60	0.28	0.16	-	9.79	0.17	0.09	-	22.09
10	59.00	7.10	0.71	17.00	0.37	0.17	-	10.03	0.22	0.10	-	41.73
9	59.00	7.27	1.28	17.30	0.41	0.14	-	10.21	0.24	0.08	-	75.28
8	59.00	7.43	2.06	17.60	0.37	0.12	-	10.38	0.22	0.07	-	121.51
7	59.00	7.59	7.32	18.10	0.25	0.27	-	10.68	0.15	0.16	-	431.62
6	59.00	7.75	7.66	18.20	0.18	0.31	-	10.74	0.11	0.18	-	452.07
5	59.00	7.91	7.27	18.20	0.13	0.24	-	10.74	0.08	0.14	-	428.75
4	59.00	8.06	7.54	18.20	0.10	0.22	-	10.74	0.06	0.13	-	445.12
3	59.00	8.21	5.11	18.40	0.08	0.17	-	10.86	0.05	0.10	-	301.52
2	59.00	8.36	3.72	18.30	0.06	0.14	-	10.80	0.03	0.08	-	219.29
1	59.00	8.51	3.85	19.50	0.05	0.27	-	11.51	0.03	0.16	-	227.06
'Wall'	150.00	8.86	8.11	17.70	0.22	0.65	-	26.55	0.33	0.98	-	1216.95
		Total mass detected (grammes)						244.97	4.38	4.14	-	
		Theoretical total based on initial enzyme activity						197.40	11.18	10.07	-	
			Percent of total dextran at rotor wall (%)							23.55		
			Percent of total fructose at rotor wall (%)						7.53			
				Total number of active enzyme units detected (DSU)								4713.23
				Total number of enzyme units loaded (DSU)								7500.00

Table A9.1: Experimental and mass balance data for Bioreaction-Separation Run Number 6

Sample number	Sample volume (cm 3)	Radial position (cm)	Enzyme activity DSU/cm 3	Concentration (%w/w)				Mass balance (grammes)				Total DSU detected (DSU)
				Sucrose	Fructose	Dextran	Other Saccharides	Sucrose	Fructose	Dextran	Other Saccharides	
25	26.00	2.80	4.11	6.20	0.18	0.10	-	1.61	0.05	0.03	-	106.87
24	69.00	3.27	1.60	6.00	0.16	0.07	-	4.14	0.11	0.05	-	110.30
23	69.00	3.68	1.31	6.70	0.16	0.07	-	4.62	0.11	0.05	-	90.40
22	69.00	4.05	1.00	7.50	0.14	0.06	-	5.18	0.10	0.04	-	68.83
21	69.00	4.39	0.67	8.30	0.13	0.06	-	5.73	0.09	0.04	-	46.44
20	69.00	4.70	1.73	9.00	0.08	0.02	-	6.21	0.06	0.01	-	119.42
19	69.00	5.00	0.61	9.60	0.12	0.05	-	6.62	0.08	0.03	-	42.30
18	69.00	5.28	0.49	10.30	0.13	0.04	-	7.11	0.09	0.03	-	34.00
17	69.00	5.54	0.97	10.90	0.10	0.04	-	7.52	0.07	0.03	-	67.18
16	69.00	5.79	0.58	11.60	0.12	0.05	-	8.00	0.08	0.03	-	39.81
15	69.00	6.03	0.64	12.30	0.12	0.03	-	8.49	0.08	0.02	-	43.95
14	69.00	6.27	0.76	13.20	0.11	0.04	-	9.11	0.07	0.03	-	52.25
13	69.00	6.49	0.90	14.40	0.10	0.06	-	9.94	0.07	0.04	-	62.20
12	69.00	6.71	0.94	14.90	0.09	0.06	-	10.28	0.07	0.04	-	64.69
11	69.00	6.92	0.94	15.80	0.10	0.08	-	10.90	0.07	0.06	-	64.69
10	69.00	7.12	0.55	16.10	0.12	0.12	-	11.11	0.08	0.08	-	38.15
9	69.00	7.32	0.83	16.80	0.12	0.11	-	11.59	0.08	0.08	-	57.22
8	69.00	7.51	1.26	17.40	0.11	0.14	-	12.01	0.07	0.10	-	87.08
7	69.00	7.70	0.76	17.70	0.13	0.16	-	12.21	0.09	0.11	-	52.25
6	69.00	7.88	1.11	17.90	0.12	0.18	-	12.35	0.08	0.12	-	76.30
5	69.00	8.06	0.81	18.20	0.14	0.24	-	12.56	0.10	0.17	-	55.56
4	69.00	8.24	0.67	18.20	0.14	0.22	-	12.56	0.10	0.15	-	46.44
3	69.00	8.41	0.50	18.30	0.15	0.22	-	12.63	0.10	0.15	-	34.83
2	69.00	8.58	0.54	18.40	0.15	0.23	-	12.70	0.10	0.16	-	37.32
1	69.00	8.74	0.83	18.40	0.14	0.31	-	12.70	0.09	0.21	-	57.22
gel	65.00	8.89	7.40	18.00	0.17	1.02	-	11.70	0.11	0.66	-	481.25
		Total mass detected (grammes)						239.56	2.22	2.52	-	
		Theoretical total based on initial enzyme activity						246.91	2.45	2.21	-	
			Percent of total dextran at rotor wall (%)							26.26		
			Percent of total fructose at rotor wall (%)						5.00			
				Total number of active enzyme units detected (DSU)								2036.96
				Total number of enzyme units loaded (DSU)								2500.00

Table A9.2: Experimental and mass balance data for Bioreaction-Separation Run Number 7

Sample number	Sample volume (cm 3)	Radial position (cm)	Enzyme activity (DSU/cm 3)	Concentration (%w/w)				Mass balance (grammes)				Total DSU detected (DSU)
				Sucrose	Fructose	Dextran	Other Saccharides	Sucrose	Fructose	Dextran	Other Saccharides	
26	0.00	2.60	0.00	0.00	0.00	0.00	-	0.00	0.00	0.00	-	0.00
25	96.00	3.28	0.23	4.20	0.93	0.42	-	4.03	0.89	0.40	-	21.75
24	68.00	3.68	8.95	7.80	0.49	0.26	-	5.34	0.34	0.18	-	611.99
23	69.00	4.05	4.54	8.60	0.68	0.32	-	5.94	0.47	0.22	-	314.12
22	69.00	4.39	0.28	11.00	0.87	0.44	-	7.60	0.60	0.30	-	19.17
21	69.00	4.71	1.66	12.00	1.09	0.67	-	8.30	0.76	0.46	-	115.04
20	69.00	5.00	0.55	12.70	1.13	0.56	-	8.78	0.78	0.39	-	38.35
19	69.00	5.28	1.86	13.00	0.73	0.51	-	8.99	0.50	0.35	-	128.46
18	69.00	5.54	0.66	13.60	0.62	0.39	-	9.40	0.43	0.27	-	45.38
17	69.00	5.80	8.11	14.40	0.10	0.00	-	9.95	0.07	0.00	-	560.81
16	69.00	6.04	7.72	14.90	0.06	0.00	-	10.30	0.04	0.00	-	533.97
15	69.00	6.27	5.96	15.40	0.37	0.12	-	10.65	0.26	0.08	-	411.90
14	69.00	6.49	4.66	16.00	0.33	0.14	-	11.06	0.23	0.10	-	322.11
13	69.00	6.71	4.74	16.60	0.39	0.17	-	11.47	0.27	0.12	-	327.86
12	69.00	6.92	5.60	17.00	0.34	0.14	-	11.75	0.24	0.10	-	387.29
11	69.00	7.13	4.60	17.80	0.41	0.21	-	12.30	0.28	0.15	-	317.63
10	69.00	7.32	4.80	18.30	0.34	0.19	-	12.65	0.23	0.13	-	332.01
9	69.00	7.52	3.87	18.60	0.31	0.22	-	12.86	0.21	0.15	-	267.46
8	69.00	7.70	3.36	19.00	0.40	0.28	-	13.13	0.28	0.19	-	232.31
7	69.00	7.89	5.02	19.20	0.18	0.21	-	13.27	0.13	0.15	-	347.35
6	69.00	8.07	8.21	19.60	0.14	0.42	-	13.55	0.10	0.29	-	567.52
5	69.00	8.24	6.27	19.60	0.16	0.53	-	13.55	0.11	0.37	-	433.31
4	69.00	8.41	7.21	19.60	0.20	0.64	-	13.55	0.14	0.44	-	498.50
3	69.00	8.58	5.97	19.60	0.23	0.84	-	13.55	0.16	0.58	-	412.86
2	69.00	8.75	10.00	19.70	0.27	1.36	-	13.62	0.19	0.94	-	691.19
1	69.00	8.91	11.18	19.60	0.44	1.24	-	13.55	0.30	0.86	-	772.67
gel	12.00	8.94	18.22	19.10	0.65	2.14	-	2.29	0.08	0.26	-	168.00
								271.43	8.07	7.47	-	
								235.88	10.80	9.73	-	
										3.44		
									0.99			
												8879.00
												11000.00

Total mass detected (grammes)
Theoretical total based on initial enzyme activity
Percent of total dextran at rotor wall (%)
Percent of total fructose at rotor wall (%)
Total number of active enzyme units detected (DSU)
Total number of enzyme units loaded (DSU)

Table A9.3: Experimental and mass balance data for Bioreaction-Separation Run Number 8

Sample number	Sample volume (cm 3)	Radial position (cm)	Enzyme activity DSU/cm 3	Concentration (%w/w)				Mass balance (grammes)				Total DSU detected (DSU)
				Sucrose	Fructose	Dextran	Other Saccharides	Sucrose	Fructose	Dextran	Other Saccharides	
-	0.00	2.60	Assay problems	0.00	0.00	0.00	-	0.00	0.00	0.00	-	Assay problems
19	40.00	2.90		1.98	2.75	1.64	-	0.79	1.10	0.66	-	
18	94.00	3.51		1.56	7.39	6.35	-	1.47	6.94	5.97	-	
17	94.00	4.02		5.59	7.45	5.62	-	5.26	7.00	5.28	-	
16	94.00	4.48		8.75	7.52	5.46	-	8.23	7.07	5.13	-	
15	94.00	4.90		14.17	6.97	3.87	-	13.32	6.55	3.64	-	
14	94.00	5.28		18.45	5.37	3.72	-	17.34	5.05	3.50	-	
13	94.00	5.64		22.55	4.22	2.72	-	21.19	3.97	2.56	-	
12	94.00	5.97		25.07	4.09	2.65	-	23.56	3.85	2.49	-	
11	94.00	6.29		28.11	3.56	1.98	-	26.43	3.35	1.86	-	
10	94.00	6.59		29.72	2.89	2.02	-	27.93	2.72	1.90	-	
9	94.00	6.88		30.19	2.78	1.93	-	28.38	2.62	1.81	-	
8	94.00	7.16		32.43	2.28	2.56	-	30.48	2.15	2.40	-	
7	94.00	7.42		31.25	2.18	2.47	-	29.37	2.05	2.32	-	
6	94.00	7.68		35.58	1.43	2.89	-	33.45	1.34	2.72	-	
5	94.00	7.93		39.73	1.29	3.76	-	37.34	1.21	3.53	-	
4	94.00	8.17		42.69	1.46	2.87	-	40.13	1.37	2.70	-	
3	94.00	8.41		42.47	1.11	3.08	-	39.92	1.04	2.89	-	
2	94.00	8.63		42.27	1.16	2.72	-	39.73	1.09	2.56	-	
1	94.00	8.86		41.43	1.90	3.52	-	38.94	1.79	3.31	-	
Gel	18.00	8.90		38.05	2.41	5.63	-	6.85	0.43	1.01	-	
Total mass detected (grammes)								470.12	62.68	58.23	-	
Theoretical total based on initial enzyme activity								441.89	84.16	75.84	-	
Percent of total dextran at rotor wall (%)										1.74		
Percent of total fructose at rotor wall (%)									0.69			
Total number of active enzyme units detected (DSU)												-
Total number of enzyme units loaded (DSU)												-

Table A9.4: Experimental and mass balance data for Bioreaction-Separation Run Number 13

Sample number	Sample volume (cm 3)	Radial position (cm)	Enzyme activity DSU/cm 3	Concentration (%w/w)				Mass balance (grammes)				Total DSU detected (DSU)
				Sucrose	Fructose	Dextran	Other Saccharides	Sucrose	Fructose	Dextran	Other Saccharides	
-	0.00	2.60	0.00	0.00	0.00	0.00	-	0.00	0.00	0.00	-	0.00
19	55.00	3.01	4.49	0.92	8.00	11.35	-	0.51	4.40	6.24	-	246.96
18	90.00	3.57	4.08	1.35	8.47	9.30	-	1.22	7.63	8.37	-	367.38
17	90.00	4.06	3.54	2.53	8.02	7.54	-	2.28	7.22	6.79	-	318.40
16	90.00	4.50	3.27	3.08	9.27	7.60	-	2.77	8.35	6.84	-	293.90
15	90.00	4.89	4.63	6.35	6.90	5.36	-	5.72	6.21	4.82	-	416.36
14	90.00	5.26	5.17	7.52	6.63	4.56	-	6.77	5.96	4.11	-	465.35
13	90.00	5.60	5.71	9.31	6.04	4.43	-	8.38	5.44	3.99	-	514.33
12	90.00	5.93	6.26	11.13	6.49	4.88	-	10.02	5.84	4.39	-	563.32
11	90.00	6.23	6.80	13.31	5.81	4.87	-	11.98	5.23	4.39	-	612.30
10	90.00	6.52	6.26	16.96	3.07	5.63	-	15.26	2.77	5.07	-	563.32
9	90.00	6.80	5.99	19.54	5.52	3.48	-	17.59	4.97	3.13	-	538.82
8	90.00	7.07	4.76	22.61	2.37	2.85	-	20.35	2.14	2.56	-	428.61
7	90.00	7.33	5.03	24.16	2.05	4.45	-	21.74	1.84	4.01	-	453.10
6	90.00	7.58	4.35	26.15	2.26	3.18	-	23.54	2.04	2.86	-	391.87
5	90.00	7.82	3.81	28.65	2.28	2.64	-	25.79	2.05	2.38	-	342.89
4	90.00	8.06	3.27	31.73	2.17	2.01	-	28.56	1.96	1.81	-	293.90
3	90.00	8.29	2.45	33.60	1.57	2.94	-	30.24	1.41	2.65	-	220.43
2	90.00	8.51	2.31	33.84	1.18	1.85	-	30.46	1.06	1.67	-	208.18
1	95.00	8.73	3.67	35.27	2.02	3.36	-	33.51	1.92	3.19	-	349.01
gel	70.00	8.90	7.43	32.83	4.58	6.96	-	22.98	3.21	4.87	-	520.10
		Total mass detected (grammes)						319.63	81.64	84.12	-	
		Theoretical total based on initial enzyme activity						406.04	144.76	130.44	-	
			Percent of total dextran at rotor wall (%)							5.79		
			Percent of total fructose at rotor wall (%)						3.93			
				Total number of active enzyme units detected (DSU)								8108.54
				Total number of enzyme units loaded (DSU)								16000

Table A9.5: Experimental and mass balance data for Bioreaction-Separation Run Number 15

Sample number	Sample volume (cm 3)	Radial position (cm)	Enzyme activity DSU/cm 3	Concentration (%w/w)				Mass balance (grammes)				Total DSU detected (DSU)
				Sucrose	Fructose	Dextran	Other saccharides	Sucrose	Fructose	Dextran	Other saccharides	
-	0.00	2.60	0.00	0.00	0.00	0.00	-	0.00	0.00	0.00	-	0.00
18	40.00	2.90	0.00	2.10	6.61	6.61	0.59	0.84	2.64	2.64	0.24	0.00
17	95.00	3.51	6.01	2.79	6.45	6.49	0.54	2.65	6.13	6.17	0.51	240.38
16	95.00	4.03	7.21	1.44	6.85	6.45	0.52	1.36	6.50	6.12	0.49	685.10
15	95.00	4.50	3.61	1.09	5.27	4.88	0.40	1.03	5.01	4.64	0.38	342.55
14	95.00	4.91	3.37	1.57	6.94	6.90	0.54	1.49	6.59	6.56	0.51	319.71
13	95.00	5.30	2.88	1.92	7.29	7.50	0.65	1.83	6.93	7.12	0.62	274.04
12	95.00	5.66	6.49	2.17	6.67	6.92	0.54	2.06	6.34	6.58	0.51	616.59
11	95.00	6.00	2.16	3.79	7.46	8.13	-	3.60	7.09	7.72	-	205.53
10	95.00	6.31	2.88	4.97	5.58	5.90	-	4.72	5.30	5.61	-	274.04
9	95.00	6.62	4.57	6.40	6.54	7.32	-	6.08	6.22	6.96	-	433.89
8	95.00	6.91	6.01	6.57	6.14	6.78	-	6.24	5.83	6.44	-	570.91
7	95.00	7.19	7.69	7.62	6.53	7.22	-	7.24	6.21	6.86	-	730.77
6	95.00	7.46	16.59	6.75	5.78	5.29	-	6.41	5.49	5.03	-	1575.72
5	95.00	7.72	16.11	8.44	6.23	6.34	-	8.01	5.92	6.02	-	1530.05
4	95.00	7.97	13.46	9.43	6.32	6.39	-	8.96	6.01	6.07	-	1278.85
3	95.00	8.21	11.30	9.90	6.41	6.58	-	9.41	6.09	6.25	-	1073.32
2	95.00	8.45	10.82	9.99	6.20	6.19	-	9.49	5.89	5.88	-	1027.64
1	95.00	8.68	15.14	10.83	6.07	5.53	-	10.28	5.77	5.25	-	1438.70
Gel	95.00	8.90	20.00	6.72	10.58	14.00	1.25	6.38	10.05	13.30	1.19	1900.00
								91.71	116.02	121.23	-	
								91.41	152.92	137.80	-	
										10.97		
									8.67			
												14517.79
												18417

Total mass detected (grammes)

Theoretical total based on initial enzyme activity

Percent of total dextran at rotor wall (%)

Percent of total fructose at rotor wall (%)

Total number of active enzyme units detected (DSU)

Total number of enzyme units loaded (DSU)

Table A9.6: Experimental and mass balance data for Bioreaction-Separation Studies; Run 16

Sample number	Sample Volume (cm 3)	Radial position (cm)	Enzyme activity DSU/cm 3	Concentration (%w/w)				Mass balance (grammes)				Total DSU detected (DSU)
				Sucrose	Fructose	Dextran	Other saccharides	Sucrose	Fructose	Dextran	Other saccharides	
-	0.00	2.60	-	0.00	0.00	0.00	-	0.00	0.00	0.00	-	0.00
14	95.00	3.27	0.73	13.65	1.35	1.06	-	12.97	1.28	1.01	-	69.76
13	95.00	3.82	5.00	15.28	1.36	1.07	-	14.51	1.29	1.02	-	474.67
12	95.00	4.31	4.24	16.60	1.01	0.97	-	15.77	0.96	0.92	-	402.57
11	95.00	4.74	4.15	18.12	1.03	1.10	-	17.21	0.98	1.05	-	394.23
10	95.00	5.14	2.51	19.05	0.74	0.75	-	18.10	0.71	0.71	-	238.29
9	95.00	5.51	3.68	19.09	0.62	0.67	-	18.14	0.59	0.64	-	349.64
8	95.00	5.86	3.33	20.75	0.57	0.60	-	19.71	0.54	0.57	-	316.20
7	95.00	6.18	3.47	21.30	0.43	0.66	-	20.23	0.41	0.63	-	329.78
6	95.00	6.49	4.56	23.60	0.54	0.51	-	22.42	0.51	0.48	-	432.93
5	95.00	6.79	4.76	24.16	0.57	0.48	-	22.95	0.54	0.46	-	452.16
4	95.00	7.07	4.01	25.85	0.44	0.41	-	24.56	0.42	0.39	-	380.48
3	95.00	7.34	4.45	26.78	0.55	0.43	-	25.44	0.52	0.41	-	422.29
2	95.00	7.61	4.69	26.35	0.58	0.22	-	25.04	0.55	0.21	-	445.59
1	409.00	8.70	3.77	27.52	0.58	0.15	-	112.56	2.37	0.01	-	1541.36
'Wall'	106.00	8.90	5.22	22.4	0.82	2.24	-	23.74	0.87	2.37	-	553.32
		Total mass detected (grammes)						398.79	12.55	11.46	-	
		Theoretical total based on initial enzyme activity						399.03	14.01	12.63	-	
		Percent of total dextran at rotor wall (%)								20.71		
		Percent of total fructose at rotor wall (%)							6.92			
				Total number of active enzyme units detected (DSU)								7685.16
				Total number of enzyme units loaded (DSU)								8000.00

Table A9.7: Experimental and mass balance data for Bioreaction-Separation Run Number 17

Sample number	Sample Volume (cm 3)	Radial position (cm)	Enzyme activity DSU/cm 3	Concentration (%w/w)				Mass balance (grammes)				Total DSU detected (DSU)
				Sucrose	Fructose	Dextran	Other saccharides	Sucrose	Fructose	Dextran	Other saccharides	
-	0	2.60	0.00	0.00	0.00	0.00	-	0.00	0.00	0.00	-	0.00
16	95	3.27	5.55	14.48	1.89	0.69	-	13.76	1.79	0.66	-	527.46
15	95	3.82	4.85	15.20	1.76	0.64	-	14.44	1.67	0.61	-	460.77
14	95	4.31	5.36	17.87	1.61	0.51	-	16.98	1.53	0.48	-	509.28
13	95	4.74	5.74	19.00	1.73	0.53	-	18.05	1.64	0.50	-	545.65
12	95	5.14	5.23	21.11	1.45	0.62	-	20.06	1.38	0.59	-	497.15
11	95	5.51	3.57	21.60	1.54	0.72	-	20.52	1.47	0.68	-	339.52
10	95	5.86	3.83	23.40	1.22	0.67	-	22.23	1.16	0.64	-	363.77
9	95	6.18	3.57	24.55	1.19	0.78	-	23.32	1.13	0.74	-	339.52
8	95	6.49	5.49	24.49	1.04	0.87	-	23.26	0.99	0.83	-	521.40
7	95	6.79	4.98	25.85	0.87	0.82	-	24.56	0.82	0.78	-	472.90
6	95	7.07	5.23	26.78	0.86	0.94	-	25.44	0.82	0.90	-	497.15
5	95	7.34	4.53	28.04	0.95	1.00	-	26.64	0.90	0.95	-	430.46
4	95	7.61	4.34	27.48	0.87	1.13	-	26.10	0.82	1.08	-	412.27
3	95	7.86	4.53	28.58	1.01	1.08	-	27.15	0.96	1.03	-	430.46
2	95	8.11	4.59	28.80	0.92	1.18	-	27.36	0.87	1.13	-	436.52
1	199	8.60	5.48	26.12	1.52	2.25	-	24.81	1.44	2.14	-	1090.52
'Wall'	126	8.90	6.23	25.57	2.78	4.28	-	83.09	2.94	4.54	-	784.98
		Total mass detected (grammes)					-	409.57	18.88	16.99	-	
		Theoretical total based on initial enzyme activity					-	384.62	29.46	26.54	-	
		Percent of total dextran at rotor wall (%)								26.70		
		Percent of total fructose at rotor wall (%)							15.59			
				Total number of active enzyme units detected (DSU)								7671.53
				Total number of enzyme units loaded (DSU)								8000.00

Table A9.8: Experimental and mass balance data for Bioreaction-Separation Run Number 18

Sample number	Sample Volume (cm 3)	Radial position (cm)	Enzyme activity DSU/cm 3	Concentration (%w/w)				Mass balance (grammes)				Total DSU detected (DSU)
				Sucrose	Fructose	Dextran	Other Saccharides	Sucrose	Fructose	Dextran	Other Saccharides	
16	0	2.60	Assay problems	0.00	0.00	0.00	-	0.00	0.00	0.00	-	Assay problems
15	108	3.35		0.00	6.36	3.32	-	0.00	6.04	3.15	-	
14	108	3.96		0.00	8.15	5.17	-	0.00	7.74	4.91	-	
13	108	4.49		0.00	8.37	5.89	-	0.00	7.95	5.59	-	
12	108	4.96		0.00	8.35	6.79	-	0.00	7.93	6.45	-	
11	108	5.40		0.00	9.46	7.35	-	0.00	8.98	6.99	-	
10	108	5.80		0.00	11.09	6.37	-	0.00	10.54	6.05	-	
9	108	6.17		0.00	11.45	5.72	-	0.00	10.88	5.43	-	
8	108	6.52		0.00	12.88	7.49	-	0.00	12.24	7.12	-	
7	108	6.86		0.00	13.31	11.00	-	0.00	12.64	10.45	-	
6	108	7.17		0.00	11.63	9.53	-	0.00	11.05	9.05	-	
5	108	7.48		0.00	12.08	10.67	-	0.00	11.48	10.14	-	
4	108	7.77		0.00	12.44	12.62	-	0.00	11.82	11.99	-	
3	108	8.05		0.00	12.24	13.35	-	0.00	11.63	12.68	-	
2	108	8.33		0.00	12.77	15.97	-	0.00	12.13	15.17	-	
1	108	8.59		0.00	13.95	14.60	-	0.00	13.25	13.87	-	
'Wall'	325	8.90		0.00	16.32	21.34	-	0.00	15.50	20.28	-	
Total mass detected (grammes)								0.00	158.02	141.26	-	
Theoretical total based on initial enzyme activity								0.00	161.96	145.94	-	
Percent of total dextran at rotor wall (%)										14.35		
Percent of total fructose at rotor wall (%)									9.81			
Total number of active enzyme units detected (DSU)												-
Total number of enzyme units loaded (DSU)												-

Table A9.9: Experimental and mass balance data for Bioreaction-Separation Run Number 19

Sample number	Sample Volume (cm 3)	Radial position (cm)	Enzyme activity DSU/cm 3	Concentration (%w/w)				Mass balance (grammes)				Total DSU detected (DSU)
				Sucrose	Fructose	Dextran	Other Saccharides	Sucrose	Fructose	Dextran	Other Saccharides	
16	0	2.60	0.00	0.00	0.00	0.00	0.00	0.00	0.00	0.00	0.00	0.00
15	115	3.39	8.68	0.00	5.79	5.11	0.44	0.00	6.66	5.88	0.51	1996.40
14	115	4.03		0.00	5.49	5.25	0.50	0.00	6.31	6.04	0.58	
13	115	4.59	16.37	0.00	6.11	4.87	0.51	0.00	7.03	5.60	0.59	3765.10
12	115	5.08		0.00	5.80	5.30	0.50	0.00	6.67	6.10	0.58	
11	115	5.53	13.42	0.00	6.55	6.29	0.37	0.00	7.53	7.23	0.43	3086.60
10	115	5.94		0.00	7.26	6.18	0.55	0.00	8.35	7.11	0.63	
9	115	6.33	14.77	0.00	7.58	7.15	0.53	0.00	8.72	8.22	0.61	3397.10
8	115	6.70		0.00	6.89	6.01	0.45	0.00	7.92	6.91	0.52	
7	115	7.04	19.06	0.00	6.66	6.24	0.62	0.00	7.66	7.18	0.71	4383.80
6	115	7.37		0.00	6.93	6.38	0.50	0.00	7.97	7.34	0.58	
5	115	7.69	16.38	0.00	6.96	6.06	0.53	0.00	8.00	6.97	0.61	3767.40
4	115	7.99		0.00	6.51	5.71	0.69	0.00	7.49	6.57	0.79	
3	115	8.29	24.27	0.00	6.61	5.73	0.47	0.00	7.60	6.59	0.54	5582.10
2	115	8.57		0.00	7.09	6.31	0.52	0.00	8.15	7.26	0.60	
1	60	8.71	19.77	0.00	6.82	5.91	0.36	0.00	4.09	3.55	0.22	1186.20
'Wall'	85	8.90		0.00	6.10	9.30	0.55	0.00	5.19	7.91	0.47	
		Total mass detected (grammes)						0.00	115.34	106.43	8.94	
		Theoretical total based on initial enzyme activity						0.00	130.19	117.32	0.00	
		Percent of total dextran at rotor wall (%)								7.43		
		Percent of total fructose at rotor wall (%)							4.50			
				Total number of active enzyme units detected (DSU)								27164.70
				Total number of enzyme units loaded (DSU)								50000.00

Table A9.10: Experimental and mass balance data for Bioreaction-Separation Run Number 20

Sample number	Sample Volume (cm 3)	Radial position (cm)	Enzyme activity DSU/cm 3	Concentration (%w/w)				Mass balance (grammes)				Total DSU detected (DSU)
				Sucrose	Fructose	Dextran	Other Saccharides	Sucrose	Fructose	Dextran	Other Saccharides	
18	0	2.60		0.00	0.00	0.00	0.00	0.00	0.00	0.00	0.00	
17	92	3.25	16.26	6.01	3.25	3.61	0.00	5.53	2.99	3.32	0.00	2991.84
16	92	3.79		6.31	4.01	3.22	0.00	5.81	3.69	2.96	0.00	
15	92	4.26	22.14	7.02	4.23	3.47	0.00	6.46	3.89	3.19	0.00	4073.76
14	92	4.69		7.43	4.22	3.39	0.00	6.84	3.88	3.12	0.00	
13	92	5.08	16.34	8.28	4.89	3.11	0.00	7.62	4.50	2.86	0.00	3006.56
12	92	5.44		9.24	4.12	3.10	0.00	8.50	3.79	2.85	0.00	
11	92	5.78	17.72	10.15	4.44	3.60	0.00	9.34	4.08	3.31	0.00	3260.48
10	92	6.10		11.55	4.63	3.82	0.00	10.63	4.26	3.51	0.00	
9	92	6.41	18.53	12.21	4.75	4.17	0.00	11.23	4.37	3.84	0.00	3409.52
8	92	6.70		13.88	4.72	4.17	0.00	12.77	4.34	3.84	0.00	
7	92	6.97	14.16	14.52	4.86	4.08	0.00	13.36	4.47	3.75	0.00	2605.44
6	92	7.24		15.11	4.88	4.51	0.00	13.90	4.49	4.15	0.00	
5	92	7.50	16.84	15.91	4.91	5.44	0.00	14.64	4.52	5.00	0.00	3098.56
4	92	7.75		16.42	5.52	5.82	0.00	15.11	5.08	5.35	0.00	
3	92	7.99	12.45	17.81	5.14	5.69	0.00	16.39	4.73	5.23	0.00	2290.80
2	92	8.23		17.10	4.82	5.74	0.00	15.73	4.43	5.28	0.00	
1	56	8.37	10.34	17.30	5.37	6.59	0.00	9.69	3.01	3.69	0.00	579.04
'Wall'	85	8.90		8.76	8.26	14.94	2.14	7.45	17.26	31.22	4.47	
Total mass detected (grammes)								190.97	87.79	96.50	4.47	
Theoretical total based on initial enzyme activity									127.49	114.89	0.00	
Percent of total dextran at rotor wall (%)										32.35		
Percent of total fructose at rotor wall (%)									19.66			
Total number of active enzyme units detected (DSU)												25316
Total number of enzyme units loaded (DSU)												47250

Table A9.11: Experimental and mass balance data for Bioreaction-Separation Run Number 21

APPENDIX A10

Computer Program Used to Model the Combined Centrifugal Bioreaction-Separation Process

```
C       FORTRAN PROGRAM SJS10.FOR
C       BY  S.  J.  SETFORD AND L.  E.  TADDEI
C       29 JUNE 1992

C       BATCH CENTRIFUGAL BIOREACTION-SEPARATION MODEL

C       PROGRAM TO SOLVE THE SET OF PARTIAL DIFFERENTIAL
C       EQUATIONS FOR SUCROSE, DEXTRAN AND FRUCTOSE,
C       DERIVED FROM THE MATHEMATICAL MODEL FOR THE
C       BATCH CENTRIFUGAL BIOREACTOR-SEPARATOR

C       S.  J.  SETFORD/CHEMICAL ENGINEERING AND APPLIED
C       CHEMISTRY DEPARTMENT
C       VAX FORTRAN V5.6-119

C       $1$DUA16:[SETFORDSJ]SJS10.FOR;

        PROGRAM BATCH
        DIMENSION S(0:500,0:500),D(0:500,0:500),F(0:500,0:500),
     +  SC(3),BETA(3)

        REAL SCONC,VM,KM,DT,DX,W2,SC,R,KAY,BETA,
     +  VOL,RAD1,RAD2,RAD3,RDP,DIMLGH,ACTLGH
        INTEGER X,T

        OPEN(UNIT=7,FILE='SJS10INP.;',STATUS='OLD')
        OPEN(UNIT=6,FILE='RESSJS10',STATUS='NEW')

C       INPUTS DATA FROM FILE SJS10INP.

C       SEDIMENTATION COEFFICIENTS AND ANGULAR VELOCITY
            WRITE (6,70)
            WRITE (6,71)
            WRITE (6,72)
            WRITE (6,73)
            READ (7,*) SC(1),SC(2),SC(3),W2
            WRITE (6,*) SC(1),SC(2),SC(3),W2

C       INITIAL SUCROSE CONCENTRATION AND SAMPLE VOLUME
            WRITE (6,74)
            WRITE (6,75)
            READ (7,*)  SCONC,  VSAM
            WRITE (6,*) SCONC,  VSAM

C       KINETIC CONSTANTS VMAX AND KM
            WRITE (6,76)
            READ (7,*) VM,  KM
            WRITE (6,*) VM,  KM

C       TOTAL RUN TIME,  DX AND DT VALUES
            WRITE (6,77)
            WRITE (6,78)
            READ (7,*) TT,  DX,  DT
            WRITE (6,*) TT,  DX,  DT

C       PROGRAM STARTS PRELIMINARY CALCULATIONS

C       CALCULATION OF THETA AND DTHETA
        THETA=SC(2)*W2*TT*60
        DTHETA=SC(2)*W2*DT
```

```
      WRITE (6,*) 'THETA, DTHETA'
      WRITE (6,*)  THETA, DTHETA

      WRITE (6,*) 'THE BETA VALUES ARE'
C     CALCULATION OF BETA
      DO 5 K=1,3

      BETA(K)=0.646*(SC(K)/SC(2))*(DX/DTHETA)
      WRITE (6,*)  BETA(K)

    5 CONTINUE

C     CALCULATION OF KINETIC CONSTANTS

      R=VM/(SCONC*SC(2)*W2)
      KAY=KM/SCONC
      WRITE (6,*) 'THE R & KAY VALUES ARE: '
      WRITE (6,*)  R,  KAY

C     CALCULATION OF NUMBER OF DISTANCE
C     AND TIME INCREMENTS

      P=NINT(1/DX)
      BCF=NINT(THETA/DTHETA)
      WRITE (6,*) 'THE P & BCF VALUES ARE: '
      WRITE (6,*)  P,  BCF

C     CALCULATION OF THE INITIAL RADIAL
C     POSITION INITIALLY OCCUPIED BY THE ENZYME

      VOL=(163.3+VSAM)
      RAD1=VOL/(7.67*3.14159265)
      RAD2=SQRT(RAD1)
      RAD3=RAD2-2.6
      RDP=RAD3/6.3
      LRP=NINT(RDP*P)
      WRITE(6,*) ' THE LRP VALUE IS'
      WRITE(6,*) LRP


C     BOUNDARY CONDITIONS IN VOLUME OF BIOREACTOR
C     INITIALLY OCCUPIED BY SAMPLE PULSE

      DO 10 X=1,LRP

      S(X,0)=1
      D(X,0)=0
      F(X,0)=0

   10 CONTINUE

C     BOUNDARY CONDITIONS IN REMAINING BIOREACTOR
C     VOLUME

      DO 20 X=LRP+1,P

      S(X,0)=0
      D(X,0)=0
      F(X,0)=0
```

```
20      CONTINUE


        DO 30 T=0,BCF

        S(0,T)=0
        D(0,T)=0
        F(0,T)=0

30      CONTINUE

C       GRID PROPAGATION LOOPS

        X=0

        DO 50 L=1,P

        X=X+1
        T=-1

        DO 60 M=0,BCF

        T=T+1

              IF(S(X,T).LT.0)THEN
                 S(X,T)=1E-10
              ENDIF

              IF(D(X,T).LT.0)THEN
                 D(X,T)=1E-10
              ENDIF

              IF(F(X,T).LT.0)THEN
                 F(X,T)=1E-10
              ENDIF


        REAC=S(X,T)*R*DTHETA/(S(X,T)+KAY)

        S(X,T+1)=S(X,T)-(BETA(1)*(S(X,T)-S(X-1,T)))-REAC
        D(X,T+1)=D(X,T)-(BETA(2)*(D(X,T)-D(X-1,T)))+(0.47368*REAC)
        F(X,T+1)=F(X,T)-(BETA(3)*(F(X,T)-F(X-1,T)))+(0.52632*REAC)

60      CONTINUE

50      CONTINUE

        WRITE(6,91)
        WRITE(6,87)
        WRITE(6,88)
        WRITE(6,89)'DIST','SUCROSE CONC','DEXTRAN CONC',
     +  'FRUCTOSE CONC'
        WRITE(6,90)  'INCREMENT',  '(DIM)',  '(DIM)','(DIM)'

        DO 105     X=1,P
         DIMLGH=X/P
         WRITE(6,*) DIMLGH,S(X,BCF),D(X,BCF),F(X,BCF)

105     CONTINUE
```

```
C       CALCULATION OF CONCENTRATIONS IN %W/V

        SMULT=SCONC*100

        WRITE(6,91)
        WRITE(6,92)
        WRITE(6,89)'DIST', 'SUCROSE CONC', 'DEXTRAN CONC',
     +  'FRUCTOSE CONC'
        WRITE(6,90)'INCREMENT', '(%W/V)', '(%W/V)', '(%W/V)'

        DO 106 X=1,P

         ACTLGH=(X*6.3)/P
         SND=S(X,BCF)*SMULT
         DND=D(X,BCF)*SMULT
         FND=F(X,BCF)*SMULT
         WRITE(6,*) ACTLGH,SND,DND,FND

  106   CONTINUE

   70   FORMAT(2X,'INPUT VALUES FOR SEDIMENTATION')
   71   FORMAT(2X,'COEFFICIENTS')
   72   FORMAT(2X,'(SC(C),SC(D),SC(F)) AND ANGULAR')
   73   FORMAT(2X,'VELOCITY SQUARED')
   74   FORMAT(2X,'INPUT VALUES FOR CHARGE CONC (CO)')
   75   FORMAT(2X,'PULSE CONC (C-DASH) AND PULSE VOLUME')
   76   FORMAT(2X,'INPUT MICHAELIS CONSTANTS (KM AND VMAX)')
   77   FORMAT(2X,'INPUT TOTAL RUN TIME (MINS) AND DISTANCE')
   78   FORMAT(2X,'AND TIME INCREMENTS')
   87   FORMAT(2X,'CONCENTRATION PROFILES IN DIMENSIONLESS')
   88   FORMAT(2X,'UNITS')
   89   FORMAT(3X,A,5X,A,5X,A,5X,A)
   90   FORMAT(2X,A,7X,A,10X,A,10X,A)
   91   FORMAT(10X)
   92   FORMAT(2X,'CONCENTRATION PROFILES AT END OF RUN')


        CLOSE(7)
        CLOSE(6)

        END
```